

Department of Radiology
Grady Memorial Hospital
80 Butler Street, S. E.
Atlanta, Georgia 30303

THE PHYSICAL ASPECTS OF DIAGNOSTIC RADIOLOGY

Michel M. Ter-Pogossian, Ph.D.

Professor of Radiation Physics, The Edward Mallinckrodt Institute
of Radiology, Washington University School of Medicine,
St. Louis, Missouri

WITH A FOREWORD BY WENDELL G. SCOTT, M.D.

WITH 257 ILLUSTRATIONS

Hoeber Medical Division



Harper & Row, Publishers
New York, Evanston, and London

Radiative Interaction of Electrons with Matter—General or White Radiation (<i>Bremsstrahlung</i>)	27
Efficiency of X-ray Production by Radiative Interaction	31
Direction of General Radiation Emission	33
Characteristic or Line X-Radiation	33
X-Ray Spectrometry	38
Attenuation Spectrometry	39
Diffraction and Interference X-Ray Spectrometry	43
Wave Diffraction and Interference	43
Refraction, Reflection, Diffraction, and Interference of X-Rays	49
X-Ray Diffraction Spectrometry	50
Scintillation X-Ray Spectrometry	54
Other Methods of X-Ray Spectrometry	57
X-Ray Spectroscopic Analysis of Matter	57
References	63
(III) INTERACTION OF X-RAYS WITH MATTER	64
Attenuation of an X-Ray Beam by Matter	64
Exponential Attenuation of X-Rays	64
Half-Value Layer (<i>HVL</i>)	67
Mean Free Path	70
Attenuation Coefficients	70
X-Rays and Particles of Matter	72
Interaction of X-Rays with Atoms, or Coherent Scattering of X-Rays (Thomson Effect)	72
Interaction of X-Rays with Electrons	74
Photoelectric Effect	74
Auger Effect and Fluorescence Yield	77
Compton Effect	77
Interaction of X-Rays with Nuclei	84
Pair and Triplet Production	84
Annihilation Radiation	86
Photodisintegration	87
Components of the Attenuation Coefficient	88
Compton and Photoelectric Attenuation in Compounds and Mixtures of Elements	90
Average Electron Density—Effective Atomic Number	91
References	95
(IV) X-RAY APPARATUS	96
History of X-Ray Tubes	97

Modern X-Ray Tubes	100
The Focal Spot	103
Rotating Anodes	106
X-Ray Tube Housing	107
X-Ray Tube Ratings	107
Maximum Voltage Ratings	107
Maximum Energy Ratings	112
Special Purpose X-Ray Tubes	117
Grid-Control X-Ray Tube	117
Beryllium-Window X-Ray Tubes	121
Stereo X-Ray Tubes	121
Space Charge—Field-Emission X-Ray Tubes	121
Monochromatic Radiation X-Ray Tubes	124
X-Ray Power Supplies—Transformers	127
High Voltage Transformers	129
Autotransformers	129
X-Ray Circuits	129
Self-Rectified Circuits	130
Current Rectifiers	131
Vacuum Tube Rectifiers (Thermionic Rectifiers, or Valve Tubes)	131
Solid State (or Barrier Layer) Rectifiers	132
Half-Wave Rectified Circuits	133
Full-Wave Rectified Circuits	134
Three-Phase Circuits	134
Six-Pulse, Six-Rectifier Circuits	136
Six-Pulse, Twelve-Rectifier Circuits	137
Twelve-Pulse, Twelve-Rectifier Circuits	137
Switching Tube X-Ray Circuits (Dynapulse Circuits)	139
X-Ray Generator Ratings	143
X-Ray Auxiliary Circuits	144
X-Ray Timers	146
Calibration of Timers—Spinning Top	147
References	149

**(V) THE RADIOLOGIC EXAMINATION, PART A: THE X-IRRADIATION
AND THE GENERATION OF INFORMATION 150**

Acquisition of Information by Means of X-Rays	150
X-Radiation Energy Spectrum in Diagnostic Radiology	151
Accelerating Potentials in Diagnostic Radiology	152
X-Ray Spectra	154
Filtration	155
Inherent Filtration	156

Added Filtration	158	
Attenuation of X-Rays in the Patient	160	
Attenuation of X-Rays in Fat	160	
Attenuation of X-Rays in Soft Tissues and Body Fluids		162
Attenuation of X-Rays in Bone	166	
Attenuation of X-Rays in Liver	168	
Contrast Media	169	
Comparison of Biologic Structures by Relative Contrast		171
High Voltage Radiography	176	
Low Energy Radiography—Mammography	183	
References	183	
(VI) THE RADIOLOGIC EXAMINATION, PART B: THE RADIOLOGIC IMAGE, AND THE RETRIEVAL OF INFORMATION	185	
Quality of the Radiologic Image	185	
Limitations Imposed by the Uncertainty Principle		185
Limitations Imposed by the Information-Carrying Capacity of the Beam	186	
Statistical Nature of the Radiologic Image		186
Poisson Distribution	187	
Standard Deviation	189	
Statistical Fluctuations	190	
Contrast, Resolution, and Unsharpness	192	
Extracting Information from the Radiologic Image	193	
Luminescence: Fluorescence and Phosphorescence	194	
Theory of Luminescence of Inorganic Crystals	195	
Radiationless Transition	198	
Storage Phosphors	198	
X-Ray Luminescent Screens	199	
Efficiency of X-Ray Screens	202	
Intensifying Screens	204	
Fluoroscopic and Photofluorographic Screens	206	
X-Ray Image Intensifier Input Screens	208	
Recording the Radiologic Image	208	
X-Ray Film	208	
Exposure	209	
Photographic Density	209	
Characteristic Curve of Film	209	
Radiographic Contrast, Subject Contrast, and Film Contrast		212
Film Densities in Diagnostic Radiology	217	
Film Latitude	217	
Film Sensitivity (Speed)	222	
Comparison of Characteristic Curves for Light and X-Rays		225

The Reciprocity Law and Its Failure	226
Base Density—Fog	227
Sensitivity of Radiographic Film to X-Rays	229
Sensitivity of Radiographic Film to Screen-Generated Light	231
Intensification Factor	234
Film Processing	234
Granularity, Graininess, Resolving Power, and Sharpness	238
References	239

(VII) THE RADIOGRAPHIC IMAGE 241

Image Conversion Quality of Screen-Film Systems	241
Modulation Transfer Function	241
Line Spread Function	244
Radiographic Mottle	249
Noise X-Ray Photons	252
Scattered X-Ray Photons	252
Effect of Scattered Radiation on Radiologic Image	260
X-Ray Grids	263
Terminology	263
Contrast Improvement Factor	264
Selectivity	266
Grid Ratio	269
Lead Content	271
Focus-Grid Decentering	271
Lateral Decentering—Angulation Error	272
Focus-Grid Distance Decentering	274
Comparison of Focus-Grid Distance Decentering and Lateral Decentering	275
Moving Grids	277
Cross Grids	278
Grid Strips	279
Grid Interspace Material	280
Reduction of Scattered Radiation by Distance	282
Unsharpness in Radiologic Examinations	283
Geometric Unsharpness (Penumbra)	283
Unsharpness Contributed by Image Conversion	287
Total Unsharpness and Detail-Recording Capability of Radiographic Systems	289
References	291

(VIII) THE FLUOROSCOPIC EXAMINATION 293

Vision at Low Luminance Levels—Scotopic Vision	294
---	------------

Scopic Visual Acuity and Statistical Fluctuations	298
Scopic Vision and the Fluoroscopic Examination	300
Statistical Fluctuations, Contrast, and Image Perceptibility	301
Statistical Fluctuations in Fluoroscopy: Comparison with Radiography	302
Statistical Fluctuations and Image Perceptibility in Fluoroscopy	305
References	306

(IX) X-RAY IMAGE INTENSIFICATION 307

Fluoroscopic X-Ray Image Intensification	307
Fluoroscopic X-Ray Image Intensifiers	308
X-Ray Image Intensifier Tubes	309
Intensification Factor—Brightness Gain	312
X-Ray Image Intensifier Tube Performance	315
Two-Stage X-Ray Intensifier Tubes	318
Light Amplifier Tube X-Ray Image Intensifiers	320
X-Ray Image Scanning Systems—Television Systems	322
Vidicon and Image Orthicon Television Pickup Tubes	322
Television Circuits and Resolution	326
Scanning—Vertical Resolution	326
Horizontal Resolution	327
Target Underscanning	327
Image Orthicon Television Chain X-Ray Intensifier	328
Television Chain X-Ray Intensifier Tube Combinations	331
Other X-Ray Scanning Television Intensifiers	333
Solid State X-Ray Intensifiers	334
Contrast Perceptibility Improvement by Image Intensification	336
References	339

(X) CINEFLUOROGRAPHY—PHOTOFLUOROGRAPHY 341

X-Ray Cinematography (Roentgen Cinematography)	341
Direct and Indirect Methods of X-Ray Cinematography	342
The X-Ray Unit in Cinefluorography	344
Synchronization in Cinefluorography	345
Nonsynchronized Systems	345
Synchronized Systems	346
Brightness Control	347
X-Ray Image Intensifiers for Cinefluorography	348
The Optical System in Cinefluorography	349
Cameras for Cinefluorography	355

Image Monitoring During Cinefluorography	356
Direct Image Monitoring	356
Television Monitoring	359
Film for Cinefluorography	362
16mm Versus 35mm Film	362
Film Characteristics	364
Negative and Reversal-Type Films	365
Recording the Cinefluorographic Television Image	366
Kinefluorography	366
Video Tape Recording in Cinefluorography	367
Comparison of Cinefluorography, Kinefluorography, and Video-tape Recording	368
Projectors for Cinefluorographic Film	370
Image Quality in Cinefluorography	371
Radiation Exposure in Cinefluorography	374
Photofluorography (Fluorography)	375
References	380
(XI) RADIATION DOSIMETRY: UNITS AND INSTRUMENTATION	382
Quality and Quantity of X-Radiation	382
Radiation Exposure—The Roentgen	384
Roentgens, Rads, and Photons	385
X-Ray Dosimetry	388
Ionization Dosimetry	390
Saturation Voltage	391
Free-Air Standard Ionization Chamber	392
Thimble Ionization Chambers	394
Electronic Equilibrium	396
The Bragg-Gray Relation	396
Air-Equivalent Thimble Ionization Chamber	397
Condenser Ionization Chamber	397
Photographic Dosimetry	399
Scintillation Dosimetry	401
Phosphors Used in Scintillation Dosimetry	401
Optical Light Coupling	405
Photomultiplier Tubes	407
Electronic Circuitry Associated with Scintillation Detectors	407
Scintillation Techniques in X-Ray Dosimetry	410
References	413
Index	415

FOREWORD

This book, devoted to the application of radiation physics for the improvement and advancement of diagnostic radiology, has been seriously needed for a long time. In fact, it is surprising how little attention has been paid by most radiation physicists to the field of diagnostic radiology. Perhaps this is because the field of radiation therapy—emerging from the era when dosage was estimated, when the correlation of dosage and skin reaction was evolving, when the value of fractionation and protraction of dosage was established—absorbed their concentration; then followed orthovoltage therapy, supervoltage therapy machines, radioactive isotope teletherapy and, now, megavoltage therapy, with the perfection of the betatron and linear accelerator. During this evolution nuclear medicine also emerged as a medical specialty. The physics of radiation therapy now appears to have reached a plateau, thus presenting an opportunity to look at diagnostic radiology and to see how the radiation physicist might apply his talents to this discipline rich with opportunities.

Diagnostic radiology has grown and expanded more rapidly than most other medical specialties. It deals with far more patients, demands more intricate examinations, requires more complex equipment, and utilizes more space than do many other hospital departments. Diagnostic radiology is a latent field ready for the radiation physicist to explore and study. With the development of radiologic techniques for cardiovascular angiography, cerebral angiography, lymphangiography, and mammography only three major organs in the body remain invisible to the inscrutable and objective eye of the roentgen beam—the liver, the pancreas, and the spleen.

The introduction of these new procedures came so fast that many refinements are now necessary—new techniques must come; new materials of greater efficiency will be substituted for those now in use; more efficient x-ray equipment awaits development; x-ray tubes of miniaturized focal spots are needed to probe the fine vascular and lymphatic vessels of the body; even development of disposable x-ray tubes for high instantaneous

exposures is possible, offering a breakthrough for new diagnostic procedures.

The techniques and the equipment for the intensification of the fluoroscopic image, while practical today, are in their infancy when considered with what remains to be done with the recording of the image for study by television, cine, magnetic tape—not to mention the possibilities for the computer analysis of such images.

With the advent of Medicare and the ever-increasing patient load for diagnostic study the necessity arises for the mechanization and automation of the examinations, since this is the way in which large numbers of patients may be handled. The increasing shortage of radiologists will require the radiation physicist to produce equipment capable of meeting this demand.

The time has come when the radiation physicist must work hand-in-hand with the diagnostic radiologist, just as he has in the past with the radiation therapist, to bring about the necessary advances. One stimulates the other, and the two by cooperation and hard work will meet the problems and evolve satisfactory solutions.

Dr. Michel Ter-Pogossian is one of the first of the radiation physicists to sense the opportunities for contributions that are inherent in diagnostic radiology. He comes unusually well equipped. He works in a large institution, The Edward Mallinckrodt Institute of Radiology, which houses all the radiation activities for the Barnes Hospital, Washington University School of Medicine Medical Center. Thus he has been the consultant to a very busy department of diagnostic radiology. This has given him an insight into their problems, and as the demands on his time in radiation therapy were eased he was able to focus more of his attention on diagnostic problems.

Dr. Ter-Pogossian has already made major contributions in this field by the development of the monochromatic x-ray beam for enhancing the roentgen image when iodinated contrast solutions were employed for angiographic and urographic examinations, and also by his more recent development of new intensifying screens employing potassium iodide instead of calcium tungstate.

The present volume is both an expansion of the lectures that Dr. Ter-Pogossian delivers to his classes on radiation physics and a critical review of the existing technology. Present throughout its pages are the author's creative imagination and his awareness of the possibilities that can come from the application of radiation physics to diagnostic problems. Enough new material is presented so that the volume is of interest not only to the intern and the resident in radiology but also the experienced radiologist. The latter should sense the possibilities that are apparent for the advancement of his specialty by the intensive application of radiation physics. Most chapters are abundantly illustrated with lucid diagrams and explanations for even the most complicated physical problems.

One of the great services which radiation physicists can and do render to diagnostic radiology is the perfection of existing radiologic techniques and

equipment to minimize the radiation exposure to the patient. Although much remains to be done, their studies of this problem have already helped in reducing patient exposure from radiation. This will be an ever present problem for which the radiation physicist must assume a major responsibility.

We hope this book will stimulate every radiologist to see the practical and research advantages that a full-time radiation physicist can bring to a department of diagnostic radiology. In fact, extra dividends can be anticipated by the department having a radiation physicist working exclusively in diagnostic radiology, just as they have been realized in radiation therapy. Such a partnership holds great promise and Dr. Ter-Pogossian is one of the prophets.

WENDELL G. SCOTT, M.D.

*Professor of Clinical Radiology, Washington
University School of Medicine, St. Louis, Missouri*

PREFACE

The purpose of this book is to provide resident physicians who are training in diagnostic radiology with a text and a source of references on the physical aspects of their discipline. I do hope that radiologists, advanced x-ray technologists, radiation physicists, x-ray engineers, and perhaps x-ray equipment manufacturers may also find it useful.

I wrote this book because of my conviction that the study of the physical aspects of diagnostic radiology is insufficiently represented in the teaching curriculum of radiologists, and that this field has not been adequately explored by either radiation physicists or by x-ray equipment manufacturers. Several excellent texts on the physics of radiation therapy have been written, radiation physicists are often active members of departments of radiation therapy, and, until very recently, most of the questions in physics for certification by the American Board of Radiology were in the domain of radiation therapy. Such a close association between physics and radiation therapy has proved to be very fruitful. Indeed, one can defend the thesis that most of the progress made in radiation therapy resulted from the understanding and application of radiation physics. It is my opinion that even greater benefits can be derived from a thorough understanding and from the application of physical principles in the field of diagnostic radiology.

The organization of the book and the selection of material included were governed by an attempt to develop the fundamental physical principles that underlie the application of radiation to diagnostic radiology. This was done with the purpose of providing the radiologist with a basic background to allow him to understand thoroughly and, hopefully, to improve, in cooperation with physicists and equipment manufacturers, the tools of his trade. While many aspects of x-ray technology are included in this text, in all instances I have attempted to emphasize the basic concepts embodied in techniques or instrumentation rather than the changing hardware.

This book can be understood with little preparation in mathematics. Although a certain number of formulas and derivations of formulas are

included, I have always attempted to make the final equations understandable, even by individuals who are allergic to calculus. A number of subjects have been omitted because I felt that they were not sufficiently important to justify lengthening a book that, after all, will be used by very busy residents in radiology. For example, I did not feel that at this time a discussion of radioisotope radiography was justifiable. Other subjects, such as radiation protection, were excluded because they are very well treated in other texts.

ACKNOWLEDGMENTS

This book is based on a series of lectures given to the resident physicians at the Edward Mallinckrodt Institute of Radiology. Notes were taken and edited by Dr. Donald F. Rayl, who, at the time, was one of our residents, and I am glad to acknowledge his very able assistance in helping me start this book.

Several sections have been adapted with only minor modifications from other authors. I am particularly grateful to Dr. W. Hondius Boldingh of the Philips Company and to Mr. George M. Corney of the Eastman Kodak Company for allowing me to borrow their excellent studies on x-ray grids and on the sensitometric properties of x-ray films, respectively. A major portion of the section on x-ray tubes was kindly supplied by Mr. Thomas H. Rogers of The Machlett Company.

I find it difficult to acknowledge personally the help of every individual and of every company which was extended to me in writing this book. I should like, however, to express generally my great appreciation to all the manufacturers of x-ray equipment and supplies who almost invariably cooperated in contributing very generously their time and much of the illustrative material to be found here.

I am very grateful to Mr. John O. Eichling for his advice and for proof-reading my manuscript. I should like to thank Miss Marilyn J. Harris for both her talent and, particularly, for her angelic patience in preparing a great portion of the illustrative material. Last, but not least, I should like to express my appreciation to Mrs. Golda M. Rain for her excellent secretarial help in preparing the manuscript.

St. Louis, Missouri

MICHEL M. TER-POGOSSIAN, PH.D.

SYMBOLS AND ABBREVIATIONS USED IN TEXT

A	ampere(s)
A	mass number
\AA	angstrom(s)
a	linear acceleration
B	luminance; Bucky factor of grid
b	lateral decentering distance (grid)
C	coulomb(s)
C	capacitance
$C_{a,b}$	contrast between areas a and b
C_{\min}	minimum perceptible contrast (threshold contrast)
c	velocity of light ($\cong 3 \times 10^{10}$ cm sec ⁻¹)
cd	candela(s)
cgs	centimeter-gram-second
D	photographic density; absorbed ionizing radiation dose; distance between strips of a grid
d	strip thickness of a grid
e	elementary charge
e	base of natural logarithms
E	energy (energy of rest mass of electron: 82×10^{-8} erg, or 5.1×10^5 eV)
esu	electrostatic unit(s)
eV	electron volt(s)
F	force; energy fluence; luminous flux; width of focal spot
f	focal length of lens
f_0	focal distance of grid
$f/$	f -number (ratio of focal length to aperture diameter) of an optical system
ft-L	foot lambert(s)
G	total luminance gain; gravitational constant
G_F	flux gain
G_M	minification gain
h	Planck's constant ($= 6.6256 \times 10^{-27}$ erg sec); thickness of grid; height of grid strips
$h\nu$	photon quantum

<i>HVL</i>	half-value layer ($T_{1/2}$)
<i>I</i>	intensity of x-radiation or light (also called energy flux density or energy fluence rate)
in.	inch(es)
J_m	number of ion pairs formed per gram of gas
<i>K</i>	contrast improvement factor
<i>k</i>	contrast reduction factor; threshold signal-to-noise ratio of human eye
keV	kiloelectron volt(s) (1 keV = 10^3 eV)
kV _p	kilovolt(s) at peak potential
L	lambert(s)
lm	lumen(s)
lx	lux
<i>M</i>	linear magnification of an optical system
<i>m</i>	mass
m_e	rest mass of electron: 9.11×10^{-28} g
mA	milliampere(s) (1 mA = 10^{-3} A)
mAs	milliampere-second(s)
MeV	million electron volt(s) (1 MeV = 10^6 eV)
mL	millilambert(s) (1 mL = 10^{-3} L)
mR	milliroentgen(s) (1 mR = 10^{-3} R)
<i>N</i>	number of photons (quanta number)
<i>n</i>	frequency of electromagnetic waves; photon flux
<i>P</i>	lead content of grid
P_N	probability of occurrence of <i>N</i> events
<i>Q</i>	charge of capacitor
R	roentgen(s)
<i>R</i>	resistance
<i>r</i>	grid ratio
r_c	grid ratio of cross grid
s_m	mass stopping power (energy dissipated by electron flux per unit mass of medium) (or S/ρ , see Table XI-1)
sr	steradian(s)
<i>T</i>	optical transmission
$T_{1/2}$	half-value layer (<i>HVL</i>)
<i>t</i>	time
U_F	width of penumbra (geometric unsharpness)
U_m	width of motion unsharpness
U_s	geometrical unsharpness
<i>V</i>	loss factor of grid ($1 - T_p$); potential difference
<i>v</i>	velocity
<i>W</i>	work; average energy expended by ionizing particles in forming one pair of ions
W	watt(s)
W_0	binding energy of an electron in the atom
<i>X</i>	radiation exposure
<i>x</i>	thickness of absorber
<i>Z</i>	atomic number
α	angulation error in grid

δ	increase in width of shadow cast by grid due to lateral decentering; linear dimension of smallest perceptible image with a contrast C
η	clean-up factor (efficiency) of a grid ($1 - T_s$)
gamma	tangent of slope of characteristic film curve
κ	linear attenuation coefficient for pair and triplet interactions
λ	wavelength of radiation
μ	linear (?) attenuation coefficient of x-radiation
μ/ρ	mass attenuation coefficient
μ_{en}/ρ	mass energy absorption coefficient
Φ	fluence (particle fluence)
φ	angle of recoil electron; flux density (particle flux density)
π	linear attenuation coefficient for photodisintegration interactions
Σ	selectivity of grid
σ	standard deviation of a number N subject to statistical fluctuations; linear attenuation coefficient for Compton interactions
σ_0	linear attenuation coefficient for Thomson interactions
τ	linear attenuation coefficient for photoelectric interactions; decay constant of phosphor
θ	angle of photon scattering; mean free path of x-ray photons in an absorber; angular divergence
ω	solid angle

(Introduction)

THE DISCOVERY OF X-RAYS

X-rays (or roentgen rays) were discovered by the German physicist, Wilhelm Conrad Röntgen, on November 8, 1895, while he was investigating the possibility that some radiation could pass through substances opaque to light.¹

At the time of his discovery, Röntgen was experimenting with cathode rays, which are accelerated electrons generated by means of a Hittorf-Crookes tube. The Hittorf-Crookes tube is a glass envelope containing gas at a pressure of a fraction of a millimeter of mercury and fitted with two electrodes separated by a distance of a few centimeters. A difference of potential of a few thousand volts is maintained between the electrodes, generally by means of a Ruhmkorff induction coil. Figures 0-1 and 0-2 show a Hittorf-Crookes tube and a Ruhmkorff coil, respectively, used by Röntgen at the time of his discovery.

In a Hittorf-Crookes tube cathode rays are generated in the following manner: The rarefied gas contained in the tube is partially ionized. The positive ions are accelerated by the electric field established between the electrodes of the tube and strike the cathode with sufficient energy to release electrons from its surface. The electrons thus released, being negatively charged, are accelerated by the electric field toward the anode. These accelerated electrons are called cathode rays. When their velocity is sufficient, they may overshoot the anode and strike the glass of the tube, as shown in Fig. 0-3, where they interact with the glass to produce x-rays. (See also Chapter IV, section on "X-Ray Tubes.") Unless the accelerating potential applied to the tube is extremely high, the cathode rays are absorbed in the glass surface which they strike and cannot escape the envelope of the tube.

When a Hittorf-Crookes tube is operated with a gas pressure between 0.1 and 0.001 mm of mercury, the cathode ray beam is visible as a bluish

¹ The reader interested in the early history of x-rays is urged to read the excellent book by Otto Glasser entitled *Wilhelm Conrad Röntgen and the Early History of the Roentgen Rays* (Ref. 1).

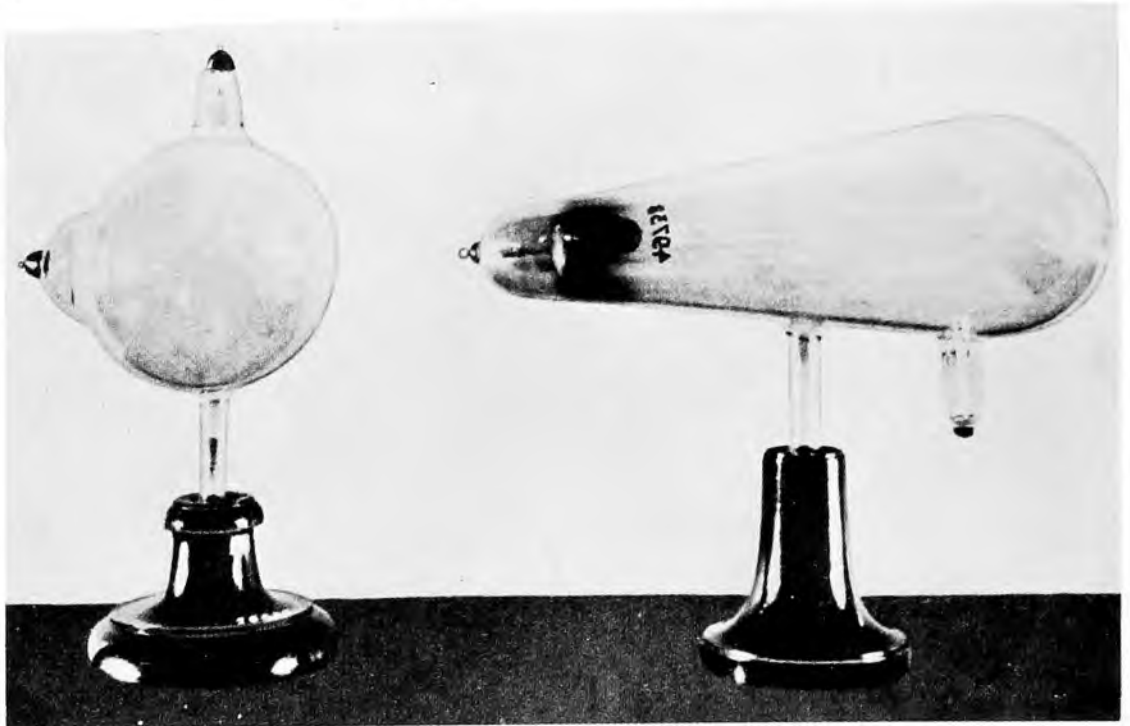


FIG. 0-1. Hittorf-Crookes tube used in Röntgen's laboratory at the time of his discovery of x-rays. The actual tube used in the discovery of x-rays has not been identified. (*Deutsche Museum in Munich. Photograph courtesy of Siemens Co.*)

fluorescence extending from the cathode toward the anode. This fluorescence is produced by the emission of radiant energy by the molecules of the gas subsequent to their excitation by bombardment with cathode rays. When the gas pressure in the tube is reduced below 0.001 mm of mercury, the cathode rays are no longer visible because of the low probability of their collisions with gas molecules.

There are several versions of Röntgen's discovery of x-rays. The following account is based on an article which appeared in McClure's Magazine early in 1896 and was written by H. J. W. Dam, a reporter who interviewed Röntgen shortly after the discovery (Ref. 2).

3.6.3 On November 8, 1895, while experimenting with cathode rays, Röntgen noticed the fluorescence of a paper screen covered with barium platino-cyanide crystals that was placed some distance from the Hittorf-Crookes tube. Barium platino-cyanide crystals fluoresce when struck by cathode rays, and paper screens covered with these crystals were used extensively as detectors for this radiation. The fluorescence observed by Röntgen occurred only when cathode rays were generated in the tube. The fluorescence could not be stimulated by visible light emanating from the cathode ray tube because the tube was covered by a shield opaque to light. (According to one version of Röntgen's discovery (Ref. 3), he was at the time "looking for invisible rays.") Nor could the fluorescence be attributed to the cathode

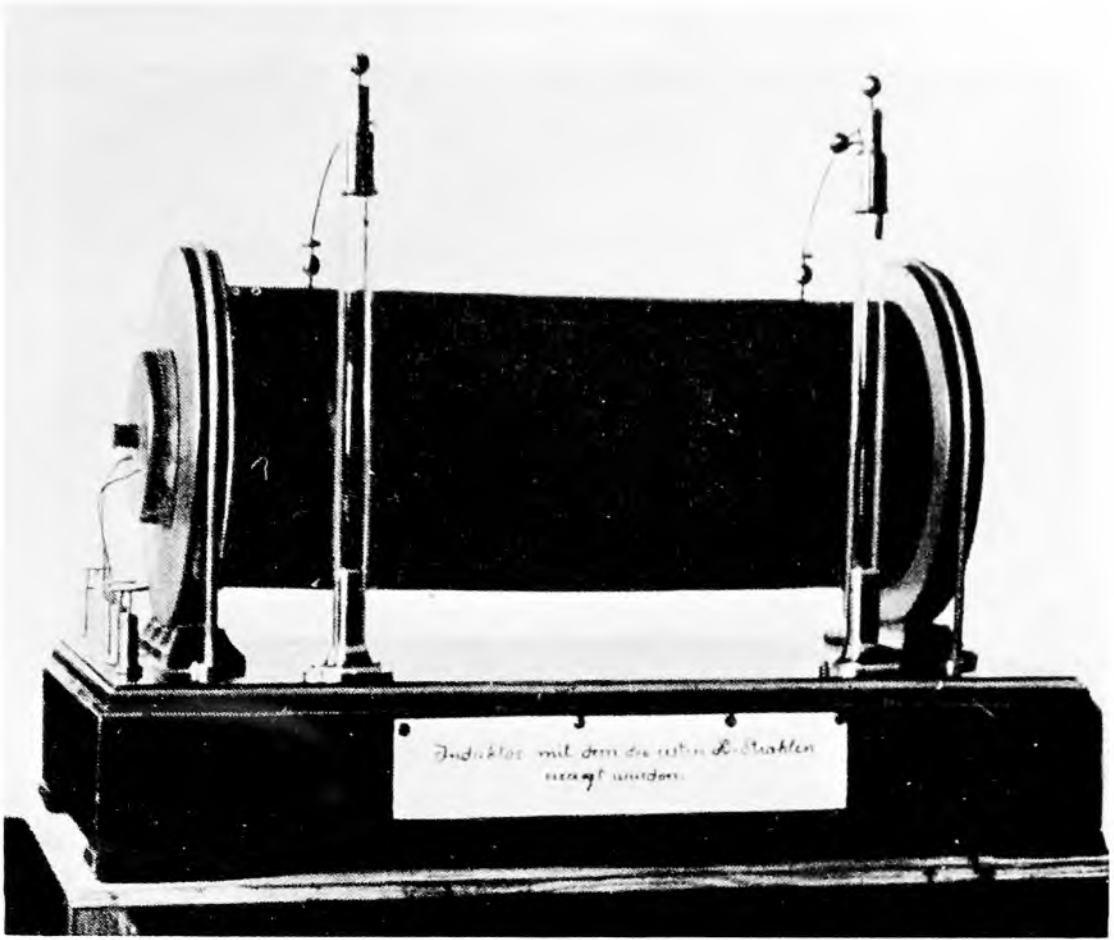


FIG. 0-2. Ruhmkorff induction coil used in Röntgen's laboratory.
(Deutsche Museum in Munich, Photograph courtesy of Siemens Co.)

FIG. 0-3. Schematic diagram of the generation of cathode rays and x-rays by means of an induction coil and a Crookes tube.

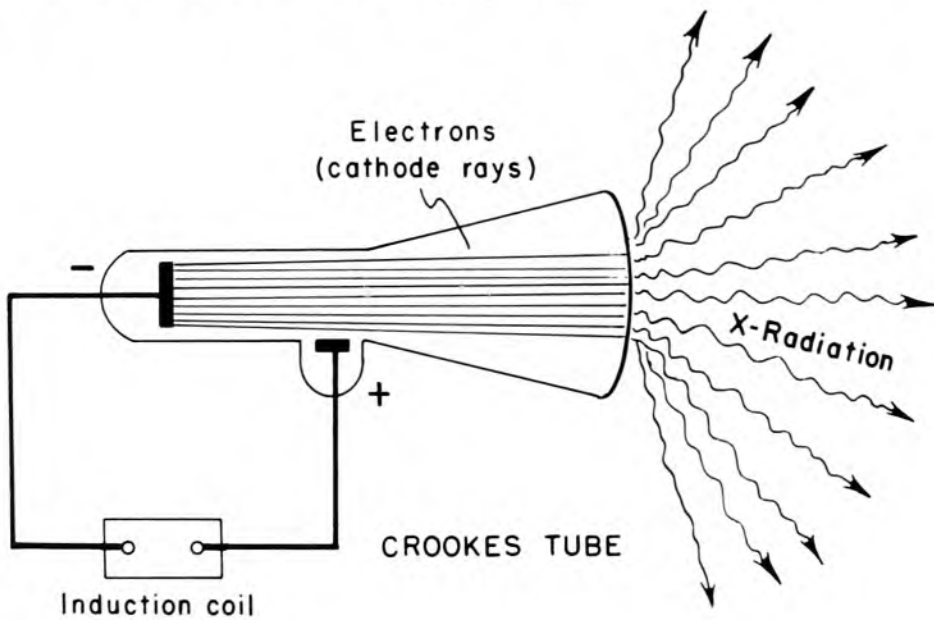




FIG. 0-4. One of the first radiographs of a living hand, exposed by Röntgen on December 22, 1895. (*Original plate in the Deutsche Museum in Munich. Photograph courtesy of Siemens Co.*)



FIG. 0-5. Perhaps the first angiogram, exposed in 1896 by Hascheck in Vienna. Amputated hand injected with a contrast medium containing mercury. (*Photograph courtesy of Siemens Co.*)

radiation, because under the conditions of Röntgen's experiment, the electrons could not escape the glass envelope of the tube. Röntgen concluded that he was observing a hitherto unknown radiation far more penetrating than cathode rays and which was emanating from the wall of the Hittorf-Crookes tube when struck by cathode rays.

Röntgen's first report of the discovery consisted of a preliminary communication (Ref. 4) to the President of the Physical Medical Society of

Würzburg, dated December 1895, in which, for the sake of brevity, he referred to the physical manifestation observed as "x-rays." At the time of this report Röntgen was unaware of the true nature of the x-radiation. He suspected a kinship to ultraviolet light, but his attempts to achieve refraction, reflection, or polarization of x-rays were unsuccessful (Ref. 4).

In an astonishingly short period of time after his discovery, Röntgen thoroughly investigated, and in most instances correctly interpreted, many of the physical properties of x-rays. With further experimentation, he discovered that shadows were cast upon the screen when objects were placed between it and the Hittorf-Crookes tube. These shadows were usually not completely opaque to radiation, but the depth of the shadows increased with the thickness and density of the interposed objects. He also noted that photographic plates wrapped in paper opaque to light were exposed when placed in the same position as the screen. Röntgen exposed what is probably the first medical radiograph as early as December 22, 1895 (Ref. 1), when he made an x-ray picture of a living hand. The original plate, a reproduction of which is shown in Fig. 0-4, is kept in the Deutsche Museum in Munich.

Early after Röntgen's observation that x-rays could penetrate parts of the human body to reveal internal structure, this radiation was applied in clinical medicine. At first, "Röntgen pictures" of the extremities were made in great numbers, and what is probably the first angiogram (Fig. 0-5) was made as early as January 1896 by Hascheck in Vienna (Ref. 5) by injecting via the brachial artery an amputated hand with Teichmann's mixture of lime, cinnabar (mercuric sulfide), and petroleum.

Röntgen's discovery of x-rays is remarkable in the history of science in two respects: (1) In less than two months, between his first observation of the new physical phenomenon and his report of this discovery, Röntgen succeeded in investigating and interpreting correctly many of the physical properties of this new radiation. (2) A very short time after the discovery of x-rays, this radiation was widely applied as a new medical tool of such importance that it justified the creation of a new medical specialty.

Among many other honors bestowed upon him, Röntgen was awarded the first Nobel Prize for Physics in 1901.

REFERENCES

1. GLASSER, O.: *Wilhelm Conrad Röntgen and the Early History of the Roentgen Rays*. Springfield, Ill., Thomas, 1934.
2. DAM, H. J. W.: The new marvel in photography. *McClure's Magazine* 6:403 (April), 1896.
3. MCKENZIE DAVIDSON, J.: The new photography. *Lancet* I:795, 875 (March 21), 1896.
4. RÖNTGEN, W. C.: On a new kind of rays. *Erste Mitt. Sitzgsber. physik.-med. Ges. Würzburg*, 137 (Dec. 1895). Translated by A. Stanton in: *Nature* (Lond.) 53:274 (Jan. 23), 1896.
5. HASCHECK, E., and LINDENTHAL, O. T.: A contribution to the practical use of the photography according to Röntgen. *Wien. klin. Wochenschr.* 9:63 (Jan. 23), 1896.

(I) CLASSIFICATION OF PHYSICAL MANIFESTATIONS

All physical manifestations can be classified into one of the following four categories: matter, force, energy, and radiation.

MATTER

Matter is defined as that physical manifestation possessing mass. Any physical manifestation having the properties exhibited by mass is matter; and, conversely, anything that does not possess mass is not matter. This definition establishes a common denominator for physical manifestations as different as solids, liquids, gases, and subatomic particles. It also distinguishes between matter and energy. Although energy can be converted into matter and, vice versa, matter can be converted into energy, energy does not possess the properties exhibited by mass. In addition to possessing mass, matter can also carry an electric charge which may be either positive or negative in sign.

FORCE

If a mass is at rest, it remains at rest; if it is moving, the velocity is constant unless the mass is acted upon by a force. Force is defined as an agent which modifies the state of rest or the state of motion of mass. Any modification of a state of rest or a state of motion can be expressed as acceleration. Force is therefore equal to mass times acceleration:

$$F = ma.$$

All masses exert upon each other a force of attraction, referred to as gravitation. If two masses m and m' are placed at a distance r from each other, they exert upon each other a force of attraction the magnitude of which is expressed by

$$F = G \frac{mm'}{r^2},$$

where F is the force of attraction and G is the constant of gravitation.

In the centimeter-gram-second (cgs) system of units, which is the system most commonly used in physics, masses are expressed in grams, forces are expressed in dynes, and the gravitational constant G is 6.670×10^{-8} dyn $\text{cm}^2 \text{g}^{-2}$. By definition, a force of one dyne imparts an acceleration of one centimeter per second per second to a mass of one gram.

Matter may also carry an electric charge. The electric charge may be positive or negative. A charge can be defined as exerting a force on another charge. The force between two charges of equal sign is repulsive, and the force between two charges of different signs is attractive. The magnitude of the force exerted between two point charges placed in a vacuum is given by

$$F = \frac{qq'}{r^2},$$

where q and q' are the magnitudes of the charges, and r is the distance between them. It should be noted that the above definition embodies two concepts: (1) A charge can exert a force only on another charge; it does not affect mass. (2) A charge can interact with another charge only if these charges are associated with matter. Since the definition of force involves the acceleration of mass, an electric charge could not be acted upon by a force unless it were associated with mass.

The unit of charge is defined as that charge which, when placed one centimeter from an identical charge in a vacuum, will repel it with a force of one dyne. This unit of charge is referred to as one electrostatic unit of charge (esu). Electric charges are quantized, i.e., all charges encountered in nature are equal to an integer times a given charge—the charge of the electron. This charge is approximately equal to 4.80×10^{-10} electrostatic cgs units. Thus, in nature it is impossible either to observe or transfer electrical charges smaller than this value.

In addition to gravitational and electrostatic forces, many other forces (magnetic, nuclear, etc.) have been observed. They are, however, of little importance in this text.

Fields

A field of force is an expression of the spatial distribution of the intensity of a force or forces. Another definition of this term is: any region of space where a mass is acted upon by a force or forces. The nature of the force or forces involved determines the nature of the field. Thus, matter may be subjected to gravitational, electrostatic, magnetic, or other fields of forces.

WORK AND ENERGY

Energy is the ability of a system to perform work. Both energy and work are expressed in the same units. Work is the product of a force and the dis-

placement of the point of application of this force. This relationship can be expressed by

$$W = Fs,$$

where W is the work performed by the force F displacing its point of application by this distance s . Because force is equal to mass times acceleration (ma), work can also be expressed as

$$W = mas.$$

For example, to raise a steel ball from the floor to any given height requires performing a certain amount of work. In this example, the force involved is equal and opposite in sign to the gravitational attraction between the mass of the steel ball and the mass of the earth, and the displacement is equal to the height to which the ball is raised. It should be noted that the force exerted upon a mass in the gravitational field of the earth is referred to as the "weight" of this mass. A system capable of performing work is said to possess energy, and the energy expended in performing the work is numerically equal to the work performed.

All forms of energy can be classified as potential energy or kinetic energy. A system is said to possess potential energy if it is capable of performing work because of its position or its state. For example, a steel ball placed at a certain distance from the center of the earth (therefore in the gravitational field of the earth) is said to possess potential energy because the force of gravity can perform a certain amount of work in pulling the mass of the ball closer to the center of the earth. Chemical energy is another form of potential energy. A gallon of gasoline is capable of performing a certain amount of work because of the chemical energy stored in its molecules; the system possesses energy because of chemical forces which, if released, can produce work.

Kinetic energy is the ability of a moving mass to perform work. Thus, a bullet fired by a rifle or a steel ball falling from a certain height possesses kinetic energy. Kinetic energy can be converted into potential energy, and vice versa. Thus, if a steel ball is allowed to fall from a certain height toward the center of the earth, its potential energy is converted into kinetic energy.

The unit of work or energy in the cgs system is the erg. It is equal to a force of one dyne displacing its point of application by one centimeter. The erg is not a unit particularly suited for the measurement of the energies involved in radiology because of two reasons: (1) the erg is too large to describe the important energy exchanges, and (2) the energies involved are usually those of the motion of electric charges in an electric field. Consequently, it is desirable to allow for these two limitations in the definition of a unit of work or energy suitable for use in radiology.

The unit of energy most commonly used in radiology is the electron volt

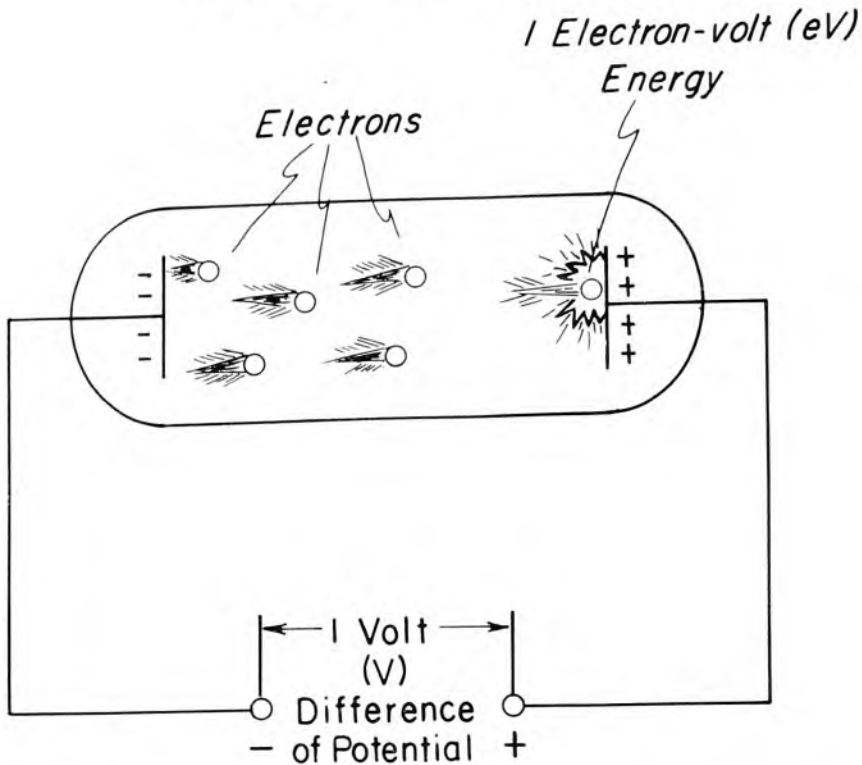


FIG. I-1. Illustration of definition of the electron volt.

(eV). It is by definition the energy of an electron raised to a potential of one volt. It is also equal to the kinetic energy of an electron accelerated by an electric field of one volt. This unit of energy can be pictured in the following manner: An evacuated envelope contains two parallel electrodes (Fig. I-1) connected to a source of electricity such that the difference of potential between the electrodes is one volt. If one electron is released at the negative electrode, it will be attracted by the positive electrode and accelerated up to the point where it strikes the positive electrode. The kinetic energy thus acquired by the accelerated electron is one electron volt. In this example the work was performed by the electrostatic force acting upon the charge of the electron.

The electron volt is a small unit. It is equal to approximately 1.602×10^{-12} erg. Multiples of the electron volt, such as the kiloelectron volt (keV), equal to 10^3 eV, and the million electron volt (MeV), equal to 10^6 eV, are commonly used in the field of radiology. The electron volt, which is a unit of energy, should not be confused with the volt, which is a unit of electrical potential.

MASS-ENERGY EQUIVALENCE

The concept that mass could be converted into energy and, conversely, that energy could be converted into mass was developed on a purely theo-

retical basis by Albert Einstein. Since the development of the fundamental principle in 1905, the conversion of both mass into energy and energy into mass has been demonstrated experimentally. A striking example of the conversion of mass into energy is the development of atom bombs and their sequelae. The conversion of energy into mass is easily observed in the laboratory in the case of pair production; this phenomenon will be discussed in some detail in Chapter III.

Mass and energy are not measured in the same units. They are not equal quantities, but one can be converted into the other under favorable circumstances. The equivalence between mass and energy is mathematically expressed by Einstein's formula

$$E = mc^2,$$

where E is equal to the energy equivalent to the mass m , and c is the velocity of light. For example, the energy equivalent to the mass of an electron at rest (see Table XI-6, Chapter XI) can be determined as follows:

$$m \text{ (mass of the electron)} = 9.11 \times 10^{-28} \text{ g}$$

$$c \text{ (velocity of light)} = 3 \times 10^{10} \text{ cm sec}^{-1}$$

$$E \text{ (energy equal to the rest mass of the electron in the cgs system)} \\ = 9.11 \times 10^{-28} \times (3 \times 10^{10})^2 = 82 \times 10^{-8} \text{ erg}$$

or

$$E = \frac{82 \times 10^{-8} \text{ erg}}{1.6 \times 10^{-12} \text{ (erg/eV)}} = 5.1 \times 10^5 \text{ eV.}$$

Thus, the conversion of one electron at rest into energy yields approximately 510,000 eV; and, vice versa, 510,000 eV is required to produce the mass of one electron.

FUNDAMENTAL PARTICLES

Matter manifests itself in the form of fundamental particles. The term "fundamental" refers to the fact that these particles cannot be divided into smaller entities. This definition, however, is misleading because many of the so-called fundamental particles have been divided into smaller particles. Thus, the neutron is known to break down into an electron and a proton. A list of a number of fundamental particles and some of their properties is shown in Table I-1.

This table is a compilation of the properties of a certain number of elementary particles. Many of these "elementary particles" are not stable and decay to other "elementary particles." The photon, which is listed in this table as a particle, is a bundle of energy carried by electromagnetic radiation. Photons do not possess mass and, consequently, they cannot be considered

TABLE I-1. Characteristics of Some Elementary Particles^a

Particle	Symbol	Charge ^b	Mass (in grams)	Mean life (in seconds)
Photon	γ	0	0	stable
Leptons				
Neutrino	ν	0	0	stable
Electron	e^-	-1	9.1085×10^{-28}	stable
Positron	e^+	+1	9.1085×10^{-28}	stable
(Muon)	μ^-	-1	0.18834×10^{-24}	2.212×10^{-6}
(Muon)	μ^+	+1	0.18834×10^{-24}	2.212×10^{-6}
Mesons				
	π^\pm	± 1	0.248829×10^{-24}	2.55×10^{-8}
	π^0	0	0.240647×10^{-24}	2.2×10^{-16}
	K^\pm	± 1	0.880411×10^{-24}	(K^+) 1.22×10^{-8}
	K^0		} 0.887363×10^{-24}	50% K_1 50% K_2
	K_1			1.00×10^{-10}
	K_2			$6.1(+1.6/-1.1) \times 10^{-8}$
Baryons				
Proton	p	+1	1.67243×10^{-24}	stable
Neutron	n	0	1.67474×10^{-24}	1.013×10^3
	Λ	0	1.988207×10^{-24}	2.51×10^{-10}
	Σ^+	+1	2.12019×10^{-24}	0.81×10^{-10}
	Σ^-	-1	2.1344×10^{-24}	1.61×10^{-10}
	Σ^0	0	2.1266×10^{-24}	$< 0.1 \times 10^{-10}$
	Ξ^-	-1	2.3501×10^{-24}	1.28×10^{-10}
	Ξ^0	0	2.336×10^{-24}	1.5×10^{-10}

(one event)

^a From Barkas and Rosenfeld (Ref. 1). Some values are taken from the NBS Miscellaneous Publication 253 (Ref. 2) (see also Table XI-6 in Chapter XI).

^b The charge of one electron (4.802810^{-10} esu) is unity.

to be matter. Under suitable circumstances, however, the energy carried by a photon can be converted into an equivalent amount of matter.

Negative electrons are found in all atoms. They carry the smallest charge observed in nature, called elementary charge. Positive electrons (called positrons) cannot exist for a long period of time in our universe. They combine with a negative electron, and the mass of the two particles is converted into two photons emitted at 180 degrees from each other. These photons are called annihilation radiation. Neutrons and protons are the building blocks for nuclei. They have about the same mass and are approximately 1836 times heavier than electrons. In free space, neutrons decay with a mean life of approximately 1000 seconds to a proton and a negatively charged electron.

When bound in a stable nucleus, neutrons are stable. In a radioactive nucleus, a neutron may be converted into a proton, thus improving the stability of this nucleus.

Neutrinos are elusive particles, as they carry practically no mass and no charge. Their existence, originally postulated to "balance the books" in beta-ray decay, has recently been experimentally observed.

Mesons, which are particles with a mass greater than that of the electron, are usually produced when very high energy particles interact with matter. Mesons are unstable particles that decay to electrons, protons, neutrons, neutrinos, or other mesons.

Mesons can be classified into three general categories: the μ mesons (leptons) have a mass approximately 200 times greater than that of the electrons, and decay to positive or negative electrons and neutrinos. The π and K mesons have a mass approximately 300 times that of the electron and they decay to μ mesons and neutrinos. The baryons include very heavy mesons which carry a mass greater than that of the proton. These mesons may decay to protons or neutrons and μ mesons (leptons).

A certain number of particles observed in our universe are called "antiparticles." They are identical to "normal" particles but of opposite charge. Antiparticles cannot exist for long periods of time in our universe; they undergo annihilation when they encounter their stable counterparts. For example, the antiparticle of the electron is the positron. The proton also has an antiparticle, called the antiproton, which has the same mass as the proton but a negative charge. The antiproton, like other antiparticles, cannot exist in our universe and is rapidly annihilated by interaction with a proton. Recently the existence of an antideuteron was reported.

Science fiction writers like to postulate the not inconceivable existence in space of stable antimatter composed of antiparticles with respect to our own universe.

Atoms

In the immediate, accessible universe, that is to say, the earth and the planets, fundamental particles tend to conglomerate. Most of the matter exists in the form of aggregates of fundamental particles rather than in the form of free particles. Fundamental particles tend to associate with one another because of forces that exist between them. One of these forces is the electrostatic force of attraction between particles carrying opposite charges. Other forces, referred to as nuclear forces, exist between heavy particles such as protons and neutrons. Gravitational forces play a negligible role in these aggregates.

One of the simpler of these aggregates consists of the bond between a proton and a neutron. Such a particle is called a deuteron; it carries the one positive electric charge of the proton and has a mass approximately equal to the sum of that of a proton and that of a neutron. A more complex aggregate

consists of a package composed of two protons and two neutrons; it is called an alpha particle. It carries two positive charges and its mass is roughly equal to twice that of the deuteron. In these examples the particles are held together by nuclear forces. Another type of combination consists of a proton attracting and holding in its immediate vicinity an electron. Such a structure is held together by the electrostatic attraction between the proton and the electron. In such a combination the electron may be found at any distance from the proton, but it more probably occupies an orbit at a given distance from the centrally located proton. A still more complex configuration can be achieved when an alpha particle, which carries two positive charges, attracts to its vicinity two electrons.

The combination of an aggregate of protons and neutrons, called nucleus, and of peripheral electrons is called an atom. From the mechanical standpoint the structure of an atom is maintained by a balance between centrifugal force, which tends to cast the electron away from the nucleus, and an electrostatic force of attraction between the positively charged nucleus and the negatively charged electrons, which maintains them within the atom. The number of positive charges in the nucleus, which is equal to the number of protons in that cluster, determines certain properties of the atom forming the cluster. These properties define a chemical element. The simplest element is hydrogen: it is composed of one proton and one electron. More complex atoms contain more protons and, consequently, more peripheral electrons. Ninety-two elements are found in the earth's crust, and to this date, an additional 11 elements have been artificially produced by man. The last element produced is called lawrencium in honor of the late Dr. E. O. Lawrence of the University of California. It is quite probable that additional elements will be artificially produced in the future.

In a neutral atom, the number of electrons is equal to the number of positive charges carried by the nucleus. Atoms are three-dimensional structures. The electrons travelling about the nucleus may occupy any position in the vicinity of that nucleus, with the greatest probability in well-defined shells. Atomic dimensions vary depending upon the element under consideration. The nuclei are approximately 10^{-12} cm in diameter, whereas the diameter of the whole atom is of the order of 10^{-8} cm. Between the nucleus and the electrons there is therefore vacuum; structurally the atom can be considered as a very thinly populated region of space. The "emptiness" of an atom can be exemplified by the following picture: If an atomic nucleus were increased to the size of a grain of sand, the surrounding space occupied by the electrons would occupy a large convention hall with the "nuclear" grain of sand in the center. Considering these relative space factors in atoms composing matter, it becomes apparent that a freely moving high-speed electron may go through a large number of atoms before colliding with any form of matter.

Nuclei are composed of protons and neutrons. These particles are called

nucleons. Nucleons are bound together by nuclear forces that are considerably greater than the electrostatic force of repulsion between protons. The positive charge of an atom is due to the number of contained protons. Neutrons add mass but no charge. Since the mass of a proton or a neutron is approximately 1836 times that of an electron, the mass of an atom is derived mainly from the nucleus. The number of protons in the nucleus defines an element and is usually referred to as its atomic number, symbolized by the letter Z . All atoms of a given element have the same atomic number.

Isotopes are atoms with nuclei containing the same number of protons but a different number of neutrons. The isotopes of a given element all have identical chemical properties, but they differ in their physical properties. Most naturally occurring elements are composed of a mixture of several isotopes. Isotopes may be either stable or unstable. An isotope with an imbalance between the number of protons and neutrons is unstable, and such instability results in the expulsion of energy, usually in the form of a particle. This disintegration is called radioactivity and results in a change of the nucleus. This process continues until a stable isotope results. The total number of protons and neutrons in the nucleus of an element is referred to as its mass number and is usually represented by the letter A . The number of neutrons in the nucleus of an isotope can be found by subtracting the atomic number Z from the mass number A .

The chemical properties of elements recur in a cyclic manner with increasing atomic number; and the grouping of elements on the basis of similarity of chemical properties results in the periodic table of elements.

In an atom, the electrons tend to occupy a series of well-defined shells about the nucleus. The distance between the nucleus and each one of these consecutive shells depends upon the atomic number of the atom. The electrostatic attraction between an electron and the nucleus depends strongly upon the distance between them; and, therefore, each atomic shell can be considered as the locus of electrons attracted to the same degree by the nucleus. Thus, a shell defines an energy level. The attractive force depends both upon the atomic number of the nucleus and upon the diameter of the shell under consideration. The greater the diameter of the shell, the lower is the electrostatic attraction. In graphic illustrations of the different energy levels, atoms are usually represented as having a central nucleus with electrons placed in surrounding concentric rings, each ring representing an energy level (Fig. I-2).

The atomic shells surrounding the nucleus are designated by letters. The shell nearest to the nucleus is referred to as the K-shell, the next as the L-shell, the third as the M-shell, and so on. It should be noted that this is an oversimplification of the atomic shell structure; in fact, most shells are subdivided into a series of subshells.

The different electronic shells can contain only a given maximum number of electrons. Thus, the K-shell contains at the most two electrons; the

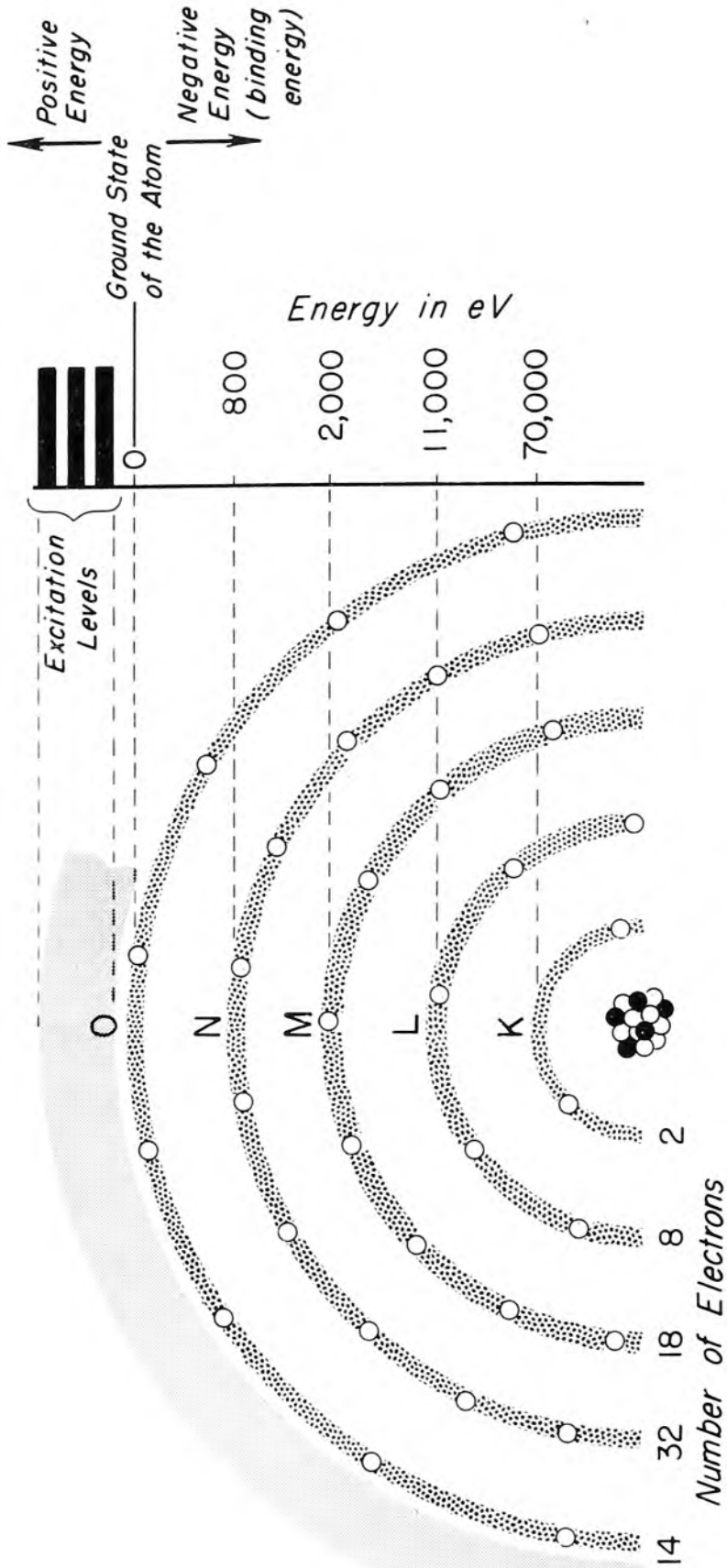


FIG. I-2. Schematic representation of a tungsten atom.

L-shell, eight electrons. The maximum number of electrons permitted in the various shells¹ is as follows:

K-shell	2 electrons
L-shell	8 electrons
M-shell	18 electrons
N-shell	32 electrons
O-shell	50 electrons
P-shell	72 electrons
Q-shell	98 electrons

5.3.3

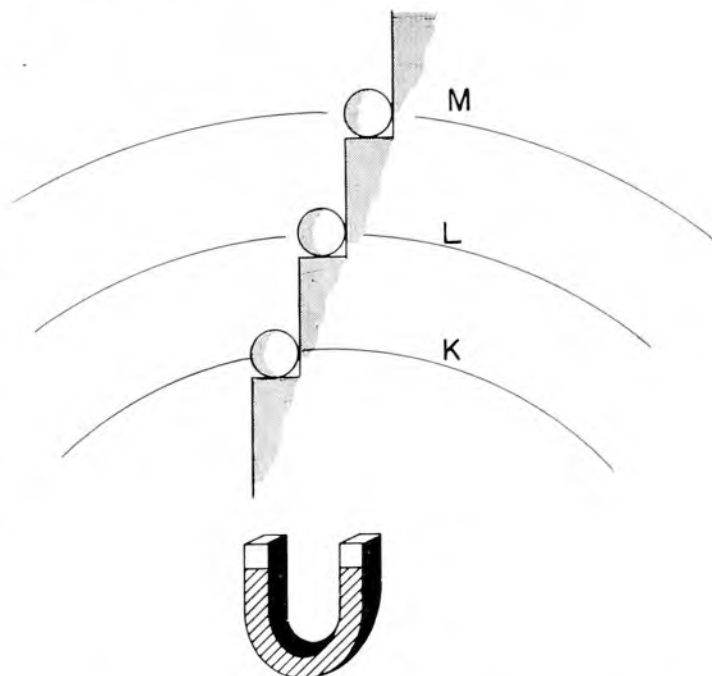
The number of electrons in the different shells and subshells and the sequence in which the electronic shells are filled with increasing atomic number follow rules that can be predicted by wave mechanics. In general, the shells are filled in the order K, L, M, N, etc., and when a certain element has its outermost shell filled to capacity, the next element in the periodic table has an additional shell with one electron in it. There are numerous exceptions to this general pattern. Because of overlapping of electron energy levels between different shells the outermost shell of any atom never contains more than eight electrons. The existence of the rare earths and other transition elements results from this overlap of electron energy levels.

The electrons in an atom are bound to the nucleus by an electrostatic force of attraction. A certain amount of energy is therefore required to remove an electron from its shell. This energy is referred to as the binding energy of the electron in the shell under consideration. Because the electrostatic force of attraction between the nucleus and the electron is inversely proportional to the square of the distance separating them, the binding energy increases from the periphery of the atom to the nucleus. Thus, the binding energy of an electron in the K-shell is greater than the binding energy of an electron in the L-shell, and the latter is greater than the binding energy of an electron in the M-shell. It should be noted that the binding energy is not energy possessed by the electron, but is rather an amount of energy that the electron is missing to be free from the attraction of the nucleus. The binding energy can be considered as negative energy. Thus, although the binding energy in the K-shell of an atom is greater than the binding energy in the L-shell, the electrons in the L-shell possess more energy than the electrons in the K-shell because of the fact that they have less negative energy.

The concept of binding energy can be illustrated by drawing an analogy between an atom and a steel ball attracted by a strong magnet, the steel ball being allowed to occupy a series of steps at different distances from the mag-

¹ It should be noted that, according to theoretical considerations, a nucleus with an atomic number greater than 137 cannot exist. Thus the total number of electrons in an atom cannot exceed 137.

FIG. I-3. Illustration of the concept of binding energy in an atom. Analogy with the attraction between a steel ball at different distances from a magnet. As is the case between the nucleus and the electrons in the atom (Fig. I-2), the attraction between the magnet and the steel ball decreases with increasing distance between them.



netic field (Fig. I-3). The magnetic force between the magnet and the ball is similar to the electrostatic attraction between the nucleus and an electron in the sense that it is inversely proportional to the square of the distance between the two. Thus, the more steps the steel ball is away from the centrally located magnet, the smaller the magnetic force exerted upon it, and the lower its binding energy. The ball in the K-level is attracted by a strong magnetic field and firmly held (tightly bound electron), whereas in the M-level it is attracted by a force of considerably lesser magnitude (loosely bound electron) and will require less energy to be removed from the system.

If, in an atom, an electron is transferred from one orbit into another orbit of greater binding energy, a certain amount of energy equal to the difference between the binding energy of the two shells is released. This energy is usually released in the form of radiation. Conversely, if an electron is moved from a shell of high binding energy to a shell of lower binding energy, energy must be supplied in a quantity equal to the difference between the binding energies of the shells under consideration. In the steel ball-magnet image of the atom, the above transition can be pictured as one of the steel balls falling from one step to another step closer to the magnet. In the process energy must be released, and this energy is observed as kinetic energy of the ball striking the landing step. On the other hand, moving a steel ball from a step close to the magnet to one farther away requires expenditure of energy to overcome the magnetic attraction between the ball and the magnet. Table I-2 lists the binding energies of some electronic shells (K-shell and L-shell and its subshells) in selected atoms as a function of their atomic number. The binding energy of the outer electrons is low, and therefore the latter require little energy to be displaced from the atom.

TABLE I-2. Binding Energies of Electronic Shells for Various Elements^a

Atomic number	Element	Binding energy of shell (in keV)			
		K	L _I	L _{II}	L _{III}
1	Hydrogen	0.0136			
6	Carbon	0.283			
8	Oxygen	0.531			
11	Sodium	1.08	0.055	0.034	0.034
13	Aluminum	1.559	0.087	0.073	0.072
14	Silicon	1.838	0.118	0.099	0.098
19	Potassium	3.607	0.341	0.297	0.294
20	Calcium	4.038	0.399	0.352	0.349
26	Iron	7.111	0.849	0.721	0.708
29	Copper	8.980	1.100	0.953	0.933
35	Bromine	13.475	1.794	1.599	1.552
47	Silver	25.517	3.810	3.528	3.352
53	Iodine	33.164	5.190	4.856	4.559
56	Barium	37.410	5.995	5.623	5.247
74	Tungsten	69.508	12.090	11.535	10.198
79	Gold	80.713	14.353	13.733	11.919
82	Lead	88.001	15.870	15.207	13.044
92	Uranium	115.591	21.753	20.943	17.163

^a From Fine and Hendee (Ref. 3).

Molecules

The chemical properties of an element consist of the ability of this element to combine with one or more other atoms of the same element or of different elements to form combinations with properties different from those of any of the constituents. The combination of two or more atoms belonging to the same or different elements is called a molecule.

The bond between the atoms of the molecule consists generally of one or more electrons bound in the electrostatic fields of both nuclei. Different types of bonds can be achieved involving one, two, four, or more electrons shared by two atoms. The chemical activity, and consequently the type of bond that can be achieved between atoms, depends upon the structure of their outer shell of electrons. If the outer shell is completely filled, it can neither give up nor accept any electrons easily, and such an atom is chemically inert. On the other hand, if a large number of either electrons or vacancies are available in the outer shell, such an atom will be capable of forming a large number of different bonds and will be chemically active.

Thus, the chemical properties of different atoms depend on the structure of their outer electron shells.

The strength of chemical bonds depends upon the type of bond under consideration. In general, the energy of chemical bonds is of the order of a few electron volts.

RADIATIONS

In the context of this book, radiation can be defined as the propagation of energy through space or through matter. This definition excludes such manifestations as sound because sound cannot travel through a vacuum.

All radiations can be classified into one of two categories: corpuscular and electromagnetic radiations.

Corpuscular Radiations

Corpuscular radiations consist of moving particles of matter. The size of these particles may vary over a wide range. For example, a bullet fired by a rifle can be looked upon as a corpuscular radiation. The latter, however, is an extreme extension of the definition of the term; in general, corpuscular radiation is composed of accelerated submolecular particles. The energy carried by corpuscular radiation consists of the kinetic energy of the moving particle and is equal to $\frac{1}{2}mv^2$, where m is the mass of the particle and v its velocity. If a particle travels with a velocity approaching that of light, the expression for the energy of the radiation becomes more complex.

Corpuscular radiation may be composed of either charged particles or neutral particles. The interaction of these radiations with matter depends upon three factors: (1) size of the particle, (2) velocity of the particle, and (3) charge carried by the particle. In general, this interaction consists of an exchange of energy between the radiation and the particles in matter of the same size or nature as the corpuscular radiation. Thus, if the radiation is composed of atom-sized particles, it interacts with atoms. If the particles are smaller, the interaction will occur at the subatomic level. If the particles are electrons, they will interact with electrons in matter. If the particles are nuclei, they will collide with nuclei. It should be noted that there are a great number of exceptions to this rule. Thus, high energy electrons may interact with nuclei, or the energy of a corpuscular radiation interacting with matter may be converted into another form of radiation such as electromagnetic radiation.

Typical corpuscular radiations are: alpha rays, which consist of accelerated helium nuclei; protons, which are accelerated hydrogen nuclei; and, of particular importance in this text, accelerated electrons. Moving electrons are called beta rays if they are emitted by radioactive nuclei, or cathode rays if the electrons are accelerated by some other method. The interaction of electrons with matter consists primarily of elastic (billiard ball type) collisions with other electrons. In general, accelerated electrons penetrating

into matter lose their energy gradually in a series of such collisions. With a considerably lower probability electrons may lose their energy either by producing electromagnetic radiation, or they may interact directly with nuclei. The latter interaction occurs only with high energy electrons and results in the production of a radioactive nucleus.

Electromagnetic Radiation

Electromagnetic radiation consists of a transport of energy through space as a combination of an electric field and a magnetic field, both of which vary in magnitude as a function of time and space. Many physical manifestations, such as x-rays, light, infrared and ultraviolet radiations, and radio waves, are electromagnetic radiations.

The physical properties of electromagnetic radiations can be fully explained only if these radiations are looked upon as possessing a dual nature, namely, waves and particles. The concept of the dual nature of electromagnetic radiations means that certain physical properties exhibited by these radiations can be explained only if they are assumed to be particles; other properties are those of a wave propagation. It is important to note that electromagnetic radiations are *not* composed of both particles and waves, but rather that the same physical phenomenon exhibits a dual nature. In general, any attempt to develop a visual concept of electromagnetic radiations leads to an image in conflict with physical observations. It is, therefore, preferable to consider separately the wave and particle natures of electromagnetic radiations, keeping in mind, however, that they represent two facets of the same phenomenon.

Wave Nature of Electromagnetic Radiation. The wave concept of the nature of electromagnetic radiation resides in the cyclic propagation of this phenomenon as shown in Fig. I-4, exhibiting maxima and minima. The transport of this wave does not require any supporting medium, as it may travel in vacuum. Electromagnetic waves are characterized by: (1) their velocity of propagation, which, in the vacuum, is about 3×10^{10} cm per sec (velocity of light, usually symbolized by the letter c); (2) their wavelength λ , which is a function of the energy of the radiation and is measured in units of length; and (3) by the frequency n , which is equal to the number of cycles per unit time and is related to the wavelength λ by the formula

$$n = \frac{c}{\lambda}$$

The wave nature of electromagnetic radiation is demonstrated by the fact that this radiation undergoes interference, diffraction, refraction, reflection, and polarization (see Chapter II).

Corpuscular Nature of Electromagnetic Radiation. The particle nature of electromagnetic radiation must be assumed because the energy carried by this radiation is always transported in the form of discrete "bundles" or

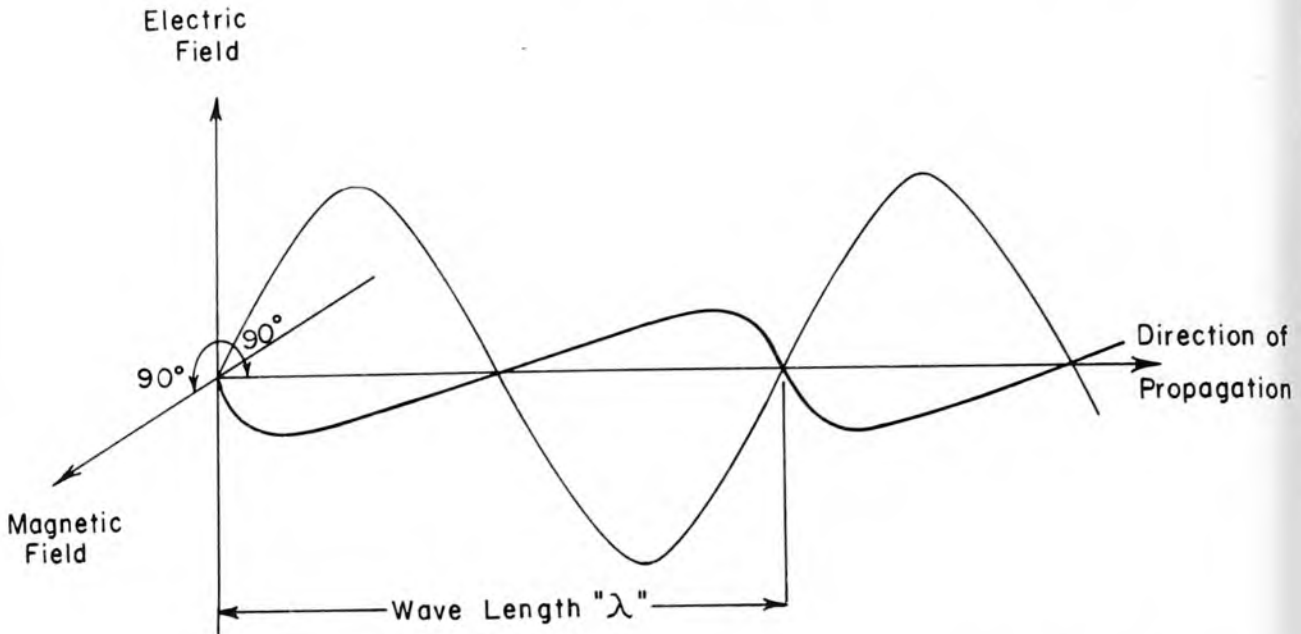


FIG. 1.4. Propagation of electromagnetic radiation composed of an electric field and a magnetic field in planes perpendicular to each other.

“quanta.” These bundles are called photons. Photons do not possess mass. They travel with the velocity of light, c . The energy of a given electromagnetic radiation is expressed by the energy carried by each photon composing this radiation; for example, the term “one million electron volt gamma radiation” means that each photon of this gamma radiation carries the energy of 1 MeV.

Energy of Electromagnetic Radiation. The energy carried by each photon represents the minimum “unit” of energy or “quantum” (plural “quanta”) carried by the radiation; and the total energy carried by the radiation is expressed in multiples of the energy carried by a single photon. Thus, the minimum amount of electromagnetic radiation is one single photon. The energy carried by a photon is related to the frequency of the electromagnetic radiation by the formula

$$E = hn,$$

where E = energy carried by 1 photon,

n = the frequency of the electromagnetic radiation expressed in cycles per unit time (for example, cycles per sec),

h = Planck’s constant, and hn = “quantum” of energy.

Planck’s constant is a universal constant in nature relating the energy of an electromagnetic radiation to its frequency. The dimensions of this constant are energy multiplied by time. Thus, when this constant is multiplied by the frequency n , which has the dimensions of 1/time, or t^{-1} , the result has the dimensions of energy. The numerical value of Planck’s constant depends upon the system of units used. In the cgs system, the value of

Planck's constant (see Table XI-6, also Ref. 2) is

$$h = 6.6256 \times 10^{-27} \text{ erg sec.}$$

In the cgs system the energy of the radiation is expressed in ergs. In radiology, the energy of electromagnetic radiation is expressed in electron volts rather than in ergs. A convenient conversion factor for the wavelength of an electromagnetic radiation into the energy carried by its photon is 12.398 keV angstroms, so that

$$E = \frac{12.4 \text{ keV angstroms}}{\lambda \text{ (wavelength in angstroms)}}$$

Physical Properties of Electromagnetic Radiation. All electromagnetic radiations share the following physical properties:

1. They travel in the vacuum with the velocity of light c , which is $2.997925 \times 10^{10} \text{ cm sec}^{-1}$ (Ref. 2).
2. They travel in straight lines. The radiation can be deflected from its original direction, but the new trajectory is also linear.
3. When interacting with matter, they are either absorbed or scattered.
4. Their interaction with matter may result in their reflection, refraction, or diffusion.
5. They are unaffected by either magnetic or electric fields.
6. They can be polarized.
7. They produce interferences.

In addition to the above properties, electromagnetic radiations exhibit a large number of different physical properties that depend upon the energy of the photons and that may not be shared by radiations of different energies. This dependence of some physical properties of radiations of identical nature allows their classification into different groups according to their energy. Figure I-5 shows a classification of electromagnetic radiations according to their energy and wavelength. These different categories are not sharply defined as a function of energy, and between them there is, in general, a wide area of overlap.

Ionizing Electromagnetic Radiation. When radiations interact with atoms or molecules,² the interaction takes one of the following forms: (1) elastic collision, (2) excitation, or (3) ionization. An *elastic collision* consists of an interaction between the corpuscles or photons of the radiation with an atom or molecule as a whole. In such a collision the atom or molecule behaves as a particle, and the atomic substructure does not intervene in the interaction. There is conservation of momentum and kinetic energy. The energy acquired by the atom or molecule is kinetic; it is therefore set in motion, which is usually vibrational. In turn, the kinetic energy of the atom or molecule is dissipated as heat in a series of collisions with neighboring atoms or molecules.

Excitation is an interaction between radiation and an electron belonging

² The interaction of electromagnetic radiation with nuclei is discussed in Chapter III.

THE PHYSICAL ASPECTS OF DIAGNOSTIC RADIOLOGY
ELECTROMAGNETIC RADIATIONS

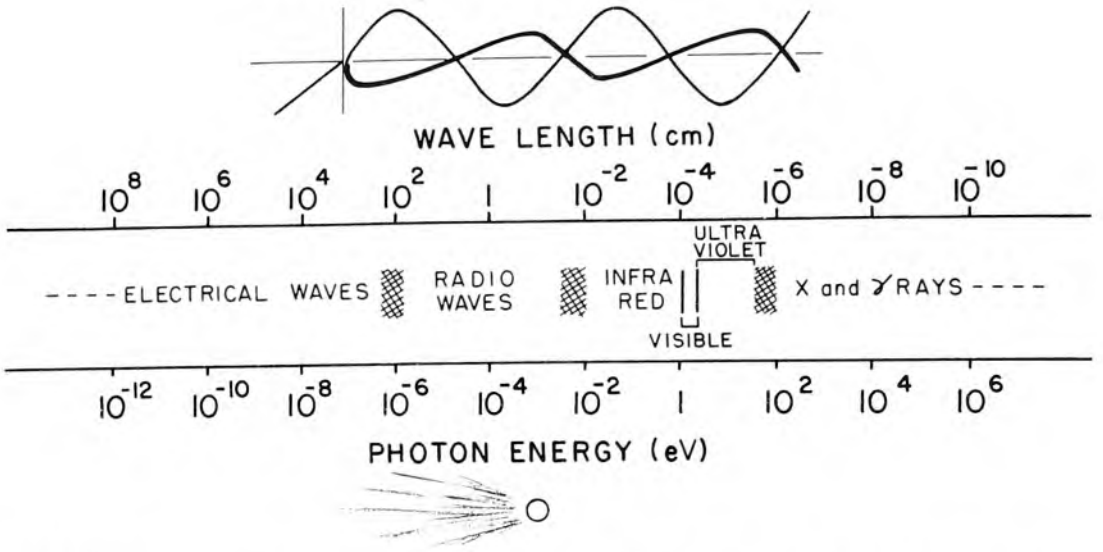


FIG. I-5. Electromagnetic radiations classified as functions of their energies and wavelengths.

to the target atom or molecule. A portion of the radiation energy is transferred to the electron, which is thereby raised to a higher energy level. The atom or molecule to which it belongs is thus raised to an excited state. The atom or molecule returns to its stable state by expelling its energy of excitation either in the form of long-wave electromagnetic radiation (fluorescence), by using it to form chemical bonds, or in the form of heat.

If the energy transferred by the radiation to an electron in the target atom or molecule is sufficiently high to remove the electron from the atom or molecule, then the process is called *ionization*. In this process a pair of ions is formed; the positive ion is the atom or molecule positively charged because of the loss of an electron, and the negative ion is the ejected electron. The energy required to remove an electron from an atom or molecule varies with the binding energy of the electron. The minimum amount of energy required to ionize an atom or molecule is equal to the binding energy of the electron or electrons having the lowest binding energy. This energy is called the critical energy for the atom or molecule. If a radiation carries per corpuscle (corpuscular radiation) or per photon (electromagnetic radiation) energy equal or superior to the critical energy of an atom or molecule, the radiation is said to be ionizing for this atom or molecule.

The critical energy for various substances varies over a wide range. Table I-3 lists a few of these values. Thus, a radiation may be ionizing for a given substance and not ionizing for another with a higher critical energy. In general, when ionizing radiation is absorbed in matter, the probability of either of the above three processes (elastic collision, excitation, or ionization) to occur depends on the energy transferred.

TABLE I-3. Ionization Energies
in Electron Volts

	Ionization energy (in eV)
Gas or vapor	
H	13.56 ^a
H ₂	15.9 ^a
O	13.6 ^a
O ₂	13. ^a
He	24.5 ^a
K	4.2 ^a
Condensed state	
Proteins	7.75 to 10.02 ^b

^a From Stranathan (Ref. 4).

^b From Setlow, Watts, and Douglas (Ref. 5).

An important constant in radiology is the average amount of energy spent by ionizing radiation for the formation of one pair of ions in air. This constant is symbolized by W_{air} and is equal to about 34 eV (Ref. 6). W_{air} is equal to the ratio of the energy dissipated in air by ionizing radiation and of the number of pairs of ions formed. It should be noted that W_{air} is not the critical energy for air, which is approximately 17 eV. In air, the energy dissipated by ionizing radiation is nearly equally divided between ionizations on one hand and excitations and elastic collisions with atoms and molecules on the other.

REFERENCES

1. BARKAS, W. H., and ROSENFELD, A. H.: *Data for Elementary-Particle Physics*. Los Angeles, The University of California, Lawrence Radiation Laboratory, VCRL-8030 Rev. April 1963.
2. *General Physical Constants Recommended by NAS-NRC, Adopted by National Bureau of Standards*. NBS Misc. Publ. 253. Washington, D.C., U.S. Government Printing Office, November 1963.
3. FINE, S., and HENDEE, C. F.: X-ray critical absorption and emission energies in kev. *Nucleonics* 13 (No. 3): 36-37, 1955.
4. STRANATHAN, J. D.: *The Particles of Modern Physics*. Philadelphia, Blakiston, 1948.
5. SETLOW, R., WATTS, G., and DOUGLAS, C.: "Inactivation of Proteins by Vacuum Ultraviolet Irradiation," in *Proceedings of the First Biophysics Conference*, ed. by Quastler, H., and Morowitz, H. J. New Haven, Yale University Press, 1959.
6. *International Commission on Radiological Units and Measurements (ICRU)*. NBS Handbook 62. Washington, D.C., U.S. Government Printing Office, 1956.

(II)

ORIGIN AND NATURE OF X-RAYS

X-rays are ionizing electromagnetic radiations that result from the conversion of either the kinetic or the potential energy carried by electrons into electromagnetic radiation.

This definition embodies the three concepts that uniquely define x-rays: (1) X-rays are electromagnetic radiations and therefore possess all the physical properties shared by these radiations. (2) X-rays are ionizing, which means that x-ray photons carry sufficient energy to ionize atoms and molecules (this energy must be in excess of about 10 eV). (3) X-rays are generated as a result of the conversion of either the potential or the kinetic energy carried by electrons into another form of energy. This qualification distinguishes x-rays from gamma rays, which are ionizing electromagnetic radiations emitted by radioactive nuclei. Consequently, the distinction between x-rays and gamma rays rests entirely upon their origin. In the absence of information about its origin, a gamma-ray photon is indistinguishable from an x-ray photon.

INTERACTION OF ELECTRONS WITH MATTER— COLLISIONAL INTERACTIONS

When electrons interact with matter, they lose energy by one of several processes, such as resonance absorption, collision with nuclei and electrons, excitation of atoms, radiative interaction, and electrodisintegration of nuclei (Ref. 1). In the energy range between a few electron volts and a few million electron volts, electrons interact with matter mostly by one of the following processes: (1) by inelastic collisional interactions with bound electrons, resulting in the excitation and/or the ionization of the struck atom, or (2) by radiative interactions, resulting in the emission of x-rays. The relative probabilities of collisional and radiative electron interactions depend on the energy of the interacting electrons and on the atomic number of the absorber (see under "Characteristic or Line X-Radiation").

In collisional interactions, the transfer of energy from an electron possess-

ing kinetic energy to an electron bound in an atom raises the atom to a higher energy level. The excited atom returns to a lower energy state either by the emission of a low-energy electromagnetic radiation (light or ultraviolet radiation) or by the dissipation of this energy in the form of heat. If the energy of the moving electron is sufficiently high to overcome the binding energy of the interacting bound electron, ionization occurs. The secondary electron displaced from the absorber, which is called a delta ray, loses its energy through excitation, ionization, or other interaction. The positive ion either recaptures a free electron or attaches itself to another atom or molecule.

The rate of loss of energy for a fast electron is small, so that collisions of such an electron do not result in an appreciable deviation from its original direction. Thus, the direction of the moving electron remains relatively unaffected and its trajectory is nearly a straight line. However, as the energy of the moving electron is dissipated and the rate at which it exchanges energy with matter becomes greater, collisions result in the deflection of the impinging electron from its original direction. Thus, the trajectory of a high energy electron in matter exhibits usually a straight portion followed by a broken line until the electron is finally brought to rest. Over a wide range of energies, the range of electrons in matter depends only on the cross-sectional density of the absorber (Fig. II-1) and is little affected by the atomic number.

X-rays are generated as a result of the loss of energy of electrons interacting with matter through two different processes: (1) radiative interaction of electrons with matter, which consists in the deceleration of electrons in the electric field of a nucleus, and (2) rearrangement of electrons in an atom which was deprived of one of its tightly bound electrons subsequent to a collisional interaction with the high energy electron. The first process results in the production of those x-rays which are referred to as white or general radiation, or *Bremsstrahlung*. The photons produced by the second process are called characteristic radiation.

Radiative Interactions of Electrons with Matter—General or White Radiation (*Bremsstrahlung*)

When an electron travels in the vicinity of a nucleus, the negative charge of the electron is acted upon by the positive charge of the nucleus. Thus, the mass of the electron is subjected to an attractive force which deflects the electron from its original direction and the electron is decelerated (Fig. II-2a). The energy lost by the electron under these circumstances is emitted in the form of an x-ray photon. This process is called radiative interaction of an electron with matter, and the x-radiation thus produced is referred to as general radiation, white radiation, or *Bremsstrahlung* (German for "braking radiation").

The amount of energy lost in a radiative interaction, and consequently

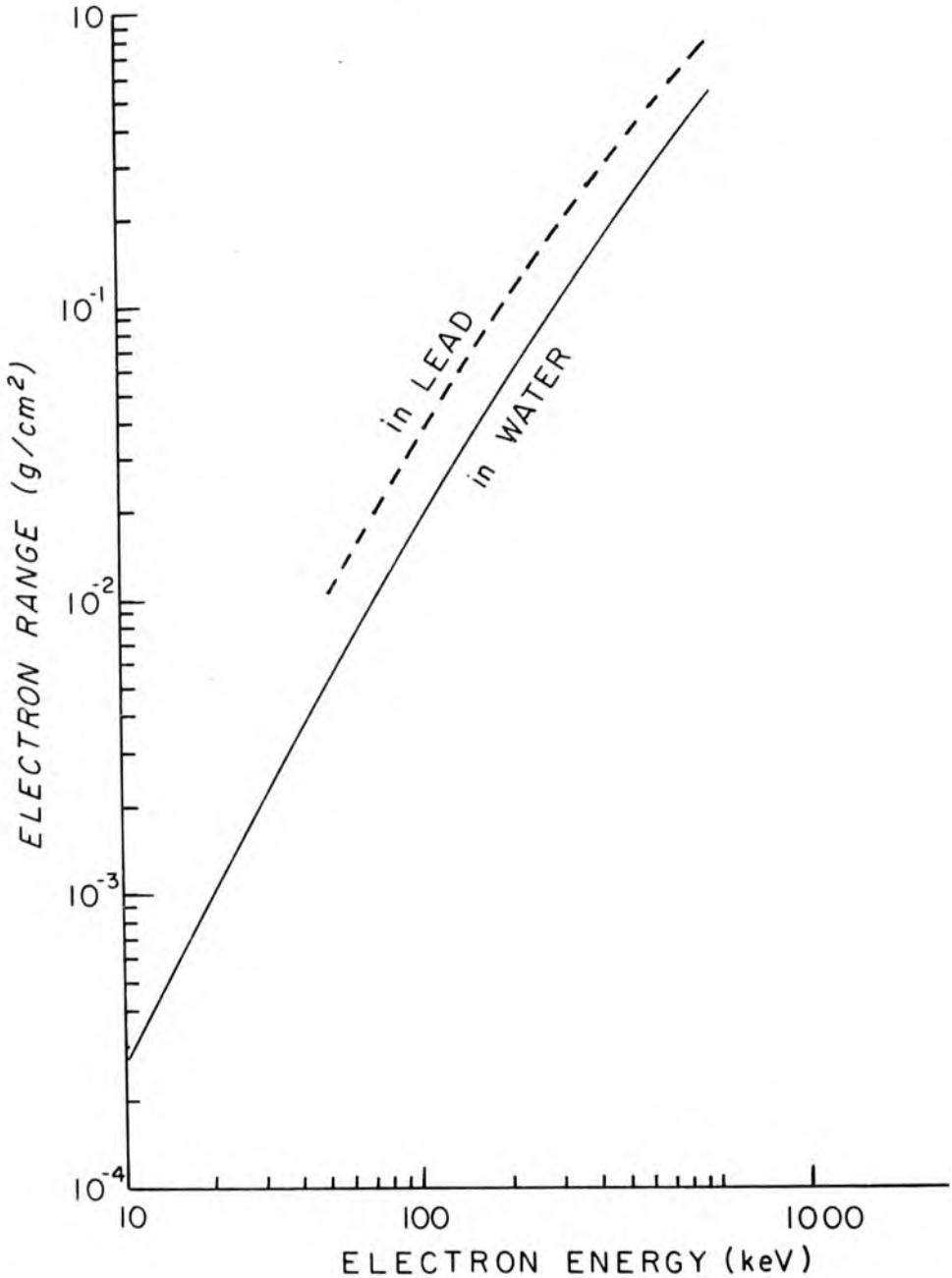


FIG. II-1. Electron range versus energy in lead and in water. In this case range means amount of material required to dissipate all the electron energy.

the energy of the x-ray photon emitted, depends on (1) the distance between the electron and the nucleus, (2) the energy of the electron, and (3) the charge of the interacting nucleus. An extreme form of this interaction consists in the "collision" between the electron and the nucleus, in which case the energy of the emitted photon is equal to the total kinetic energy of the impinging electron (Fig. II-2b). Thus, the deceleration of electrons in matter by radiative interaction results in the emission of x-ray photons with ener-

gies ranging from a low value up to the total kinetic energy of the interacting electrons.

The intensity of the x-radiation produced by radiative interaction as a function of electron energy can be predicted by the quantum theory of radiation (Ref. 2). A qualitative discussion of this subject (Ref. 3) follows:

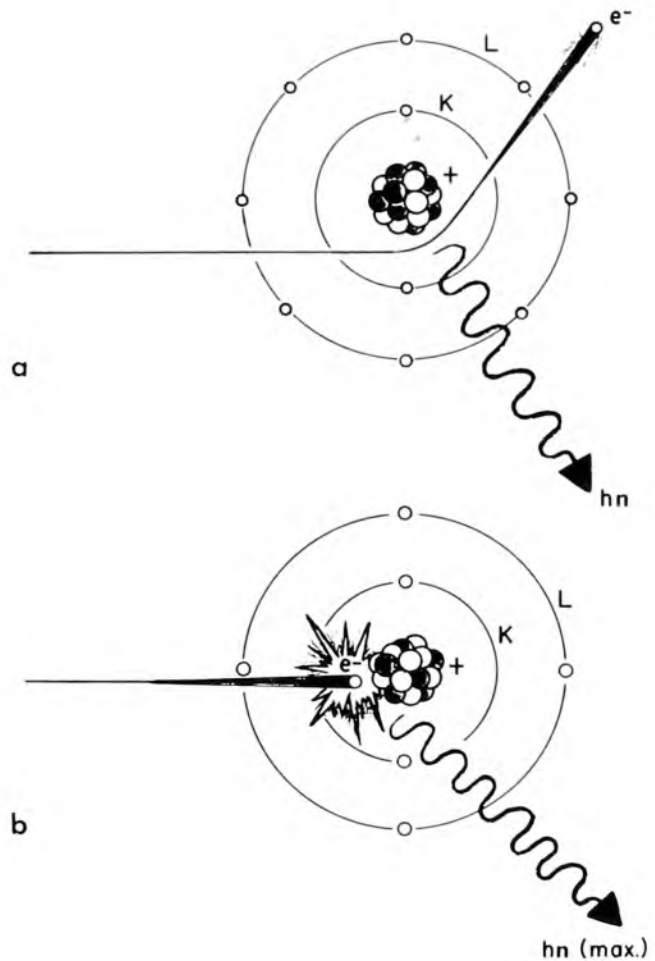
Assume a beam of monoenergetic electrons each carrying an energy E interacts with a thin absorber. The term "thin absorber" introduces the assumption that the amount of material encountered by the electrons is so thin that they may undergo only one interaction while passing through the absorber. Under the circumstances the energy of the electrons impinging upon the absorber is not degraded in multiple interactions, and all the interactions, whether collisional or radiative, occur with monoenergetic electrons (electrons carrying the same energy). Figure II-3a shows the predicted spectral distribution of the intensity of the x-radiation emitted as a function of photon energy for a thin target. The constancy of radiation intensity with radiation energy shows that the number of photons emitted is inversely proportional to the energy at which they are emitted. Thus, twice as many photons are emitted with an energy $E/2$ as with an energy E . The total energy radiated is proportional to the area under the curve in Fig. II-3a.

FIG. II-2. Generation of general or white radiation (*Bremsstrahlung*) by interaction between an electron and a nucleus.

a impinging electron is deflected and decelerated

b total kinetic energy of impinging electron is converted into x-radiation

hn energy of generated photon



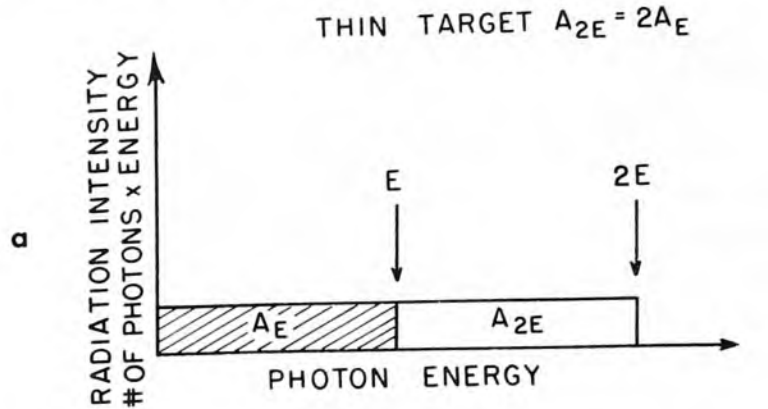
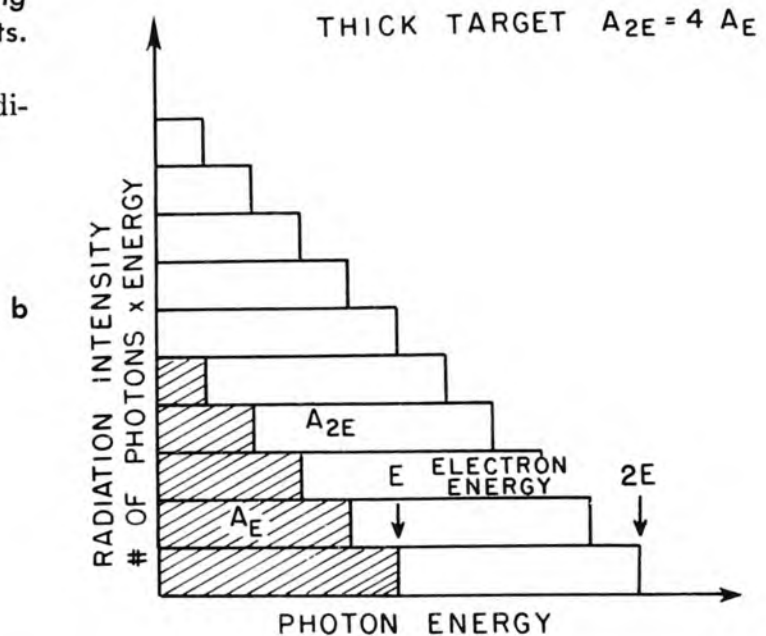


FIG. II-3. Bremsstrahlung
in thin and thick targets.
E electron energy
A intensity of x-radiation generated



The elementary theory also predicts that the total energy radiated is proportional to the atomic number of the absorber; thus, in a thin absorber the amount of energy lost by electrons through radiative interactions is proportional to the energy of the electrons and to the atomic number of the absorber. This result has been verified experimentally for lower-energy electrons (below 100 keV) but is only approximately correct for higher energies (Ref. 4).

The above discussion is valid only for thin targets. When a beam of monoenergetic electrons interacts with a thick target, the energy of the electrons is rapidly degraded through a series of collisional and radiative interactions. In the study of the radiation emitted by a thick target, it can be assumed that the target is composed of a number of thin targets each of them exposed to monoenergetic electrons of increasingly lower energy. The radiation intensity spectrum thus achieved can be obtained graphically by the super-

imposition of the various spectra obtained for thin targets, as shown in Fig. II-3b. The thick target spectrum is no longer rectangular and exhibits a predominance of low energy radiation. As the energy of the beam of electrons impinging upon a thick target increases, the total amount of energy emitted is altered. The area under the curve (the spectral distribution), which is proportional to the total amount of energy emitted, increases more rapidly with energy than in the case of the thin target. The area under the curve is proportional to the energy of the photons multiplied by the intensity of the radiation, since both of these quantities increase linearly with the energy of the impinging electrons; therefore the total amount of energy radiated is proportional to E^2 . As is the case for thin targets, the intensity of the radiation emitted by thick targets is proportional to the atomic number of the absorber. Thus, the intensity of the general x-radiation emitted by a thick target is approximately proportional to

$$I \propto Z \times E^2.$$

Efficiency of X-Ray Production by Radiative Interaction. The generation of x-rays by the radiative deceleration of electrons in matter is in competition with collisional interactions, which result mostly in the dissipation of the electronic energy as heat. Although most of the electron energy lost by collisional interactions is dissipated in the form of heat, a small fraction of this energy may be re-emitted as so-called characteristic radiation.

The efficiency of the production of x-rays can be expressed as the percentage of the total amount of energy dissipated by the electrons in the absorber. The efficiency of production of x-rays by radiative interactions is proportional to: (1) the square of the energy of the interacting electrons (as shown above) and (2) the square of the atomic number of the absorber, Z . The dependence of the efficiency on the square of the atomic number of the absorber is predicted by the classical theory of the deceleration of a charged particle in an electric field (Ref. 3).

It should be noted that while the efficiency of the radiative process *per atom* is proportional to Z^2 , the efficiency *per unit cross-sectional density of material traversed* (g/cm^2) is proportional only to Z because the number of atoms per gram of any element is inversely proportional to Z .

Figure II-4 shows a plot of the fraction of electron energy radiated as x-rays in water and in lead as a function of electron energy. It is apparent that for low energy electrons the efficiency of x-ray production is extremely low. In lead, for electrons with a kinetic energy of 100 keV (0.1 MeV), the efficiency of x-ray production is only of the order of 1.0%. However, as the energy of the impinging electron increases, probability of radiative interactions also increases rapidly to reach a plateau where practically all the energy of the electrons is converted into radiation.

Since the shape of the distribution of the general radiation is independent of Z , the efficiency of production of x-rays for any element can be extrap-

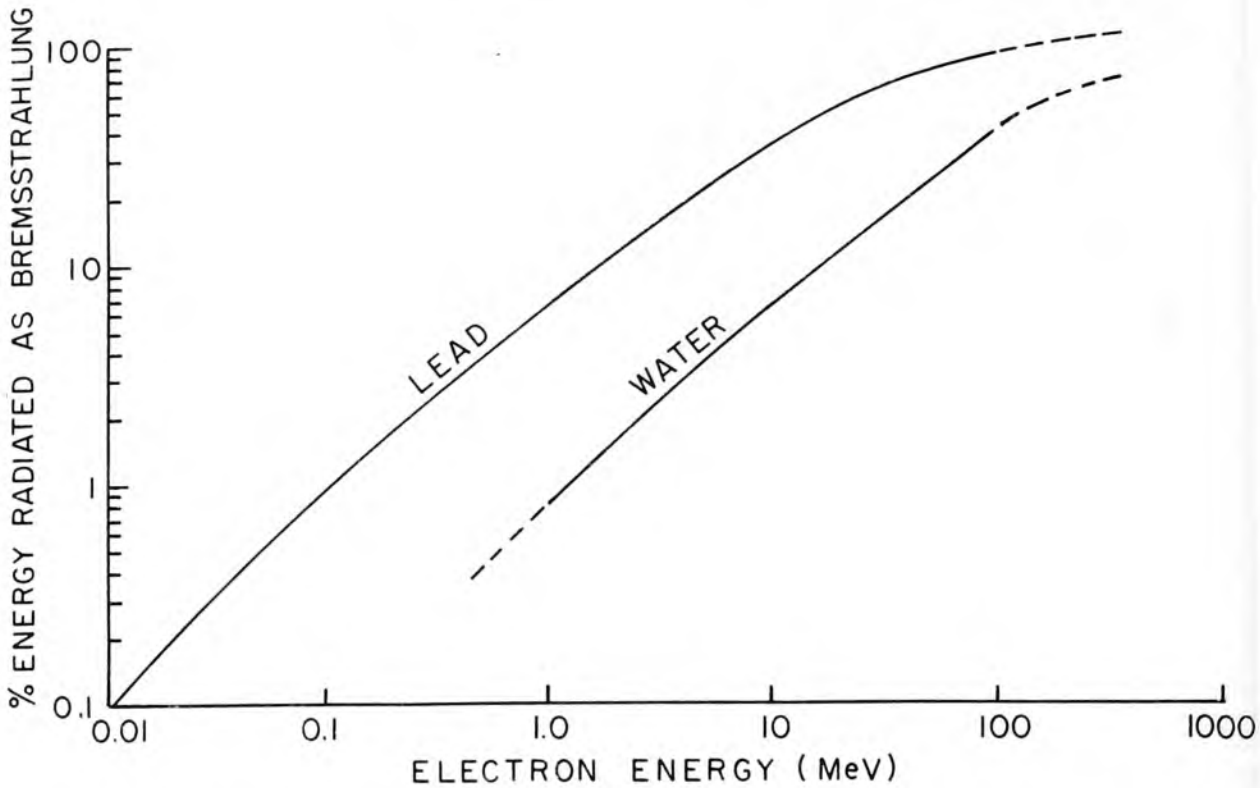


FIG. II-4. Percentage of electron energy radiated as *Bremsstrahlung* in lead and in water, as a function of electron energy. Logarithmic plot.

olated from the curves shown in Fig. II-4. For example, the efficiency of x-ray production in tungsten is given by

$$\frac{I_W}{I_{Pb}} = \frac{Z_W}{Z_{Pb}}$$

where I_W and I_{Pb} are the relative amounts of the x-radiation produced in tungsten and in lead, respectively, and Z_W and Z_{Pb} are the atomic numbers of tungsten and lead, respectively.

Since

$$\frac{Z_W}{Z_{Pb}} = \frac{74}{82} = 0.9$$

and, from Fig. II-4, the efficiency of x-ray production in lead by 100 keV (0.1 MeV) electrons is approximately 1.0%, the production of x-rays by the deceleration of 100 keV (0.1 MeV) electrons in tungsten is

$$I_W = \frac{Z_W}{Z_{Pb}} \times I_{Pb} = 0.9 \times 1.0\% = 0.9\%,$$

while 99.1% of the energy for these electrons is converted into heat. (Efficiency at 60 keV for lead: 0.6%.)

The above example is typical of the situation encountered in diagnostic radiology, where the target uniformly used is tungsten and most of the clinical examinations are carried out with x-rays generated by electrons accelerated between about 60 and 100 keV.

Direction of General Radiation Emission. The direction of emission of x-rays generated by radiative interactions in a thin target is related to the direction of the electrons creating them. At low energies, of the order of 100 keV, the radiation intensity is maximum in a direction perpendicular to the travel of the electrons. In this energy range, very few x-rays are emitted in a forward direction with respect to the direction of the electrons, and practically none are emitted backwards. As the energy of the electrons increases, x-rays have a tendency to be emitted in the forward direction, and the angle between the maximum x-ray intensity and the direction of the electrons decreases from 90 degrees to 0 degrees for high energy electrons. At 20 MeV, the angle of distribution of the x-radiation with respect to the direction of the electrons forms a very narrow cone.

The above relationships are valid only for thin targets in which the x-radiation is generated by electrons unaffected by other interactions. In thick targets, and for low energy electrons, the direction of the impinging electrons is rapidly modified by interactions either collisional or radiative, and the direction of the emitted x-radiation, although perpendicular to the direction of the traveling electrons, is no longer related to the direction of the primary beam before interacting with the target. Thus, for low energy electrons and in a thick target, the direction of the x-radiation produced is, for all practical purposes, isotropic with respect to the direction of the impinging electrons. This situation prevails for the generation of x-rays in conventional diagnostic radiology.

For high energy electrons (of the order of 1 MeV), collisional interactions in the target have little influence on their direction; therefore in that energy range there will be little difference in the angular distribution of x-rays between thin and thick targets. For high energy electrons, the angular distribution of the x-radiation produced even in a relatively thick target, forms an acute cone having for its axis the direction of the primary beam of electrons and a decreasing solid angle as a function of increasing electron energy.

Characteristic or Line X-Radiation

While general radiation is produced by radiative interactions of electrons, x-rays are also generated as a result of collisional interactions of electrons with tightly bound electrons. The radiation thus produced is called the characteristic or line radiation, and it is generated as follows (Fig. II-5):

1. An electron impinging upon matter undergoes a collisional interaction with a tightly bound electron, for example, with an electron bound in the K-shell of one of the atoms in the target material.
2. The interaction results in the ejection of the K electron from its shell.

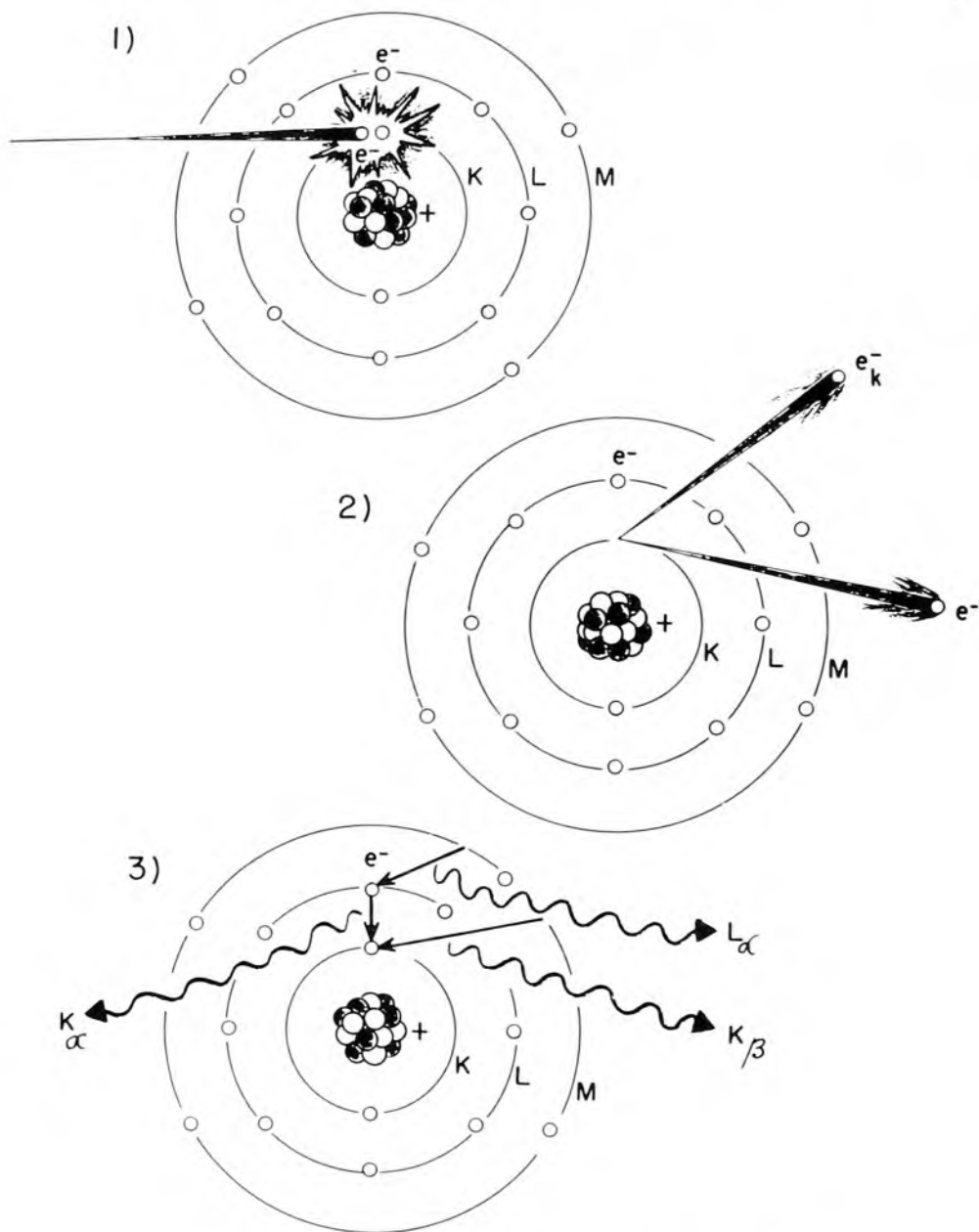


FIG. II-5. Generation of characteristic radiation.

- L_α x-ray photon emitted on transition of M electron to L-shell
- K_β x-ray photon emitted on transition of M electron to K-shell
- K_α x-ray photon emitted on transition of L electron to K-shell

The energy of the impinging electron is used to overcome the binding energy of the ejected electron and the remainder of the kinetic energy of the impinging electron is shared with the ejected K electron. This process can occur only if the kinetic energy of the impinging electron is at least equal to the binding energy of the shell where the interaction takes place. Following the interaction, both the initial electron and the ejected electron lose their kinetic energy away from the atom where the original interaction took place.

3. The struck atom is left with an unoccupied space or vacancy in its K-shell. Such a structure is unstable, and the vacancy in the K-shell is rapidly replenished by an electron usually falling from the next shell (L-shell). The transition of the electron from the L-shell to the K-shell results in a loss of potential energy by the L electron equal to the difference between the binding energy of the K- and L-shells. The energy thus lost by the L electron is radiated as a single x-ray photon with an energy equal to the energy of the transition.

4. The transition of the L electron to the K-shell leaves the L-shell unfilled. The vacancy in the L-shell is in turn replenished by an electron usually from the M-shell. Then, the vacancy created in the M-shell must in turn be replenished from another shell, and so on. Each electronic transition from one shell to another shell of higher binding energy results in the emission of an x-ray photon with an energy equal to the energy of the transition.

Thus, the displacement of an electron from one of the inner shells of an atom results in an avalanche of electronic transitions that consist in occupying, in sequence, a vacancy in a shell provided by the previous transition. Each one of the transitions results in the emission of one x-ray photon, and the sum of the energies of the x-ray photons emitted is equal to the binding energy of the shell from which the first electron was ejected.

These electronic transitions result in the emission of a series of x-ray photons with energies that are specific of both the atom and the particular shell in which the interaction took place. For example, if the collisional interaction takes place in the K-shell of tungsten, the interaction results in the excitation of the tungsten K series.

Photons of different energies are emitted for transitions occurring between different subshells of an atom and a vacancy in a higher binding-energy shell (Table II-1). For example, transitions between the K-shell and the three subshells of the L-shell result in the emission of the K_{α} series, as shown in Table II-1. Transitions from the M-subshells to the K-shell result in the K_{β} series, and so on (see also Fig. II-5). Some of the transitions are more probable than others and therefore result in the emission of more intense x-ray lines. Some "forbidden" transitions do not occur because of quantum mechanical restrictions.

Because the energy of the x-ray photons emitted by the described process is characteristic of the shell of the atom in which the interaction takes place, this radiation is referred to as "characteristic radiation" or "line radiation." Table II-1 shows the energy of a certain number of characteristic lines for various atoms.

The excitation of a series of lines in a given atom can take place only if the energy of the impinging electron is sufficient to eject the electron from the shell corresponding to that series. For example, the binding energy of the K-shell in tungsten is equal to approximately 69 keV. A 50 keV electron impinging upon a tungsten target is not capable of exciting the tungsten-

TABLE II-1. Characteristic Radiation Energies in keV^a

Z	Element	K Series					L Series				M Series		N Series			
		K _{β2}	K _{β1}	K _{α1}	K _{α2}	L _{γ1}	L _{β2}	L _{β1}	L _{α1}	L _{α2}	M _I -M _{III}	M _I -M _{VI}	N _{IV} -N _{VI}			
8	Oxygen				0.523											
20	Calcium		4.012	3.691	3.688					0.344		0.341				
29	Copper	8.976	8.904	8.047	8.027					0.948		0.928				
47	Silver	25.454	24.942	22.162	21.988	3.519	3.348			3.151		2.984	2.978			
53	Iodine	33.016	32.292	28.610	28.315	4.800	4.507			4.220		3.937	3.926			
74	Tungsten	69.090	67.233	59.310	57.973	11.283	9.959			9.670		8.396	8.333		2.40 ^b	2.21 ^b
82	Lead	87.343	84.922	74.957	72.794	14.762	12.620			12.611		10.549	10.448		3.208 ^b	
92	Uranium	114.549	111.289	98.428	94.648	20.163	16.425			17.218		13.613	13.438		4.516 ^b	

Line	Transition	Line	Transition
K _{α1}	K-L _{III}	L _{α1}	L _{III} -M _V
K _{α2}	K-L _{II}	L _{α2}	L _{III} -M _{IV}
K _{β1}	K-M _{III}	L _{β1}	L _{II} -M _V
K _{β2}	K-N _{II} /N _{III}	L _{β2}	L _{III} -M _V
K _{β3}	K-M _{II}	L _{γ1}	L _{II} -N _V

^a From Fine and Hendee (Ref. 5).

^b From Compton and Allison (Ref. 9).

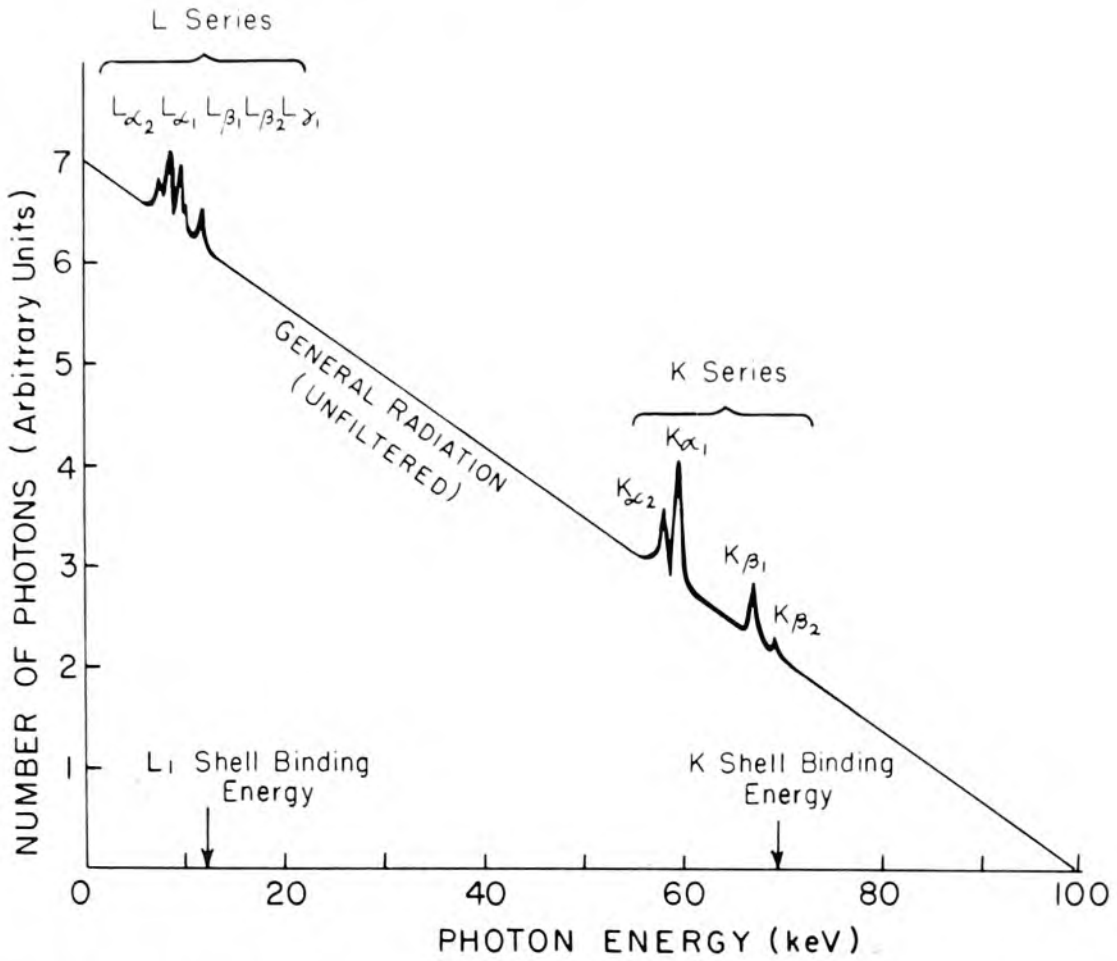


FIG. II-6. X-ray spectrum in tungsten, showing the superimposition of characteristic x-ray lines over the continuous distribution of the general radiation.

TABLE II-2. Relative Intensities of Characteristic and General Radiations for a Tungsten Target

Tube voltage ^a (kV _p)	Relative number of x-ray photons emitted	
	Characteristic radiation (%)	General radiation (%)
80	10	90
100	19	81
120	24	76
150	28	72

^a Three-phase 12-pulse rectified circuit with only inherent filtration.

characteristic K series; on the other hand, since the binding energy of the L-shell in tungsten is only 12 keV, the 50 keV electron may excite the L series in that target.

The energy spectrum of the characteristic x-radiation appears as a series of sharp lines superimposed over the general radiation, as shown for tungsten in Fig. II-6. The relative intensities of the characteristic radiation and the general radiation vary with the energy of the impinging electrons and the atomic number of the absorber, as shown for a tungsten target in Table II-2.

X-RAY SPECTROMETRY

X-ray spectrometry is the analysis of the composition of an x-ray beam. The composition of an x-ray beam is fully defined by: (1) the number of photons in the beam, and (2) the photon energies. X-ray spectrometry consists therefore of the study of one of these variables as a function of the other. Most commonly the results of such a study are expressed in terms of the distribution of the number of photons as a function of their energies, the graphic representation of which represents an x-ray spectrum.

Different methods of analysis can be applied to the study of the spectral distribution of energies in an x-ray beam. Thus, instead of representing a plot of the number of photons per energy interval, an x-ray spectrum may also represent the intensity of radiation per energy interval. The *intensity* of the radiation is equal to the number of photons per energy interval times their energies. The intensity spectrum can be calculated from the "number-of-photons" spectrum by multiplying the ordinate of each point by its abscissa. The area under the number-of-photons-versus-energy spectrum is equal to the total number of photons emitted over the energy range studied. The area under the intensity-versus-energy curve is equal to the total energy carried by the x-ray beam in the energy range studied.

The choice of the type of spectrum used in a given study depends on the requirements of the study and also on the experimental apparatus used in the determination of the spectral distribution of the radiation. The conversion of one type of spectral presentation to the other is simple.

The energy spectrum of a beam of x-rays can be obtained either by calculation or by experimental determination by means of an x-ray spectrometer. Various physical principles have been applied in the design of different types of x-ray spectrometers. However, all x-ray spectrometers embody two fundamental components: a detector sensitive to x-ray photons and a device capable of distinguishing between photons of different energies, referred to as the analyzer.

Detectors can be classified according to the different physical principles they embody for the detection of x-ray photons. The most important classifications are: (1) photographic emulsions, (2) ionization chambers, (3) Geiger and proportional counters, and (4) scintillation counters. These devices are discussed in Chapter XI.

Based on this classification, detectors for x-ray photons can be separated into two main categories:

1. *Counters*. These detectors are sensitive to the number of photons striking them, and their response is independent of the energy of the photons. A typical example of this category is the Geiger-Müller counter.

2. *Integral Detectors*. These detectors record the total amount of energy carried by the photons, rather than the number of photons striking them. Ionization chambers and photographic emulsions are integral detectors. Proportional counters and scintillation counters can be operated either as counters or as integral detectors (Ref. 6).

The use of a counter-type detector in an x-ray spectrometer results in obtaining the data in the form of a number-of-pulses versus energy-interval spectrum. On the other hand, the use of an integral detector provides an energy-carried versus energy-interval spectrum. Both detector types are used in x-ray spectrometry.

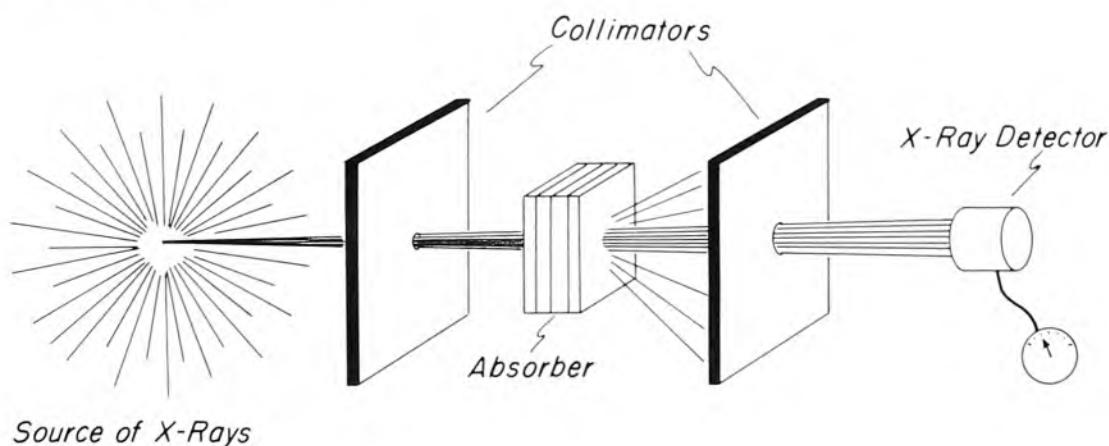
The energy analysis of an x-ray beam is usually achieved by either attenuation, diffraction, or scintillation spectrometry.

Attenuation Spectrometry

The attenuation of x-rays in matter depends on: (1) the energy of the x-radiation, (2) the atomic number of the absorber, and (3) the total amount of absorber present. The relation between these three factors is discussed in detail in Chapter III. Because of the dependence of the attenuation of x-rays on their energy, it is possible to perform a spectroscopic analysis of an x-ray beam by studying its rate of attenuation in matter.

The apparatus used in such studies is schematically shown in Fig. II-7. It consists of: (1) the source of x-rays to be analyzed; (2) a collimating device, which reduces the size of the x-ray beam to a narrow pencil; (3) a series of absorbers that can be interposed in the path of the x-radiation; and

FIG. II-7. Schematic diagram of apparatus used for study of the attenuation of x-rays in matter.



(4) of a detector sensitive to x-rays. The collimating device is usually a hole in a lead plate. The chemical nature of the absorbing material used is determined by the maximum energy of the radiation to be analyzed, because of the strong dependence of the attenuation of x-rays on the atomic number of the absorber (Chapter III). For low energy radiation of the order of 10 keV, the absorber used is usually composed of low atomic-number elements such as beryllium or carbon. For higher energies, from 10 to 100 keV, aluminum is most often used. For radiation of up to approximately 400 keV, copper is used, and for even higher energies, lead.

The physical form of the absorber is usually a series of plates of increasing thickness. However, in some experiments, the absorber used may be a solution of increasing concentration.

Attenuation spectrometry consists of the study of the intensity of the x-ray beam as a function of the amount of absorber interposed. The results of such a study are, in general, represented as a plot of radiation intensity versus amount of absorber traversed, as shown in Fig. II-8, 1(A). The intensity of the transmitted radiation is plotted as a percentage of the impinging beam, and the amount of absorber can be expressed either as thickness (for example, in centimeters), or in terms of mass per unit area (g/cm^2). If the radiation studied is monochromatic (monoenergetic), which means composed of photons carrying the same energy, the attenuation of this radiation is represented by the relationship

$$I = I_0 e^{-\mu x}.$$

In this equation, I is the intensity of the transmitted radiation, I_0 is the intensity of the incident radiation, e is the base of natural logarithms, μ is the attenuation coefficient, and x is the amount of material traversed (see also Chapter III, Equation (2)).

This equation is represented by the exponential curve shown in Fig. II-8, 1(A). The same function plotted with semilogarithmic coordinates is represented by a straight line, as shown in Fig. II-8, 1(B).

A useful parameter for the representation of the rate of attenuation of radiation in matter is the half-value layer (HVL , or $T_{1/2}$), which is the amount of absorber required to reduce the intensity of the impinging radiation by a factor of 2 (see also Chapter III, under "Half-Value Layer"). The half-value layer can be determined graphically from either the linear plot in Fig. II-8, 1(A) or from the semilogarithmic plot in Fig. II-8, 1(B). The mathematical relationship between the half-value layer and the attenuation coefficient (see also p. 67) is

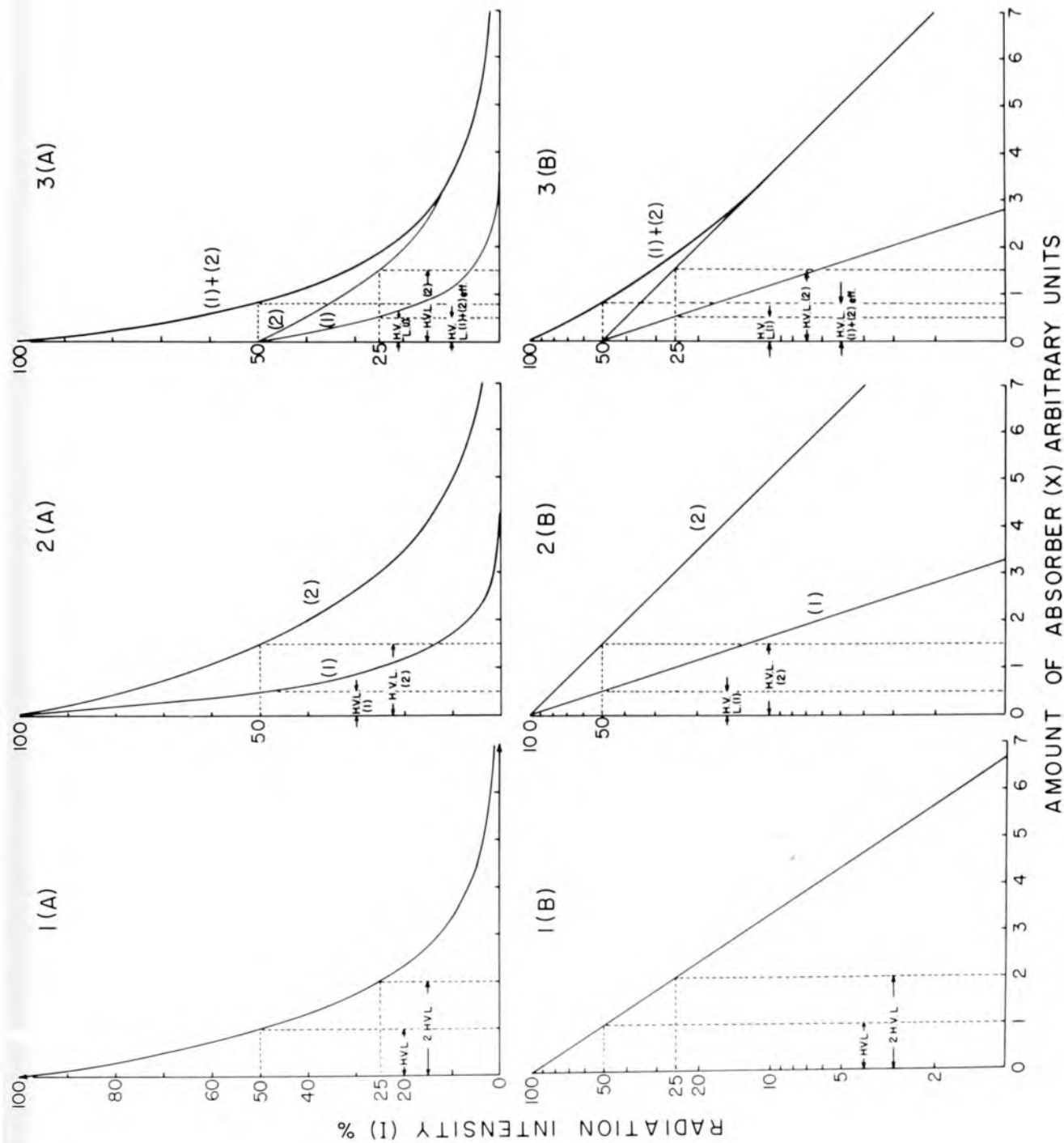
$$HVL = \frac{0.693}{\mu}.$$

The half-value layer depends on the energy of the radiation and on the nature of the absorber. For a given absorber the half-value layer is usually

FIG. II-8. Attenuation of x-rays versus amount of absorber.

1(A) attenuation curve of monoenergetic photons
2(A) attenuation curves for two photon beams of different energies (Beam 1 lower in energy than Beam 2)
3(A) compound attenuation curve for a beam of x-rays composed of 50% photons with Energy 1 and 50% photons with Energy 2

1(B), **2(B)**, and **3(B)** semi-logarithmic plots of **1(A)**, **2(A)**, and **3(A)**, respectively
HVL half-value layer



greater for higher energy radiation (harder radiation) than for lower energy radiation (soft radiation). Figure II-8, 2(A) shows a plot of the attenuation of a softer and a harder monoenergetic radiation in the same absorber; Fig. II-8, 2(B) is the semilogarithmic plot of the same curves.

If the radiation studied is polychromatic (polyenergetic), which means composed of photons of different energies, its attenuation curve in matter is composed of the sum of the exponential absorption curves for the different energies contained in the beam of x-rays. Figure II-8, 3(A) shows the attenuation curve obtained for an x-ray beam composed of photons of two different energies. It should be noted that the compound curve coincides at its tail end with the simple exponential curve representing the attenuation of the higher energy photons. This is due to the fact that the softer photons are rapidly removed from the beam and play a lesser role in the attenuation curve for larger amounts of absorber. Figure II-8, 3(B) is a semilogarithmic representation of the attenuation curve for the polyenergetic radiation shown in Fig. II-8, 3(A). The compound curve obtained by adding the straight attenuation lines for energies (1) and (2) is no longer a straight line. Hence, if the semilogarithmic plot of the attenuation of x-rays in matter is not a straight line, it indicates that the radiation is polyenergetic. It is apparent in Fig. II-8, 3(B) that the compound attenuation curve (1) + (2) becomes a nearly straight line towards its high attenuation end, which is due to the fact that the beam of x-rays is depleted of softer photons and becomes nearly monochromatic.

The half-value layer for polychromatic radiation varies as the energy of the radiation is modified by selective absorption. If the amount of absorber interposed is sufficiently great to remove most of the soft radiation, thus reducing the radiation to relatively monochromatic photons, the half-value layer may become constant. The first half-value layer for a polychromatic radiation is referred to as the effective half-value layer and is a measure of the effective energy of the photons in the radiation. The effective half-value layer, and consequently the effective energy of polychromatic radiation, is modified by the addition of absorbers that selectively remove the softer photons. The half-value layer of monochromatic radiation is not modified by absorption.

Attenuation spectrometry is a simple but crude method of analysis of an x-ray beam. It does not permit an accurate measure of the distribution of photons as a function of their energies. On the other hand, the method supplies the following information: (1) whether or not the radiation studied is monochromatic; (2) if the radiation is polyenergetic, the semilogarithmic plot of the attenuation curve allows a crude study of the distribution of the photon energies; (3) a relatively accurate measurement of the maximum energy carried by the x-ray photons; and (4) determination of the effective energy of the radiation studied, which information is of value in diagnostic roentgenology.

Diffraction and Interference X-Ray Spectrometry

The spectrometric analysis of a beam of x-rays by diffraction and interference provides the most accurate method for this purpose. This form of spectrometry utilizes the wave properties of x-radiation. Among other tests, the wave nature of the x-radiation was established on the basis of its successful diffraction and interference. The property of undergoing diffraction and interference is shared by all wave-type transfers of energy. Because of the importance of these phenomena in the identification of x-rays as a wave-type propagation of energy and in x-ray spectrometry, the subjects of diffraction and interference are discussed in some detail in the following paragraphs.

Wave Diffraction and Interference. When two trains of waves emitted in phase intersect at any point in space, they either reinforce each other's effect at that point or interfere destructively with each other. Thus, the total effect contributed by both trains of waves at the point of intersection may be either greater or smaller than the effect produced by either wave. If the two waves are in phase at the point of intersection, which means that their crests and troughs coincide, the resulting energy is equal to the sum of their energies. If the two waves are out of phase in such a fashion that the crest of one wave coincides with the trough of the other, then the resulting energy is equal to the difference between their energies. Interference is characteristic of any wave propagation of energy; thus, sound waves and waves produced by a disturbance on the surface of a liquid exhibit this phenomenon. The interaction of electromagnetic radiations does also result in interference. This is one of the major reasons why electromagnetic radiation must be regarded as wave propagation of energy.

Interference exhibited by electromagnetic waves has been extensively studied with light (Refs. 7 and 8). The phenomenon cannot be demonstrated experimentally with two difference sources of light, because it has been impossible to establish two sources of light that emit radiation in phase. The electromagnetic radiation emitted by a source of light varies continuously in phase, and therefore it is impossible to predict with any accuracy the phase of the radiation emitted by such a source. This difficulty may be overcome by splitting the light emitted by a single source into two overlapping beams; thus, the two beams are always in phase, and interferences may be observed in the area where the two beams overlap.

Different methods can be used for splitting the light emitted by a single source into two separate overlapping beams. For example, it can be achieved by the use of two plane mirrors set up in such a fashion that there is a small angle between their planes (Fresnel bi-mirrors). This arrangement is pictured in Fig. II-9. The two mirrors provide two virtual images of the source *S*, and interferences can be observed in the shaded region where the two beams of light emitted by the images intersect. At any given point *P* in this zone of overlapping, there is enhancement or reduction of light intensity, depending

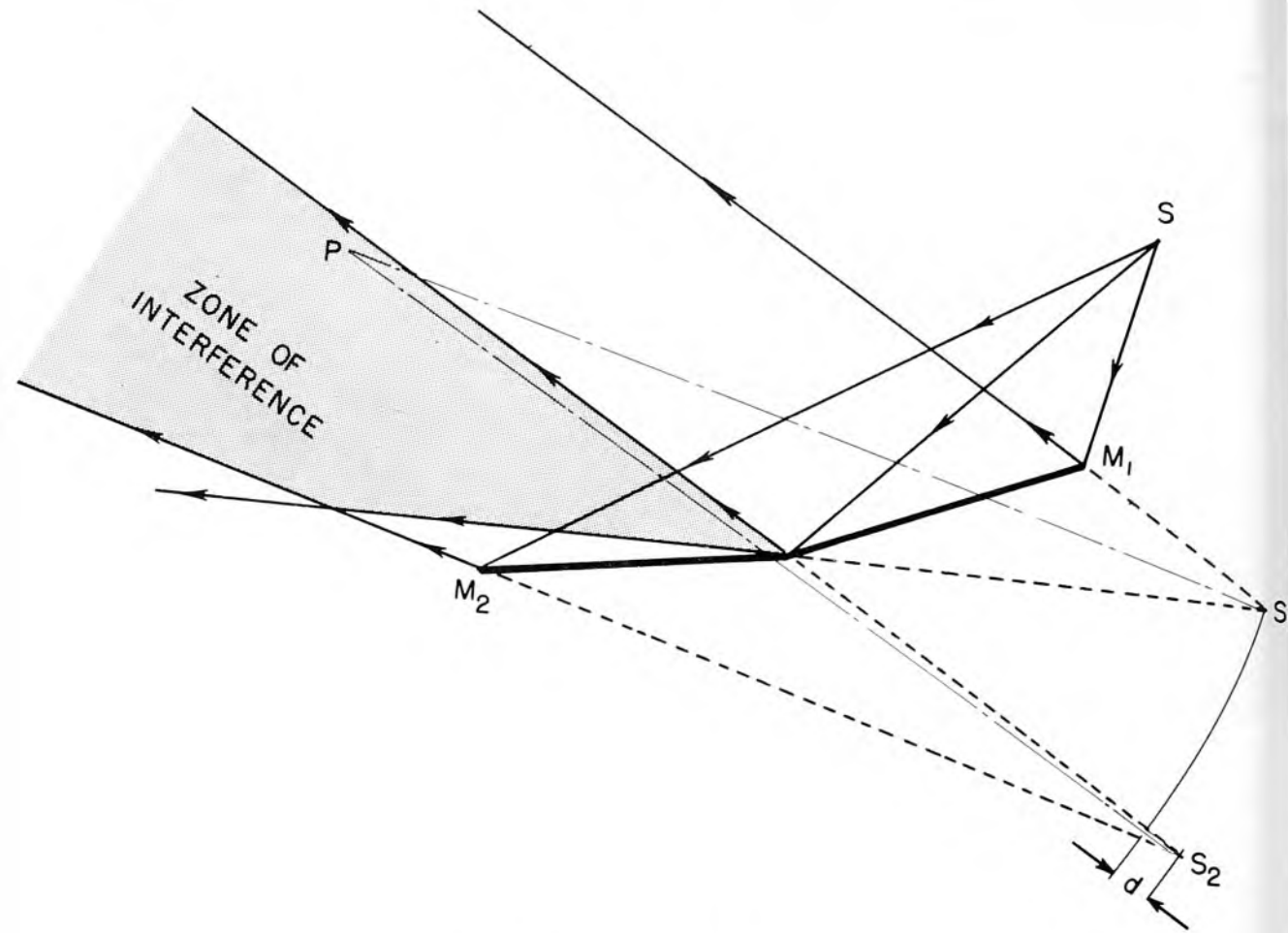


FIG. II-9. Fresnel bi-mirrors.

M_1 and M_2 plane mirrors

S source of light

S_1 and S_2 images of the source of light S formed by mirrors M_1 and M_2

d difference between optical paths between point P and images S_1 and S_2 , respectively

on the difference d between the optical paths from this point to the two virtual sources of light S_1 and S_2 . If this difference is equal to zero, that is, if the point is equidistant from both S_1 and S_2 , or if this difference is equal to one wavelength or an integer times one wavelength ($n\lambda$), then the radiations from the sources S_1 and S_2 are in phase at the point P and there is reinforcement of light. On the other hand, if the difference is equal to one-half of one wavelength, or an odd number of half wavelengths, the beams are out of phase and their interference results in depression of light.

The described experiment is carried out with monochromatic light. If a polychromatic source of light is used, the extinction and reinforcement of the light, which are dependent upon the wavelength, occur in different

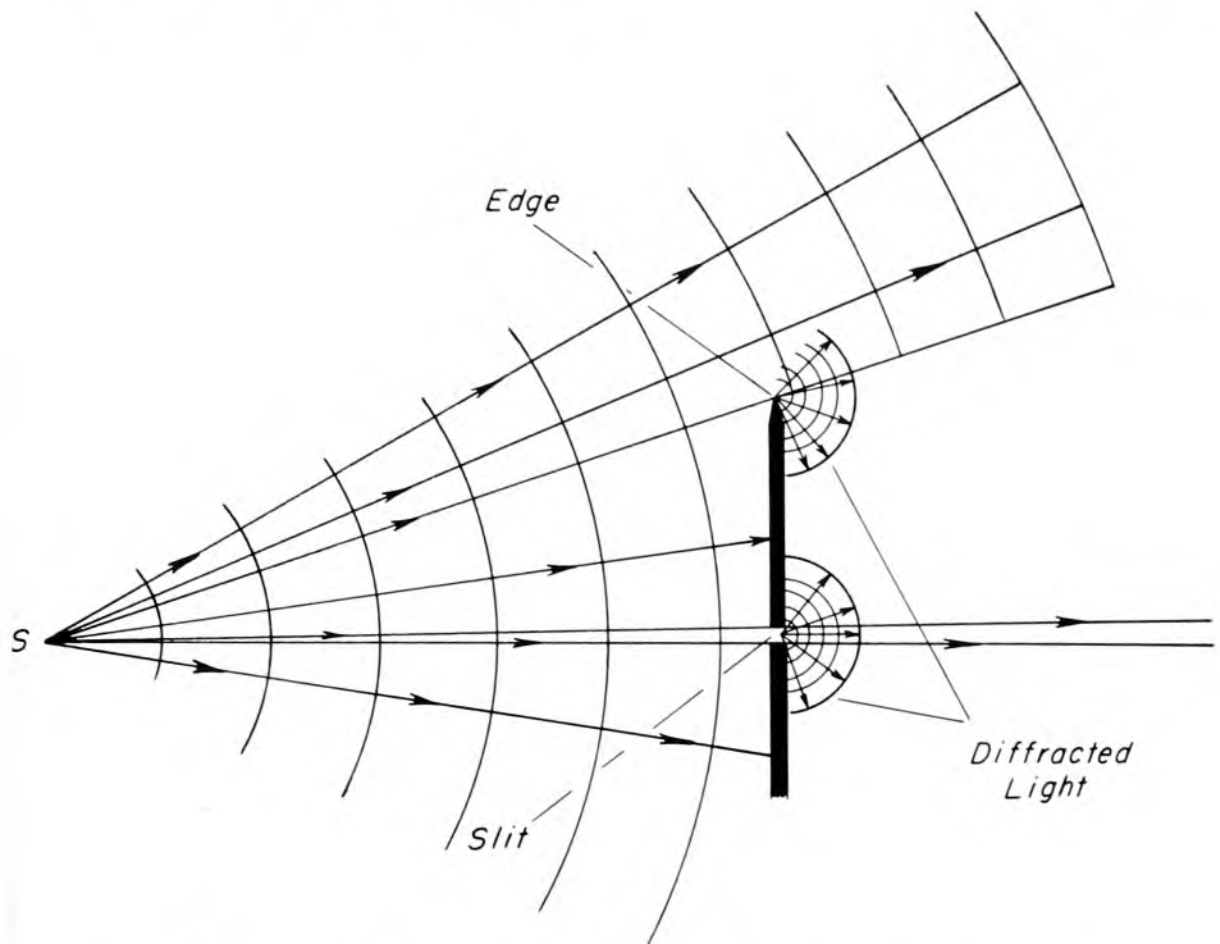


FIG. II-10. Diffraction of light either by a sharp edge or by a slit.
S light source

positions for different wavelengths. In this manner the system provides a method for the analysis of a polychromatic beam of light into its different components; in other words, it provides a method for light spectroscopy.

The device most commonly used for high-resolution light spectroscopy is a diffraction grating. The diffraction grating utilizes two properties of waves: interference and diffraction.

Diffraction is the ability of waves to be bent or diffracted from their original direction when they encounter the sharp edge of an absorber, or a slit. In diffraction the edge of the absorber, or the slit, can be considered as a secondary source emitting light in phase with the primary source, as shown in Fig. II-10.

Most often a diffraction grating is composed of a series of slits that are used to diffract the light from the source to be analyzed. Technically, a diffraction grating can be constructed in a variety of ways. The most important consists in scribing a series of equally spaced parallel lines either on a glass plate or on a mirror. The scratches are opaque to light while the areas

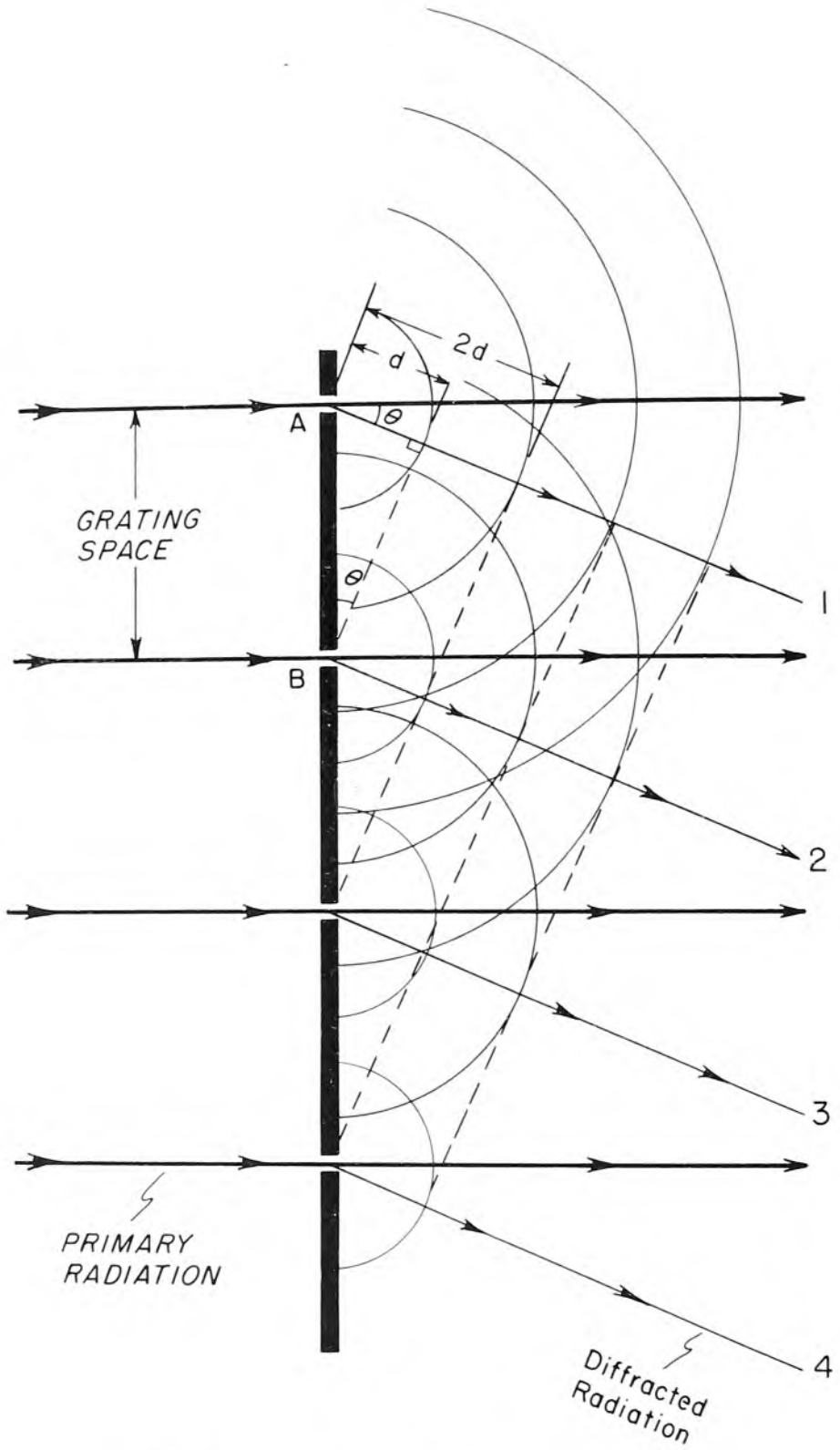


FIG. II-11. Principle of a diffraction grating.

d difference in optical path length between beams diffracted by adjacent slits
 θ angle of diffraction

between them act as slits, either by transmission in the case of the glass plate or by reflection in the case of the mirror. The scribed glass plate is called a transmission diffraction grating, while the scribed mirror is called a reflection diffraction grating. The number of lines per unit length is of the order of 10,000 per centimeter for a good grating. The importance of this factor will become apparent later in the text.

A diffraction grating (Fig. II-11) functions as follows: A parallel beam of light is directed against the grating. A certain portion of the light is unaffected by the grating and travels in a straight line. The remainder of the light is diffracted by the slits of the grating at different angles from the original direction. The difference between the optical paths of two beams of light diffracted by a given angle, θ , from the original direction of the light by two adjacent slits of the grating is equal to d , as shown in Fig. II-11. This difference d is related to the angle of diffraction θ and to the grating space AB by the formula

$$d = AB \sin \theta.$$

Thus, the difference between the optical paths of light beams diffracted at an angle θ by two adjacent slits is constant for a given diffraction grating. The difference in optical paths between a beam of light scattered at an angle θ and a beam of light scattered at the same angle but by a slit twice removed from the first one is equal to twice this constant, and so on, and the difference between the length of the optical paths of the beams of light diffracted at a given angle is equal to an integer times that constant.

If the difference in the length of optical paths, d , is equal to the wavelength λ of the component of the light emitted by the source under study, that particular wavelength is reinforced by interference in the direction θ , while all the other wavelengths are reduced in intensity. On the other hand, for another angle of diffraction, another wavelength is enhanced at the expense of all the others, and so on. Therefore, the diffraction grating analyzes polychromatic light into its components.

The apparatus used for the spectrometry of light by means of a diffraction grating is shown in Fig. II-12. It consists of the following elements: (1) the source of light to be analyzed, (2) a lens that converts the divergent beam of light emitted by the source into a parallel beam, (3) a grating, and (4) a second lens that focuses all the rays of light impinging upon it at a given angle to the same point. The light which passes through the diffraction grating unaffected and which therefore is parallel to the axis of the two lenses is then focused in the center of the image formed by the second lens. All the other components of the beam of light that have been diffracted by the grating are projected on both sides of the central unaffected ray at angles that increase with increasing wavelength. Thus, red light, which has a longer wavelength than blue light, is diffracted at a greater angle.

It should be noted that a diffraction grating provides several spectra. The

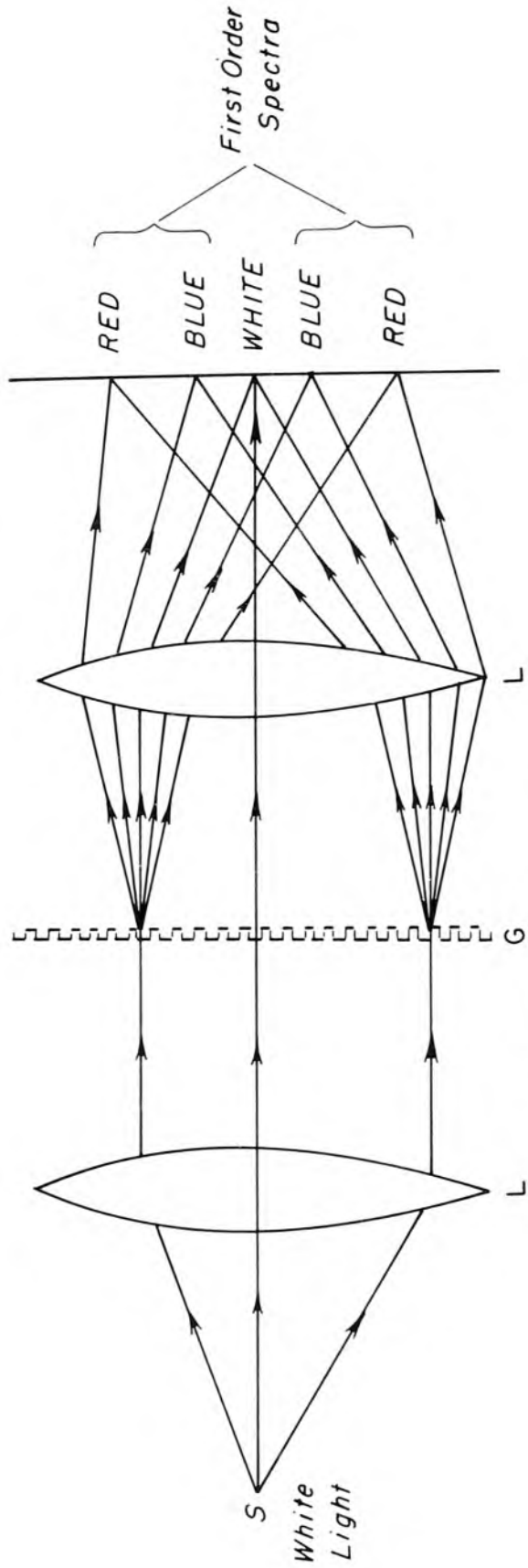


FIG. II-12. Diffraction grating spectrometer.

- S source of light
- L lenses
- G grating

first spectrum is obtained when the distance d between the paths of beams scattered by two adjacent slits is equal to one wavelength, the second is obtained when the distance is equal to two wavelengths, the third, to three wavelengths, and so on. The first spectrum is called the first order spectrum, the second, the second order spectrum, and so on. The resolution that can be achieved by means of a diffraction grating is inversely proportional to the distance AB between its slits. Indeed, the smaller the distance AB, the greater the angle of diffraction for a given wavelength. The efficiency of an optical grating can be expressed as the percentage of the impinging light that is actually utilized in forming the different spectra. This efficiency depends on the total number of lines in the grating.

Refraction, Reflection, Diffraction, and Interference of X-Rays. Early after the discovery of x-rays, several similarities of this radiation with light were noticed. Many experiments were carried out in an attempt to establish further identity between the physical properties of x-rays and those of light. Röntgen (Ref. 4) himself attempted unsuccessfully to observe the refraction of x-rays by means of prisms made of various materials such as hard rubber, aluminum, and water. The early attempts to observe diffraction patterns obtained with x-rays passing through very narrow slits produced equivocal results (Ref. 9).

The lack of success of the early experiments was due to inadequate instrumentation rather than to faulty theory. Since then, interference, diffraction, reflection, and refraction of x-rays have been successfully produced in the laboratory. In 1919, Stenström (Ref. 10), experimenting with long-wavelength x-rays, found that their reflection from crystalline sugar and gypsum did not obey Bragg's law. He interpreted that failure as being due to a partial refraction of the x-radiation in the crystal. Later, Duane and Patterson (Ref. 11) and Siegbahn (Ref. 12) observed the same small discrepancies in crystalline calcite. These experiments pointed to an index of refraction for the employed crystals smaller than 1. Since the index of refraction of a substance for an electromagnetic radiation is equal to the velocity of light in the vacuum divided by the velocity of propagation of that radiation in the substance, an index of refraction smaller than 1 observed for x-rays indicates therefore that this radiation travels in the substance with a velocity greater than that of light.

On the basis of these results, Compton reasoned that total reflection could be observed with x-rays, provided the angle between the radiation and the reflecting surface is sufficiently small, almost glancing, "just as light in a glass prism is totally reflected from a surface separating the glass from the air if the light strikes the surface at a sufficiently sharp angle" (Ref. 9). In 1923, Compton demonstrated experimentally the reflection of x-rays from surfaces of glass and silver through angles of several minutes, and from these experiments he deduced the index of refraction of the deflectors for the radiation used (Ref. 13).

Walter in 1924 (Ref. 14) and Rabinov in 1925 (Ref. 15), using extremely thin slits and monochromatic x-rays, succeeded in obtaining excellent diffraction patterns. The first spectral analysis of an x-ray beam by means of dispersion in a prism was accomplished by Larsson, Siegbahn, and Waller in 1924 (Ref. 16). In these experiments the x-rays struck the prism at a glancing angle slightly greater than the critical angle for total reflection of the radiation. The use of such small angles explained the success of these experiments as compared to the earlier experiments, which were carried out with a crystal prism set for minimum deviation. Later, in 1932, Kellström (Ref. 17) obtained interference with x-rays by means of the classical Fresnel bi-mirror used at very small angles. The angle between the mirrors was of 19.6 seconds of arc, and the wavelength of the radiation used was 8.3 Å. Further experiments demonstrated abundantly that the reflection and the refraction of x-rays are functions of the index of refraction and of the absorption in the refracting medium, just as the reflection and the refraction of light are.

The focusing of x-rays by means of refraction by lenses, although possible, is of little practical value because of the very small differences between the indices of refraction of most substances for this radiation and the integer 1. A similar situation prevails for the reflection of x-rays, which occurs with such low efficiency and at such small angles that the use of mirrors for the focusing of x-ray beams is not very efficient. Although focusing of x-ray beams is used in bent crystal spectrometers, x-ray beams cannot be for practical purposes focused and are always either divergent or nearly parallel at great distances from the source.

X-Ray Diffraction Spectrometry. Optical spectrometry resolves polychromatic light into its monochromatic components either by means of a prism or, if higher resolution is required, by means of a diffraction grating. It may appear that either method can also be applied to the spectrometry of x-radiation. Although the analysis of the polyenergetic x-ray beam into its components by means of a prism has been achieved by Larsson, Siegbahn, and Waller (Ref. 16), this method is of little practical value because of the poor dispersion obtained.

The construction of a diffraction grating for x-ray spectrometry presents the following technical problems: The design of a diffraction grating is governed by the energy of the electromagnetic radiation to be analyzed; and the width of the slits in the case of a transmission grating, or the width of the reflecting surfaces in the case of a reflection grating, must be of the order of magnitude of the wavelength of the radiation to be diffracted. Also, the diffraction spacing must be of the same order of magnitude. If the grating space is large with respect to the wavelength of the radiation to be analyzed, then the angle of diffraction is too small to be practical. An efficient diffraction grating for the spectral analysis of an x-ray beam in the 50 keV energy range requires a grating composed of either extremely narrow slits or extremely narrow reflecting surfaces, separated by a distance of the order of

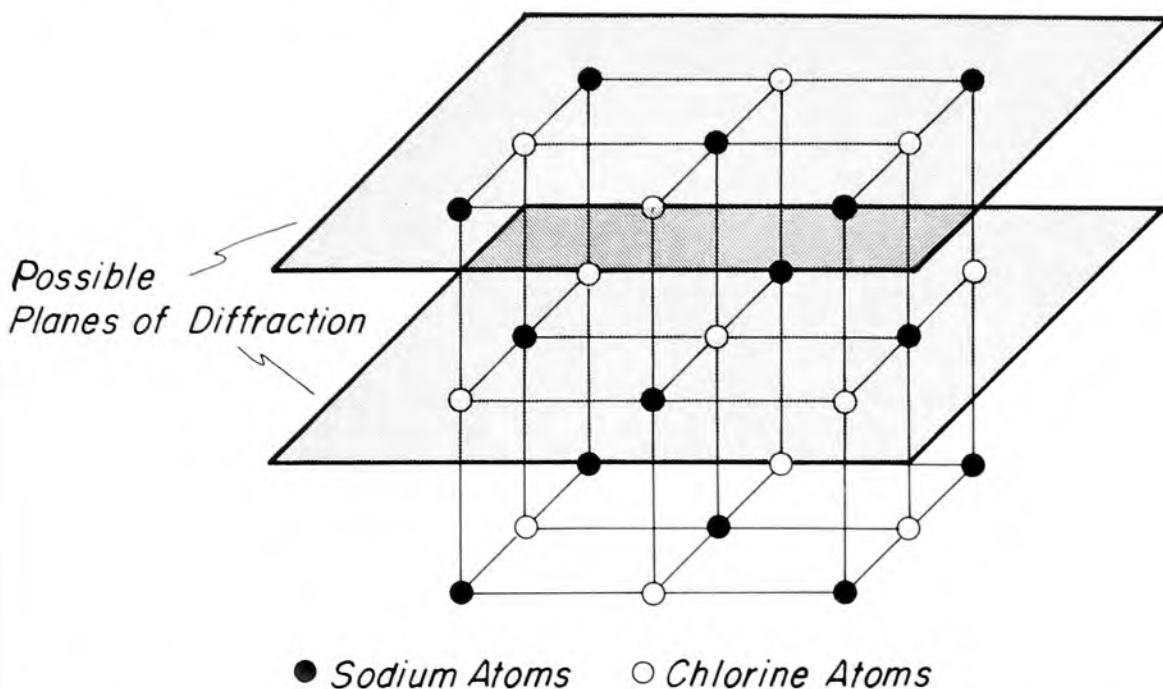


FIG. II-13. Crystalline structure of sodium chloride, showing atomic planes that form natural diffraction gratings.

1 Å. The construction of such a grating presents serious problems. It should be noted, however, that conventional reflection-type diffraction gratings have been successfully used in conjunction with x-rays by using them at an extremely small angle. The glancing angle of irradiation is necessary in this case, first, to achieve the reflection of x-rays, and second, to reduce the apparent grating space.

The difficulty of constructing an efficient diffraction grating for x-rays was circumvented when von Laue and his co-workers (Ref. 18) demonstrated that crystals could be used as natural gratings for the diffraction of x-rays. The atoms or molecules of organic or inorganic crystals are distributed in an orderly manner forming a series of different planes, which can be defined as regions of space containing high concentrations of particles (Ref. 19). These planes can be classified into different groups. All the planes in one group contain the same arrangements of atoms, and they are parallel. Planes belonging to different groups intersect each other at angles that are characteristic of the crystal. Figure II-13 shows the crystalline structure of sodium chloride and two series of atomic planes. The crystalline planes are nearly perfectly flat, and the distances between those of one group are constant. However, distances vary both from crystal to crystal and for different groups of planes within the same crystal. The order of magnitude of these distances is about 1 Å. A crystal may be regarded as a three-dimensional diffraction grating with a grating space well suited for x-ray diffraction. The experimental test by von Laue of the usefulness of crystals as

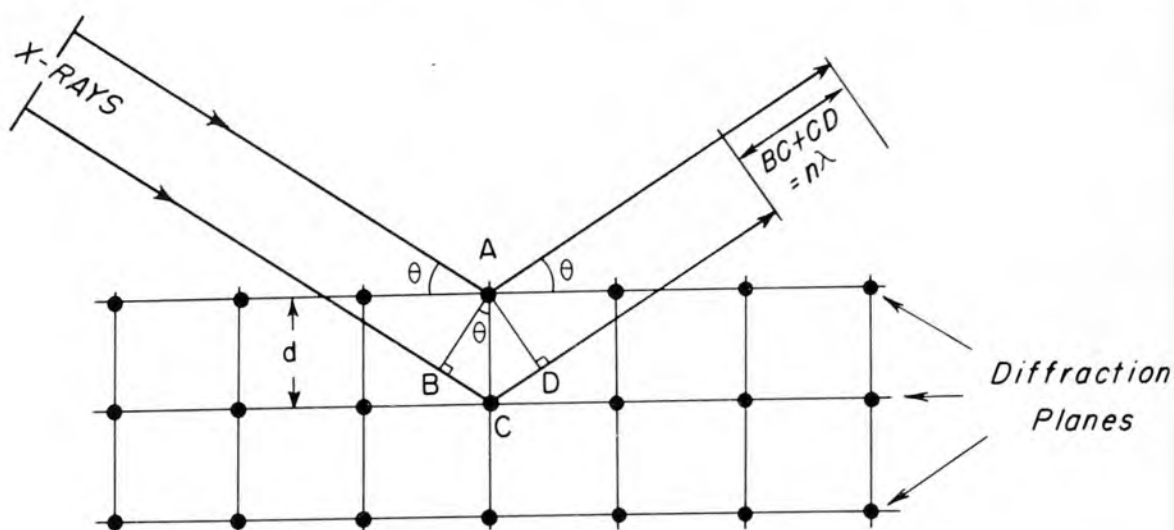


FIG. II-14. Diffraction of x-rays by a crystal. The two beams will show reinforcement of the radiation because difference in their lengths ($BC + CD$) is equal to $n\lambda$ where n is an integer.

diffraction gratings was successful, and provided an extremely refined method for x-ray spectrometry.

In x-ray diffraction spectrometry, crystals are used as reflection diffraction gratings. When a beam of x-rays impinges upon a crystal, the x-rays are reflected by the different crystalline planes, as shown in Fig. II-14. The difference in length between the paths of rays diffracted by two adjacent planes is equal to $BC + CD$, which in turn is equal to

$$2d \sin \theta.$$

If the difference in length $BC + CD$ between the optical paths is equal to the wavelength λ of the radiation or to λ times an integer n , so that

$$n\lambda = 2d \sin \theta,$$

then the optical beams are in phase and the radiation diffracted by the two adjacent planes is reinforced. Wavelengths other than λ or $n\lambda$ undergo destructive interference for this angle. This relationship is called Bragg's law. A typical Bragg-type spectrometer is shown schematically in Fig. II-15.

A plot of the intensity of radiation measured at an angle θ versus the angle θ provides a spectral analysis of the beam of radiation impinging upon the crystal. Although the Bragg spectrometer allows good resolution of soft x-rays, it suffers from several deficiencies, particularly from: (1) a low resolving power for short wavelength radiation; (2) overlap of the direct beam of

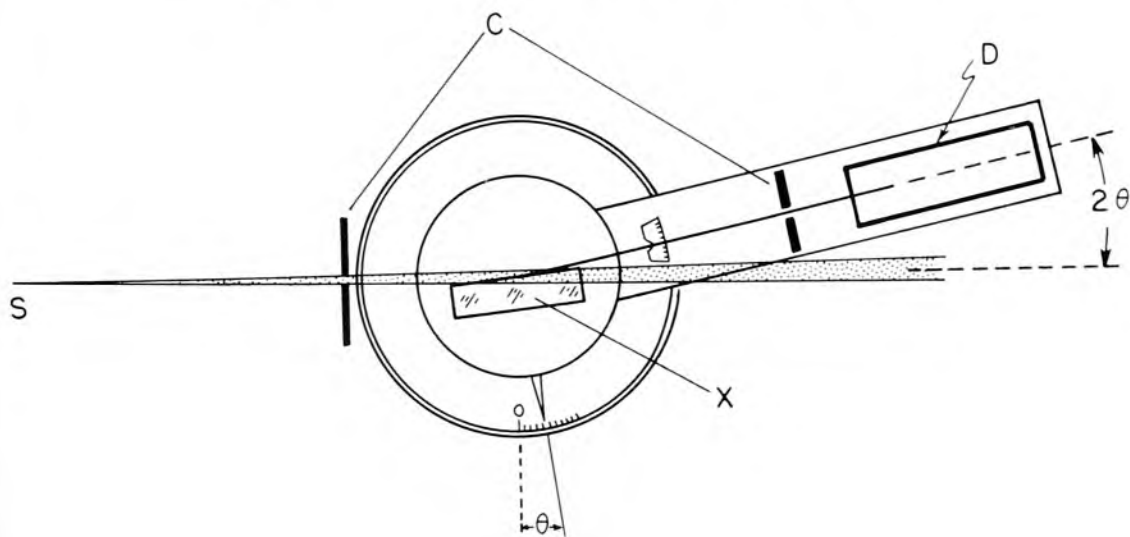
radiation and scattered radiation over the low wavelength spectrum; and (3) low efficiency of the apparatus. The latter point can be clarified by a comparison between the Bragg x-ray spectrometer and the optical grating spectrometer shown in Fig. II-12. The analysis of the electromagnetic radiation is carried out in a similar fashion in the two spectrometers. However, in the optical spectrometer the radiation diffracted by the entire grating is utilized in the formation of the spectra by focusing the light diffracted by each slit by means of a lens. In the Bragg spectrometer, only an extremely small segment of the crystal is used in the analysis of the x-ray beam; because lenses are practically inoperative with x-radiation, no gathering of radiation is possible; and thus the efficiency of the system is drastically reduced.

The above shortcomings of the Bragg spectrometers are partially corrected in the curved (bent)-crystal diffraction spectrometers (Fig. II-16). In this family of instruments, the analyzing crystal is mechanically bent in order to achieve a partial focusing of the beam of x-rays in a manner somewhat similar to that achieved by means of optical curved mirrors. Curved-crystal x-ray spectrometers have been designed both for reflection operation and transmission operation. These instruments, at this time, represent probably the most perfect x-ray diffraction spectrometers in the sense that they embody both a relatively high efficiency and a very high resolution.

In conclusion, diffraction x-ray spectrometers provide an excellent method

FIG. II-15. Bragg spectrometer.

- S source of x-rays
- C collimators
- X crystal
- D radiation detector
- θ angle between beam of x-rays and surface of crystal



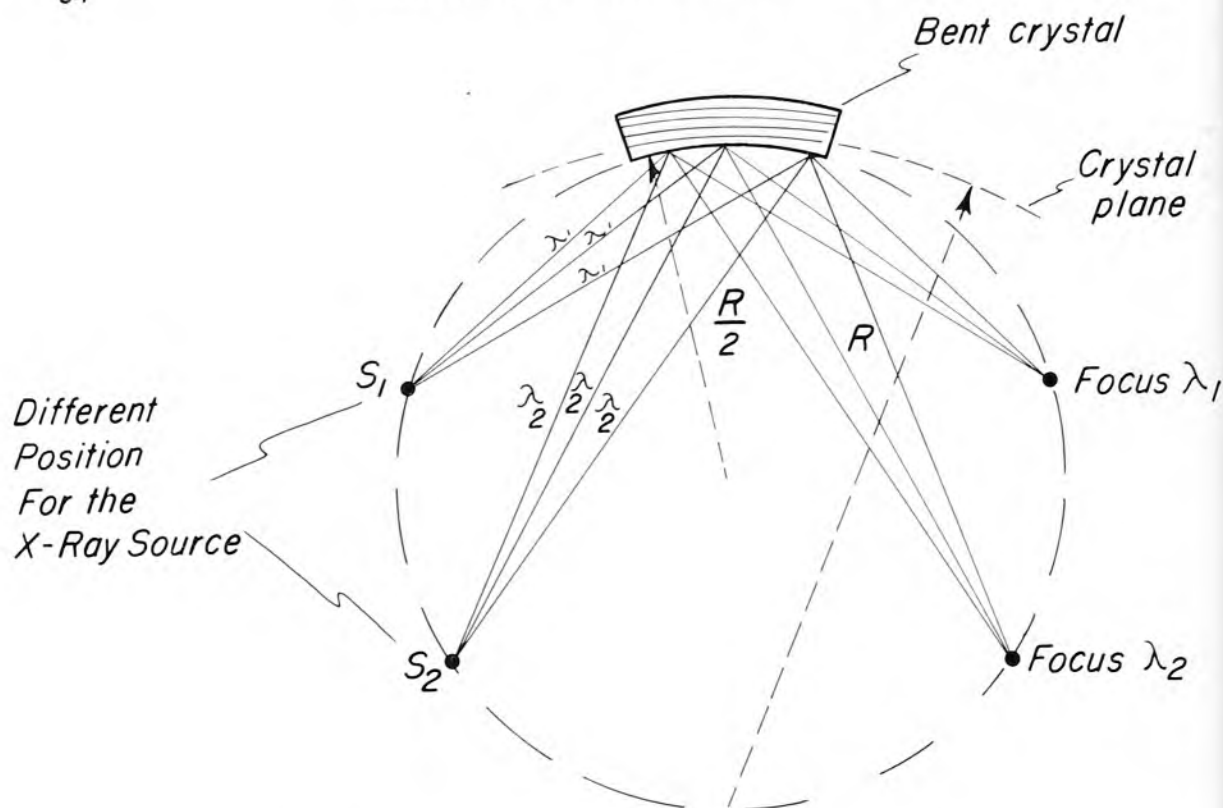


FIG. II-16. Bent-crystal x-ray spectrometer.

S_1 and S_2 different positions of source of x-rays
 R radius of curvature of the crystal
 λ_1 and λ_2 wavelengths of x-rays

for the analysis of x-ray spectra. The main deficiencies of the diffraction methods are: (1) low efficiency and (2) relative complexity of the apparatus.

Scintillation X-Ray Spectrometry

Scintillation spectrometry of x-rays is based on the property of certain substances, particularly certain crystals, to convert the energy dissipated by ionizing radiation within them into flashes of light; these substances are usually referred to as phosphors. The intensity of the flash of light thus generated is proportional to the amount of energy dissipated by the ionizing radiation within the phosphor (Refs. 20 and 21). The theory of this process is discussed in Chapter VI.

A scintillation spectrometer is composed of the following elements (Fig. II-17): (1) a phosphor in which the energy of the impinging x-radiation is converted into flashes of light; (2) a photomultiplier tube that converts the light impinging upon it into electrical pulses that are proportional in amplitude to the intensity of the light flash "seen" by the tube; and (3) a pulse height discriminator, which is an electronic circuit capable of sorting elec-

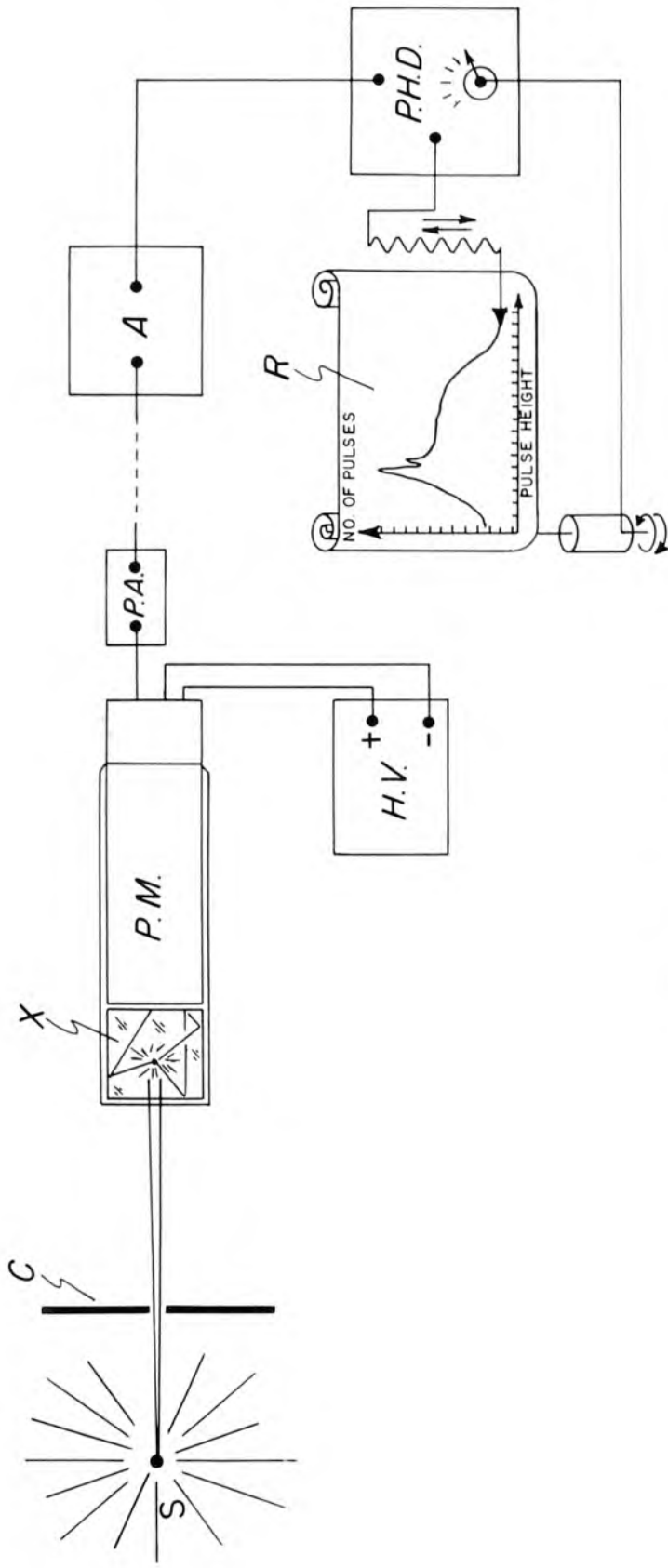


FIG. II-17. Scintillation spectrometer.

- S source of x-rays
- C collimator
- X phosphor (crystal)
- P.M. photomultiplier tube
- H.V. high-voltage power supply
- P.A. preamplifier
- A amplifier
- P.H.D. pulse height discriminator
- R recorder

trical pulses according to their height. In addition to these fundamental components, the operation of the photomultiplier tube also requires the use of a highly regulated high-voltage power supply.

The scintillation spectrometer functions as follows: (1) An x-ray photon is stopped within the phosphor, thus transferring its energy to the phosphor material. (2) This energy is converted with a certain efficiency into a light pulse of magnitude proportional to the energy of the impinging photon. (3) The light thus emitted enters the photomultiplier tube and is converted there into an electrical pulse proportional in height (usually measured in volts) to the amount of light generated by the phosphor. (4) The electrical pulse supplied by the photomultiplier is fed into the pulse height discriminator, which records the number of pulses and their heights.

A plot of the number of pulses provided by the pulse height discriminator versus the height of the pulses corresponds to the spectral distribution of the x-ray photons absorbed in the phosphor. It should be noted that if two photons are absorbed simultaneously within the phosphor, the flash of light produced corresponds in intensity to the sum of the energy of the photons absorbed and is recorded by the pulse height discriminator as a single pulse, which leads to a faulty concept of the energy carried by a single photon. Such an occurrence, however, is rare if precautions are taken to carry out scintillation spectrometry with relatively low-intensity x-ray beams.

Scintillation spectrometry requires that the photon energy be completely dissipated within the phosphor. For that reason, a phosphor of high atomic number is selected. The phosphor material most commonly used for x-ray spectroscopy is sodium iodide activated with thallium. This phosphor is an efficient scintillator that is relatively opaque to x-rays and converts a large percentage of the ionizing radiation energy into light.

< The main advantage of scintillation spectrometers over diffraction spectrometers is their high efficiency. In a scintillation spectrometer each photon stopped in the phosphor is utilized in the spectral analysis, and, in general, the size of the phosphor is selected in such a fashion that the x-radiation to be studied is absorbed within it with an efficiency of nearly 100%. In contrast, in a diffraction spectrometer, an infinitesimal fraction of the x-ray photons striking the crystal is used in the spectral analysis, most of the photons emitted by the source being wasted from the standpoint of the analysis.

The resolution of scintillation spectrometers is limited by several physical factors, the most important ones being: (1) the light collection efficiency of the phosphor; (2) the efficiency of the photo cathode; (3) the efficiency of the collection of electrons in the photomultiplier tube; and (4) the lack of linearity of the amplifier system used in the electronics of the apparatus. The resolution of the best scintillation spectrometers is considerably worse than that of diffraction spectrometers.

Scintillation spectrometers are difficult to use for low energy x-radiation

below approximately 10 keV because in that region the light pulses produced in the phosphor compete with thermal noise in the photomultiplier tube, and the latter tends to overshadow the signal fed to the tube. Nevertheless, scintillation spectrometers are reliable and simple instruments which are very widely used in the analysis of x-ray spectra.

Other Methods of X-Ray Spectrometry

In addition to the above methods, x-ray spectrometry can and has been carried out through the application of several other physical phenomena. For example, proportional counters are widely used for the purpose. When an x-ray photon dissipates energy within the sensitive volume of a proportional counter, the magnitude of the electrical pulse subsequent to the discharge of the proportional counter is proportional to the amount of energy dissipated and, in turn, the pulse height distribution of such electrical pulses can be obtained by means of an electronic analyzer identical to that used in scintillation spectrometry. Proportional counters are particularly useful for the spectrometry of low-energy x-rays.

Another method of x-ray spectrometry is based on the fact that when x-rays interact with matter their energy is transferred to electrons. The energy distribution of these electrons can be studied by means of magnetic spectrometers, and the spectral distribution of the primary photons can be deduced from the electron spectrum thus obtained. This method has been extensively used in the spectrometry of gamma rays but is of little consequence in x-ray spectrometry (Ref. 20). More recently, very high resolution lithium-drifted germanium solid-state x-ray spectrometers have been developed (Ref. 22).

X-Ray Spectroscopic Analysis of Matter

The diffraction of x-rays by matter provides an excellent method for the determination of both the interspace between the planes containing the molecules or atoms of the substance to be analyzed and the direction of these planes. A typical arrangement for such a study is shown in Fig. II-18. It is similar to the original arrangement used by von Laue to show x-ray diffraction. The image obtained by that method on a photographic plate is shown in Fig. II-19. Such a pattern is referred to as Laue spots. The pattern of the spots was interpreted by Bragg as being the reflection of the incident beam of x-rays by the crystalline planes. The interpretation of the position and intensity of the spots allows a very accurate determination of the distribution and pattern of the molecules within a particular solid.

X-ray diffraction has become a very powerful tool in the study of solid states. The method is particularly important in the study of the molecular structure of biologic systems. It should be noted that x-ray diffraction is now

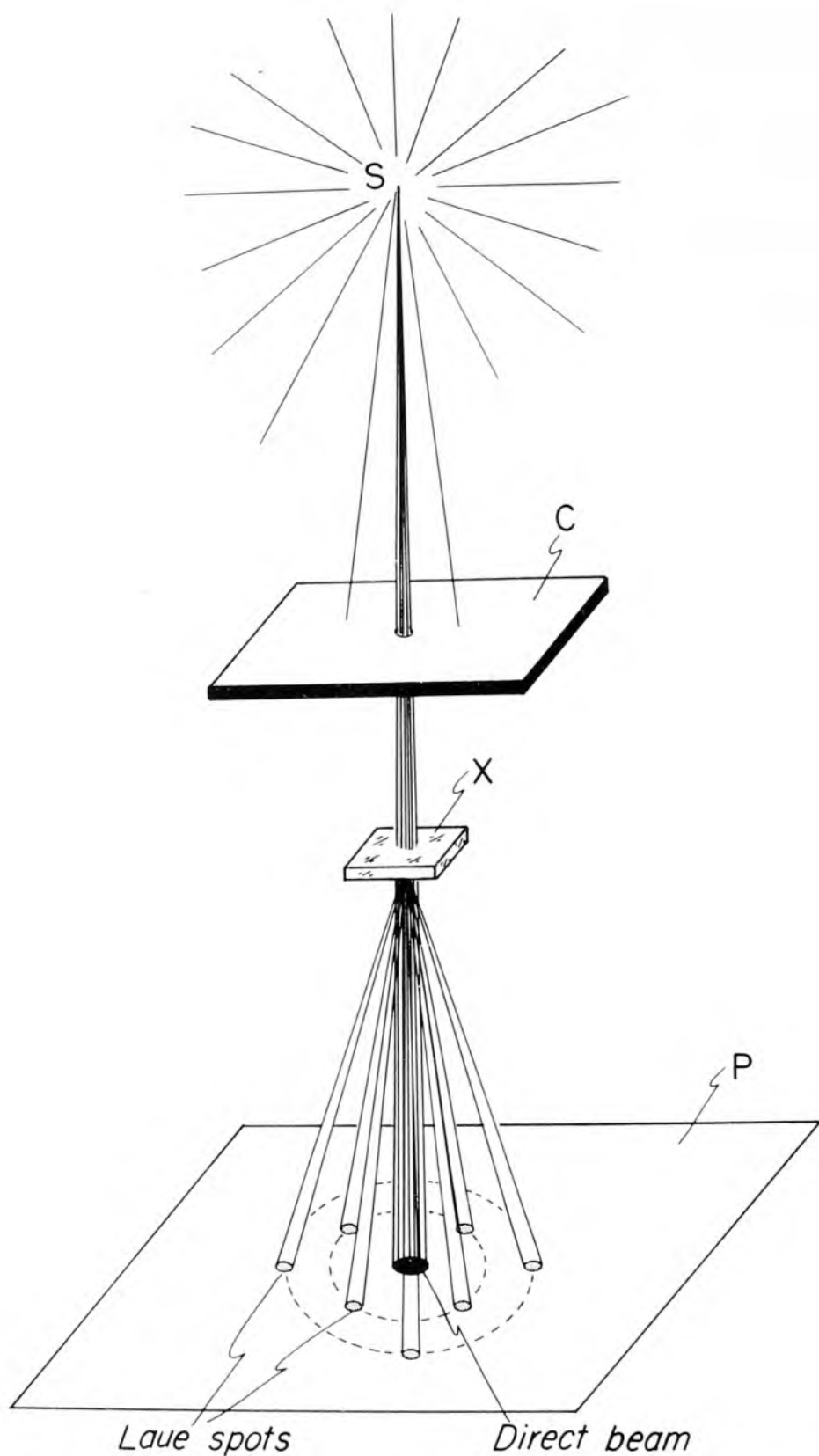


FIG. II-18. Apparatus for study of crystals by diffraction of x-rays.
 S source of x-rays X crystal
 C collimator P photographic film

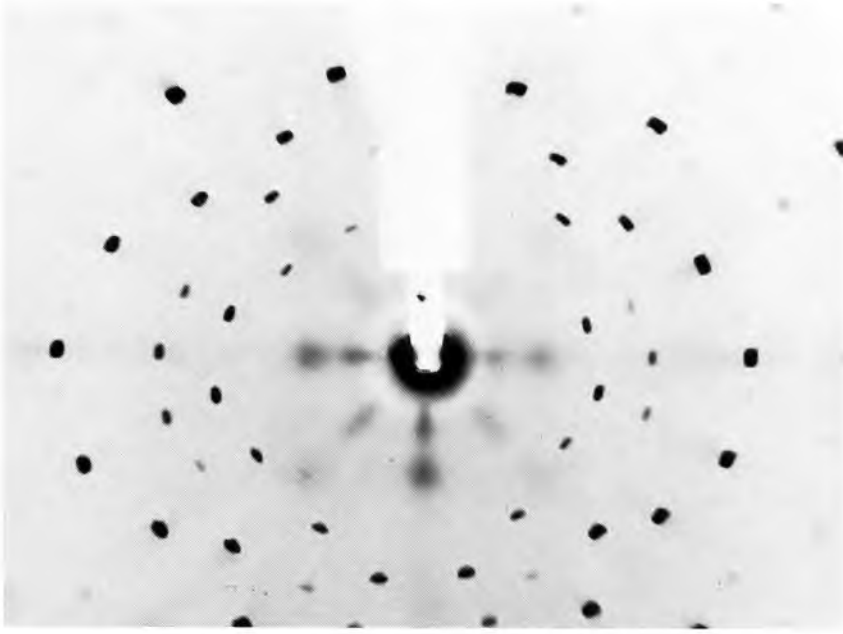


FIG. II-19. Laue diffraction pattern obtained by method illustrated in Fig. II-18.
(Courtesy of Picker X-Ray Corporation.)

probably much more important as an analytic tool in the study of matter and in chemical analysis than as a method for x-ray spectrometry.

Analysis by x-ray spectroscopy is similar to that by optical spectrometry in the sense that it consists of the determination of either the absorption (attenuation) of x-radiation by the sample to be analyzed or the emission of the x-radiation spectrum of the sample. Thus, two forms of x-ray spectroscopic analysis are used: attenuation analysis and emission or fluorescence analysis.

Attenuation analysis is based on the strong dependence of the attenuation of x-radiation at a given energy on the atomic number of the absorber (Chapter III). In this application the x-ray diffraction apparatus is used in a manner similar to the optical monochromator in optical spectrometry.

Emission or x-ray fluorescence analysis consists in exposing the sample to be analyzed to polychromatic x-rays and in studying the spectral distribution of the x-ray radiation re-emitted as fluorescence radiation, which is characteristic of the composition of the irradiated sample (Chapter III). An x-ray diffraction spectrometer used in the determination of the spectral distribution of fluorescent radiation is shown in Figs. II-20 and II-21.

X-ray spectroscopic analysis is an accurate and sensitive method for the determination of the elemental composition of the unknown sample (Fig. II-22). The method differs from optical spectroscopic analysis in two main respects: (1) The x-ray method provides the analysis of the elements present in the sample. It is unaffected by their chemical bonds. (2) The x-ray method is nondestructive for samples not affected by x-rays.

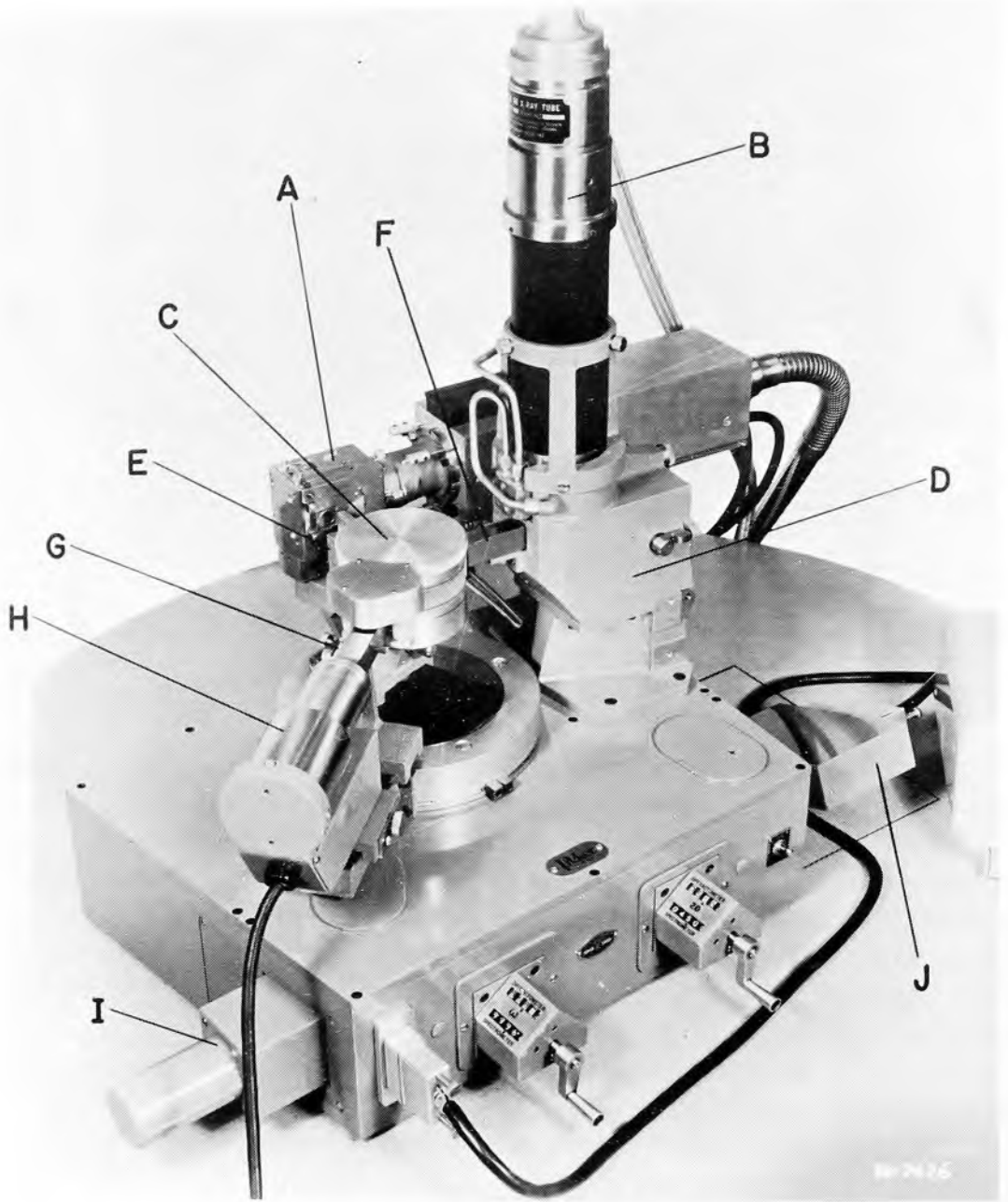


FIG. II-20 (Legend on opposite page).

FIGS. II-20 and II-21. Picker Spectrodiffractometer for x-ray fluorescence analysis and diffraction techniques.

- A diffraction x-ray tube
 - B spectroscopy x-ray tube
 - C flat sample holder for diffraction, and analyzing crystal holder for spectroscopy (shown with a helium chamber in place)
 - D sample chamber for spectroscopy
 - E diffraction incident-beam collimator and slit support
 - F beam tunnel
 - G diffracted beam collimator and slit support for diffraction, and soller slit support for spectroscopy
 - H radiation detector
 - I high speed motor and clutch
 - J angle encoder for automatic operation
- (Courtesy of Picker X-Ray Corporation.)*

FIG. II-21.



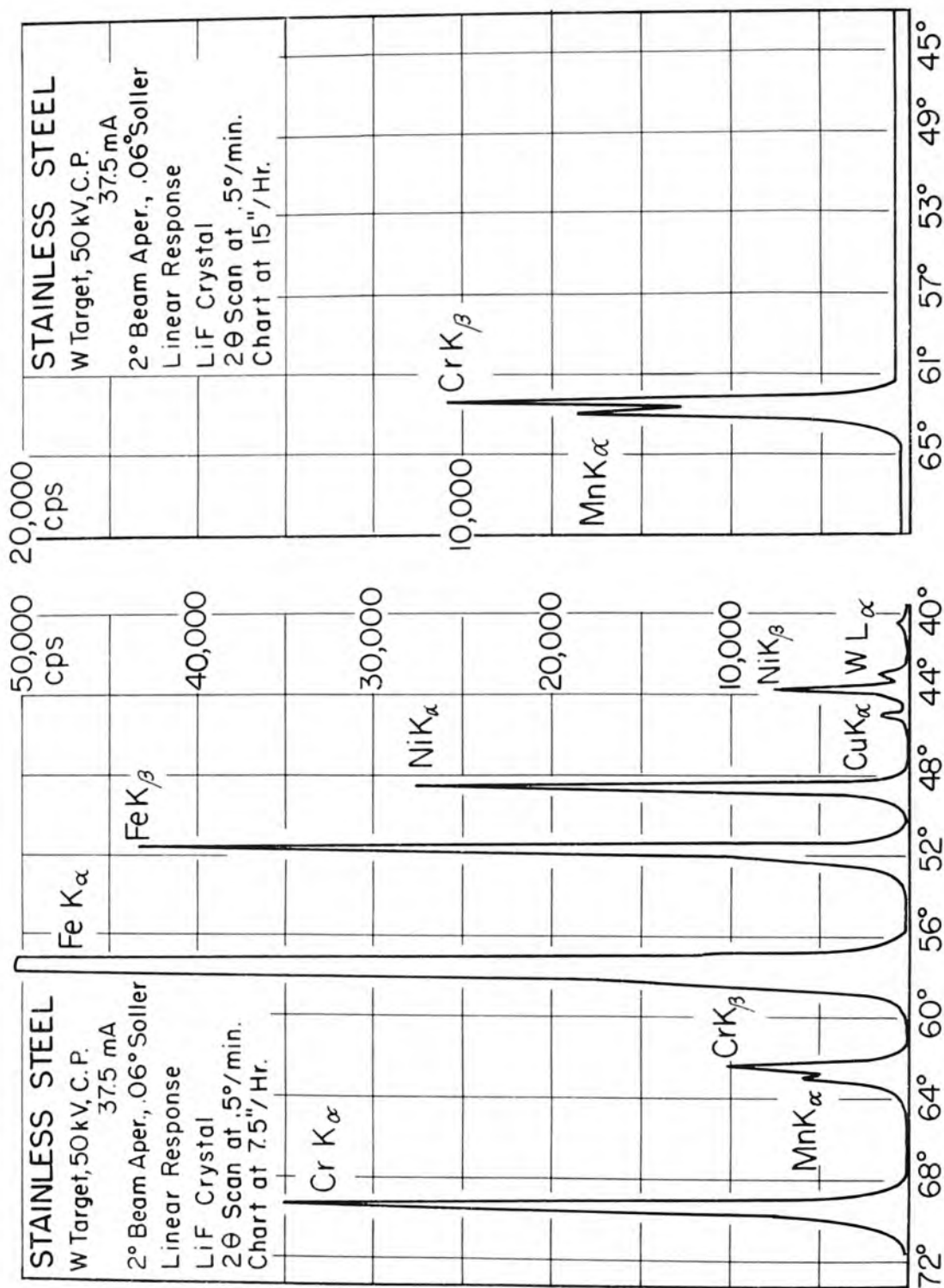


FIG. II-22. X-ray fluorescence analysis of a sample of stainless steel.
(Courtesy of Picker X-Ray Corporation.)

REFERENCES

1. JOHNS, H. E., and LAUGHLIN, J. S.: "Interaction of Radiation with Matter," in *Radiation Dosimetry*, ed. by Hine, G. J., and Brownell, G. L. New York, Academic Press, 1956.
2. HEITLER, W.: *The Quantum Theory of Radiation*, 2nd ed. New York, Oxford University Press, 1944.
3. JOHNS, H. E.: *The Physics of Radiology*, 2nd ed. Springfield, Ill., Thomas, 1953.
4. EVANS, R. D.: *The Atomic Nucleus*. New York, McGraw-Hill, 1955.
5. FINE, S., and HENDEE, C. F.: X-ray critical absorption and emission energies in kev. *Nucleonics* 13(#3):36, 1955.
6. SNELL, A. H., ed.: *Nuclear Instruments and Their Uses*, vol. 1. New York, Wiley, 1962.
7. JENKINS, F. A., and WHITE, H. E.: *Fundamentals of Optics*, 3rd ed. New York, McGraw-Hill, 1957.
8. ROSSI, B.: "Optics," in *Principles of Physics Series*. Reading, Mass., Addison-Wesley, 1957.
9. COMPTON, A. H., and ALLISON, S. K.: *X-rays in Theory and Experiment*, 2nd ed. New York, Van Nostrand, 1935.
10. STENSTRÖM, W.: Dissertation. Lund, 1919.
11. DUANE, W., and PATTERSON, R. A.: *Phys. Rev.* 16:526, 1920.
12. SIEGBAHN, M.: *Compt. Rend.* 173:1350, 1921, and 174:745, 1922.
13. COMPTON, A. H.: *Phil. Mag.* 45:1121, 1923.
14. WALTER, B.: *Ann. d. Phys.* 74:661, 1924, and 75:189, 1924.
15. RABINOV, I. I.: *Proc. Natl. Acad. Sci. U.S.* 11:222, 1925.
16. LARSSON, A., SIEGBAHN, M., and WALLER, I.: *Naturwiss.* 12:1212, 1924, and *Phys. Rev.* 25:235, 1925.
17. KELLSTRÖM, G.: *Nov. Act. Reg. Soc. Sci. Uppsal.* 8:#5, 1932.
18. FREIDRICH, W., KNIPPING, P., and VON LAUE, M.: *Ber. Bayer. Akad. Wiss.* 303:1912.
19. BRAGG, W. L.: *Proc. Cambridge Phil. Soc.* 17:43, 1912.
20. BELL, P. R.: "The Scintillation Method," in *Beta- and Gamma-Ray Spectroscopy*, ed. by Siegbahn, K. New York, Interscience, 1955.
21. PRICE, W. J.: *Nuclear Radiation Detection*. New York, McGraw-Hill, 1958.
22. SHIRLEY, D. A.: Applications of germanium gamma-ray detectors. *Nucleonics* 23(#3):62, 1965.

(III) INTERACTION OF X-RAYS WITH MATTER

ATTENUATION OF AN X-RAY BEAM BY MATTER

The interaction of x-rays with matter at the atomic and subatomic levels can be explained only by assuming the corpuscular nature of this radiation. The wave nature of the x-radiation clarifies only a few of the phenomena involved in the exchange of energy between this radiation and matter.

A beam of x-rays impinging upon any form of matter is attenuated. This attenuation consists in the removal of x-ray photons from the beam by two processes: (1) absorption of the photons in matter, and (2) scattering of the photons out of the beam. Absorption of an x-ray photon by matter consists in the transfer of the total energy carried by the photon to the absorber; after such an interaction the x-ray photon ceases to exist as such. Scattering of an x-ray photon by matter consists in the deflection of the photon from its original direction; in general, this interaction results in the transfer of some of the energy carried by the photon to the absorber.

Both absorption and scattering result in the exchange of energy between the radiation and the matter encountered and subsequent depletion of the energy of the x-ray beam. The study of this interaction can be divided into two areas: (1) determination of the mathematical relationship governing the attenuation of a beam of x-rays impinging upon an absorber, and (2) qualitative and quantitative study of the physical phenomena involved in the exchange of energy between the x-ray photons and the absorber. This division into two categories is legitimate because of the fact that the equation governing the depletion of an x-ray beam traversing matter can be derived statistically without the knowledge of the physical interactions involved between the photons and the absorber.

Exponential Attenuation of X-Rays

The derivation of the mathematical equation relating the attenuation of a beam of x-rays to the amount of matter traversed can be derived statistically by making the following four assumptions:

1. A beam of x-rays is composed of small particles (photons).
2. From the standpoint of interactions with photons, matter is composed of discrete particles separated by distances large with respect to the size of these particles. In other words, the assumption is made that a photon may either interact with a particle of matter or slip unaffected between these particles.
3. The interaction between an x-ray photon and a particle of matter does not affect the other photons in the beam. It should be noted that at this point no assumption is made as to the nature of the particles composing the absorber. These particles can be either molecules, atoms, electrons, or nuclei. Furthermore, no assumption is made as to the uniformity of the particles encountered. Thus, interactions between photons and matter could occur at the molecular, atomic, electronic, or nuclear levels simultaneously, without affecting the validity of the derivation of the mathematical expression governing the attenuation of the x-ray beam.
4. The interaction between a photon and one of the particles of matter results in the removal of the photon from the beam either by scattering or by absorption.

The first assumption is supported by our understanding of the corpuscular nature of x-rays. The second assumption is supported by the experimental observation that in a beam of x-rays directed against an absorber, a certain number of photons are able to traverse the absorber unaffected. Thus, any absorber must exhibit a certain number of "holes" as far as the x-radiation is concerned and is not comparable to a homogeneous impenetrable shield. The third assumption is merely a statement of the fact that the life history of each x-ray photon is independent of the others, and that the photons are not connected by any forces and should be treated as independent particles. Finally, the fourth assumption is derived from experimental observations showing that if a photon interacts with a particle of matter, the exchange of energy involved results either in the removal of the photon from the beam by absorption or in its deflection from its original direction. The situation where a photon loses its energy to an absorber without deflection from its original direction does not occur.

The picture presented by the above assumptions can be visualized as a large number of particles emitted in a beam and directed against a network of other particles in such a fashion that the distances between the absorber particles are large with respect to the physical dimensions of either particles involved.

Under these assumptions, the number of interactions occurring between the photons in an x-ray beam and the matter particles in a given thickness of absorbing material is proportional to the number of photons impinging upon the absorber. This can be expressed mathematically by

$$\frac{\Delta N}{N} = -\mu \Delta x.$$

The greek letter Δ placed before a number indicates a change in that number. In this formula, ΔN denotes the number of photons interacting, and therefore removed from the beam, in the absorber of thickness Δx ; N is the number of photons impinging upon the absorber; and μ is a constant. The minus sign is introduced in the formula to indicate that the interactions result in the removal of the photons from the beam. The above equation can also be written as

$$\frac{\Delta N}{N} \cdot \frac{1}{\Delta x} = -\mu, \quad (1)$$

where $\Delta N/N$ represents the number of photons removed from the beam per incident photon for each thickness increment Δx in which the interaction takes place. This equation expresses the fact that the fraction of photons removed from the beam per unit thickness of absorbing material is constant and is equal to μ .

The dimensions of the constant μ can easily be obtained from Equation (1); $\Delta N/N$ is a ratio of two numbers with the same dimensions and is therefore dimensionless; Δx is expressed in units of length. Therefore, dimensionally μ is expressed as 1/length, or "per unit length," or length⁻¹. If we assume that the thickness of the absorber is equal to 1 unit of length, the physical meaning of μ becomes apparent as that fraction of photons removed from the beam by 1 unit length of absorber. The constant μ is called the linear attenuation coefficient for x-rays; and, as will be shown later, it depends both on the nature of the absorber and on the energy of the radiation used.

The above expression relating the attenuation ΔN of the x-ray beam to the thickness of the absorber Δx is valid only if the thickness of the absorber Δx does not alter appreciably the number of photons N in the x-ray beam. This condition is fulfilled only if Δx is very small. A real absorber does not fulfill this requirement and it can be visualized as a stack of a large number of layers each with a very small thickness, Δx . Equation (1) applies to each one of the layers, but the number of photons N impinging on each successive layer is gradually reduced by the previous layers. The fraction of photons removed from the beam is, however, constant in each one of the layers Δx . Thus, for example, if the first layer Δx attenuates the beam by 10%, 90% of the remaining photons impinge upon the second layer, which again attenuates the beam by 10%, thus removing 9% of the original photons and allowing 81% of the original photons to impinge upon the third layer Δx . The latter in turn attenuates the beam by another 10%, equal to 8.1% of the original beam, and so on. It should be noted that this calculation is valid only if the layer Δx is made infinitely thin in such a fashion that there is no variation in the number of photons traversing Δx .

The total attenuation of an x-ray beam by an absorber of finite thickness x can be calculated by dividing this absorber into an extremely large number

of very thin layers, and by carrying out the summation of the attenuation achieved by each one of these layers. This is accomplished by integrating the expression $dN/dx = -\mu N$ as follows:

$$\int_{N_0}^N \frac{dN}{N} = -\mu \int_0^x dx.$$

The integration of the number of photons is carried out from N_0 , which is the number of photons impinging upon the absorber, to N , the number of photons emerging from the absorber; and the integration of dx is carried out from 0 to x , which is the thickness of the absorber under consideration. The result of this integration is the equation

$$N = N_0 e^{-\mu x}. \quad (2)$$

In this equation, which shows the relationship between the attenuation of an x-ray beam by an absorber of thickness x and the linear attenuation coefficient μ for the radiation and the material under consideration, e is the base of natural logarithms which is a constant approximately equal to 2.718. The equation can be represented graphically with Cartesian coordinates by plotting the number of photons N along the vertical axis (ordinate) and the absorber thickness x along the horizontal (abscissa), as shown in Fig. III-1. The curve thus obtained is exponential in nature and its shape merely reflects the fact that x-rays are attenuated in matter at a constant rate. A discussion of the influence of the attenuation coefficient upon the slope of the exponential curve is found in Chapter II, under "Attenuation Spectrometry."

If Equation (2) is plotted with semilogarithmic coordinates in such a fashion that the logarithm of N is plotted versus x , then the resulting curve is a straight line, as shown in Fig. III-2. This representation is convenient in many applications.

Half-Value Layer (*HVL*)

The half-value layer is a constant that characterizes conveniently the attenuation of a beam of x-rays in a given absorber. This constant, often symbolized by $T_{1/2}$, is equal to the amount of absorber required to reduce the number of x-ray photons passing through it to one-half. Most commonly the amount of absorber is expressed as thickness, and the dimensions of the half-value layer are those of length, such as millimeters, centimeters, inches, or other units of length. Under certain circumstances, when the amount of material interposed in the path of a beam of x-rays is expressed as mass per unit area (g/cm^2) or number of atoms per unit area (atoms/cm^2), then the half-value layer is also expressed in these units (see under "Attenuation Coefficients").

The relation between the half-value layer and the attenuation coefficient

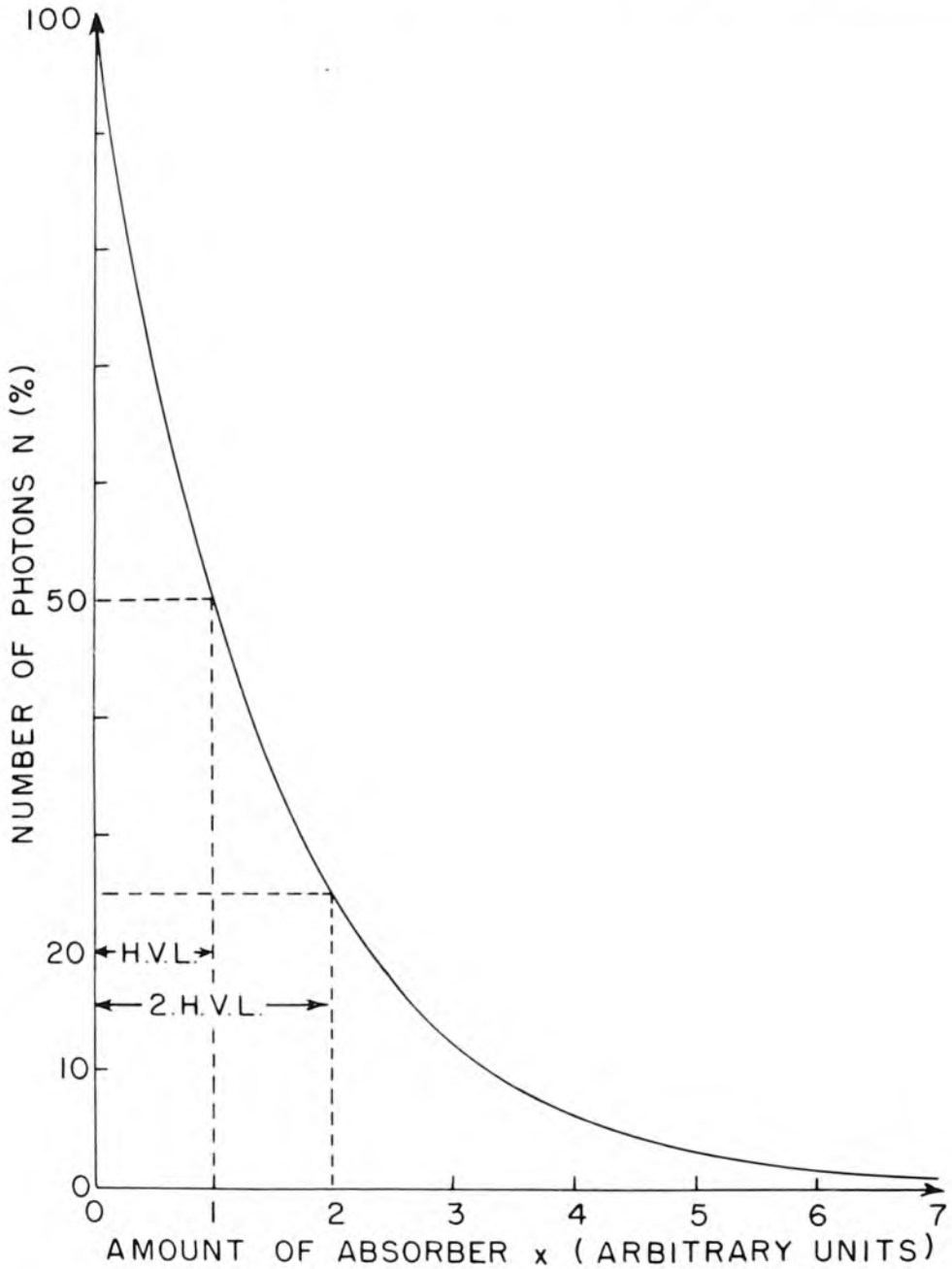


FIG. III-1. Attenuation of monoenergetic photons in matter
(linear plot of $N = N_0 e^{-\mu x}$).

can be determined as follows: The attenuation of a beam of x-rays in a given absorber, expressed by Equation (2), can be rewritten

$$\frac{N}{N_0} = e^{-\mu x},$$

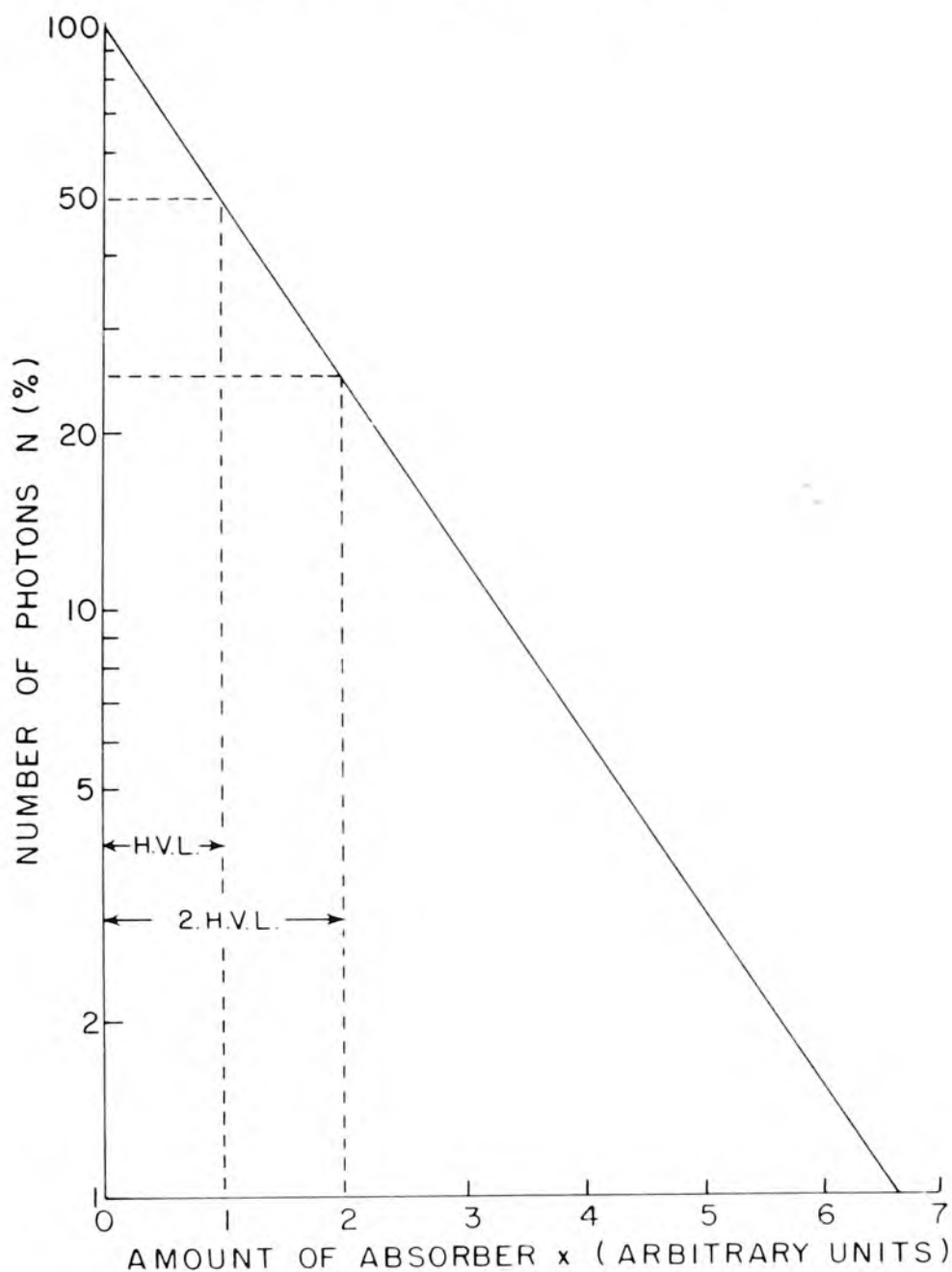
where the ratio N/N_0 is equal to the attenuation of the x-ray beam.

If the amount x of absorber interposed in the path of the beam is equal to one half-value layer ($T_{1/2}$), the attenuation N/N_0 is equal to $1/2$, and the equation can be written

$$\frac{1}{2} = e^{-T_{1/2}\mu}. \quad (3)$$

By taking the logarithm to the base e of both sides of Equation (3) it

FIG. III-2. Attenuation of monoenergetic photons in matter (semilogarithmic plot of $N = N_0 e^{-\mu x}$).



becomes

$$\log_e \frac{1}{2} = -\mu T_{1/2} \log_e e.$$

By definition, $\log_e e = 1$. Therefore, the above equation becomes

$$\log_e \frac{1}{2} = -\mu T_{1/2}$$

or

$$\begin{aligned} \log_e 2 &= +\mu T_{1/2} \\ \log_e 2 &= \sim 0.693; \end{aligned}$$

therefore,

$$T_{1/2} = \frac{0.693}{\mu} \quad (4)$$

which is the relationship between $T_{1/2}$ and μ .

The interposition in the path of an x-ray beam of one half-value layer of absorber attenuates it by a factor of 2. Two half-value layers result in an attenuation by a factor of 4, three half-value layers, by a factor of 8, and so on. The attenuation factor obtained with n half-value layers is equal to 2^n .

Mean Free Path

The mean free path θ of a beam of x-ray photons in a given absorber is defined as the mean distance traveled by one photon before it undergoes one interaction, and is equal to the reciprocal of the attenuation coefficient μ :

$$\theta = \frac{1}{\mu} \quad (5)$$

Since from Equation (4) μ is equal to $0.693/T_{1/2}$, the mean free path is equal to the half-value layer divided by 0.693 or multiplied by the reciprocal of 0.693, which is 1.45. Therefore,

$$\theta = T_{1/2} \times 1.45. \quad (6)$$

Attenuation Coefficients

In the above discussion, the amount of material placed in the path of an x-ray beam is expressed in terms of the thickness of the material present. Under certain circumstances, it is more convenient to express the quantity of an absorber in units other than length. For example, the method of expressing the amount of absorber as mass per unit area (g/cm^2 or lb/in^2) presents several advantages. In particular, it eliminates the need for qualifying the physical form of the absorber. Thus, if water is used as an absorber, a given number of grams per square centimeter of water is equivalent to the

same number of grams per square centimeter of steam although the thicknesses of the two absorbers differ considerably. Another advantage of this method of expression is derived from the fact that for high-energy x-radiation, the attenuation is nearly independent of the atomic number and depends only on the mass of material traversed; for practical purposes a given number of grams per square centimeter of lead is equivalent, from the attenuation standpoint, to the same number of grams per square centimeter of aluminum or of any other material, although the equivalent thicknesses of these materials vary considerably. In other applications it may be convenient to express the amount of absorber in electrons or in atoms per square centimeter.

If the amount of the absorber is expressed in certain units, the corresponding attenuation coefficient is expressed in reciprocal units. Thus, if the amount of absorber is expressed in centimeters of thickness (length), for example, the corresponding absorption coefficient is called *linear* attenuation coefficient and is expressed in cm^{-1} units. If the amount of material is expressed as mass per unit area, for example in g/cm^2 , the corresponding attenuation coefficient will be expressed in cm^2/g . The different attenuation coefficients commonly used are listed in Table III-1.

TABLE III-1. X-Ray Attenuation Coefficients

Units of absorber	Units of attenuation coefficient ^a	Units of half-value layer
length: (cm)	linear (μ) (cm^{-1})	cm
mass per unit area: (g/cm^2)	mass $\left(\frac{\mu}{\rho}\right)$ (cm^2/g)	g/cm^2
number of electrons per unit area: (electrons/ cm^2)	electronic $\left(\frac{\mu}{\rho \cdot N_0}\right)$ ($\text{cm}^2/\text{electron}$)	electrons/ cm^2
number of atoms per unit area: (atoms/ cm^2)	atomic $\left(\frac{\mu Z}{\rho \cdot N_0}\right)$ (cm^2/atom)	atoms/ cm^2

^a N_0 = number of electrons per gram; Z = atomic number of absorber; and ρ = density of absorber.

The reason for expressing the attenuation coefficient in units that are reciprocals of the units used for measuring the amount of absorber is readily apparent from Equation (2):

$$N = N_0 e^{-\mu x} \quad \text{or} \quad \frac{N}{N_0} = e^{-\mu x}.$$

Both sides of any equation must be expressed in the same units, otherwise the equation is meaningless. The ratio N/N_0 is a pure number, it is dimensionless. Therefore, to balance this equation, the expression $e^{-\mu x}$ must also be dimensionless. Since x is expressed in the units used for the amount of absorber, the attenuation coefficient μ must be expressed in reciprocal units in such a fashion as to render their product dimensionless.

The half-value layer of an absorber for a given x-radiation is expressed in the units used for the amount of absorber interposed. Thus, if the absorber thickness is measured in units of length, the half-value layer will be measured in units of length. If the amount of absorber is measured in g/cm^2 , the half-value layer is expressed in g/cm^2 , and so on (see Table III-1).

X-RAYS AND PARTICLES OF MATTER

The interaction of x-rays with matter takes place at a submolecular level because the forces which bind atoms together within a molecule are too weak to intervene in these interactions. Thus, x-rays interact only with atoms, electrons, and nuclei. An absorber attenuates an x-ray beam identically whether it is composed of a mixture of atoms or whether the same atoms are bound within the absorber to form chemical compounds. In any problem involving the interaction of x-rays with matter it is sufficient to specify the atomic mixture of the form of matter studied, disregarding its molecular composition. In some forms of interactions even the atomic composition of the absorber may become unimportant, and a given absorber may be adequately defined by the number of electrons per unit volume, regardless of the forces involved in binding these electrons together and the nuclear charges involved. In general terms, x-ray photons interact with particles of matter at a scale that is determined both by the size of the particle and the energy of the x-ray photon. Thus, low-energy x-ray photons may interact with an atom as a whole; higher energy photons will have a greater tendency to interact with tightly bound electrons in inner electronic shells; and, finally, the interaction of very high energy photons takes place at the nuclear level. It should be noted that this rule contains a number of what may appear to be glaring contradictions. They are not exceptions to the rule, but their explanation is outside the scope of this text.

Interaction of X-Rays with Atoms, or Coherent Scattering of X-Rays (Thomson Effect)

The interaction of an x-ray photon with a whole atom results in the deflection of the direction of travel of the photon, or scattering of the

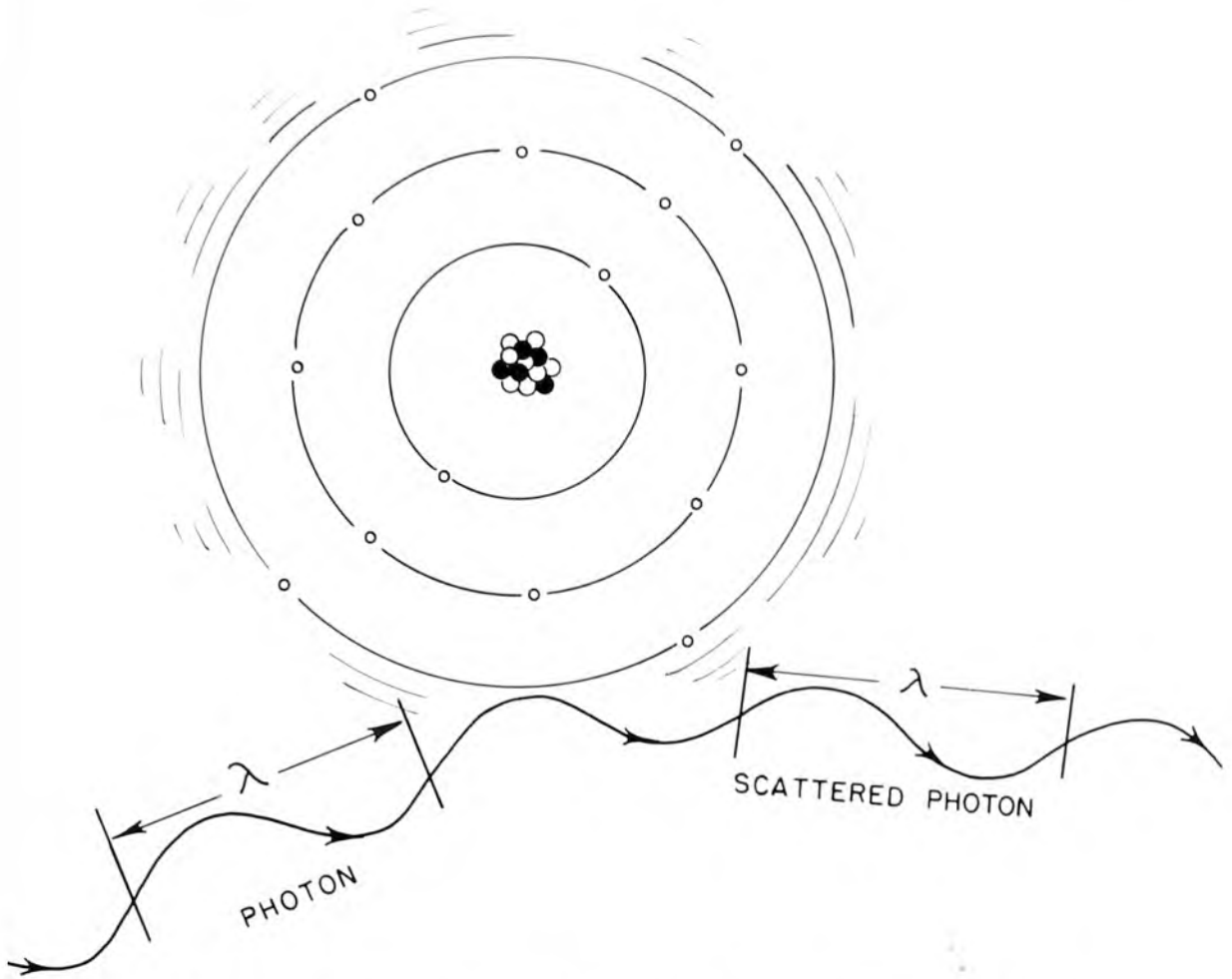


FIG. III-3. Thomson, or classical or coherent scattering of x-rays.

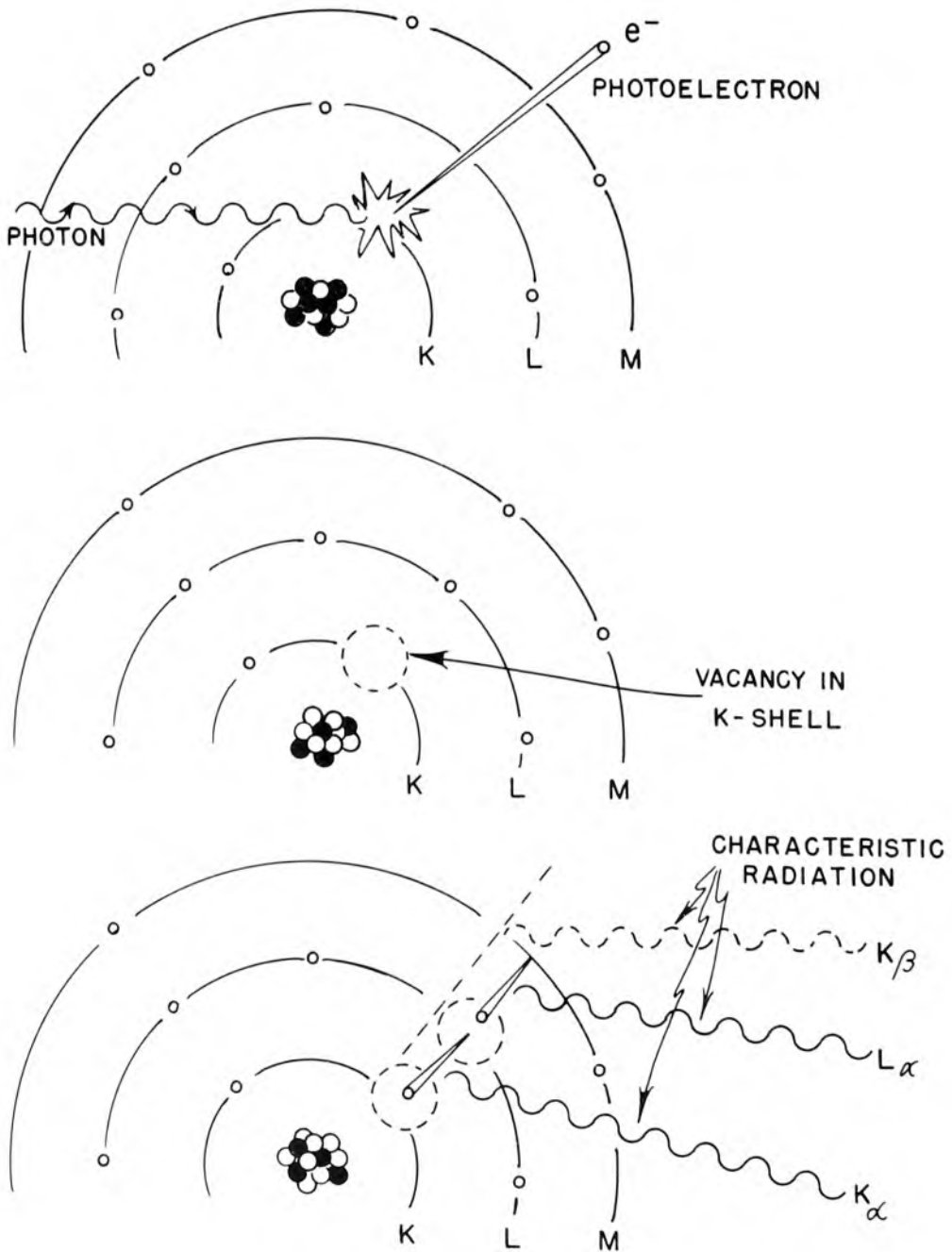
photon from its original direction, without loss of energy to the atom (Fig. III-3). Coherent scattering (Thomson scattering) is also referred to as classical scattering because it can be completely explained on the basis of the classical theory of electromagnetic radiation, which does not embody the corpuscular nature of x-radiation. In this form of interaction the x-ray wave transfers energy to the atom, which is thereby set into vibration and re-emits electromagnetic radiation in phase and equal in energy with the incident radiation (therefore called "coherent" radiation) but deflected from its original direction. This form of re-emission of radiation is very similar to the emission of radio waves by an antenna in which the electrons are set in vibrational motion and emit electromagnetic radiation. Coherent scattering can take place only if the wavelength of the electromagnetic radiation is of the same order of magnitude as the atomic dimensions. Since the diameter of an atom is of the order of 10^{-8} cm, as shown in Chapter I, coherent scattering takes place only for x-ray photons with an energy of the order of a few kiloelectron volts, and is consequently unimportant in diagnostic roentgenology.

It should be noted that the manifestations that establish the wave nature of x-rays, such as reflection, refraction, diffraction, and polarization, are due to coherent scattering. All other forms of interaction of x-rays with matter require the use of the corpuscular concept of electromagnetic radiations.

Interaction of X-Rays with Electrons

Photoelectric Effect. The photoelectric effect consists of the interaction of an x-ray photon with an electron tightly bound in an atom and is usually

FIG. III-4. Photoelectric effect.



accompanied by the emission of an x-ray photon characteristic of the absorber (Fig. III-4). This interaction results in the absorption of the photon, in the sense that all of its energy is transferred to the electron and the photon ceases to exist as such. The energy hn transferred from the photon to the electron is divided into two parts: (1) the energy W_0 required to overcome the binding energy of the electron and to free it from its shell, and (2) the remaining energy E_{kin} , which is carried away by the ejected electron in the form of kinetic energy. This transfer of energy can be described by the equation

$$hn = E_{\text{kin}} + W_0, \quad (7)$$

where h is Planck's constant and n is the frequency of the x-radiation. Eventually, the kinetic energy of the electron is dissipated in matter, usually away from the atom where the photoelectric effect took place.

A photoelectric interaction can take place in a given atomic shell only if the energy of the incident photon is sufficient to overcome the binding energy of the electron in the shell under consideration. The removal of the electron from its atomic shell by photoelectric effect results in the creation of a vacancy in the shell. This vacancy is filled in a very short period of time by an electron falling into it usually from the next shell. In turn, the newly created vacancy in the following shell is replenished from the next shell, and so on (see Fig. III-4). This process is identical in all points to the replenishment of an electron shell vacancy created by the ejection of an electron by electron collision, as described in Chapter II. The cascade-type replenishment of electronic shells following a photoelectric interaction results in the emission of the x-radiation characteristic (sometimes called fluorescent radiation) of the shell and atom under consideration.

The probability for an impinging photon to undergo photoelectric interaction with an absorber depends on the energy of the photon and on the atomic composition of the absorber. Photoelectric interaction occurs with a particularly high probability when the energy of the impinging photon is just sufficient to eject an electron from the shell in which the interaction takes place. A graphic representation of the probability of the photoelectric effect to occur in various absorbers as a function of x-ray photon energy exhibits a series of discontinuities corresponding to the binding energies of the electronic shells of the atoms of the absorber (Fig. III-5).

The probability for a photoelectric interaction to occur also varies with the following three variables: (1) It varies with $(hn)^{-N}$ (except in the vicinity of an orbital absorption edge), where hn is the interacting photon energy and N is a number that changes slowly with the atomic number Z of the absorber and with photon energy. In the diagnostic energy range, and for low- Z absorbers, N is equal to about 3 (Ref. 1). (2) The probability, *per electron*, is approximately proportional to Z^3 . Since an atom contains Z electrons, the photoelectric effect *per atom* is proportional to Z^4 . (3) The

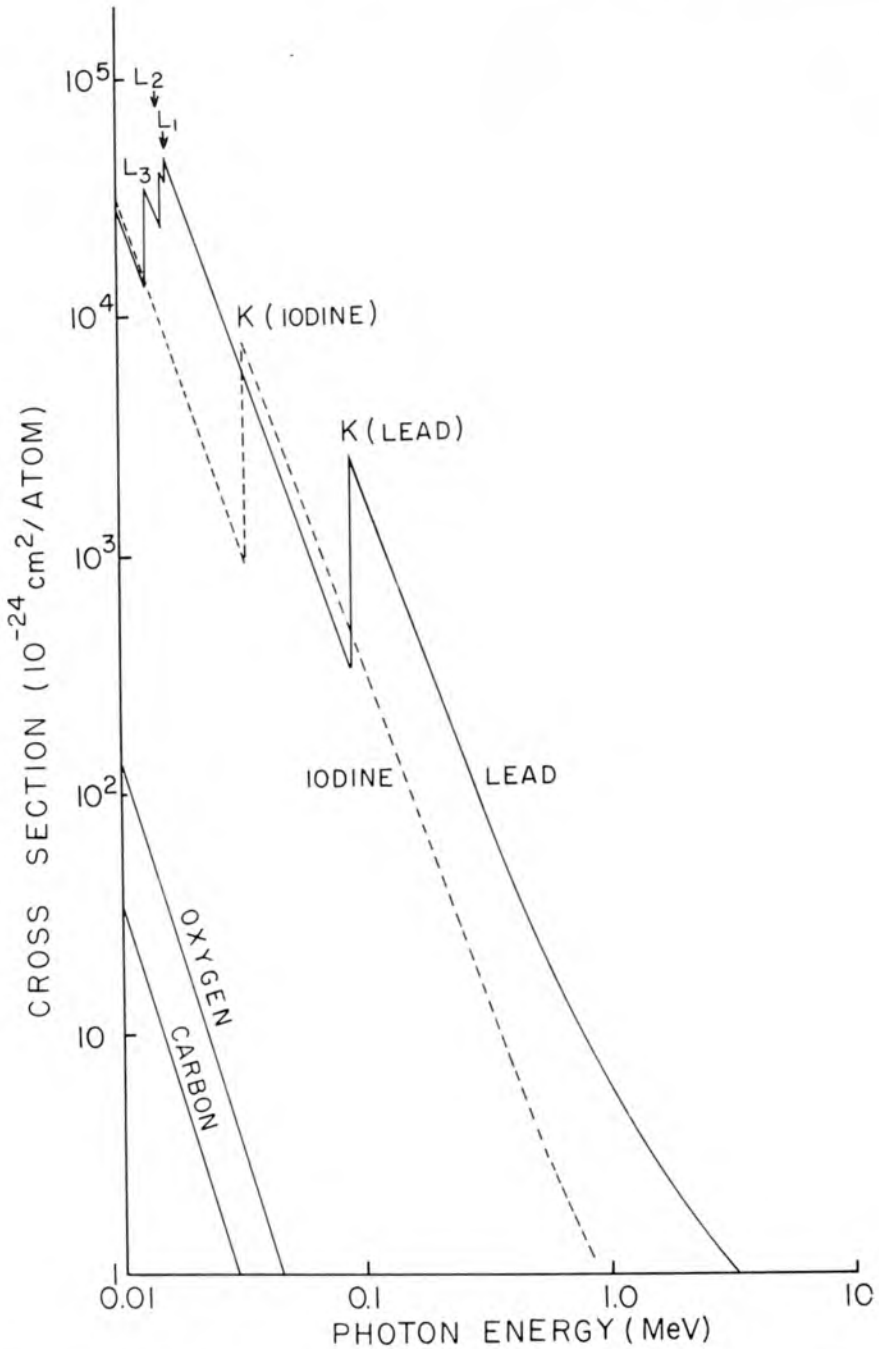


FIG. III-5. Photoelectric cross sections for carbon, oxygen, iodine, and lead. (For a definition of cross section see footnote to page 84.)

probability for a photoelectric interaction to occur is greater in a tightly bound shell than in a shell with a lower binding energy. With photons carrying sufficient energy to dislodge an electron from the K shell of an atom, approximately 80% of the photoelectric interactions take place in that shell (Ref. 1).

It is apparent from the above that the photoelectric effect occurs with

high probability for low energy photons and in high atomic-number elements.

A photoelectric interaction is usually accompanied by the emission of x-rays characteristic of the absorbing medium. If the atomic number of the absorber is low, the energy of the characteristic radiation is also low, and the photon thus emitted is usually absorbed in the immediate vicinity of the absorbing atom. On the other hand, if the atomic number of the absorber is high, the energy of the characteristic radiation is also high and these photons may travel to great distances away from the original absorbing atom.

The direction of travel of the ejected electron (photoelectron) with respect to that of a photon undergoing a photoelectric interaction depends on the energy carried by the electron. If the energy of the photoelectron is low, then it is emitted predominantly at right angles with respect to the direction of the incident photon. As the energy carried by the electron increases, it tends to be emitted at smaller angles with respect to the photon.

3 **Auger Effect and Fluorescence Yield.** The energy expended by a photon undergoing a photoelectric interaction in dislodging the photoelectron from its shell is not always emitted in the form of characteristic radiation photons. Instead, this energy may be utilized in ejecting an electron from a shell of lower binding energy. Usually, if a photoelectric interaction occurs in the K-shell of an atom, the vacancy in that shell is filled by an L electron, and the energy thus available, which is equal to the difference between the binding energies of the K- and L-shells is emitted as a photon. Sometimes, this energy may be utilized to dislodge another electron from the L-shell or another shell of lower binding energy. The electron thus ejected from the L-shell and escaping the atom is referred to as an Auger electron. The kinetic energy of such an electron is equal to the difference between the binding energies of the K- and L-shells of the atom under consideration minus the binding energy of the shell from which it originated, the latter being the energy expended to dislodge the Auger electron from its shell. The emission of an Auger electron can be visualized as a photoelectric interaction between the characteristic radiation emitted by an atom and an electron contained in one of the outer shells of the same atom. It should be noted, however, that this picture is not strictly true, in the sense that no characteristic photon is created in such a transition. The Auger effect always competes with the emission of the characteristic radiation.

The ratio of the number of characteristic radiation photons emitted by a given shell to the number of x-ray photons absorbed by photoelectric effect is called the fluorescence yield for the shell under consideration. The fluorescence yield is a number smaller than one because of the competition between characteristic radiation emission and Auger electron emission. Typical values of the fluorescence yield for various elements in the K-shell are shown in Table III-2.

4 **Compton Effect.** The Compton effect consists of the interaction between an x-ray photon and either a free electron or an electron loosely bound in one

TABLE III-2. Fluorescence Yield in the K-Shell

Element	Z	Fluorescence yield ω_K
Sulfur	16	0.049
Calcium	20	0.120
Nickel	28	0.359
Molybdenum	42	0.733
Iodine	53	0.863
Tungsten	74	0.945
Uranium	92	0.963

From Wapstra, Nijgh, and van Lieshout (Ref. 2).

of the outer shells of an atom. In a Compton interaction the law of conservation of momentum does not allow the transfer of the total energy carried by the photon to the electron. (It should be noted that in the case of a photoelectric interaction, total transfer of energy from a photon to an electron is made possible because of transfer of momentum to a third particle, namely, the atom in which the struck electron is bound.) Thus, the Compton interaction consists in the deflection or scattering of the impinging photon from its original direction, with loss of some energy which is gained by the recoiling electron.

The Compton interaction is represented in Fig. III-6. The loss of energy suffered by the interacting photon, which is equal to the energy gained by the electron, is governed by the angle of scattering. The mathematical relationship between these quantities is obtained by an approach identical with that to the study of the behavior of two colliding balls. In both cases, the relationship between the angle of scattering and the amount of energy transferred from one particle to the other is obtained by equating the energy and the momentum of both particles before and after collision. The fundamental difference between the Compton interaction and the collision between a moving and a stationary ball stems from the fact that the balls possess mass, whereas in the case of the Compton interaction the moving photon does not possess mass although it carries both energy and momentum; otherwise, the behavior of both the recoiling electron and the scattered photon is parallel to the situation encountered in the collision of two balls. Thus, if the photon interacts "head-on" with the electron, the photon is "scattered" back in its original direction and the electron is projected forward. In such a collision the photon suffers maximum energy loss. On the other hand, if the collision is of the "glancing" type, very little energy is transferred to the electron, which recoils at right angles from the original direction of the photon; and the scattered photon continues almost in a straight line with its original direction. Between these two extreme cases there is an infinite

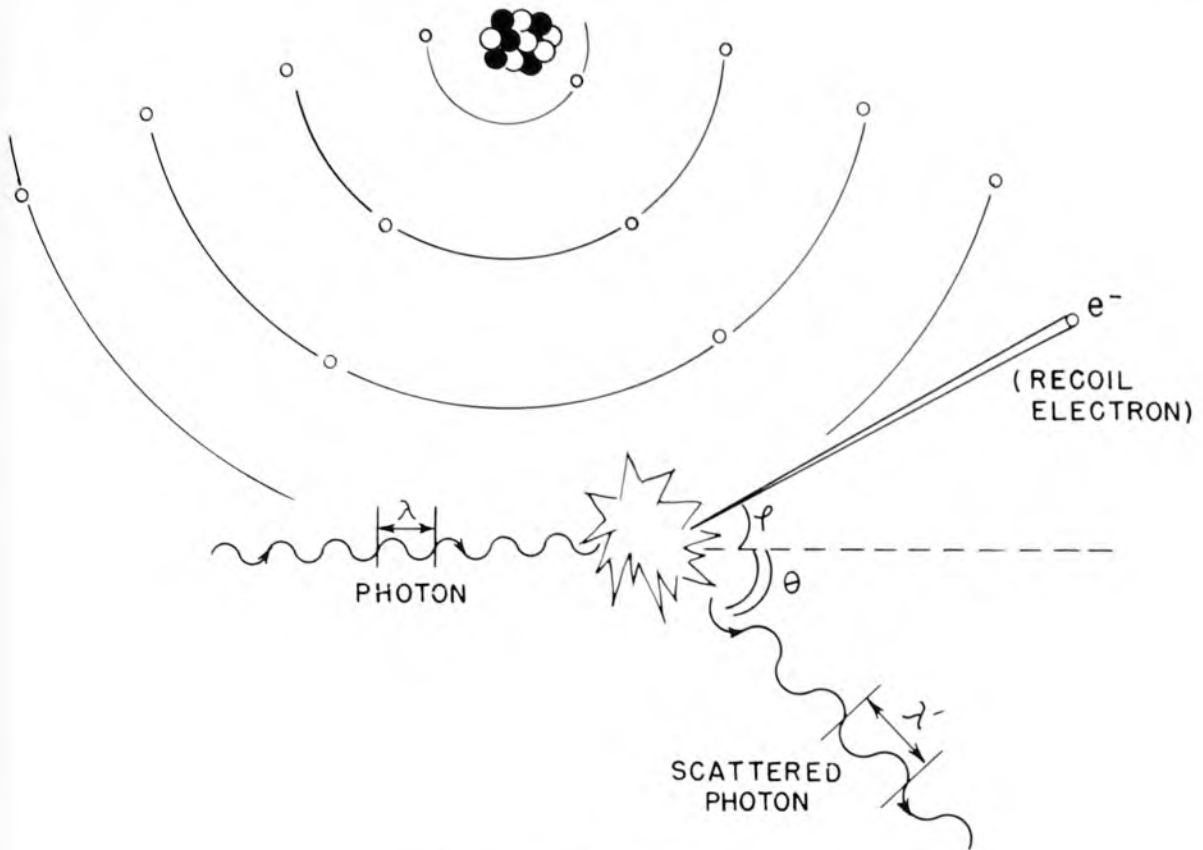


FIG. III-6. Compton effect.

θ angle of photon scattering
 φ angle of recoil electron

number of angles of scattering, each one of them resulting in the recoil of an electron at a well-defined angle and carrying a well-defined energy (Fig. III-7).

The equations relating the variables in a Compton interaction are:

1. Change in wavelength as a function of the angle of scattering:

$$\lambda' - \lambda = \Delta\lambda \text{ (in angstroms)} = 0.0241(1 - \cos \theta) \quad (8)$$

where λ = wavelength of incident photon, λ' = wavelength of scattered photon, and θ = angle of scattering (Fig. III-6).

2. Relation between the angle of scattering and the angle of the recoil electron:

$$\cot \theta = \left(1 + \frac{hn}{0.511} \right) \tan \frac{\varphi}{2} \quad (9)$$

where φ = angle of recoil electron and hn = energy of impinging photon in MeV.

The maximum and minimum transfer of energy from the photon to the electron can be obtained from Equation (8): $\Delta\lambda$ assumes its maximum value

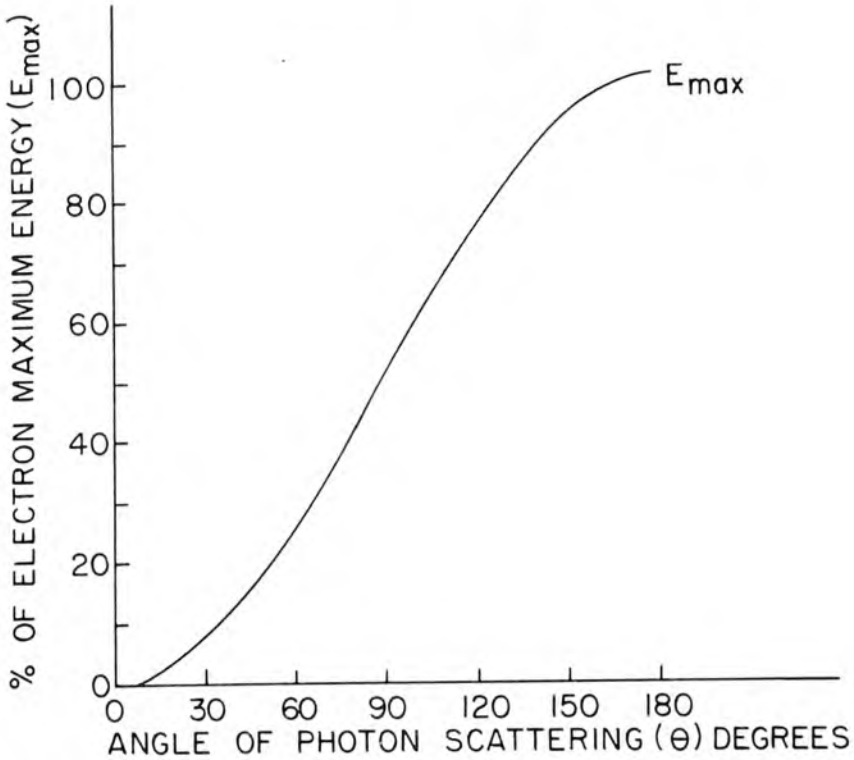


FIG. III-7. Relationship in a Compton interaction between angle of scattering and energy transferred to the electron.

when the expression $(1 - \cos \theta)$ is maximum. Since the cosine of an angle varies only between $+1$ and -1 , $(1 - \cos \theta)$ takes a maximum value when $\cos \theta$ is equal to -1 , which occurs for $\theta = 180$ degrees. Thus, there is maximum transfer of energy from the photon to the electron when the photon is scattered back and the electron travels in the forward direction. Under these circumstances the maximum change in wavelength, $\Delta\lambda$, is equal to $2 \times 0.0241 = 0.0482 \text{ \AA}$. Conversely, the minimum transfer of energy occurs when the expression $(1 - \cos \theta)$ is equal to zero. This occurs when $\cos \theta$ is equal to 1 , or when $\theta = 0$ degrees. Under these circumstances, $\Delta\lambda$ is equal to zero, and therefore there is no transfer of energy from the photon to the electron.

An interesting consequence of Equation (8) is that the maximum change in wavelength, $\Delta\lambda$, experienced by the impinging photon (0.0482 \AA) is independent of the energy of the impinging photon. If the wavelength of the impinging photon is long with respect to 0.0482 \AA ($hn < 50 \text{ keV}$, for example), the maximum change in wavelength represents only a small percentage of the energy carried by the photon, and the recoiling electron receives comparatively little energy. Under these circumstances, the scattered radiation differs only slightly in energy from the impinging photon. On the other hand, with impinging photons of increasing energy (reduced

TABLE III-3. Maximum Energy Transferred in a Compton Interaction

Incident photon energy $h\nu$ (MeV)	Incident photon wavelength λ (\AA)	180° scattered photon energy $h\nu'$ (MeV)	180° scattered photon wavelength λ' (\AA)	$\Delta\lambda = \lambda' - \lambda$ $= 0.048 \text{ \AA}$	Energy of recoil electron (MeV)	% of primary photon energy carried by recoil electron
0.010	1.24	0.0096	1.288	0.048	0.0004	4
0.050	0.250	0.0416	0.298	0.048	0.0084	17
0.100	0.124	0.072	0.172	0.048	0.028	28
0.500	0.0250	0.170	0.073	0.048	0.330	66
1.000	0.0124	0.205	0.0604	0.048	0.795	80
10.000	0.00124	0.252	0.0492	0.048	9.748	97

DIFFERENTIAL CROSS SECTION FOR
THOMSON AND COMPTON SCATTERING
OF X-RAYS, AS A FUNCTION OF THE
ANGLE OF SCATTERING (θ)

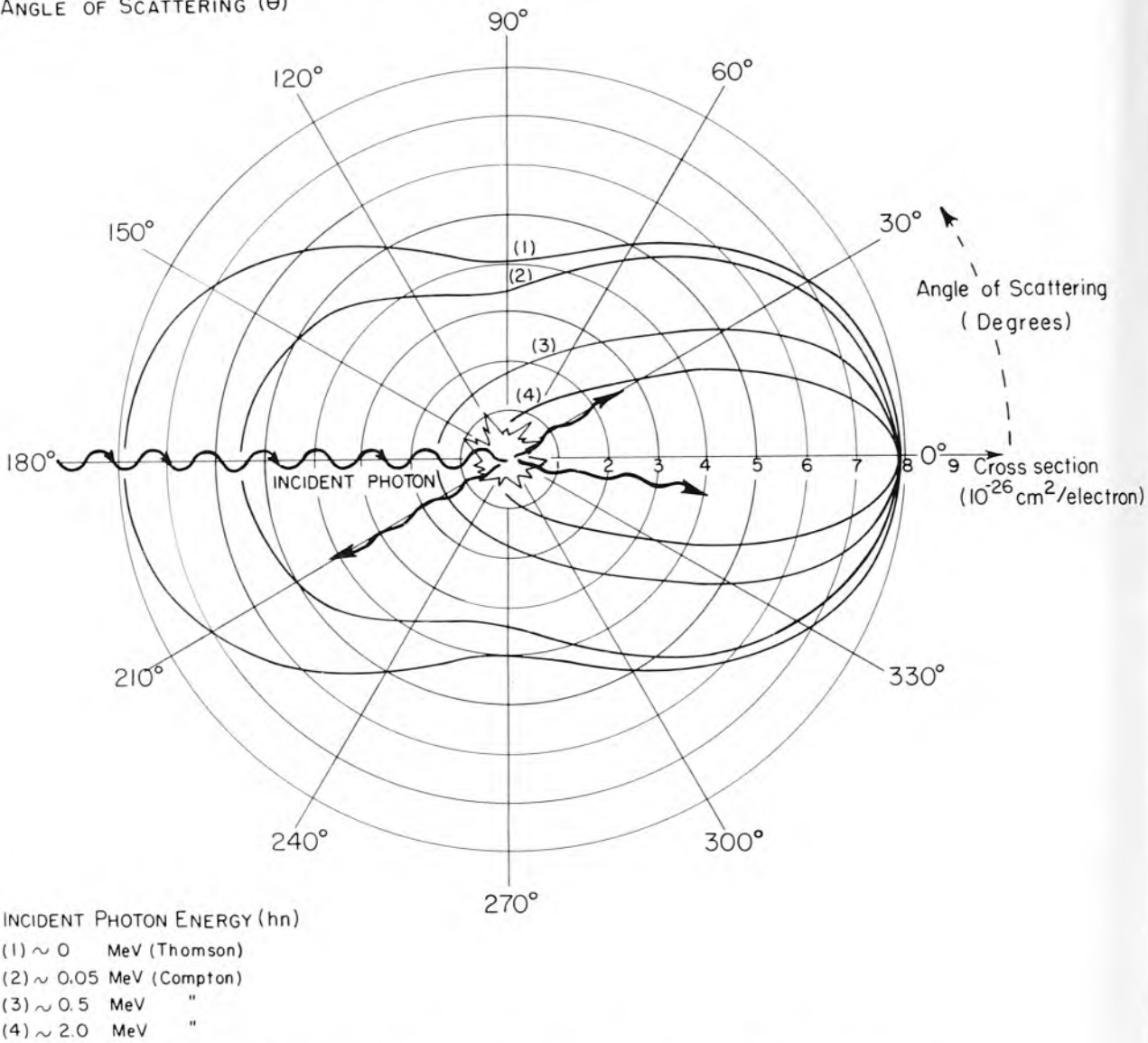


FIG. III-8. Angular distribution of scattered photons.
(Adapted from Davisson, Ref. 4.)

wavelengths), the value 0.0482 becomes proportionally more important; and, at higher energies ($hn > 100$ keV), a large percentage of the energy of the impinging photon is transferred to the recoiling electron. Table III-3 gives the maximum energy that can be transferred by x-ray photons of 10, 50, 100, and 500 keV, and 1 and 10 MeV to the recoil electron by Compton interaction.

As the energy of photons undergoing a Compton interaction increases, the energy of the radiation scattered at large angles approaches constant values, which are 0.511 and 0.260 MeV for 90- and 180-degree scattered photons,

respectively. From Equation (8)

$$\begin{aligned}\Delta\lambda_{90^\circ} &= \lambda' - \lambda = 0.0241 \text{ \AA} \\ \Delta\lambda_{180^\circ} &= \lambda' - \lambda = 0.0482 \text{ \AA}.\end{aligned}$$

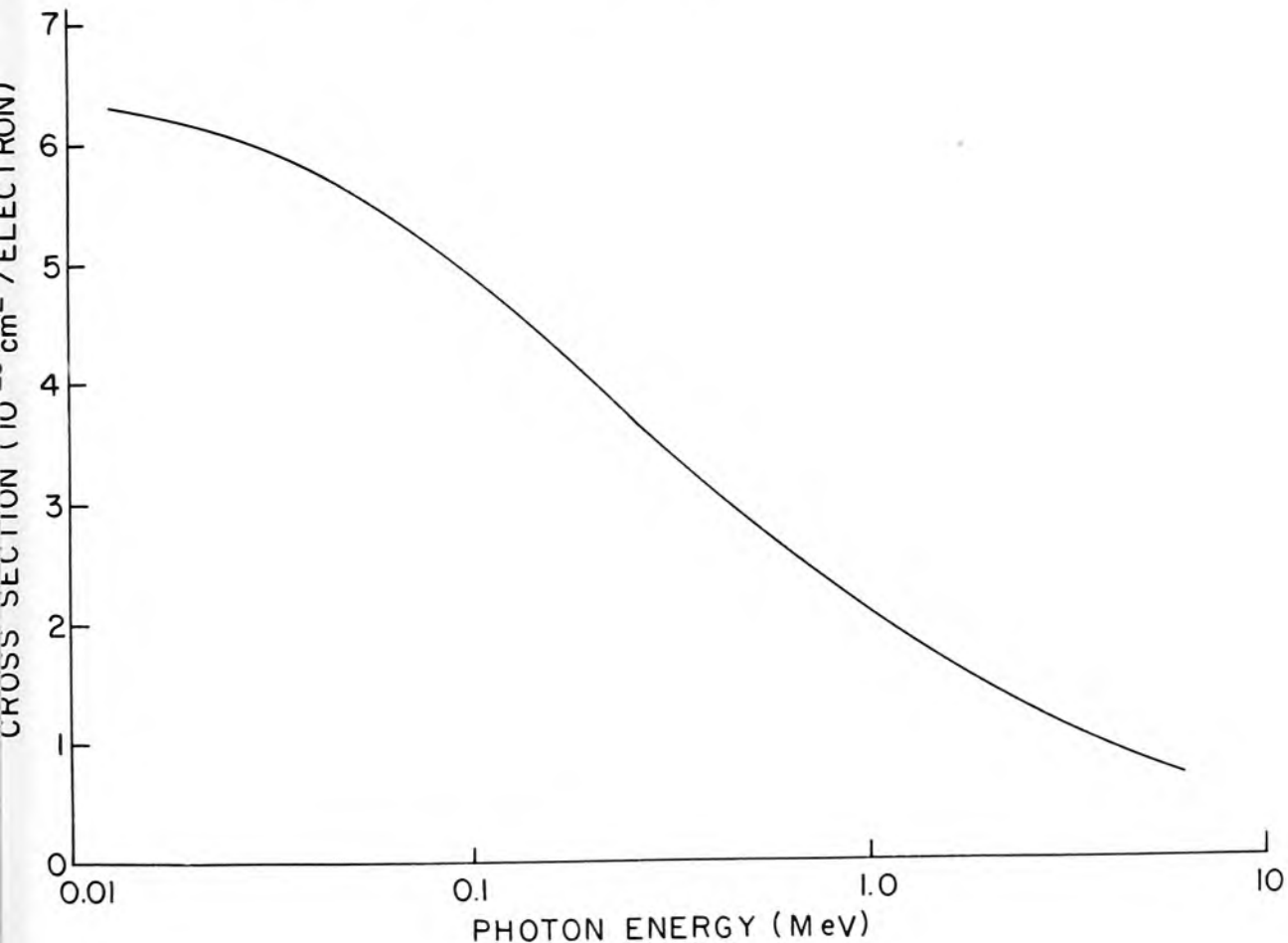
If the wavelength of the impinging photon, λ , decreases with respect to $\Delta\lambda$, then λ' approaches $\Delta\lambda$ and

$$\text{for } \lambda \leq \Delta\lambda \begin{cases} \lambda'_{90^\circ} \rightarrow \Delta\lambda_{90^\circ} = 0.0241 \text{ \AA} \quad (hn = 0.511 \text{ MeV}) \\ \lambda'_{180^\circ} \rightarrow \Delta\lambda_{180^\circ} = 0.0482 \text{ \AA} \quad (hn = 0.260 \text{ MeV}). \end{cases}$$

The angular distribution of scattered photons by Compton effect is given in Fig. III-8. It is apparent that for relatively low energies the photons are scattered almost isotropically, with a minimum number of photons scattered at 90 degrees and with about the same number of photons scattered at 0 and at 180 degrees. As the energy of the photons increases, forward scattering increases.

Because the Compton effect is an interaction involving a free or loosely

FIG. III-9. Electronic cross section for Compton interactions as a function of photon energy. (Adapted from Davisson, Ref. 4.)



bound electron, this interaction depends only on the number of electrons in the absorber and it is unaffected, *per electron*, by the atomic number of the atom containing the electron. Since the number of electrons per atom is equal to the atomic number, the Compton effect *per atom* is proportional to its atomic number. The probability of the Compton effect to occur decreases as the energy of the interacting photon increases. Figure III-9 is a plot of the cross section¹ for Compton interactions per electron as a function of photon energy.

Interaction of X-Ray Photons with Nuclei

5 **Pair and Triplet Production.** Pair production is the conversion of the energy of an x-ray photon into matter. This phenomenon is a form of interaction of x-ray photons with matter because it occurs only in the vicinity of a nucleus. There is an exchange of momentum and of a small amount of energy between the photon and the absorber.

Energy can be converted into matter, as was discussed in Chapter I. Pair production occurs when a high energy photon travels sufficiently close to a nucleus to interact with it. In this interaction the energy of the photon is converted into two electrons—one negatively charged and the other (positron) positively charged. Inasmuch as after the interaction the photon ceases to exist, this interaction is also a form of absorption of x-rays (Fig. III-10).

Pair production can occur only if the energy carried by the photon is sufficiently high for the creation of two electrons. The mass of one electron at rest is equivalent to an energy of approximately 0.511 MeV (see Chapter I, under "Mass-Energy Equivalence"). Thus, the creation of two electrons requires the interacting photon to carry an energy of at least 1.022 MeV. Since a photon does not carry an electrical charge, the creation of a negatively charged electron, by pair production, requires the creation of a positron to counterbalance the charge thus created.

Pair production cannot take place in free space because the presence of a nucleus is necessary for conservation of momentum. Indeed, conservation of momentum is not achieved between the photon and the two electrons created, and part of the momentum carried by the photon is taken up by the nucleus. There is no known mathematical relation between the angles formed by the negative and positive electrons because of the fact that the equation for such a relation includes the momentum acquired by the nucleus, which is unknown.

If the energy of a photon undergoing pair production exceeds the energy

¹ The cross section is a measure of the probability of an interaction between two bodies; it is expressed as the effective area presented by a target. The target may be an electron, a photon, a nucleus, an atom, or some other particle. (In the case of the Compton effect, the target is an electron.) The projectile impinging upon the target may be a particle or, as is the case in the Compton effect, a photon. The cross section is measured in units of area, usually cm^2 ; the unit of cross section is the barn, which is equal to 10^{-24} cm^2 .

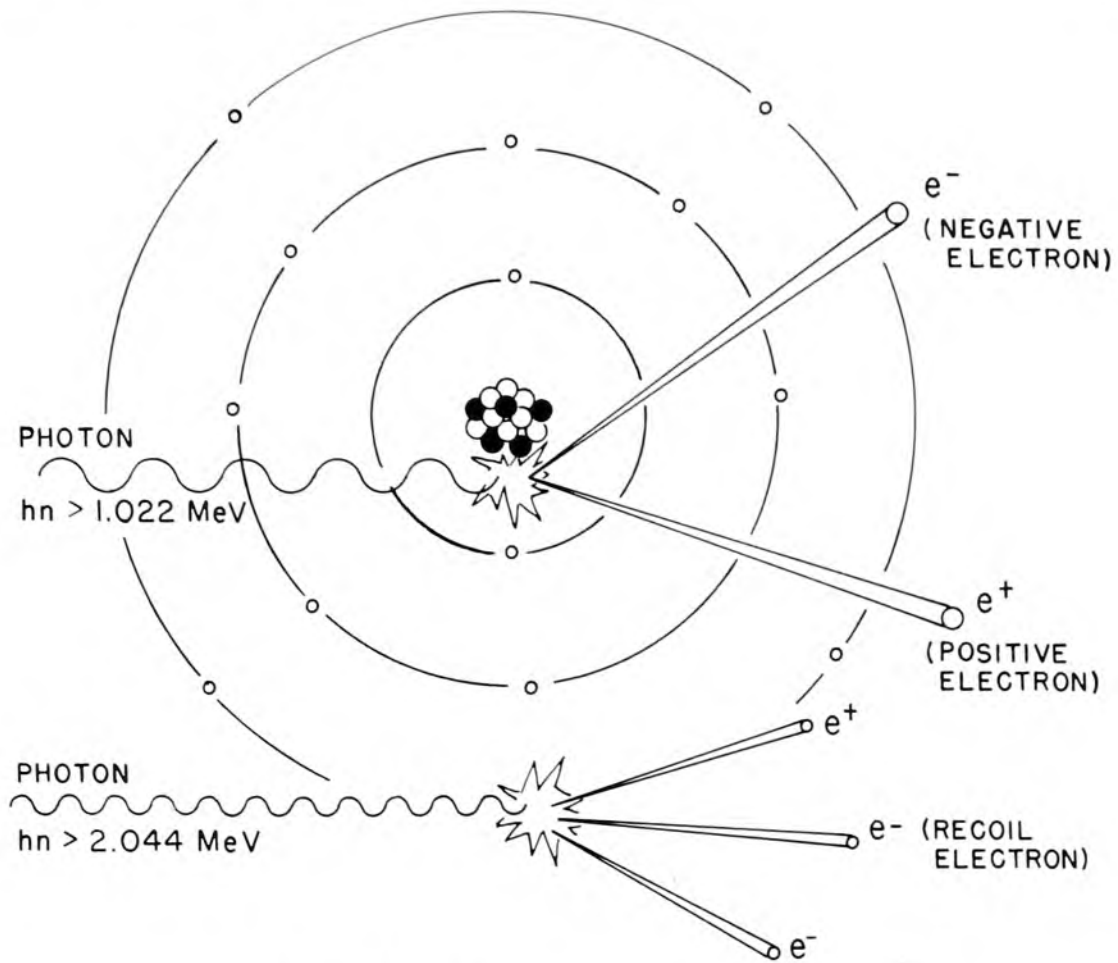


FIG. III-10. Pair and triplet production.

required for the formation of the two electrons, the excess energy is shared by the two new electrons as kinetic energy. The energy acquired by the interacting nucleus is negligibly small because of its large mass compared to that of the electron. For all practical purposes the energy of the interacting photon is divided between the 1.022 MeV required for the formation of the two electrons and their kinetic energies.

The energy threshold for pair production, as stated, is 1.022 MeV, and the probability of this process to occur increases with increasing photon energy, as shown in Fig. III-11.

The conversion of photon energy into matter may also occur in the vicinity of an electron. The process is referred to as triplet production (Fig. III-10) because the interacting electron is also set in motion along with the other two electrons formed in the process. The energy threshold for triplet production is 2.044 MeV—twice as high as for pair production.

In contrast with the photoelectric and Compton effects, the probability of both pair or triplet production to occur increases with increasing photon energy and is proportional to the square of the atomic number of the

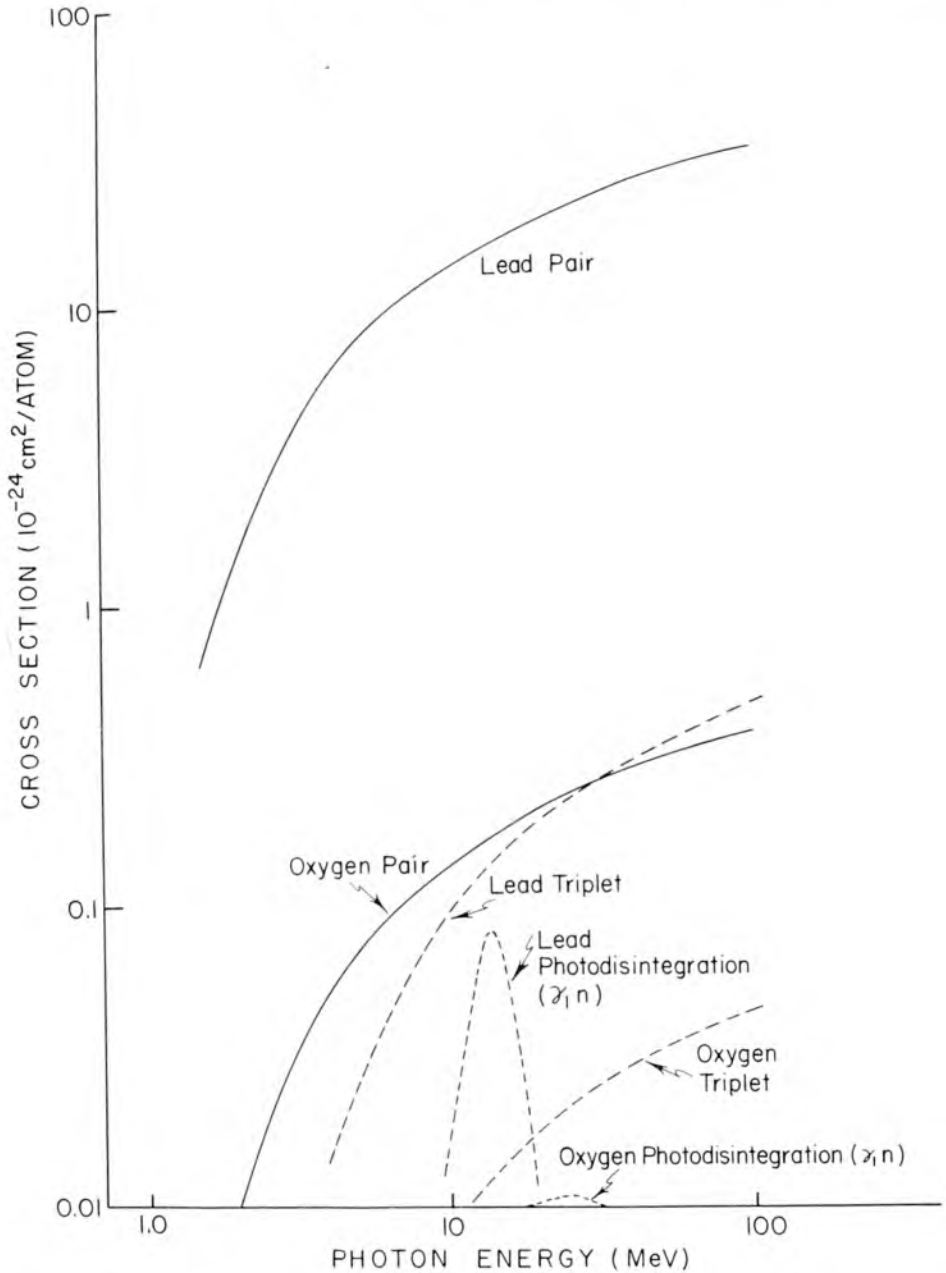



FIG. III-11. Cross sections in oxygen and lead for pair and triplet production and photodisintegration, as a function of photon energy.

absorber (Fig. III-11). Both pair and triplet production are high energy processes that play no role in present-day diagnostic radiology. 

Annihilation Radiation. After the creation of a pair of electrons by either pair or triplet production, the fate of the two electrons is similar only for a short period of time. Both electrons lose their energy, as described in Chapter II, usually by excitation and ionization, until they are brought to rest. The negatively charged electron remains free until it is captured by an atom or a molecule requiring an additional electron. The fate of the posi-

tively charged electron at that point is different from its negative counterpart, because positively charged electrons cannot exist in nature for long periods of time. When brought to rest, the positively charged electron interacts with a negatively charged electron and their masses are annihilated, creating thus two photons at 0.511 MeV each. It should be noted that the annihilation of a positron may occur but with a low probability before it is brought to rest. These two photons, which are called "annihilation radiation," are emitted at 180 degrees one from the other (Fig. III-12). Thus the matter created by the conversion of the energy of a photon into two electrons is reconverted into two photons.

Photodisintegration. Photodisintegration is the interaction between a high energy photon and a nucleus, resulting in the expulsion from the struck nucleus of either a neutron, a proton, an alpha particle, or some other nuclear particle or cluster of particles. Under certain circumstances two particles may be ejected, such as two neutrons, a neutron and a proton, or other combinations. To the extent that in photodisintegration all the energy of the photon is transferred to the nucleus and the photon ceases to exist, photodisintegration is a form of absorption of x-rays (Fig. III-13).

Photodisintegration can take place in a nucleus only if the energy of the photon is sufficiently high to overcome the binding energy holding a nuclear particle in the nucleus. The binding energy of nuclear particles within the nucleus varies with the atomic number of the nucleus; it is of the order of 10 to 15 MeV for light elements (with a few exceptions such as beryllium and deuterium, for which the threshold energies are about 2 and 1.5 MeV) and approximately 7 MeV for heavy elements. Thus, photodisintegration may take place in light elements, with few exceptions, only if the energy of the impinging photon is at least 10 to 15 MeV, and in heavy or high atomic-

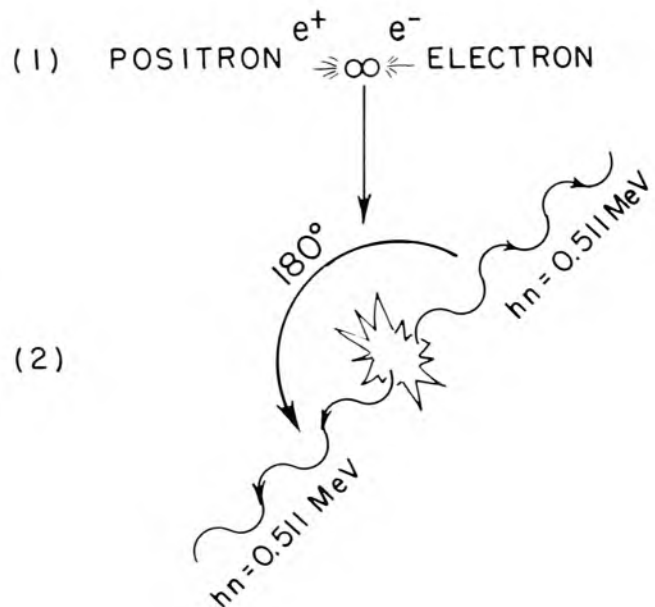


FIG. III-12. Annihilation radiation.

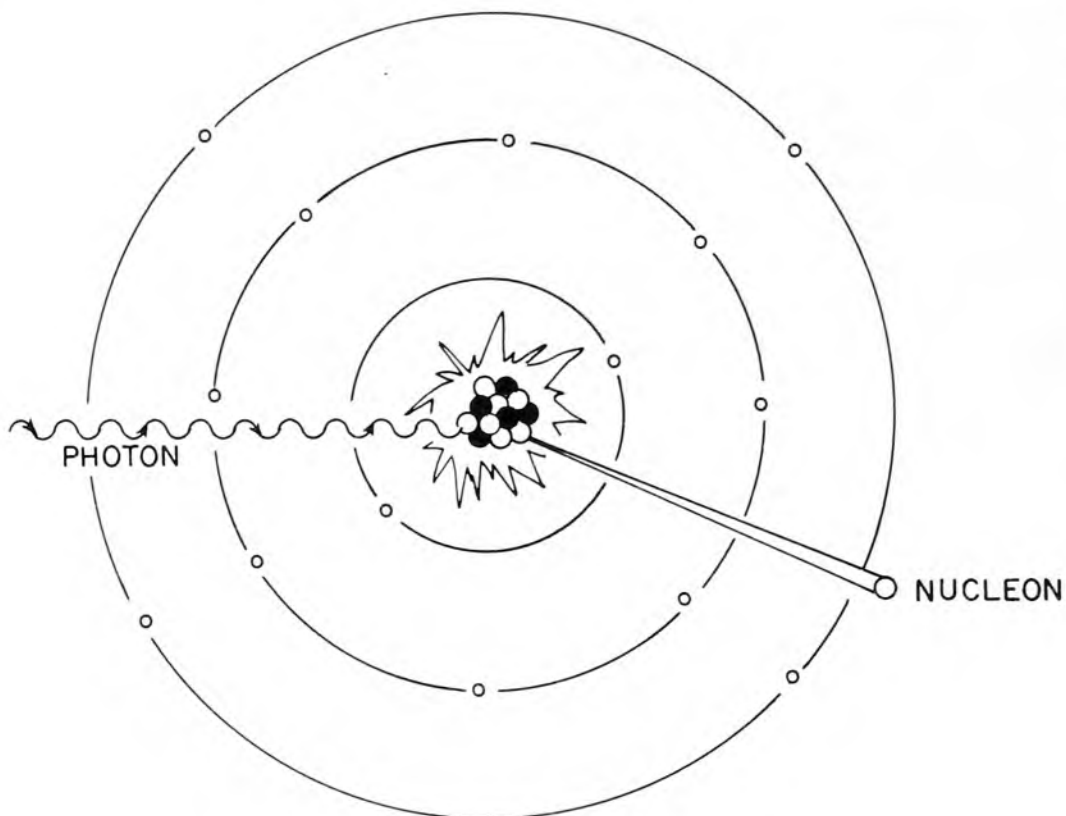


FIG. III-13. Photodisintegration.

number elements with photons carrying an energy of at least 7 MeV. In any given element photodisintegration, therefore, is characterized by a threshold value equal to the minimum energy required to displace a nucleon from the nucleus. As shown in Fig. III-11, the cross section for photodisintegration increases rapidly with the energy of the impinging photon, and decreases after reaching a maximum value.

The interaction is characterized by a resonance energy value. In general, after the ejection of the nucleon, the nucleus is in an unstable state and returns to stability by radioactive decay.

Photodisintegration is a high energy phenomenon that is of no consequence in modern radiology.

Components of the Attenuation Coefficient

In Equation (2), $N = N_0 e^{-\mu x}$, which describes the attenuation of a beam of x-ray photons in matter, the linear attenuation coefficient μ embodies the different forms of interaction of x-rays with matter and can be written as follows:

$$\mu = \sigma_0 + \tau + \sigma + k + \pi, \quad (10)$$

where σ_0 , τ , σ , k , and π are, respectively, the linear attenuation coefficients for Thomson, photoelectric, Compton, pair and triplet, and photodisintegration interactions. The relative contribution of each one of these effects to the attenuation of the beam of x-rays varies with the energy of the interacting photons and with the composition of the absorber. In certain circumstances some of these effects may not contribute at all to the attenuation of the beam. Photons with energies less than 1.022 MeV do not interact either by pair or triplet formation or by photodisintegration. In high atomic-number materials, low energy photons interact mostly by photoelectric absorption, and all the other interactions may become negligible. The relative importance of these different modes of absorption as a function of the energy of the impinging photon in different materials is discussed in Chapter V.

The attenuation coefficient μ expresses the rate of attenuation of x-rays that results from both absorption and scattering of x-rays. The attenuation coefficient μ may be regarded as the sum of a "true" absorption coefficient and a "scatter" absorption coefficient. For the same reason, it is useful to express the Compton coefficient σ as the sum of the "true" Compton absorption coefficient (σ_a), which expresses the energy transferred by the impinging photon to the electron, and the "scatter" coefficient (σ_s), which represents the portion of energy carried by the scattered photon, thus:

$$\sigma = \sigma_a + \sigma_s, \quad (11)$$

where σ is the total Compton coefficient, σ_a the true absorption coefficient, and σ_s the scatter coefficient.

It should be noted that even in interactions resulting in total transfer of the energy of the impinging photon, a large fraction of this energy may escape the absorber. For example, in photoelectric absorption, some of the higher-energy characteristic photons may be lost by the absorber, particularly if the interaction takes place in a high- Z element. Also in pair production, the annihilation radiation may escape the absorber. In general, the energy transferred to particles is dissipated in the absorber, while the energy carried by secondary or scattered photons tends to escape.

The validity of the above statement is limited by a number of exceptions: for example, secondary electrons can easily escape a thin absorber, and low-energy characteristic photons produced in low- Z elements may easily be stopped in the absorber. Table III-4 summarizes the qualitative energy transfers in x-ray photon interactions.

Although five modes of x-ray attenuation were discussed in this chapter, only photoelectric and Compton interactions are important in diagnostic radiology. Indeed, Thomson scattering occurs at energies too low and pair and triplet production and photodisintegration occur at energies too high to be of any consequence in diagnostic radiology. For that reason, in the

TABLE III-4. Qualitative Energy Transfers in X-Ray Photon Interactions

Type of interaction	Fate of impinging photon	Energy transferred to	Characteristic sequelae
Thomson, classical or coherent scattering σ_0	scattered	none	
Photoelectric effect τ	no longer exists	bound electron	emission of characteristic radiation and Auger electrons
Compton effect, absorption σ_a	scattered	free electron	
Compton effect, scatter σ_s			
Pair and triplet production k	no longer exists	electron (1 or 2) and positron	generation of annihilation radiation
Photodisintegration π	no longer exists	nucleon	transmutation of a nucleus, usually to a radioactive form

remainder of this text only photoelectric and Compton interactions between x-rays and matter will be considered.

Compton and Photoelectric Attenuation in Compounds and Mixtures of Elements

The attenuation of x-rays in matter is unaffected by chemical bonds. If either a mixture or a compound of various elements is interposed in the path of a beam of x-rays, the contribution of each element to the attenuation of the beam is identical to that produced by the element if it were present alone in the amount equal to its content in the mixture or the compound.

The calculation of the attenuation of x-rays in a compound or a mixture can be carried out (1) by determining the attenuation of the radiation in each one of the elements contained in the mixture or the compound in the amount equal to the fractional content of that element, and (2) by multiply-

ing the attenuations thus observed with each other. For example, the attenuation of 50 keV x-rays in 10 g/cm² of water (equal to 10 cm of water because the density of water is 1 g/cm³) can be calculated as follows:

1. The composition by weight of water is 89% oxygen and 11% hydrogen. Therefore, 10 g/cm² of water represent 8.9 g/cm² of oxygen and 1.1 g/cm² of hydrogen. The mass attenuation coefficients of 50 keV x-rays in oxygen and hydrogen are (Ref. 3): oxygen, 0.207 cm²/g; hydrogen, 0.335 cm²/g. On the basis of these coefficients, the attenuation of x-rays in 8.9 g/cm² of oxygen and 1.1 g/cm² of hydrogen can be calculated by the formula

$$\frac{N_0}{N} = e^{+\mu x}, \quad (12)$$

where N_0 is the number of x-ray photons impinging upon the absorber, N is the number of x-ray photons transmitted by the absorber, N_0/N is the attenuation of the beam of x-rays, e is the base of natural logarithms, μ is the mass attenuation coefficient expressed in cm²/g, and x is the amount of absorber expressed in g/cm². The application of the above formula² yields the following attenuations:

$$\frac{N_0}{N} \text{ for } 8.9 \text{ g/cm}^2 \text{ of oxygen} = 6.29$$

and
$$\frac{N_0}{N} \text{ for } 1.1 \text{ g/cm}^2 \text{ of hydrogen} = 1.45.$$

2. The attenuation of 50 keV x-rays in 10 g/cm² of water is equal to the product of the attenuation in its components:

$$\frac{N_0}{N} (\text{water}) = \frac{N_0}{N} (\text{oxygen}) \times \frac{N_0}{N} (\text{hydrogen}) = 6.29 \times 1.44 = 9.07.$$

This means that about 90% of the impinging x-ray photons are removed from the beam by 10 cm of water.

Average Electron Density—Effective Atomic Number

The above method for the calculation of the attenuation of x-rays in a mixture or a compound of various elements does not provide an easy method

² It should be noted that Equation (12), $N_0/N = e^{+\mu x}$, is obtained from Equation (2) (pp. 67 and 68), $N/N_0 = e^{-\mu x}$, by taking the reciprocal of both sides of the equation, which yields

$$\frac{N_0}{N} = \frac{1}{e^{-\mu x}} = e^{+\mu x}.$$

Equation $N/N_0 = e^{-\mu x}$ gives the ratio of the number of transmitted photons to the number of incident photons as a function of μ and x , while equation $N_0/N = e^{+\mu x}$ expresses the ratio of the number of incident photons to the number of transmitted photons as a function of μ and x .

of comparison of the attenuation of x-rays in two different compounds, particularly if the compounds are complex. It is sometimes useful to evaluate the attenuation of x-radiation in a mixture or a compound by assuming that they behave as a single element, without evaluating separately the attenuation properties of each one of their component elements.

If it is assumed that only Compton and photoelectric interactions are of importance in this study (see the section, "Components of the Attenuation Coefficient," above), then the mixture or the compound taken as a single element must exhibit Compton (σ) and photoelectric (τ) absorption coefficients identical to the combined Compton and photoelectric absorption coefficients of its components. Both Compton and photoelectric effects consist of the interaction of photons with electrons. Both of these effects, therefore, depend on the number of electrons encountered by the impinging photons in an absorber. The two effects differ, however, in that Compton interactions are independent of the binding energy of the electrons involved and are therefore independent of the atomic number of the element contributing the electrons, while photoelectric interactions are strongly dependent on the binding energy of the interacting electrons.

The Compton contribution to the attenuation properties of a mixture or a compound of elements is solely determined by the average electron density of the absorber. The electron density can be expressed either as the number of electrons per gram of absorber (el/g) or as the number of electrons per centimeter of absorber (el/cm), depending on whether the amount of absorber interposed in the beam is expressed in grams per square centimeter or in terms of centimeters.

The photoelectric effect, per electron, is approximately proportional to the third power of the atomic number of the nucleus binding the interacting electron (Z^3). Thus, the photoelectric attenuation in a mixture or a compound of elements depends both on the average electron density and on the atomic number of the component elements. Mayneord (Ref. 5) has defined the concept of "effective atomic number" for a compound or a mixture. By definition, the effective atomic number of a mixture or a compound of elements is the atomic number of an element which exhibits a photoelectric attenuation identical to the combined photoelectric attenuations of the elements in the mixture or the compound. The effective atomic number (Z_{eff}) can be determined by the formula

$$Z_{\text{eff}} = \sqrt[2.94]{a_1 Z_1^{2.94} + a_2 Z_2^{2.94} + a_3 Z_3^{2.94} + \dots}, \quad (13)$$

where a_1 , a_2 , and a_3 are the electron fractions bound in elements Z_1 , Z_2 , and Z_3 , respectively, of the mixture or the compound.

Thus, the average electron density and the effective atomic number determine respectively the Compton and the photoelectric attenuations of a mixture or a compound of several elements. The application of the above two

factors to the calculation of the attenuation of x-rays in a compound is demonstrated in the following example which consists, as in the previous section, of the determination of the attenuation of 50 keV x-rays in 10 g/cm² of water:

1. The composition by weight of water is 89% oxygen and 11% hydrogen.

2. The electron densities of these elements are: oxygen, 3.012×10^{23} el/g; hydrogen, 5.997×10^{23} el/g (Ref. 3). (The electron density of an element is determined by dividing the Avogadro number by the atomic weight of the element under consideration and by multiplying the ratio thus obtained by the atomic number of the element.)

3. The electronic contributions of oxygen and hydrogen to one gram of water are:

$$\text{for oxygen: } 3.012 \times 10^{23} \times 0.89 = 2.681 \times 10^{23}$$

$$\text{for hydrogen: } 5.997 \times 10^{23} \times 0.11 = 0.659 \times 10^{23}$$

which by addition result in an electronic density for water of 3.340×10^{23} el/g. The fractional contributions of these electrons are:

$$\text{for oxygen: } \frac{2.681}{3.340} = 0.80,$$

$$\text{for hydrogen: } \frac{0.659}{3.340} = 0.20.$$

It should be noted that 11% per weight of hydrogen contributes 20% of the electrons in water because of the greater electron density in hydrogen than in oxygen.

4. The effective atomic number of water is obtained by substituting in Equation (13) as follows:

$$Z_{\text{eff H}_2\text{O}} = \sqrt[2.94]{0.80 \cdot Z_{\text{O}}^{2.94} + 0.20 \cdot Z_{\text{H}}^{2.94}} = 7.42,$$

where Z_{O} and Z_{H} are the atomic numbers of oxygen and hydrogen, respectively.

Thus, from the standpoint of the Compton and photoelectric attenuations of x-rays, water behaves as a substance with an electron density of 3.340×10^{23} el/g and with an effective atomic number of 7.42.

Knowledge of the electron density and of the effective atomic number of a substance allows the determination, either by calculation or by extrapolation from experimental values, of both the Compton and the photoelectric absorption coefficients of this substance.

In general, the x-ray absorption coefficients of a complex substance are derived by extrapolation from the listed values of these coefficients for the element with an atomic number nearest to the effective atomic number of the complex substance. For example, the Compton ($\sigma_{\text{H}_2\text{O}}$) and photoelectric

($\tau_{\text{H}_2\text{O}}$) mass absorption coefficients for 50 keV x-rays in water can be extrapolated from the listed values of these coefficients for nitrogen, as follows:

1. Nitrogen has an atomic number 7, with an electron density of 3.011×10^{23} el/g. Water has an effective atomic number of 7.42, with an electron density of 3.340×10^{23} el/g.

2. The Compton and photoelectric mass attenuation coefficients for 50 keV x-rays in nitrogen are (Ref. 3):

$$\begin{aligned} \text{Compton: } \sigma_{\text{N}} &= 0.178 \text{ cm}^2/\text{g}; \\ \text{photoelectric: } \tau_{\text{N}} &= 0.016 \text{ cm}^2/\text{g}. \end{aligned}$$

3. The Compton attenuation is proportional to the number of electrons encountered by the photons; therefore the Compton mass absorption coefficient in water ($\sigma_{\text{H}_2\text{O}}$) can be extrapolated from the Compton mass absorption coefficient in nitrogen by the formula

$$\begin{aligned} \sigma_{\text{H}_2\text{O}} &= \sigma_{\text{N}} \times \frac{\text{el. den.}_{\text{H}_2\text{O}}}{\text{el. den.}_{\text{N}}} = 0.178 \text{ cm}^2/\text{g} \times \frac{3.340 \times 10^{23}}{3.011 \times 10^{23}}; \\ \sigma_{\text{H}_2\text{O}} &= 0.198 \text{ cm}^2/\text{g}. \end{aligned}$$

4. The photoelectric attenuation is proportional (a) to the third power of the atomic number of the element binding the interacting electrons and (b) to the number of electrons encountered by the x-ray photons. The photoelectric absorption coefficient in water can be extrapolated from the photoelectric absorption coefficient in nitrogen by multiplying the latter (a) by the third power of the ratio of the effective atomic number of water to the atomic number of nitrogen, and (b) by the ratio of the electron density of water to the electron density of nitrogen, as follows:

$$\begin{aligned} \tau_{\text{H}_2\text{O}} &= \tau_{\text{N}} \times \left(\frac{Z_{\text{eff H}_2\text{O}}}{Z_{\text{N}}} \right)^3 \times \frac{\text{el. den.}_{\text{H}_2\text{O}}}{\text{el. den.}_{\text{N}}} \\ &= 0.016 \text{ cm}^2/\text{g} \times \left(\frac{7.42}{7} \right)^3 \times \frac{3.340 \times 10^{23}}{3.011 \times 10^{23}}; \\ \tau_{\text{H}_2\text{O}} &= 0.021 \text{ cm}^2/\text{g}. \end{aligned}$$

The total mass absorption coefficient of 50 keV x-rays in water, assuming only Compton and photoelectric attenuations, is equal to:

$$\mu_{\text{H}_2\text{O}} = \sigma_{\text{H}_2\text{O}} + \tau_{\text{H}_2\text{O}} = 0.198 \text{ cm}^2/\text{g} + 0.021 \text{ cm}^2/\text{g} = 0.219 \text{ cm}^2/\text{g}.$$

The attenuation of 50 keV x-rays in 10 cm of water is given by

$$\frac{N_0}{N} = e^{+0.219 \times 10} = 8.93.$$

This figure is equal, within 1.5%, to that obtained on p. 91, in item 2.

REFERENCES

1. HINE, G. J., and BROWNELL, G. L., eds.: *Radiation Dosimetry*. New York, Academic Press, 1956.
2. WAPSTRA, A. H., NIJGH, G. J., and VAN LIESHOUT, R.: *Nuclear Spectroscopy Tables*. Amsterdam, North-Holland Publishing Co., 1959.
3. JOHNS, H. E.: *The Physics of Radiology*, 2nd ed. Springfield, Ill., Thomas, 1961.
4. DAVISSON, C. M.: "Interaction of Gamma-Radiation with Matter," in *Beta- and Gamma-Ray Spectroscopy*, ed. by Siegbahn, K. New York, Interscience, 1955.
5. MAYNEORD, W. V.: The significance of the röntgen. *Acta Int. Union against Cancer* 2:271, 1937.

(IV)

X-RAY APPARATUS

X-rays are generated when moving electrons are decelerated in matter. Therefore, apparatus designed for the generation of x-rays embody the following elements: (1) a source of electrons; (2) a system capable of accelerating electrons; and (3) a structure, usually called a target, in which the energy of the accelerated electrons is converted into x-radiation.

Electrons cannot be readily accelerated if they are trapped in matter. Consequently, in an x-ray apparatus the space between the source of the electrons and the target must be either evacuated or must contain a gas at a sufficiently low pressure to minimize the probability of collisions between the accelerated electrons and the gas molecules. To achieve this purpose, both the source of the electrons and the target are usually contained within an envelope that is either completely or almost completely evacuated. The structure containing the source of electrons and the target is called the x-ray tube.

The acceleration of electrons may be achieved by a variety of different methods. Electrons can be accelerated in a circular orbit by means of a rapidly varying magnetic field (Ref. 1). This method is employed in betatrons, which are widely used in radiation therapy. Another method of acceleration consists in allowing a packet of electrons to ride the crest of a traveling radio-frequency electromagnetic wave (Ref. 1). (This method of gaining acceleration is comparable to that achieved in the sport of surfboarding, where velocity is gained by riding a water wave.) The method is used in traveling-wave linear accelerators, which produce the high-energy x-rays mostly applied in radiation therapy.

In diagnostic radiology electrons are accelerated almost exclusively by means of an electric field established between the source of the electrons and the target in such a fashion that the source of the electrons is negatively charged (cathode) and the target (anode) is positively charged with respect to the source of the electrons. The negatively charged electrons are repelled by the cathode and attracted by the target, thus acquiring an energy that is

determined by the magnitude of the electric field between the two electrodes. The source of electricity that provides the acceleration of the electrons in the x-ray tube is commonly called the generator.

In addition to the two basic components of x-ray apparatus—x-ray tube and generator—a large number of other components are also included for the purpose of controlling and measuring the radiation produced.

HISTORY OF X-RAY TUBES

The first tube used by Röntgen for the generation of x-rays consisted of a partially evacuated glass envelope that contained two electrodes maintained at a high difference of potential. The electrons required for the production of x-rays in such a tube were generated as follows: The rarefied gas in the envelope was partially ionized. The positive ions, attracted by the cathode, struck the cathode with sufficient energy to release electrons from the metal of the cathode. The electrons released by the cathode were accelerated by the electric field between the two electrodes. After traveling in a nearly straight line, the accelerated electrons struck the glass of the tube opposite the cathode, as shown in Fig. (0-3). The deceleration of the electrons in the glass of the tube produced x-rays. Thus, in the first x-ray tube the electrons, produced by ionic bombardment of the cathode, were accelerated by an electric field, and the target of the tube was that portion of the glass envelope which was struck by the accelerated electrons, or cathode rays.

The usefulness of x-radiation in clinical diagnostic applications became apparent a short time after its discovery, and attempts were made to improve the design of Röntgen's original tube. The glass target of the first x-ray tube was quite large in area and did not lend itself to high resolution radiology. One of the early steps in the improvement of the x-ray tube was the reduction of the target size. This was accomplished by focusing the beam of electrons at a metallic target introduced into the glass envelope. Effective focusing of the electron beam can be achieved by giving the cathode a concave surface facing the target of the x-ray tube. Such a surface shapes the electric field that accelerates the electrons and concentrates the lines of force of this field on a small area of the anode (target).

The material used for the construction of the target must fulfill three criteria for the efficient production of x-rays: (1) It must have a high atomic number; (2) it must be a good conductor of heat; and (3) it must have a high melting point. The target must have a high atomic number because, as shown in Chapter II, the efficiency of x-ray production is proportional to the atomic number of the material in which the electrons are decelerated. Thus, from the standpoint of efficiency, the target material should have the highest atomic number possible. Unfortunately, as shown in Chapter II, the production of x-rays is an inefficient process, most of the energy of the decelerated electrons in an x-ray tube being converted into heat, and the generation of a considerable amount of heat in the target results in im-

posing conditions (2) and (3) upon the target material—it must have a high melting point and it must be a good heat conductor to dissipate the heat.

As a rule, the selection of the target material results from a compromise between the above criteria. Early in the history of the development of x-ray tubes, the conclusion was reached that the most suitable material for an x-ray tube target was tungsten, although platinum was also used in early tubes. The tungsten was imbedded in copper to provide better dissipation of heat. Tungsten has a relatively high atomic number (74) and high melting and boiling points (3370° C and 5900° C, respectively) (Ref. 2). Because copper has a higher heat conductivity than tungsten, the dissipation of heat is sometimes achieved by means of a heavy copper block in which the tungsten target is imbedded (Fig. IV-1).

Gas x-ray tubes were used extensively in diagnostic roentgenology in spite of certain serious drawbacks, the most important of which were: (1) unreliable tube operation due to variation of the partial pressure of the gas, which modified the character of the x-radiation emitted; and (2) the relatively low intensity of the x-radiation they generated. The first deficiency could be partially corrected by controlling the gas pressure with various gas regulators. With these devices gas could be released according to need, and the early radiologists were forever adjusting the gas pressure in their x-ray tubes to obtain reproducible results in their examinations (Fig. IV-2). The capacity of these tubes was limited by (1) the low intensity of the cathode rays produced by ionic bombardment and (2) the cooling of the target.

In 1913, W. D. Coolidge developed an x-ray tube, the basic design of which, with minor modifications, is still used in diagnostic radiology (Fig. IV-3). Coolidge's improvement consisted in replacing the unreliable electron source of the early gas tubes by a hot filament. Hot metals emit electrons. This phenomenon, called the Edison effect, results from subjecting electrons to sufficient thermal agitation to overcome their binding energy and allow them to escape the atoms in which they are bound. The number of electrons thus "boiled off" depends on the nature of the heated metal and on its temperature. In a Coolidge x-ray tube, the metallic filament is usually made of tungsten and is heated by the passage of an electric current. It should be noted that a source of electrons can be produced by heating a metal by any method; however, an electric current passing through a filament seems to be the most convenient solution to this problem.

The Coolidge tube is completely evacuated because there is no need for gas in the tube; the presence of gas molecules is only a hindrance in the operation of a tube where electrons are supplied by a hot filament. It should be noted, however, that the quality of the vacuum in a Coolidge tube is not very critical. Indeed, the high velocity electrons have a relatively low probability for collision with gas molecules, and a glow-type discharge occurs in a partially evacuated tube only for relatively high gas pressures.

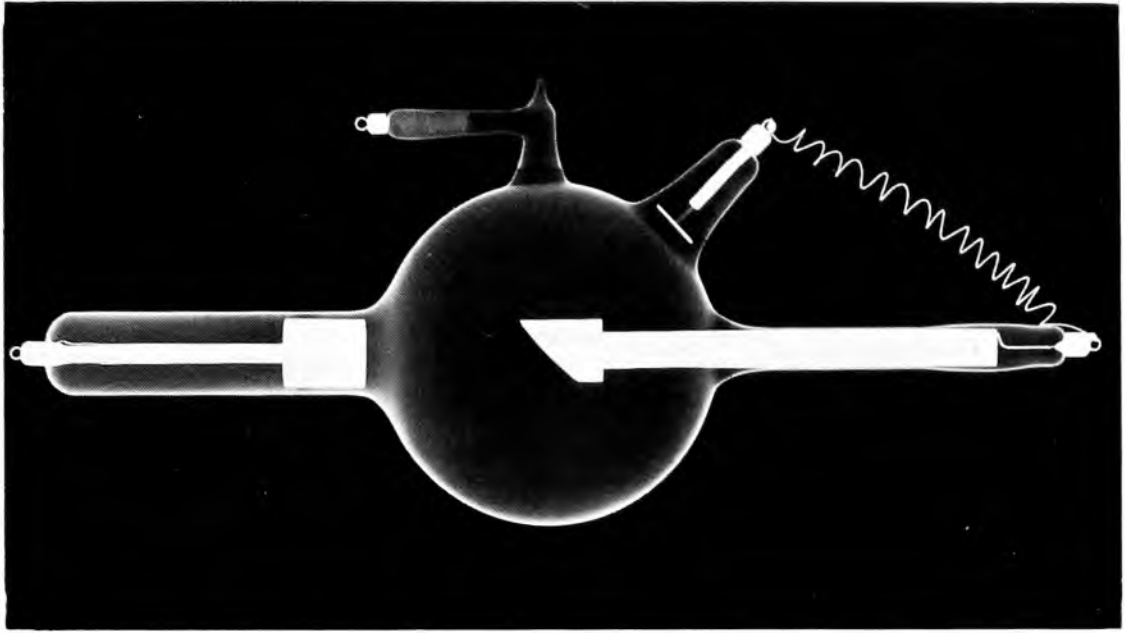


FIG. IV-1. Radiograph of an early gas x-ray tube.



FIG. IV-2. Picture of an early x-ray tube with gas pressure control device.
(Courtesy of General Electric Company.)

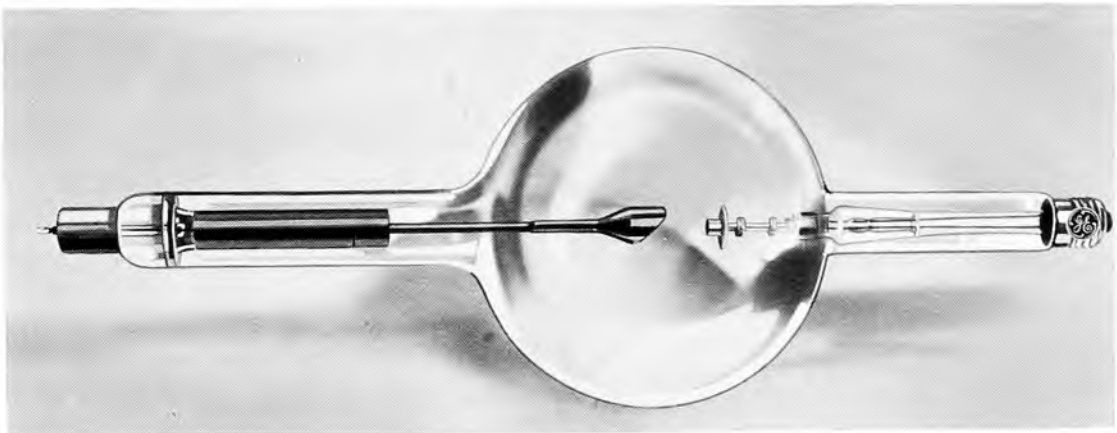


FIG. IV-3. Early model of Coolidge tube.
(Courtesy of General Electric Company.)

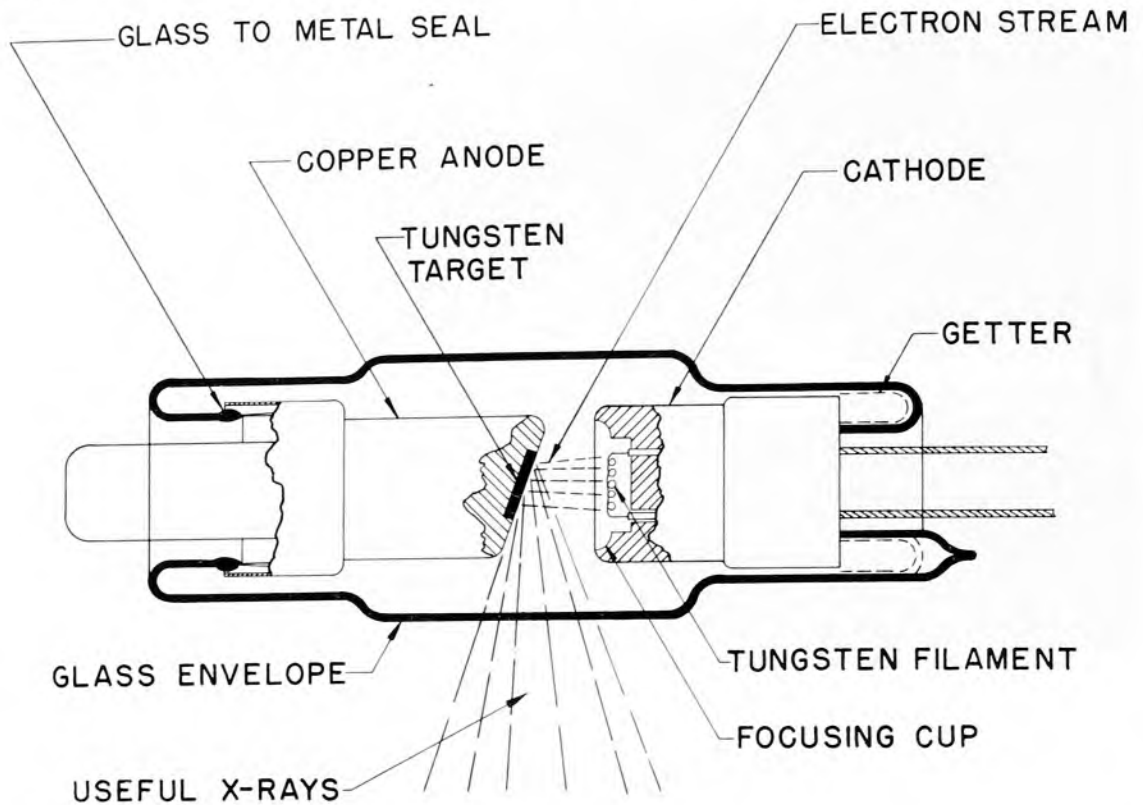


FIG. IV-4. Diagram of stationary anode x-ray tube with getter.
(Courtesy of Dunlee Corporation.)

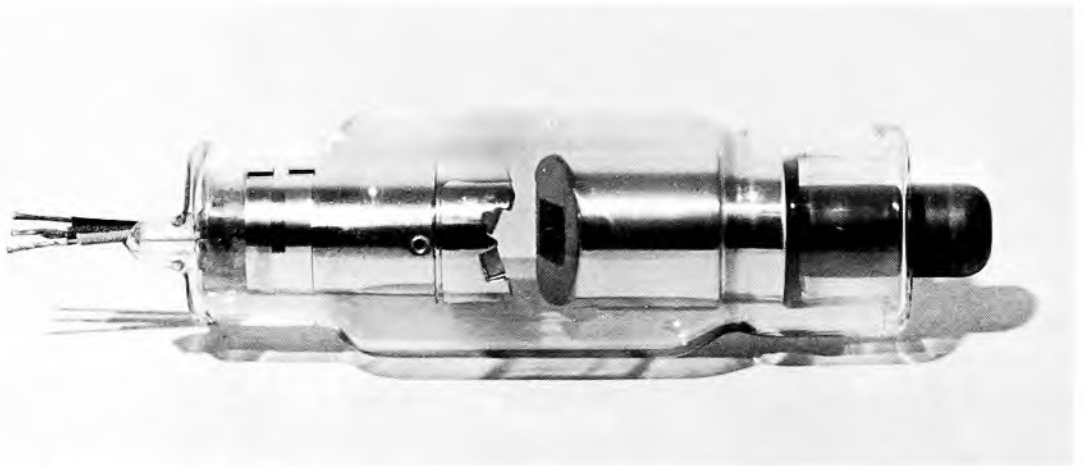


FIG. IV-5. Stationary anode double-focus x-ray tube (Aeromax).
(Courtesy of Machlett Laboratories, Inc.)

MODERN X-RAY TUBES

With a few technical modifications, the modern tubes used in diagnostic roentgenology are basically identical to the Coolidge x-ray tube. The envelope of the tube is usually made of glass and may have different shapes or sizes depending upon the purpose of the tube. The cathode is usually a

tungsten filament that is heated by means of an electric current (Figs. IV-4 and IV-5). This filament is contained in a semicylindrical structure that focuses the electrons emitted by the filament onto a target (Fig. IV-6). The target may be either solid tungsten or tungsten imbedded in copper or backed by some other metal such as molybdenum. The potential difference (voltage) between the anode and the cathode is maintained by means of a generator which will be discussed later on.

In conventional radiography the voltage applied is of the order of 100 kV. The quality of the x-ray beam produced by the tube depends upon two factors: the number of electrons striking the target per unit time, and the energy of the electrons. The number of electrons flowing in an x-ray tube varies with the temperature of the filament, which can be regulated by altering the filament current. The x-ray tube current is limited by the power which can be supplied by the generator.

In diagnostic radiology, the x-ray source should be as small as possible to reduce "geometrical unsharpness" (Chapter VI), and the x-ray exposure should be made in the shortest period of time. These two conditions are translated in the x-ray tube as a high electron flux impinging on a small

FIG. IV-6. Cathode structure of a modern double-focus rotating-anode x-ray tube. Each filament supplies electrons to a focus of different size. Note the focusing structure of the cathode.



FIG. IV-7. Damage caused to x-ray tube anodes by excessively high electron flux.

Top stationary anode

Bottom rotating anode which remained stationary during the exposure (stationary melt)

(Courtesy of Machlett Laboratories, Inc.)



target. The combination of these factors results in a considerable amount of heat applied in a short period of time on a small target; under the circumstances, the main limitation in the operation of an x-ray tube is the ability of the target to withstand heat without damage (Fig. IV-7).

The Focal Spot

The resolution achieved in an x-ray examination depends strongly on the size of the focal spot of the x-ray tube used (see Chapter VII). Therefore considerable efforts are always made to reduce the focal spot to the smallest size compatible with the heat dissipation capability of the target used, and most of the improvements that distinguish one diagnostic tube from another consist of the different and more efficient methods they incorporate for dissipating the heat generated in the target. One of the very early approaches to the solution of this problem consisted in slanting the plane of the target at an obtuse angle with respect to the beam of x-rays. Thus the surface presented by the target to the electronic bombardment was a narrow rectangle, and the projection of this rectangle in a direction perpendicular to the stream of electrons (the apparent focal spot) was a square of considerably smaller

FIG. IV-8.

- A target angulation in a stationary anode tube
 - B target angulation in a rotating anode tube
- (Courtesy of Machlett Laboratories, Inc.)

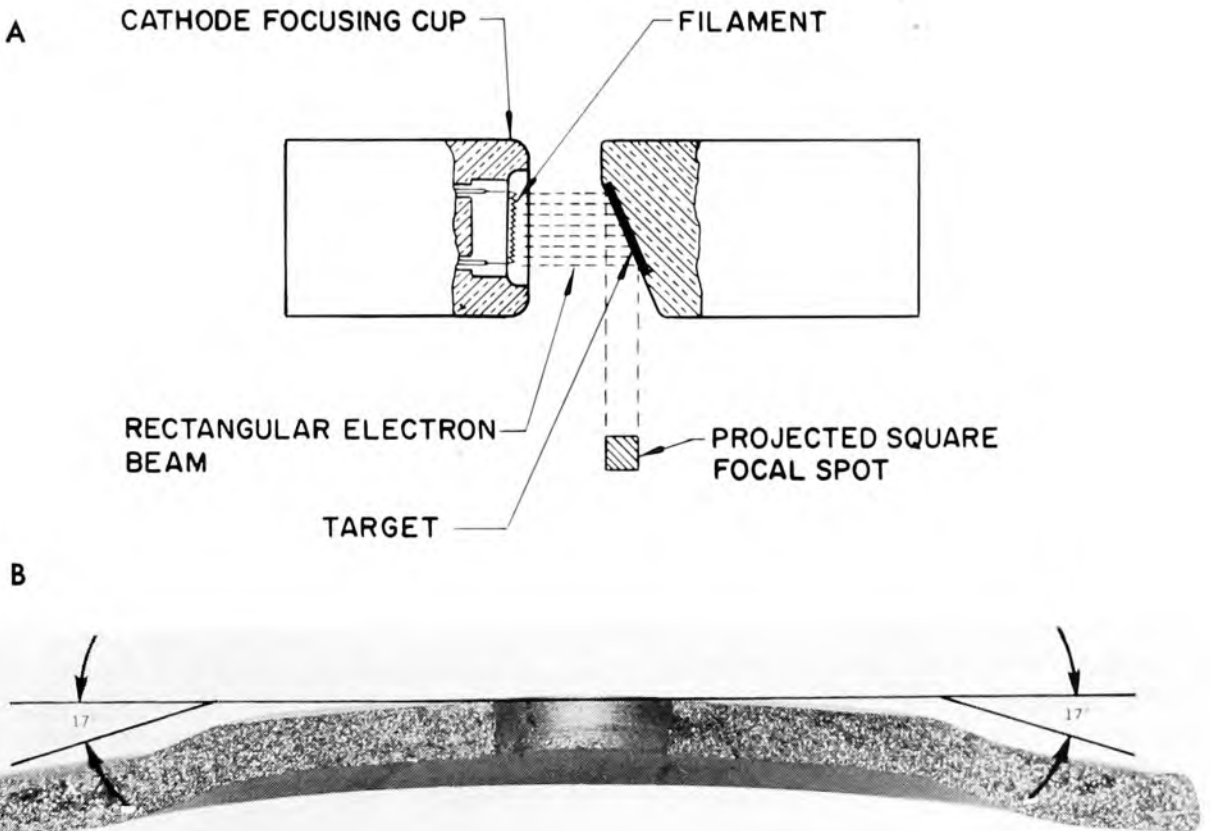
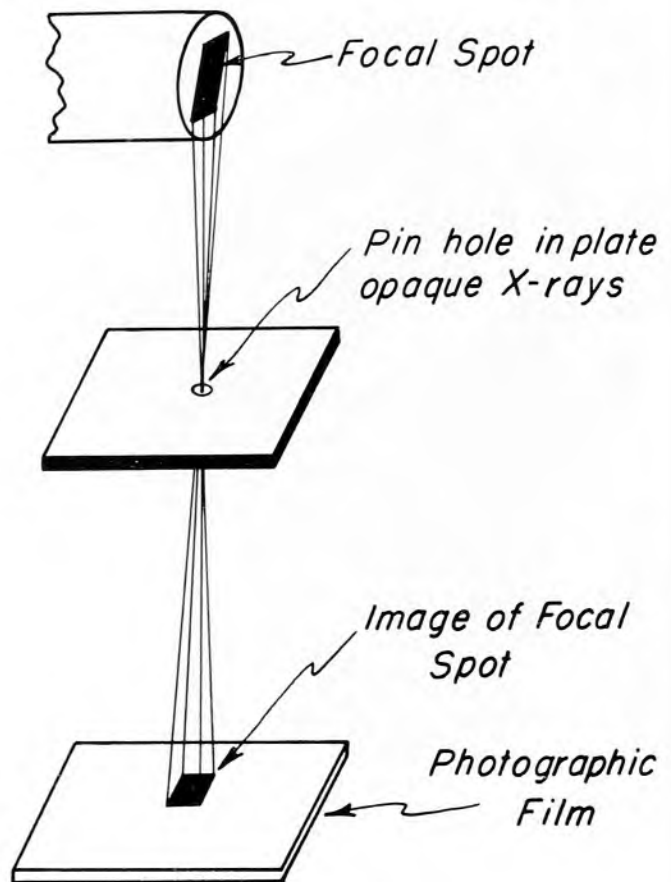


FIG. IV-9. Principle of pinhole camera used in obtaining photographs of x-ray tube focal spots.



area (Fig. IV-8). By this method the target area could be increased without increasing the size of the apparent focal spot. This method is widely used in diagnostic radiology today, and most targets are sloping at an angle of the order of 20 degrees. As shown in Fig. IV-8, the area of the projected focal spot is equal to the area of the focal spot divided by the sine of the angle of the target. Since $\sin 20 \text{ degrees} = 0.342$, the area of the tube's target is approximately three times greater than that of the apparent focal spot. The angulation of the target, however, results in a lack of uniformity of the x-ray beam which is tolerable only for target angles greater than about 16 to 20 degrees (Ref. 20).

Angulation of the target provides focal spots that are approximately square in shape with side dimensions varying approximately between 0.3 and 2.5 mm. Special tubes with smaller (0.1 mm) or larger focal spots have been built. Most modern radiographic examinations are carried out with 1-mm (high resolution) and 2-mm (examination of thick parts) focal spots.

The size of the focal spot in an x-ray tube can be determined by using a pinhole camera, the principle of which is illustrated in Fig. IV-9. In order to obtain good resolution by means of a pinhole camera, the size of the pinhole must be small with respect to the size of the focal spot to be measured. The International Commission of Radiological Units and Measurements



FIG. IV-10. Pinhole photographs of stationary anode tube (*top*) and rotating anode tube (*bottom*). Note greater intensity of off-focus radiation with rotating anode. (Courtesy of Zed J. Atlee (Ref. 20) and The Dunlee Corporation.)

(ICRU) (Ref. 7) recommends the following pinhole diameters:

- 0.03 mm for focal spot sizes below 1.0 mm,
- 0.075 mm for focal spot sizes from 1 to 2.5 mm.

Pinhole camera pictures of x-ray tubes reveal that in addition to the focal spot there are other sources of radiation within the x-ray tube (Ref. 8). X-radiation originating in areas different from the focal spot is called off-focus or extrafocal radiation.

Off-focus radiation is mostly produced by electrons scattered by the target and which strike metallic surfaces in the x-ray tube (Refs. 9 and 20). While any surface struck by stray electrons in the tube becomes a source of off-focus radiation, most of this radiation is contributed by tungsten surfaces because of the considerably higher atomic number of this metal than that of other components of x-ray tubes. Thus, off-focus radiation is particularly intense in x-ray tubes in which a large surface of tungsten can be "seen" through the exit port. Rotating anode tubes, with a large exposed area of tungsten (see next section), generate a particularly large amount of off-focus radiation. Pinhole pictures of rotating tubes show that the whole front surface of the anode disk is a source of off-focus x-rays (Fig. IV-10). The off-focus radiation, which may represent up to 25% of the "on-focus" radiation, results in undesirable artifacts in radiology. The amount of off-focus radiation reaching the film may be reduced by collimating the x-ray beam close to the target (Ref. 8).

Rotating Anodes

In low-capacity x-ray tubes the cooling of the target may be achieved by air or water. In the high-capacity x-ray tubes required in most modern radiologic techniques, a considerable increase in the capacity of the target to withstand heat is achieved by using a rotating anode. This, in effect, consists in spreading the electronic bombardment of the target over a wide area without altering the size of the focal spot (Fig. IV-11). The rotation of the anode is accomplished by attaching the latter to the rotor of a motor contained within the vacuum of the x-ray tube (Fig. IV-12). The stator of the motor is located outside of the vacuum, as shown in Fig. IV-13. The speed of anode rotation obtained in modern x-ray tubes may be as high as 10,000 rpm.

Many difficulties had to be solved in the development of rotating anode tubes (Refs. 3 and 4). For example: (1) The high speed of the rotating anode required excellent bearings. (2) The heat generated in the tube posed several serious problems because of the low tolerance of certain bearing materials to heat. (3) The bearings had to be capable of operating over a wide range of temperature. (4) The lubrication of the vacuum-enclosed "hot" rotor, impractical with liquid lubricants, presented another problem; it was solved by the use of metallic lubricants (lead, gold, barium, or silver). (5) Early rotating anode tubes were fitted with an anode composed of a rotating copper

block fitted with a thin tungsten target; such anodes were not successful because the high temperature gradient between the hot tungsten target and the cooler copper disc resulted in "peeling" of the target (Ref. 5) (Fig. IV-14).

Modern rotating anodes are made of either solid tungsten, as shown in Fig. IV-8B, or of a "sandwich" of different metals such as a rhenium-tungsten layer backed by molybdenum (Ref. 6). A further improvement in x-ray tubes, both of the fixed and rotating anode types, consists in fitting the cathode with two filament structures, providing two focal spots of different size (Fig. IV-6).

In the overwhelming majority of roentgenographic examinations the x-radiation is generated by means of rotating anode tubes. Stationary anode tubes are mostly used in dental radiography, in low capacity portable x-ray units, and in some out-dated fluoroscopic installations.

X-RAY TUBE HOUSING

In modern diagnostic x-ray installations the x-ray tube, commonly referred to as the insert, is contained in a housing that fulfills the following purposes: (1) it serves as a mechanical support for the x-ray tube; (2) it provides electrical insulation for the high voltage applied to the x-ray tube; and (3) it provides radiation shielding (rayproofing).

An x-ray tube housing (Fig. IV-15) is composed of a metallic container fitted with insulated connections for the shockproof cables that connect the x-ray tube to the generator. If the insert is of the rotating anode type, the stator which provides the magnetic field for the rotation of the rotor is contained in the housing. The housing is generally filled with oil, which provides electrical insulation and serves as a medium for the dissipation of heat generated in the insert. The oil exchanges heat between the x-ray tube and the outside of the housing both by radiation convection and conduction; the outside of the housing may be cooled by forced air circulation. During tube operation the temperature of the oil rises, and provision must be made within the x-ray tube housing for the thermal expansion of that medium. This is accomplished by the use of metallic bellows which allow a variation of the volume of the oil. The bellows may also be connected to a safety switch to prevent operation of the x-ray tube if the heat capacity of the housing is exceeded. Lead shielding is provided in the housing to reduce the intensity of the x-radiation outside the useful beam.

X-RAY TUBE RATINGS

X-ray tubes are rated for maximum voltage and maximum energy (Ref. 10).

Maximum Voltage Ratings

The maximum voltage rating for an x-ray tube is the maximum instantaneous voltage that, under specified conditions, can be applied to the tube

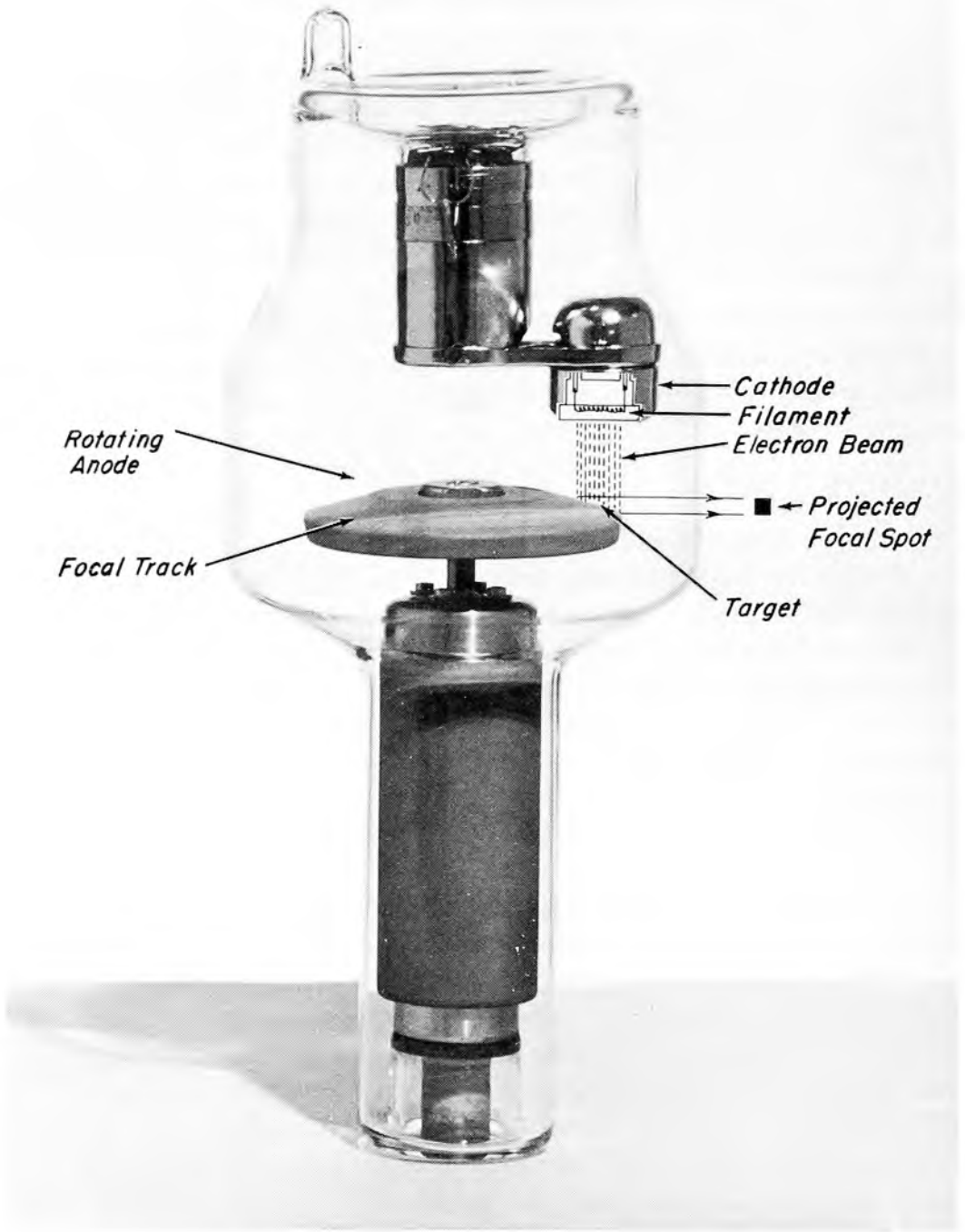


FIG. IV-11. Rotating anode x-ray tube.
(Courtesy of Machlett Laboratories, Inc.)

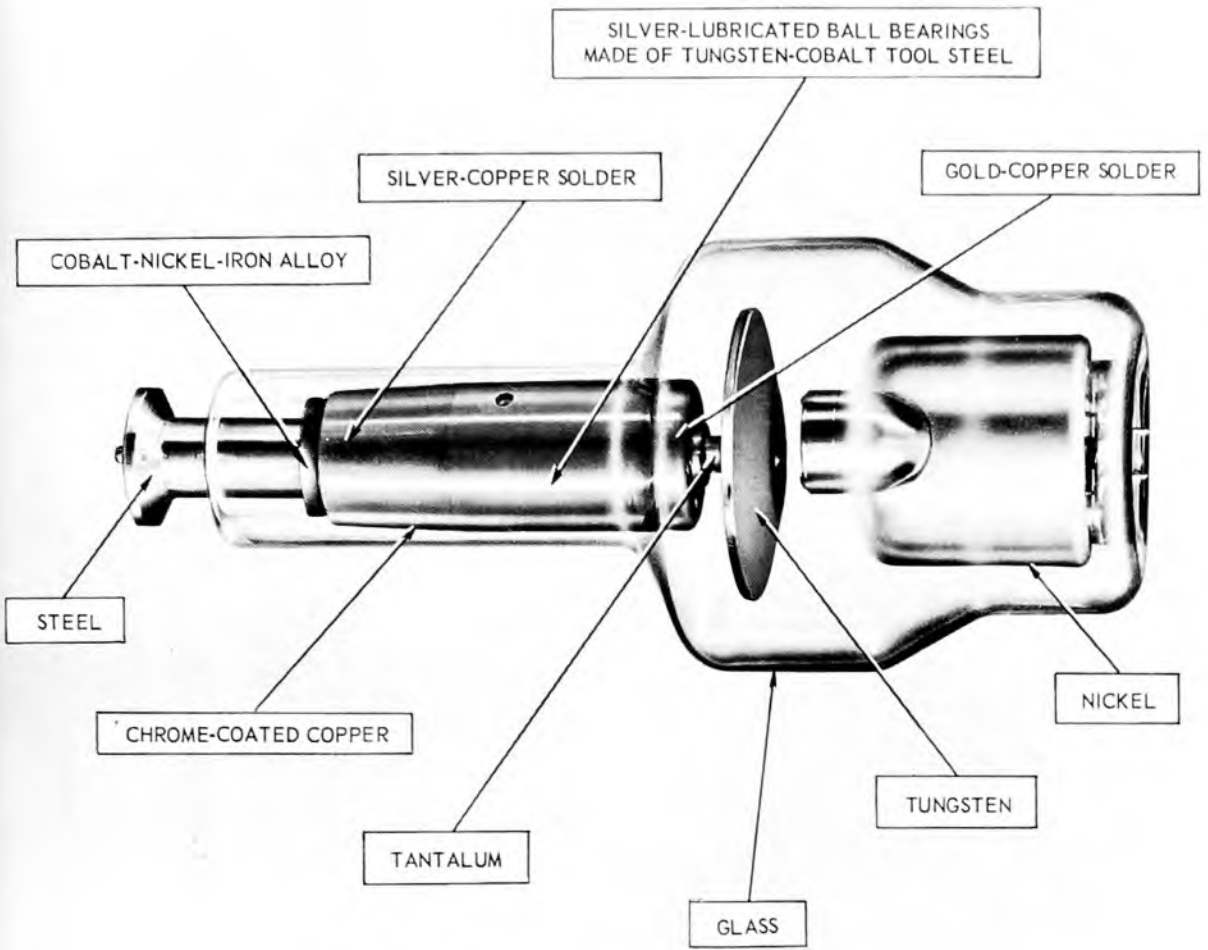


FIG. IV-11 (Continued). Rotating anode x-ray tube.
(Courtesy of General Electric Company.)

FIG. IV-12. Target and rotor of rotating anode x-ray tube, showing bearings.
(Courtesy of Machlett Laboratories, Inc.)

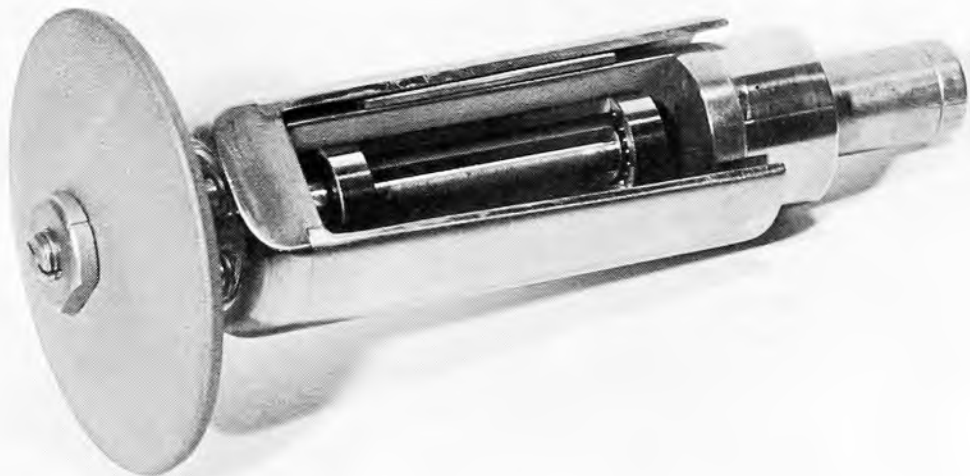




FIG. IV-13. External winding (stator) used to rotate rotating anode in x-ray tube. Dynamax "50" bulkhead. (Courtesy of Machlett Laboratories, Inc.)

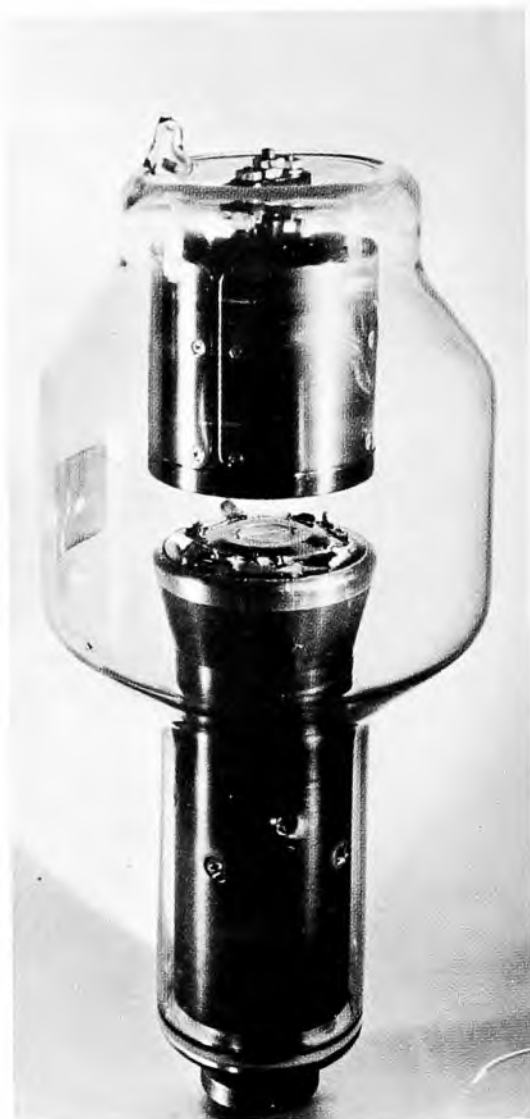
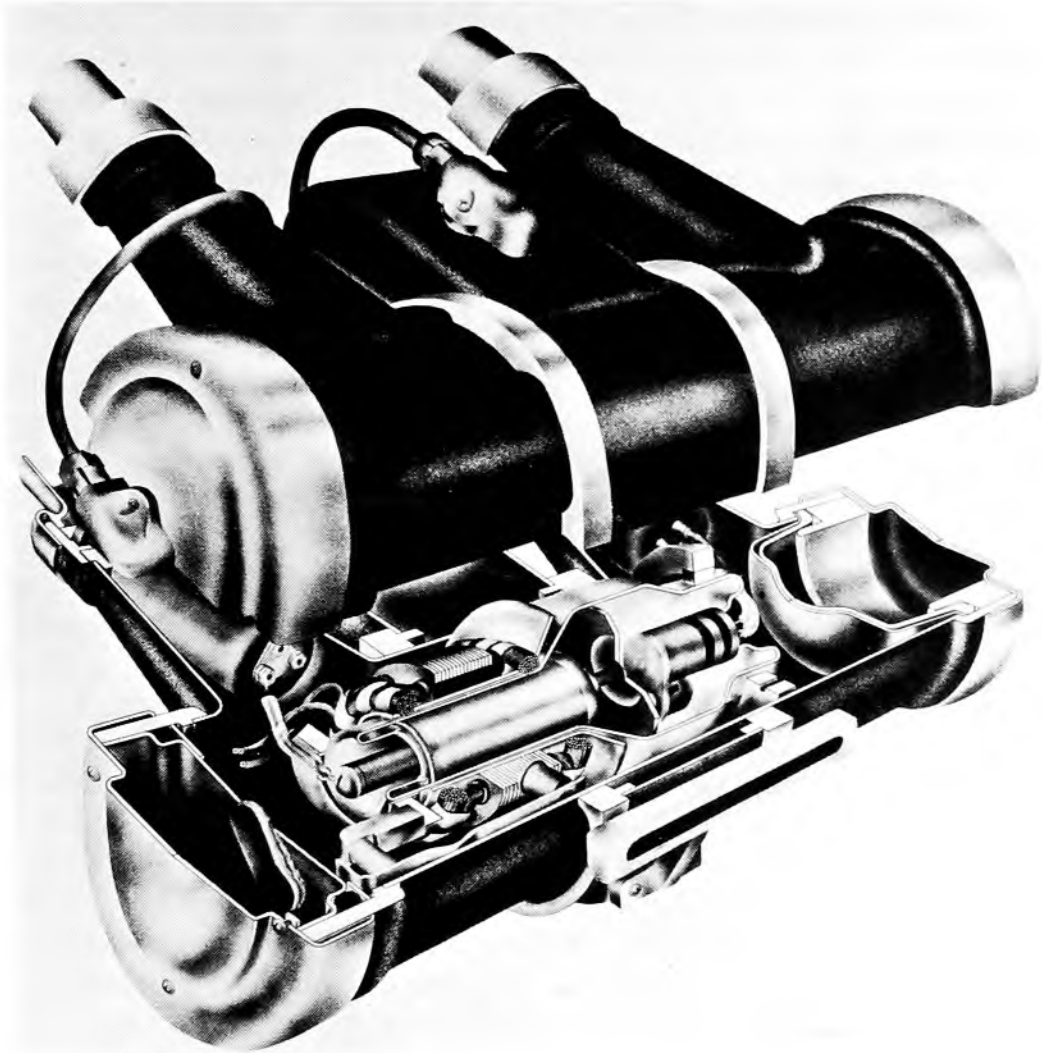


FIG. IV-14. Early rotating anode tube with tungsten-covered copper anode, showing damage due to tungsten "peeling." (Courtesy of Machlett Laboratories, Inc.)

without damage. Maximum voltage ratings depend on such factors as: (1) rectification of the voltage applied to the tube, (2) voltage balance in the generator transformer, and (3) possible voltage surges in the circuit; because these factors may subject the tube to a voltage higher than the planned steady-state operating voltage. For example, an x-ray tube used in a self-rectified circuit is subjected to a higher voltage during the nonconducting half-cycle than during the conducting half-cycle when the tube draws a current from the generator and thus produces a drop in potential. Also, in three-phase full-wave rectified circuits, the voltage to the ground may be 15% greater than the voltage at the terminals because the voltage pulsations at each terminal are out of phase with one another (Ref. 10). In general, x-ray tubes are capable of withstanding transient surges of voltage that exceed their steady-state tube voltage ratings without damage, because of

FIG. IV-15. X-ray tube (insert) in its housing.
(Courtesy of Machlett Laboratories, Inc.)



the engineering safety factors in the insulation of the tubes; however, surges exceeding 10% of the maximum voltage rating are considered excessive.

Maximum Energy Ratings

Most of the electrical energy supplied to an x-ray tube during the production of x-rays is converted into heat. This heat flows through the various components of the tube, raises their temperature, and is finally dissipated outside the tube. The rise in temperature of any component depends on: (1) its heat capacity, (2) its ability to dissipate heat, and (3) the rate at which heat is applied. The maximum energy ratings of the different components in a tube are determined by their ability to dissipate heat and withstand high temperatures.

The electrical energy supplied to an x-ray tube is proportional to the voltage applied, the current flowing through the tube, and the time of operation. It is therefore convenient to express this energy, and also the maximum energy ratings of x-ray tubes, in units of peak voltage (in kilovolts) \times tube current (in milliamperes) \times time of exposure (in seconds). The product $1 \text{ kV}_p \times 1 \text{ mA} \times 1 \text{ sec}$ is called a heat unit.

In a stationary-anode x-ray tube, heat is generated and transferred as follows: (1) The accelerated electrons are stopped in the target, practically all their energy is converted into heat, and the temperature of the target is raised to a high value. (2) Most of this heat, with the exception of a small percentage radiated by the focal spot, is transferred by conduction to the copper anode. This heat is temporarily stored by the anode, thus raising its temperature. (3) The heat of the anode is dissipated into the oil and the tube housing, where it is again temporarily stored until dissipated into the atmosphere.

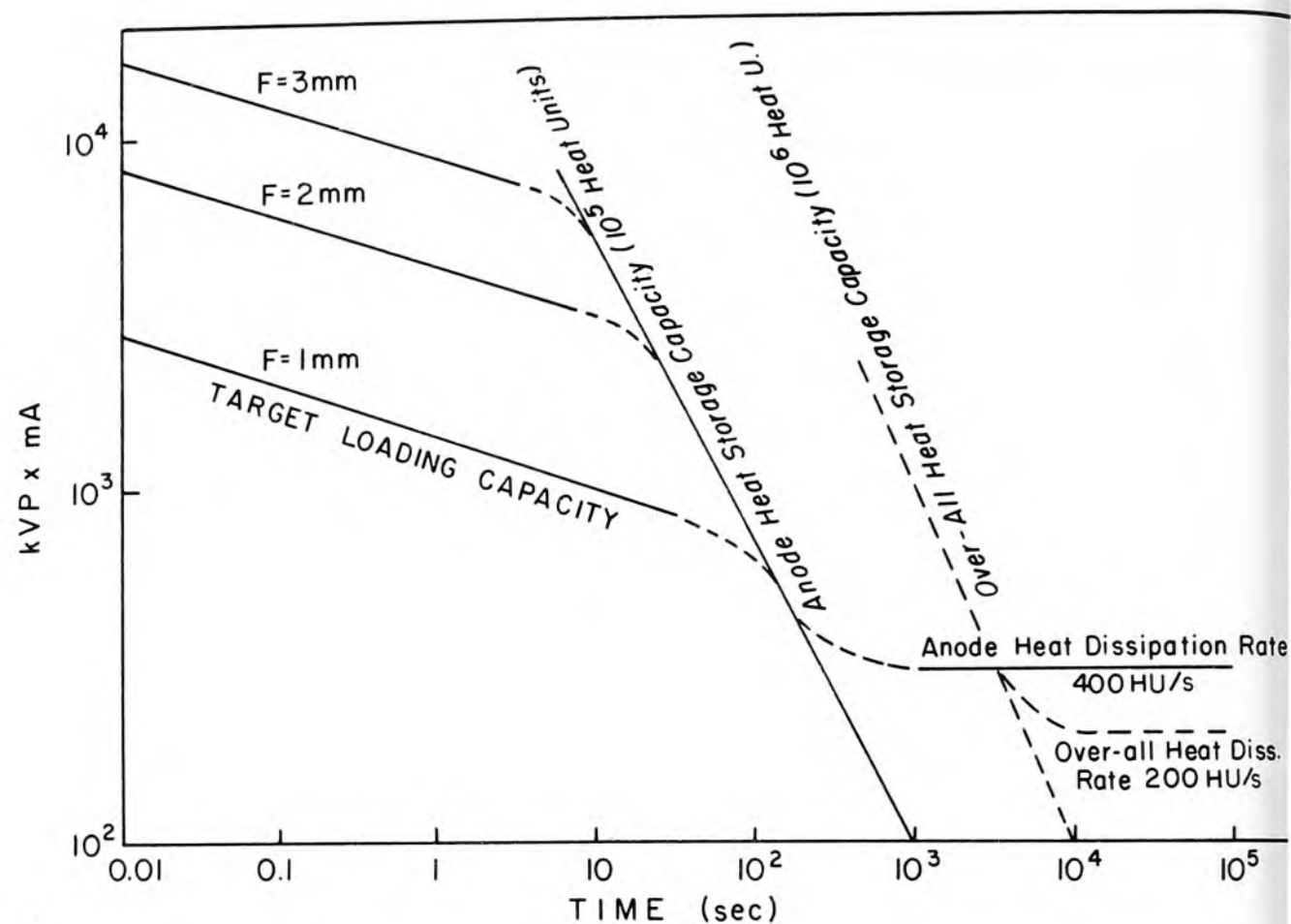
The first limiting factor in this chain of events is the temperature reached by the target at the focal spot. The temperature of the tungsten target must remain below the melting point of that metal, and the temperature of the surface of the copper anode in contact with the tungsten must remain below the melting point of copper. The maximum energy rating for the target is proportional to its area. A typical loading capacity for a tungsten target backed with copper is approximately 200 watts/mm² of focal area per second. This factor varies to a certain degree depending on the size of the target, because of lateral conduction of heat (Ref. 10).

The limit imposed on the maximum energy rating of an x-ray tube can be conveniently shown as a line on a plot of the voltage applied to the x-ray tube multiplied by the tube current ($V \times \text{mA}$) versus time (t) (Fig. IV-16A). The region of the plot located under the limiting line includes all the permissible loadings, while the area above the line corresponds to loadings which would damage the tube. The limits imposed on the maximum energy rating of the tube by the loading capacity of the target are represented by a series of curves for different focal spot sizes.

The heat generated in the target (minus the fraction radiated by the target) is transmitted by conduction to the anode structure. The important factor in the maximum rating of an anode structure is its heat storage capacity, which is a measure of the number of heat units that can be accumulated before the anode structure reaches an undesirably high temperature. If there were no dissipation of heat from the anode structure, the maximum energy rating for the tube due to the anode heat storage capacity would be represented as a straight line in Fig. IV-16A, corresponding to the value of the anode heat storage capacity. It should be noted that the limitation imposed by the anode structure on x-ray tube capacity is independent of the focal spots size, and it is controlled by a series of factors such as the melting point of the anode material, the heat-resistant characteristics of the seal, the degree of outgassing, etc. (Ref. 10). The anode structure, however, is not thermally insulated, and it dissipates heat; thus, even after the heat storage capacity of the anode structure is used up, the x-ray tube can still be operated, provided the energy input does not exceed the rate of heat dissipation, which in Fig. IV-16A is represented by a horizontal line. Thus in Fig. IV-16A, the area located below the lines formed by the target loading capacity, the anode heat storage capacity, and the anode heat dissipation rate corresponds to permissible tube loadings, while the area above represents excessive loadings.

In modern x-ray tubes the heat transfer to the anode structure is rapidly transmitted to the oil in the housing, mostly by radiation. Therefore, the heat storage capacity of the whole housing must be taken into account in the determination of the maximum energy rating of the tube. The heat storage capacity of the anode plus the tube housing structure is, in general, considerably larger than the heat storage capacity of the anode alone. However, the over-all heat dissipation rate of the unit is lower than that of the anode alone. Typical values of these ratings that were used in Fig. IV-16A are: anode heat storage capacity, 100,000 units; anode heat dissipation rate, 400 units/sec; over-all heat storage heat capacity, 1 million units (anode structure plus housing); over-all heat dissipation rate, 200 units/sec.

The maximum energy ratings of rotating anode tubes are determined in a manner similar to that of stationary anode tubes. The main difference of a rotating anode tube is that the effective area of the target is considerably increased by the rotation of the anode and that a considerably higher instantaneous loading capacity than for a stationary target results. Rotating anode tubes are often constructed with solid tungsten anodes. Indeed, there is no need for good thermal conductivity in the anode structure because the heat is distributed over a wider area of the anode by its rotation. Thus, with a solid tungsten anode there is no limitation imposed by the melting point of copper. It should be noted that the transmission of heat from the anode to the oil of the housing occurs mostly by radiation, and it is proportional to the fourth power of the temperature of the radiator. Some rotating anodes



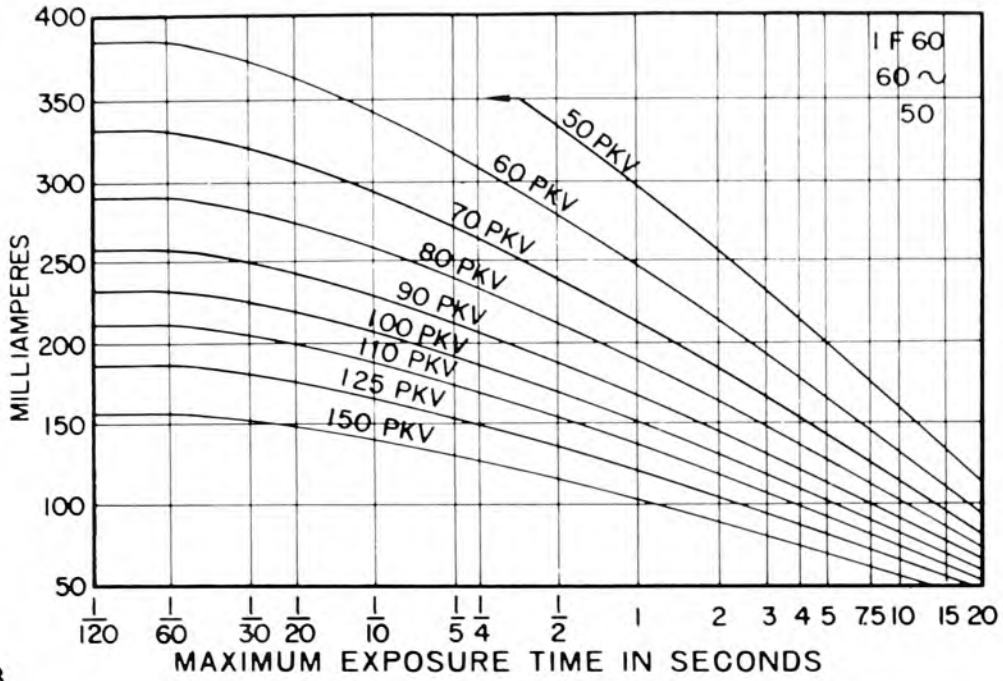
A

FIG. IV-16.

A Chart expressing individual exposure ratings for 20-degree line focus x-ray tube with tungsten target and copper anode. (Courtesy of T. H. Rogers (Ref. 10) and Machlett Laboratories, Inc.)

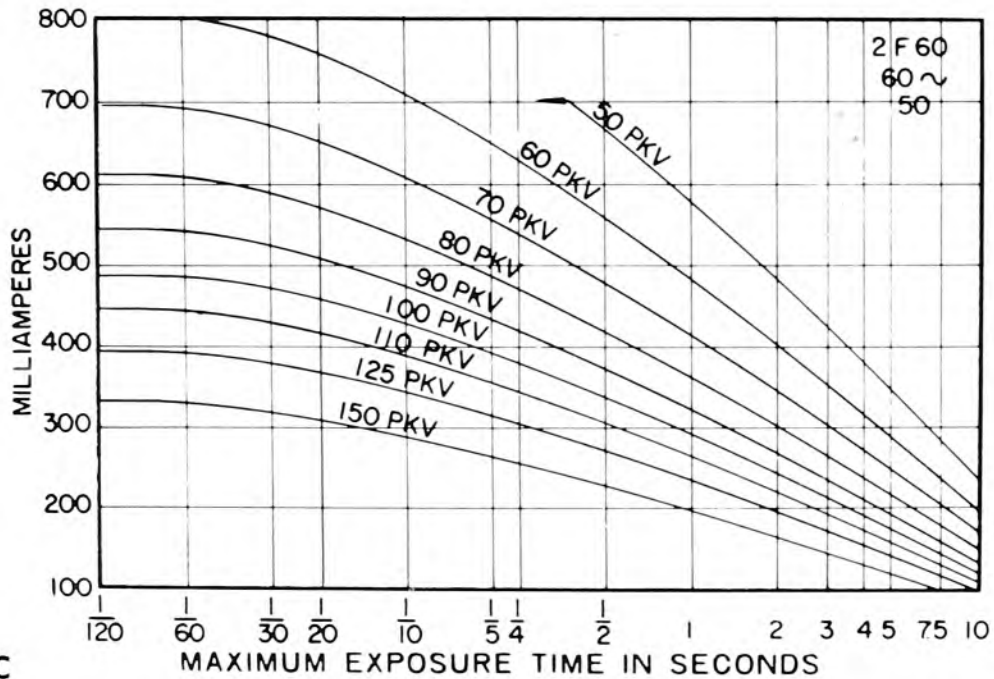
B and C (opposite) Target rating charts for a Dynamax "50" rotating-anode x-ray tube (full-wave, single-phase, 60-cycle stator operation), for two different targets with effective focal spot sizes of 1.0 and 2.0 mm, respectively. The charts show the relationship between tube current and maximum exposure time which can be used without damage to the target, for different peak kilovoltages applied to the tube. For example, at 100 kV_p, a tube current of 200 mA can be safely applied to the target with an effective focal spot size of 1.0 mm, for a maximum exposure time of about $\frac{1}{8}$ sec (25 mAs). On the other hand, the target with an effective 2.0-mm focal spot can withstand the same current with the same tube voltage for about 3.5 sec (700 mAs). (Courtesy of Machlett Laboratories, Inc.)

Effective Focal Spot Size — 1.0 mm



B

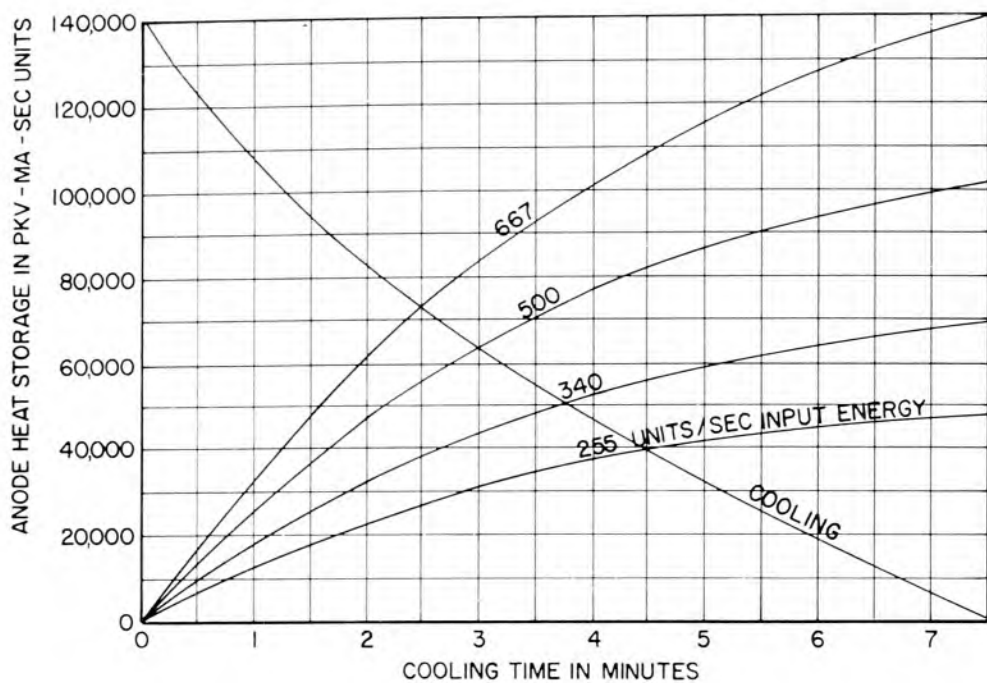
Effective Focal Spot Size — 2.0 mm



C

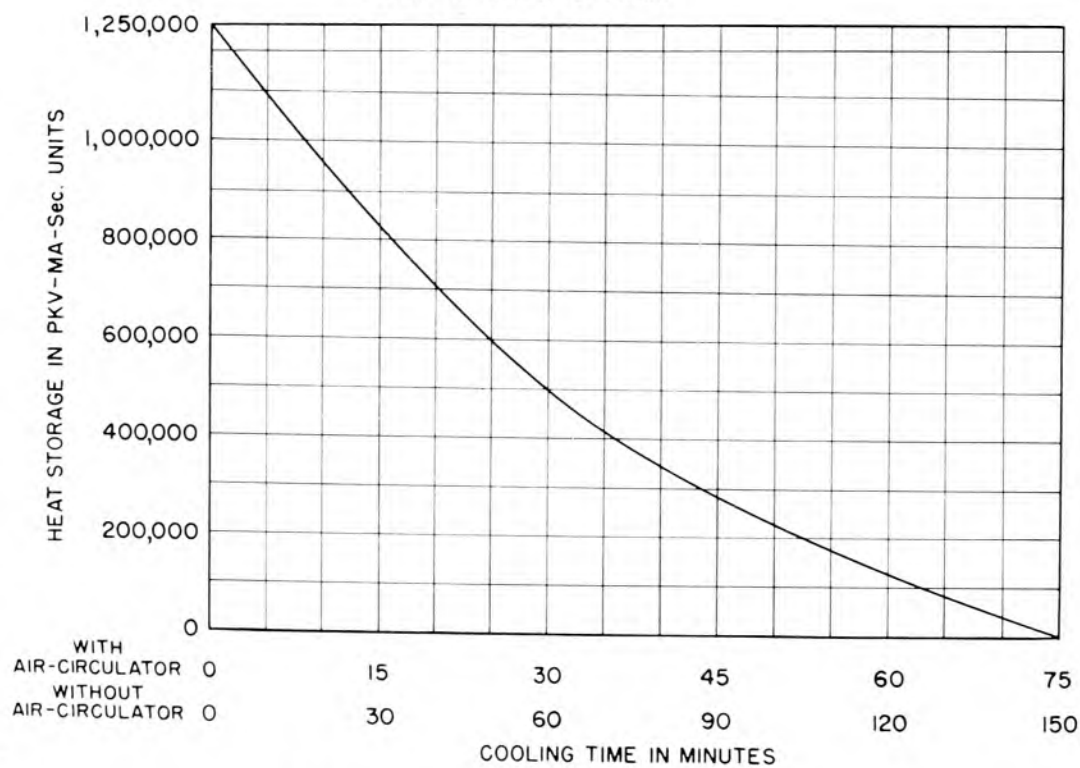
FIG. IV-16B and C (Legend on opposite page).

ANODE THERMAL CHARACTERISTICS



D

HOUSING COOLING CHART



E

FIG. IV-16D and E (Legend on opposite page).

have been constructed with blackened surfaces to improve their heat emissivity. Figures IV-7 and IV-17 show different forms of stationary anode damage caused by overload. Figure IV-18 shows different rotating anode damages.

The maximum energy ratings for x-ray tubes are usually expressed as rating charts. Two types are commonly used. The first is a plot of milliamperes versus maximum exposure time for different peak kilovoltages. The other, a plot of anode heat units versus time, expresses the maximum number of heat units that can be delivered to the tube in a given period of time. It is particularly useful when a number of exposures are to be made in rapid succession. Typical rating charts are shown in Figs. IV-16B through E.

SPECIAL PURPOSE X-RAY TUBES

Special requirements imposed upon x-ray tubes have resulted in tube designs different from the more conventional ones described above. Among the special-purpose tubes, grid control, beryllium window, and stereo x-ray tubes are currently used in diagnostic radiology. Others, such as monochromatic radiation tubes and particularly field-emission x-ray tubes, may find clinical applications in the future.

Grid-Control X-Ray Tube

The grid-control x-ray tube contains, in addition to the two conventional components of an x-ray tube—the filaments and the target—a third electrode called the control grid. This tube functions like a conventional vacuum tube triode, which contains three electrodes: an electron-emitting cathode, an anode, and a grid placed between the anode and the cathode. If a potential difference is established between the anode and the cathode and electrons travel from the cathode to the anode, an electric current flows through the tube if the grid does not carry any potential, because electrons can travel

FIG. IV-16. D and E (opposite) The anode thermal characteristics chart shows:

- 1 anode heat storage capacity (140,000 heat units)
- 2 rate at which the anode heat storage capacity is filled up for different input energy rates
- 3 rate of heat dissipation of the anode (cooling) as a function of time. If the energy input is 667 heat units/sec, the anode heat storage capacity is reached, in spite of heat dissipation, in 7.5 min. On the other hand, the tube can be operated indefinitely without damage to the anode with an input energy of 500 heat units/sec. The cooling curve allows the determination of the cooling time required after exposures resulting in loading the anode to its full heat storage capacity.

The housing cooling chart shows:

- 1 heat storage capacity of the tube housing (1,250,000 heat units)
- 2 rate of cooling of the housing, with and without air circulator

(Courtesy of Machlett Laboratories, Inc.)

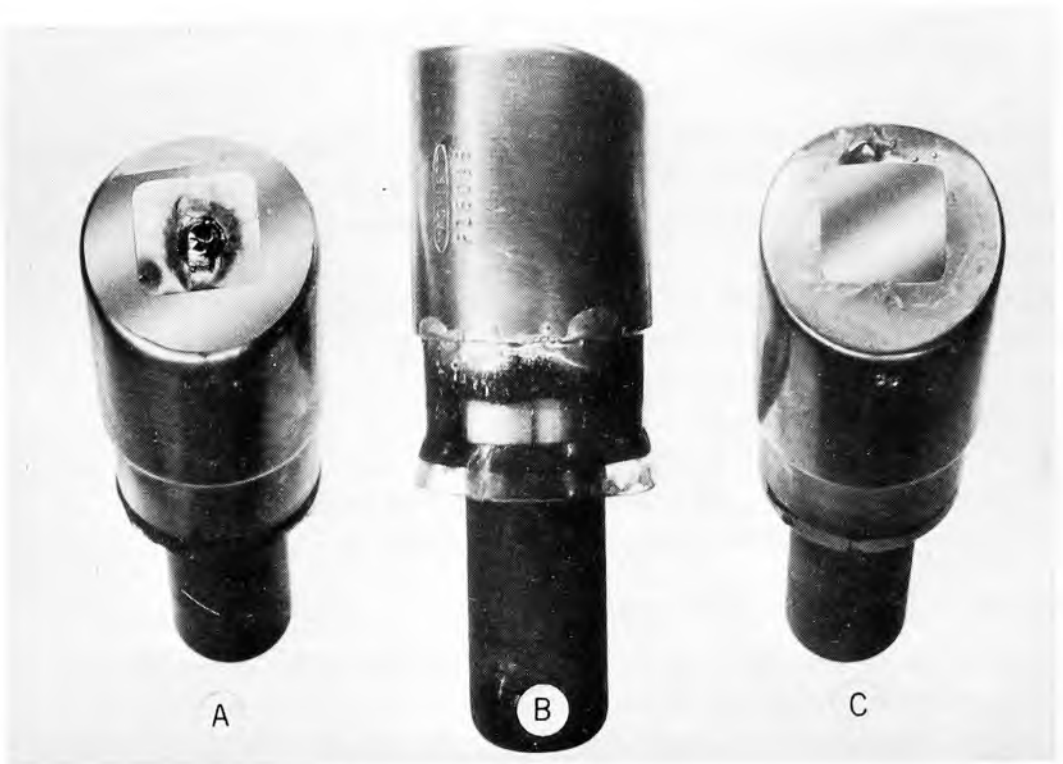
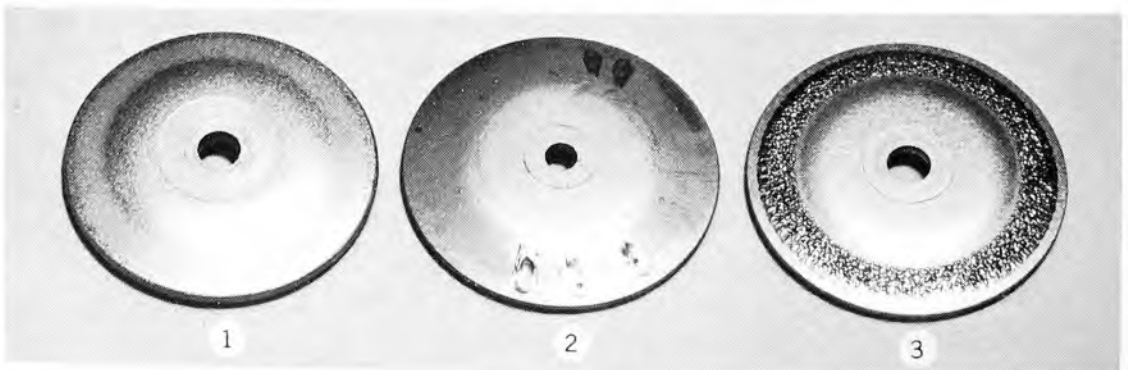


FIG. IV-17. Effect of overloading stationary anodes.

- A** focal spot overheated by short-duration overload
 - B** anode seal destroyed by exceeding the heat storage capacity
 - C** copper surrounding target melted by too long an exposure at high intensity
- (Courtesy of T. H. Rogers (Ref. 10) and Machlett Laboratories, Inc.)*

FIG. IV-18. Effect of overloading rotating anodes.

- 1** effect of normal use
 - 2** effect of heavy exposure during start-up or coasting down of the rotating anode. The multiple melted areas result from the pulsing of the electron beam, by the pulsed nature of the high voltage applied to the tube during the x-ray exposure. This form of damage, which occurs only if the x-ray tube is energized by a pulsating circuit, is called "spinning top effect" because of the similarity of the origin of the multiple melts with the multiple images obtained with a spinning top used in calibrating x-ray timers (see Fig. IV-42). Damage is usually caused by inadequate motor control circuitry allowing exposure before full rotor speed is reached.
 - 3** damage resulting from exceeding the anode storage capacity
- (Courtesy of Machlett Laboratories, Inc.)*



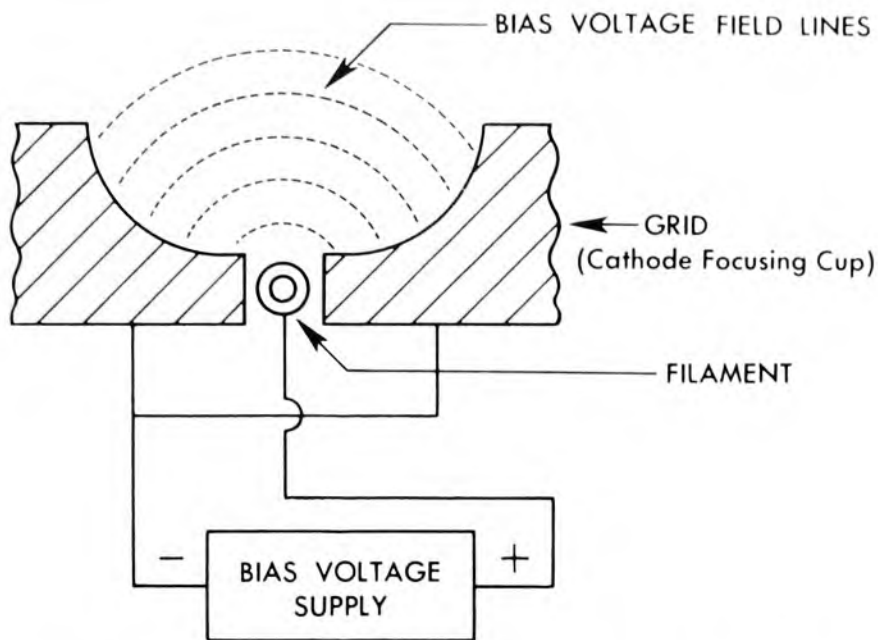
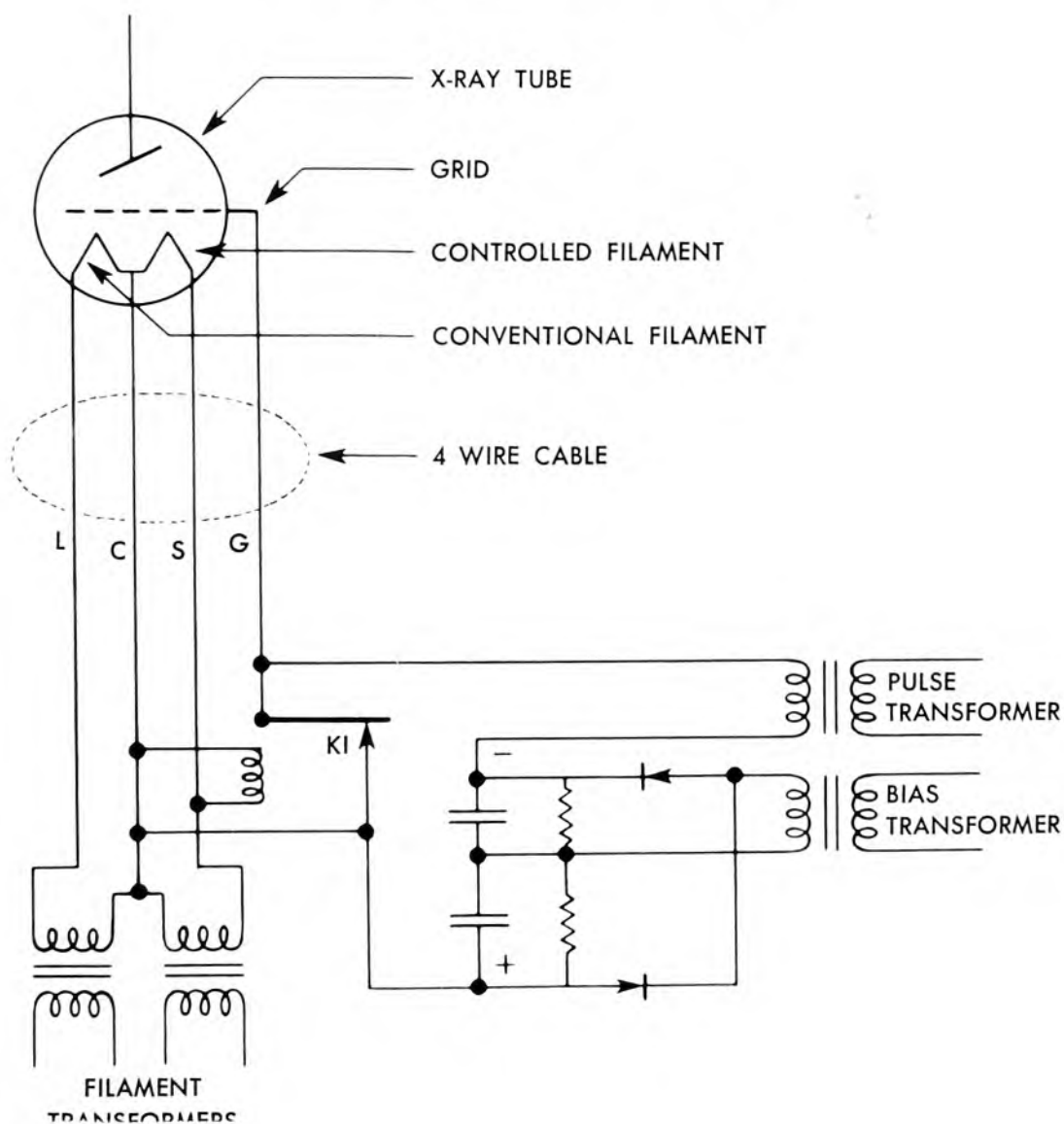


FIG. IV-19. Grid-control x-ray tube. Simplified sectional schematic diagram of grid control and beam-forming structure for cut-off condition. (Courtesy of Machlett Laboratories, Inc.)

FIG. IV-20. Circuit for grid-control x-ray tube. (Courtesy of Machlett Laboratories, Inc.)



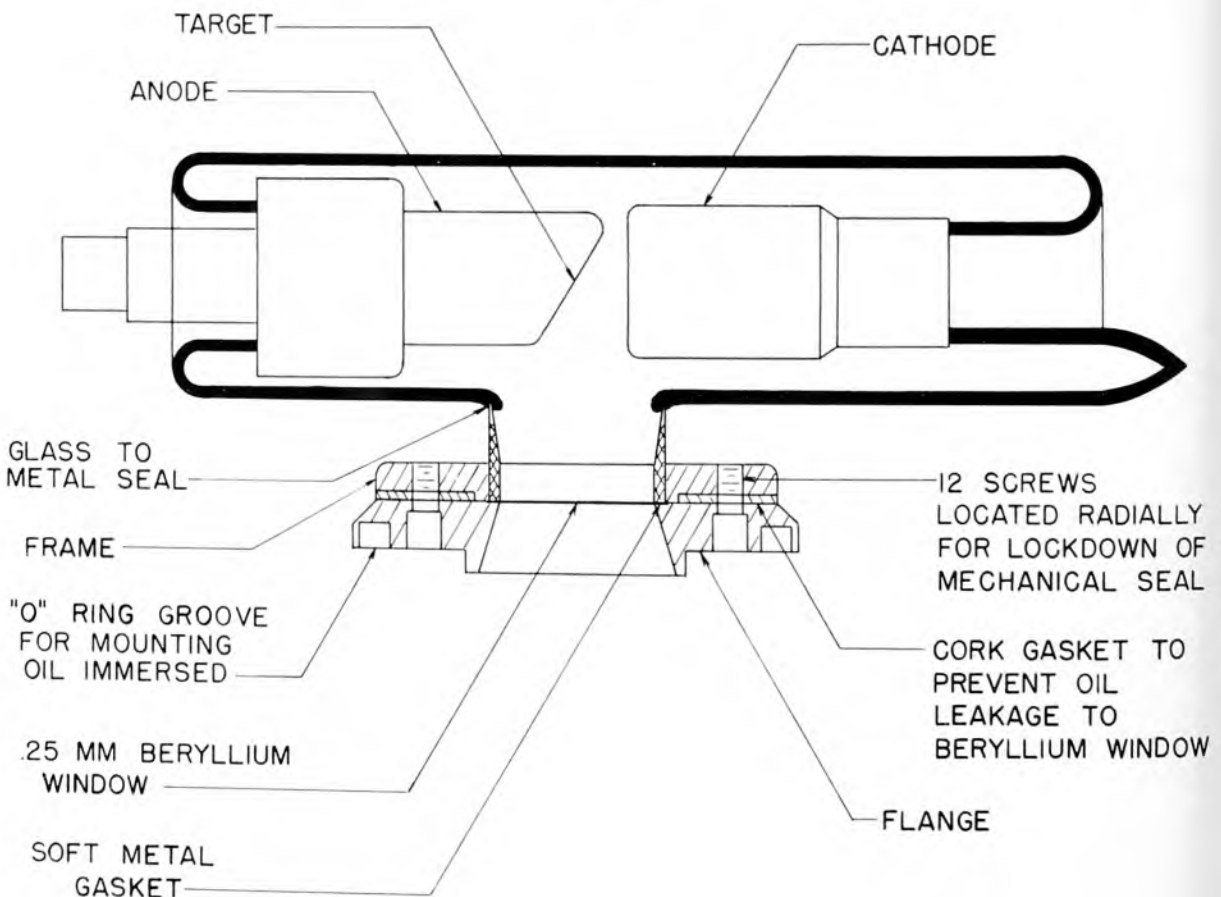
unimpeded between the interstices of the grid. On the other hand, if the potential of the grid is made negative with respect to the cathode, its potential interferes with the travel of the electrons. In this manner the current flowing through the tube may be controlled by the grid potential. A relatively small change in grid potential may alter appreciably the current flowing through the tube.

In the grid control tube the third electrode is the focusing cathode which surrounds the filament (Fig. IV-19). In a conventional x-ray tube this structure is maintained at the same potential as the filament. In the grid control tube the potential of the focusing cup can be varied by means of the circuit shown in Fig. IV-20.

Thus, if the potential of the control electrode (grid) is negative with respect to the filament, electrons do not leave the cathode and no current flows through the x-ray tube. When the control electrode is switched to a potential equal to that of the filament, electrons are accelerated in the tube and x-rays are produced. The control electrode acts as an on-off switch for the x-ray tube.

In a grid control tube, as in a vacuum tube triode, a small variation of

FIG. IV-21. Stationary anode beryllium-window x-ray tube.
(Courtesy of Dunlee Corporation.)



potential allows the control of relatively large currents. The grid control tube is of particular value in diagnostic roentgenology when very short x-ray exposures are required (cardiac angiography) and also in cinefluorography (Chapter IX). *amplify*

Beryllium-Window X-Ray Tubes

Certain radiologic examinations require the use of particularly low-energy x-rays. Conventional x-ray tubes are unsuitable for that purpose because most of the low energy radiation is absorbed in the glass envelope of the tube. This difficulty may be circumvented by fitting a conventional x-ray tube with a beryllium window (Ref. 11). Beryllium, because of its low atomic number ($Z_{\text{Be}} = 4$) exhibits a considerably lower absorption coefficient for low energy x-rays than glass, and beryllium-window x-ray tubes are capable of supplying much "softer" radiation than all-glass tubes. Stationary (Fig. IV-21) as well as rotating anode beryllium-window x-ray tubes have been constructed.

It should be noted that x-ray tubes fitted with beryllium windows are potentially hazardous because the beryllium window allows the escape of a large portion of the soft-component of the x-radiation produced in the tube. This component is difficult to detect with radiation-measuring instruments conventionally available in an x-ray department. Thus, an x-ray tube fitted with a beryllium window may be the unrecognized source of intense x-radiation.

Stereo X-Ray Tubes

X-ray tubes with two separate targets are used for stereoscopic diagnostic examinations (Figs. IV-22 and IV-23).

Space Charge—Field-Emission X-Ray Tubes

Space charge is the electric charge acquired by a volume of space due to the presence within it of charged particles. In an x-ray tube the maximum electron flux that can be produced by thermionic emission (emission of electrons by a hot cathode) is limited by the space charge created by the emitted electrons around the cathode, as follows:

The space charge produced by the electrons the filament emits is determined by the balance between the number of electrons emitted per unit time and the rate of removal of the electrons from the vicinity of the cathode. If the flux of emitted electrons is greater than the rate of removal, the space charge builds up and interferes with the thermionic emission until it is sufficiently high to prevent further thermionic emission altogether. At that point an increase in cathode temperature does not result in a rise of electron flux.

Under normal conditions of operation the electron flux in a conventional x-ray tube is not limited by space charge. However, if very short exposures are attempted the cathode is required to emit a high flux of electrons and

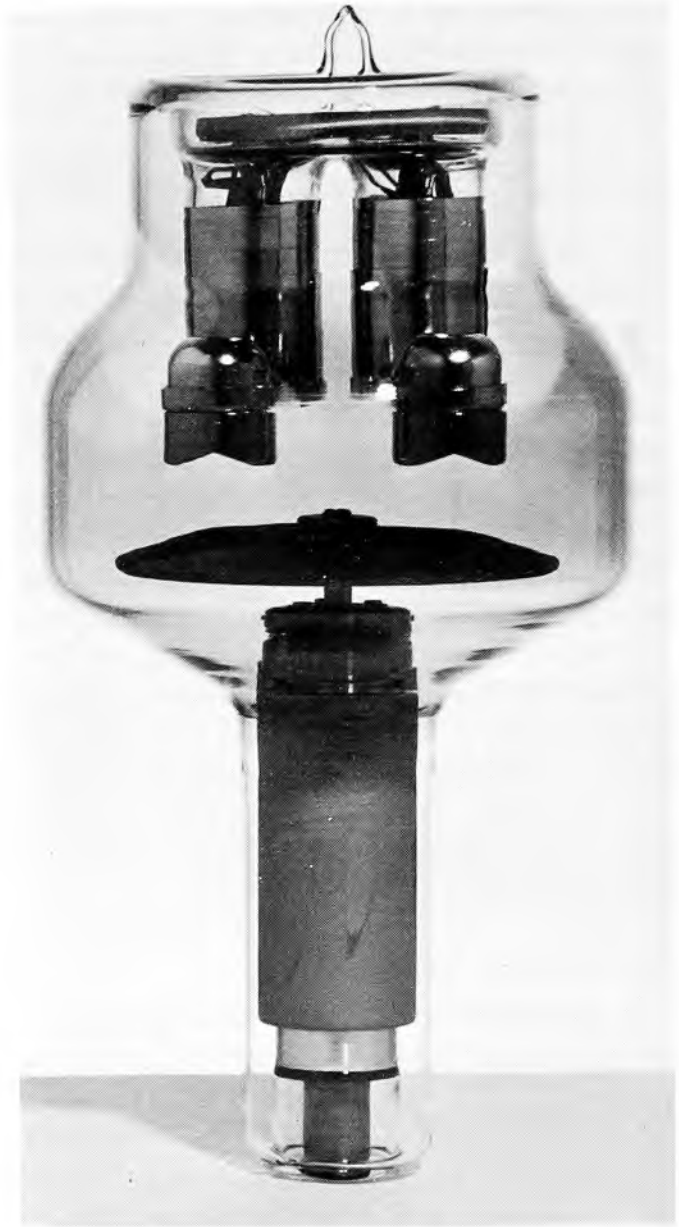


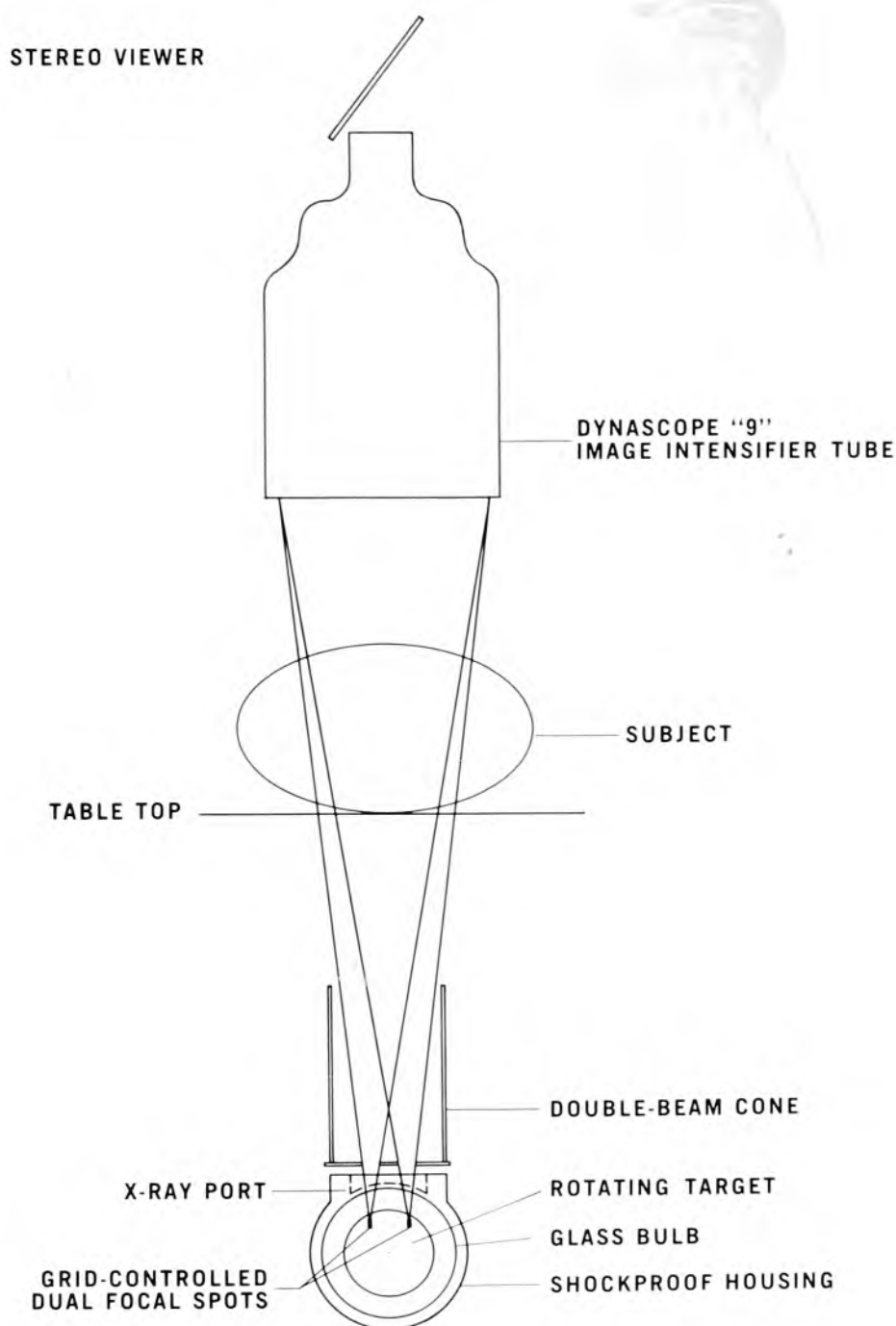
FIG. IV-22. X-ray tube for stereoradiologic examinations (Stereo Dynamax). (Courtesy of Machlett Laboratories, Inc.)

space charge limits the tube current. Space charge limitation in such exposures can be overcome by the use of x-ray tubes in which electrons are extracted from the cathode by field emission.

The principle of field emission was described by R. W. Wood in 1897. An x-ray apparatus which embodies that principle (made by the Field Emission Corporation, McMinnville, Oregon) (Ref. 12) is used for ultrashort (less than $1 \mu\text{sec}$) radiography. The field-emission x-ray tube differs from a conventional x-ray tube mainly by the method used in obtaining the electrons. In the conventional x-ray tube thermal emission is used, while in field emission tubes the electrons are pulled from the cathode, which is not necessarily heated, by means of a high electric field in the vicinity of the cathode. This high electric field is achieved by designing this electrode in the shape of

a sharp metallic needle with a tip diameter of about 1μ (Ref. 13) (Fig. IV-24). Under suitable circumstances, it is possible to draw a current of about 1 A from such a cathode. The current in a field emission tube is not limited by space charge as it is in "hot-cathode" electronic emission (thermionic emission) because the electrons are removed by the high electric field as

FIG. IV-23. Stereofluoroscopy.
(Courtesy of Machlett Laboratories, Inc.)



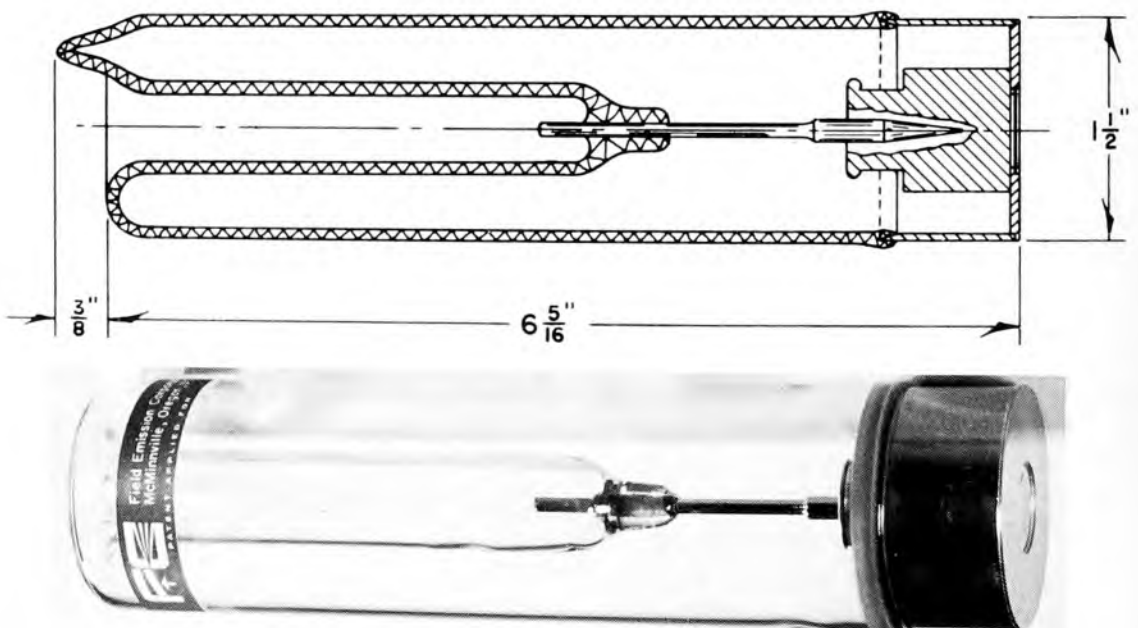
soon as they are pulled off the metal. Field-emission x-ray tubes require a power supply capable of delivering a large amount of energy in an extremely short period of time. Heating the field-emitting cathode increases the current density achieved; this mechanism has been referred to as TF (thermal-field) emission (Ref. 12).

Field-emission x-ray units capable of producing pulses of x-rays considerably shorter than $1 \mu\text{sec}$ are used in radiography of very fast events, such as the detonation of explosive charges, the penetration of bullets in various materials, and the deformation of organs of experimental animals decelerated or accelerated to high G-values (Figs. IV-25 and IV-26). To this date, field-emission x-ray units have not been widely used in diagnostic radiology because they exhibit two drawbacks: (1) the focal spot size in field emission tubes currently available is larger than in conventional x-ray tubes, and (2) these tubes can be operated only at relatively high voltages, which results in the emission of high energy radiation not particularly suited for radiologic examinations.

Monochromatic Radiation X-Ray Tubes

X-radiation with a relatively narrow energy spread over a desired range can be obtained by using an x-ray tube having a target that emits characteristic radiation with the desired energy and by reducing the intensity of the general radiation by filtration. The characteristic radiation emitted by an x-ray target represents only 15 to 20% of the total intensity of the beam

FIG. IV-24. Diagram of photograph of field emission x-ray tube.
(Courtesy of Field Emission Corporation.)



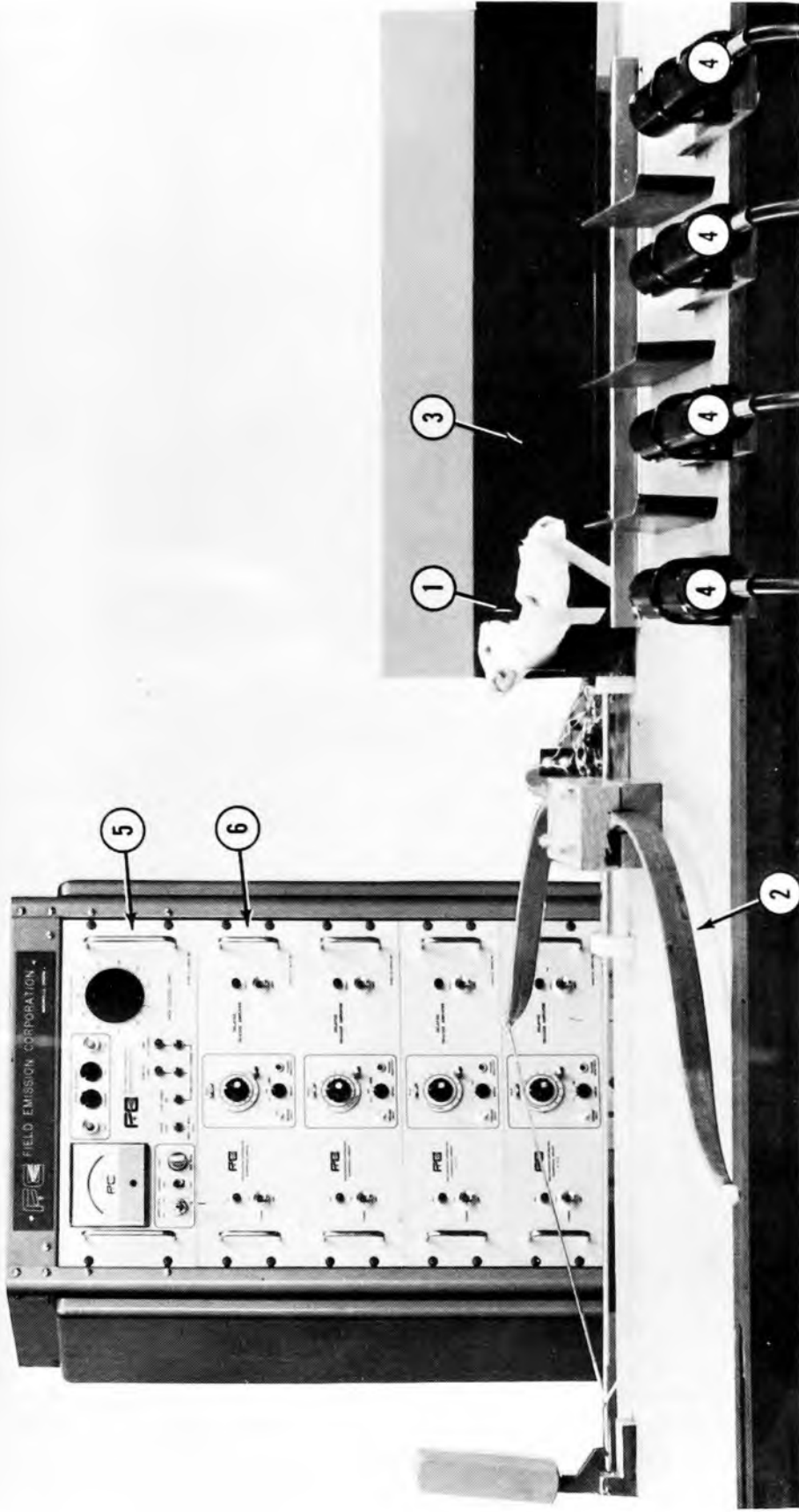


FIG. IV-25. Four-field emission x-ray tube system for the study of the displacement of internal organs under a 30-G acceleration. The four x-ray tubes (4) are located along the track of a guinea pig (1) that is accelerated by a crossbow (2) past a stationary x-ray film (3). The dc supply and the trigger amplifier/delay units are shown at (5) and (6). Pulsers (not shown) are located in the bottom of the cabinet. (Courtesy of Field Emission Corporation.)

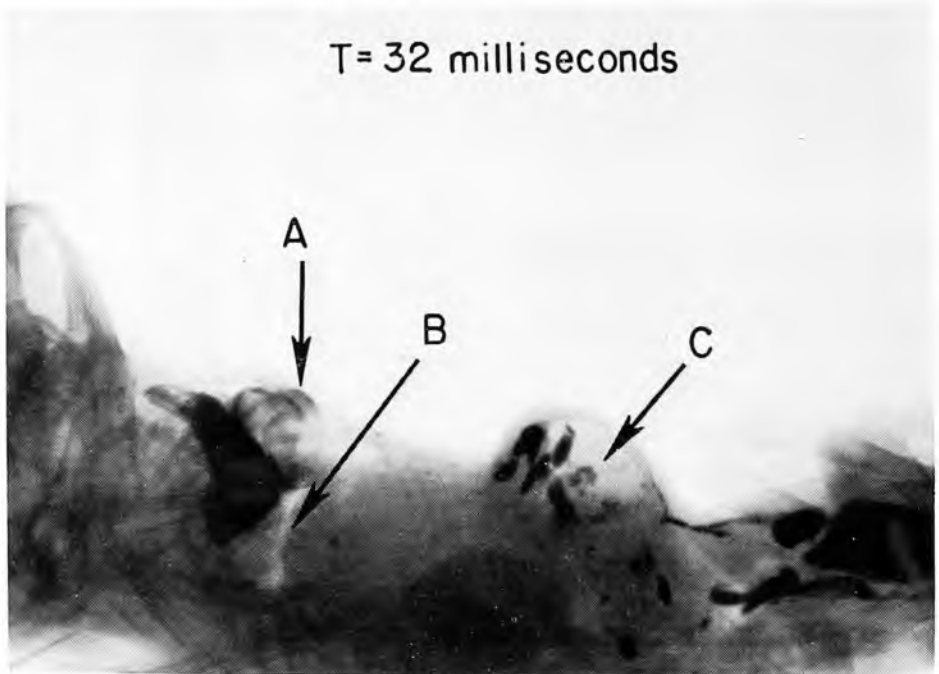
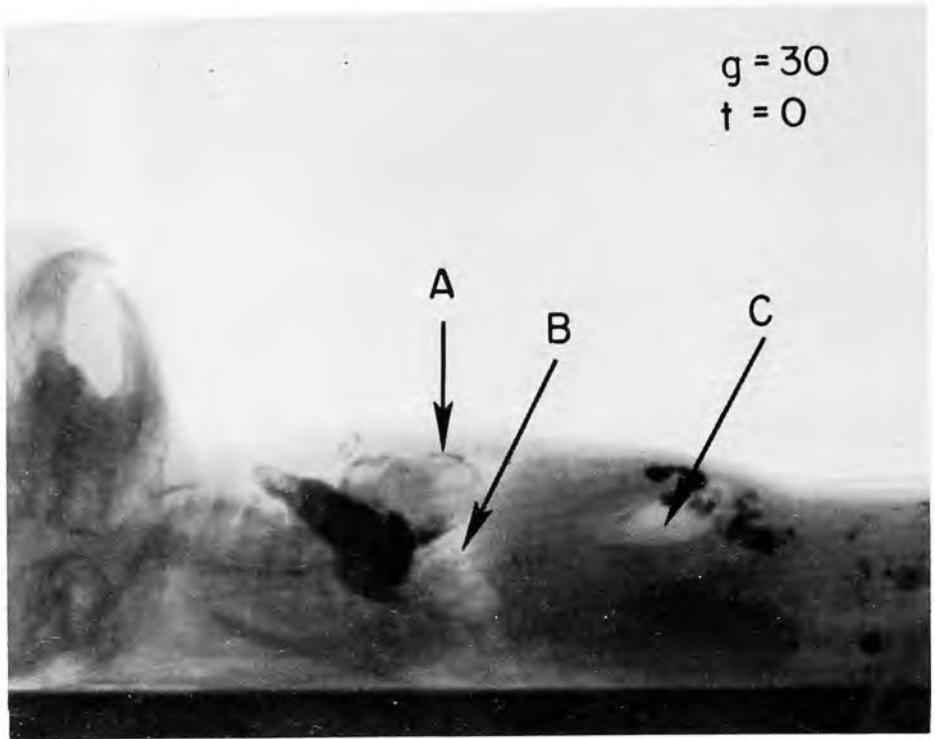


FIG. IV-26. Radiographs obtained with the system shown in Fig. IV-25.
 A compression of the heart
 B motion of diaphragm
 C transposition of a gas bubble and heavy intestine
 (Courtesy of Field Emission Corporation.)

(Ref. 14). This percentage, however, can be enhanced by filtering out a considerable fraction of the photons with greater than required energies by means of an absorber having a photoelectric K-absorption peak at an energy slightly higher than that of the photons to be transmitted. Such higher energy-selective filtration is possible because the photoelectric absorption coefficient for any element passes through a low value for photons with energies slightly lower than the K-binding energy of the absorber. X-ray tubes containing iron, cobalt, chromium, copper, molybdenum, or other metals as targets for the generation of the characteristic radiation of these elements are widely used in x-ray diffraction studies.

A possible value of the use of monochromatic x-rays in diagnostic radiology, as has been pointed out by several authors (Refs. 14-16), lies in the enhancement of radiographic contrast of organs made opaque by contrast media. Radiographs of such organs exhibit particularly high contrast if monochromatic x-rays with an energy matching the absorption peak of the contrast medium are used in preference to polychromatic radiation. Oosterkamp (Ref. 14) has shown that when iodine contrast media are used and a relatively thick part of the body is examined, the use of monochromatic x-rays of suitable energy improves contrast by a factor of approximately 1.5, as compared to conventional polychromatic radiography; the improvement achieved is even higher for thinner parts of the body.

X-ray tubes with either stationary or rotating anodes have been developed for the generation of monochromatic x-rays most suited for high absorption in iodine. The target element used in these tubes is cerium, and the radiation obtained is further monochromatized by filtration with cerium absorbers. Although tests performed with these tubes confirmed the theoretical usefulness of monochromatic radiation, these x-ray tubes proved to be impractical in radiography because of the low intensity of the radiation they are capable of producing. The use of x-ray image intensifiers may render radiography with monochromatic radiation more practical.

X-RAY POWER SUPPLIES—TRANSFORMERS

The high potential difference required to accelerate electrons in an x-ray tube is usually achieved by a transformer. Transformers are also used extensively in x-ray circuits to provide electrical power to the filament of the x-ray tube and to the filaments of the rectifier tubes, if such are used. A transformer is also used in adjusting the voltage supply of the x-ray tube.

A transformer basically consists of a ferromagnetic core with two conductive windings about it. The combination of the iron core and the electrical windings may assume a variety of forms. For example, the two windings may be superimposed, or only a single winding may be used (autotransformer) (Fig. IV-27). One of the windings of the transformer, called the primary winding, is connected to a source of alternating current. The secondary winding is connected to the transformer load.

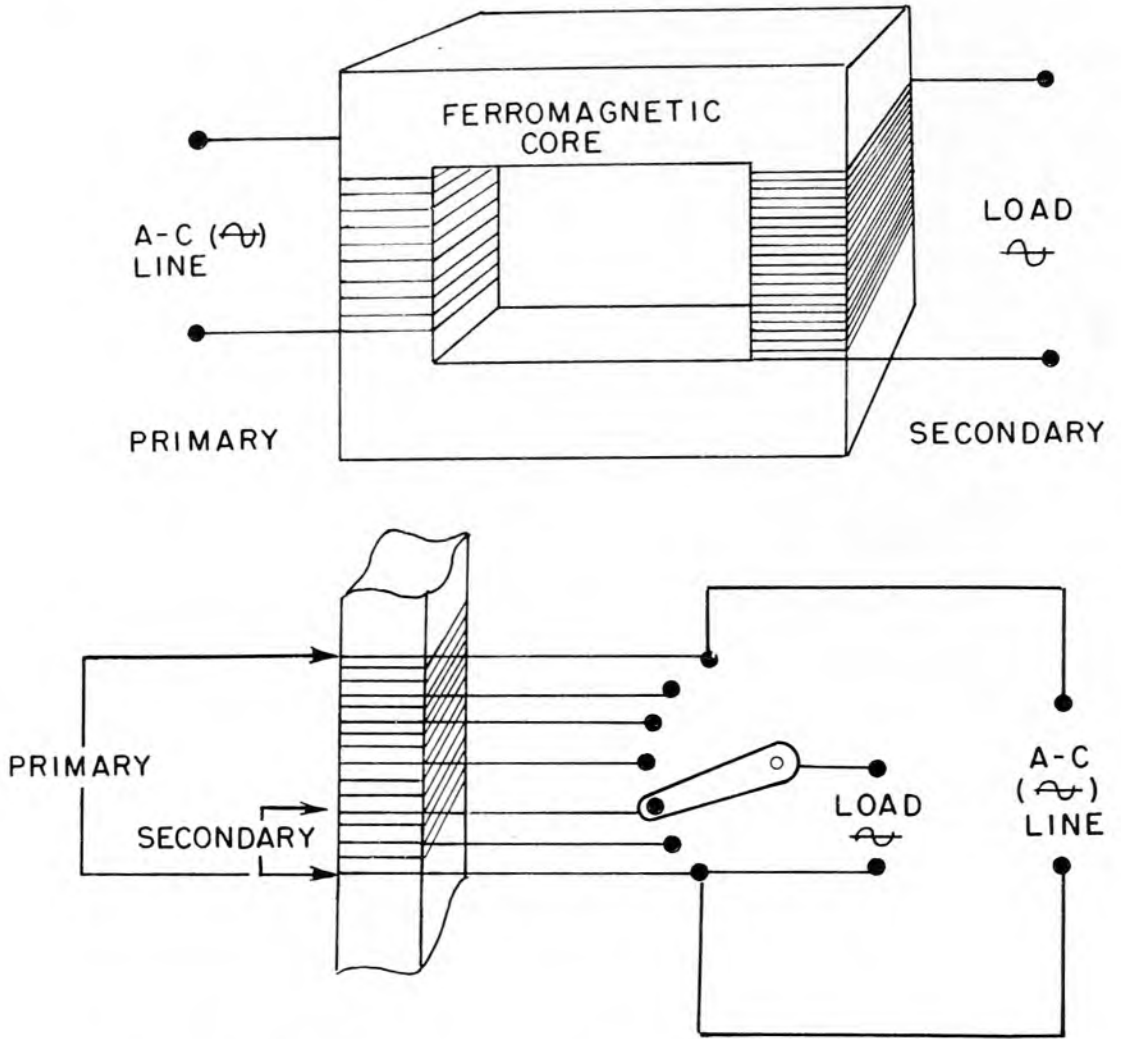


FIG. IV-27. Two-winding transformer (upper) and autotransformer (lower).

A transformer functions as follows: The alternating current flowing through the primary winding produces in the core a magnetic flux that varies cyclicly. The changing flux induces in the primary winding an electromotive force of self-induction, and in the secondary winding an electromotive force of mutual induction. (It should be noted that in a transformer connected to a source of direct current, no electromotive force of induction is observed because the operation of a transformer requires a variable magnetic field.) The voltage induced in the secondary winding of the transformer is equal to the voltage applied to the primary winding multiplied by the ratio of the number of turns of wire in the primary and secondary windings. If the number of turns is greater in the secondary winding, the voltage induced is also greater, and the transformer is a step-up transformer. If the primary winding contains more turns than the secondary winding, the transformer is a step-down transformer.

Transformers function with an efficiency of 90 to 99%. The small power losses are mostly caused by heat generated in the wires (copper loss) or by hysteresis or eddy currents in the magnetic core. Core losses can be minimized by suitable design and by selection of the proper metal. If the secondary winding of a transformer is left open, the electromotive force of self-induction generated in the primary circuit prevents passage of current in this winding, with the exception of a small current due to transformer losses.

High Voltage Transformers

The electric potential difference between the electrodes of an x-ray tube is achieved by means of a step-up high-voltage transformer, which brings a standard ac line voltage of 220 V and usually 60 cycles to the desired voltage of about 100,000 V. The high voltage developed in the secondary winding of such a transformer requires suitable insulation, which is usually achieved by immersing the transformer in oil. In most x-ray generators the midpoint of the secondary winding is grounded. Under such conditions the high voltage is divided into two, one side of the transformer being above ground potential and the other, below. Such a connection simplifies the insulation of the transformer load, balances the circuit with respect to ground, and permits the measurement of the load current at near-ground potential.

It is interesting to note that when x-rays were discovered by Röntgen, the high voltage source used was a special type of transformer called a Ruhmkorff induction coil (see Fig. 0-2). Although the windings are very similar to those of a modern transformer, the current flowing through the primary winding is a direct current interrupted by means of an electric switch, rather than an alternating current.

Autotransformers

The autotransformer is a step-down transformer and is widely used in x-ray circuits to alter the voltage applied to the primary winding of the high voltage transformer. The autotransformer embodies a single winding that is used both as primary and secondary (Fig. IV-27). A series of tabs are provided on the windings, allowing connection in the secondary circuit with a variable number of turns of wire. The fraction of the turns included in the secondary circuit determines the proportion of voltage reduced. The autotransformer provides a method for reducing voltage with very little power loss. If a rheostat were used for the same purpose, a large portion of the electric power would be dissipated in the form of heat.

X-RAY CIRCUITS

The electronic circuitry used in the operation of an x-ray-producing apparatus can be divided into two broad categories: (1) a high voltage circuit, which is at high electrical potential with respect to the ground, and

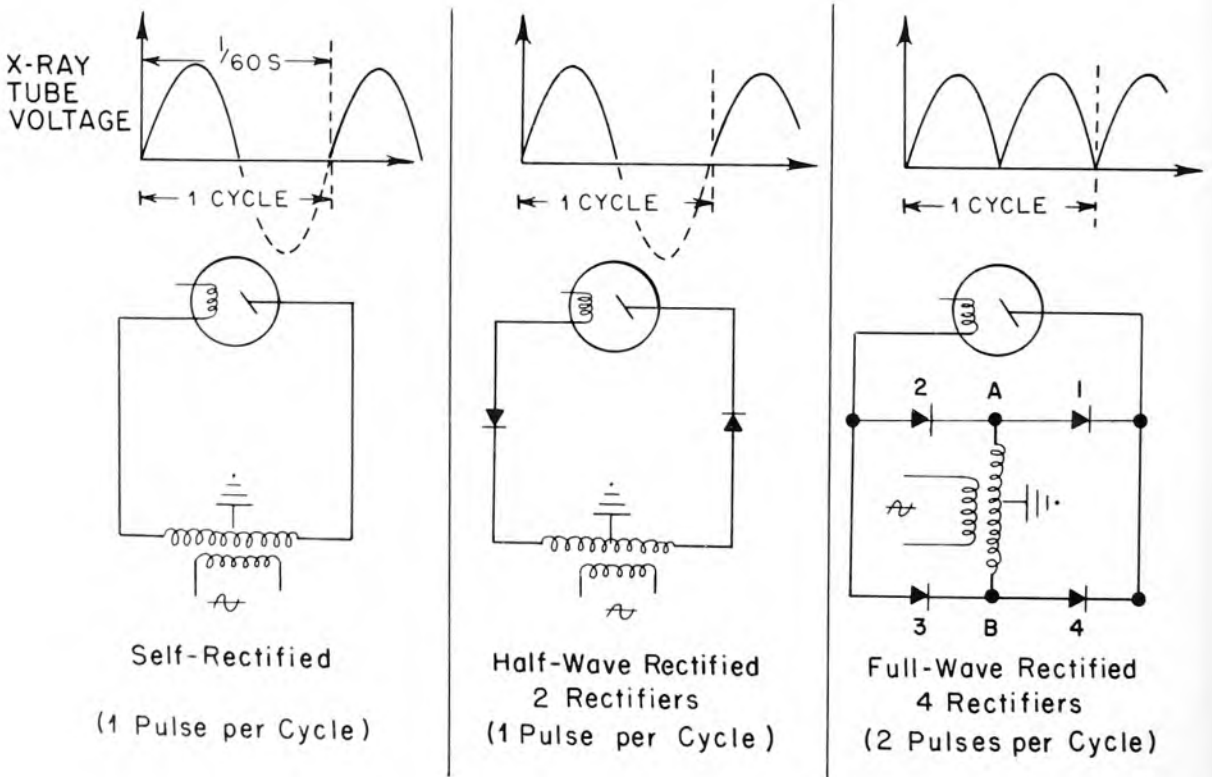
consequently of difficult access during the operation of the apparatus, and (2) a low-voltage primary circuit used to control the radiation beam.

Self-Rectified Circuits

The simplest high voltage circuit used in diagnostic radiology—the self-rectified circuit—consists of an x-ray tube connected to the secondary terminals of a high voltage transformer. The voltage at the secondary terminals of the transformer varies in a sinusoidal manner as a function of time, as shown in Fig. IV-28. However, the flow of electrons in the x-ray tube can take place only when the filament of the tube is at a negative potential with respect to the target. Thus, the x-ray tube conducts and produces radiation only during that half of the ac cycle when the polarity of the high voltage transformer is correct for electron acceleration. During the half-cycle when the target is negative with respect to the filament, the x-ray tube does not conduct, and no current flows through the circuit.

The self-rectified circuit, although very simple, suffers from the following serious deficiency: If a target of the x-ray tube becomes sufficiently hot to emit an appreciable number of electrons, the tube may become conductive during the half-cycle when the target is negative with respect to the filament. During such “back emission” the unfocused electrons may strike the glass envelope and other components of the tube, and damage them. Self-rectified

FIG. IV-28. Single-phase ac diagnostic x-ray circuits.



circuits can be used only for low-capacity x-ray production, and care must be taken to prevent the target from reaching a high temperature.

In the modern radiologic armamentarium, self-rectified circuits are used only in portable x-ray units. Even in these units there is now a tendency to abandon such circuits.

Current Rectifiers

Instead of self-rectified circuits, current rectifiers are included in the x-ray circuit to prevent an x-ray tube from conducting in a direction opposite to the one for which it is designed. A current rectifier is a structure that allows the flow of electricity in only one direction. Two types of rectifiers are commonly used in x-ray circuits: (1) vacuum tube rectifiers, and (2) solid state or barrier rectifiers.

Vacuum Tube Rectifiers (Thermionic Rectifiers, or Valve Tubes). A vacuum tube rectifier is usually composed of an evacuated glass envelope containing two electrodes: (1) the filament (cathode), usually made of tungsten (sometimes thoriated to increase electronic emission), and (2) the anode (or plate), which may be constructed in a variety of shapes and which is generally made of tantalum (Fig. IV-29). The vacuum tube rectifier functions in a manner similar to an x-ray tube placed in a self-rectified circuit. The filament of the rectifier tube is heated and emits electrons. If a potential difference is established between the anode and the cathode, a current flows through the tube, but only if the filament is at a negative potential with respect to the plate. If this condition is not fulfilled, the rectifier does not allow passage of current.

The vacuum-tube rectifier cathode is designed to produce a large number of electrons, and the anode presents a large surface placed as close to the cathode as arcing allows. Such a design results in low electrical resistance: a small drop in potential between the cathode and the anode (of the order of 2 to 3 kV) is sufficient to cause current to flow. A low "voltage drop" in a rectifier is desirable because this drop lowers the voltage applied to the x-ray tube.

When a vacuum tube rectifier is placed in an x-ray circuit the potential difference causing current to flow through the circuit is approximately 50 times greater in the x-ray tube than in the rectifier. Thus, the amount of electrical energy dissipated in the form of heat in the anode of a rectifier is relatively low as compared to the energy dissipated in the x-ray tube anode. Inasmuch as this energy is measured by the drop of potential across the tube multiplied by the intensity of the current circulating through it, in a typical situation the energy dissipated in the x-ray tube is about 50 times greater than that dissipated in the vacuum tube rectifier.

Vacuum tube rectifiers are rated in terms of maximum inverse voltage (voltage applied with a polarity opposite to the operation of the rectifier) and maximum load current, the latter for continuous and intermittent loads.

Vacuum tube rectifiers emit x-rays owing to the deceleration of electrons in the plate. Although the energy and the intensity of the radiation thus produced are low because of the low accelerating voltage in the rectifier (about 2 to 3 kV), vacuum tube rectifiers may present a certain radiation hazard and must be shielded.

Solid State (or Barrier Layer) Rectifiers. Solid state rectifiers are based on the property of certain semiconductors to exhibit a lower resistance to

FIG. IV-29.

- A vacuum rectifier (valve tube) commonly used in radiology
B radiograph showing the filament structure

A



B



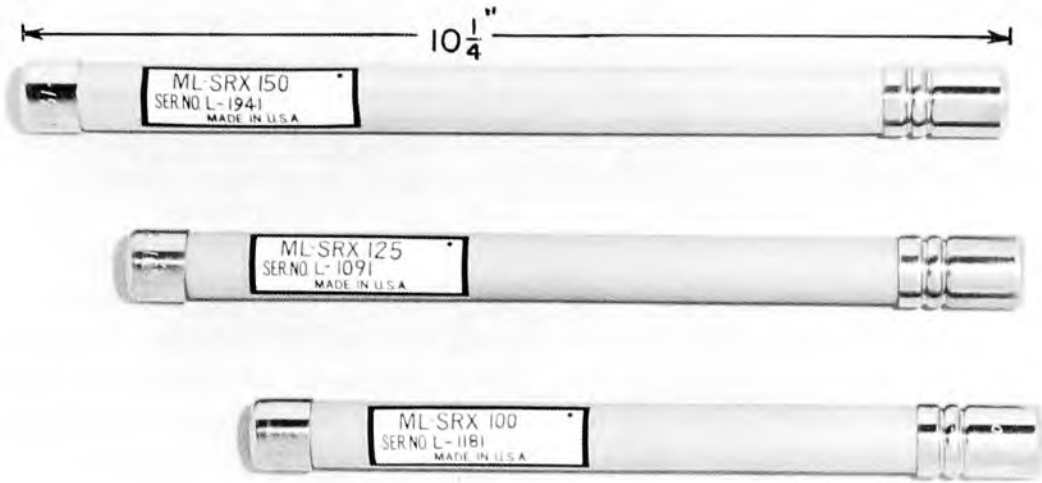


FIG. IV-30. Silicon rectifiers.
(Courtesy of Machlett Laboratories, Inc.)

the passage of electric current in one direction than in the opposite direction. Substances such as selenium, copper oxide, germanium, and silicon exhibit this property.

Selenium solid state rectifiers are widely used in x-ray circuits. They are composed of a thin deposit of selenium on an aluminum plate covered by a thin layer of tin-cadmium alloy (Ref. 17). Such a cell conducts in one direction readily but can withstand a difference of potential of approximately 60 V in the opposite direction. By stacking a sufficient number of such cells, it is possible to obtain a rectifier capable of withstanding the high voltages used in x-ray circuits. For example, a stack capable of withstanding a 100 kV_p inverse voltage contains about 1600 cells (100,000 V/60 V per cell). Selenium rectifiers suffer from the disadvantage of exhibiting an undesirably greater forward voltage drop than vacuum tube rectifiers.

More recently, silicon rectifiers suitable for x-ray high-voltage circuits have become available (Fig. IV-30). These rectifiers have a particularly low voltage drop (of the order of 200 V), which is considerably lower than that of selenium rectifiers or even vacuum tube rectifiers. Silicone rectifier cells (also called junctions) can withstand a considerably higher maximum inverse voltage (10 to 20 times higher) than selenium rectifiers. This property allows the construction of compact solid state rectifiers. Silicone rectifiers are so superior to any other form of rectification currently available that they probably will, in spite of their price, completely replace vacuum tube rectifiers.

Half-Wave Rectified Circuits

Half-wave rectified x-ray circuits have one or more frequently two rectifiers, usually of the vacuum tube type, interposed between the x-ray tube

and the secondary winding of the high voltage transformer, as shown in Fig. IV-28. The rectifiers allow the flow of electrons in the x-ray circuit during the half-cycle when the polarity of the transformer terminals is suitable for the production of x-rays, and they protect the x-ray tube against back currents during the other half of the cycle. Half-wave rectified x-ray circuits are not used to any appreciable extent in diagnostic radiology.

Full-Wave Rectified Circuits

Both self-rectified and half-wave rectified circuits supply the x-ray tube with a power of correct polarity only during one half-cycle of the alternating current provided by the transformer, and radiation is produced only during this half of the ac cycle. The full-wave rectified circuit corrects this situation by reversing the polarity of the connections between the x-ray tube and the secondary winding of the high voltage transformer during each half-cycle. This is accomplished by the use of four rectifiers connected as shown in Fig. IV-28. The circuit functions as follows: When terminal A of the secondary winding of the high voltage transformer is positive, rectifiers 1 and 3 conduct, connecting the anode of the x-ray tube to terminal A and the cathode of the x-ray tube to terminal B. During this half-cycle rectifiers 2 and 4 do not conduct and thereby isolate the anode from terminal B and the cathode from terminal A. During the following half-cycle terminal A is negative and terminal B is positive, and rectifiers 2 and 4 conduct, connecting the cathode to terminal A and the anode to terminal B. Rectifiers 1 and 3 do not conduct during the second half-cycle.

Thus, an x-ray tube connected to a full-wave rectified circuit utilizes the complete cycle of the alternating current supplied by the transformer. It should be noted, however, that the voltage across the x-ray tube varies from zero to the maximum potential and then back to zero during each half-cycle, as is the case in half-wave and self-rectified circuits.

Full-wave rectified circuits are widely used in medium- and high-capacity x-ray circuits. Most of the diagnostic x-ray examinations carried out in this country are performed by means of full-wave rectified x-ray circuits.

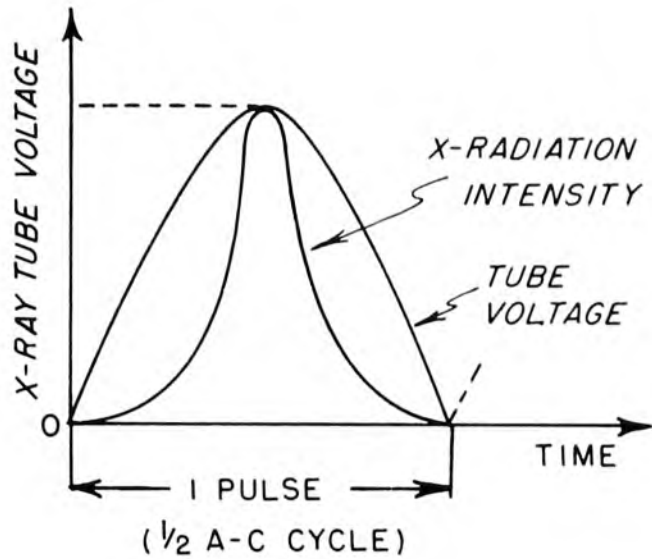
Three-Phase Circuits

All the x-ray circuits so far described supply the x-ray tube with voltages that vary continuously between zero and the maximum voltage supplied by the transformer. This variation in voltage has the following disadvantages:

1. During the portion of the cycle when the voltage is appreciably lower than the maximum value at the crest of the cycle, x-rays are produced with low efficiency and the accelerated electrons contribute mostly heat to the target (Fig. IV-31). Because heat tube ratings impose stringent limits on radiologic examinations, such waste of the heat storage of the tube is undesirable.

2. Most of the low-energy x-radiation produced during the lower voltage

FIG. IV-31. Generation of x-rays by pulsating voltage.



portion of the cycle is absorbed either by the tube housing, the filter, or, which is worse, by the patient, and contributes little to the examination.

3. The intensity of the radiation produced is lowered by the fact that no radiation is generated during a large part of the exposure time.

4. The timing of short radiographic exposures is complicated by the necessity of synchronizing them with the sine waves of the alternating voltage.

The generation of constant or nearly constant potential for x-ray tubes in diagnostic radiology can be accomplished by the rectification of three-phase alternating current.

Normal household alternating current, as obtained from a two-conductor electric line, is referred to as single-phase alternating current. In a single-phase source of electricity, both the voltage and the current vary between the two connectors as a sine function of time. Three-phase electric current is transported by means of three wires in such a fashion that the sinusoidal variation of the current is out of phase by one-third of one cycle between any set of two wires; so that, if the duration of one cycle is $\frac{1}{60}$ sec, the two currents are $\frac{1}{180}$ sec out of phase (Fig. IV-32). Any set of two conductors of a three-phase line supplies single-phase alternating current. Alternating current is usually generated and transported in three-phase form, and single-phase current is obtained by tapping two conductors of a three-phase line.

The generation and transmission of electric power as a three-phase alternating current presents many practical advantages over single-phase alternating current. Three-phase current is also more convenient than single-phase for energizing high-power electric motors; for that reason, three-phase alternating current is usually available in areas where high electric power is required.

Three-phase transformers have three primary windings and three secondary windings. These windings may be connected in star, Y, or delta

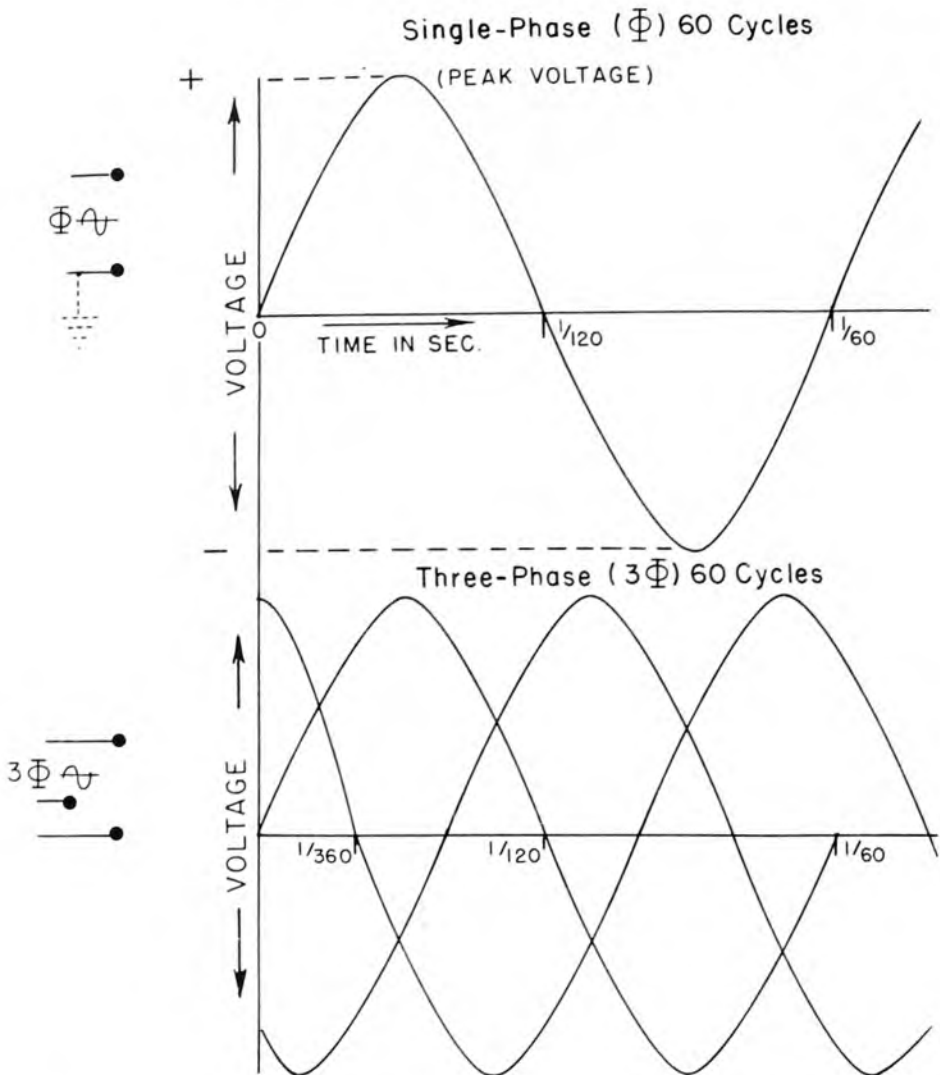


FIG. IV-32. Voltage variation as a function of time in single-phase and three-phase currents.

fashion (Fig. IV-33). Two types of three-phase circuits are of interest in diagnostic radiology: six-pulse and 12-pulse circuits.

Six-Pulse Six-Rectifier Circuits. A three-phase six-pulse circuit is shown in Fig. IV-34.

The primary winding of the high voltage transformer in this circuit is connected in delta fashion, and the secondary in star fashion. The rectification is achieved by means of six solid state rectifiers; vacuum tube rectifiers are generally not used in three-phase circuits.

This circuit supplies six pulses of voltage to the x-ray tube per ac cycle. (For comparison, a single-phase full-wave rectified circuit supplies two pulses per cycle.) The theoretical variation of the voltage supplied by the circuit to the tube (voltage ripple) is about 13% of the maximum (as compared to

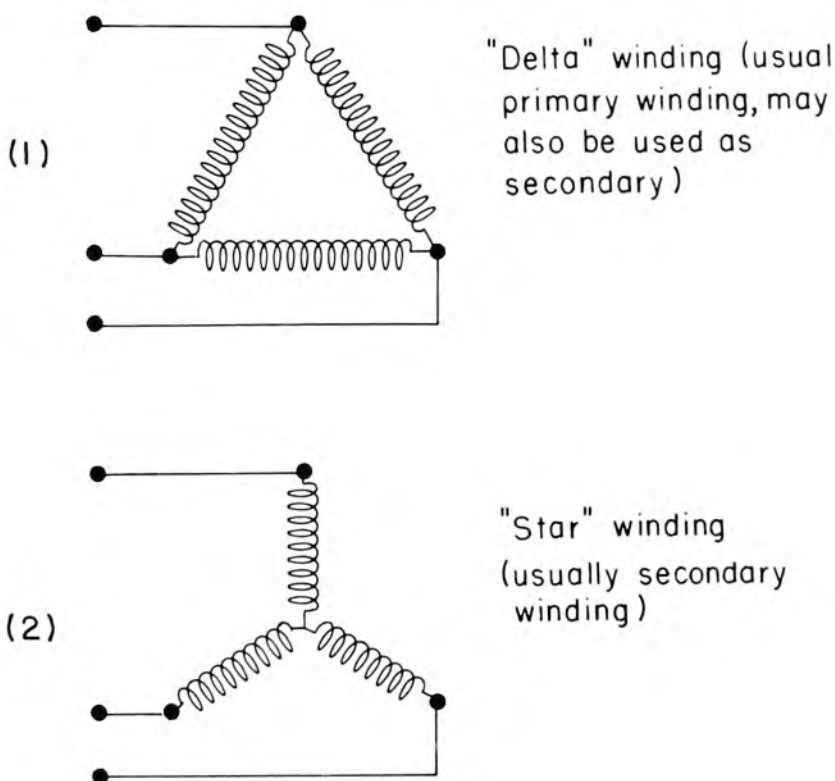
100% for a two-pulse circuit) (Fig. IV-35). One of the deficiencies of this circuit is that it is not balanced with respect to ground.

Six-Pulse Twelve-Rectifier Circuits. This circuit (Fig. IV-34) utilizes a transformer with two secondary windings in phase and 12 rectifiers. The rectification achieved by this circuit is six pulses per cycle. This circuit is an improvement over the six-pulse six-rectifier circuit because it is balanced with respect to ground.

Twelve-Pulse Twelve-Rectifier Circuits. This circuit (Fig. IV-34) utilizes a transformer with a primary winding connected in delta, and two secondaries one of which is delta-connected and the other, star-connected. This arrangement can be regarded as being composed of two separate six-pulse transformers which are out of phase with one another by one-twelfth of one cycle. The rectification of these 12 pulses results in a voltage as shown in Fig. IV-35. The ripple of this voltage is only 3%, and for practical purposes the tube potential is constant.

Three-phase circuits in x-ray apparatus present a certain number of complications as compared to single-phase circuits: (1) The adjustment of the primary voltage in three-phase circuits requires the use of three autotransformers. (2) A more serious difficulty is encountered in starting and terminating an exposure. In inductive circuits, such as transformers, it is always desirable to close or open a switch, interrupting or making the circuit, only

FIG. IV-33. Three-phase transformer windings.



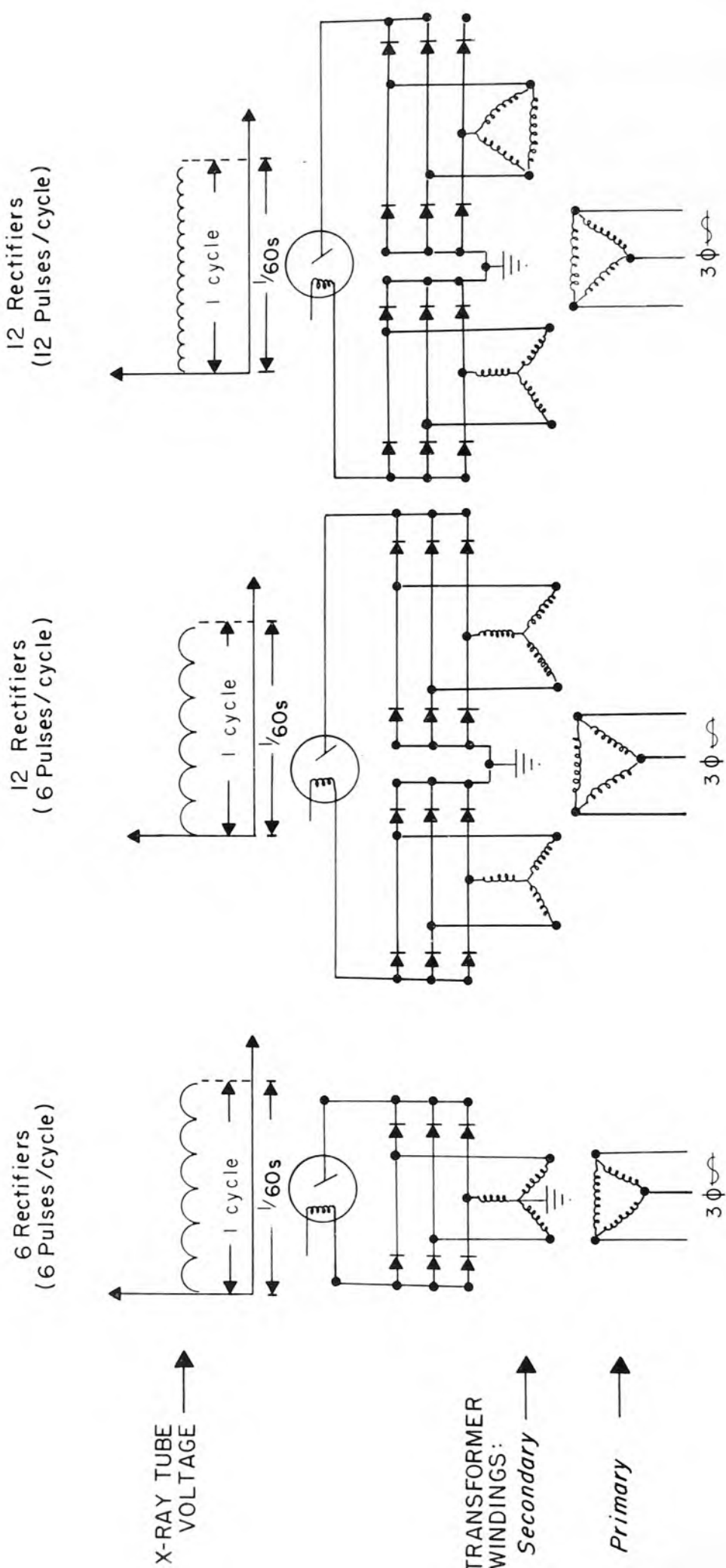


FIG. IV-34. Three-phase ac circuits used in diagnostic radiology.

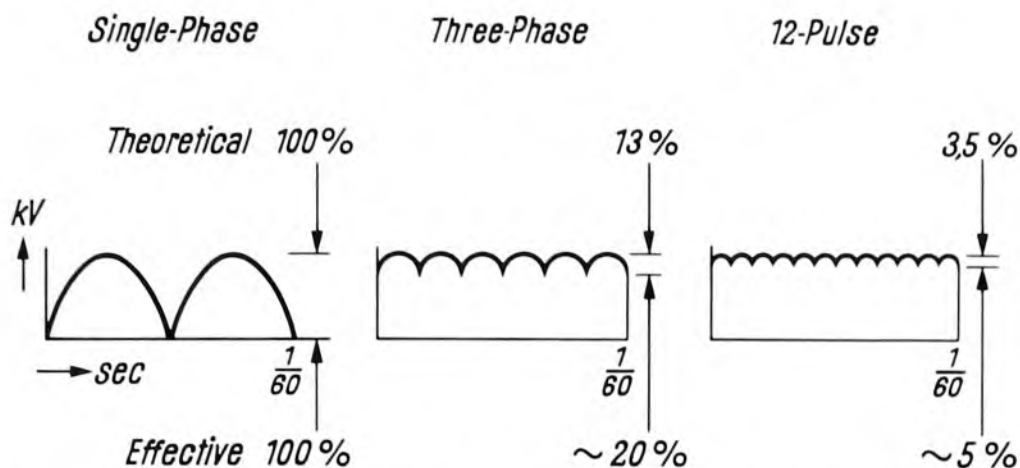


FIG. IV-35. Voltage (dc) ripple in single-phase two-pulse and three-phase 12-pulse circuits. (Courtesy of Siemens Company.)

at zero load in order to prevent surges of current that may damage some components of the circuit. In a single-phase circuit, contacting is made when the voltage passes through a zero value (every $\frac{1}{120}$ sec). In a three-phase circuit, when one of the phases reaches a zero value, the other two are at about 85% of peak value, and contacting at zero load is not possible. This difficulty is solved by phasing in the contactors in such a fashion that they open and close in sequence rather than simultaneously. This method of contacting reduces the transient currents without suppressing them completely. These transients are further dampened by the relatively high resistance of the selenium rectifiers commonly used in these circuits, and which act as surge suppressors.

Three-phase circuits offer the following advantages over single-phase power supplies: (1) They supply more power to the x-ray tube per unit time and therefore allow for shorter exposures (Fig. IV-36). (2) The intensity of the x-radiation generated for a given tube current is considerably higher. (3) The radiographic quality of the x-radiation produced by a three-phase circuit is superior because it contains less soft radiation. (4) With a three-phase circuit the x-ray tube is utilized more efficiently because its target is not subjected to low energy electrons, which use up the heat storage of the tube while emitting little x-radiation (Fig. IV-37).

When particularly high intensity radiation is required in diagnostic examinations, three-phase equipment offers an excellent solution to the problem because of the high radiation output for a given tube current.

Switching Tube X-Ray Circuits (Dyapulse Circuits)

In most x-ray circuits the exposure is controlled by a contactor placed in the primary circuit (low voltage) of the high voltage transformer. The purpose of the contacting system is to phase the instant of contact with the sine

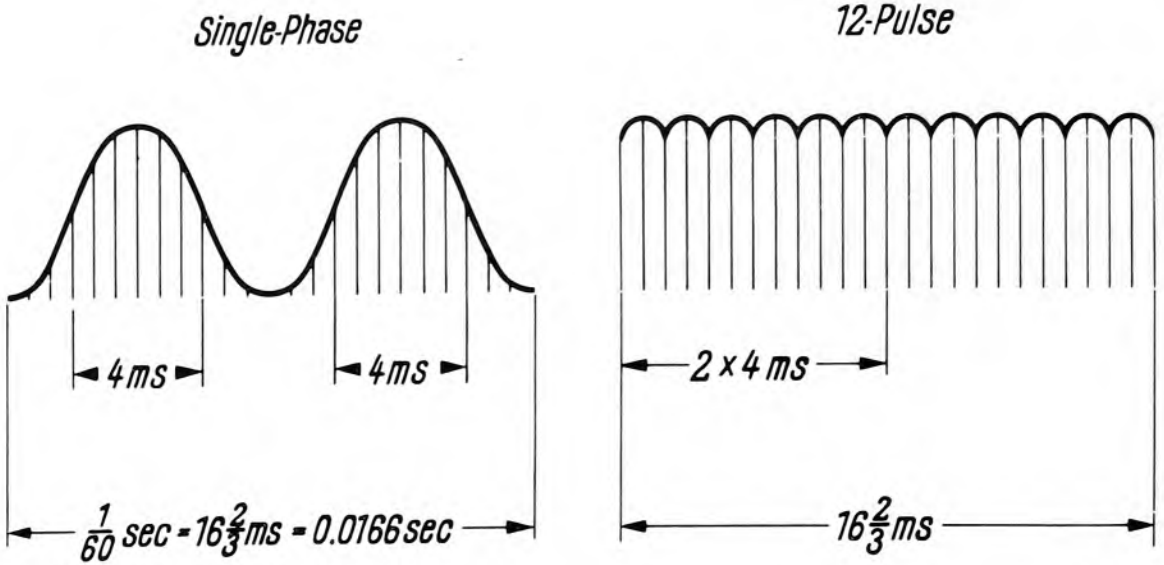
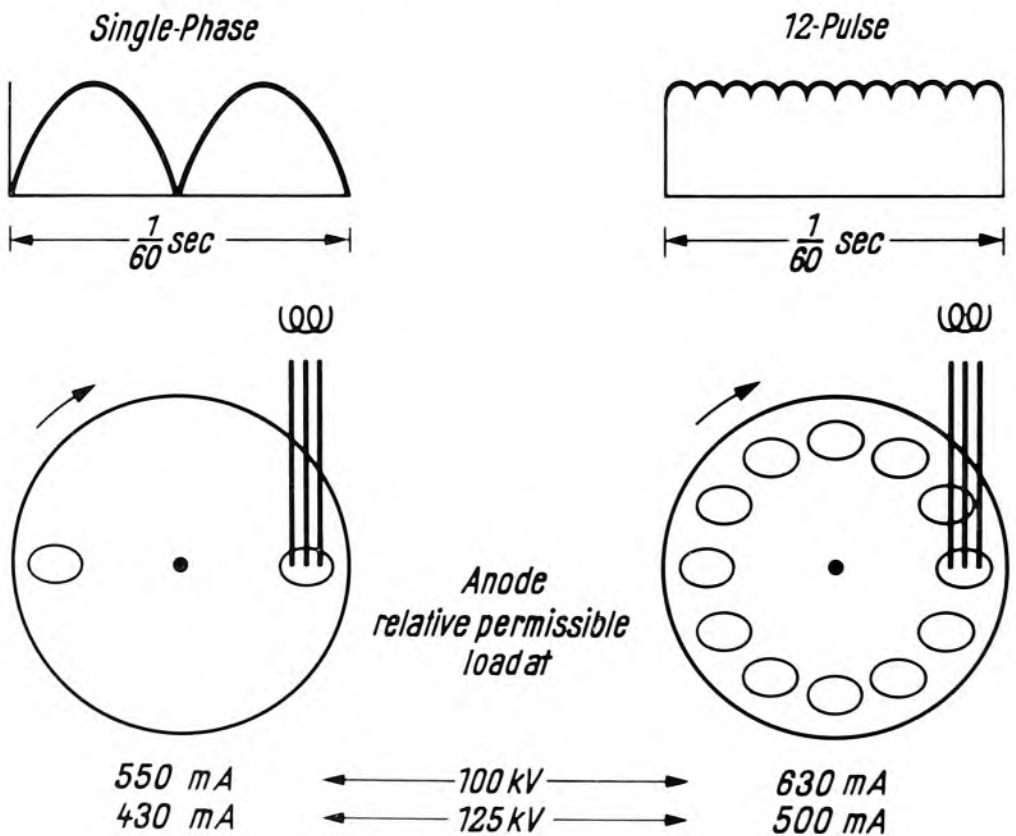


FIG. IV-36. Radiographic exposure with single-phase and three-phase 12-pulse circuits. (Courtesy of Siemens Company.)

FIG. IV-37. Tube loading for single-phase and three-phase 12-pulse circuits. (Courtesy of Siemens Company.)

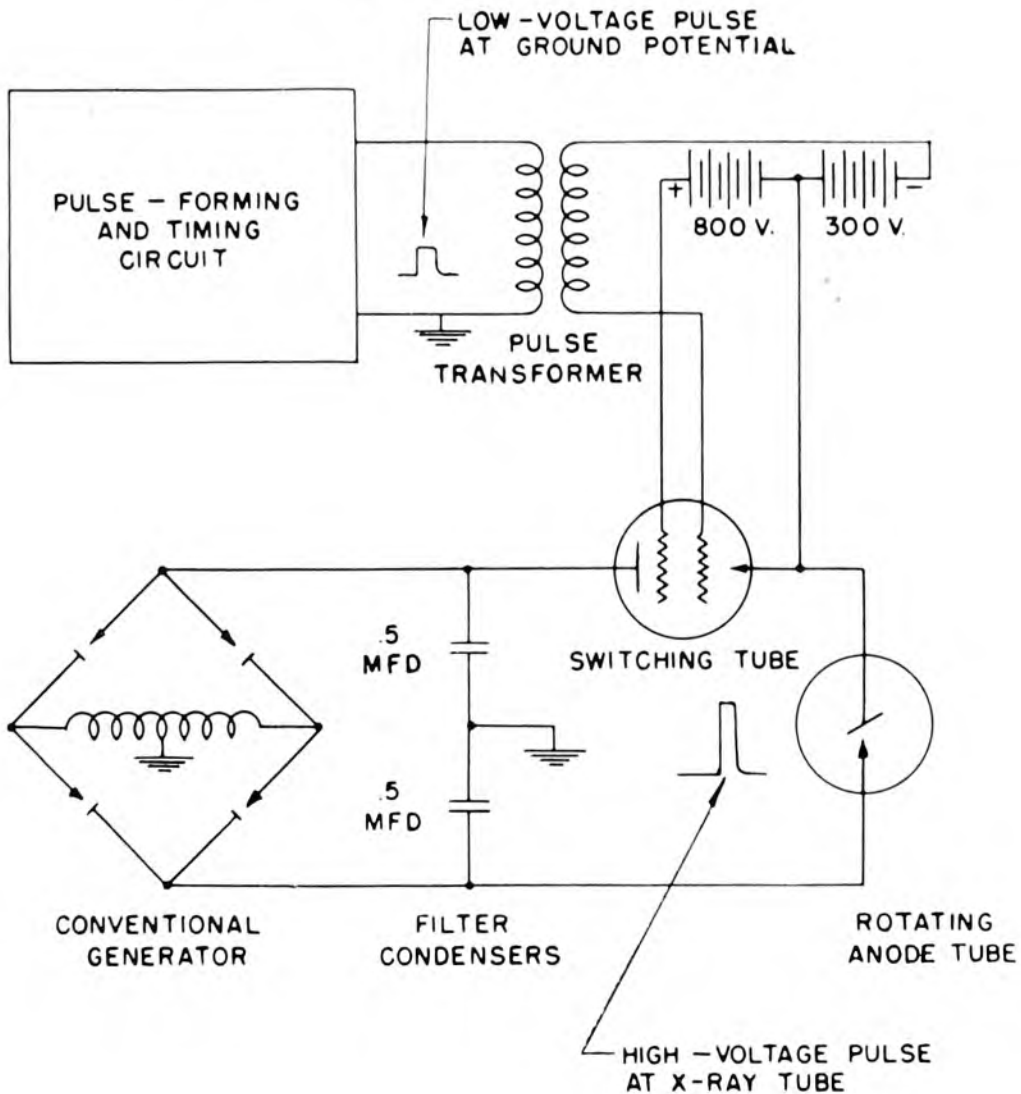


wave input voltage in such a fashion that contact is either made or interrupted when the load of the secondary circuit is at its minimum value. This phasing is done to avoid potentially harmful current transients (Ref. 18). In general, it limits the possible exposures to integral multiples of one half-cycle duration for the ac current used. With a single-phase 60-cycle input, the useful exposure is limited to approximately $\frac{1}{120}$ sec. (The half-cycle $\frac{1}{120}$ sec exposure is equal in effect to a $\frac{1}{240}$ sec exposure because radiographically effective radiation is produced only during approximately one-half of the pulse.) The 12-pulse three-phase system described in the previous section allows exposures of the order of $\frac{1}{360}$ sec. Even shorter exposures have been obtained with three-phase circuits by increasing the frequency of the ac current used.

(3) Another method of obtaining exposures of the order of 0.001 sec consists

FIG. IV-38. "Dynapulse" switching circuit.

(Courtesy of Machlett Laboratories, Inc.)



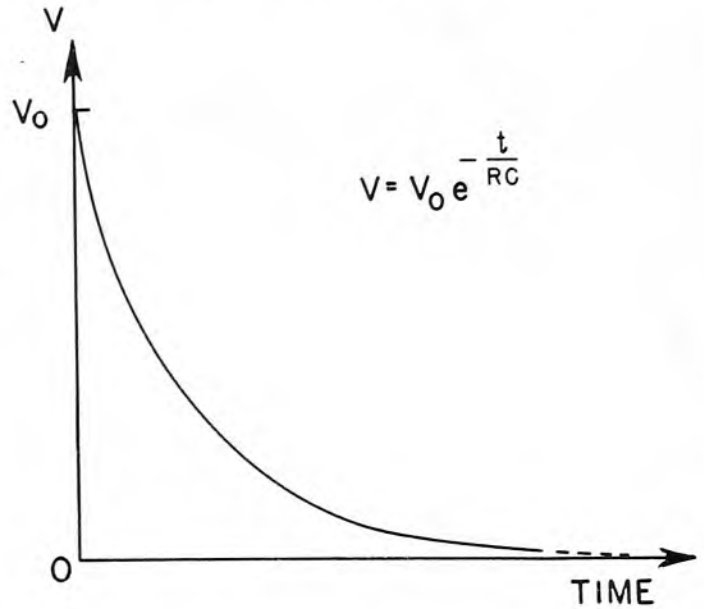


FIG. IV-39. Discharge of a capacitor.

in placing the x-ray switch on the high voltage side of the circuit. Mechanical switches are inadequate for this purpose; controlled electron-flow vacuum tubes (switching tubes) are employed.

Figure IV-38 shows a high-voltage electronic switching tube x-ray circuit ("Dynapulse" circuit). In this circuit the high voltage is supplied to the x-ray tube by means of capacitors that are charged by a transformer-rectifier combination. The switching is achieved by means of a high-voltage switching tetrode and the exposure is controlled by means of a circuit that controls the grids of the switching tube. The purpose of the capacitors in the circuit is to supply the needed power to the x-ray tube independently of ac cycling.

A capacitor is a structure capable of storing electricity and delivering it when needed. It is composed of two electrical conductors, which may assume a variety of shapes, separated by an insulator (dielectric). When a potential difference V is established between the electrodes of a capacitor, the capacitor acquires a charge Q as follows:

$$Q = CV,$$

where C is a constant characterizing the capacitor, called the capacitance. Theoretically, a capacitor can be made to store a charge as great as desired by increasing the potential difference. In practice, the potential difference is limited by the insulation between the electrodes.

When a charged capacitor is connected to a resistor (or any other load), the electrical charge escapes the capacitor and the potential difference between its electrodes decreases exponentially as a function of time (t) according to the equation

$$V = V_0 e^{-t/RC},$$

where V_0 is the potential difference between the electrodes of the capacitor at time 0, R is the resistance of the resistor, and C is the capacitance of the capacitor (Fig. IV-39).

The Dynapulse circuit shown in Fig. IV-38 consists of the following elements: (1) a high-voltage full-wave rectified circuit charging continuously, (2) two capacitors which discharge into the x-ray tube when the switching tube is conducting, and (3) an electronic switching tube.

The switching tube is a four-electrode vacuum tube (tetrode) the conductivity of which is controlled by a pulse-forming circuit. The x-ray tube is energized for periods of time so short that the potential difference across the condenser does not drop appreciably and the x-ray tube is energized by what amounts to a constant potential. Oscilloscope tracings of the voltage supplied by the condensers are shown in Fig. IV-40. In typical exposures carried out with a dynapulse circuit, which are of the order of a few milliseconds, the voltage applied to the x-ray tube drops only a few percent of the maximum value.

The dynapulse circuit allows frequent high-intensity short x-ray exposures that are impossible with other circuits of identical capacity. Repetitive exposures with the dynapulse circuit are limited by the rate of recharge of the capacitors by the generator.

Dynapulse circuits are particularly useful in radiologic examinations when extremely short exposures are desirable, particularly in serial angiography.

X-RAY GENERATOR RATINGS

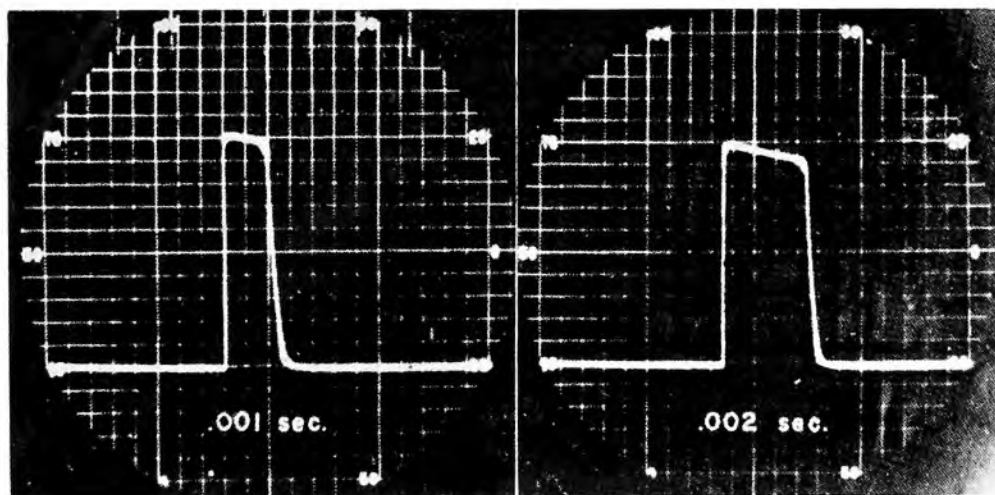
X-ray generators are rated on the basis of the maximum voltage they can supply and the maximum electrical power they can deliver. The electrical power supplied by a generator is proportional to the difference of potential multiplied by the current flowing through the circuit. Therefore, the maximum current that a generator can withstand without damage varies with

FIG. IV-40. Oscilloscope tracings of potential applied to x-ray tube by "Dynapulse" circuit for:

Left 0.001-sec exposure

Right 0.002-sec exposure

(Courtesy of Machlett Laboratories, Inc.)



the voltage at which it is operated. A typical x-ray generator may be rated as follows:

$$\begin{array}{l} \text{Maximum voltage—150 kV} \\ \text{Maximum currents—} \left\{ \begin{array}{l} 500 \text{ mA at 150 kV} \\ 800 \text{ mA at 125 kV} \\ 1000 \text{ mA at 100 kV or below} \end{array} \right. \end{array}$$

X-RAY AUXILIARY CIRCUITS

A typical circuit for a diagnostic x-ray unit is shown in Fig. IV-41. In addition to the high voltage circuit, the operation of the unit requires additional electrical power to heat the filaments of the x-ray tube and of the vacuum rectifiers. Because the input power of an x-ray installation is ac, this form of current is used for heating the filaments. Typically, the current flowing through an x-ray tube filament varies approximately from 2 to 6 A with an applied voltage of about 3 to 14 V. The rectifier tube filaments are operated at about 10 V and circulate approximately 10 to 12 A.

The electrical power for both x-ray and rectifier filaments is supplied by means of step-down transformers which reduce the input voltage to the desired value. The input power is often supplied by a winding of the auto-transformer. It should be noted that both the x-ray and the valve tube filaments are periodically at high voltage with respect to the ground potential, and therefore the step-down transformers used to energize the filaments must be insulated for these voltages. This purpose is achieved by separating the secondary winding of the step-down transformer from the iron core by a distance of several inches and by immersing the whole transformer in a bath of insulating oil.

The rectifier filament is operated at constant current. The current flowing through the x-ray tube filament, on the other hand, is varied to control the x-ray tube current. The x-ray filament current may be controlled by altering the primary voltage applied to the step-down filament transformer by means of different resistors connected in series in the circuit (see Fig. IV-41). This control is critical because a small variation of the x-ray filament current results in a large variation of the x-ray tube current. In some x-ray installations the filament transformer current is indicated on a meter.

The x-ray tube current can be measured by connecting a milliammeter anywhere in the circuit of the secondary winding of the high voltage transformer. It is, however, undesirable to place the meter in a portion of the circuit that is at a high potential with respect to ground, because the insulation of such a meter from the ground potential would present serious problems. To alleviate this difficulty, the milliammeter measuring the tube current is generally placed close to the ground potential, as shown in Fig. IV-41, where the insulation of the meter need not exceed a few volts.

The voltage applied to the x-ray tube could be measured by installing a

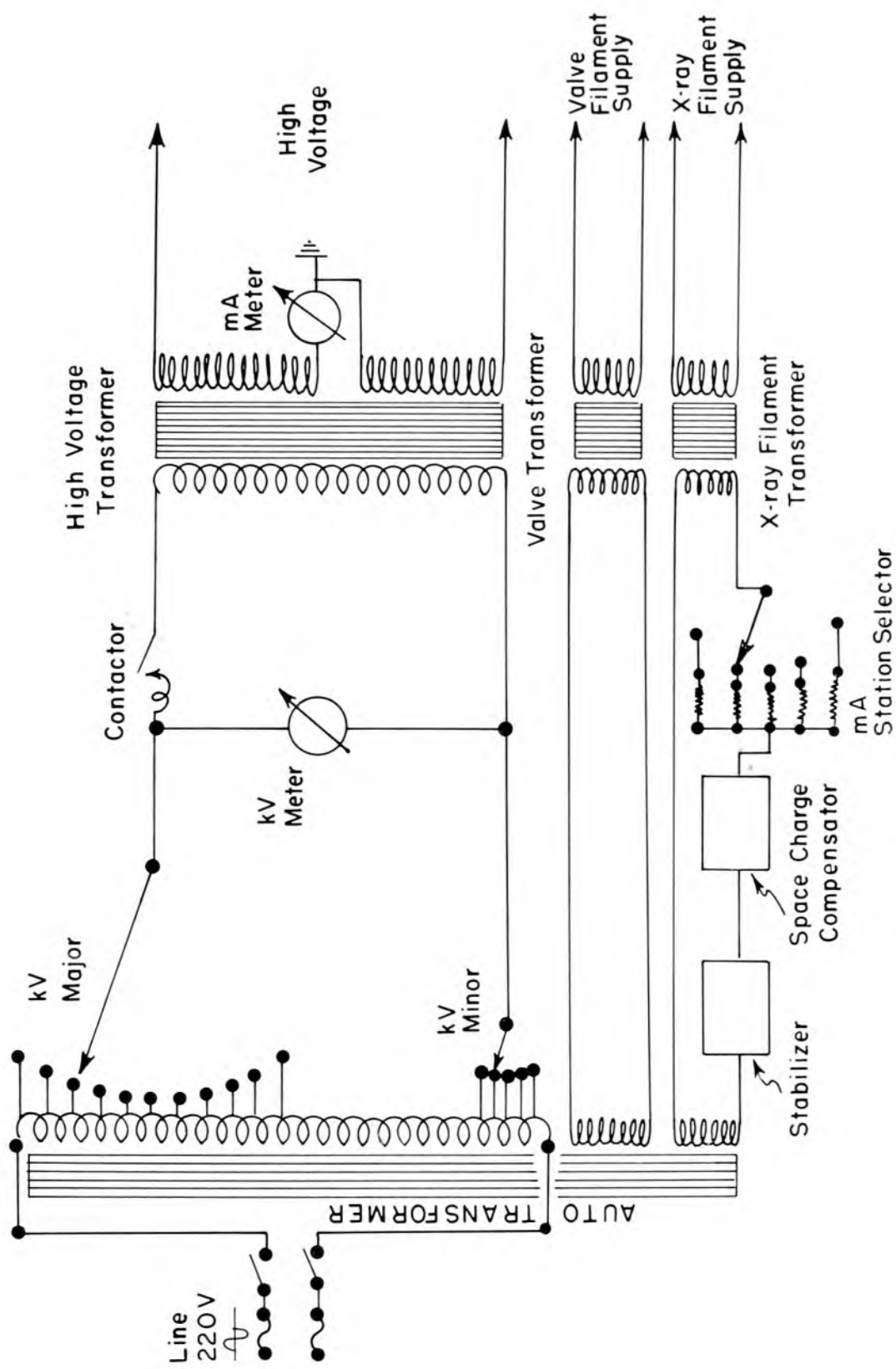


FIG. IV-41. Control circuit for diagnostic x-ray unit.

voltmeter between the high voltage terminals of the x-ray transformer. Such a system, however, would also result in insulation difficulties. Therefore, the voltmeter measuring the x-ray tube voltage is connected in the primary circuit of the high voltage transformer; the voltage measured is proportional to the voltage applied to the x-ray tube.

The x-ray tube voltage is varied by means of an autotransformer with coarse (major) and fine (minor) controls (Fig. IV-41). The x-ray switch (contactor) previously discussed is also placed in the primary circuit of the high voltage transformer. It should be noted that the voltage adjustment in the primary of the transformer and the consequent adjustment of the potential difference across the x-ray tube are always accomplished with the x-ray switch (contactor) in the "off" position, and the switch is closed only when the primary voltage has been adjusted to the desired value. This precaution must be taken to prevent arcing in the contacts of the autotransformer due to self-inductance in the circuit, and to avoid current surges in the circuit. Arcing would rapidly damage the contacts of the autotransformer.

X-RAY TIMERS

The duration of an x-ray exposure is usually limited by means of a timer connected in series with the primary circuit of the high voltage transformer. Different types of timers are used in diagnostic x-ray circuits. Interval or synchronous timers close and open the x-ray circuit by means of a synchronous motor. They are adequate for relatively long x-ray exposures, but they cannot be relied upon for exposures shorter than approximately $\frac{1}{20}$ sec for the following reasons: (1) It is difficult to obtain an accurate timing of periods shorter than $\frac{1}{20}$ sec by means of a mechanical device. (2) When an interval timer is used for short exposures, the amount of radiation generated by the x-ray tube may vary widely for a given time interval, depending on the number of electrical pulses included in the time interval.

To overcome these difficulties in short x-ray exposures, impulse timers are used. These electronic timers are based on the use of thyatron tubes (Fig. X-4) triggered in phase with the alternating current in such a fashion that they close the x-ray circuit for a predetermined number of pulses, or during a fraction of one pulse. Electronic impulse timers are reliable for exposures as short as $\frac{1}{120}$ sec.

Another timer that is gaining acceptance in more advanced x-ray circuits is the milliampere-second meter (mAs timer). This apparatus controls the delivery to the x-ray tube of a predetermined amount of electrical charge expressed in milliampere-seconds. The device is based on the use of a capacitor charged by an amount of electricity that is proportional to the charge flowing to the x-ray tube. The accumulation of electrical charges in the capacitor raises its potential, and when a predetermined potential is reached, i.e., when a predetermined amount of electricity has been delivered to the x-ray tube, the mAs timer interrupts the flow of electricity through the circuit.

Some timers delimit the x-ray exposure on the basis of a predetermined amount of radiation to be delivered to the radiographic film. Among these instruments phototimers and ionization timers are particularly important.

X A phototimer (Ref. 19) consists of a photomultiplier tube optically connected to a fluorescent "pickup" screen. The screen may be placed behind an x-ray cassette and thus be exposed to the radiation escaping the cassette, or it may be placed between the patient and the cassette, thus absorbing a negligibly small amount of the useful radiation. In the latter case, optical coupling between the screen and the photomultiplier tube may be achieved by means of a plastic sheet acting as light guide. Phototimers are also extensively used in cinefluorography, where a portion of the light from the output screen of the x-ray image intensifier is guided by a mirror, or other optical coupling, to the photomultiplier tube. The electric current generated in the photomultiplier tube, which is proportional to the amount of radiation absorbed per unit time in the pickup screen, is used to charge a capacitor and raises its potential. The capacitor is connected to the grid of a thyratron, and when the grid potential reaches a predetermined value, the thyratron conducts, and thereby interrupts the x-ray exposure.

An ionization timer ("Iontomat") (Ref. 6) is composed of an ionization chamber that is placed between the film and the source of radiation. The current generated by the x-radiation in the ionization chamber is fed to a current-integrating device which interrupts the x-ray exposure.

Phototimers and ionization timers are useful devices widely used in diagnostic radiology.

Calibration of Timers—Spinning Top

Timers of x-ray units supplying pulsating voltage to the x-ray tube can be calibrated by a simple device called "spinning top" (or "spin top"). The spinning top used in radiology (Fig. IV-42) is a circular disc, made of a material relatively opaque to x-rays, with a small aperture, or window, near its periphery. The disc is attached to a vertical axis supported by bearings to allow free rotation. The spinning top is used by (1) placing it on x-ray film under the unit to be calibrated, (2) setting it into motion by a twist of the fingers, and (3) exposing a radiograph timed by the timer to be calibrated. The radiograph thus obtained consists of the shadow of the disc with a series of images of the window exposed by the pulsation of the x-ray beam (Fig. IV-42). Since the pulsation frequency of the x-ray beam is known, the count of the number of images of the window allows the determination of the time of exposure. For example, for a full-wave rectified circuit with a frequency of 60 cycles per second, the number of x-ray pulses is 120 per second. If with such a unit the number of images of the spinning top window is 12 (Fig. IV-3) then the exposure timed is $\frac{1}{10}$ sec. The speed of rotation of the spinning top during calibration must be such as to provide several images of the window. Spinning tops are inaccurate unless several pulses are encompassed within

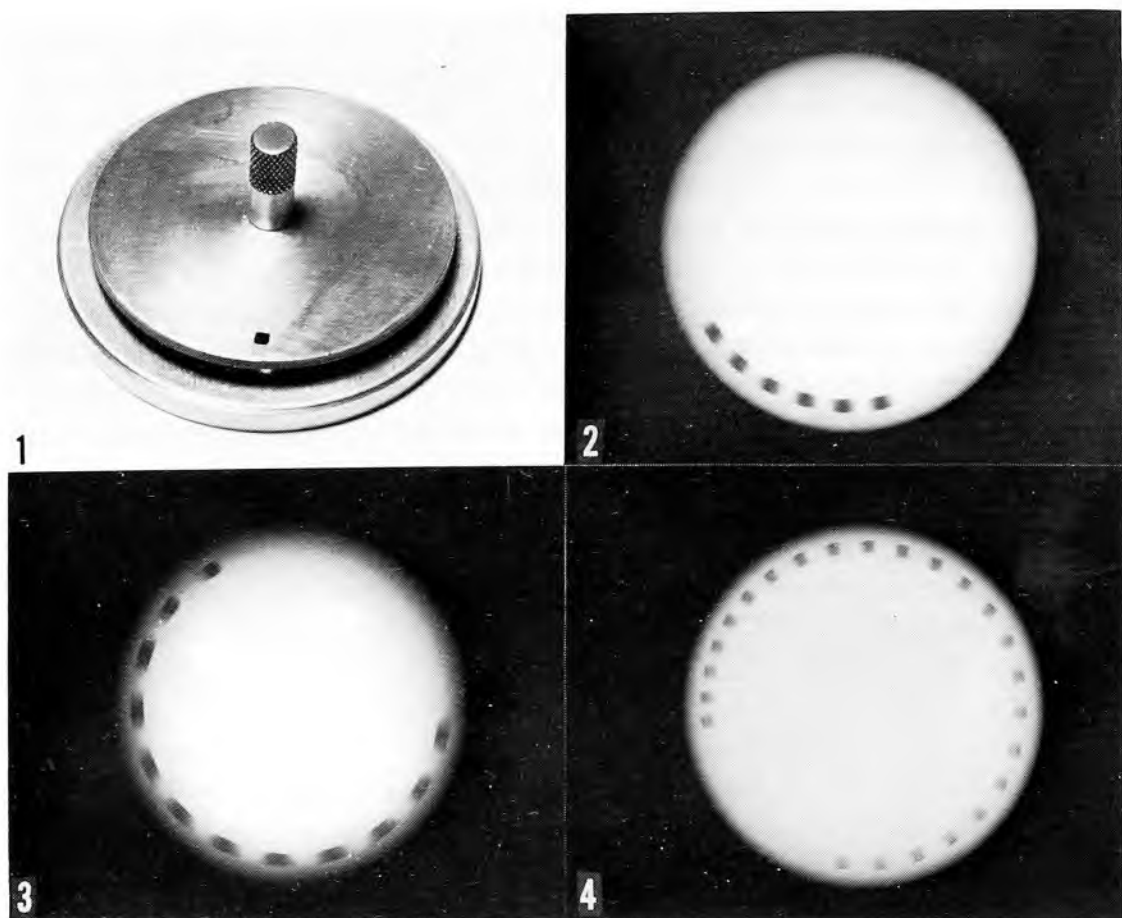


FIG. IV-42. Spinning top for calibration of x-ray timers.

- 1 photograph of spinning top, showing window provided in the x-ray opaque brass disk
- 2 radiograph of spinning top exposed by a full-wave rectified 60-cycle x-ray unit (120 x-ray pulses/sec). Since six images of the window appear on the radiograph during the exposure, the exposure consisted of 6 x-ray pulses, or

$$\frac{6 \text{ pulses}}{120 \text{ pulses/sec}} = \frac{1}{20} \text{ sec}$$

- 3 radiograph of spinning top exposed with the same x-ray unit as in 2, with an exposure time of $\frac{1}{10}$ sec (12 x-ray pulses)
- 4 $\frac{1}{5}$ -sec exposure (24 x-ray pulses)

Note the increasingly shorter distance between the images of the window resulting from the slowing down of the spinning top during exposure (counter-clockwise rotation of the spinning top).

the exposure. They cannot be used with constant potential circuits or with exposures shorter than one pulse.

REFERENCES

1. LIVINGSTON, M. S., and BLEWETT, G. P.: *Particle Accelerators*. New York, McGraw-Hill, 1962.
2. HODGMAN, C. D., WEAST, R. C., and SELBY, S. M., eds.: *Handbook of Chemistry and Physics*. Cleveland, Ohio, Chemical Rubber Publishing Company, 1959-1960.
3. KASTEN, R. F., and ASMUS, C.: Fundamentals of bearing design for rotating anode type x-ray tubes. *Dunlee Digest* (Dunlee Company) 8(#4):2, 1964.
4. MACHLETT, R. R., and ROGERS, T. H.: An improved vacuum bearing system for rotating anode tubes. *Cathode Press* (Machlett Company) 6: Fall, 1951.
5. ROGERS, T. H.: Dynamax 20, the only double focus light-weight rotating-anode x-ray tube. *Cathode Press* (Machlett Company) 2: Fall, 1951.
6. Siemens-Reininger-Werke AG, Erlangen, Germany.
7. *Method of Evaluating Radiological Equipment and Materials*. Recommendations of the International Commission on Radiological Units and Measurements (ICRU), NBS Handbook 89. Washington, D.C., U.S. Government Printing Office, 1962.
8. MATTSSON, O.: Practical photographic problems in radiography. *Acta Radiol.*, Suppl. 120:85 1955.
9. BOWERS, A., and vDTUUK, J. H.: Secondary electrons in x-ray tubes. *Physica* 12:274, 1932.
10. ROGERS, T. R.: Factors involved in the determination of an expression of x-ray tube ratings. *Cathode Press* (Machlett Company) 8(#4):13, 1951.
11. ROGERS, T. H.: Beryllium window x-ray tubes and their uses. *Cathode Press* (Machlett Company) 5(#1):4 and 38, 1948.
12. DYKE, W. P., FLOYD, R., and GRUNDHAUSER, F. J.: High dose rate x-ray sources with development of a light-weight diagnostic unit. *Radiology* 76:257, 1961.
13. DYKE, W. P., FLOYD, R., ANDERSON, R., and GRUDHAUSER, F. J.: *On the Application of Field Emission to Medical Instrumentations*. McMinnville, Ore., Field Emission Corporation.
14. OOSTERKAMP, W. J.: Monochromatic x-rays for medical fluoroscopy and radiography? *Medica Mundi* (Philips Company) 7(#3):68, 1961.
15. TER-POGOSSIAN, M.: Monochromatic roentgen rays in contrast media roentgenography. *Acta Radiol.* 45:313, 1956.
16. JACOBSON, B., and MACKAY, R. S.: Radiological contrast-enhancing methods. *Adv. Biol. Med. Physics* 6:201, 1958.
17. JOHNS, H. E.: *The Physics of Radiology*, 2nd ed. Springfield, Ill., Thomas, 1961.
18. ROGERS, T. H.: An electronic switching system for ultrashort rapidly repeated exposures in angiocardiology. *Cathode Press* (Machlett Company) 13(#1):12, 1956.
19. MORGAN, R. H.: A photoelectric timing mechanism for the automatic control of roentgenographic exposure. *Amer. J. Roentgen.* 48:220, 1942.
20. ATLEE, Z. J., and PERRY, J. T.: "Roentgen Rays: Tubes, Ratings and Performance of Rotating Anode X-Ray Tubes," in *Medical Physics*, vol. 3, ed. by Glasser, O. Chicago, Year Book, 1960.

(V)

THE RADIOLOGIC EXAMINATION, Part A: The X-Irradiation and the Generation of Information

A study of the influence of physical factors upon the radiologic examination requires the understanding of the various steps involved in acquiring information by this method of analysis.

The study of any system by physical means consists of the observation of the perturbation resulting when the system interacts (exchanges energy) with another physical system. For example, the visual study of an object consists of the observation of the light photons that are reflected or absorbed when the object is illuminated. Chemical analysis is the observation of the chemical changes produced when the substance under study interacts chemically with another substance. A metallic object located in a nonconductive medium of different density may be discovered by the perturbation it produces when the medium containing it is subjected either to a field of electromagnetic radiation or to the field of gravity.

The amount of information that can be gathered by the perturbation of a physical system by another is determined by (1) the nature and amount of the interactions between the system under study and the perturbed system, and (2) the nature and amount of information that can be extracted from the perturbed system. Under ideal circumstances no information is lost between these two steps, and all the information coded by the perturbed system is utilized in the study. In general, however, the amount of information extracted from the perturbed system is considerably lower than the amount it carries. The *maximum* amount of information that can be derived from two interacting physical systems can be predicted; and while it is desirable to extract the maximum information available, it is futile to attempt to extract more information from the perturbed system than it carries.

ACQUISITION OF INFORMATION BY MEANS OF X-RAYS

Diagnostic radiology consists of the interpretation of information acquired by the examination of the opacity to x-rays of a biologic system. The purpose

of Chapters V and VI is to evaluate the different steps by which a beam of x-rays extracts information from the part examined, and to determine what fraction of the information thus coded in the beam of x-rays is utilized in the examination.

From the standpoint of the acquisition of information, there are three steps in a radiologic examination: (1) the part to be examined is exposed to a beam of x-rays, (2) the beam of x-rays is perturbed by interacting with the part examined, and (3) the information carried by the perturbed x-ray beam is translated into a form suitable for interpretation. The first two steps consist in generating information, and the third is the retrieval of the information generated.

The perturbation of the beam of x-rays by the part under examination consists in the removal of photons from the beam, and the information carried by the x-radiation emerging from the examined part is coded as a variation in the number of x-ray photons per unit area (photon fluence). This change in photon fluence is the only variable utilized for extracting information in diagnostic radiology. In this respect diagnostic radiology differs from optical examination which generally utilizes two variables, namely, fluence of light photons and their energy or color. It is interesting to note that most diagnostic x-ray examinations are carried out with polyenergetic x-ray beams and that the distortion of the spectral distribution of the photon energies by the examined part is not utilized in the examination.

The generating of information in diagnostic radiology, then, consists of the attenuation of a beam of x-rays by the examined part. The factors that affect the attenuation of a beam of x-ray photons by matter are described in Chapter III. The influence of these factors depends on the energy of the x-ray photons and the nature and amount of material traversed.

X-RADIATION ENERGY SPECTRUM IN DIAGNOSTIC RADIOLOGY

The energy spectrum of the photons originating from an x-ray tube depends upon three factors: (1) the nature of the target of the x-ray tube, (2) the electric field accelerating the electrons, and (3) the nature and amount of absorbing materials interposed in the path of the beam that escapes from the tube. The first two factors determine the spectral distribution of the energy of the photons emitted by the target of the x-ray tube. However, as it emerges from the x-ray tube housing, this spectrum is profoundly altered by selective absorption of some of the photons by the glass envelope of the x-ray tube and by absorbers embodied in those parts of the x-ray tube housing that are interposed in the path of the beam. In the context of this presentation, the spectral distribution of the radiation inside the tube envelope is of little interest, and only the radiation emerging from the tube will be studied.

Most x-ray tubes used in diagnostic radiology contain a tungsten target (a few exceptions are discussed in Chapter IV). Thus, in the present content,

the three factors affecting the energy spectrum of the radiation emitted by an x-ray tube (namely, target material, potential applied, and influence of the tube envelope and housing) can be reduced to a single variable—the accelerating potential applied to the x-ray tube.

Accelerating Potentials in Diagnostic Radiology

The voltage applied to x-ray tubes in diagnostic x-ray units either may vary as a sine function of time, if it is supplied by a single-phase rectified circuit; or it may be relatively constant in time if supplied by either a three-phase 12-pulse circuit, or a “Dyapulse” type of generator. The three-phase six-pulse generator falls between the above two categories and supplies a voltage which varies as a function of time, but between narrower limits than observed with a single-phase rectified circuit. Other forms of electrical potential may conceivably be applied to x-ray tubes, but at this time it appears that the above categories encompass the great majority of diagnostic x-ray installations.

The accelerating voltage supplied by a full-wave or half-wave rectified circuit varies between zero and a maximum value, and returns to zero according to a sine function (see Fig. IV-28). The number of such cycles per unit time depends on the frequency of the alternating current applied to the transformer, and on whether the circuit is of the full- or half-wave type. In most installations in the United States the frequency of the alternating current is 60 cycles per second, and therefore full-wave and half-wave generators supply, respectively, 120 and 60 cycles per second.

The voltage of an alternating current varies sinusoidally as a function of time, between zero and a maximum value (peak voltage), with a change in polarity every half-cycle. A conventional voltmeter connected to an alternating circuit cannot follow the rapidly changing difference of potential, and voltmeters designed for the measurement of alternating potentials are constructed to indicate a potential equivalent to the potential of a direct current that carries the same amount of energy as the alternating current. This potential, called the root mean square (rms) potential, is equal to the maximum potential reached by the alternating current divided by the square root of ($\sqrt{2} = 1.414$). In an x-ray circuit, the voltmeter that indicates the voltage supplied by the generator to the x-ray tube is inserted, as discussed in Chapter IV, in the primary circuit of the high voltage transformer, and the voltmeter reading is the maximum or “peak” value of the voltage induced on the high voltage side of the circuit (kV_p).

The waveform of the potential supplied by an x-ray generator is distorted as it is conducted to the x-ray tube. The distortion is mostly due to the electrical capacitance of the shielded cables that connect the generator to the tube. The cables act as two capacitors interposed in the tube circuit: they are charged when potential is applied to the tube and thereby reduce its peak potential, and the charge thus stored is released into the tube when

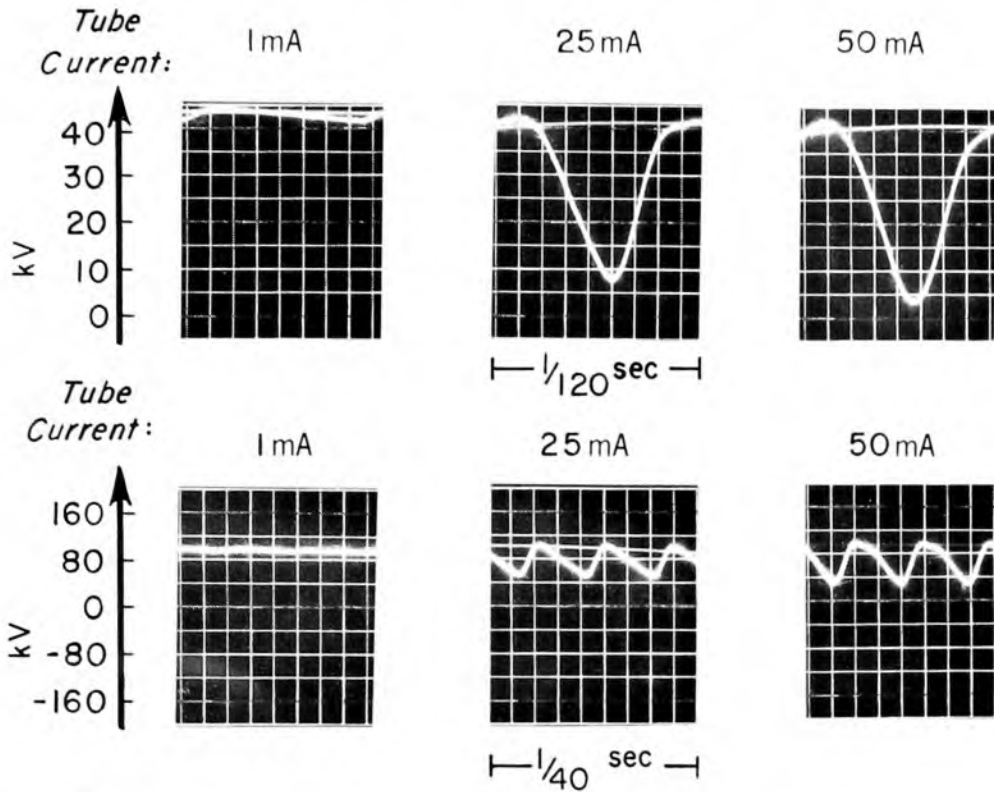


FIG. V-1. Effect of capacitance of cables on waveform of voltage supplied to x-ray tube.

Generator single-phase full-wave rectification

Cables 20 feet

Top 50 kV_p; 1, 25 and 50 mA

Bottom 100 kV_p; 1, 25, and 50 mA

It is apparent that, for a low tube current, the tube is supplied with nearly constant potential owing to the capacitance of the cables. The influence of cable capacitance on waveform is more pronounced for higher tube voltage.

the potential supplied by the generator decreases. The magnitude of this effect depends (1) on the capacitance of the cables, which is proportional to their length (2) on the x-ray tube current, and (3) on the voltage applied. With long cables and low tube currents this effect is important (Fig. V-1).

The x-ray production rate of a tube connected to a full-wave rectified circuit is cyclic in time, with a frequency equal to that of the potential applied to the tube; however, the curve of this rate does not follow that of the potential applied to the tube. The x-ray curve (see Fig. IV-31) is more "peaked" than the voltage curve because the efficiency of the x-ray production is strongly dependent on the accelerating potential applied to the tube.

In Chapter IV, various x-ray generators with circuits that supply x-ray tubes with nearly constant potential were discussed. The three-phase 12-pulse rectified circuit, which is probably the constant potential circuit

most widely used in diagnostic radiology, delivers a potential with a "ripple" of only 3% of the peak potential achieved. It should be noted that this "ripple" is for all practical purposes erased by the capacitance of even short cables.

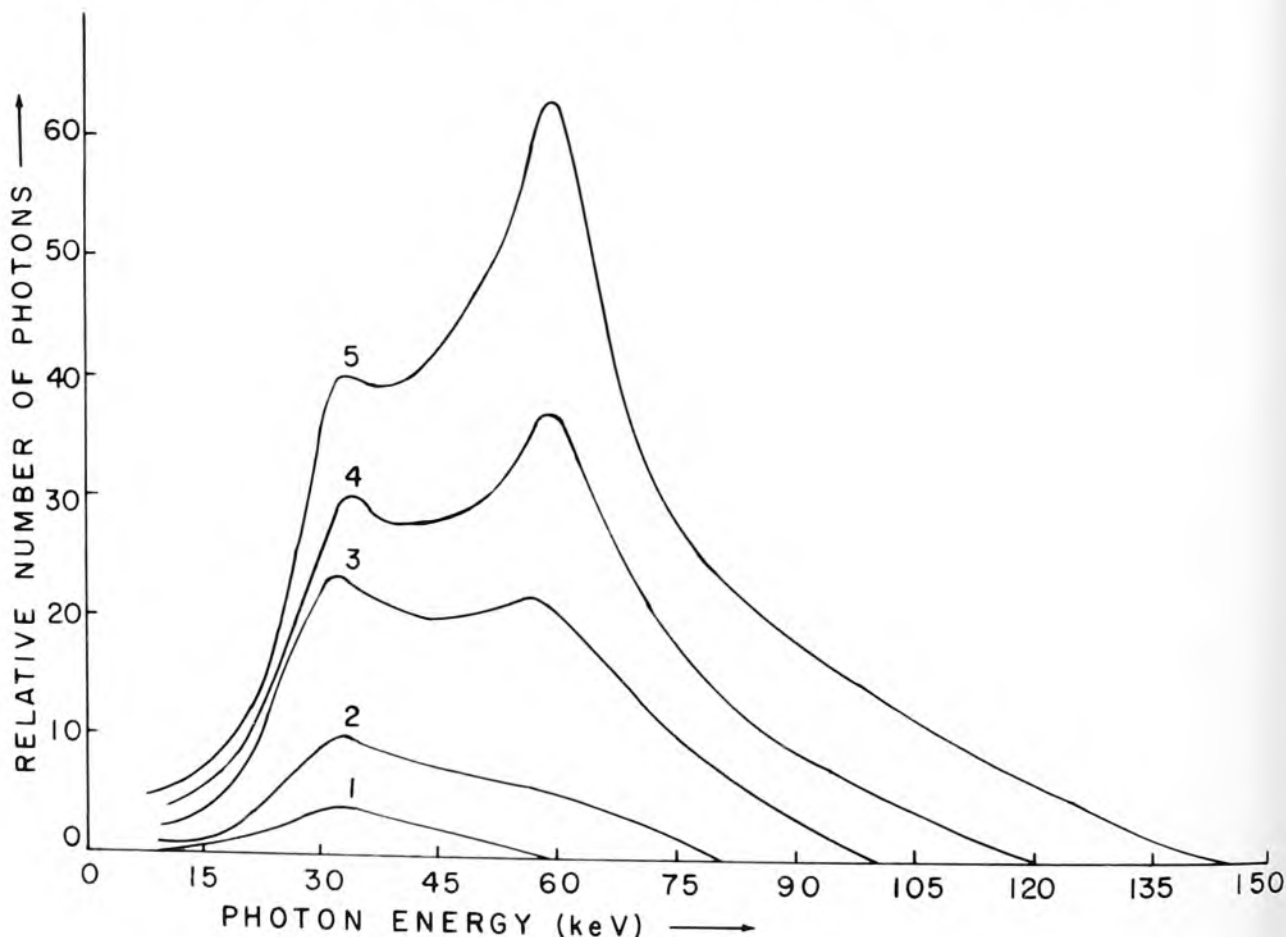
X-Ray Spectra

Figure V-2 shows the spectral distributions of x-ray photons generated by different accelerating potentials applied to an x-ray tube energized with a three-phase 12-pulse rectified circuit. These spectra are typical of most constant potential circuits. For the same accelerating potential and therefore for the same maximum photon energy, the radiation produced by a pulsating circuit (Fig. V-3) is not as rich in high energy photons as the radiation generated at constant potential.

The contribution of the K-characteristic radiation from the tungsten

FIG. V-2. Spectra of x-rays generated with different accelerating potentials and same tube current.

Generator three-phase 12-pulse circuit, inherent filtration
 1 60 kV_p 2 80 kV_p 3 100 kV_p 4 120 kV_p 5 150 kV_p



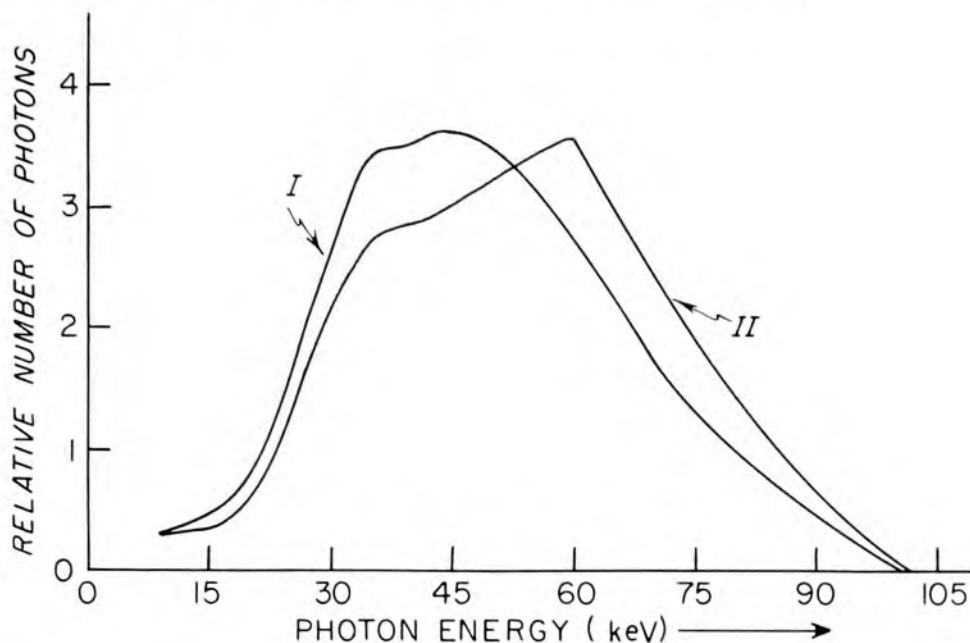


FIG. V-3. Comparison of spectra of 100 kV_p x-rays generated with:
 I single-phase (full-wave) circuit
 II three-phase 12-pulse circuit
 Filter 3 mm Al added
 Spectra normalized for equal number of photons

x-ray tube target, as a function of accelerating potential, is shown in Fig. V-2.

FILTRATION

The attenuation of a beam of polychromatic (polyenergetic) x-rays by an absorber usually results in the alteration of the spectral distribution of the x-ray photons. This effect, which stems from the unequal attenuation of photons having different energies, is called filtration. Filtration occurs because, in most instances, the attenuation coefficient of a substance for x-rays varies with photon energy. This rule suffers a few exceptions: for example, equal attenuation of photons having different energies takes place when these energies encompass a high or low value of the attenuation coefficient owing either to a photoelectric absorption discontinuity,¹ or to a transition from one mode of attenuation to another.

Filtration does not take place with a beam of monoenergetic x-rays. With such radiation all photons exhibit the same attenuation coefficient, and the interposition of an absorber results in attenuation without alteration of the energy distribution.

¹ The value of the photoelectric attenuation coefficient, plotted versus photon energy, exhibits a series of discontinuities for photon energies equal to the electronic shells of the absorber.

In general, the attenuation of x-rays in matter increases with decreasing photon energies, and the filtration of a beam of x-rays results in the relatively greater depletion of lower energy photons than higher energy photons. In this way filtration produces an increase in the mean energy of a poly-energetic beam of x-rays. This effect is sometimes referred to as "hardening" of an x-ray beam. Under certain circumstances filtration may result in the removal of a relatively greater number of higher energy photons than lower energy photons, with the unusual result of a decrease in mean energy. This occurs when a large fraction of the higher energy photons have energies equal to a photoelectric attenuation peak of the filtering material. Under these circumstances the lower energy photons are absorbed to a lesser degree because the attenuation coefficient of the filter exhibits a relative minimum at each photoelectric discontinuity.

Both photoelectric and Compton effects may contribute to filtration because the probabilities of both of these modes of attenuation decrease with increasing photon energy. However, photoelectric attenuation results in a considerably more selective filtration (relatively greater number of low energy photons removed) than Compton attenuation because of the much stronger energy dependence of the former process. In the diagnostic x-ray energy range filtration by Compton effect is minimal.

In radiologic examinations x-radiation is subjected to three forms of filtration: (1) the filtration of the x-ray beam as it passes through absorbers inherent in the structure of the x-ray tube and its housing (inherent filtration), (2) the additional filtration of the x-ray beam emerging from the tube housing by absorbers placed in the path of the beam with the purpose of reducing the number of low energy photons (added filtration), and (3) the filtration of the x-ray beam as it passes through the organs and parts of the patient examined.

Inherent Filtration

The x-radiation emerging from a tube housing is filtered by various absorbers the presence of which is required for the operation of the tube. In a modern x-ray tube this filtration, called inherent filtration, takes place in three structures: (1) the glass envelope of the x-ray tube, (2) the oil insulation that surrounds the tube, and (3) the window in the tube housing, usually made of plastic, which contains the oil and allows the radiation to escape from the tube housing. In low-capacity x-ray tubes the cooling oil and the tube housing window may be absent.

Table V-1 shows the inherent filtration of a typical diagnostic-type rotating-anode tube. The glass envelope of the x-ray tube is responsible for most of the attenuation of the radiation because of its higher effective atomic number than oil and Bakelite, which are both organic compounds the contribution of which to inherent filtration is negligible. For photons having energies below 50 keV the attenuation of x-rays in glass (silicon dioxide)

TABLE V-1. Inherent Filtration for Typical Diagnostic X-Ray Tube^a

Absorber	Thickness (mm)	Aluminum equivalent ^b (mm)
Glass envelope	1.4	0.78
Insulating oil	2.36	0.07
Bakelite window	1.02	0.05

^a From Trout (Ref. 1).

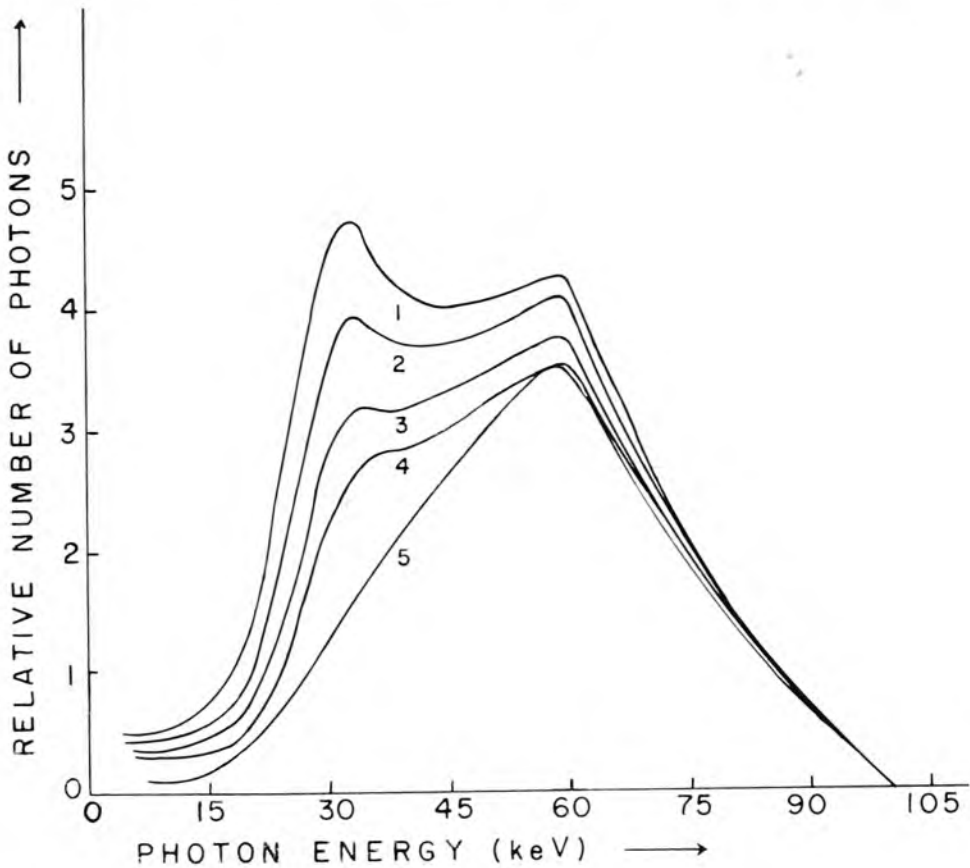
^b Thickness of aluminum resulting in same filtration as the absorber.

takes place by photoelectric interactions predominately. For higher energy photons, Compton interactions become more probable.

The inherent filtration of an x-ray tube effectively removes low energy photons, which explains the difference between the spectral distribution of x-ray photons actually emerging from an x-ray tube (Fig. V-4) and the

FIG. V-4. Effect of added filtration on spectral distribution of 100 kV_p x-rays (three-phase 12-pulse circuit).

- 1 inherent filtration, including collimator
- 2 1 mm Al 3 2 mm Al 4 3 mm Al 5 0.125 mm Cu



theoretical shape of the radiation spectrum as produced by the target (see Fig. II-6).

Added Filtration

The x-radiation emerging from the tube housing, although depleted of a certain number of low energy photons by inherent filtration, still exhibits a broad spectral distribution containing a number of photons with energies considerably lower than the mean energy of the beam. The presence of these low energy photons in the x-ray beam is undesirable in diagnostic radiology because their absorption by the part to be examined is greater than that of the higher energy photons, and they contribute little to the examination and much to the highly undesirable irradiation of the patient. It is therefore desirable to reduce further the number of low energy photons in the beam already filtered by inherent filtration. This is accomplished by interposing a filter between the tube housing and the patient. The nature and the amount of filter material are determined by (1) the energy of the radiation to be filtered and (2) the degree of "hardness" to be achieved.

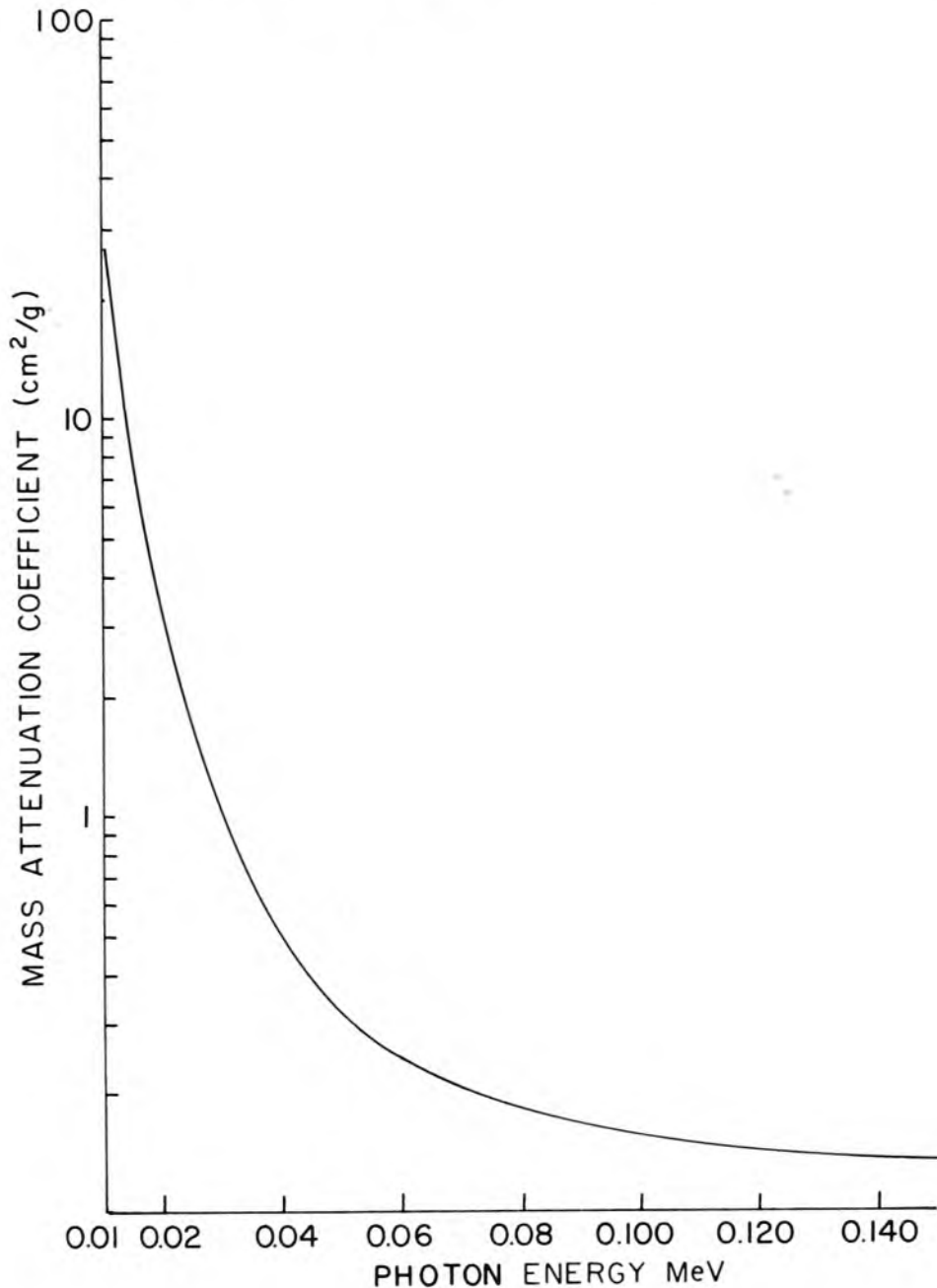
Under ideal conditions the filter should remove all unwanted photons without affecting the useful radiation. Unfortunately, ideal filters do not exist, and the removal of low energy photons is always accompanied by the loss of a certain number of higher energy photons. The performance of a filter can be rendered optimum by making it of a substance having an attenuation coefficient that is particularly high for low energy photons and that decreases rapidly with increasing photon energy. Such energy dependence is typical of photoelectric attenuation, and filters are therefore made of elements that attenuate mostly by photoelectric effect in the low energy region of the radiation to be filtered. In conventional diagnostic radiology, aluminum is the material generally used for added filtration. The attenuation of x-rays in aluminum takes place mostly by photoelectric effect for photons with energies up to 50 keV, and decreases rapidly with increasing photon energy, as shown in Fig. V-5.

The filtration of higher-energy x-rays, generated by peak voltages between 100 and 200 kV, is more effectively achieved with copper than with aluminum because of the greater attenuation of higher energy photons in copper, as shown in Fig. V-6. In general, the use of a higher atomic-number filter results in the removal of higher energy photons.

It is difficult to determine the ideal amount of filtration for a given diagnostic procedure. Although increasing the filtration means depressing the number of low energy photons, it also reduces the number of high energy photons available for the examination. Many authors agree on the desirability of adding about 2 mm of aluminum to the inherent filtration in conventional-range diagnostic procedures. Figure V-4 shows the alteration of the spectrum of a beam of x-rays traversing 1, 2, and 3 mm of aluminum and

0.125 mm of copper. It is apparent that after the addition of 1 mm of aluminum further filtration does not appreciably alter the distribution of the radiation energy. The comparison of the filtration effect produced by 3 mm of aluminum and 0.125 mm of copper on 120 keV_p x-radiation, generated by a constant potential circuit, shows that copper filtration is more effective in removing low energy photons than the 3-mm aluminum filter (Fig. V-6).

FIG. V-5. X-ray attenuation coefficient for aluminum as a function of photon energy. (From values of Grodstein, Ref. 11.)



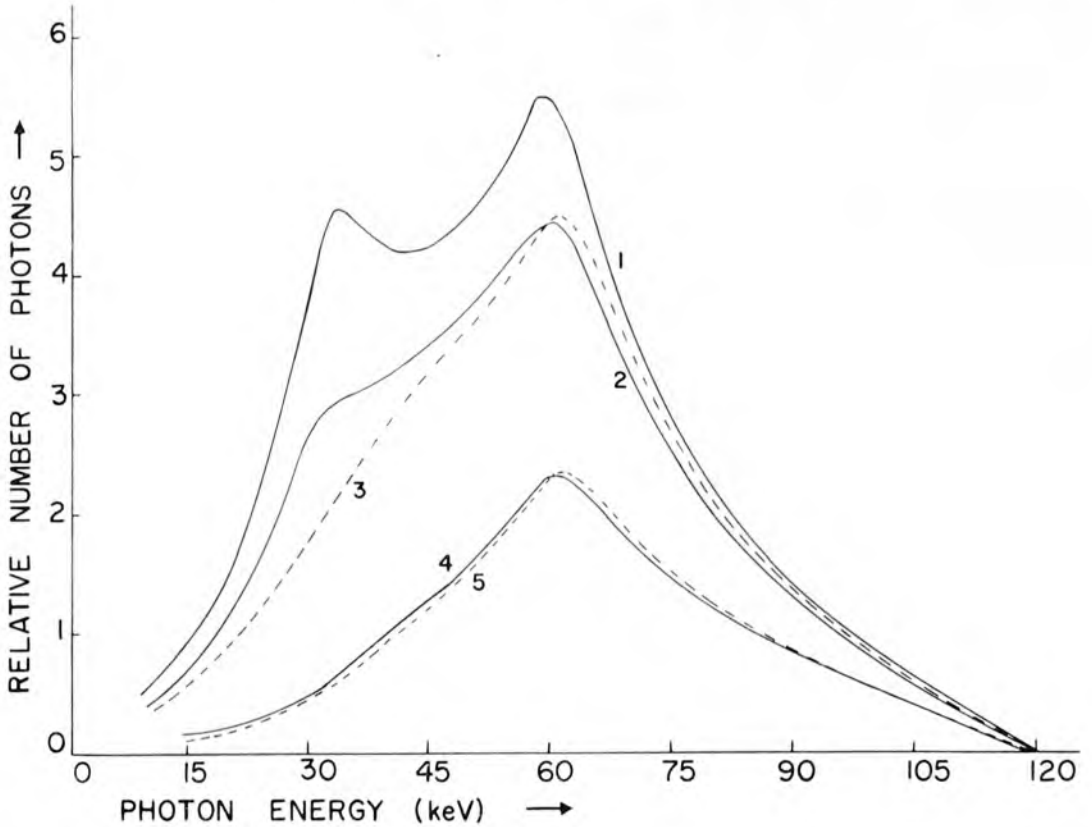


FIG. V-6. Effect of added filtration on the spectral distribution of 120 kV_p x-rays (three-phase 12-pulse circuit) and distortion of the filtered radiation by 10 cm of water.

- 1 inherent filtration
- 2 3 mm Al
- 3 0.125 mm Cu
- 4 3 mm Al and 10 cm water
- 5 0.125 mm Cu and 10 cm water

✕✕ ATTENUATION OF X-RAYS IN THE PATIENT

The rate of attenuation and the consequent filtration suffered by an x-ray beam as it traverses the part examined during a radiologic diagnostic procedure depends on the atomic composition of the structures encountered by the x-ray photons. From the standpoint of their opacity to x-rays, all anatomic structures encountered in clinical radiology can be classified according to their effective atomic numbers into three categories: adipose tissues (fat); soft tissues (with the exclusion of fat) and body fluids; and bone.

Attenuation of X-Rays in Fat

There is a wide variation in the chemical composition of adipose tissues, depending both on the particular adipose tissue under consideration and the

age of the individual. However, from the standpoint of x-ray attenuation a reasonably representative effective atomic number and an average electron density for all human fat can be determined. The percentage composition of adult human adipose tissue (Refs. 2 and 3) is as follows:

Water	23.02%
Protein	5.85%
Carbohydrate	<0.1%
Ether-extractable lipid	71.57%

The percentage composition of the lipid is:

Cholesterol	0.3%
Phospholipid	<0.1%
Triglyceride	99.5%

On the basis of this chemical composition the effective atomic number of human fat is 6.3, with an electron density of 3.34×10^{23} electrons per gram (Table V-2).

The relative contribution of photoelectric and Compton interactions to the attenuation of x-rays in human fat is shown in Fig. V-7. Figure V-8

TABLE V-2. Elemental Composition, Electron Density, and Effective Atomic Number of Fat, Muscle, Water, and Bone

	Fat (adult human adipose tissue)	Muscle (striated)	Water	Bone (femur)
Percentage composition (by weight)				
Hydrogen	11.2 ^a	10.2 ^b	11.2	8.4 ^b
Carbon	57.3 ^a	12.3 ^b		27.6 ^b
Nitrogen	1.1 ^a	3.5 ^b		2.7 ^b
Oxygen	30.3 ^a	72.9 ^b	88.8	41.0 ^b
Sodium		0.08 ^b		
Magnesium		0.02 ^b		0.2 ^b
Phosphorus		0.2 ^b		7.0 ^b
Sulfur	0.06 ^a	0.5 ^b		0.2 ^b
Potassium		0.3 ^b		
Calcium		0.007 ^b		14.7 ^b
Electron density (el/g)	3.34×10^{23}	3.32×10^{23}	3.34×10^{23}	3.19×10^{23}
Effective atomic number (Z_{eff})	6.3	7.4	7.4	11.6

^a From Todd and West (Ref. 2), Hirsh et al. (Ref. 3), and Hilditch (Ref. 4).

^b From Johns (Ref. 7).

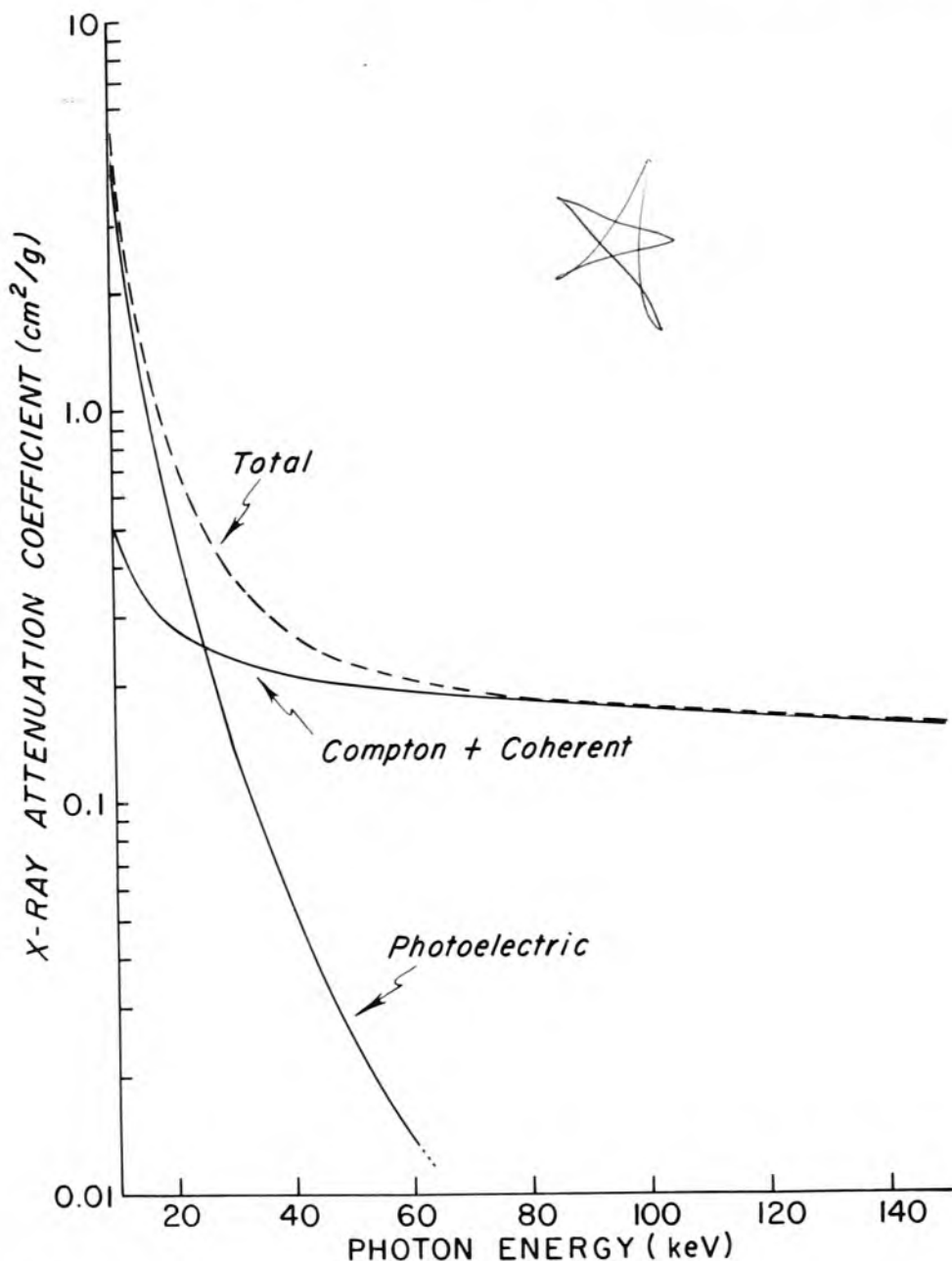


FIG. V-7. Contribution of photoelectric and Compton interactions to the attenuation of x-rays in fat. (From values of Grodstein, Ref. 11.)

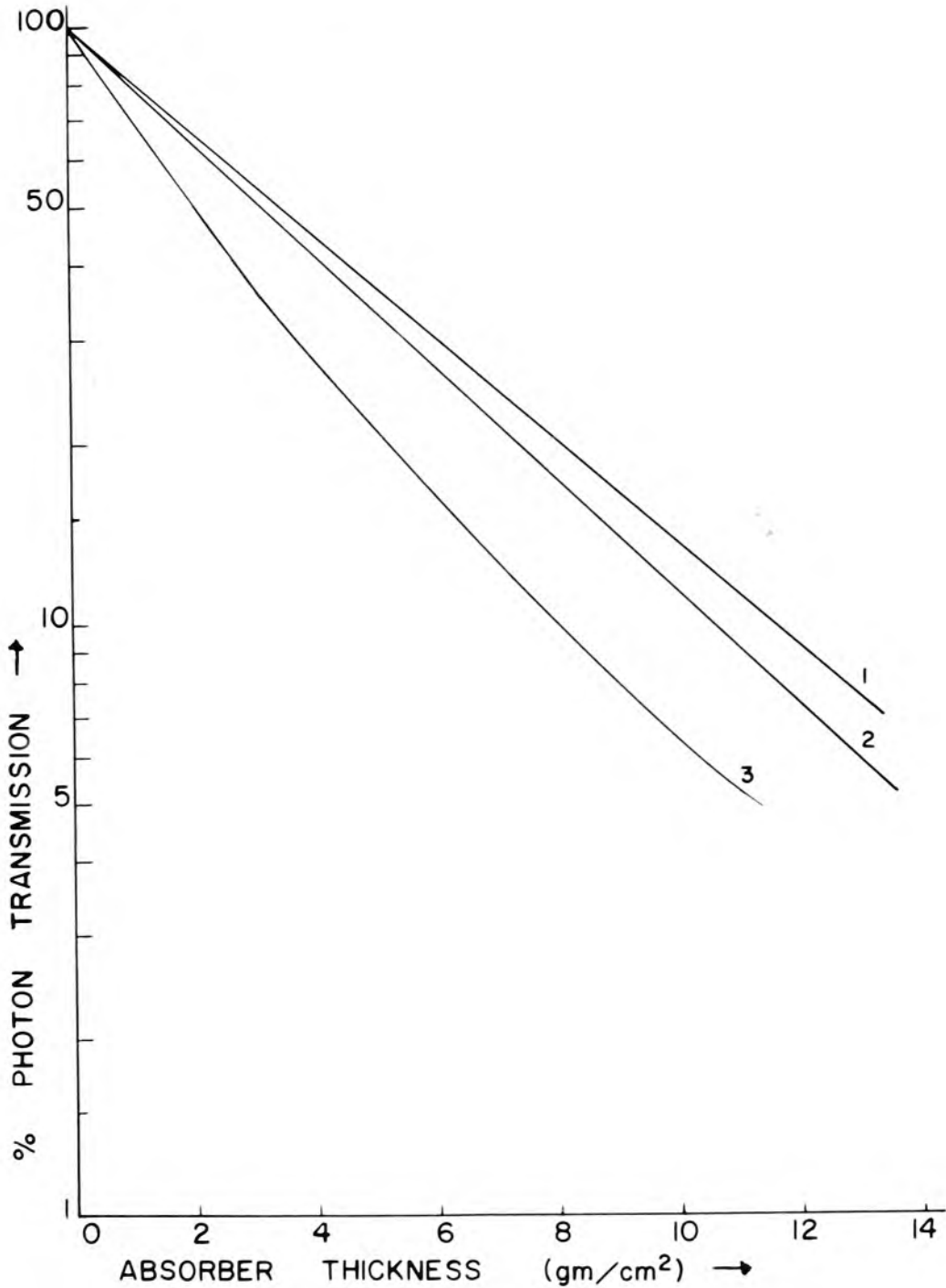
shows the attenuation of 100 keV_p x-rays in mineral oil, which is representative of human fat.

Attenuation of X-Rays in Soft Tissues and Body Fluids

The attenuation of x-rays in soft tissues and in body fluids is governed by the interaction of x-ray photons with low atomic-number elements, because neither electrolytes nor high atomic-number trace elements are found in

sufficient concentrations in these parts to affect appreciably their effective atomic numbers. The effective atomic numbers of different soft tissues (except fat) and of various body fluids do not differ appreciably from that of muscle, this value being 7.4 (Table V-2). The electron density of muscle is 3.32×10^{23} electrons per gram. For practical purposes, these values are

FIG. V-8. Narrow-beam attenuation of 100 kV_p x-rays in (1) mineral oil, (2) water, and (3) a medium ("mock" bone) having an effective atomic number and an electron density similar to those of bone.



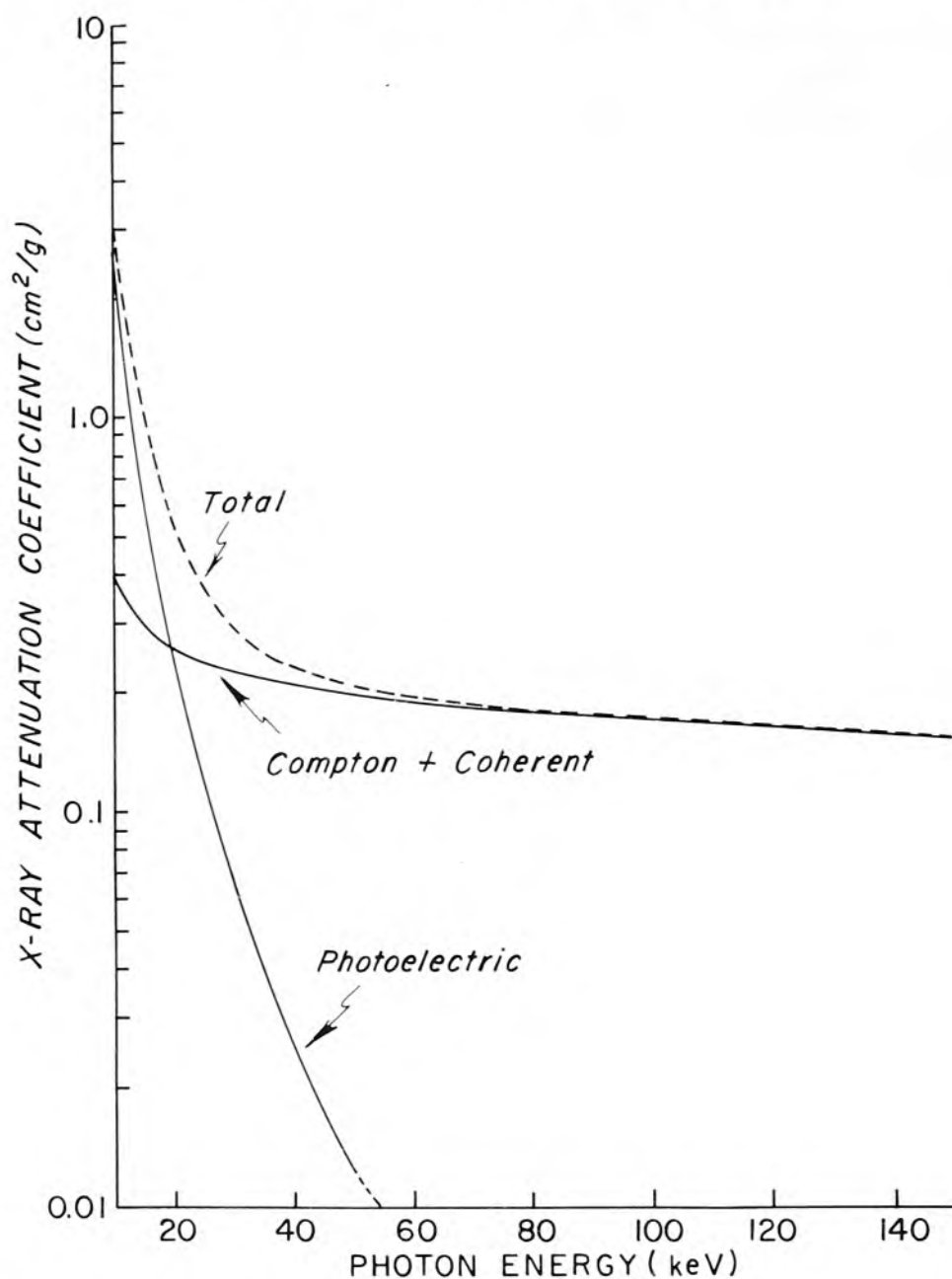


FIG. V-9. Contribution of photoelectric and Compton interactions to attenuation of x-rays in water (muscle). (From values by Grodstein, Ref. 11.)

identical with those of water. This uniformity of the effective atomic number for soft tissues and body fluids and its identity with that of water result from the predominance of water in both soft tissues (approximately 75% by weight) and body fluids (from 85 to nearly 100% by weight). The remainders of the weights of both soft tissues and body fluids consist of organic compounds having effective atomic numbers similar to that of water.

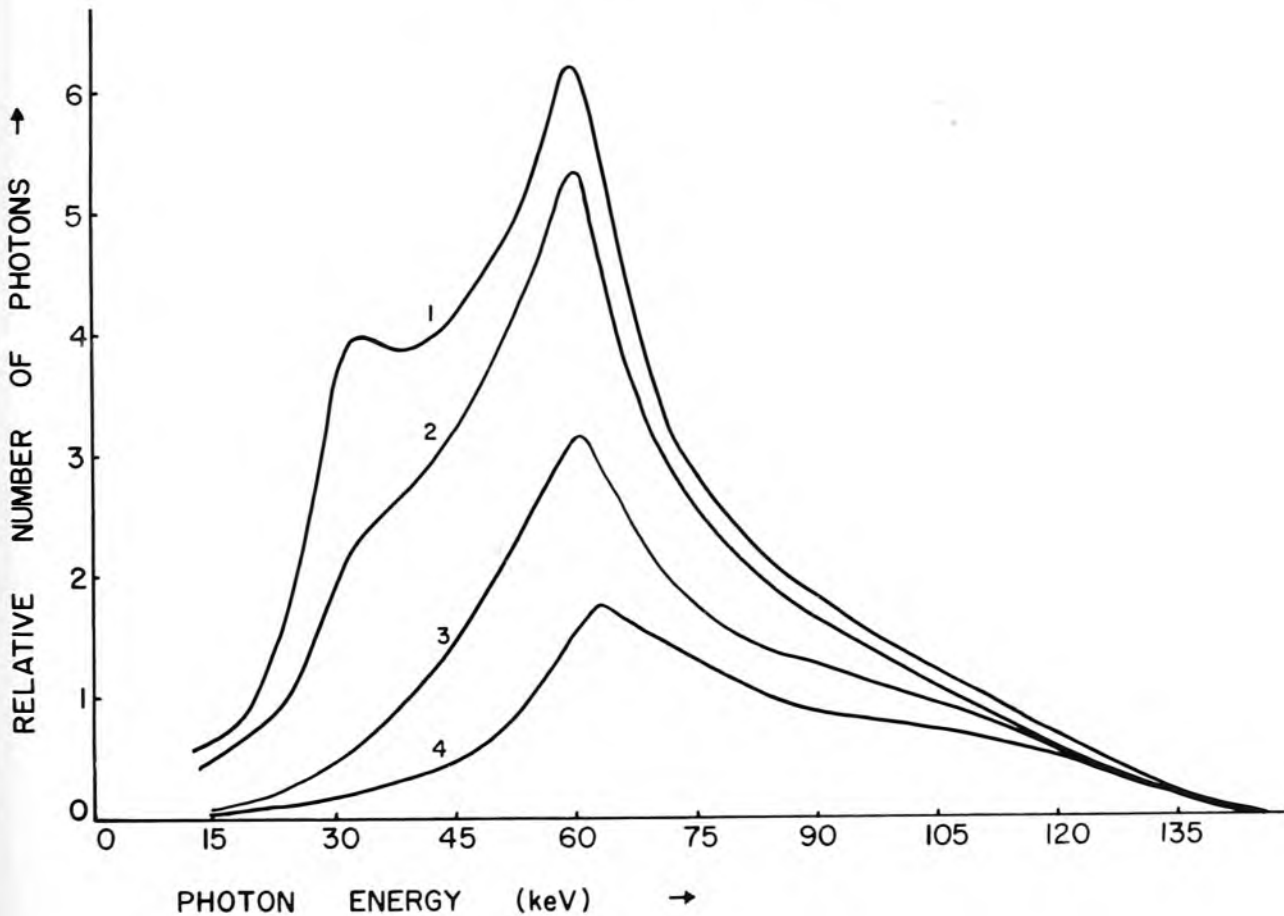
Under these circumstances the study of the attenuation of x-rays in soft

tissues and in body fluids encountered in diagnostic radiology can be considerably simplified by assuming their identity with water. The contribution of Compton and photoelectric interactions to the attenuation of x-rays in water is shown in Fig. V-9. Up to approximately 30 keV, photoelectric attenuation is important; beyond that energy, the Compton effect is mostly responsible for the attenuation of x-rays in water.

The alteration of the spectral distribution of filtered polyenergetic x-rays in water is shown in Figs. V-6, V-10, and VI-10. It is apparent that the filtration effect is moderate even for a large amount of water interposed in the path of the beam. Figure V-11 shows the attenuation of x-rays generated with various peak energies in water. The linearity of the semilogarithmic plot shows that the filtration effected by water does not alter appreciably the absorbability of the x-radiation in this medium.

FIG. V-10. Alteration of spectral distribution of 150 kV_p x-rays in 3 mm aluminum and water.

- 1 inherent filtration
- 2 3 mm Al added
- 3 3 mm Al and 10 cm water, $\times 4.0$
- 4 3 mm Al and 20 cm water, $\times 15.0$



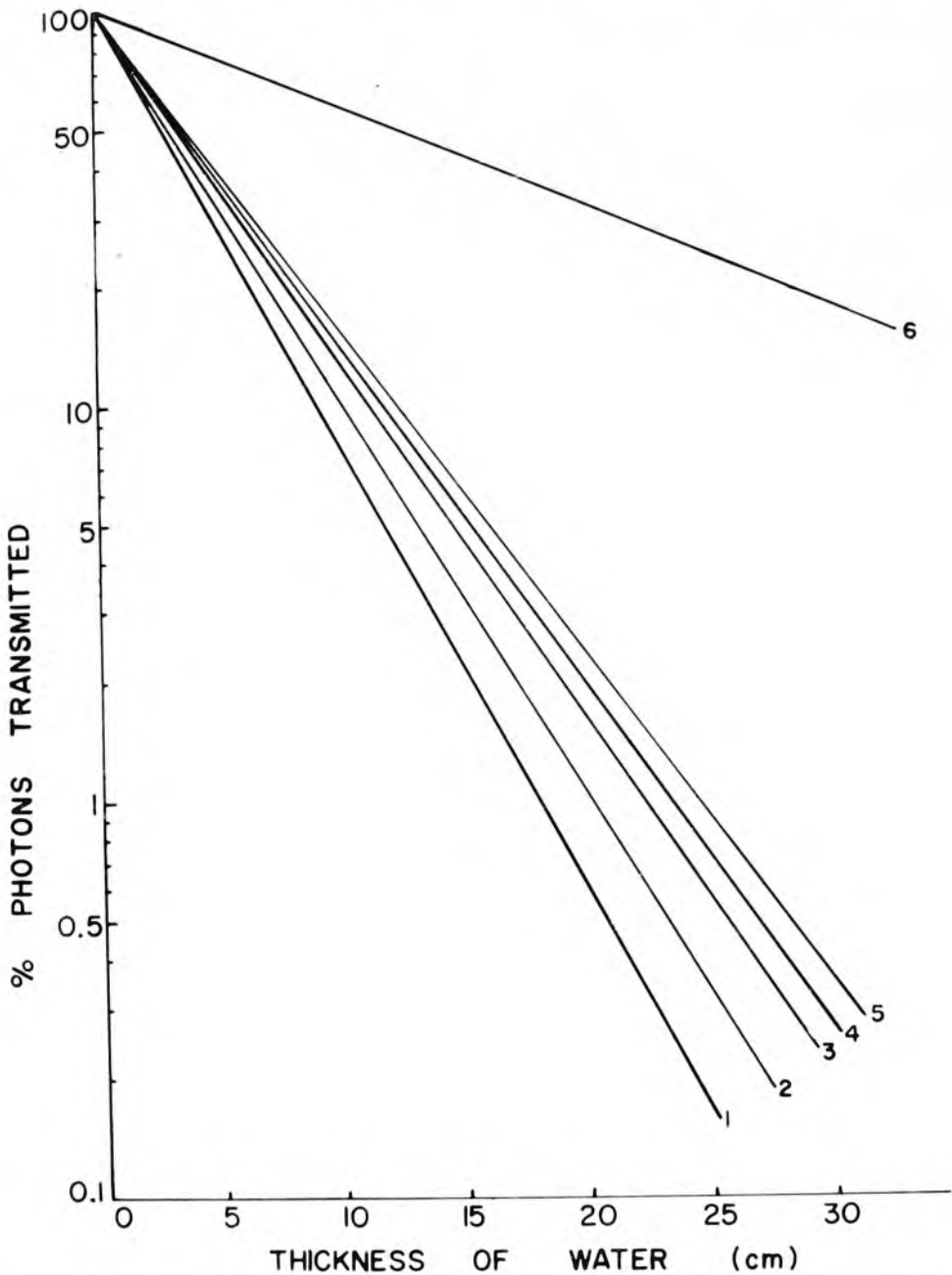


FIG. V-11. Narrow-beam attenuation of x-rays of various energies in 3 mm aluminum and water.

1 60 kV_p 2 80 kV_p 3 100 kV_p 4 120 kV_p 5 150 kV_p
 6 1200 keV γ -rays, Co^{60}

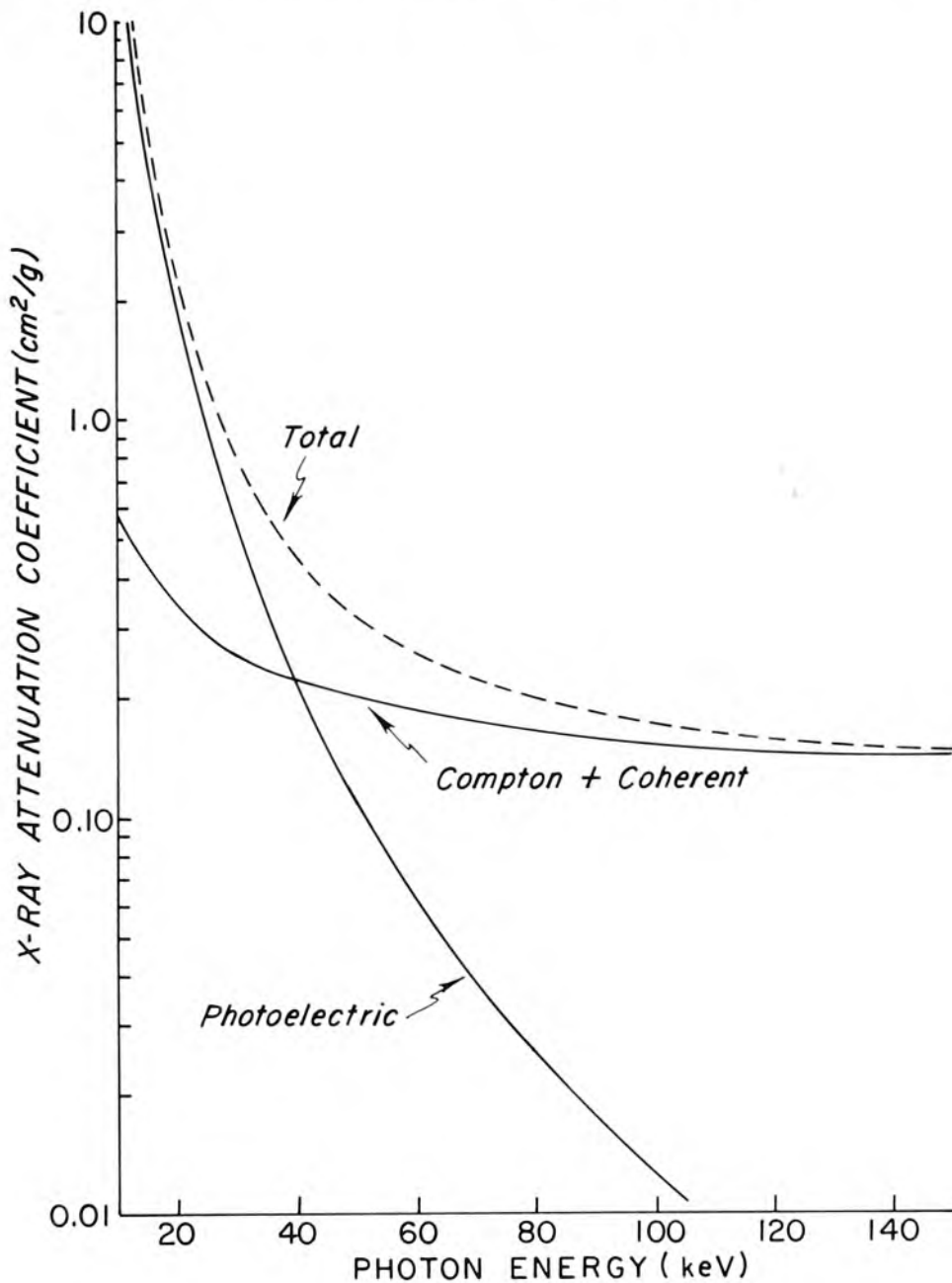
Attenuation of X-Rays in Bone

The elemental composition of bone (Table V-2) differs mainly from that of soft tissues by the presence in bone of approximately 15% by weight of calcium, which raises the effective atomic number of this tissue to the value of 11.6. Because of this relatively high effective atomic number, the photoelectric component of the attenuation of x-rays in bone is considerably

higher than that in soft tissues. Figure V-12 shows the relative contributions of photoelectric and Compton attenuations to the total attenuation of x-rays in bone. It is apparent that up to an energy of about 40 keV the attenuation in bone takes place mostly by photoelectric effect.

The attenuation of 100 keV_p x-rays in bone is shown in Fig. V-8. Because of the relatively high effective atomic number of bone and of the consequent predominance of photoelectric absorption, polychromatic x-rays are con-

FIG. V-12. Contribution of photoelectric and Compton interactions to the attenuation of x-rays in bone. (From values by Grodstein, Ref. 11.)



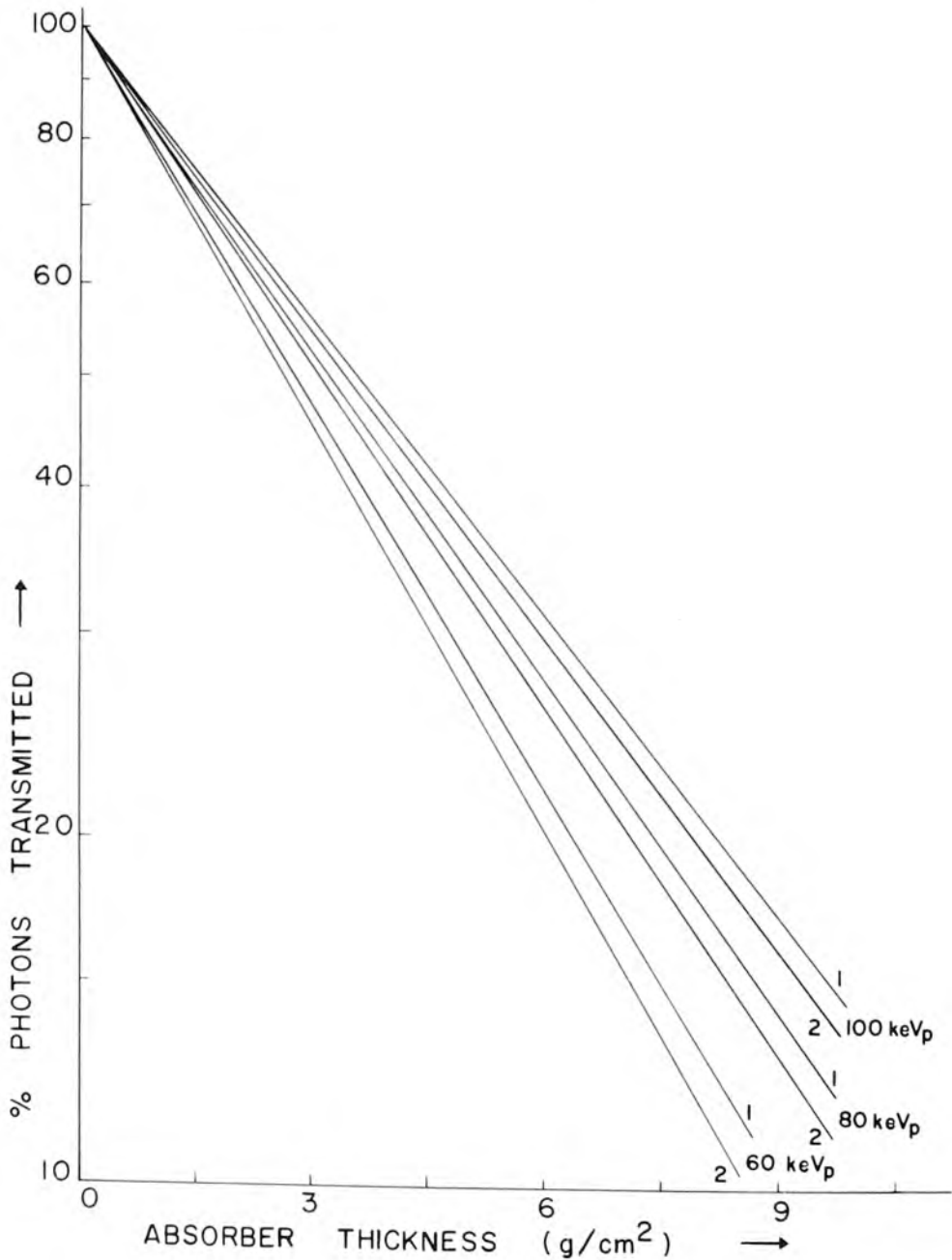
siderably "hardened" by bone, as demonstrated by the curvature of the semilogarithmic plot in Fig. V-8.

Attenuation of X-Rays in Liver

The concentration of high atomic-number elements in certain organs is considerably greater than in most soft tissues or body fluids. Such organs are the thyroid gland, which concentrates iodine selectively, and the liver and

FIG. V-13. Narrow-beam attenuation of 60, 80, and 100 kV_p x-rays in beef liver (1) and in water (2) with 3 mm Al added.

Generator Three-phase 12-pulse circuit



the spleen, in which the concentrations of tellurium are high (Ref. 5). It would appear that the concentration of high atomic-number elements in these organs renders them more opaque to x-rays, particularly to low energy photons, because of photoelectric interactions.

The attenuation of x-rays generated at various peak voltages in liver is shown in Fig. V-13. It is apparent that in spite of the relatively high tellurium content, the attenuation of x-rays in liver is lower than in water. Therefore, in spite of the high concentration of tellurium in the liver, this organ cannot be distinguished by means of a conventional roentgenographic examination from the surrounding soft tissues.

Contrast Media

Many organs and anatomic structures are not visualized by x-radiation because they exhibit the same attenuation as the tissues which surround them. For example, a blood vessel in muscle does not cast an x-ray shadow distinctive from that of muscle because the linear attenuation coefficient is the same for blood and muscle. However, the attenuation of x-rays in such structures can be altered by introducing a substance called contrast medium that has a different x-ray attenuation coefficient. The contrast medium may exhibit an attenuation coefficient either larger or smaller than that of the structure to be visualized, visualization being achieved by "contrast" with respect to adjacent tissues. The most obvious application of this method is the introduction of contrast material into body cavities, such as the rectum, the colon, the esophagus, the uterus, and others. The blood circulatory system can be visualized by the injection of contrast media into it. Some organs can be opacified with the help of their physiologic functions that concentrate the contrast media in the organs. A typical example of such an opacification is the visualization of the kidneys by intravenous injection of a contrast medium that is cleared by the kidneys.

Although in most procedures the contrast medium used increases the attenuation of x-rays in the structure or the organ to be visualized, sometimes a decrease is produced by the introduction of air into a body cavity otherwise either collapsed or filled with a body fluid. This technique is referred to as air contrast radiography and is used in the visualization of the gastrointestinal tract and the bladder, among others.

Toxicity often limits the amount of contrast material that can be safely administered. It is therefore desirable that the contrast medium exhibit a high x-ray attenuation coefficient for the radiation used. In the conventional diagnostic energy range, which comprises x-rays having peak energies below 150 keV, high attenuation of radiation can be achieved by photoelectric effect in high atomic-number elements; and contrast media most often contain high atomic number elements.

It would appear that because of the strong dependence of the photoelectric effect on the atomic number of the absorber, contrast media should

contain elements in the higher Z portion of the periodic table (for example, lead). However, throughout most of the diagnostic x-ray energy range, elements with an atomic number close to 50 exhibit a higher mass x-ray attenuation coefficient than higher atomic-number elements. This apparent paradox is due to the fact that the energy of most photons used in diagnostic radiology is insufficient to interact by photoelectric effect in the K-shell of high atomic-number elements such as lead. Under these circumstances, photoelectric absorption takes place with a relatively low probability in the L-shell of the high- Z element. On the other hand, the energy of these x-ray photons is sufficient to be highly absorbed in the K-shell of the lower- Z elements.

Figure V-14 shows a comparison of the mass attenuation coefficients for lead and iodine. For photon energies between about 33 and 88 keV, which correspond to the energies of the K -absorption edges for iodine and lead, iodine exhibits a higher attenuation coefficient than lead. Outside these limits the situation is reversed. The energy range in which iodine exhibits a higher attenuation coefficient than lead encompasses most of the photons used in diagnostic radiology. Indeed, few x-ray photons below 33 keV traverse the examined part, and few of them are generated with energies greater than 88 keV in conventional examinations. Thus, in radiologic examinations carried out with x-radiation generated by peak voltages of less than approximately 150 kV, iodine, gram per gram, is a better contrast material than lead. This also applies to the elements situated approximately in the middle of the periodic table, i.e., elements with an atomic number in the neighborhood of 50, which are superior contrast media from the radiation attenuation standpoint than heavier elements such as lead, mercury, gold, or tungsten. It is interesting to note that the two most widely used contrast media, barium and iodine, with atomic numbers of 56 and 53, respectively, are particularly suitable for the attenuation of x-rays in the conventional energy range (Ref. 6). It is probable, however, that these materials were originally selected primarily on the basis of their chemical properties and low toxicities, rather than their physical superiority with regard to x-ray attenuation.

The attenuation coefficients of medium atomic-number elements for photon energies of about 50 to 60 keV are greater than those of high atomic-number elements only if the attenuation coefficients are expressed in terms of cm^2/g (mass attenuation coefficients). The situation is reversed if linear absorption coefficients are used (cm^{-1}). In such a case, the high atomic-number elements, because of their greater densities, are better absorbers. Thus, 1 mm of lead attenuates 50 keV x-ray photons to a greater extent than 1 mm of iodine. However, because the toxicity of a contrast medium is usually determined on the basis of total mass of the material administered, the evaluation of the attenuation of x-rays in terms of mass per unit area is preferable.

Figure V-14 also shows the attenuation of x-rays in muscle (water) as

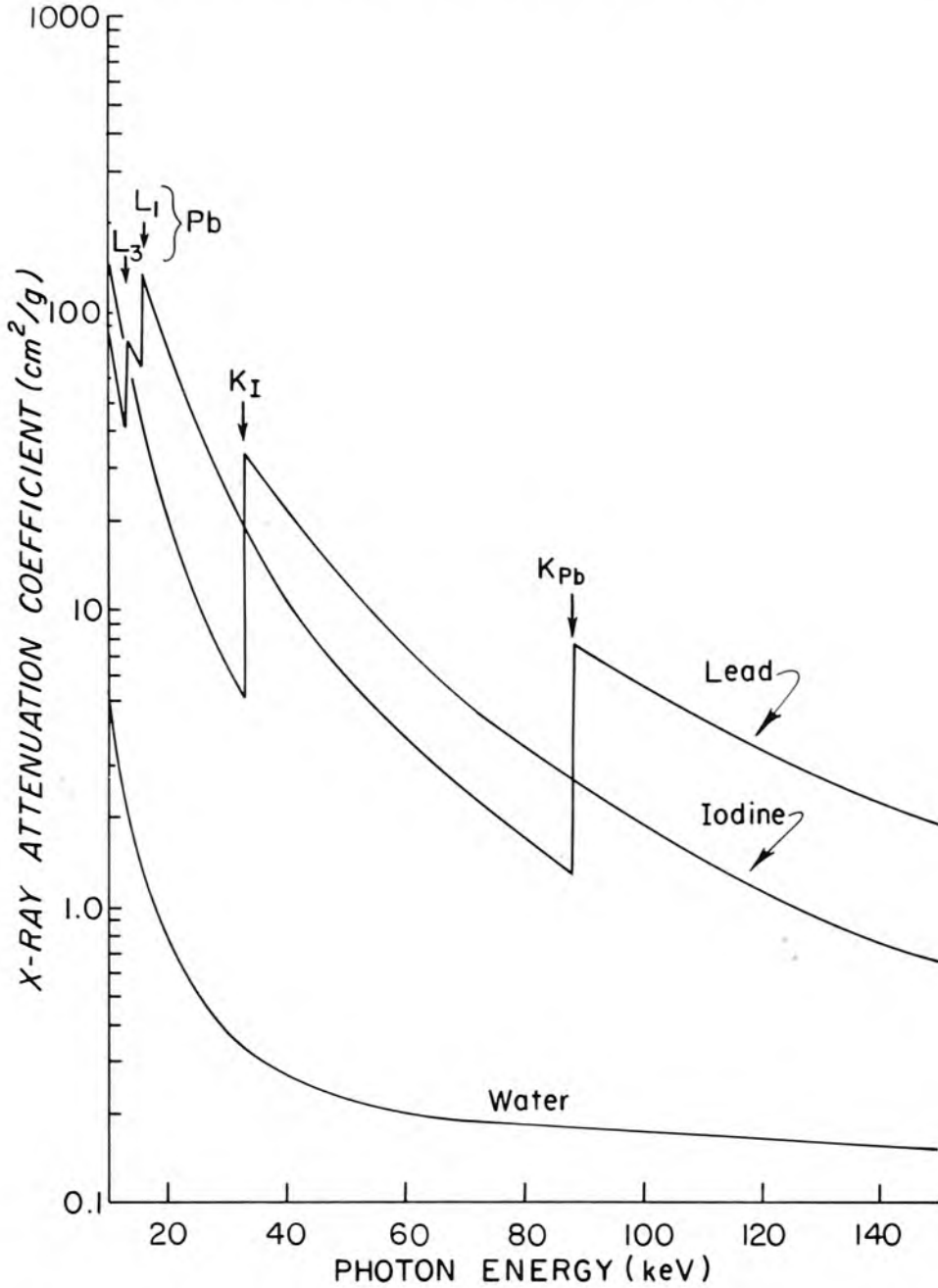


FIG. V-14. X-ray attenuation coefficients for water, iodine, and lead, as a function of photon energy. (From values by Grodstein, Ref. 11.)

compared to iodine and lead. The attenuation in both lead and iodine is so much higher than in soft tissue that it is quite obvious that the addition of even a small amount of contrast material containing these elements will enhance the opacity of a structure or organ by a considerable factor.

Comparison of Biologic Structures by Relative Contrast

Two adjacent structures can be distinguished radiologically only if there is a difference between the x-ray attenuations in the two structures. Such a

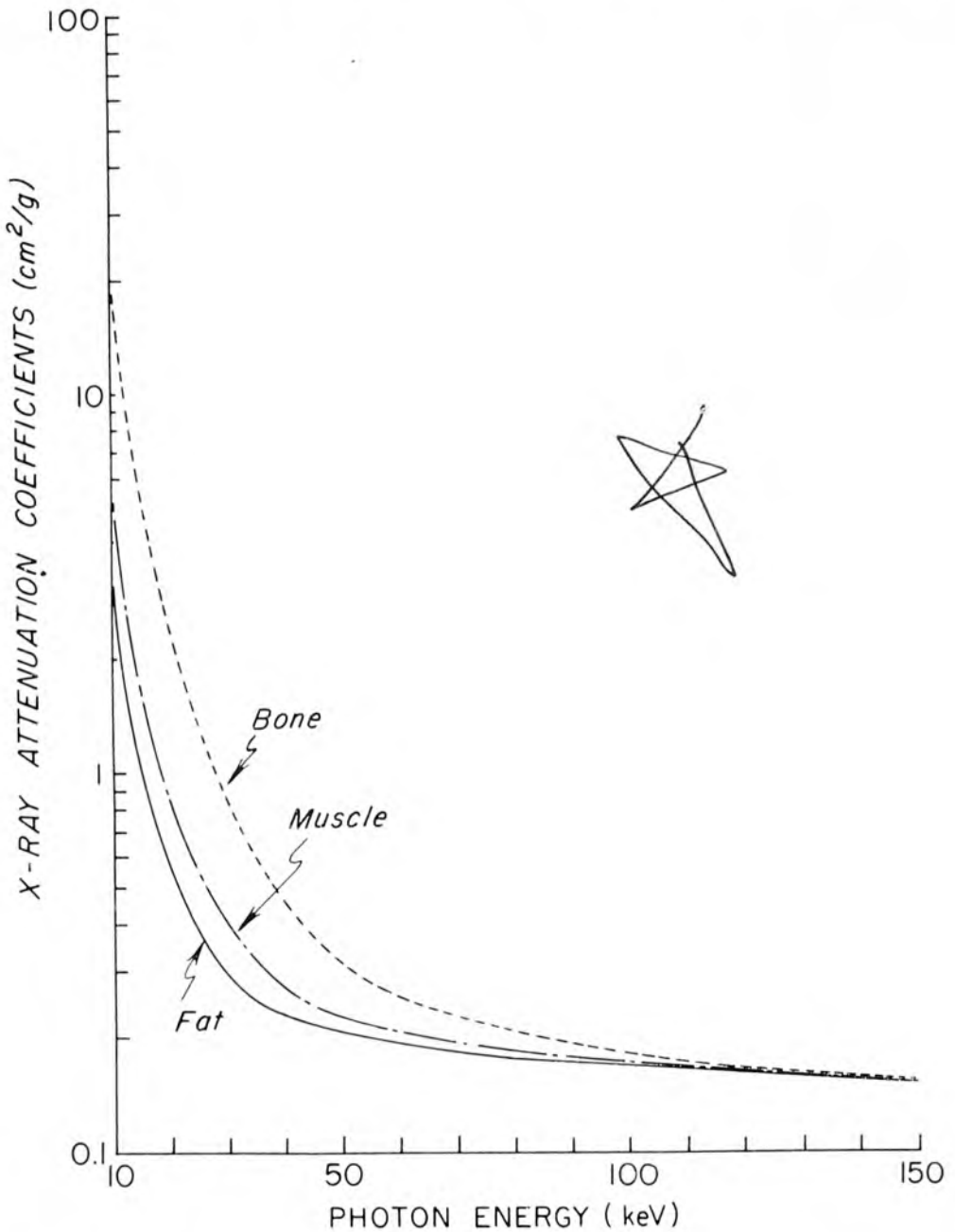


FIG. V-15. X-ray attenuation coefficients for water, fat, and bone, as a function of photon energy. (From values by Grodstein, Ref. 11.)

difference depends on the relative x-ray attenuation coefficients of the two structures and on the amounts of the two absorbers traversed. Figure V-15 shows the variations of the x-ray attenuation coefficients for bone, fat, and muscle (water) as a function of photon energy. It is apparent that the difference between these coefficients is greatest at low photon energy, that it decreases with increasing photon energy, and that it vanishes at about 120 keV. The differences exhibited at lower energies result from the contribu-

tion of photoelectric interactions, which are dependent on the effective atomic number of the absorber (Z_{eff} : fat = 6.3, muscle = 7.4, bone = 11.6) (Table V-2). At higher photon energies, with the predominance of Compton interactions, which depend only on the absorber electron density, the differences between the x-ray attenuation coefficients of fat, muscle, and bone vanish because these three tissues have almost identical electron densities (3.34×10^{23} , 3.32×10^{23} , and 3.19×10^{23} electrons per gram, respectively) (Table V-2).

It should be noted that, while the electron densities for fat, bone, and muscle are nearly equal, resulting in nearly equal Compton attenuation coefficients, their densities are different (Table V-3). Thus, equal thicknesses of fat, muscle, and bone attenuate x-rays to different degrees, even for photons having energies greater than 120 keV. In many instances the visualization of structures in radiology depends on differences in density rather than differences in attenuation coefficients. For example, a noncalcified lung tumor casts a denser shadow than the adjacent lung tissue because of a difference in density (Table V-3), although both structures have identical x-ray mass attenuation coefficients.

Table V-3. Densities of Various Human Tissues

Tissue	Density (g/cm ³)
Lung	0.32 (Ref. 8)
Fat	0.92 (Ref. 9)
Lung carcinoma	0.86 to 1.05 (Ref. 8)
Bone	1.65 to 1.85 (Ref. 10)

The structures revealed in the patient by radiologic examination can be classified as follows:

1. Muscles and body fluids. These absorbers have a density of about 1 g/cm³ and are identical with water from the standpoint of attenuation of x-rays.

2. Air pockets. From the standpoint of attenuation of x-rays an air pocket can be regarded as a vacancy in the structure in which it is found.

3. Tissues such as lung, which have a mass x-ray attenuation coefficient equal to that of muscle and water, but have a lower density.

4. Fat.

5. Bone.

6. Body structures filled with contrast media.

Figure V-16 illustrates the transmission of x-rays through a series of nodules 2 cm in diameter immersed in a 20 cm-thick water "phantom." The nodules contain respectively air, lung tissue, fat, bone, and a 10% aqueous iodine

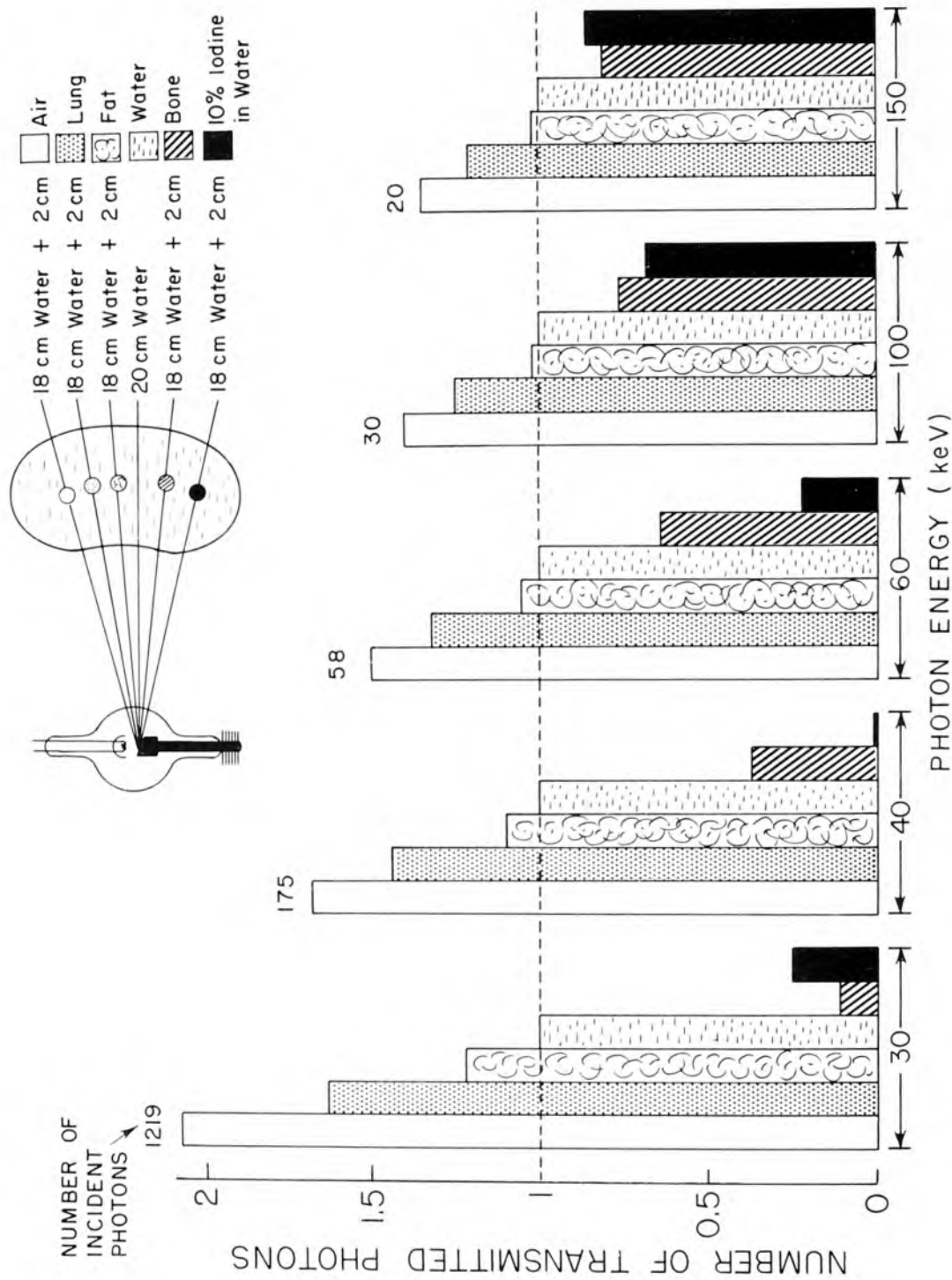


FIG. V-16. Attenuation of x-rays in 2 cm of air, lung, fat, water, bone, and 10% iodine in water, as a function of photon energy. The number of incident photons is normalized for a transmission of one photon through 20 cm of water.

solution. The number of photons impinging on the phantom has been normalized to a value corresponding to the transmission of one photon by 20 cm of water. It is apparent that the differences between the transmissions of radiation through the different absorbers, which are proportional to the contrasts between the absorbers, decrease with increasing photon energy. The relative contrast of bone and iodine reveals an interesting situation. For 30 keV photons, bone (under the described circumstances) absorbs more radiation than iodine; while for 40 keV photons the situation is reversed, so that iodine attenuates much more than bone. For 60 and 100 keV photons, iodine is still a better absorber than bone. However, the difference in absorption between these two media is reduced with increasing photon energy: for 150 keV photons, the situation has been reversed and bone is a slightly better absorber than iodine.

This effect can be explained by comparing the x-ray attenuation coefficients for bone (Fig. V-12) and iodine (Fig. V-14). The attenuation of x-rays in bone decreases with increasing photon energy. (The ratio of the x-ray attenuations in water and in bone also decreases with increasing photon energy. The cause of this effect is apparent from Fig. V-15.) On the other hand, the attenuation of x-rays in iodine in the energy range of 30 to 150 keV exhibits a discontinuity because the K absorption peak of iodine occurs at approximately 33 keV (Table II-1). Thus, for 30 keV photons the attenuation of x-rays in iodine is relatively low because these photons do not carry sufficient energy to undergo photoelectric interactions in the K-shell. At 40 keV, however, the energy of the impinging x-ray photons is greater than the binding energy of the K-shell of iodine, and the attenuation of x-rays in that medium is intense. Thereafter, with increasing photon energy, attenuation in iodine again decreases. At 150 keV the attenuation in bone surpasses that in iodine, although the attenuation coefficient for iodine is still greater than that for bone because of the greater mass per unit area (g/cm^2) of bone traversed by the radiation.

In conclusion, the maximum differential in the attenuation of x-ray photons in organs and other anatomic structures is observed for very low energy radiation, where the contribution of photoelectric attenuation is important. This differential decreases with increasing photon energy (Fig. V-17). When contrast media are used, maximum attenuation occurs for photons with energies slightly higher than the K absorption discontinuity in the element used as contrast material. For iodine, maximum attenuation occurs at a photon energy slightly greater than 33 keV. It should be noted that the high differential attenuation of low energy photons is also accompanied by a high total attenuation of the beam. Thus, as shown in Fig. V-16, a beam of 30 keV photons is attenuated by a factor of 1219 when passing through 20 cm of water, while an attenuation factor of only 20 is observed with 150 keV photons. The use of very low energy photons in diagnostic radiology, although highly desirable from the standpoint of

obtaining high contrast, is, in most instances, limited by the high total absorbability of such radiation which results in an undesirably high exposure of the patient to radiation.

HIGH VOLTAGE RADIOGRAPHY

Practically all radiologic examinations are carried out by means of x-rays generated with tube potentials under 150 kV. However, radiographic examinations have been carried out (mostly in Sweden) by means of heavily filtered x-rays generated with a potential of 200 kV; and the possibility of using x-rays in the MeV range in diagnostic radiology has been investigated by Tuddenham and his co-workers (Refs. 12 and 13). The main purpose of using higher energy radiation in diagnostic radiology is to reduce the difference in the absorption of x-rays in bone and in soft tissues in an attempt to improve the visualization of soft tissue structures overlying bone. In the conventional diagnostic x-ray energy range the contribution of the photoelectric effect to the attenuation of x-rays in bone is important; and because of its relatively high effective atomic number, bone in this radiation energy range is considerably more opaque to x-rays than soft tissues (see Sections on "Attenuation of X-Rays in Bone" and "Comparison of Biologic Structures by Relative Contrast," above). Under the circumstances the radiologic visualization of soft tissue structures which overlie bone is difficult because they are "overshadowed" by the underlying bone. For example, a radiographic examination of the chest with suitable visualization of the lung field does not show much detail of mediastinal structures because of inadequate penetration of x-rays through bone (Fig. V-18).

The use of higher energy x-rays reduces the contribution of photoelectric attenuation, and for photon energies above 120 keV, the x-ray mass attenuation for bone is practically identical with that of muscle (Figs. V-15 and V-18).

Figure V-17 shows a comparison of conventional energy and high energy radiographs. It can be seen that, although bone is still apparent on the high energy films because of its higher density than soft tissues, these radiographs show good visualization of air passages, which in the conventional examination are obscured by bone shadow.

High energy x-rays have been generated for diagnostic purposes with conventional x-ray generators (up to 200 keV_p), with resonant transformers (Refs. 12 and 13) (2,000 keV_p), and with Van de Graaff generators (2,000 keV_p) (Refs. 13 and 15). Cobalt-60 gamma radiation has also been used for this purpose (Ref. 14). For 200 keV_p radiography, conventional x-ray intensifying screens can be used; but for higher photon energies conventional

FIG. V-17. Radiographs of: **A** head; **B** chest; **C** pelvis; exposed with 70 kV_p (bottom) and 2 MV_p (top) x-rays (2 MeV Van de Graaff generator). (Courtesy of Dr. D. Cochran, Department of Radiology, University of Missouri Medical School.)



FIG. V-17A (*Legend on opposite page*).

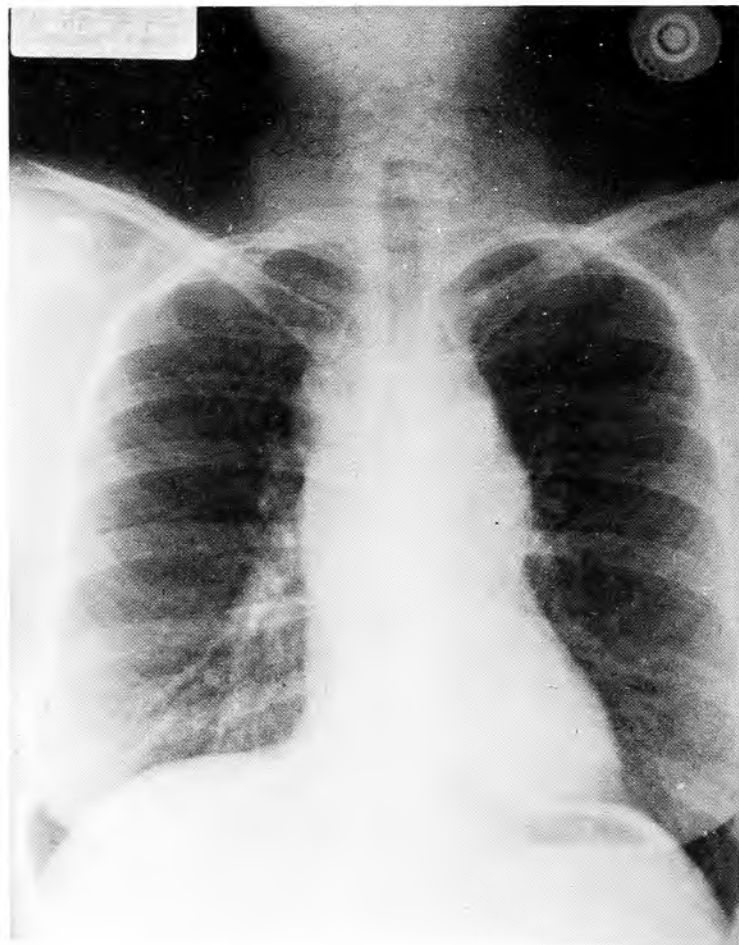
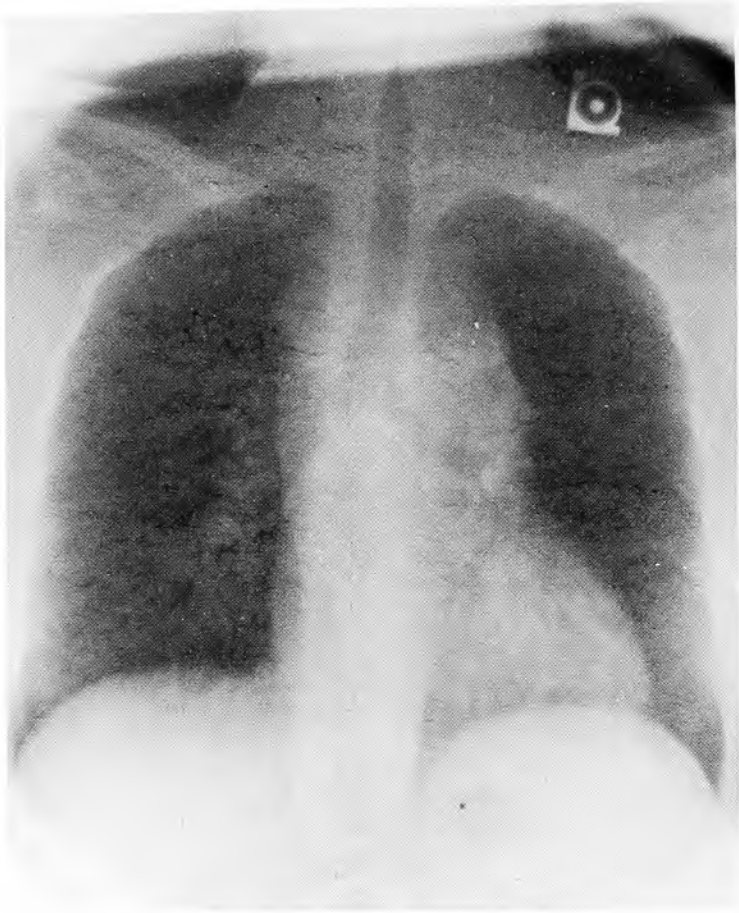


FIG. V-17B (*Legend on page 176*).

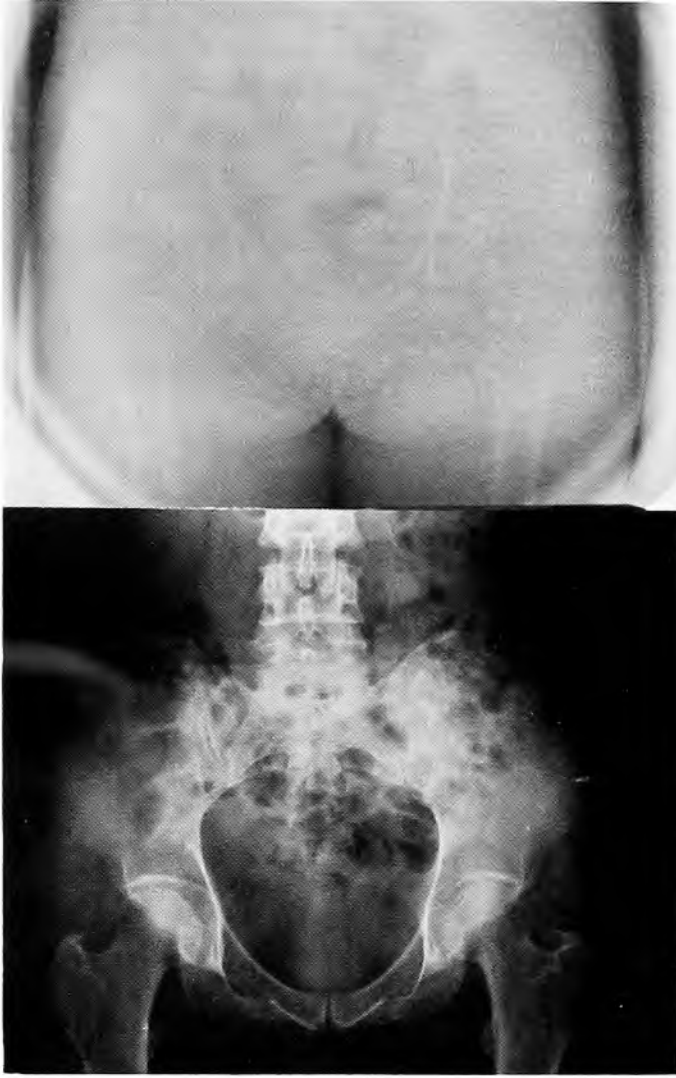


FIG. V-17C (*Legend on page 176*).

screens are too transparent to x-rays, and lead screens are used. Lead screens, which are typically 0.005 in. thick (Ref. 12), do not fluoresce in the visible range; but they generate secondary electrons subsequent to absorption of x-rays; it is these electrons that expose the film.

The use of high energy radiography has been shown to increase the visibility of mediastinal structures without overexposing the lung field (Refs. 1 and 2). High energy radiographic techniques are particularly applicable to the visualization of bronchogenic carcinoma which often escapes detection because of overlying skeletal parts (Ref. 12) for visualization of the larynx, and for field localization in radiation therapy (Refs. 14 and 15).

The main disadvantages of high energy radiography are:

1. The contrast of the examination is drastically reduced because of the low attenuation of the radiation in tissues.

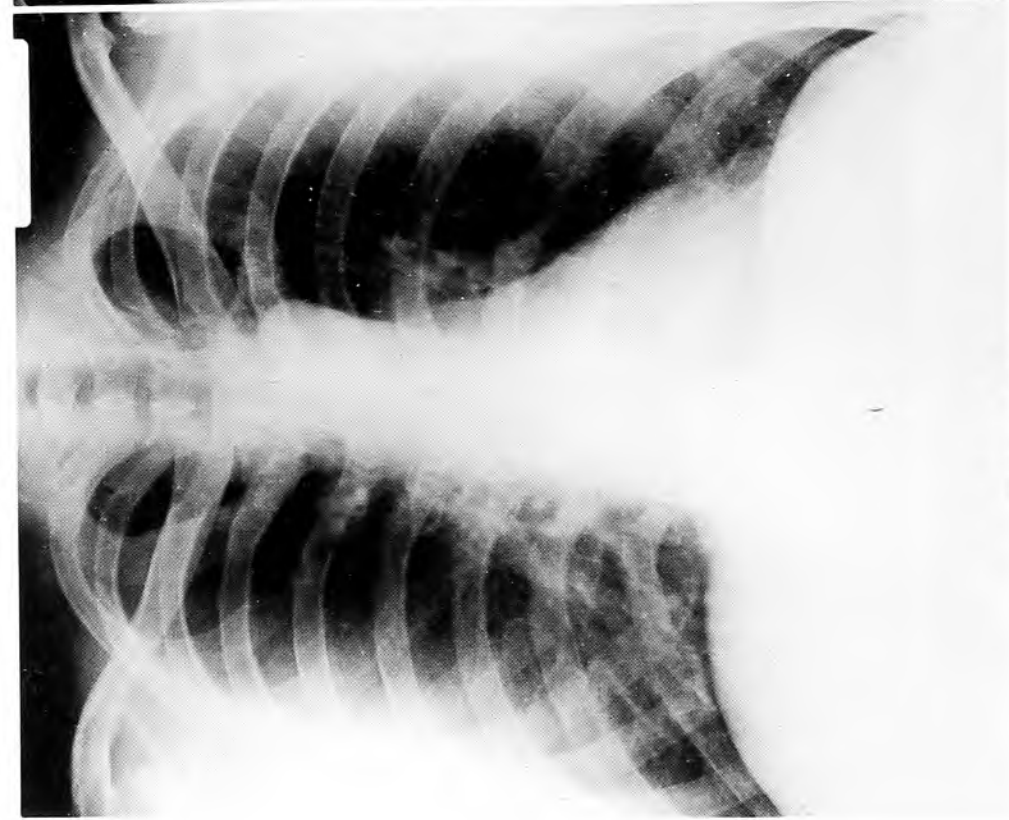


FIG. V-18A.

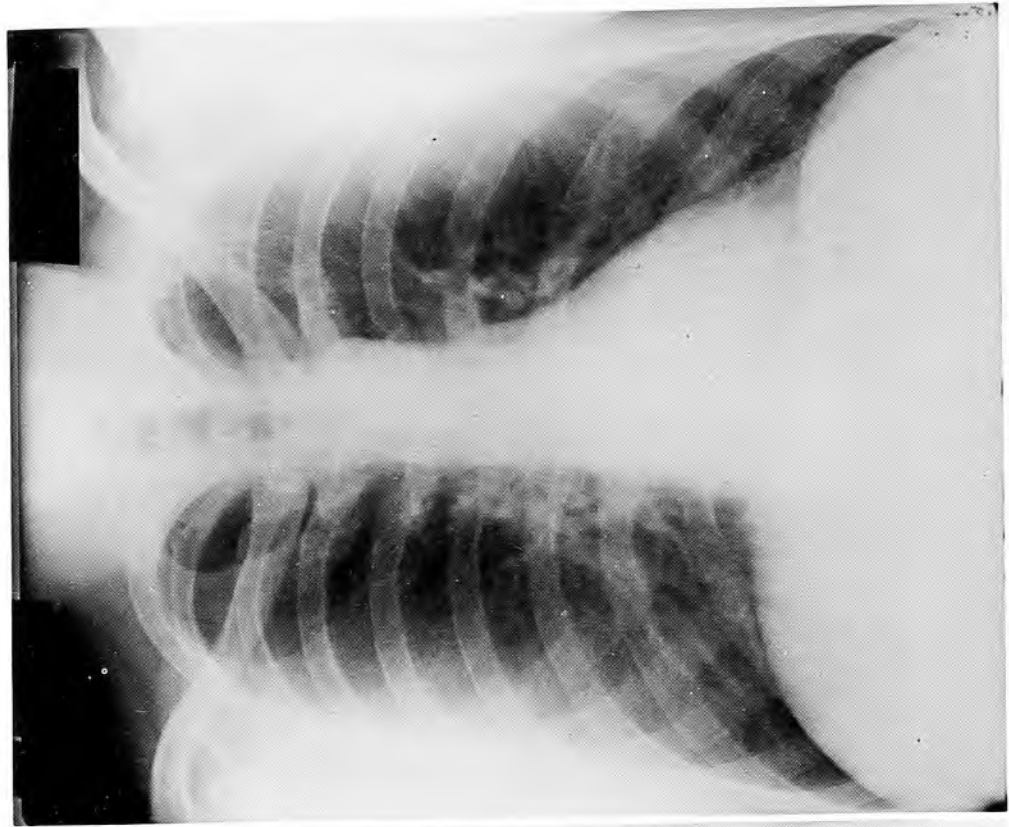


FIG. V-18B.

FIG. V-18. Three radiographs of chest of same individual exposed with different x-ray energies. Note decrease in contrast with increasing x-ray energy.

A 75 kV_p—16 mAs

B 100 kV_p—4.8 mAs

C 150 kV_p—2 mAs

Focus-film distance in all three 72 in.

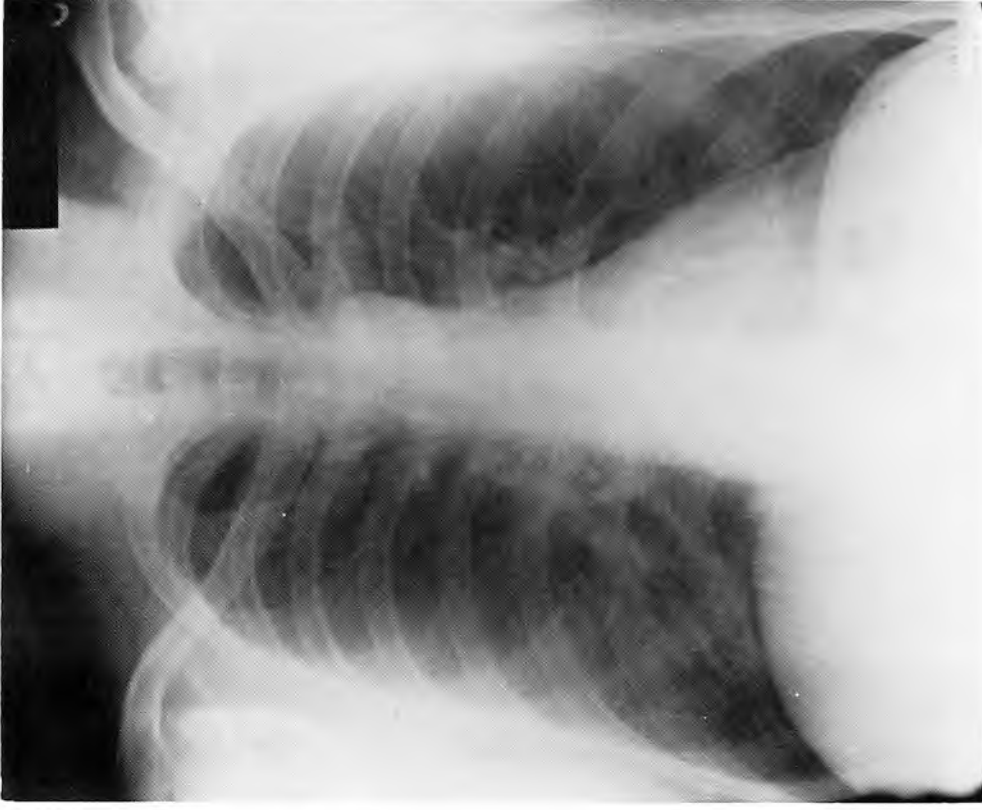


FIG. V-18C.

2. The scattered radiation generated by Compton interactions of the high energy photons is emitted mostly in the forward direction (Fig. III-8) and it is practically impossible to remove it by means of a grid because of the small angle of scattering, and because of the high penetration of the scattered radiation. This scattered radiation contributes to further reduce the contrast.

3. The dose of radiation delivered to the patient during a high energy radiographic examination is considerably higher than that of a conventional



FIG. V-19. Mammogram showing benign cyst (fibrosarcoma of breast).

Technique 30 kV_p, 300 mA, 6 sec

Focus-film distance 40 in. on Kodak Industrial Film Type M
(*Courtesy of Dr. P. Ruben Koehler, The Edward Mallinckrodt Institute of Radiology.*)

examination because little of the high energy radiation is absorbed by the screens.

LOW ENERGY RADIOGRAPHY—MAMMOGRAPHY

Certain radiographic examinations require the visualization of soft, sometimes calcified, tissue lesions that are surrounded by soft tissue. A typical example of such an examination is mammography (Ref. 16), where the breast is examined radiographically mainly for the purpose of visualizing neoplastic and also benign lesions (Fig. V-19). Radiographic examinations of this type require high soft-tissue contrast and high absorption of x-rays in calcium. Both of these factors are maximized by using the lowest possible energy radiation (see Figs. V-15 and V-16). No consideration need be given to the location of the K absorption discontinuity of calcium, which occurs at about 4 keV, because x-ray photons in that energy range are inconsequential in the examination.

The main technical problem in mammography is to generate a sufficiently intense beam of x-rays suitable for exposure of the film. The difficulty is created by a combination of four factors: (1) The process of generating the low energy x-rays required (approximately 30 kV_p accelerating voltage) is very inefficient. (2) The intensity of the low energy x-radiation produced is appreciably reduced by inherent filtration in the tube. (3) The low energy x-ray beam is much attenuated in the breast, and only a small percentage of the photons reach the film. (4) Because of the high resolution required for the examination, intensifying screens are not used.

These four factors impose a particularly heavy load on the x-ray tube (Ref. 17). Tubes fitted with beryllium windows for the purpose of reducing inherent filtration have been used in mammography. The improvement thus achieved is limited by the fact that the very low energy photons which escape the tube through the beryllium window are rapidly absorbed by the breast, and few of them contribute to the examination. For mammography, beryllium window tubes do not appear to be superior to glass window tubes.

REFERENCES

1. TROUT, E. D.: The life history of an x-ray beam. *Radiol. Tech.* 35:161, 1963.
2. TODD, W. R., and WEST, E. S.: *Textbook of Biochemistry*, 3rd ed. New York, Macmillan, 1961.
3. HIRSCH, J., FARQUHAR, J. W., AHRENS, E. H., JR., PETERSON, M. L., and STOFFEL, W.: Studies of adipose tissue in man. *Amer. J. Clin. Nutrition* 8:499, 1960.
4. HILDITCH, T. P.: *The Chemical Composition of Natural Fats*, 2nd ed. New York, Wiley, 1947.
5. *Radiobiological Dosimetry*. Recommendations of the International Commission on Radiological Units and Measurements (ICRU), Report 10E, 1962. NBS Handbook 88. Washington, D.C., U.S. Government Printing Office, 1963.
6. OOSTERKAMP, W. J.: Monochromatic x-rays for medical fluoroscopy and radiography? *Medica Mundi* (Philips Company) 7(#3):72, 1961.

7. JOHNS, H. E.: *The Physics of Radiology*, 2nd ed. Springfield, Ill., Thomas, 1961.
8. JACOBSON, L. F., and KNAUER, I. S.: Correction factors for tumor dose in the chest cavity due to diminished absorption and scatter in lung tissue. *Radiology* 67:863, 1956.
9. HODGMAN, C. D., WEAST, R. C., and SELBY, S. M., eds.: *Handbook of Chemistry and Physics*, 41st ed. Cleveland, Ohio, Chemical Rubber Publishing Company, 1959-1960.
10. *Clinical Dosimetry*. NBS Handbook 87. Washington, D.C., U.S. Government Printing Office, 1963.
11. GRODSTEIN, G.: X-ray attenuation coefficients from 10 keV to 100 MeV. NBS Circular 583, 1957.
12. TUDDENHAM, W. J., HALE, J. F., and PENDERGRASS, E. P.: Supervoltage diagnostic roentgenography. *Amer. J. Roentgen.* 70:759, 1953.
13. TUDDENHAM, W. J., GIBBONS, W. J., HALE, J. F., and PENDERGRASS, E. P.: Super-voltage and multiple simultaneous roentgenography—a new technique for the examination of the chest. *Radiology* 63:184, 1954.
14. PERRYMAN, C. R., McALLISTER, J. D., and BURWELL, J.: Cobalt-60 radiography. *Amer. J. Roentgen.* 83:525, 1960.
15. HARE, H. F., LIPPINCOTT, S. W., JR., and SAWYER, D.: Physical and clinical aspects of super-voltage rotational therapy. *Radiology* 57:157, 1951.
16. GERSHON-COHEN, J., and INGLEBY, H.: Roentgenology and pathology of cyclic disturbances in breast. *Surg. Gynec. Obstet.* 94:91, 1952.
17. KIRKA, C.: X-ray tube considerations for mammography. *Cathode Press* (Machlett Company) 18(#2), 1961.

(VI)

THE RADIOLOGIC EXAMINATION, Part B: The Radiologic Image and the Retrieval of Information

In a radiologic examination the information extracted by the x-ray beam from the examined part consists of the attenuation of this beam by the structures through which it passes. The spatial distribution of the transmitted photons in a plane perpendicular to the emerging x-ray beam, is called the radiologic or x-ray image.

QUALITY OF THE RADIOLOGIC IMAGE

The faithfulness, or quality, of the radiologic image can be defined as the ability of this image to reflect the spatial variations in the attenuation of x-rays by the examined object. For example, if two adjacent objects differ in their opacities to x-rays by 10%, a faithful radiologic image of these objects consists of two areas in which the number of photons per unit area differ by 10% and the boundary between the two areas on the image is identical with that separating the two objects. Many physical factors, such as finite size of the x-ray focal spot, scattered radiation, etc., contribute to the deterioration of the quality of a radiologic image. These factors will be discussed later in this text. First we shall examine the upper limit of the quality of the radiologic image, assuming that the variable under scrutiny is the ability of the image to "code" information.

The maximum amount of information coded in a radiologic image, which determines the quality of the image, is limited by only two factors: (1) the uncertainty principle which limits the ability of x-ray photons to interact with small structures and therefore to reproduce fine detail, and (2) the statistical fluctuations of the x-ray photons that form the radiologic image.

Limitations Imposed by the Uncertainty Principle

One of the consequences of the uncertainty principle is that, when a system is studied by its interaction with an electromagnetic radiation, the maximum resolution obtained can at best be of the magnitude of the wavelength of the radiation used. The wavelength of x-rays commonly used in

diagnostic radiology is of the order of 0.1 \AA ; therefore it is impossible to achieve a resolution greater than this in radiologic images. Since 0.1 \AA is a subatomic dimension, the restriction imposed by the uncertainty principle on the possible quality of the radiologic image is inconsequential in the present discussion.

Limitations Imposed by the Information-Carrying Capacity of the Beam

The amount of information either acquired or stored by any physical system is limited by the total number of information-carrying elements contained in the system. In the case of the radiologic image, these information-carrying (coding) elements are the number of photons per unit area; indeed, the quality of the image depends on this number. This concept can be illustrated by considering the extreme case of a radiologic examination carried out with one single photon. Under such circumstances, the radiologic image is either a blank or consists of one photon. It is apparent that in either case the information content of such an image is low. If a greater number of photons are used, for example, if the radiologic image consists of ten photons per square centimeter, the amount of information contained in the image is greater than in the previous example.

This line of reasoning indicates that the quality of the radiologic image increases with the number of photons per unit area, and that this image may reproduce faithfully the examined structure only if the number of photons per unit area is infinitely large. It may seem that the number of photons used in an actual radiologic examination is so great that from a practical standpoint the number of photons that form the image is large enough to produce an image of high quality. In practice, however, the intensity of the x-radiation used in a radiologic procedure is severely limited by the fact that it is undesirable to expose a patient to too much radiation; and, in many instances, the quality of the examination indeed suffers from the small number of photons per unit area in the image.

Statistical Nature of the Radiologic Image

The emission and absorption of x-rays are random events, the frequencies of which can be predicted only by the law of probability. For example, it is impossible to predict with certainty whether or not the interaction of an electron with the target of an x-ray tube will result in the emission of an x-ray photon. The only prediction that can be made is that the probability of such an event is equal to a certain value. The attenuation of x-rays in matter obeys the same statistical law; if a photon strikes one half-value layer of absorber it is impossible to predict whether the photon will be removed from the beam or not; all that can be said is that the probability of such an occurrence is 50%. Statistical laws, however, permit very accurate predictions concerning large numbers of events. The formation of the radiologic image results from the production and the attenuation of x-ray photons;

and because of the statistical nature of these events, the distribution of photons in the radiologic image is also subject to the laws of statistics.

In the image of an object exhibiting uniform attenuation of x-rays, the number of photons per unit area (photon fluence) over the whole surface of the image is constant only if the number of photons used is infinitely large. If a finite number of photons has been used in the examination, then the photon fluence of the image varies from area to area. These photon fluence variations obey the statistical theory of random events and are called statistical fluctuations.

These fluctuations are of particular importance if the radiologic image is formed by a small number of photons. Their influence decreases with increasing number of photons and vanishes when the number of photons reaches infinity, as can be demonstrated by the following example: Assume the radiologic image of a uniform absorber formed by the attenuation of two x-ray photons both impinging upon one square centimeter of an object that has a uniform attenuation of 50%. Under the circumstances one might expect the radiologic image to be formed by one photon per square centimeter. In practice, the photon density will vary from zero to two photons per square centimeter, with a higher occurrence of one photon per square centimeter than either zero or two. If the number of photons used in the formation of the image is increased, then the pattern becomes more uniform by a gradual reduction in the statistical fluctuations.

Poisson Distribution

The distribution of the photon fluence in a radiologic image can be expressed by plotting the number of square centimeters containing a given number of photons (frequency or probability of occurrence of a given number of events) versus the number of photons counted per square centimeter (number of events per interval). The distribution of events thus obtained, which is shown in Fig. VI-1, is called a Poisson distribution. The equation for the Poisson distribution is (Ref. 1):

$$P_N = \frac{\bar{N}^N e^{-\bar{N}}}{N!}, \quad (1)$$

where P_N = probability of occurrence of N events, N = number of events, \bar{N} = average number of events, e = base of natural logarithms, and $N!$ = factorial $N = N \times (N - 1) \times (N - 2) \times \cdots \times 1$. The probability of occurrence of a number of events in a range $\bar{N} \pm N$ is given by the area under the Poisson distribution curve between $-N$ and $+N$.

For a small number of statistical events ($\bar{N} < \text{about } 20$), the Poisson distribution is asymmetrical (Fig. VI-1A). As \bar{N} increases, the distribution approaches a Gaussian, or normal curve and becomes symmetrical (Figs. VI-1B and 1C).

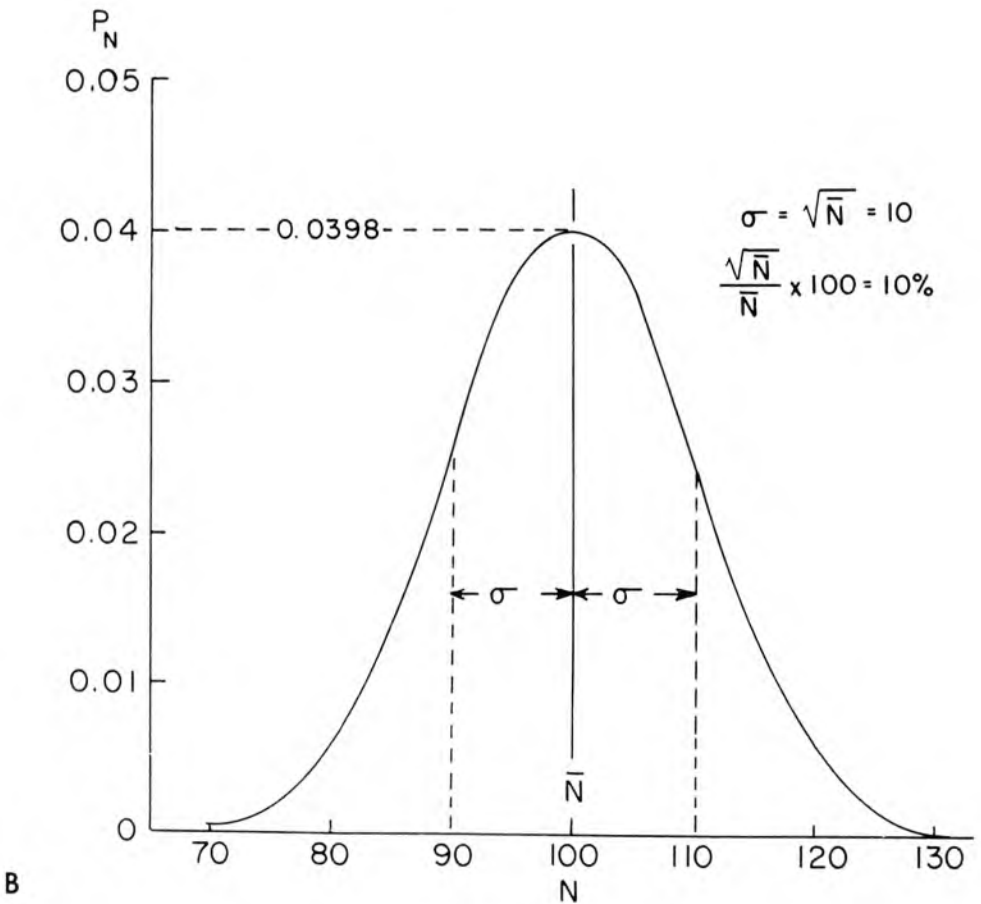
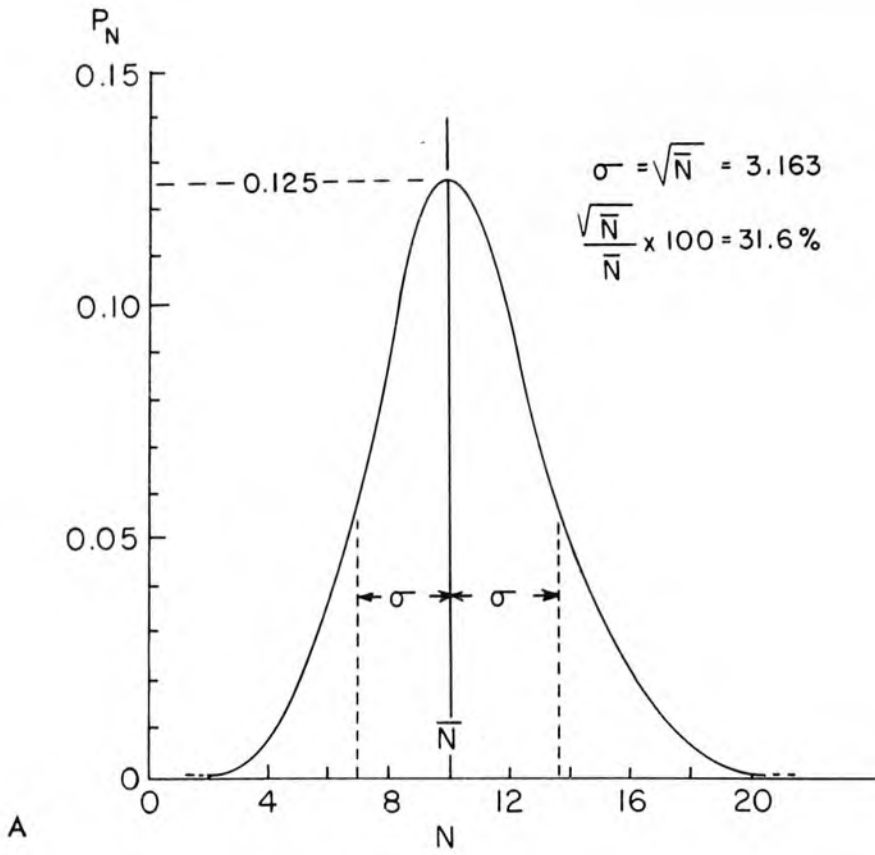


FIG. VI-1A and B (Legend on facing page).

The Poisson distribution shows that while the probability of occurrence of a number of events is greatest for an average value, there is a finite probability of occurrence of very low and very high numbers of events.

Standard Deviation

Any number of events subject to statistical fluctuation may differ from the average measure of the physical phenomenon it represents by any value, so that the exact value of a number of events subject to statistical fluctuation cannot be determined. It is, however, possible to predict that the true value of a number subject to statistical fluctuation will be found with any desired degree of probability within a certain range of the observed value.

Such an analysis, which is based on the assumption that the observed number is part of a Poisson distribution, makes use of the concept of stand-

FIG. VI-1. Poisson distributions for different average numbers of events (\bar{N}).

A $\bar{N} = 10$ B $\bar{N} = 100$ C $\bar{N} = 1000$

Note that the distribution for $\bar{N} = 10$ is asymmetrical with respect to \bar{N} . As \bar{N} increases, the Poisson distribution tends to become symmetrical and approaches a Gaussian distribution.

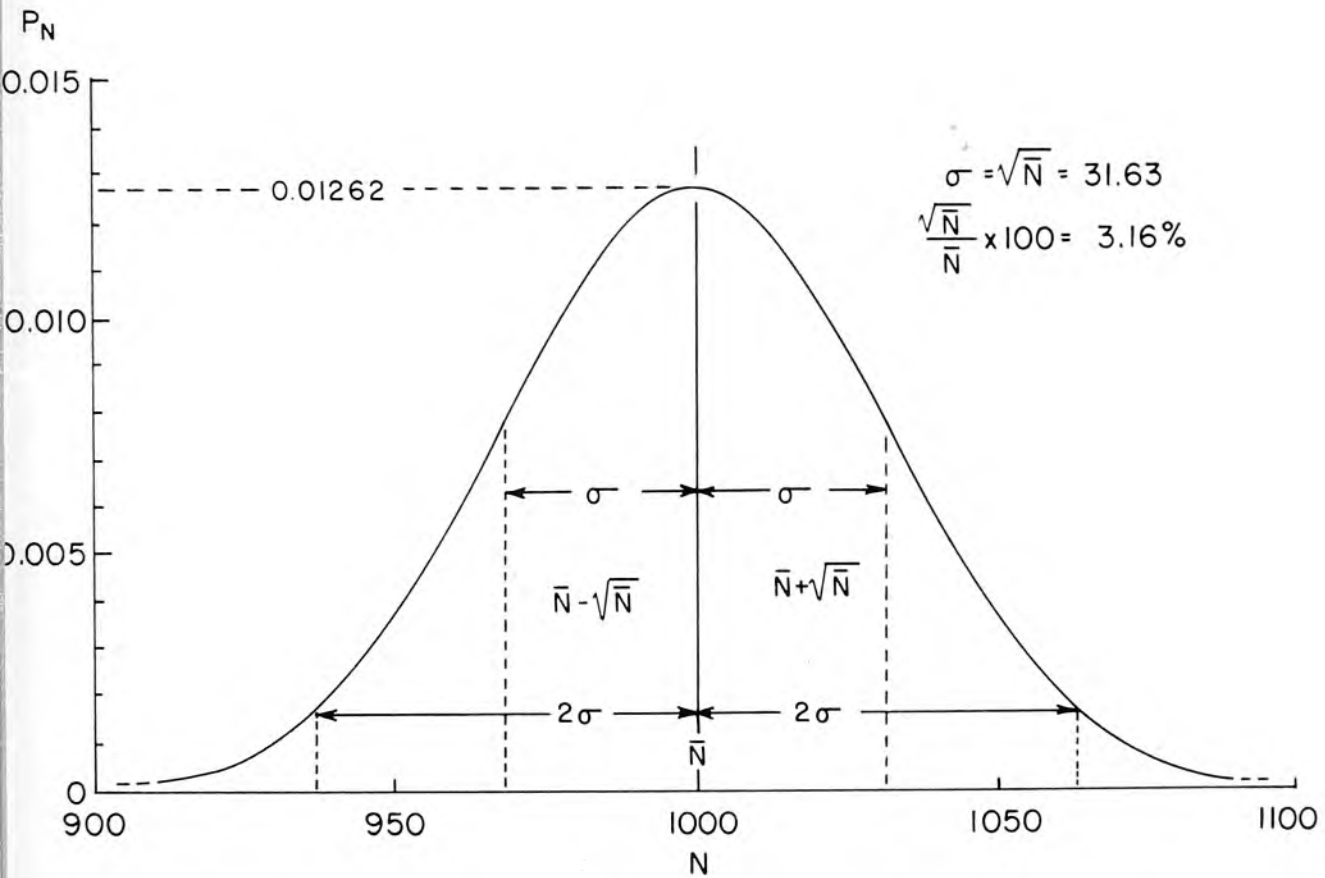


FIG. VI-1C.

ard deviation. The standard deviation σ of a number N subject to statistical fluctuation is approximately equal to

$$\sigma \simeq \sqrt{N}.$$

The probability that the true value of N is found in the interval $N \pm \sigma$ is about 68%; it is about 95% for the interval $N \pm 2\sigma$, and about 99.7% for the interval $N \pm 3\sigma$. This distribution of probabilities is due to the fact that 68% of the area of the Poisson distribution lies between $\bar{N} \pm \sqrt{\bar{N}}$, that 95% of this area is between $\bar{N} \pm 2\sqrt{\bar{N}}$, and 99.7% of this area is between $\bar{N} \pm 3\sqrt{\bar{N}}$ (Fig. VI-1).

The ratio of the standard deviation σ to the number of events N ,

$$\frac{\sigma}{N} = \frac{\sqrt{N}}{N} = \frac{1}{\sqrt{N}}, \quad (2)$$

decreases when N increases (Fig. VI-1). This means that as the number of events observed increases, the statistical fluctuations of that number vary proportionally less from the average value. When N becomes infinitely large, σ/N vanishes.

Statistical Fluctuations and Quality of the Radiologic image

The influence on the image of the statistical fluctuations in the number of photons forming the radiologic image on the quality of the latter can be demonstrated as follows (Figs. VI-2-1 and VI-2-2):

Two adjacent objects, A and B, are subjected together to two radiologic examinations. It is assumed that the attenuation of the radiation used in the two examinations is 10% greater in object A than in object B. The two radiologic examinations, which differ only in the number of x-ray photons used, are carried out as follows: (1) Examination 1 (Fig. VI-2-1) provides radiologic images of the two objects with 100 photons ($100 hn$) per mm^2 for the image cast by object A and with $110 hn$ per mm^2 for Image B. (2) Examination 2 (Fig. VI-2-2) is carried out with a number of photons ten times greater than Examination 1; or, for Image A, $N = 1000 hn$ per mm^2 ; for Image B, $N = 1100 hn$ per mm^2 .

In both examinations the Poisson distributions of the statistical fluctuations of the number of photons per square millimeter intersect. The area of overlap of the two curves is proportional to the probability of observing a reversal in the relative number of photons per mm^2 in the two images (greater number of photons per mm^2 in Image A than in Image B). It is apparent from Fig. VI-2 that in Examination 1 the area of overlap represents a larger fraction of the total area under the distributions than in Examination 2. This means that in Examination 1, owing to the frequent reversal of photon fluence, the boundary between the radiologic images of areas A and B is more "jagged" than in Examination 2, which provides a

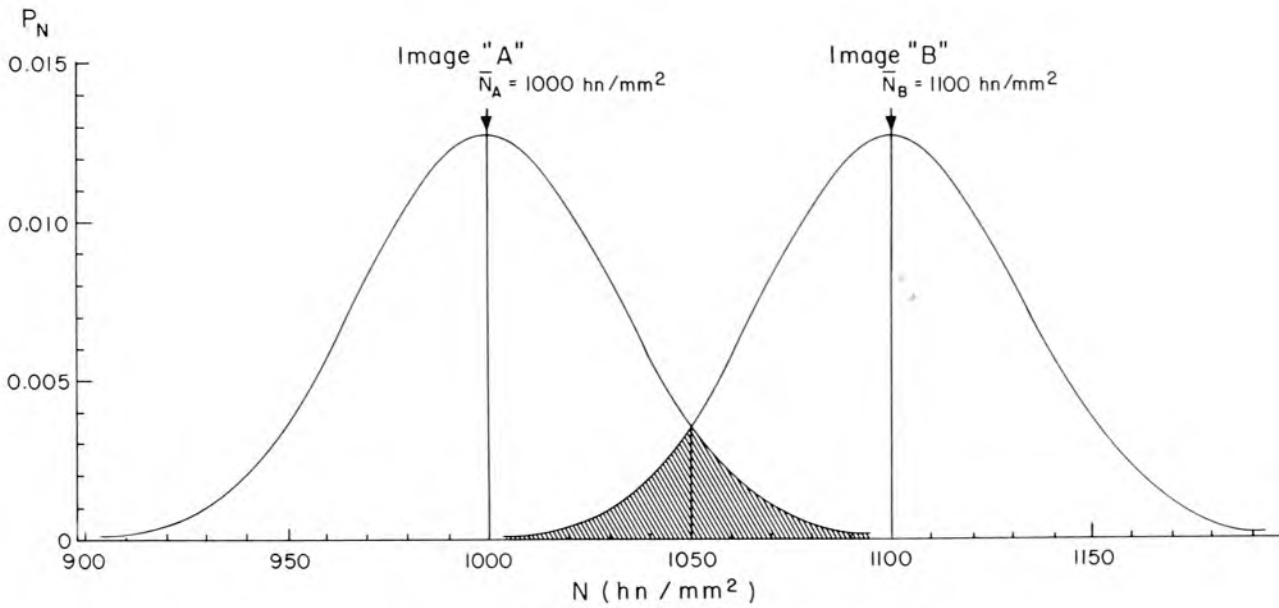
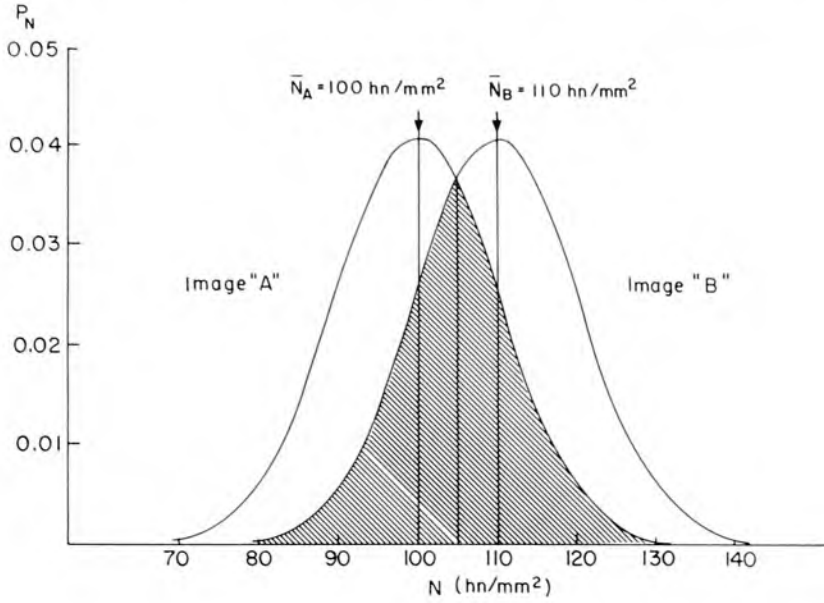


FIG. VI-2. Poisson distributions for two average numbers of photons \bar{N}_A and \bar{N}_B such that $\bar{N}_B/\bar{N}_A = 1.1$.

- 1 $\bar{N}_A = 100$ photons, $\bar{N}_B = 110$ photons
- 2 $\bar{N}_A = 1000$ photons, $\bar{N}_B = 1100$ photons.

better delineation of the two objects and consequently a better-quality radiologic image.

The statistical fluctuations in the number of photons of the radiologic image establish an upper limit for the quality of the image. The image may be adversely affected by various physical factors, such as finite focal spot size, scattered radiation, loss in resolution when the radiologic image is con-

verted into an optical image, and others. However, under no circumstances can the quality of the image be improved above the limitations of statistical fluctuations. Statistical fluctuations impose an impenetrable barrier to the improvement of the image other than by increasing the number of photons used in the examination; and any effort made to reduce the number of photons used in an examination is always accompanied with a statistical deterioration of the image.

It may seem that the number of photons used in a radiologic examination is so great that statistical fluctuations play a negligible part compared to other factors with respect to deterioration of the image. The lowest number of image-forming photons reached in a typical radiographic examination is of the order of $10^5 hn$ per mm^2 , and approximately $40 hn$ per mm^2 in a fluoroscopic examination (Chapter VIII, section on "Statistical Fluctuations in Fluoroscopy"). An analysis of these numbers shows that: (1) the quality of a radiographic examination, particularly when carried out by means of "fast" films and screens, is affected to an appreciable degree by statistical fluctuations of the photons in the radiologic image (Chapter VII, section on "Radiographic Mottle"); (2) the number of image-forming photons in a radiographic examination can, at best, be reduced by a factor of 10 before statistical fluctuations become the major factor affecting the quality of the image (Ref. 2); (3) it is now well established that the major limitation in the quality of the fluoroscopic image results from statistical fluctuations (Chapter VIII).

Contrast, Resolution, and Unsharpness

The quality of the radiologic image can be defined as its ability to reproduce faithfully the transmission of x-radiation through the examined object. This quality can be expressed quantitatively by means of three components; contrast, resolution, and unsharpness.

Contrast in a radiologic image (subject contrast—see p. 212) is usually expressed as the percentage of the x-radiation transmitted in one area of the image with respect to the radiation transmitted by the surrounding field or by the adjacent area, or as follows

$$C_{a,b} = \frac{B_a - B_b}{B_a} \times 100, \quad (3)$$

where $C_{a,b}$ is the contrast of Area a with respect to Area b, B_a is the number of photons per unit area in Area a, and B_b is the number of photons per unit area in Area b.

The *resolution* of a radiologic image is a measure of its ability to produce separate images of objects separated by a small distance. The resolution of an optical system is conventionally expressed as the number of lines per unit length which are resolved when the system is tested by an object consisting of a series of black lines on a white background, with a separation

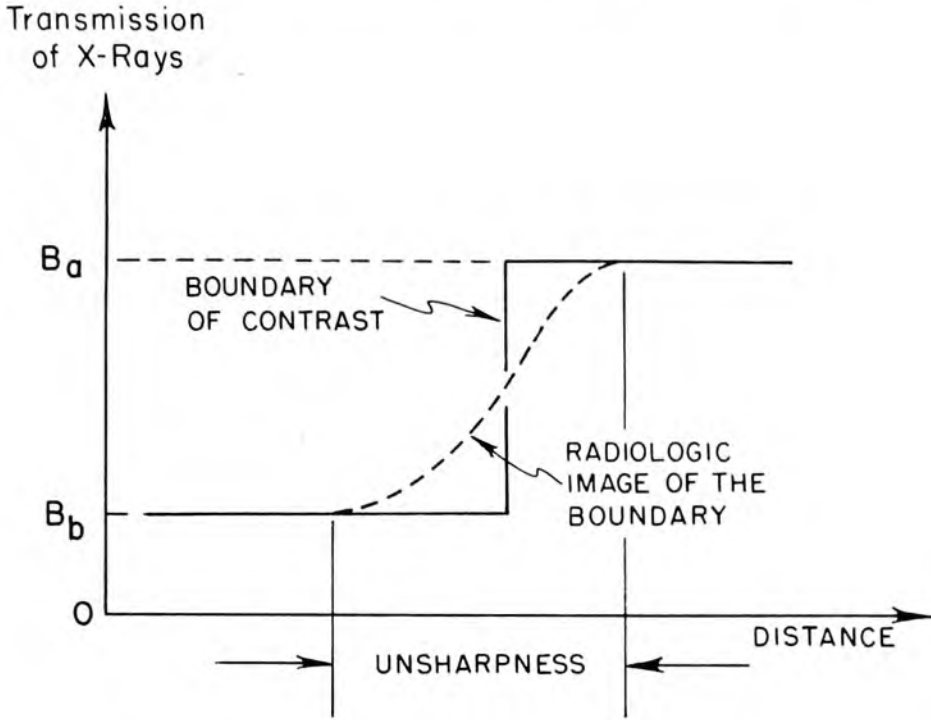


FIG. VI-3. Unsharpness at a contrast boundary.

between the lines equal to the width of the lines. In radiology, resolution can be measured in a similar manner with a test object having a series of lines transparent to x-rays set in a plate opaque to x-rays. A typical test object used for this purpose is the Buckbee-Mears reticle¹; the use of this object, however, exhibits a number of shortcomings. A better method for determination of the ability of the system to reproduce detail is the measurement of its modulation transfer function (see Chapter VII, section on "Modulation Transfer Function").

Unsharpness is a measure of the inability of the radiologic image to reproduce faithfully the boundary of a given contrast (Fig. VI-3). Contrast and unsharpness are unrelated parameters. Resolution is a function of unsharpness (see Chapter VII, section on "Unsharpness") and of contrast (see Chapter VIII, section on "Statistical Fluctuations, Contrast, and Image Perceptibility").

EXTRACTING INFORMATION FROM THE RADIOLOGIC IMAGE

Human senses are practically insensitive to x-ray photons. (This statement is not rigorously true; it has indeed been shown that the retina can be stimulated by x-ray photons. Nevertheless, this sensitivity is low.) The lens does not focus x-ray photons, and it is well known that exposure to x-rays is harmful. Consequently the human eye cannot be used to observe the radio-

¹ Buckbee-Mears Company, 245 East Sixth Street, St. Paul 1, Minn.

logic image directly. Because the information coded by the image must be extracted in a form suitable for interpretation, it is customary in diagnostic radiology to convert this information into a visual image. (It is not inconceivable that in the future other methods for extracting and presenting the information carried by the radiologic image may be used. For example, the information could be presented as a series of numbers, pulses, or graphs suitable for computer analysis without conversion into a visual image.)

The conversion of the radiologic image into an optical image is done in two steps: (1) the x-ray photons of the radiologic image are made to interact with matter, and (2) the energy thus dissipated in the absorber is converted into an optical image. The absorption of x-ray photons in matter results in a transfer of energy to electrons, and the electrons in turn transfer their energies in the form of excitations and ionizations.

Therefore, the translation of a radiologic image into an optical image means converting ionization and excitation energy into an optical image. This can be carried out by one of two methods: (1) either the ionizations and excitations are utilized to expose a photographic emulsion directly, or (2) they are first converted into electromagnetic radiation in the visible or near-visible range by means of luminescent screens. The image thus obtained is either viewed directly, as in fluoroscopy; recorded on a photographic emulsion, as in radiography and photofluorography; or reconverted into electrons and processed by an electronic system by means of an image intensifier. Other methods of conversion of ionization and excitation into a visual image, such as the use of semiconducting screens, have been attempted in diagnostic radiology. At this time, however, these methods have not yet met with much success.

The direct exposure of a photographic emulsion by x-ray photons is used infrequently, and this method will be discussed later in this chapter under "Sensitivity of Radiographic Film to X-Rays." In the overwhelming majority of examinations, the radiologic image is converted into an optical image at some stage by means of a luminescent screen.

Luminescence: Fluorescence and Phosphorescence

Certain substances have the ability to convert energy into electromagnetic radiation in the visible or near-visible range. This energy conversion is called luminescence, and the substances that share this property are called phosphors. Luminescence may be induced by various forms of energy, such as light, chemical reactions, heat, mechanical strains, ionizations, or excitations.

Fluorescence is a term applied to luminescence when the emission of radiation occurs during the exciting event or within 10^{-8} sec of its occurrence (Ref. 4). If the emission of radiation is delayed beyond 10^{-8} sec, the phenomenon is referred to as phosphorescence. The time of 10^{-8} sec corresponds approximately to the lifetime of the atomic state for an allowed transition

(Ref. 3). After excitation by ionization, the light emitted by a phosphor decays exponentially as a function of time, according to the equation

$$I_t = I_0 e^{-t/\tau}, \quad (4)$$

where I_t is the intensity of light emitted at time t ; I_0 is the intensity of light emitted at $t = 0$; τ is the decay constant of the phosphor; and t is the time after excitation.

The number of light photons emitted by a phosphor following excitation is represented by

$$N_t = N(1 - e^{-t/\tau}), \quad (5)$$

where N_t is the number of photons emitted within time t after excitation, and N is the total number of photons generated during the event.

The decay constant τ may vary from microseconds to several hours. Some phosphors may show several different decay times. The same phosphor, for example, may exhibit fluorescence followed by phosphorescence. The physical properties of some inorganic phosphors are shown in Table VI-1. 16.1.2

Phosphors may be divided into five classes according to the mechanism of their luminescence: organic crystals, liquid solutions of organic materials, solid solutions of organic materials, noble gases, and inorganic crystals (Refs. 3 and 4). In diagnostic radiology only inorganic crystals have been found to be useful phosphors; organic materials, owing to their relatively low effective atomic numbers, do not absorb x-rays efficiently and noble gases do not have a sufficiently high density.

Many different inorganic crystals have been used as phosphors. Röntgen discovered the presence of x-rays by the fluorescence they produced in barium platinocyanide crystals. Zinc sulfide, cadmium sulfide, and also the mixed sulfides of these metals are extensively used in fluoroscopy and photo-fluorography. The majority of radiographic examinations employ calcium tungstate and lead barium sulfide screens. Recently potassium iodide has been used for high-speed radiography.

Most inorganic crystal phosphors luminesce efficiently only if they contain a small amount (less than 1%) of a metallic impurity called activator. Zinc and cadmium sulfides can be activated by silver, and alkali halides (potassium, cesium, and sodium iodides, and others) by the addition of thallium. Calcium tungstate, on the other hand, fluoresces in the pure state. The usefulness of activators is explained by the theory of luminescence.

Theory of Luminescence of Inorganic Crystals. The theory of luminescence is at this time not completely understood, and the following is only a cursory discussion of the problem.

The energy states of a crystalline inorganic phosphor (for example, an activated alkali halide crystal) may be represented schematically as shown in Fig. VI-4. The diagram represents the energy bands that may be occupied by the outer electrons of the atoms forming the crystalline lattice of the

TABLE VI-1. Physical Properties of Some Inorganic Phosphors

Phosphor	Effective atomic number (Z_{eff})	Density (g/cm ³)	Wavelength of radiation emitted (Å)	Conversion ^{a,b} efficiency (%)	Decay ^b time (10 ⁻⁶ sec)	Refractive index
Calcium tungstate [CaWO ₄]	59 (Ref. 4)	6.12 (Ref. 7)	4300 (Ref. 7)	5 (Ref. 6)	>1 (Ref. 4)	1.94 (Ref. 7)
Zinc sulfide ^c (activated with silver) [ZnS(Ag)]	27 (Ref. 4)	4.1 (Ref. 4)	4500 (Ref. 4)	28 for α rays (Ref. 5); about 13 for β rays	0.04-.01 and a component of about 5 (Refs. 3, 5)	2.4 (Ref. 4)
Cadmium sulfide ^c (activated with silver) [CdS(Ag)]	44 (Ref. 4)	4.8 (Ref. 4)	7600 (Ref. 4)	probably similar to ZnS(Ag)	>1	2.5 (Ref. 4)
Cesium iodide (activated with thallium) [CsI(Tl)]	54 (Ref. 4)	4.51 (Ref. 4)	white (broad spectrum max. in red)(Ref. 5)	high	0.43-1.1 for γ rays (Ref. 5)	1.79 (Ref. 4)
Potassium iodide (activated with thallium) [KI(Tl)]	49 (Ref. 4)	3.13 (Ref. 4)	4100 (Ref. 4)	high	>1 (Ref. 5)	1.68 (Ref. 4)

^a The conversion efficiency is the efficiency with which a phosphor converts the energy dissipated within it by ionizing radiation into light energy; it is equal to: $\frac{\text{light energy emitted}}{\text{ionizing energy absorbed}} \times 100$.

^b Both the conversion efficiency and the decay time of phosphors depend on the method of their preparation and on the intensity of excitation (Ref. 1).

^c Fluorescopic screens are most often composed of mixtures of ZnS(Ag) and CdS(Ag).

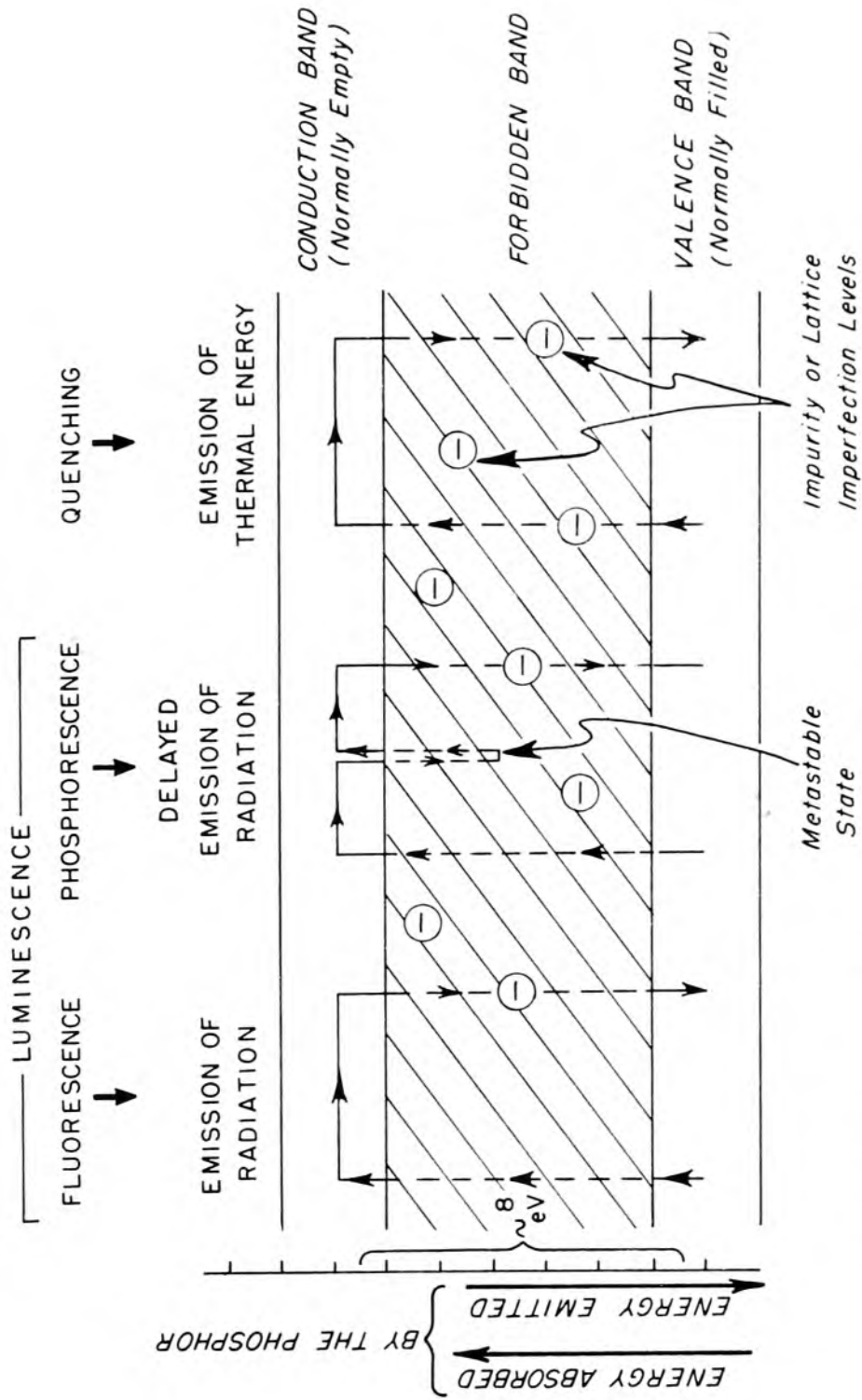


FIG. VI-4. Energy levels in an inorganic phosphor, showing lattice imperfections responsible for its luminescence.

phosphor: (1) the valence band which is normally filled; (2) the forbidden band, which represents energies that cannot be occupied by the electrons, with the exception of a certain number of vacancies provided by impurities in the crystal or by lattice imperfections; and (3) the conduction band, which is a region where electrons are strongly affected by surrounding atoms and can consequently move freely throughout the crystal, and which is a normally unoccupied band.

When energy is imparted to an electron in the valence band, this electron may be raised to the conduction band where it can move freely until it reaches an imperfection in the forbidden band. It then drops to the energy associated with the imperfection; and from that imperfection it returns to the valence band with the emission of radiation in the visible or near-visible range. This is the mechanism of *fluorescence*.

An electron raised to the conduction band may also be trapped in the forbidden band at an energy level created by one of the impurity atoms. Such a trapped electron is in a metastable state, and it will return to the valence band more or less rapidly depending on the instability of the metastable state. If energy is imparted to an electron trapped in such a metastable state, it may be raised back to the conduction band; from there it may return to the valence band via an imperfection, and with the emission of radiation in the visible range or near-visible range by fluorescence. This form of delayed fluorescence is *phosphorescence*.

The energy that separates the valence band from the conduction band is of the order of a few electron volts. Consequently the transition of an electron from the conduction band to the valence band results in the emission of a photon carrying an energy of a few electron volts. This energy corresponds to a wavelength in the visible or near-visible range.

Radiationless Transition. An electron that has been raised from the valence band to the conduction band may also lose its energy and return to the valence band by a radiationless process such as thermal energy transfer to other atoms or lattice vibration. Such a radiationless transition is referred to as *quenching*, because it competes with the emission of radiation.

Nonradiative processes are, in general, more probable than radiative processes, and the conversion efficiency of a good phosphor, which is defined as the ratio of the energy emitted in the form of radiation to the energy absorbed by the phosphor, is usually of the order of only 10 to 20% (see Table VI-1).

An interesting and useful consequence of the mechanism of luminescence is that inorganic crystals are relatively transparent to their own fluorescent radiation, because most of the optical absorption results from the transition between the valence and the conduction bands, and fluorescent photons do not carry sufficient energy to be absorbed by this process.

Storage Phosphors. In certain phosphors, electrons trapped in impurity energy levels in the forbidden band may remain in a metastable state for a

long period of time, unless some external stimulation, such as heat, allows their return to the ground state by fluorescence. Such is the case of silver-activated sodium chloride, which is capable of storing up to 3% of the energy absorbed in the crystal for a period as long as one day, unless it is heated.

X-Ray Luminescent Screens

Radiologic images are converted into optical images by means of inorganic crystalline phosphors imbedded in screens. Desirable phosphor characteristics for this purpose are: (1) A high absorption coefficient for the radiation used. (This condition calls for high effective atomic-number phosphors.) (2) A high efficiency in converting the energy dissipated by x-ray photons into light. (3) A high transparency to its own luminescence. (As pointed out above, this condition is fulfilled by most phosphors.) (4) A relatively low refractive index, which allows easy escape of the luminescent radiation from the crystal. (5) The phosphor material should be stable, relatively inexpensive, and convenient to handle in the preparation of screens.

In addition to these characteristics, shared by all x-ray phosphors, the following are specific of the radiologic application: (1) The wavelength of the radiation emitted by the phosphor must be optimum. In fluoroscopy the light emitted must be in the visible range and preferably have a wavelength in the region of maximum spectral sensitivity of the dark-adapted retina. In radiography this wavelength should fall in a desirable region within the film sensitivity curve. (2) The decay constant must not interfere with the radiologic examination. Phosphors with a long decay constant are unsuitable for rapid dynamic studies such as rapid serial radiographic examinations carried out with one set of screens and cineradiography. On the other hand, a long decay constant is tolerable in most radiographic examinations, in which a long period of time elapses between exposures carried out with one set of screens.

Most x-ray screens are composed of the following elements (Fig. VI-5): (1) a cardboard or plastic, or more rarely, a metallic plate, (2) a light-reflecting coating, (3) an active layer, composed of the finely divided phosphor material embedded in a plastic matrix, and (4) a light-transparent plastic protective layer. Some physical parameters of conventional x-ray screens are shown in Table VI-2.

An x-ray screen functions as follows: The energy dissipated in a phosphor particle subsequent to the interaction of an x-ray photon with matter is converted into a number of light photons. A large fraction of these light photons escape the crystal phosphor particle into the plastic matrix. If the direction of these photons is toward the exit face, they have a high probability of escape. If that direction is toward the reflecting coating, they are reflected back and also may escape with a relatively high probability. On the other hand, lateral diffusion of the photons into the phosphor results in

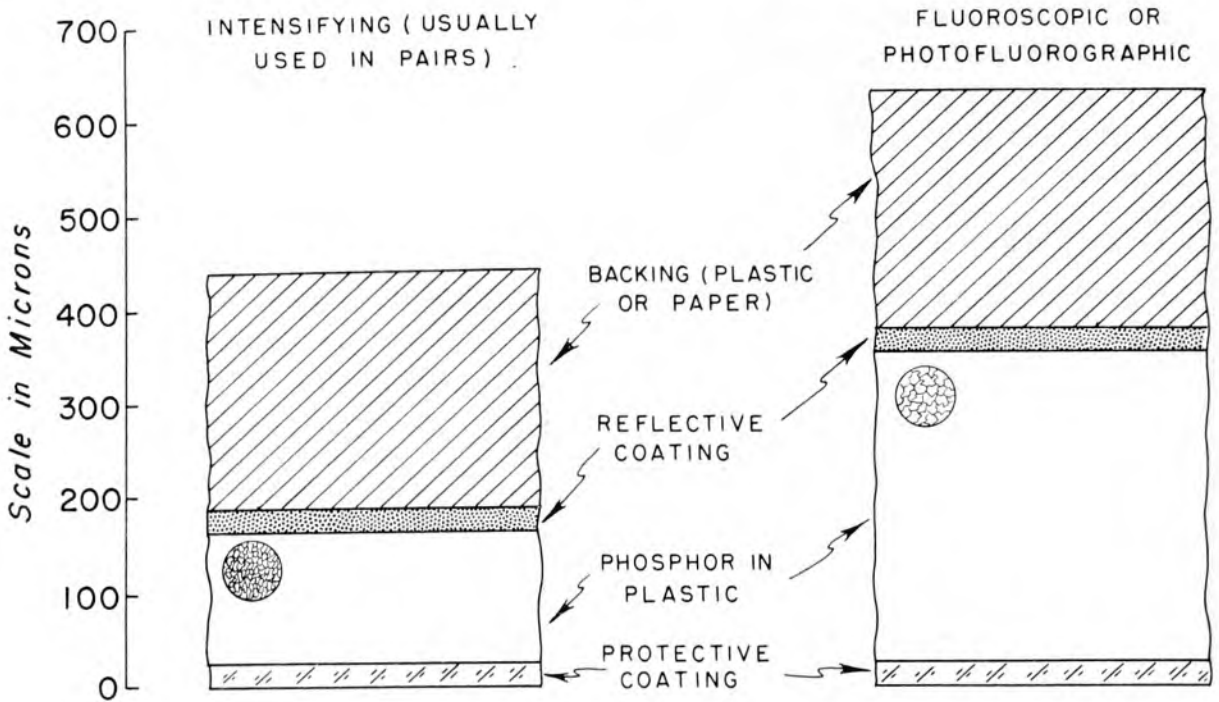


FIG. VI-5. Cross sections of typical x-ray screens.

multiple scattering and eventual absorption. This mechanism explains the structure of the screen. The reason for using the phosphor material in divided form, rather than in one solid sheet, is to prevent the lateral diffusion of the light photons and consequent loss of resolution of the optical image.

Two factors characterize the performance of an x-ray screen: (1) "speed," which is a measure of the number of light photons given off by the screen for a given x-ray energy impinging upon it; and (2) resolution, which is the ability of the screen to reproduce faithfully the radiologic image.

For a given phosphor material, the speed of the screen depends on the amount of phosphor material interposed in the path of the x-ray photons, on the conversion efficiency of the phosphor used, and on the ability of the light photons generated in the phosphor to escape the screen. Ideally, a fast screen would consist of a thick and transparent layer of phosphor. Unfortunately, these requirements conflict with those for high resolution. For high resolution in a screen, lateral diffusion of the light photons must be prevented; this may be achieved by reducing the thickness of the phosphor layer, by reducing the size of the phosphor particles, or by increasing the opacity of the phosphor layer to its own light. In practice, the structural features of an x-ray screen represent a compromise between speed and resolution, leaning towards either one depending upon the demands of the radiologic examination. Thus, high speed-low resolution screens have thick phosphor layers with large phosphor particles, and low speed-high resolution, or "high detail," screens have thin phosphor layers with small particles, and

TABLE VI-2. Physical Characteristics of X-Ray Luminescent Screens

Type of screen	Phosphor	Wave-length of fluorescence (Å)	Mass per unit area of phosphor (g/cm ²)	Phosphor layer thickness (μ)	Phosphor particle size (μ)	Resolving power ^a (lines/mm)
Intensifying Screens						
High Speed						
Front screen (TF) ^b	Calcium tungstate	4200	0.05	150	8	9 (7)
Back screen (TF) ^b	Calcium tungstate	4200	0.11	300	8	9 (7)
Hi-Speed ^c	Barium lead sulfate	3700	0.08	230	5	6.5 (9)
Medium Speed (T) ^b	Calcium tungstate	4200	0.04	100-130	4	10 (10)
Par Speed ^c	Calcium tungstate	4170	0.05	175	5	8 (10)
Detail (UD) ^b	Calcium tungstate	4200	0.02	50-75	4	14
Detail ^c	Calcium tungstate	4170	0.03	175	5	>10 (15)
KI ^c	Potassium iodide	4300	0.03	127	7	5
Fluoroscopic Screens						
(FGP) ^b	Zinc cadmium sulfide	5300	0.10	300-360	25-30	3
CB-2 ^c	Zinc cadmium sulfide	5350	0.11	350	30-40	3
Photofluorographic Screens						
E-2 ^c	Zinc cadmium sulfide	5350	0.15	540	30-40	2.5
(PFG) ^b	Zinc cadmium sulfide	5300	0.10	300-360	25-30	3 (5)
(PF) ^b	Zinc sulfide	4300	0.08	300-360	25-30	3 (6)
Type D ^c	Zinc sulfide	4450	0.11	320	20-25	5.5
X-Ray Image Intensifier Screens						
X-Ray Image Intensifier Tube						
Input Screen ^d	Zinc cadmium sulfide	5300	0.10	250-360	3-15	>2
"Cinelix" Intensifier Screen ^e	Zinc cadmium sulfide	5430	0.09	380	12-60	3.1-3.2

^a The values for the resolving power of the screens, reported by different companies, were measured by different techniques involving subjective evaluations and therefore cannot be compared. Values in left column were supplied by the respective manufacturers; values in right column (in parentheses) are from Morgan and Corrigan (Ref. 8). Other values in this table were reported by the manufacturers.

^b United States Radium Corporation, Radelin Division, Morris Plains, N.J.

^c E. I. du Pont de Nemours and Company, Wilmington, Del.

^d The Rauland Corporation, Chicago, Ill.

^e Aerojet Delft Corporation, Plainview, L.I., N.Y.

sometimes a plastic matrix made opaque by means of a dye to reduce lateral diffusion of light photons.

Efficiency of X-Ray Screens. Inasmuch as an x-ray screen is a device that converts a radiologic image of x-ray photons into an optical image of visible or near-visible photons, the efficiency of an x-ray screen can be defined as the efficiency with which x-ray photons are converted into light photons. This conversion takes place in three stages: (1) absorption of the x-ray photons in the screen, (2) conversion of the excitation and ionization energy thus dissipated in the screen into light photons, and (3) escape of the light photons from the screen. The over-all efficiency of the screen is the product of the efficiencies of these three processes. The efficiencies of these three processes can be illustrated by determining quantitatively the image conversion of 80 kV_p x-rays in a pair of medium-speed x-ray intensifying screens, as follows:

1. The mean photon energy for x-rays produced with a tube voltage of 80 kV_p, with conventional filtration, is about 50 keV ($\lambda = 0.25 \text{ \AA}$).

2. The absorption of 50 keV x-ray photons in two medium-speed calcium tungstate screens is about 30% (Fig. VI-8).

3. If the energy absorbed in the screen were converted with a 100% efficiency into light, each x-ray photon absorbed would produce 17,000 light photons with a wavelength of 4300 \AA (calcium tungstate fluorescence) (Fig. VI-7):

$$\frac{4300 \text{ \AA}}{0.25 \text{ \AA}} \cong 17,000.$$

However, the energy conversion efficiency of calcium tungstate is of the order of only 5%, and each absorbed x-ray photon results in the re-emission of about 1000 light photons only.

4. Intensifying screens are relatively transparent to their own fluorescence, and a typical value for the fraction of light escaping the screen is 50%.

5. Thus, the combined effect of these processes on one x-ray photon impinging on the screens is (Fig. VI-6):

Probability of absorption		Number of light photons generated per x-ray photon absorbed		Ability of light photons to escape screen		Number of light photons escaping screen
0.30	×	1000	×	0.5	≅	150

The above analysis, although carried out for a particular set of circumstances, is generally valid for x-ray screens in the sense that any x-ray screen acts as a photon multiplier. It should be noted that the screen extracts

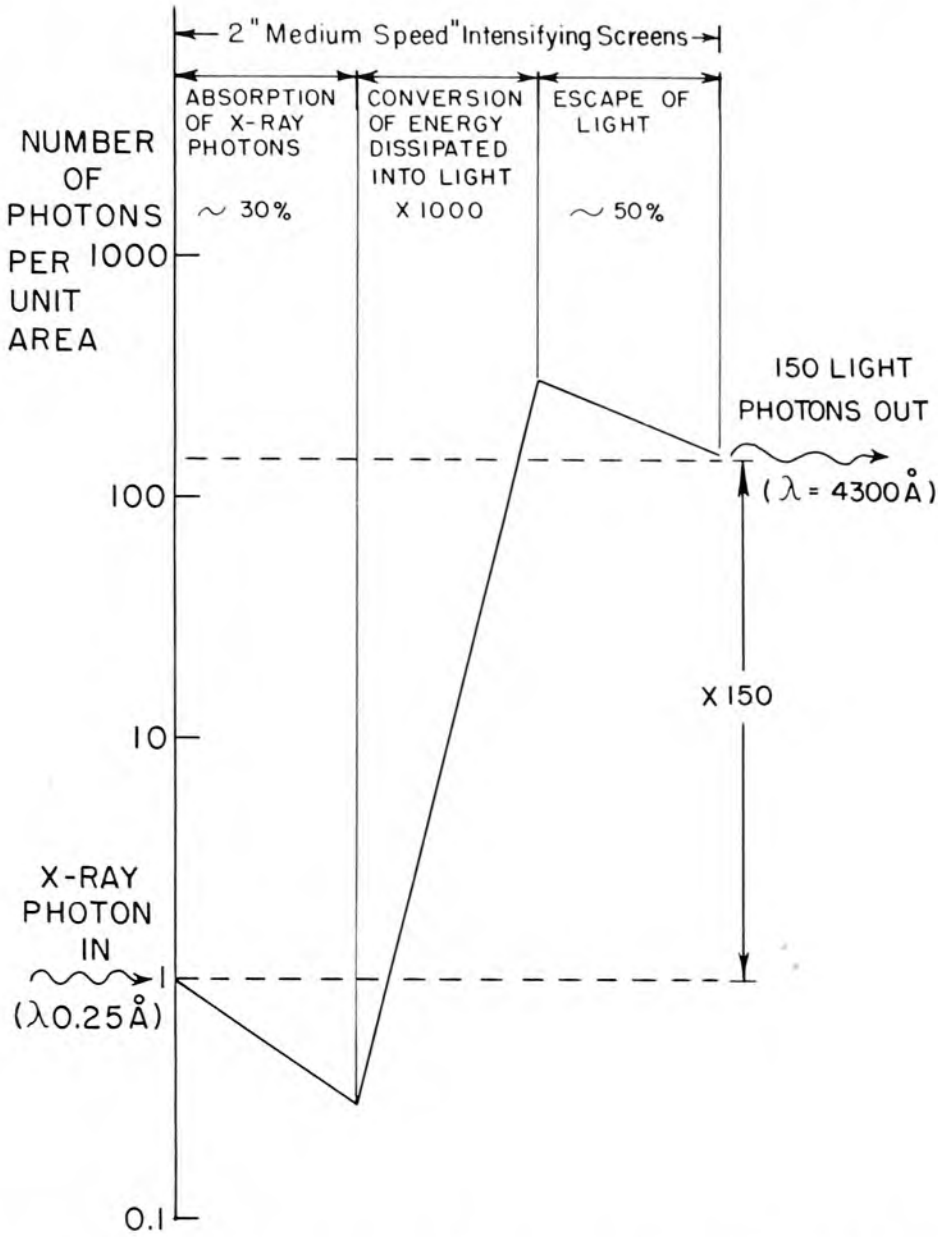


FIG. VI-6. Stages in the conversion of one x-ray photon into light by a pair of x-ray intensifying screens.

information from the radiologic image only at the first stage by stopping x-ray photons. Whatever transformations occur afterward may result in loss of information but never in gain. Under ideal conditions the screen can transfer to the emulsion as much information as was absorbed from the x-ray beam, but never more.

It is important that a large number of light photons be generated for each x-ray photon absorbed. This factor allows for a considerable loss of light photons within the screen without affecting the amount of statistical information that can be transferred from the radiologic image. The loss in

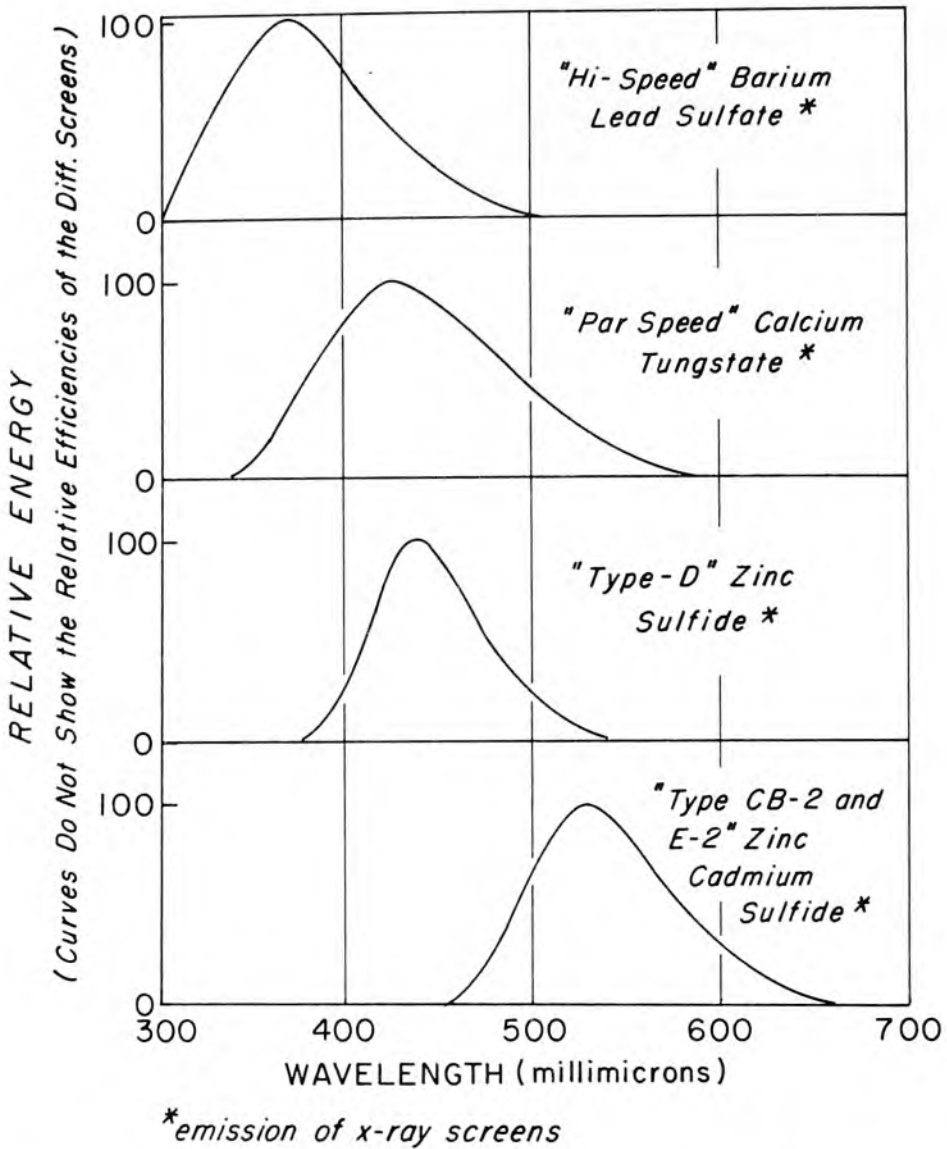


FIG. VI-7. Light emission of phosphors commonly incorporated in x-ray screens.
(Courtesy of E. I. du Pont de Nemours & Company, Inc.)

image quality during the conversion of the radiologic image into an optical image by an x-ray screen is due mostly to screen unsharpness rather than loss of photons within the screen. (See Chapter VII, section on "Unsharpness Contributed by Image Conversion.")

As the nature of the phosphor used and the structural features of x-ray screens vary with the purpose for which they are designed, the efficiencies of various types of screens must be studied separately. X-ray screens can be classified into three broad categories: (1) intensifying screens, (2) fluoroscopic and photofluorographic screens, and (3) x-ray intensifier input screens.

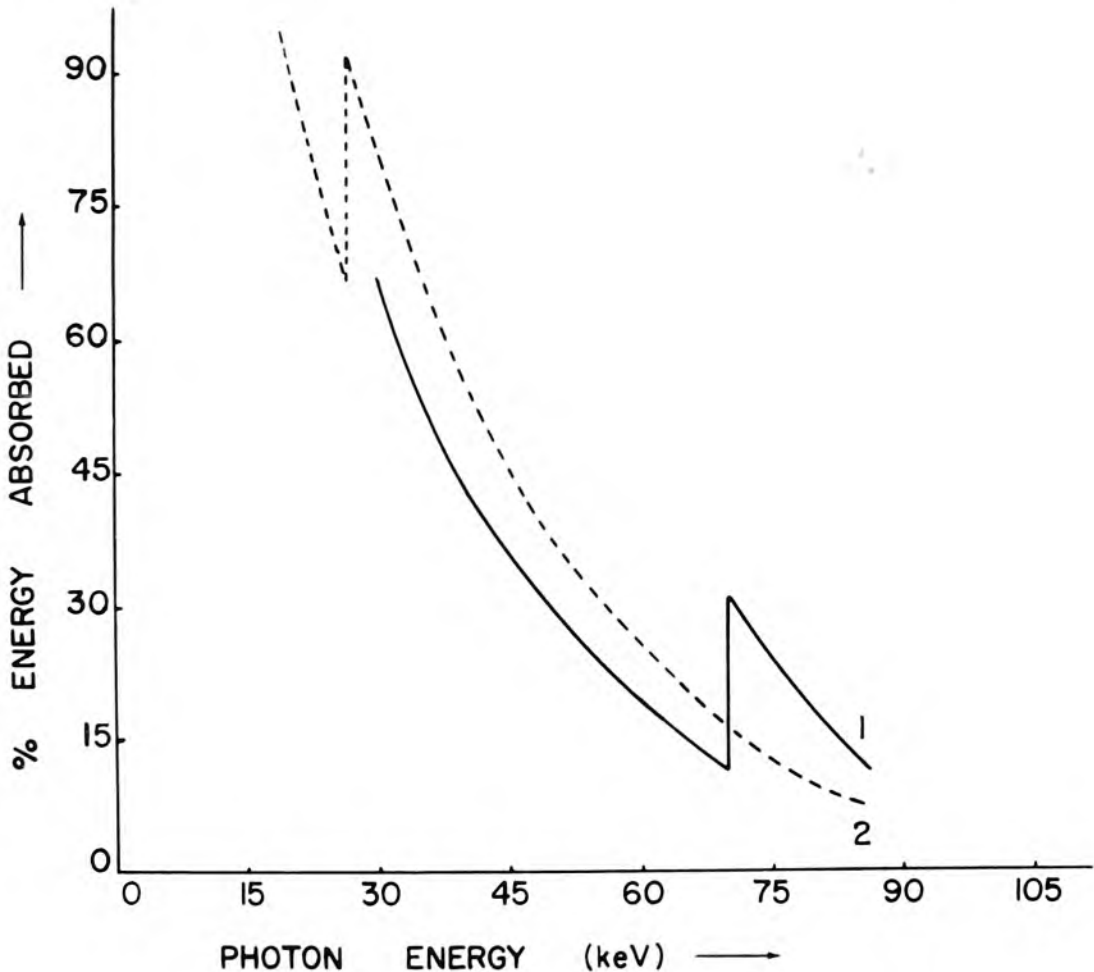
Intensifying Screens. X-ray intensifying screens are used with the x-ray photographic film that records the optical image of the screen, usually by

sandwiching a double emulsion film between two intensifying screens. Intensifying screens are usually fabricated in three grades of increasing resolution, or detail: low, medium, and high detail. The resolution of these screens varies from approximately six lines per millimeter for low detail screens, about eight to ten lines per millimeter for medium detail screens, and up to 15 lines per millimeter for high detail screens (Table VI-2). The relative "speeds" of these screens are approximately 1, 3, and 4.6, in reverse order of detail.

The phosphor most commonly used in an intensifying screen is crystalline calcium tungstate, which fluoresces with the emission of blue light (Fig. VI-7). The absorption of x-ray photons in calcium tungstate screens is

FIG. VI-8. Absorption of x-rays

- 1 in a pair of medium-speed calcium tungstate x-ray intensifying screens (Radelin T)
- 2 in a single fluoroscopic screen (Radelin FGP), as a function of photon energy. Absorption of x-rays in the fluoroscopic FGP screens is identical to that in photo-fluorographic (Radelin PFG) screens. Table VI-2 lists some physical characteristics of these screens.



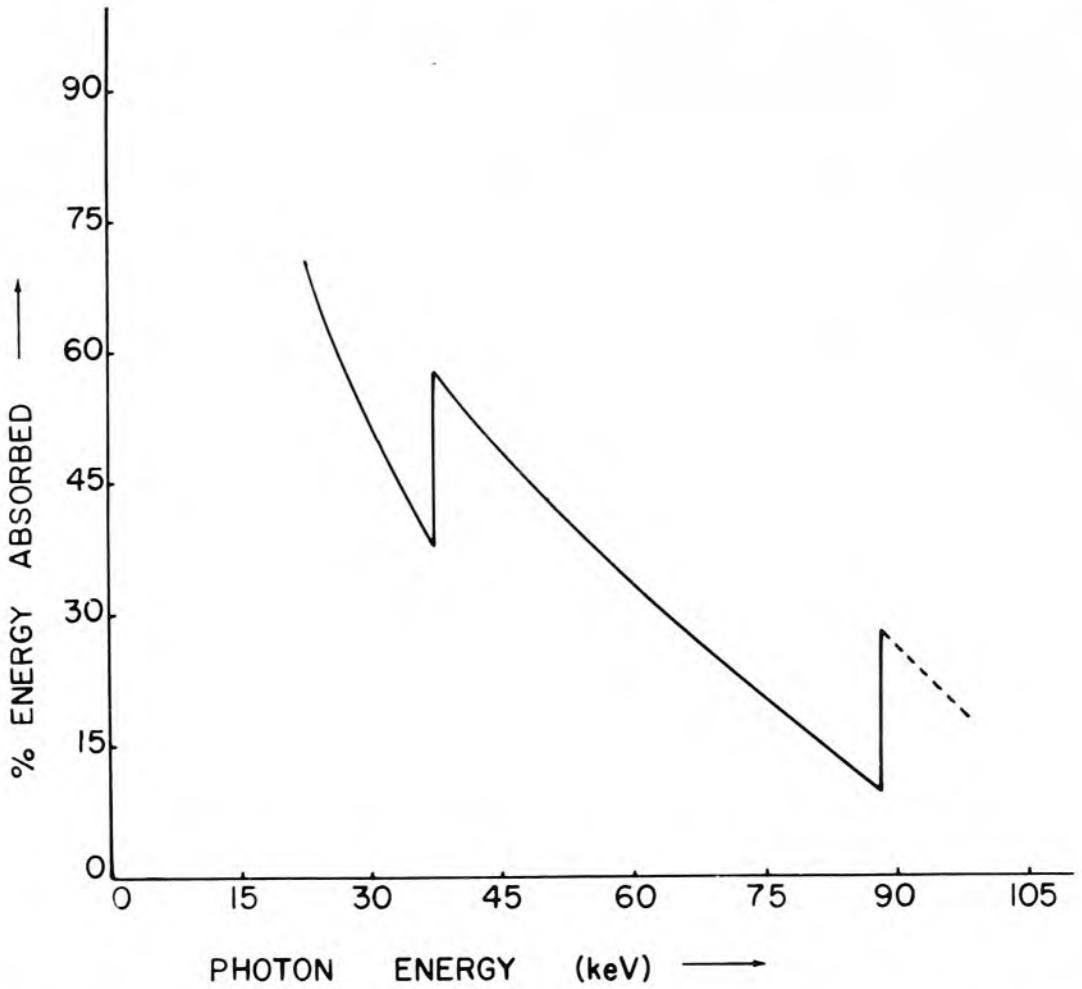


FIG. VI-9. Absorption of x-rays in a pair of high-speed barium lead sulfate x-ray intensifying screens (du Pont Hi-Speed). Table VI-2 lists some physical characteristics of these screens.

shown in Figs. VI-8 and VI-10. The conversion efficiency of calcium tungstate is of the order of 5%. This figure, however, is unreliable because of the difficulties involved in measuring conversion efficiencies. Another phosphor used in high-speed intensifying screens is barium lead sulfate, which fluoresces at 3700 Å. This phosphor is particularly useful for higher energy radiography because of its greater x-ray absorption coefficient at higher energies, as shown in Fig. VI-9. Thallium-activated potassium iodide has also been incorporated in x-ray intensifying screens. The use of this phosphor produces particularly high speed screens because of its favorable absorption of x-rays coupled with high fluorescence efficiency.

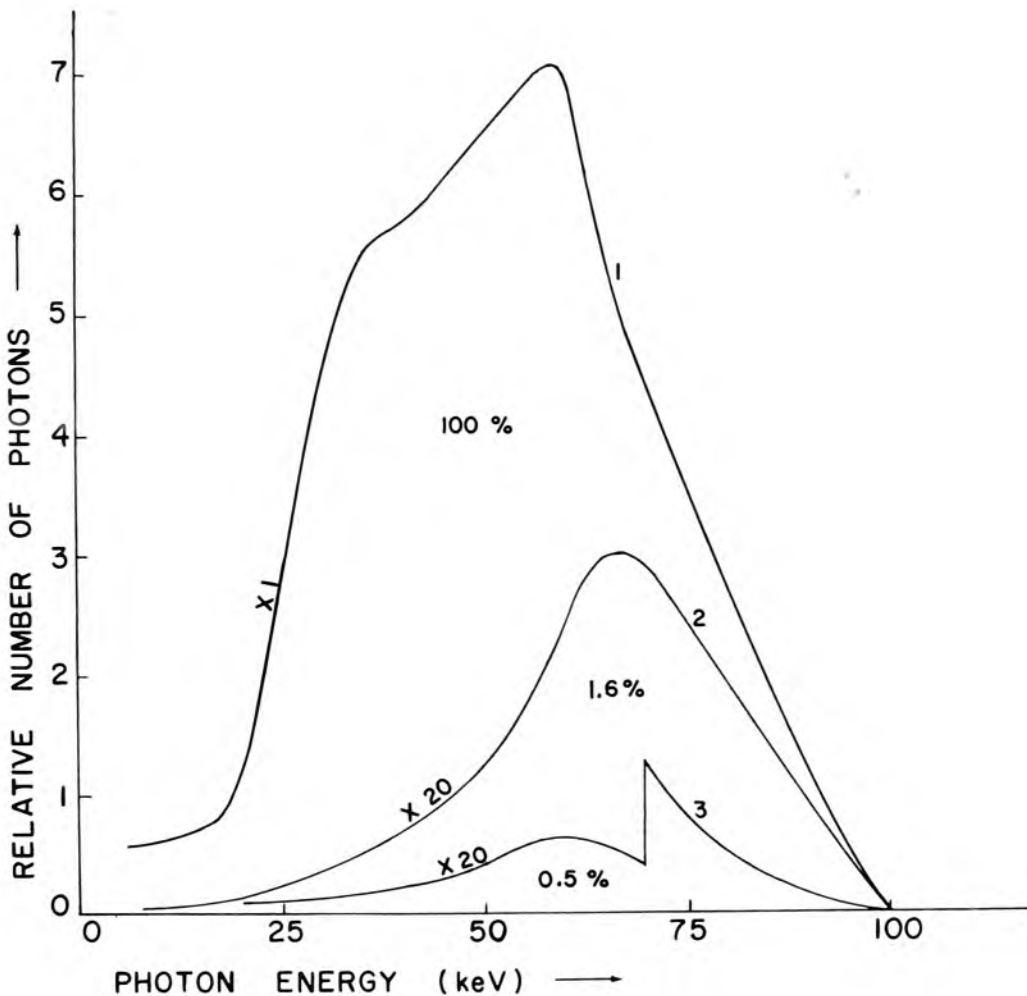
Fluoroscopic and Photofluorographic Screens. These two categories are discussed together here because both the phosphor used and the structures of these screens are practically identical. The image produced by a

fluoroscopic screen is examined visually, while the photofluorographic image is recorded by a photographic camera. Two phosphors are widely used for these screens: (1) zinc sulfide activated with silver, which fluoresces with the emission of blue light; and (2) zinc cadmium sulfide, which has a green fluorescence. The proportion of zinc sulfide to cadmium sulfide used in these screens is not constant. A typical figure is 60% zinc sulfide and 40% cadmium sulfide.

The x-ray absorption of these screens as a function of energy is shown in Fig. VI-8. The typical resolution of these screens is approximately two to three lines per millimeter. Both zinc sulfide and zinc cadmium sulfide are good phosphors, with a fluorescence efficiency probably of the order of 10 to 15% (Table VI-1).

FIG. VI-10. Spectral distributions

- 1 of 100 kV_p x-rays used in typical roentgenologic examination
- 2 of radiation transmitted by a 20-cm thick abdomen
- 3 of radiation absorbed in two medium-speed calcium tungstate x-ray intensifying screens.



X-Ray Image Intensifier Input Screens. The x-ray input screens used in most x-ray image intensifiers (Chapter VIII) are very similar in most respects to fluoroscopic screens. The phosphor most commonly used in these screens is zinc cadmium sulfide, and the energy absorption and the resolution of these screens are similar to those of conventional fluoroscopic screens. Some x-ray intensifier tubes are fitted with screens thinner than fluoroscopic screens for the purpose of achieving better resolution. However, the resolution of image intensifiers of conventional design is not strongly affected by screen thickness, and image intensifiers fitted with screens equal in thickness to fluoroscopic screens do not appear to suffer in resolution.

RECORDING THE RADIOLOGIC IMAGE

In the overwhelming majority of radiologic examinations the radiologic image is recorded on photographic film. The exceptions are processes such as xerography and magnetic tape recording. Xerography, although useful in special examinations such as mammography, is not widely used in radiology. On the other hand, magnetic tape recording appears to be very promising, particularly in cinefluorography, and will be discussed in Chapter X.

The uses of photographic film in diagnostic radiology are twofold: (1) The photographic film is used to record an optical image supplied by a screen, as in radiography with screens, photofluorography with or without x-ray image amplifiers, and cinefluorography. (2) The photographic emulsion is exposed by direct absorption of x-ray photons without the help of a luminescent screen. In this case the film is used to extract information from the radiologic image as well as to record it. This "no-screen" or "cardboard cassette" technique is used only in the radiography of thin parts.

The selection of the most suitable photographic film for a given radiographic application is a function of the relationship in a film between exposure and film processing on the one hand and film response on the other. The quantitative study of these relationships is called *sensitometry*.¹

X-Ray Film

Photographic film consists of an inert support, the film base, which is usually made of some plastic coated either on one side or on both sides with the photographic emulsion. The photographic emulsion is a gelatin base containing silver halide crystals, usually silver bromide (Fig. VI-11). The emulsion is sensitive to radiant energy either in the visible or near-visible range, or to higher energy radiation such as x-ray photons or other ionizing radia-

¹ Most of the discussion in this chapter on the sensitometric properties of x-ray films is based on George M. Corney's "Photographic Aspects of Cinefluorography" (Ref. 9), and particularly on the excellent booklet entitled "Sensitometric Properties of X-ray Films" (Ref. 10). The author is very grateful to Mr. George M. Corney and to the X-Ray Sales Division, Eastman Kodak Company, for their kind authorization to use and reproduce this material.

tions. The physical characteristics of film emulsion and base vary with their purpose. Table VI-3 shows some physical properties of x-ray films.

The theory of the photographic process is thoroughly described elsewhere (Ref. 11); it will not be discussed in this text.

Exposure. The exposure of a photographic film expresses the quantity of radiant energy incident upon the film per unit area that is responsible for producing a given density on the processed film. Exposure may be expressed in units of energy per unit area, such as ergs/cm², or in number of particles per unit area. It is often convenient to express exposure in relative terms with respect to a given reference exposure.

Photographic Density. Exposure of the photographic film results in "blackening" after processing. The unexposed film remains transparent to light. Photographic density is the measure of film blackening. The photographic density of a given area of film is numerically equal to the logarithm to the base 10 of the ratio of the intensity of light incident on that area to the intensity of the light transmitted:

$$D = \log \frac{I_0}{I_t}, \quad (6)$$

where I_0 is the intensity of the light incident on a given area of film, I_t is the intensity of the light transmitted through the area, and D is the photographic density of the area. The expression I_t/I_0 (the reciprocal of I_0/I_t), which is equal to the fraction of light transmitted by the film, is referred to as *transmittance*.

Since photographic density is the logarithm of the ratio of two quantities expressed in the same units, it is dimensionless. A density of 1 refers to a film blackening that allows the transmission of one-tenth of incident light ($\log 10 = 1$). A density of 2.0 refers to a blackening resulting in the attenuation of $\frac{99}{100}$ of incident light intensity or, in other words, in the attenuation of light by a factor of 100 ($\log 100 = 2$). The usefulness of this definition of density becomes apparent if one considers that the addition of a film with a density of 1 to another with a density of 2 results in a total density of 3, which attenuates light by a factor of 1000.

Characteristic Curve of Film. The response of a film to exposure is usually expressed graphically as a plot of the film density (ordinate) versus the logarithm of the relative exposure (abscissa). This curve is called the *characteristic curve of the film* (also, sensitometric curve; or H and D curve, after Hunter and Driffield, who first used such a curve).

Figure VI-12 shows a typical characteristic curve. It should be noted that only a portion of this curve is nearly linear. At low exposure values it exhibits a "toe," and at high exposure values it has a "shoulder." The reason for plotting exposures on a logarithmic scale in characteristic curves is that the important parameter in the comparison of relative exposures is not their difference but their ratio, and on a logarithmic scale equal ratios are sepa-

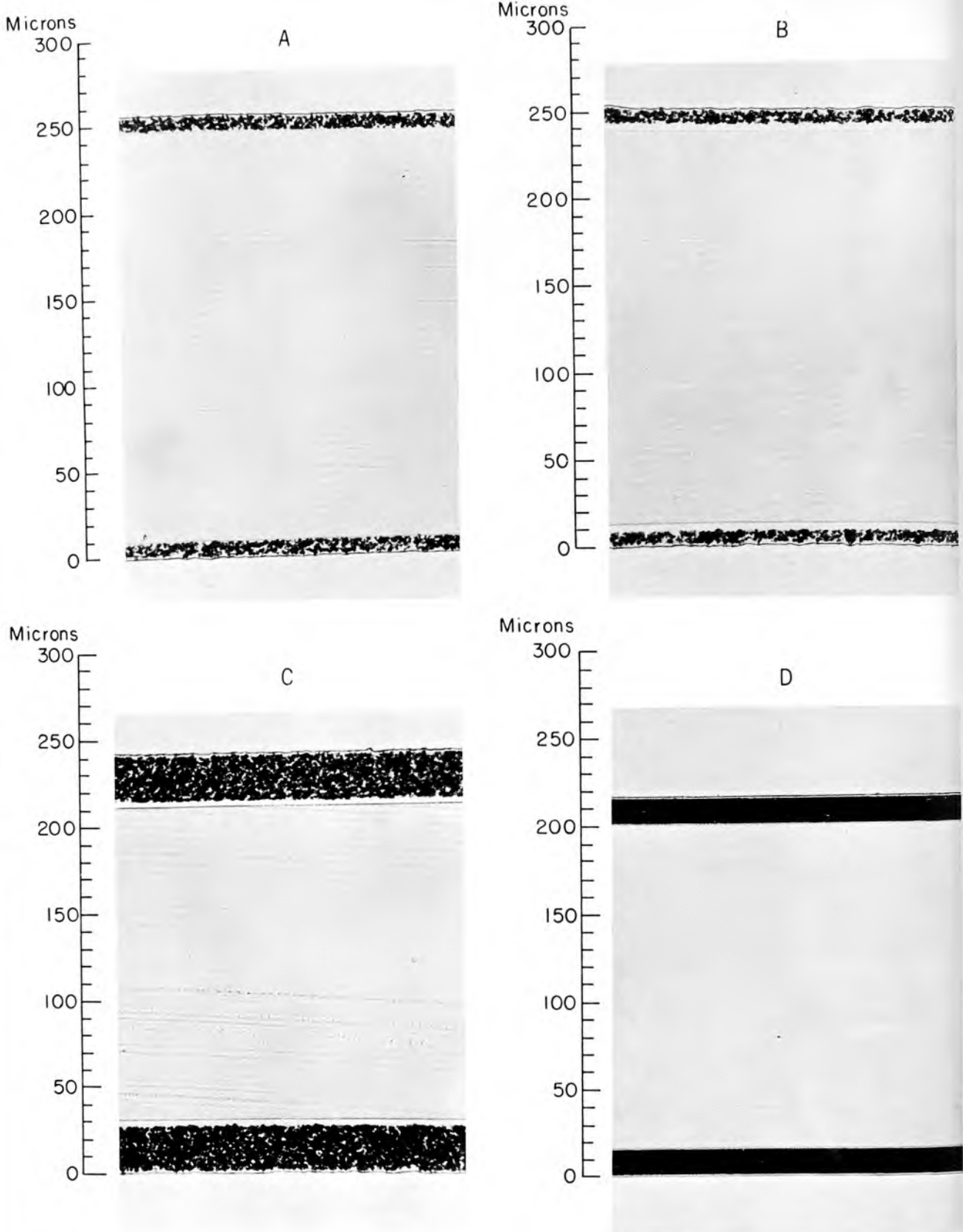
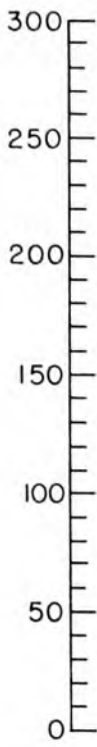


FIG. VI-11. Photomicrographs of some Kodak films used in radiology, showing the base coated with emulsion ($\times 500$). A Kodak Blue Brand Medical X-Ray Film; B Kodak Royal Blue Medical X-Ray Film; C Kodak No-Screen Medical X-Ray Film; D Kodak Industrial X-Ray Film, Type M; E Kodak Industrial X-Ray Film, Type KK; F Kodak Photofluore Film, Green Sensitive; G Kodak Photofluore Film, Blue Sensitive. Longitudinal base distortions which can be noted in the photomicrographs are due to striations from the microtome knife in cutting and to the refractive index of the mounting media. These striations are not related in any way to the uniformity of the base. (Photomicrographs supplied through courtesy of X-Ray Sales Division, Eastman Kodak Co.)

Microns



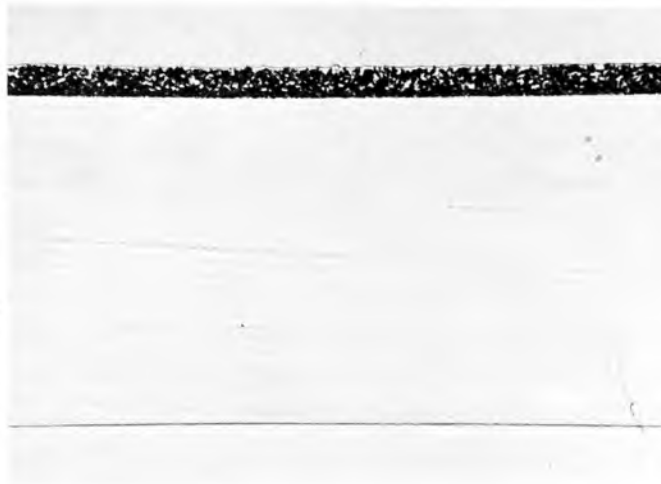
E



Microns



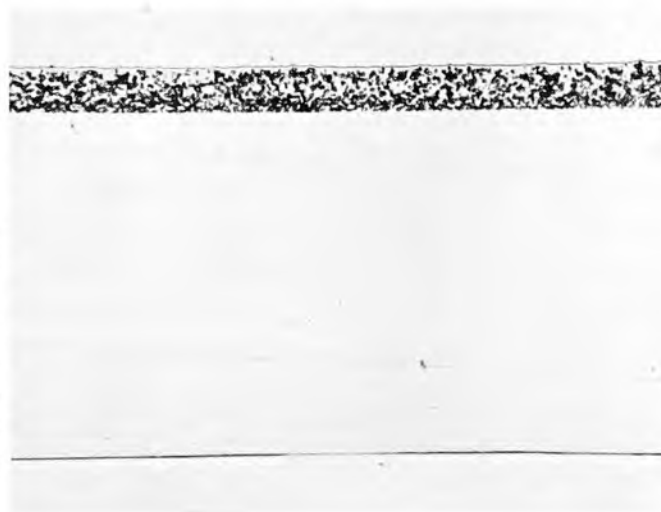
F



Microns



G



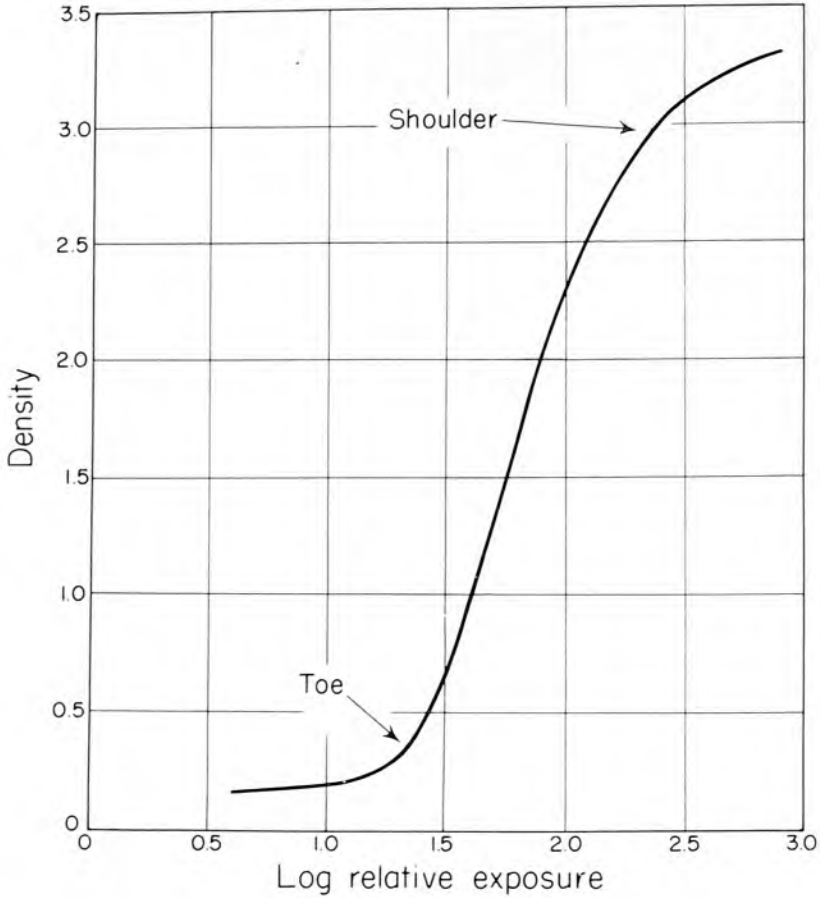


FIG. VI-12. Characteristic curve of typical medical x-ray film, exposed with calcium tungstate intensifying screens. (Courtesy of X-Ray Sales Division, Eastman Kodak Co.)

rated by the same value regardless of the absolute values of the exposures. For example, in Fig. VI-12 the interval between 0 and 1 on the log exposure scale corresponds to an exposure of from 1 to 10. This interval is identical in length to the interval between 1 and 2, which corresponds to an exposure range of 10 to 100; and it is also identical in length to the interval between 2 and 3, which corresponds to an exposure ranging from 100 to 1000.

Radiographic Contrast, Subject Contrast, and Film Contrast

The contrast between two areas on a processed film that was exposed to a radiologic image is called *radiographic contrast* and is equal to the difference between the densities of the two areas. Radiographic contrast depends on two factors: subject contrast and film contrast.

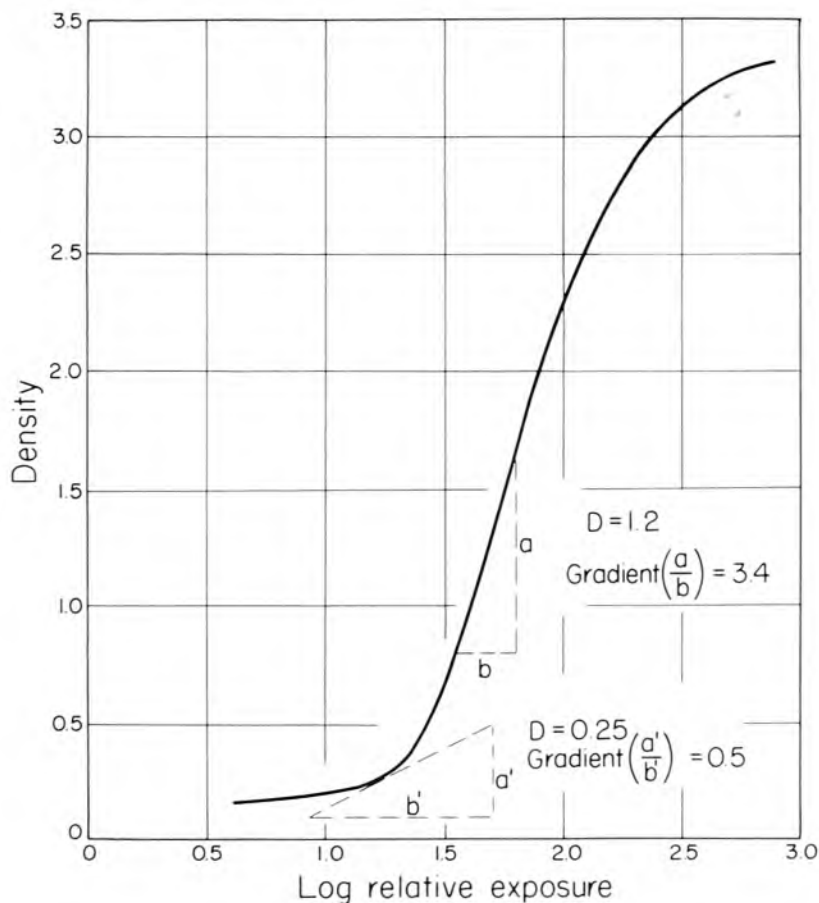
Subject contrast is defined as the contrast between two areas of the radiologic image, regardless of how it is recorded. The subject contrast between two areas is usually expressed by the ratio of the number of photons for these two areas. Subject contrast can also be conveniently expressed as a per-

centage, $[(B_a - B_b)/B_a] \times 100$, where B_a and B_b are the number of photons in the two areas, respectively (see p. 192). If the radiologic image is recorded by photographic film, the subject contrast between two areas is numerically equal to the ratio of the exposures for these two areas. Under certain circumstances subject contrast is defined as the logarithm of the ratio of the exposure for two areas.

Film contrast represents the ability of the film for translating subject contrast into radiographic contrast. Film contrast depends on (1) the film used, (2) the processing of the film, and (3) the density of the film. Film contrast is expressed quantitatively by the slope of the characteristic curve.

The slope (or gradient) of the characteristic curve is a function of film density (Figs. VI-13 and VI-14). A portion of the characteristic curve is usually nearly linear and consequently has a constant slope. The tangent of this slope is called the "gamma" of the film under consideration (Fig. VI-15) and is used to express film contrast. The usefulness of gamma is limited because many photographic films, particularly those used in radiology, have short

FIG. VI-13. Characteristic curve of screen-type film, exposed with calcium tungstate intensifying screens. Gradients have been evaluated at two points on curve. (Courtesy of X-Ray Sales Division, Eastman Kodak Co.)



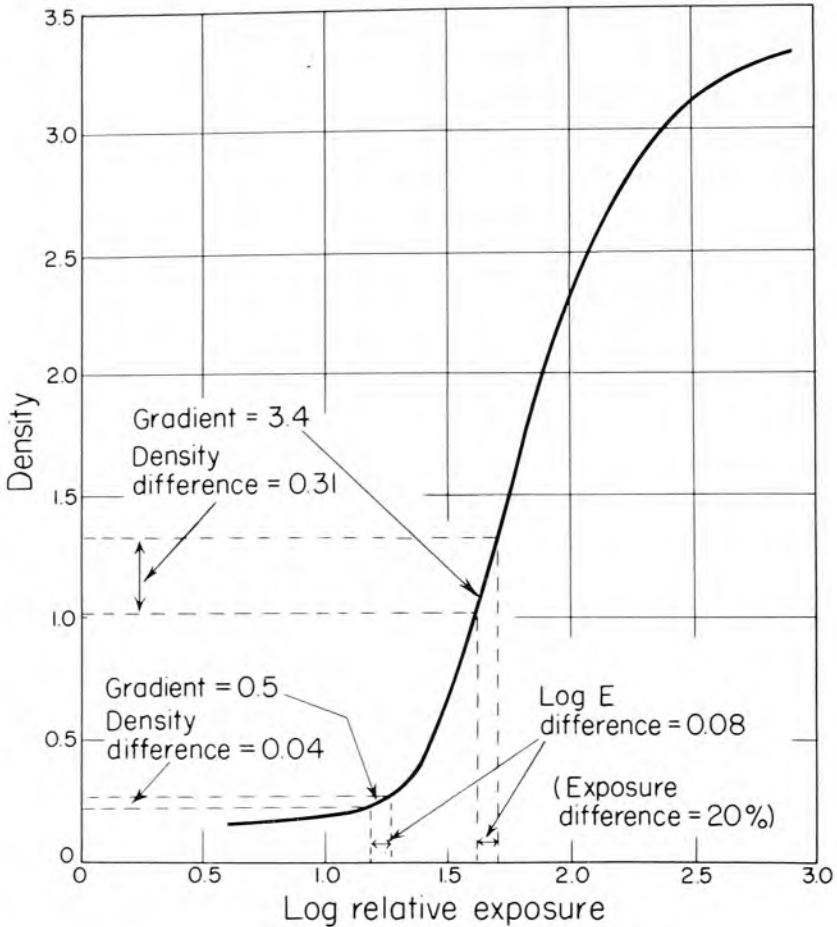


FIG. VI-14. Characteristic curve of screen-type medical x-ray film, exposed with calcium tungstate intensifying screens. The density differences for a 20% difference in exposure have been evaluated for the two values of gradient illustrated in Fig. VI-13. (Courtesy of X-Ray Sales Division, Eastman Kodak Co.)

linear portions. For this reason, film contrast is better defined by the average gradient, which is the slope of a straight line between two points of specified density (Fig. VI-15).

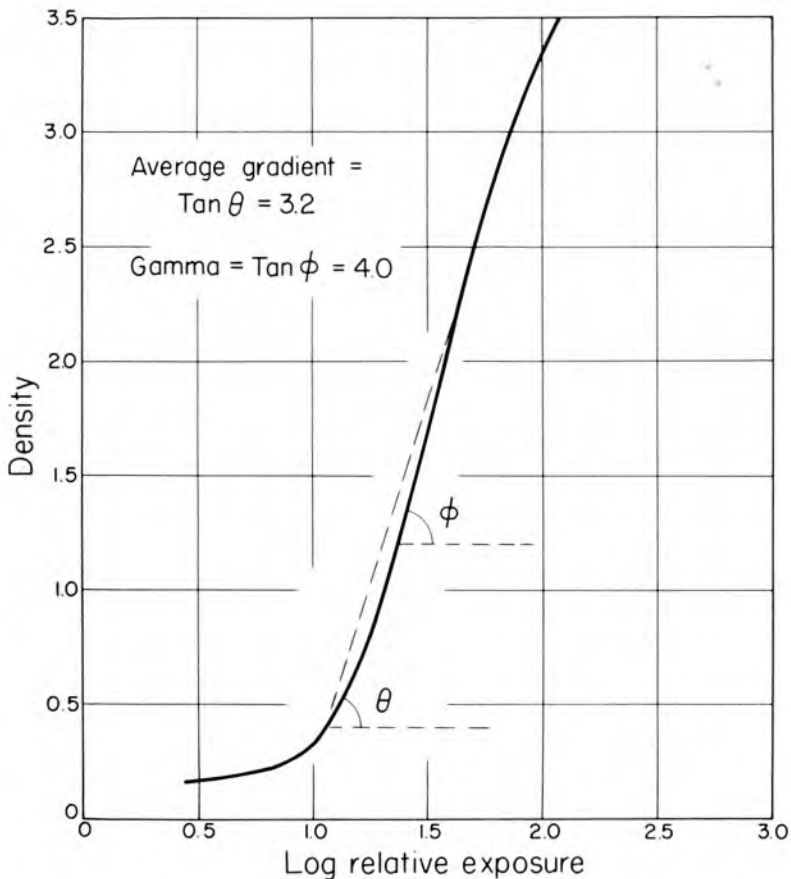
If the gradient of the characteristic curve over a given density range is equal to 1, the radiographic contrast between two areas in this density range is equal to the subject contrast. If the gradient of the curve is greater than 1, the radiographic contrast is greater than the subject contrast and the film acts as a contrast amplifier. On the other hand, if the gradient is smaller than 1, the radiographic contrast is smaller than the subject contrast and the film then dampens the contrast.

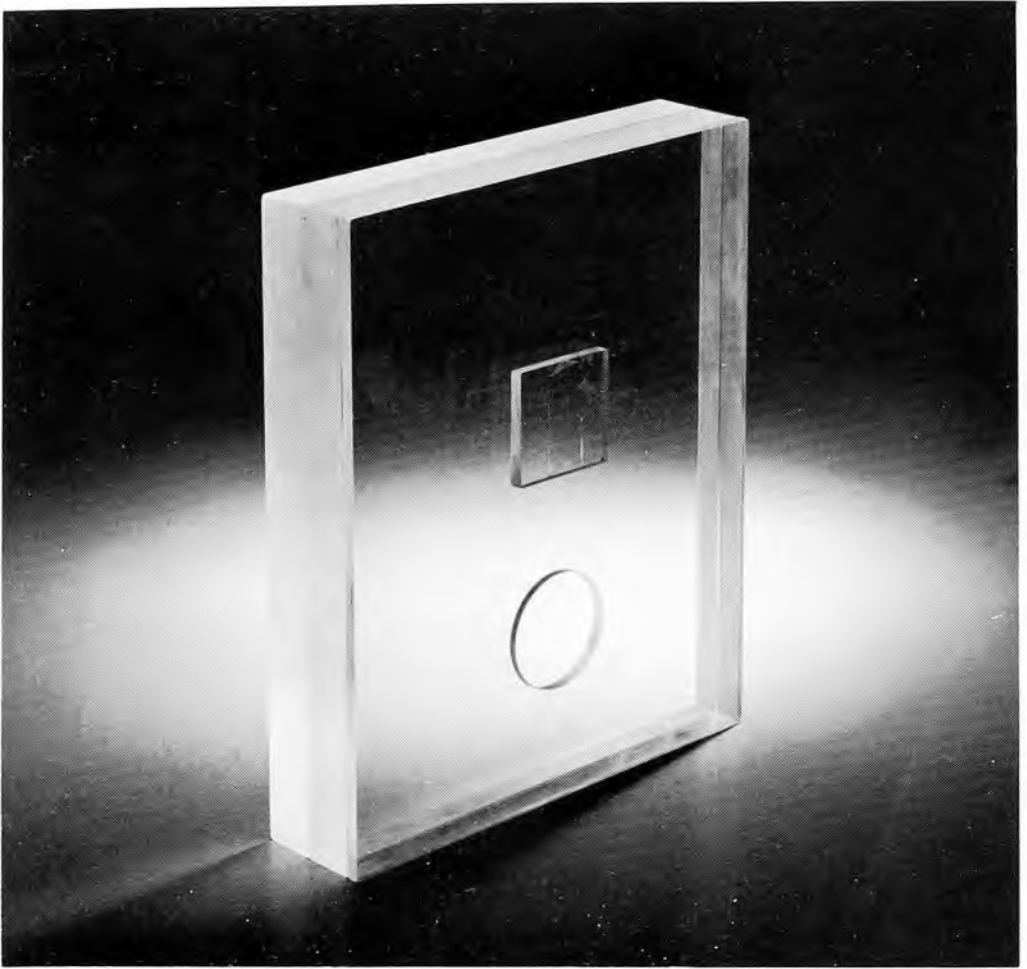
The importance of film contrast in radiography can be illustrated by the example in Fig. VI-16: B, C, and D are all radiographs of the test object A. The subject contrast in Radiographs B, C, and D was kept constant; however, the exposure varied over a wide range from B to D. It is apparent that Radiograph C exhibits the best radiographic contrast and allows the best

identification of the object examined. This variation in radiographic contrast is explained by the fact that Radiograph B was obtained by low exposure, below the "toe" of the curve, in a region of low film contrast; Radiograph D was obtained by exposure above the "shoulder" of the characteristic curve, also in a region of low film contrast; whereas Radiograph C resulted from an exposure corresponding to the maximum contrast for the film under consideration. This example shows (1) that in a roentgenographic examination structures having low subject contrast may be difficult to observe if their exposure places them in a region of low film contrast (exposure either too high or too low), and (2) that in a radiographic examination covering a broad range of densities the areas of very low and very high densities exhibit a compressed scale of densities (narrow range) as compared to the areas included in a more favorable range.

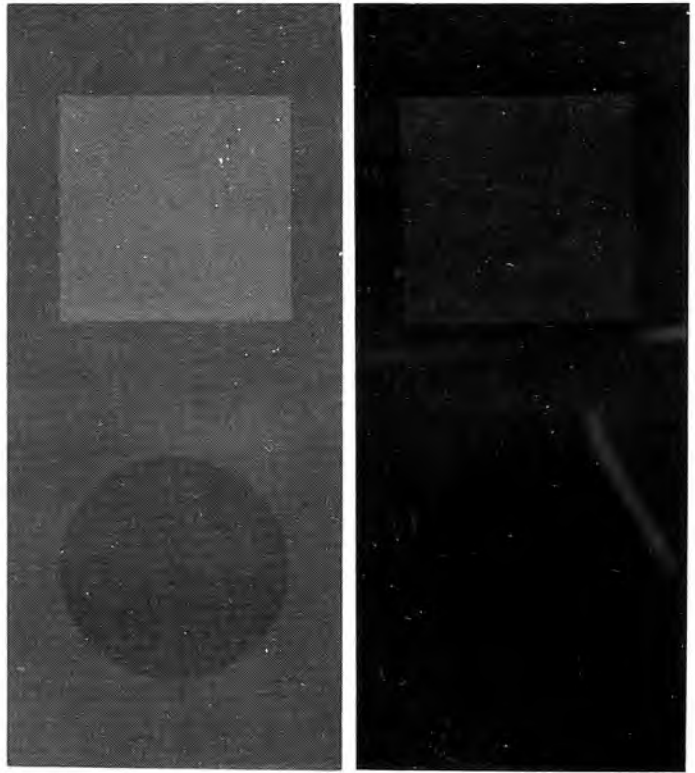
A series of characteristic curves for commonly used x-ray films are shown in Fig. VI-17, and Fig. VI-18 shows the influence of film contrast on an x-ray examination.

FIG. VI-15. Characteristic curve of screen-type x-ray film, exposed with calcium tungstate intensifying screens. Average gradient has been calculated over density range 0.25–2.00 above base and fog; gamma (slope of approximately straight portion of curve) is also indicated. (Courtesy of X-Ray Sales Division, Eastman Kodak Co.)





A



B

C

D

FIG. VI-16 (*Legend on opposite page*).

Film Densities in Diagnostic Radiology

The densities most commonly encountered in films of diagnostic value are in the range of 0.25 to 2, which corresponds to a range of transmitted radiation between a little more than 50 and 1% (see p. 209). The lower limit of the useful density range is established by the toe of the characteristic curve of the more commonly used radiographic films (Fig. VI-17). On the other hand, the upper limit of the film density is not limited by the shoulder of the characteristic curve; indeed, most screen-type films used in radiography exhibit a steep slope up to a density of about 3, and no-screen films are usable to densities much higher than that (see section on "Sensitivity of Radiographic Film to X-Rays"). The limit of 2 imposed by the radiologist on film density when exposing a radiograph stems from the following practical considerations: (1) Most medical x-ray illuminators are not sufficiently intense to give an adequate image of a film having a density greater than 2. (2) If much brighter illuminators were used in the examination of radiographs exhibiting a wide variation in density, the radiologist would be dazzled by the areas of low density and could probably not evaluate the denser areas. The solution to this problem that has been adopted by many radiologists is to use very bright illuminators of limited aperture for the study of the darker film areas.

Film Latitude. In a given range of densities the latitude of a film is a measure of the exposure range which results in these densities (Fig. VI-19). The latitude of a film varies with the reciprocal of film contrast. Thus, films with low contrast exhibit a greater latitude for a given density range than films with higher contrast. The usefulness of the concept of latitude in radiology is as follows: If a predetermined range of desirable densities is set for an examination (for example, from 0.25 to 2, as discussed above), a film with greater latitude allows a greater range of exposures than a film with lower latitude. From the standpoint of the radiologic examination this means that a film with greater latitude may, under certain circumstances, provide diagnostic images of structures that would have been outside the useful density range if a shorter latitude film had been used.

However, high film latitude means low film contrast and, consequently, a poorer presentation of the examined structures from the standpoint of detail perception. Rather than using a film with greater latitude it is usually preferable to extend, whenever possible, the useful density range (for

FIG. VI-16. A Photograph of plastic test object. B, C, D Radiographs of test object, made on a screen-type film with increasingly greater exposure times, all other radiographic factors remaining constant. Note that the structure of the test object is most easily visible in the middle range of densities, C, where the characteristic curve (see Fig. VI-12) is steepest. (Courtesy of X-Ray Sales Division, Eastman Kodak Co.)

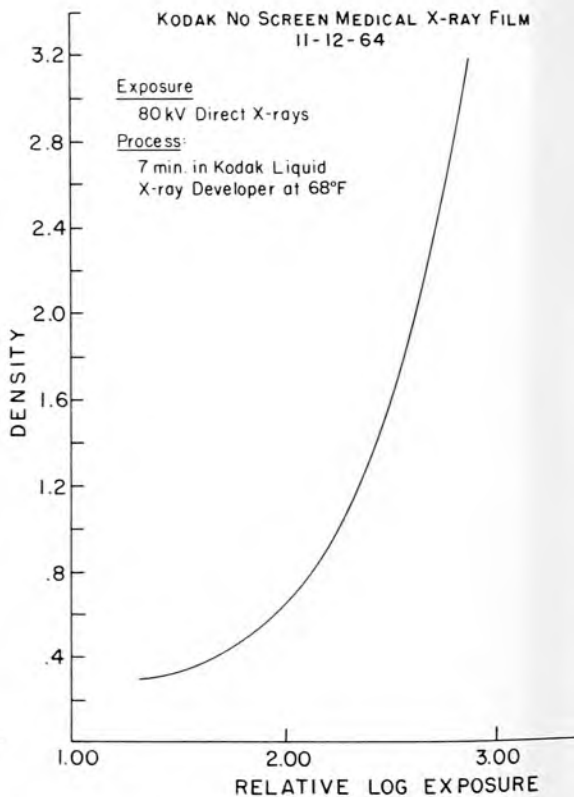
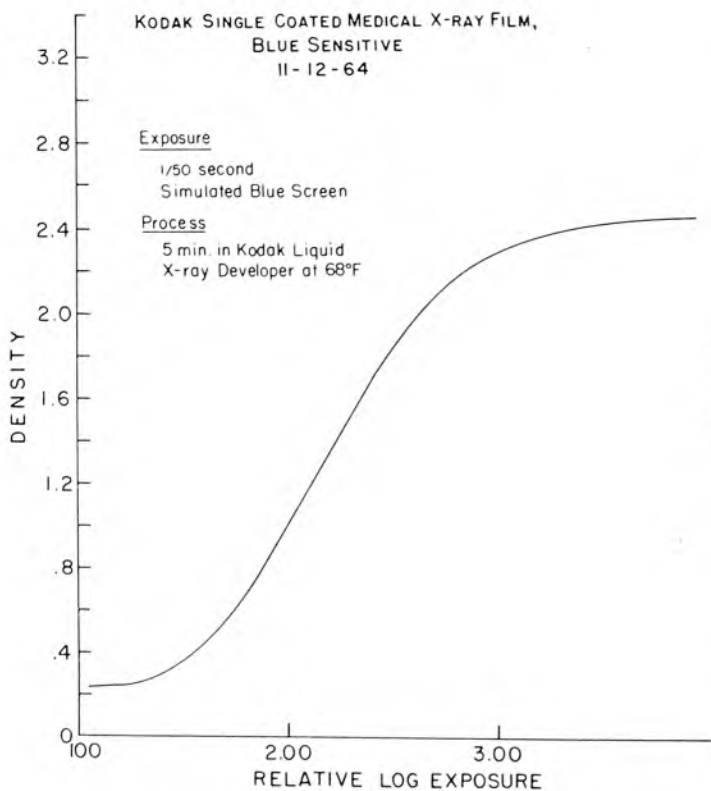
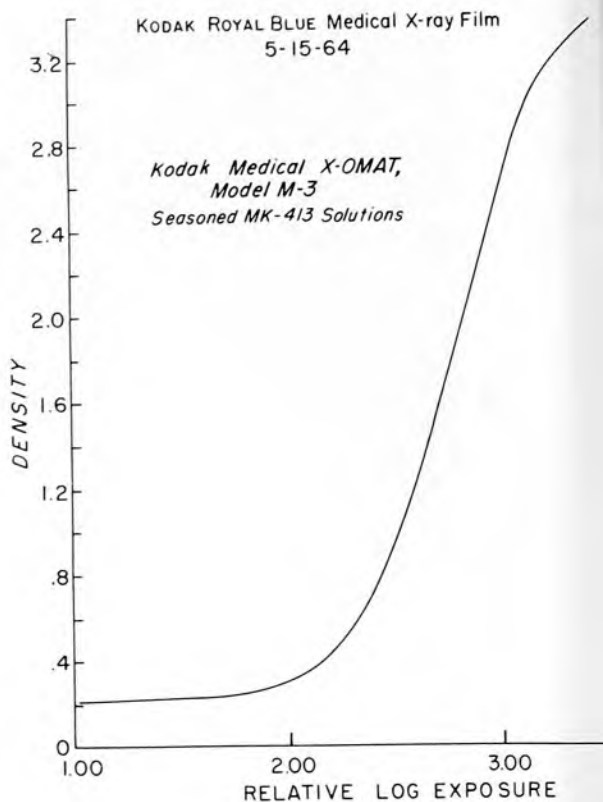
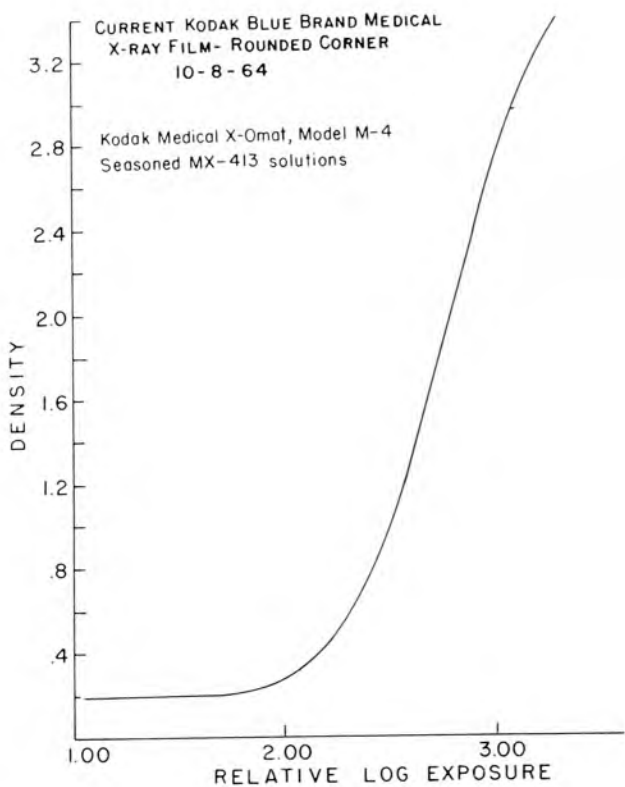


FIG. VI-17. Characteristic curves of some films used in diagnostic radiology. (Courtesy of X-Ray Sales Division, Eastman Kodak Co.; Photo Products Department, E. I. du Pont de Nemours & Company, Inc.; Ansco X-Ray Products, General Aniline and Film Corporation.)

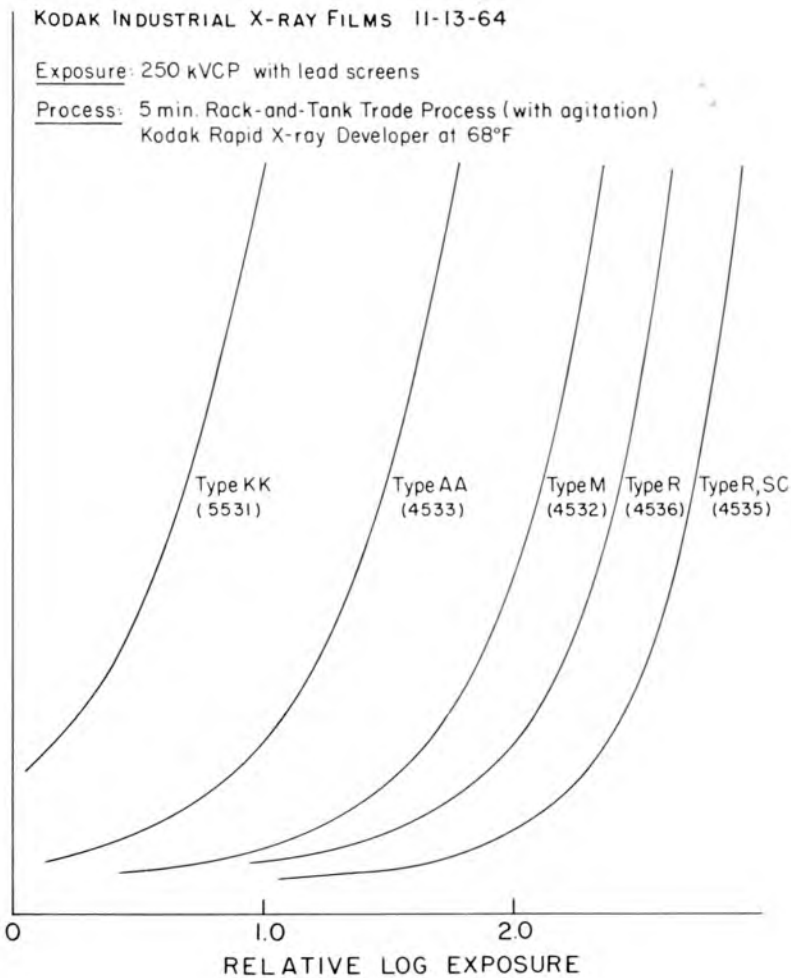
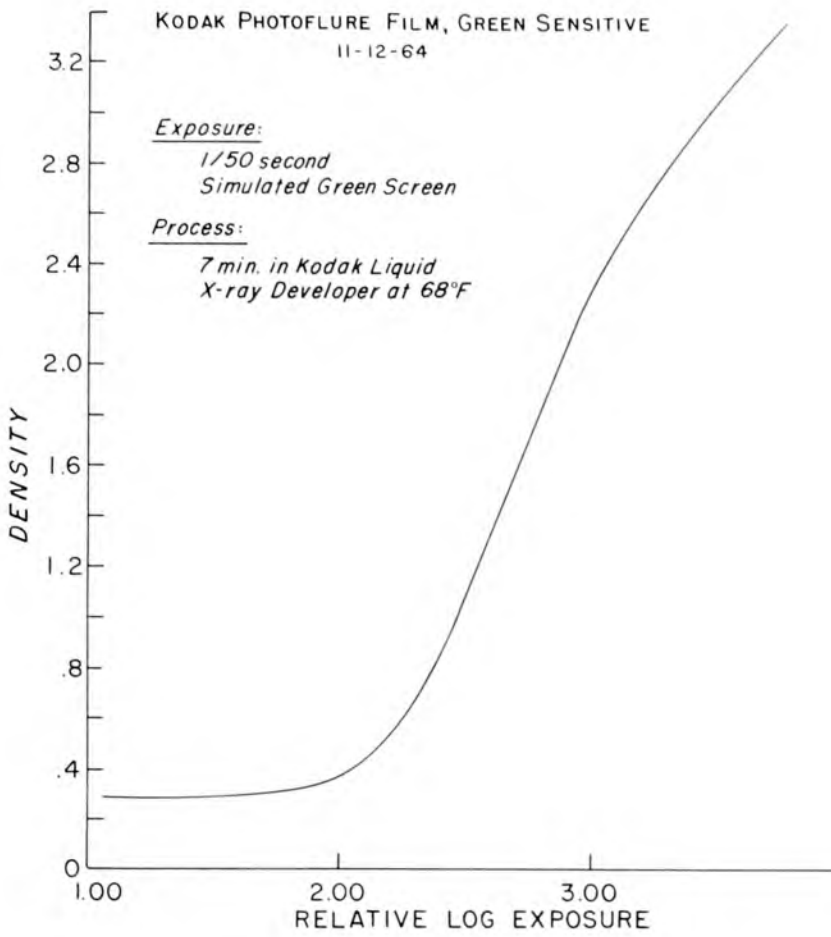


FIG. VI-17 (Continued).

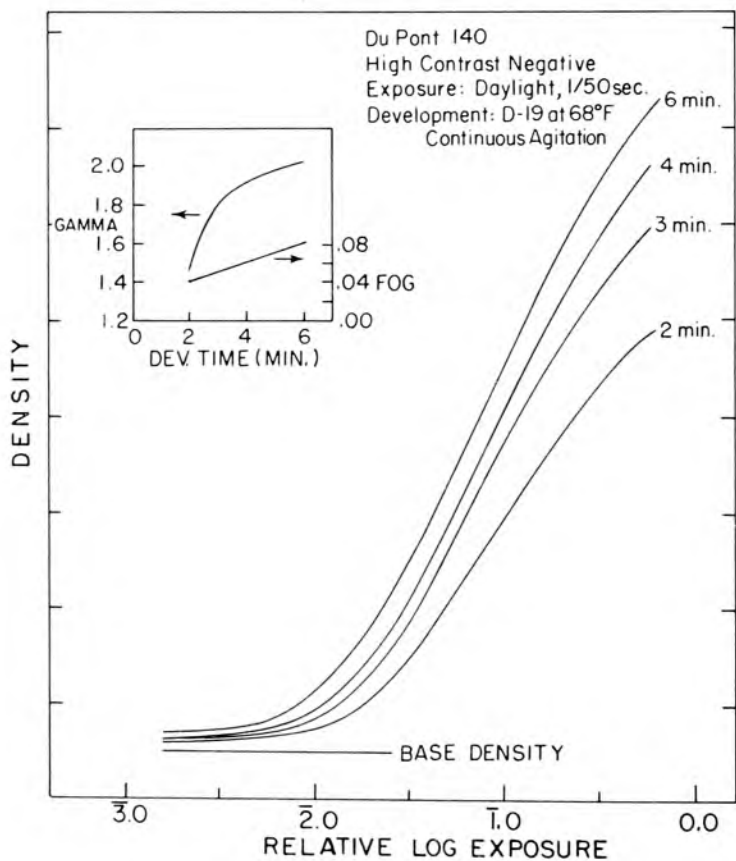
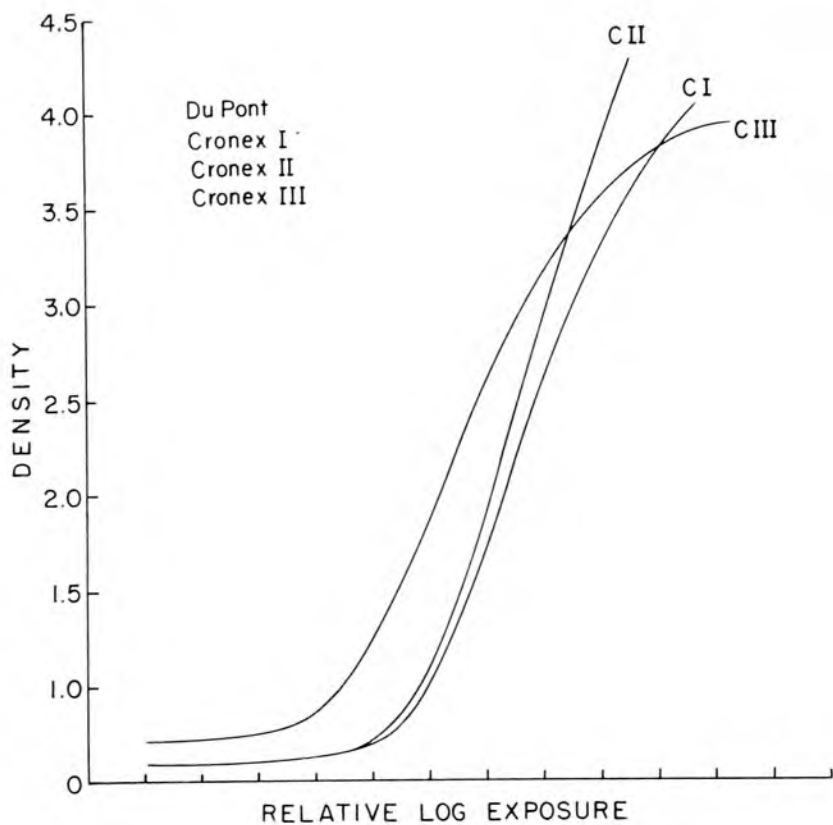


FIG. VI-17 (Continued).

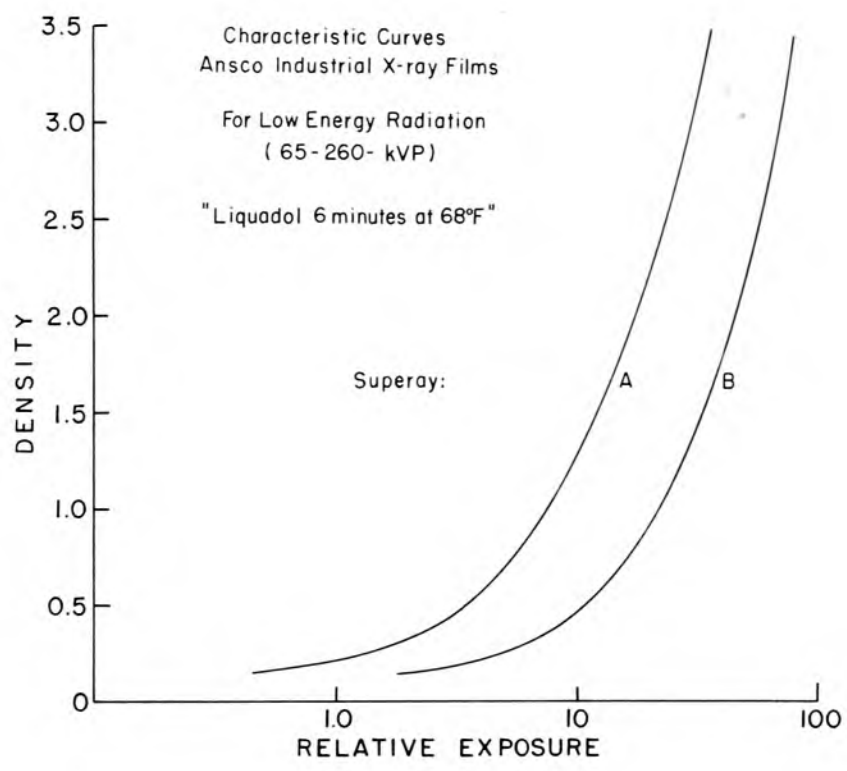
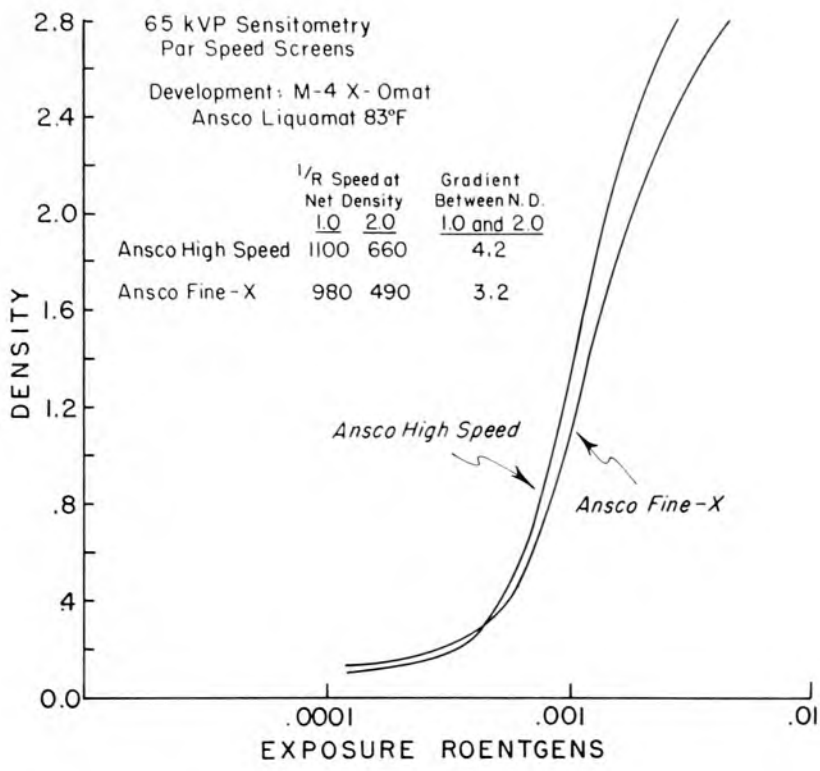


FIG. VI-17 (Continued).



FIG. VI-18. Radiographs of the phantom of a head on films having different characteristic curves.

A Cronex I B Cronex II C Cronex III

(Courtesy Photo Products Department, E. I. du Pont de Nemours & Company, Inc.)

example, through the use of high intensity illuminators) and thus to include all the structures to be examined in the useful density range without sacrifice of contrast (Fig. VI-20). It should be noted that in most radiographic examinations a considerable range of potentially useful densities is omitted at the high end of the density scale.

Film Sensitivity (Speed). The sensitivity, or the speed of a film, is defined as the reciprocal of the radiant energy exposure required to produce a given density on that film. While film contrast determines the shape of the characteristic curve of a film, film sensitivity determines the position of this curve with respect to the log exposure scale (Fig. VI-21). The sensitivity of



FIG. VI-18B and C (*Legend on opposite page*).

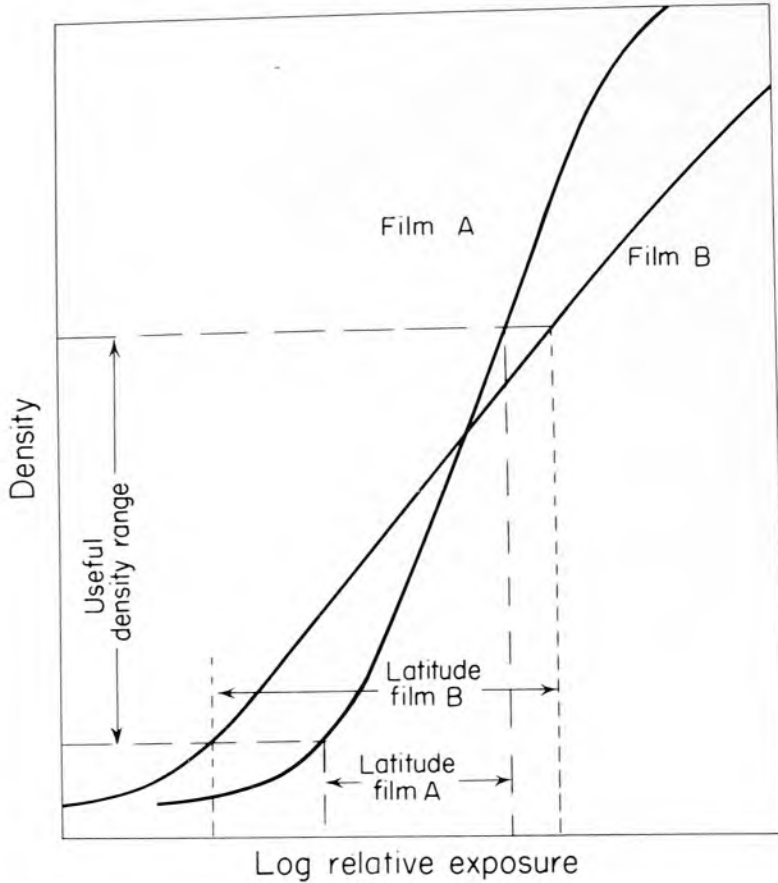


FIG. VI-19. Characteristic curves of two hypothetical radiographic films. Range of exposures that can be covered within the range of useful densities (i.e., the latitude of the film) depends upon average gradient.

A high contrast film

B low contrast film

(Courtesy of X-Ray Sales Division, Eastman Kodak Co.)

radiographic films used in conjunction with screens is measured in ergs/cm^2 required to produce a net density of 1.0 above base density and fog (see below); the sensitivity of films directly exposed to x-radiation is measured in $\text{roentgens}/\text{cm}^2$ required to produce a net density of 1.0. In many instances, film sensitivity is measured in relative units by assigning an arbitrary speed (for example, 100) to a given film. For industrial x-ray films the standard density used in the determination of film sensitivity is 1.5 (also above base density and fog), which reflects the higher densities employed in industrial radiography.

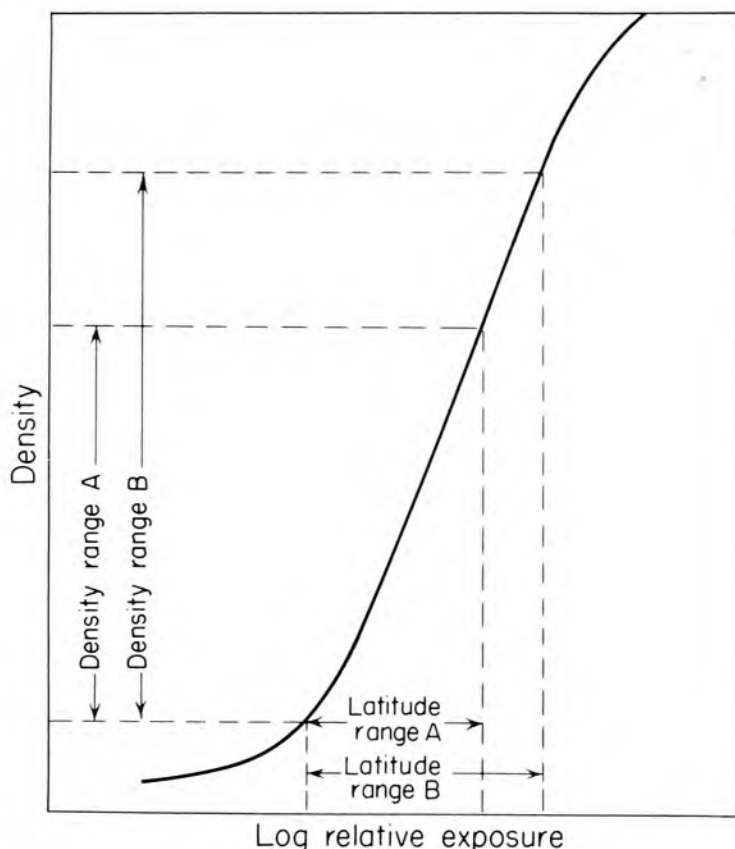
Under certain circumstances the characteristic curves for two films may cross, as shown in Fig. VI-22. In such a case the relative sensitivities of the two films may be reversed, depending on whether a density below or above the point of intersection is used as a standard. At the point of intersection the two films have equal sensitivities. It is apparent that the unqualified

expression of relative film sensitivities is sufficient only in the comparison of films with similar contrast. For films of different contrast, the comparison of sensitivities must be supplemented by their characteristic curves and by an indication of the density at which the speed was determined.

Comparison of Characteristic Curves for Light and X-Rays. The shape of the characteristic curve of an x-ray film exposed directly to x-rays is different from that of the same film exposed to the light of intensifying screens. Figure VI-23 illustrates this difference. Curves A and B have been brought together for easier comparison. The characteristic curve for the film exposed directly to x-rays (Curve B) has a longer, more sweeping toe, a less steep central portion, and a longer, more sweeping shoulder than the curve for the same film exposed with screens (Curve A). This effect is observed by radiologists who use conventional screen-type x-ray film without screens (in cardboard cassettes) and find that the contrast obtained is inferior to that obtained when the same examination is carried out with the same film but with screens.

The characteristic curve for a direct exposure film (Fig. VI-23, Curve C)

FIG. VI-20. Characteristic curve of hypothetical radiographic film. The latitude of a particular film depends upon the range of useful densities. (Courtesy of X-Ray Sales Division, Eastman Kodak Co.)



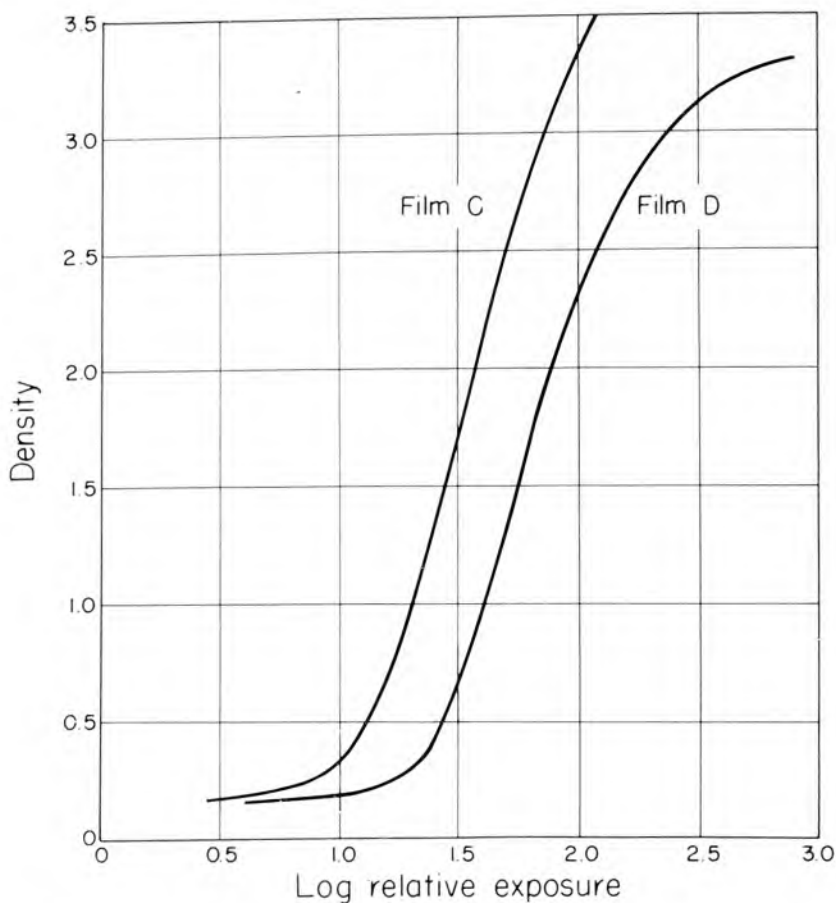


FIG. VI-21. Characteristic curves of two typical medical x-ray films, Film C being faster than Film D. Exposures made with calcium tungstate intensifying screens. (Courtesy of X-Ray Sales Division, Eastman Kodak Co.)

exhibits the same sweeping toe and sweeping shoulder as Curve B; however, the shoulder of Curve C, which occurs at densities above 6.0, is not included in the picture.

The difference between screen and direct x-ray film exposure can be also shown by a plot of net density versus relative exposure. Such a graph (Fig. VI-24) shows a straight-line relationship for the direct x-ray exposure curve. This characteristic curve is quite useful in the film dosimetry of x-rays or gamma rays.

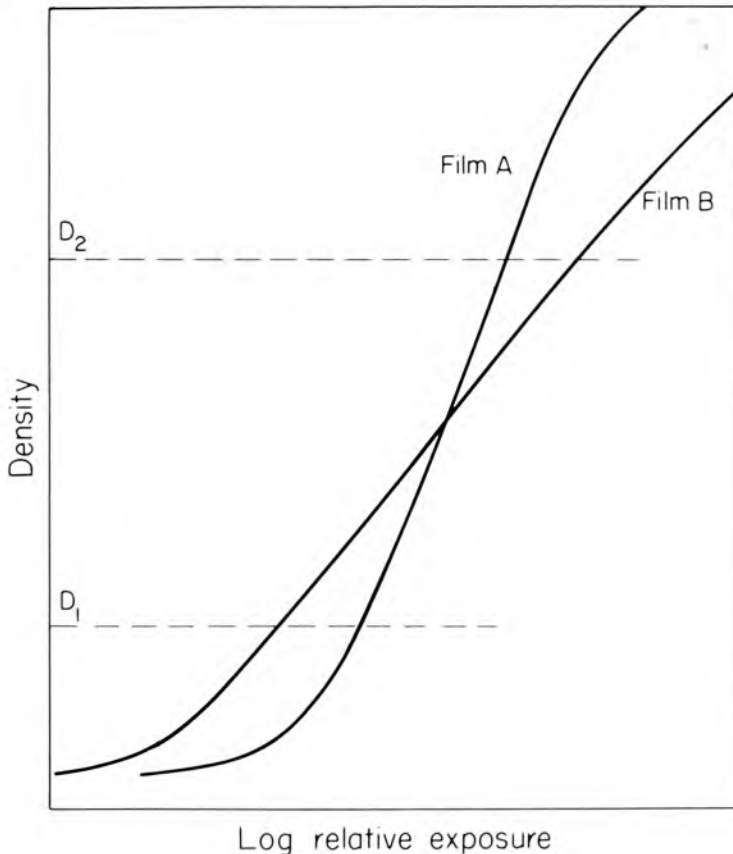
The Reciprocity Law and Its Failure. In the previous discussion it has been assumed that the relationship between exposure and density is independent of the period of time during which the exposure is applied. In other words, it was assumed that a given density produced on a film is the same whether the radiant energy is applied with high intensity over a short period of time or with low intensity over a long period of time, provided that the total amount of applied radiant energy is the same. This assumption is based on the reciprocity law, which can be stated as follows: The density of a

photographic film depends only on the exposure and is independent of the rate at which the exposure is applied.

The reciprocity law holds for radiographic film exposed directly to x-rays and also for film exposed to screens (or to any form of light) over most of the exposure rates encountered in conventional diagnostic radiology. However, if extremely short or extremely long exposures are used, the reciprocity law fails and the film appears to be in both cases less sensitive than when the same amount of light energy is delivered at an "optimum" rate. Medical x-ray films exhibit their optimum sensitivity at the exposures used routinely in radiography, and small divergences from such delivery rates do not result in appreciable errors until the exposure rate is changed by a factor of about 8.

Base Density—Fog. Unexposed photographic film exhibits a certain density after processing. This density results from base density and fog. Base density is contributed by the absorption of light in the plastic material used in the fabrication of the film base. In addition, the base of most x-ray films is tinted to produce a pleasing, colored radiograph. Such coloring adds to the base density. (Colorless x-ray films, with low base density, are also

FIG. VI-22. Characteristic curves of hypothetical high contrast Film A and low contrast Film B. Relative speeds of the two films depend upon density at which they are measured. (Courtesy of X-Ray Sales Division, Eastman Kodak Co.)



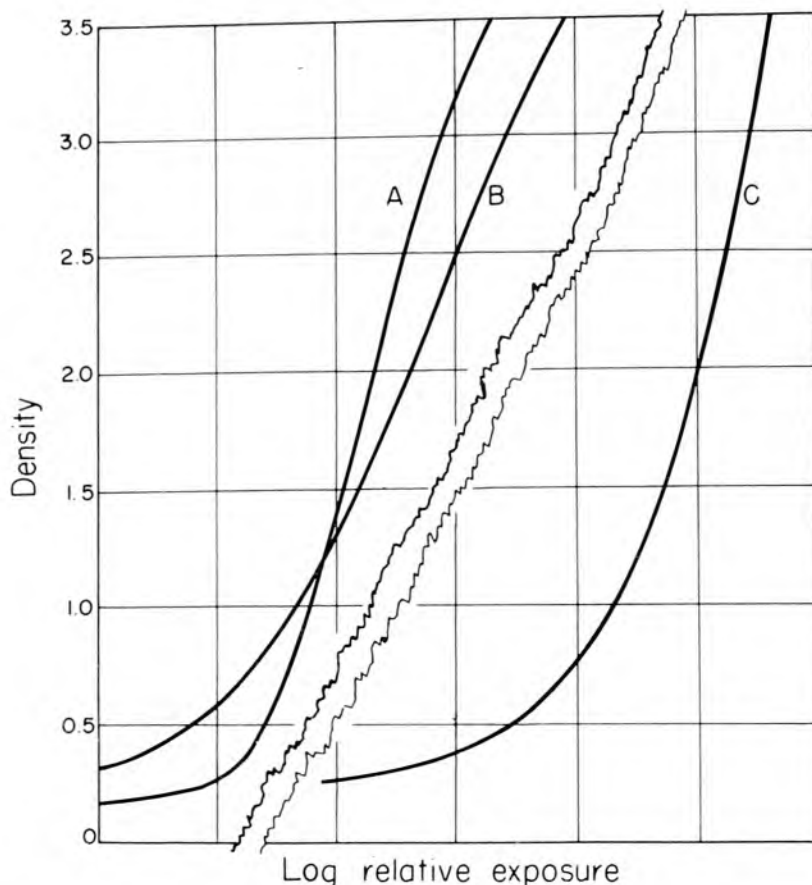


FIG. VI-23. Characteristic curves of typical screen-type x-ray film

- A** exposed to calcium tungstate intensifying screens
 - B** exposed directly to x-rays
 - C** a typical direct-exposure film exposed directly to x-rays
- (Courtesy of X-Ray Sales Division, Eastman Kodak Co.)

manufactured.) The base density varies depending on the base used in the manufacture of the film. A typical value for base density is 0.07.

Fog is the density of a film due to the development of unexposed silver halide grains. Another form of undesirable film density, also referred to as fog, results from the unplanned exposure of film to radiant energy. A common contributor to such fog is background ionizing radiation and accidental exposure to penetrating radiation from other radioactive sources. A net density of 0.2 is produced by an exposure as small as 5 mR with lightly filtered 100 kV_p x-rays on Kodak No-Screen Medical X-Ray Film, and the same density requires 10 mR with Kodak Blue Brand Medical Film (Ref. 12).

Base density does not vary with time, while fog increases with time, particularly if the film is not kept in cold storage. A typical value for density contributed by fog in a "fresh" x-ray film is about 0.05. "Fresh" unexposed processed x-ray film may exhibit a low "base-plus-fog" density of about

0.12, but this value increases with time. A base-plus-fog density in excess of 0.20 is considered objectionable.

Sensitivity of Radiographic Film to X-Rays

The conversion of the radiologic image into a radiograph by a film exposed directly to x-rays without the help of screens takes place as follows: The x-ray photons are stopped in the film, and the energy thus dissipated in the form of excitations and ionizations is recorded by the film emulsion. The sensitivity of a film to x-rays is therefore determined by (1) the absorption of x-ray photons by the film and (2) the efficiency with which excitations and ionizations are utilized in exposing the photographic emulsion.

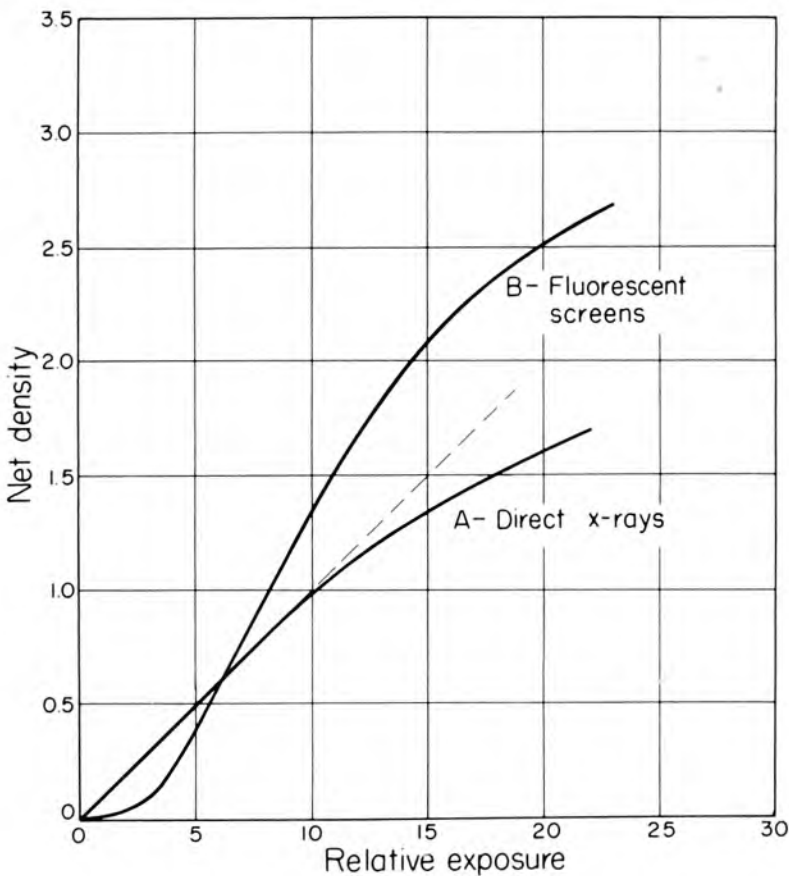
The sensitive photographic emulsion is composed of an organic gelatin matrix containing a suspension of silver bromide particles. The gelatin is nearly transparent to x-ray photons in the conventional diagnostic energy

FIG. VI-24. Net density-versus-exposure curves for a medical x-ray film

A exposed directly to x-rays

B exposed to calcium tungstate intensifying screens.

Note that at low densities the direct exposure curve is a straight line. (Courtesy of X-Ray Sales Division, Eastman Kodak Co.)



range, and most of the absorption of the x-ray photons takes place by photoelectric interactions in the silver bromide. The absorption of x-rays in x-ray films shows two relative maxima for photon energies equal to the K absorption peaks of bromine and silver (Ref. 13). The amount of silver bromide per unit area in radiographic film is small, as shown in Table VI-3, and x-ray film is relatively transparent to x-rays.

TABLE VI-3. Physical Characteristics of Some "Kodak" Films Used in Radiology

Film	Silver halide ^a (mg/cm ²)	Base (10 ⁻³ in.)	Emulsion ^{b,c} (10 ⁻³ in.)
Kodak Blue Brand Medical X-Ray Film	1.84	9	0.35
Kodak Royal Blue Medical X-Ray Film	2.10	9	0.5
Kodak No-Screen Medical X-Ray Film	7.00	7	1.2
Kodak Industrial X-Ray Film, Type M	3.30	7	0.6
Kodak Industrial X-Ray Film, Type KK	7.00	7	1.2
Kodak Photofluore Film—Green Sensitive	1.58	5.6	5
Kodak Photofluore Film—Blue Sensitive	1.80	5.6	0.8

Data supplied through the courtesy of the X-Ray Sales Division, Eastman Kodak Company, Rochester, New York. This information applies to the products as currently manufactured. The make-up of these films is subject to change without notice.

^a In the top five films, the silver halide is equally distributed between the two emulsion layers.

^b For the top five films, the emulsion thicknesses are the thicknesses of each individual emulsion.

^c Emulsion thicknesses include the thickness of any undercoat between emulsion and base.

The conversion of x-ray photon energy dissipated in the film into developable silver bromide grains is inefficient. Although a large number of silver atoms are liberated by single x-ray photons, this number is considerably lower than predictable on the basis of the amount of energy available, and it is estimated that only 5 to 6% of the energy dissipated by an x-ray beam in a photographic emulsion is utilized in liberating silver atoms (Ref. 13). The absorption of one x-ray photon renders only a few silver bromide grains developable. The efficiency with which the energy of x-ray photons dissipated in a photographic emulsion is utilized for producing a photographic effect decreases with increasing photon energy.

It should be noted that the sensitivity of a photographic film to x-rays is not determined by absorption of x-rays alone, and two photographic films of similar chemical composition and similar amounts of silver bromide per unit area but with different grain characteristics exhibit similar sensitivities to x-ray photons only at high energies. For low energy photons they may exhibit very different sensitivities (Ref. 13).

The absorption of x-rays by film and the resulting exposure can be conveniently represented by plotting the number of incident roentgens neces-

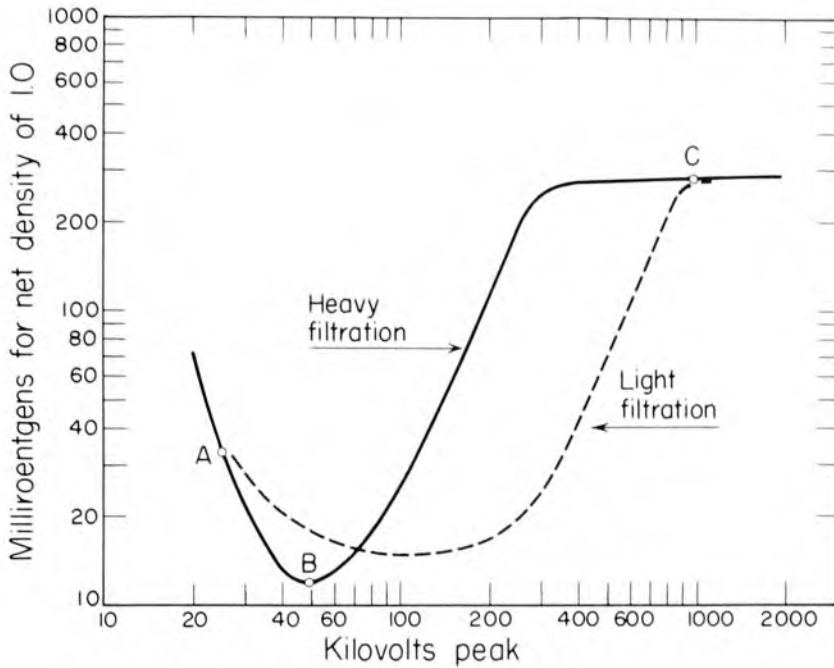


FIG. VI-25. Direct x-ray spectral sensitivity curve for typical film used for radiation monitoring, showing number of roentgens required to produce a net density of 1.0 for two radiation qualities. Characteristic curves for radiations designated A, B, and C are shown in Fig. VI-34. (Courtesy of X-Ray Sales Division, Eastman Kodak Co.)

sary to produce a density of 1 above fog versus photon energy. This relationship is shown in Fig. VI-25, where the milliroentgens required for a net density of 1 are plotted against peak photon energies for polychromatic x-radiation. It is apparent that in the diagnostic energy range, x-ray film is most sensitive to x-ray photons carrying an energy of about 45 keV, primarily because of photoelectric interactions in silver at this energy range.

Sensitivity of Radiographic Film to Screen-Generated Light

In all radiographic examinations with screens, the exposure of the film is due to light, and the direct effect of radiation on the film is negligible. This situation is obviously true in cinefluorography and in photofluorography, where the film is protected against the direct effect of x-rays. Although in cassette-type radiography the film is not protected against the direct action of x-rays, the contribution of the x-radiation to the total density of the film is in most cases of the order of 2% (see section on "Intensification Factor") and can be neglected.

A given film-screen combination can be effectively used only if the film is sensitive to the light emitted by the screen. Most screens used in radiography emit either blue or yellow-green light. Blue-emitting screens are used in cassette-type radiography, and yellow-green-emitting screens are used in photofluorography and cinefluorography; blue-emitting screens are also used

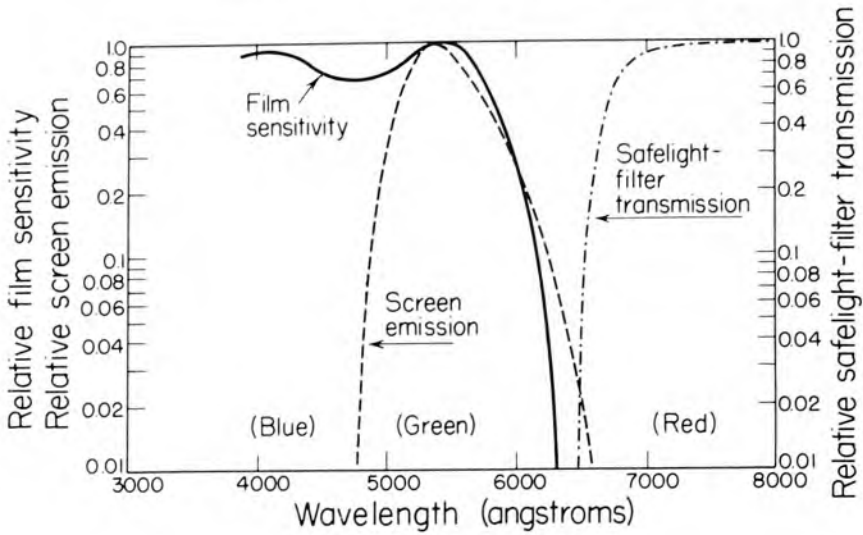
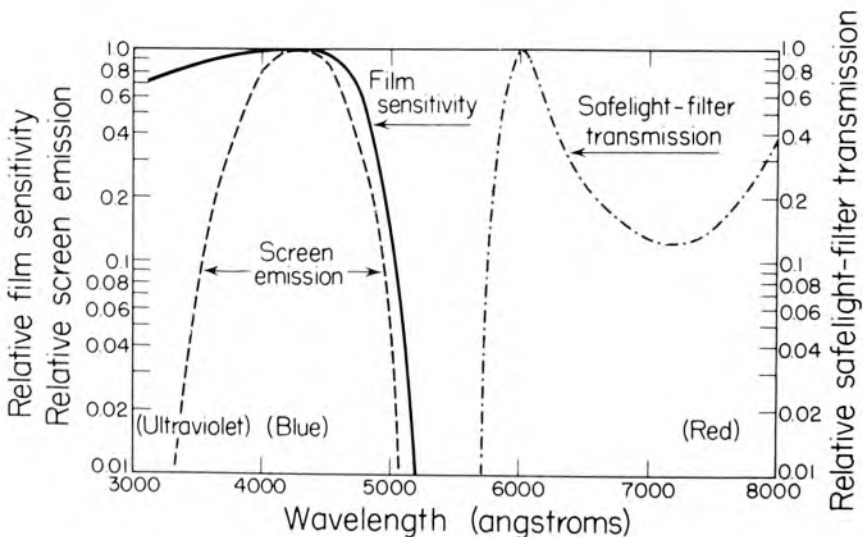


FIG. VI-26. Relative spectral sensitivity of typical screen-type x-ray film; relative spectral emission of typical calcium tungstate intensifying screen; and relative spectral transmission of amber safelight filter recommended for radiographic films. (Courtesy of X-Ray Sales Division, Eastman Kodak Co.)

in photofluorography. The spectral sensitivities of typical radiographic films are shown in Figs. VI-26 and VI-27; the spectral distribution of light emitted by x-ray screens widely used in radiography can be seen in Fig. VI-6.

It may appear that the most efficient film-screen combination is achieved when the film sensitivity curve is identical in shape to the screen emission

FIG. VI-27. Spectral sensitivity of typical green-sensitive photofluorographic film; spectral emission of typical green-emitting photofluorographic screen; and spectral transmission of dark red safelight filter recommended for use with fast green-sensitive films. (Courtesy of X-Ray Sales Division, Eastman Kodak Co.)



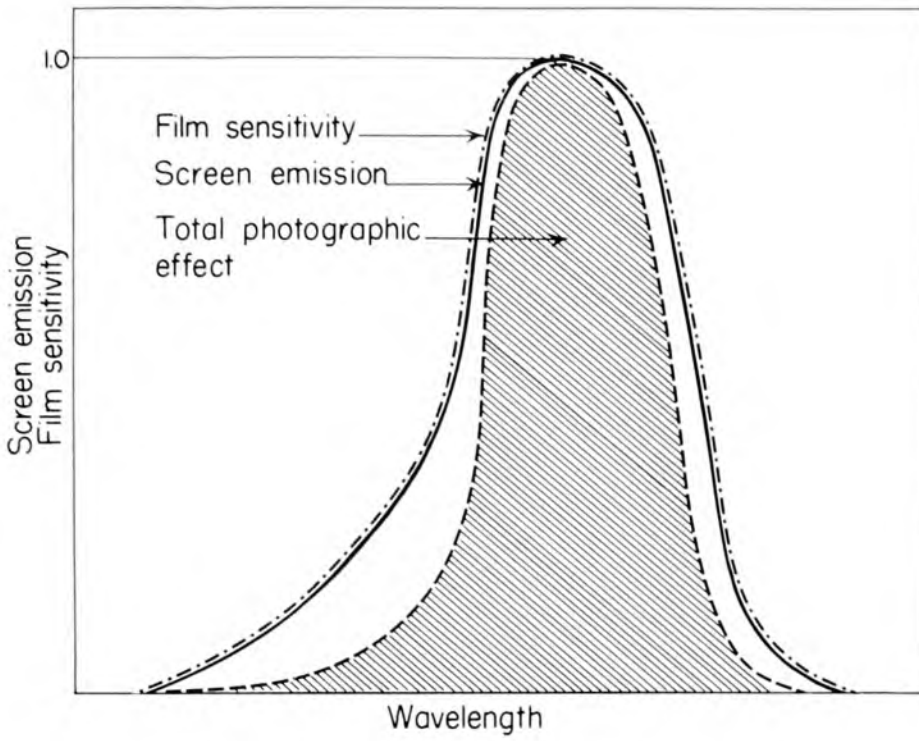
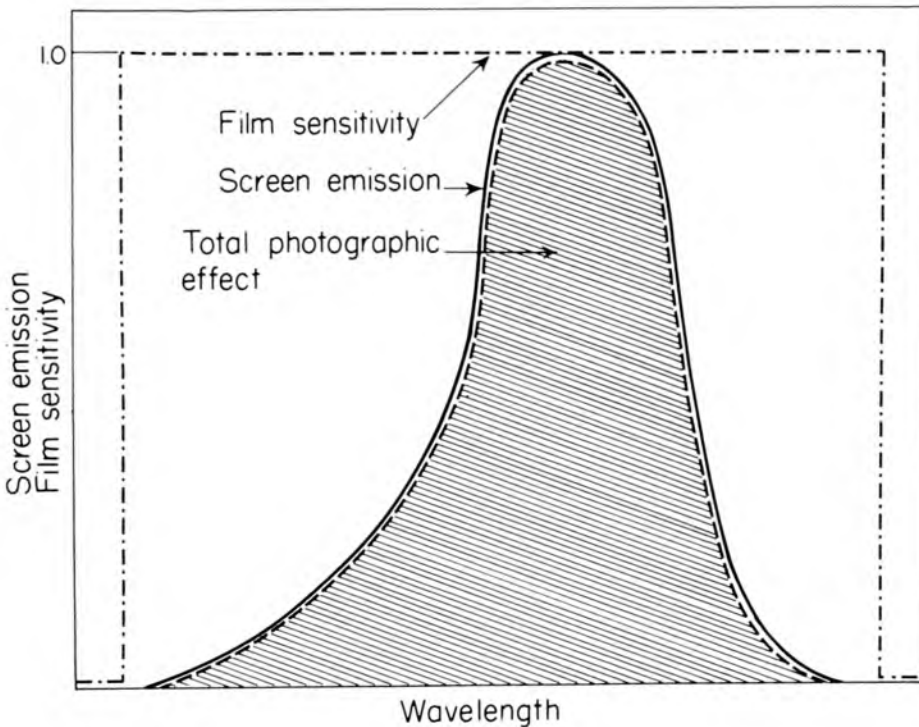


FIG. VI-28. Hypothetical curves illustrating effect of screen emission and film sensitivity on total photographic effect. Screen emission and film sensitivity exactly matched. (Courtesy of X-Ray Sales Division, Eastman Kodak Co.)

FIG. VI-29. Effect of screen emission and film sensitivity on total photographic effect. Screen emission and film sensitivity greatly different. Note that the total photographic effect is greater than in Fig. VI-28. (Courtesy of X-Ray Sales Division, Eastman Kodak Co.)



curve. The fact is that such a match would result in poor utilization of the light emitted by the screen, as shown in Figs. VI-28 and VI-29. In the situation shown in Fig. VI-28, only the light emitted having an energy corresponding to the maximum film sensitivity is utilized with high efficiency. On the other hand, if the film sensitivity is maximum for the whole energy range of the light emitted by the screen (Fig. VI-29), the photographic exposure is greater than if a close match between the curves is achieved. This situation calls for broad film sensitivity and a relatively narrow spectrum of screen emission located somewhere in the middle of the broad sensitivity distribution. Such an optimum match exists with most films used in radiography.

The relative speed and the characteristic curve of an x-ray film depend on the spectral distribution of the light emitted by the screen. Thus, the same film used with different screens may exhibit appreciably different characteristics.

The conversion of light by a photographic film into density is accomplished in two steps: (1) the light photons are stopped in the film which absorbs most of the incident light, and (2) this energy renders silver bromide grains developable. The light energy required to produce a density of 1.0 above fog, on Kodak Blue Brand Medical X-Ray Film, is about 8.5×10^{-3} ergs/cm² of incident light with a wavelength of 4360 Å. (This corresponds to 1.86×10^9 photons/cm².) (Refs. 14 and 15.)

The sensitivity dependence of a film-screen combination on x-ray photon energy is dependent only on the absorption of x-ray photons in the screen used (see screen absorption curves).

Intensification Factor

The intensification factor of a screen for a given film is the ratio of the x-ray exposures required to produce the same density (usually a density of 1.0) on the film with and without the screen. The intensification factor varies with photon energy in a complex manner because the sensitivities of both the screen and the film vary with photon energy also in a complex manner. The intensification factor of a given screen may vary depending on the film used with it. Typically, in the diagnostic x-ray range the intensification factor is approximately 40 to 50 (Ref. 16). It is interesting to note that a combination of x-ray radiographic film and calcium tungstate screens exhibits a relatively constant sensitivity to x-rays practically throughout the whole diagnostic range if exposure is expressed in roentgens (Fig. VI-30). Thus, in the voltage range from 60 to 120 kV_p, an exposure of approximately 1 mR produces a net density of 1 on medium-speed radiographic film exposed with a pair of medium-speed intensifying screens.

Film Processing

Three desirable characteristics of photographic film that affect the quality of the radiographic image are: fine grain, high contrast, and high speed. In the

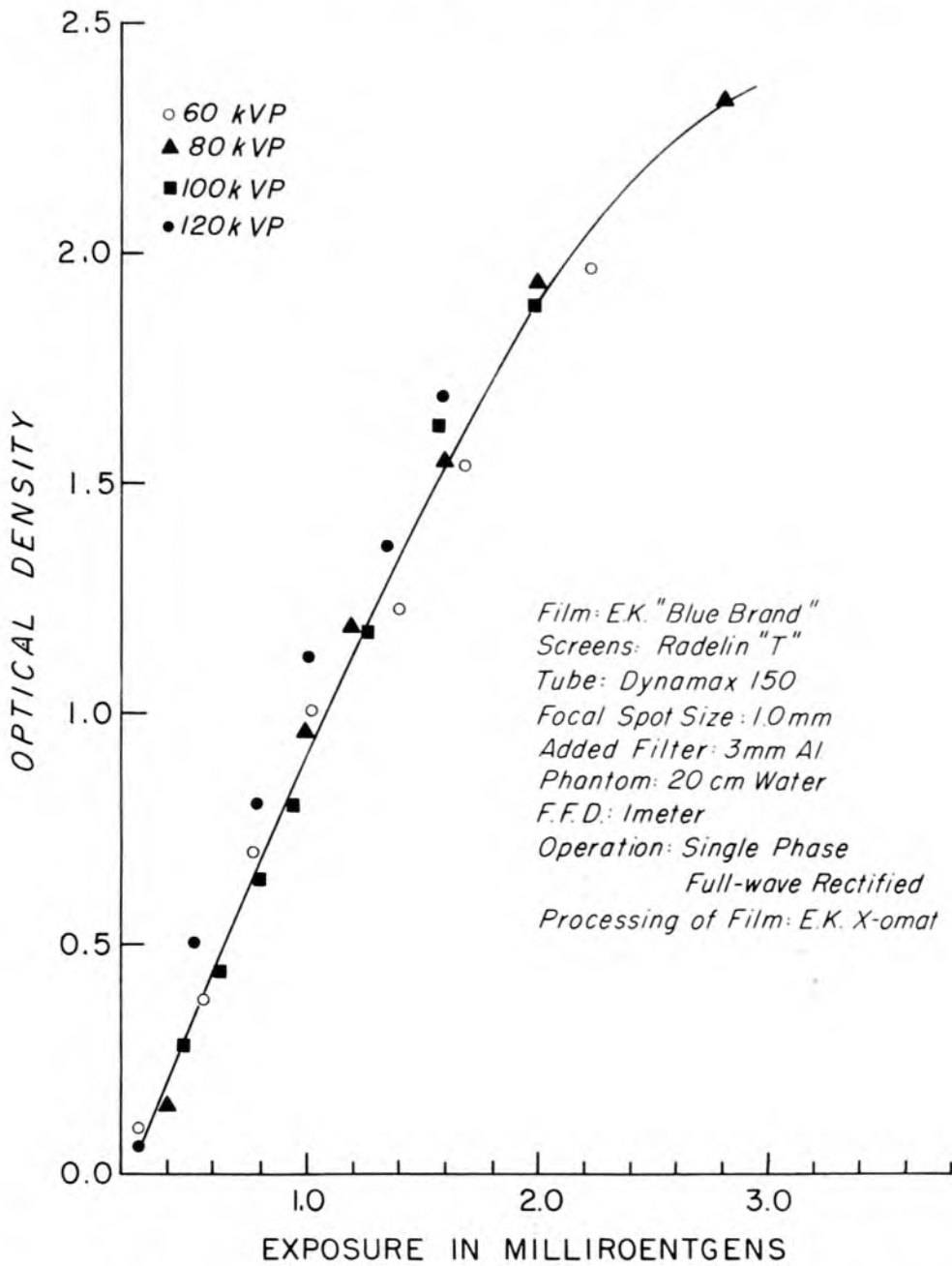


FIG. VI-30. Relationship between photographic density and radiation exposure for a film-screen combination at different peak-energy x-rays.

manufacture of a photographic emulsion any two of these three characteristics can be improved at the expense of the third one. Thus, a fine grain-high contrast film exhibits a lower speed than a fine grain-low contrast film. Also, a high speed-high contrast film is grainy. The desirability of high speed in a radiographic film is obvious. The usefulness of high contrast has been pointed out earlier in this chapter, and the graininess of the film may sometime affect resolution if fine detail is desired. Different films commercially

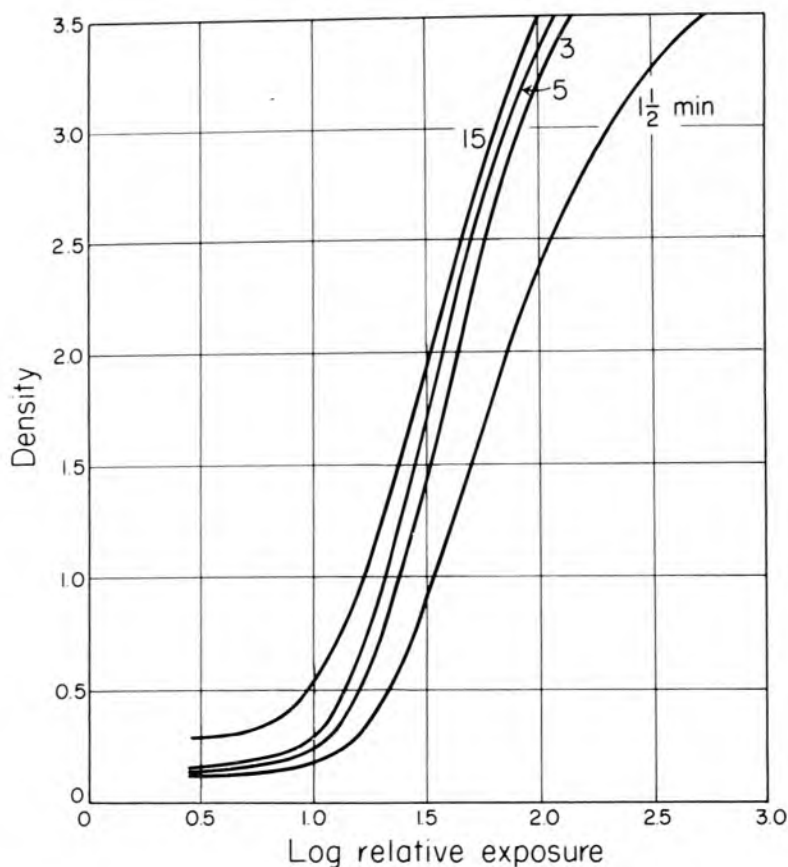


FIG. VI-31. Characteristic curves of typical screen-type x-ray film for a series of developing times at 68° F. (Courtesy of X-Ray Sales Division, Eastman Kodak Co.)

available for radiography embody different combinations of these three factors, and the selection of the proper combination depends on the type of examination for which the film is intended. Proper selection is of particular importance in cinefluorography (Chapter X).

In a given film any two of these factors may to a certain extent be enlarged at the expense of the third factor by modifying the conditions of the film processing.

Film processing consists of developing and fixing. Developing is the reduction in the photographic emulsion of exposed silver halide particles to image-forming particles of metallic silver. This chemical reaction is affected by time and temperature. Fixation consists in dissolving the silver halide particles that have not been affected by light and consequently remained unaffected by the developer. The purpose of fixation, and of subsequent washing, is to render the image stable. Fixation also hardens the gelatin and renders it more resistant to abrasion.

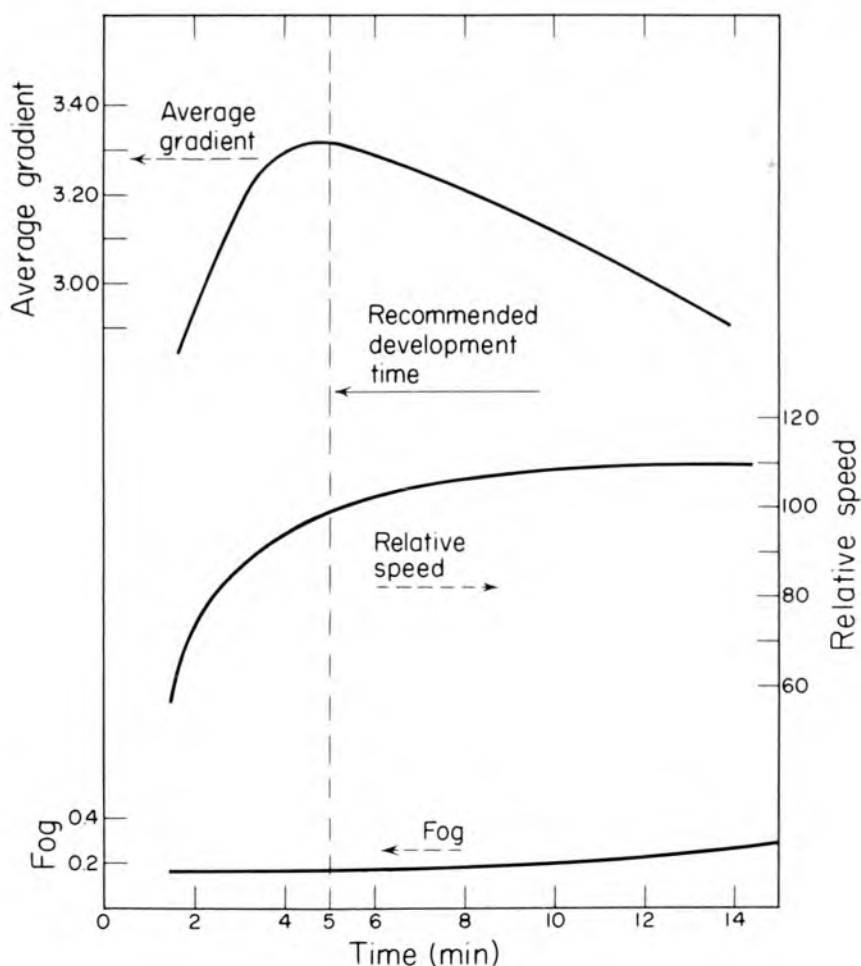
Both the speed and the contrast of a photographic film increase to a certain degree with developing time (Fig. VI-31). However, as developing time increases, the speed reaches a plateau and may even decrease. It should be

noted that increased developing time increases also the undesirable film fog. Figure VI-32 shows the relationship between speed, average gradient, and fog in a photographic film as a function of developing time. It can be seen that the recommended developing time (5 minutes for this particular film) achieves a reasonable compromise between high film contrast and relatively low fog with adequate speed.

The effect of the temperature of the developer on speed, density, and fog is shown in Figs. VI-33 and VI-34. It is apparent that developer temperature and time affect the film in a similar manner.

Fixation of the film does not appreciably affect either speed, density, or contrast. If fixation is carried out for too long a period of time, however, a decrease in film density is observed.

FIG. VI-32. Time-speed and time-average gradient curves derived from the characteristic curves of Fig. VI-19. Time-fog curve for the same developing conditions is also shown. (The relative speed at the recommended developing time of 5 min has been arbitrarily assigned a value of 100. Fog values include density of the blue film base—about 0.10.) (Courtesy of X-Ray Sales Division, Eastman Kodak Co.)



Granularity, Graininess, Resolving Power, and Sharpness (Ref. 17)

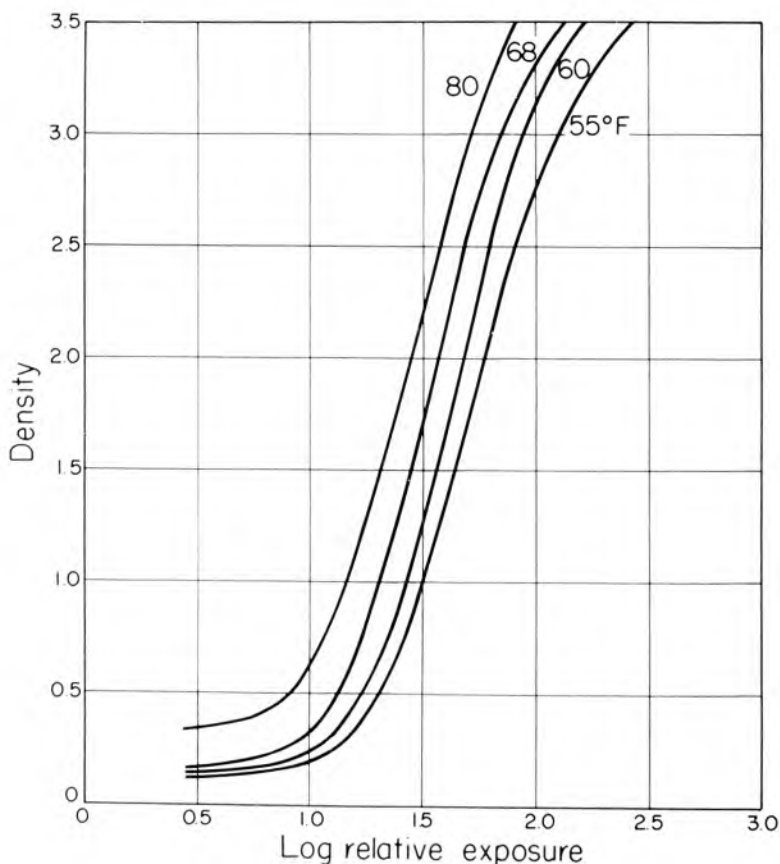
Photographic density is produced by the presence of molecular particles of silver in the processed emulsion. The *granularity* of a photographic image results from the spatial distribution of the reflecting or transmitting components of the processed film. Granularity can be measured on a film by means of a microdensitometer.

The *graininess* of a photographic image is the subjective impression of nonuniformity experienced by an individual observing the granularity.

The *resolving power* of a film is an expression of the ability of the film to record detail. Resolving power is usually measured by a line test pattern recorded photographically on the tested film. The resolving power of photographic films varies from a few lines per millimeter for low resolving power to a high value of about 200 lines/mm. Some special purpose films are made with a resolving power of 1500 lines/mm.

Sharpness is the ability of a film to reproduce a sharp boundary between contrasts. The relationship between sharpness and resolving power is complex, and a series of photographic images are not always ranked in the same

FIG. VI-33. Characteristic curves of film in Fig. VI-19, but developed for 5 min at a series of developer temperatures. (Courtesy of X-Ray Sales Division, Eastman Kodak Co.)



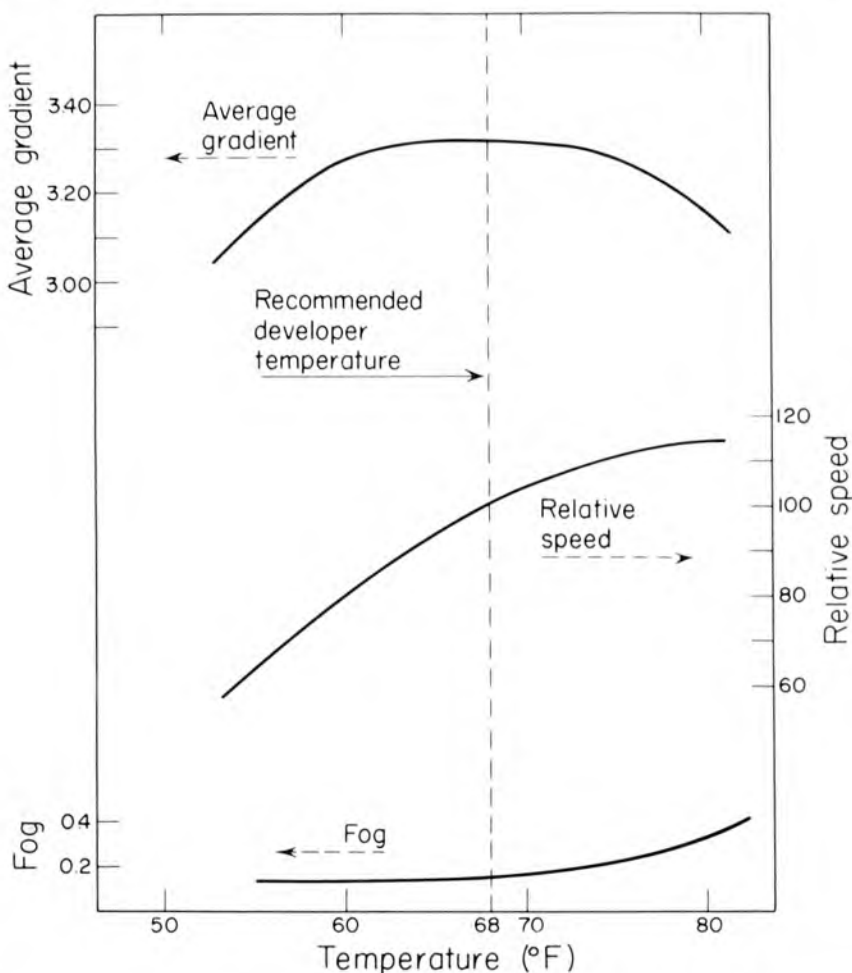


FIG. VI-34. Temperature-average gradient and temperature-speed curves derived from the characteristic curves of Fig. VI-33. Temperature-fog curve under same conditions is also shown. (The relative speed at the recommended developing time has been arbitrarily assigned a value of 100. Fog values include density of the blue film base—about 0.10.) (Courtesy of X-Ray Sales Division, Eastman Kodak Co.)

order of increasing sharpness and resolving power. The relationship between sharpness and resolving power in an emulsion can be altered by certain developers that strongly affect sharpness without altering appreciably resolving power. In general, however, resolution in x-ray films correlates well with sharpness.

REFERENCES

1. BEERS, Y.: *Introduction to the Theory of Error*. Cambridge, Mass., Addison-Wesley, 1953.
2. TER-POGOSSIAN, M.: "The Efficiency of Radiographic Intensifying Screens," in *Technological Needs for Reduction of Patient Dosage from Diagnostic Radiology*, ed. by Janower, M. L. Springfield, Ill., Thomas, 1963, pp. 215-228.
3. PRICE, W. J.: *Nuclear Radiation Detection*. New York, McGraw-Hill, 1958.

4. RAMM, W. J.: "Scintillation Detectors," in *Radiation Dosimetry*, ed. by Hine, G. J., and Brownell, G. L. New York, Academic Press, 1956.
5. MURRAY, R. B.: "Scintillation Counters," in *Nuclear Instruments and Their Uses*, vol. 1, ed. by Snell, A. H. New York, Wiley, 1962.
6. COLTMAN, J. W., EBBIGHAUSEN, E. G., and ALTAR, W.: *Physical Properties of Calcium Tungstate X-Ray Screens*. Scientific Paper No. 1279. East Pittsburgh, Pa., Westinghouse Research Laboratories, 1946.
7. GILLETTE, R. H.: Calcium and cadmium tungstate as scintillation counter crystals for gamma ray detection. *Rev. Sci. Instruments* 21:294, 1950.
8. MORGAN, R. H., and CORRIGAN, K. E., eds.: *Handbook of Radiology*. Chicago, Ill., Year Book, 1955.
9. CORNEY, G. M.: "Photographic Aspects of Cinefluorography," in *Cinefluorography*, ed. by Ramsey, G. H. S., Tristan, T. A., Watson, J. S., Weinberg, S., and Cornwell, W. S. Springfield, Ill., Thomas, 1960.
10. *Sensitometric Properties of X-Ray Films*. X-Ray Sales Division, Eastman Kodak Co., Rochester, N.Y.
11. MEES, C. E. K.: *Theory of Photographic Process*. New York, Macmillan, 1942.
12. WILSEY, R. B.: The use of photographic films for monitoring stray x-rays and gamma rays. *Radiology* 56:229, 1951.
13. SEEMAN, H. E.: Spectral sensitivity of two commercial x-ray films between 0.2 and 2.5 angstroms. *Rev. Sci. Instruments* 21:314, 1950.
14. SEEMAN, H. E.: Personal communication.
15. HERZ, R. H.: The spectral quantum- and energy-efficiency of calcium tungstate x-ray intensifying screens. *Brit. J. Appl. Physics* 7:182, 1956.
16. VAN ALLEN, W. W.: *Characteristics of Commercial X-Ray Films and Screens*. U.S. Dept. of Health, Ed., & Welfare, 1953.
17. *Kodak Plates and Films for Science and Industry*, Eastman Kodak Company, Rochester, N.Y., 1962.

(VII)

THE RADIOGRAPHIC IMAGE

IMAGE CONVERSION QUALITY OF SCREEN-FILM SYSTEMS

The screen-film system converts the x-ray image into a radiographic image suitable for visual interpretation or for some other form of analysis. Under ideal conditions, the radiographic image is identical to the radiologic image in terms of the information they contain. Unfortunately, the conversion of the radiologic image into a radiograph by the screen-film combination is always accompanied by a loss of information which is expressed as loss of detail in the recorded image.

One of the simpler methods for the evaluation of the detail-recording capability of a screen-film combination consists in comparing a test object with its radiograph obtained by means of the screen-film combination. The comparison is carried out under conditions that yield a radiologic image of high quality (reduction of geometric unsharpness, scatter, etc.). Various test objects, such as holes in metallic plates, screws, wire mesh, reticles, etc., have been used in the evaluation of screen-film systems.

A better test object, developed by Van Allen and Morgan (Ref. 1), consists of a slit of adjustable width between two blocks of lead which is moved between the film and the source of x-rays by measured increments, usually equal to the width of the slit. In this fashion a series of dark and light lines are obtained on the radiograph, and the number of lines per unit area that can be distinguished visually determines the resolution of the tested system.

These methods are suitable for testing the image-forming quality of a screen-film combination for the radiography of metallic plates, screws, wire mesh, or slits, but are not applicable to the unsharp, low-contrast structures usually examined in radiology.

Modulation Transfer Function

A method more suitable for measuring the quality of the image-forming system in diagnostic radiology is the determination of the modulation trans-

fer function. This method is also used in general photography for measuring the quality of optical image-forming systems. The parameter has been called *sine wave response*, *contrast transmission function*, *frequency response function*, etc. But in July 1961, the Subcommittee for Image Assessment Problems of the International Commission for Optics (Ref. 2) recommended the adoption of the term *modulation transfer function*.

The photon density gradient forming the contrast boundary in a radiologic image (or any density pattern or any image) can always be expressed by Fourier analysis as the summation of a series of components consisting of sine functions of various frequencies, amplitudes, and phase relationships. Thus, the ability of a screen-film combination to convert a radiographic image into a recorded optical image can be expressed as the ability of the system to faithfully reproduce sine functions. An ideal screen-film system should reproduce without distortion the amplitudes of sinusoidal spatial variations of photon densities in the radiologic image, for any frequency of these functions. This system should not alter the frequencies of the sine functions, and, in addition, should preserve the phase relationships of the sine functions. In general, a nonideal system distorts one or more of the above parameters (Ref. 3).

Amplitude distortion consists of the variation of the amplitude response of the screen-film system, as a function of the frequency of the sine function. It increases with the frequency of the sine function, until the frequency reaches a value where the system is no longer able to reproduce the function. This form of distortion results mainly from screen thickness and screen grain size. Amplitude distortion can be observed when the system is evaluated by means of a multiline test object: The frequency of the sine function is determined by the number of lines per unit length, and when this number reaches a certain value, the system is no longer capable of resolving the lines. The amplitude response of a screen-film system is shown in Fig. VII-1. It is apparent that this response drops rapidly after 1 cycle/mm, and is only 10% at 10 cycles/mm, which incidentally corresponds to the resolving power of approximately 10 lines/mm for a good screen-film system.

Harmonic distortion consists of the introduction by the screen-film system of frequencies which do not exist in the x-ray image (Ref. 3). Harmonic distortion is mainly due to nonlinear response of the film to light excitation as discussed in the previous chapter. The distortion is mostly apparent at high densities; it decreases with diminishing exposure because film response becomes more linear; and becomes again of importance at very low light intensities.

Phase distortion, which results from the inability of the screen-film system to maintain proper phase relationship between the different sinusoidal components of the x-ray image, is not of appreciable importance in radiography. It is usually introduced by optical systems such as lenses, image amplifiers,

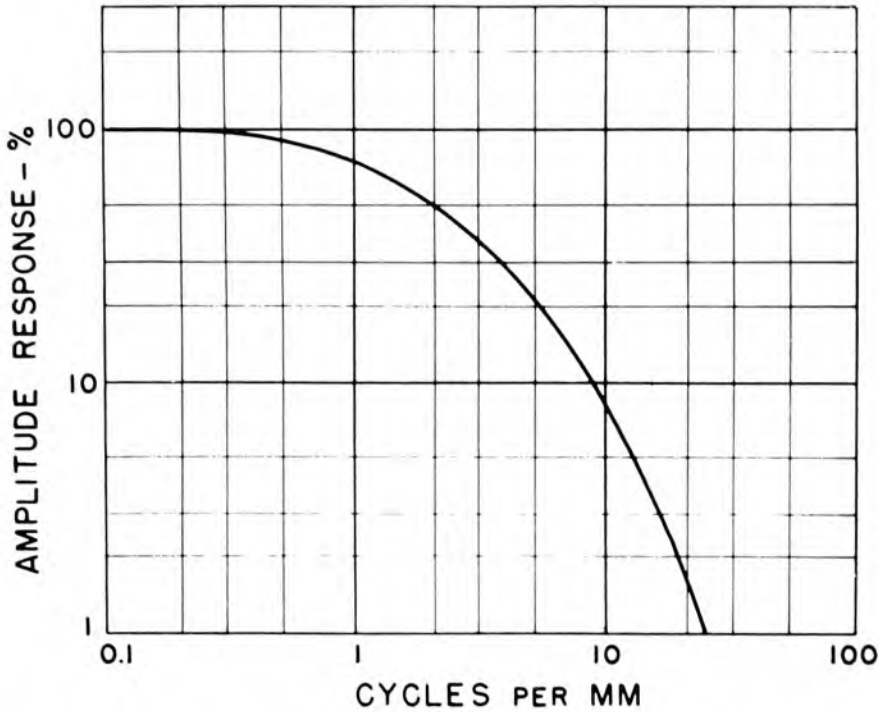


FIG. VII-1. Modulation transfer function. Sine-wave amplitude response of typical x-ray film-screen combination. (From Morgan et al., Ref. 3.)

and others, interposed between the screen and the film. Phase distortion produces blurring of the edges of examined objects (Ref. 3).

In conclusion, it appears that in diagnostic radiologic systems the most important limitation to reproducing detail is amplitude distortion (Ref. 3).

On the basis of the above, modulation transfer function can be defined as follows (Ref. 4): “The modulation transfer function of an imaging system is a measure of the ability of the system to image, frequency for frequency, a radiation pattern in which intensity varies sinusoidally in one dimension with distance in the object plane.” It may therefore appear that a good method for the determination of the quality of an image-forming x-ray system would consist in the use of a series of test objects with sinusoidal attenuation properties with different frequencies and amplitudes for the radiation used (Ref. 3).

This approach encounters the following practical difficulty: The design of a suitable test object for the sine modulation of x-rays is difficult because the attenuation of x-rays in matter is dependent on the spectral energy distribution of the radiation used and on the nature of the absorber. Thus the same test object may modulate x-rays having different energy to different extents. Secondary radiation emission and absorption unsharpness in the test object further complicate the problem (Refs. 5 and 6), and controlled modulation of x-rays by various test objects is not practical (Refs. 3 and 7).

Line Spread Function

At present one of the most attractive methods for the evaluation of the image-forming quality of film-screen combinations is determination of the line spread function (Refs. 3, 7, and 8).

The quality of a radiographic image-converting system, for example, of a screen-film combination, can be defined as the ability of the system to give a point-by-point reproduction of the x-ray image in such a fashion that for each point of the x-ray image there is a corresponding single point in the radiographic image. The distortion (blurring) introduced by the image-converting system results from the fact that the energy corresponding to a point of the x-ray image is spread over a greater area on the radiographic image.

It appears, therefore, that the most direct method for the evaluation of the quality of an image-converting system is study of the intensity distribution of the image of a point converted by this system. This intensity distribution is referred to as *point spread function* (Ref. 8). It can be determined by exposing the system to x-rays through a point aperture in a plate opaque to x-rays. The image thus obtained is then scanned by means of a microdensitometer, and the spatial distribution of the blackening of the film is a measure of the point spread function. This method involves the technical difficulties of providing an extremely small aperture and of scanning the resulting image exactly through the center of the distribution.

These difficulties can be overcome by observing the spread of a line image instead of a point image. In this case, the intensities distribution can be obtained by scanning the resulting image perpendicularly to the line obtained, and the observed spread is referred to as *line spread function*. The line spread function is a one-dimensional representation of the two-dimensional intensity distribution of the point image and is a measure of the ability of a system to form images of extended objects.

The apparatus for the determination of the line spread function of a radiographic system consists of a narrow slit between two jaws made of material highly opaque to x-rays—uranium (Ref. 7), tungsten (heavy-met) (Ref. 3), and platinum (Ref. 4) have been used for this purpose. The slit is used to collimate a beam of x-rays before it impinges upon the screen-film system to be evaluated (Fig. VII-2). The width of the slit must be sufficiently narrow so that the line spread function it produces can be considered identical to that of a dimensionless line. Typical slit width is of the order of 10μ (Refs. 3 and 4).

The line spread function is determined by scanning the image of the slit by means of a microdensitometer whose slit system is at least as narrow as that of the x-ray slit. A typical line spread function is shown in Fig. VII-3. The modulation transfer function of the screen film system can be calculated from the measured line spread function (Ref. 4). As mentioned in the section

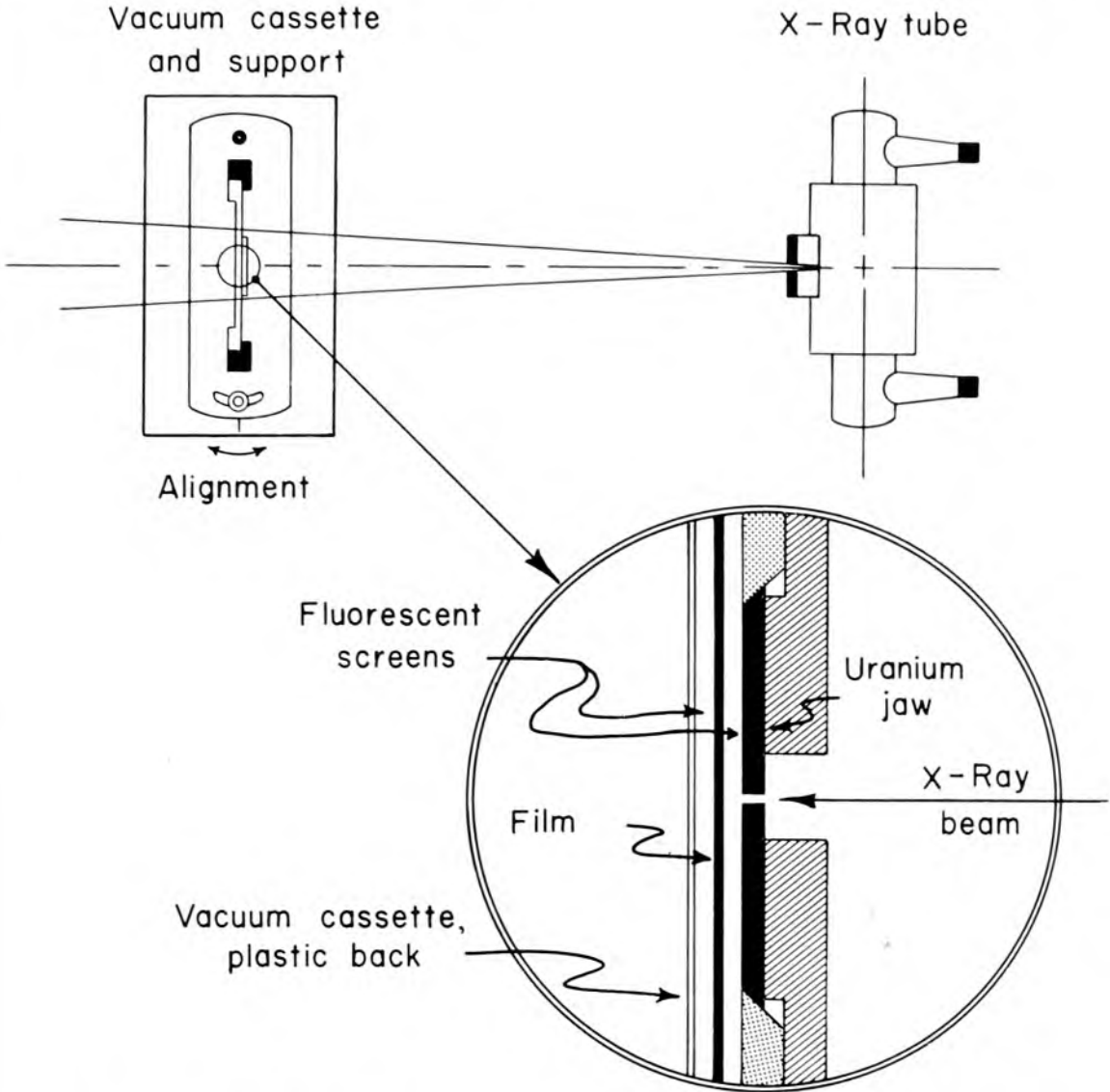


FIG. VII-2. Optical bench arrangement for making radiographic slit exposures. (From Rossmann, Ref. 2.)

on "Modulation Transfer Function," the limiting factor in detail recording capabilities of x-ray screen-film systems usually is amplitude distortion; phase distortion occurs only when an optical system is included in the system and is usually not important; and the exposures of most films is carried out in a density region where harmonic distortion is of little significance.

The line spread function for two intensifying screen-film systems is shown in Fig. VII-4. In both cases the amplitude distortion increases as image frequency rises. High speed screens demonstrate this property at lower frequencies than medium speed screens. The modulation transfer function determined from the line spread function for some typical intensifying screens is shown in Fig. VII-5.

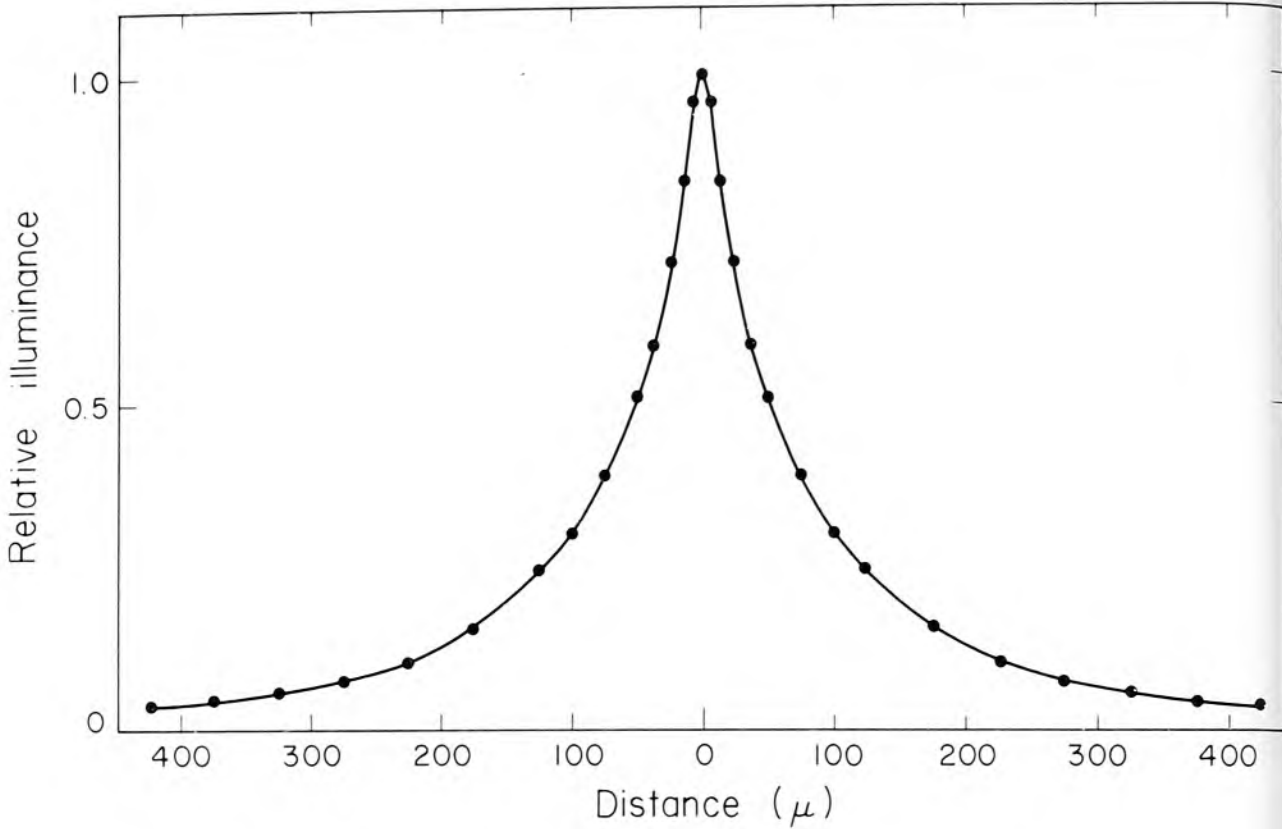


FIG. VII-3. Normalized line spread function of two medium-speed calcium tungstate intensifying screens and Kodak Blue Brand Medical X-Ray Film exposed at 70 kV_p with a 3-mm aluminum filter. (From Rossmann, Ref. 2.)

As mentioned, the most important component affecting the modulation transfer function is amplitude distortion. Figure VII-6 shows the amplitude response of various screens used in diagnostic radiology. The presentation of these curves differs from that in Fig. VII-5 mainly in the use of logarithmic coordinates. A comparison of Curves A, B, C, D, and E in Fig. VII-6 shows that the amplitude response of fluoroscopic and photofluorographic screens is poorer than that obtained with intensifying screens.

The determination of the line spread function for x-ray films exposed directly to radiation without screens is particularly difficult to determine because it requires the use of extremely narrow slits warranted by the high resolutions of such system. Figure VII-7 shows the amplitude response for a typical radiographic film.

Use of the line spread function in diagnostic radiology is not limited to the assessment of the quality of a screen-film system. This method can be used to measure the influence of each one of the components of the image-forming system, such as focal spot size (geometrical unsharpness), motion (motion unsharpness), scatter, and other factors in the image-forming quality of this system.

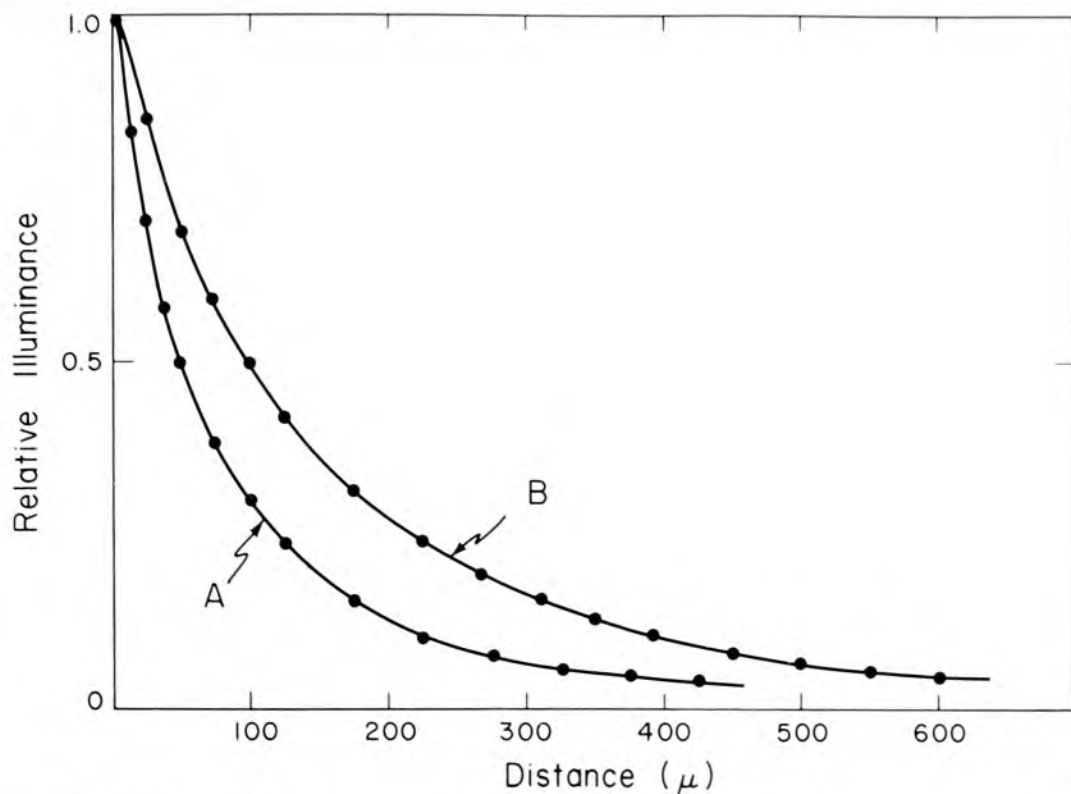
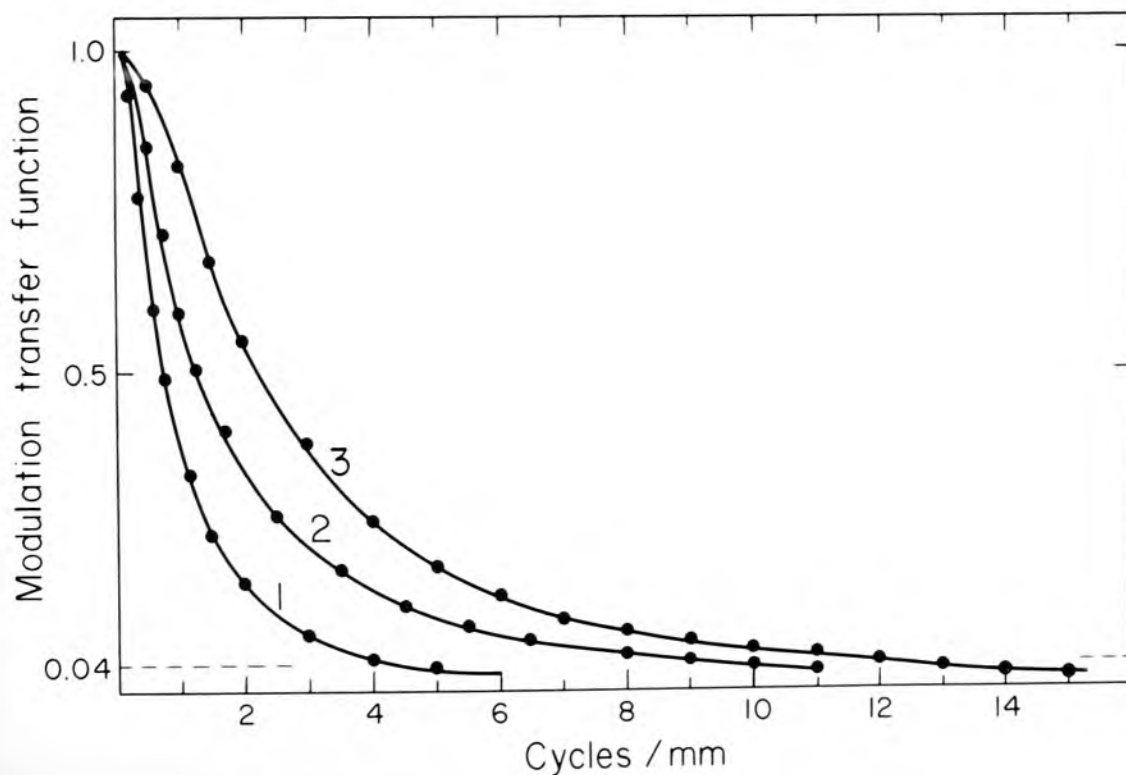


FIG. VII-4. Normalized line spread functions of two radiographic systems containing calcium tungstate screens (because of symmetry, only one-half of each function is shown).
A two medium speed screens
B two high-speed screens.

Both exposed with Kodak Blue Brand Medical X-Ray Film at 70 kV_p with a 3-mm aluminum filter. (From Rossmann, Ref. 2.)

FIG. VII-5. Modulation transfer function.

1 two fast calcium tungstate screens with Kodak Blue Brand Medical X-Ray Film
2 two medium-speed calcium tungstate screens with Kodak Blue Brand Medical X-Ray Film
3 one medium-speed calcium tungstate screen with Kodak single-coated Medical X-Ray Film Blue Sensitive 3 mm aluminum
Technique 70 kV_p, 3 mm aluminum filter; HVL, 3 mm aluminum (From Rossmann, Ref. 2.)



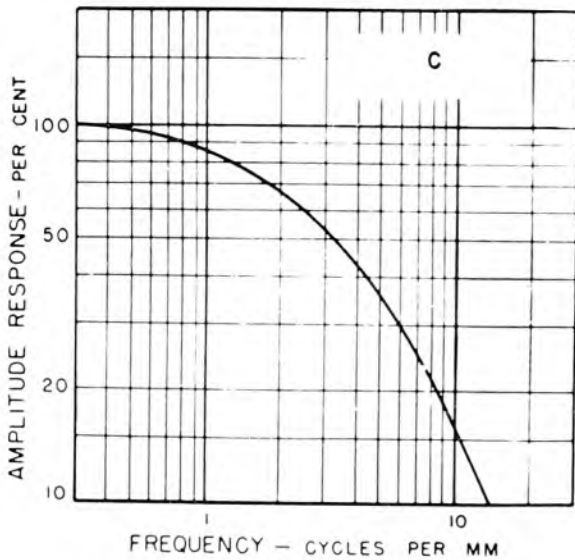
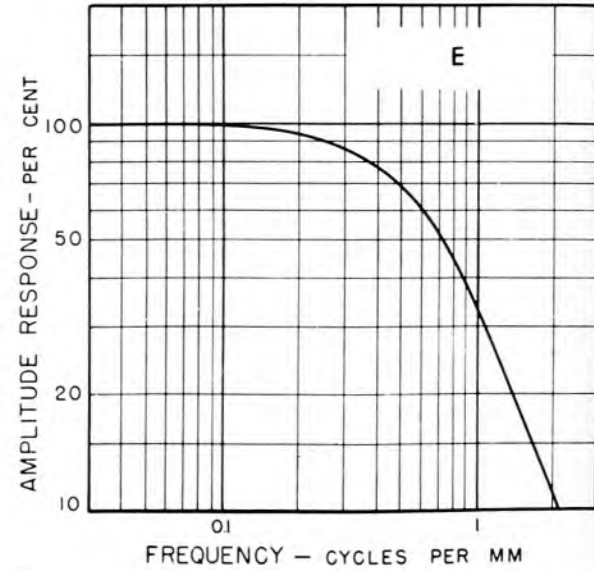
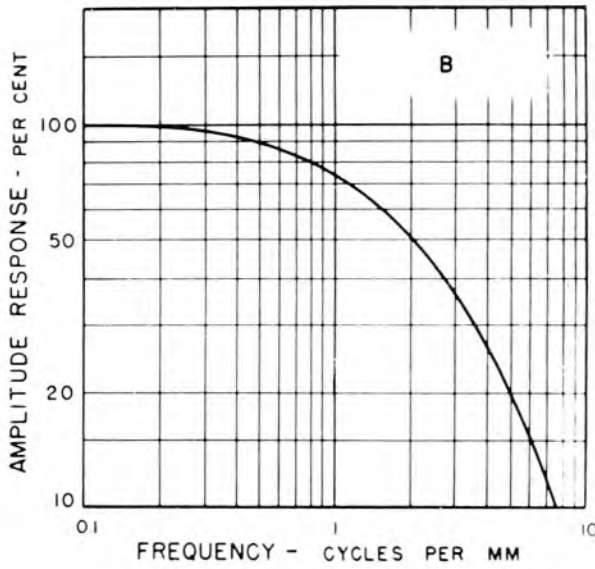
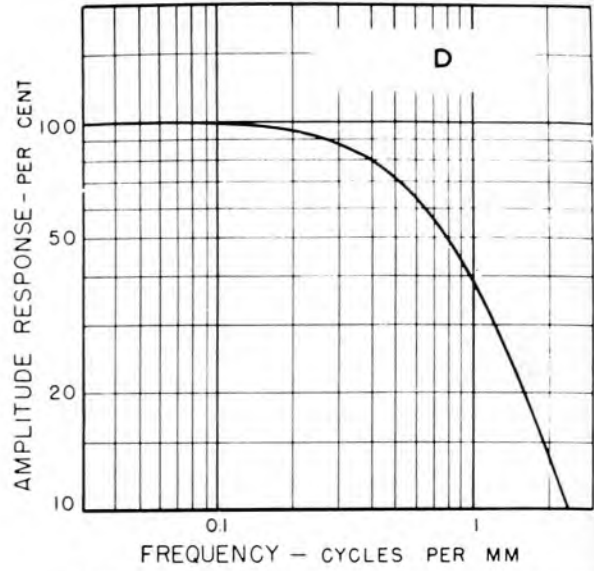
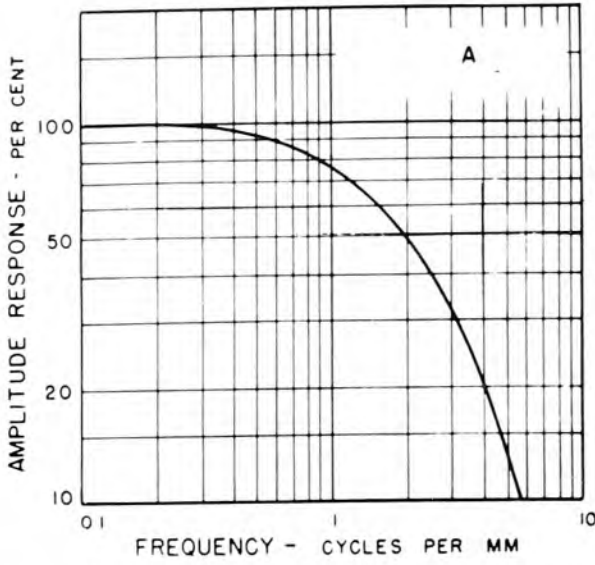


FIG. VII-6. Sine-wave amplitude response modulation transfer function characteristic of five x-ray screens.

A high speed-type intensifying screens
B medium speed-type intensifying screens

C high resolution-type intensifying screens

D typical fluoroscopic screen

E typical photofluorographic screen

(From Morgan, Ref. 3.)

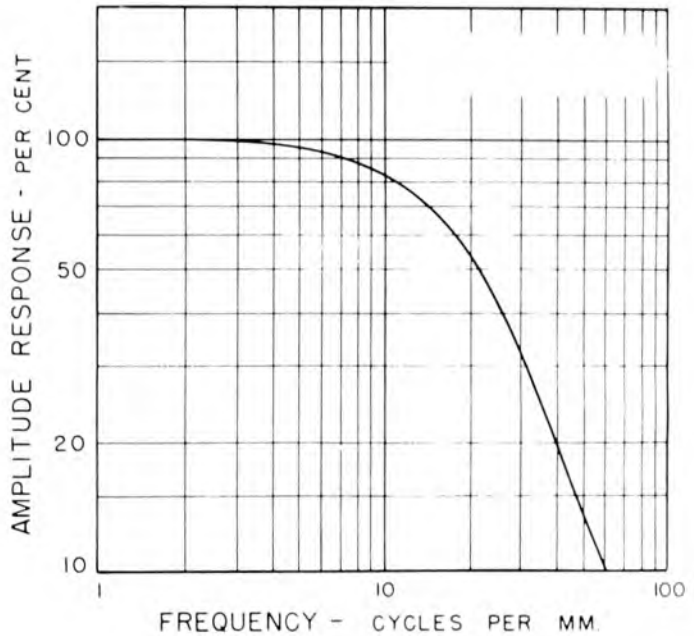


FIG. VII-7. Sine-wave amplitude response modulation transfer function characteristic of typical radiographic film exposed without intensifying screens. (From Morgan, Ref. 3.)

Radiographic Mottle

A radiograph obtained by exposing a screen-film combination to a uniform dose of radiation resulting in a film density similar to that encountered commonly in radiographic examinations (density between 0.5 and 1.0) exhibits an irregular, motley texture (Ref. 9) (Fig. VII-8). This texture is referred to as radiographic mottle (Ref. 10). Sturm and Morgan (Ref. 11) suggested that such an effect could be due to the statistical fluctuations in the number of x-ray photons per unit area responsible for the photographic image.

Cleare, Spletstosser, and Seemann (Ref. 9), and more recently Rossmann (Ref. 10) demonstrated that radiographic mottle is a combination of several components, as shown in Fig. VII-9. Quantum mottle (for quantum see Chapter I, p. 22) results from statistical fluctuations in the spatial distribution of the number of photons in the x-ray image. Structure mottle results from irregularities in the structure of the screen. Combination of quantum mottle and structure mottle is called screen mottle. Film graininess results

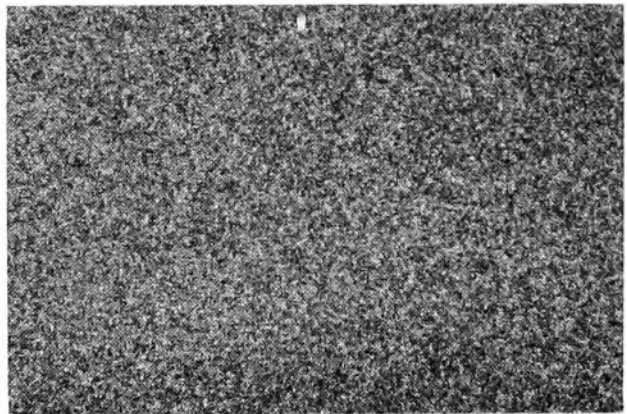


FIG. VII-8. Mottle of radiograph made with intensifying screens. (From Rossmann, Ref. 10.)

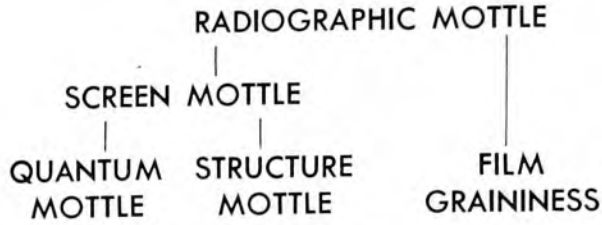


FIG. VII-9. Components of the coarse density fluctuations observed on x-ray films exposed with fluorescent screens (radiographic mottle). (Adapted from Rossmann, Ref. 10.)

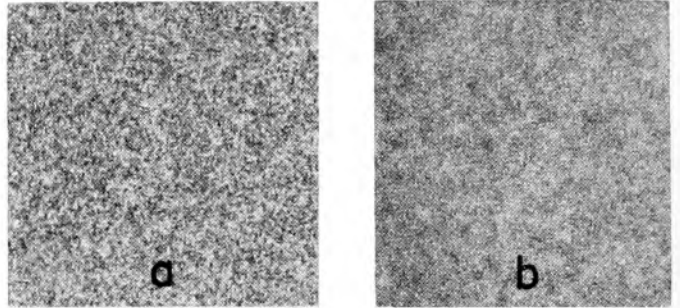
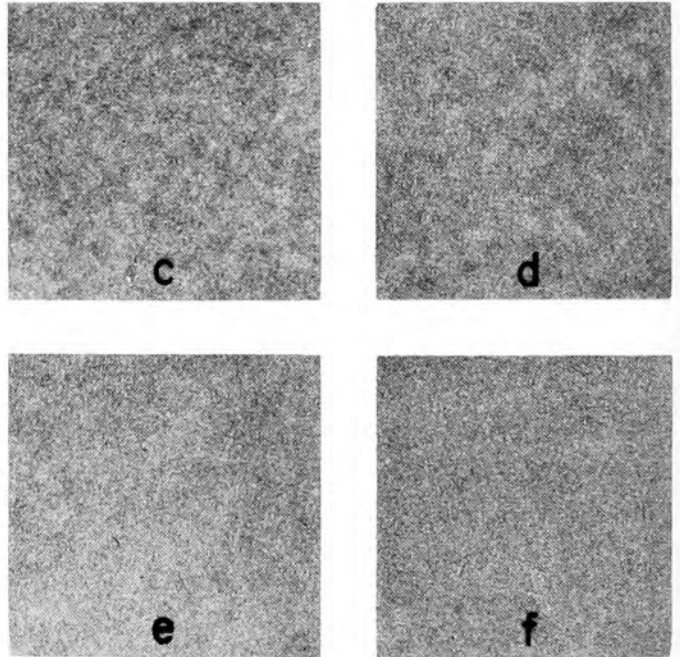


FIG. VII-10. Radiographic mottle. Air space of increasing width was introduced between screen and film.

- a intimate contact
- b 0.02 mm
- c 0.05 mm
- d 0.12 mm
- e 0.23 mm
- f 13.0 mm

(From Rossmann, Ref. 10.)



from the clumping of developed film particles and is independent of the screen. The major contributing factor to radiographic mottle is quantum mottle. In conventional radiographic examinations structure mottle and film graininess are considerably finer in structure than quantum mottle, and are completely overshadowed by the latter; their contribution to radiographic mottle can be put in evidence only by using very special techniques which are not normally encountered in diagnostic radiology.

Screen mottle is radiographically reproduced only if the screen-to-film image conversion is of good quality. If film-screen contact is poor, radiographic mottle, which is mostly due to screen mottle, is considerably reduced because of the blurring introduced by light diffusion (Fig. VII-10). A similar blurring of radiographic mottle takes place when a thicker, low resolution screen is used with high diffusion of light through the screen phosphor layer. Under extreme conditions, when the image-forming quality of the screen-film system is particularly poor, the only component of the radiographic mottle apparent on the film is film graininess. The radiographic reproduction of quantum mottle is such a good expression of the image-forming quality of a screen-film combination that the density fluctuations on the film can be used as a test pattern for the measurement of the modulation transfer function of the system (Refs. 10 and 12).

Because radiographic mottle is mostly due to quantum fluctuations, it will be particularly apparent whenever a "fast" image-forming system is used. It is particularly pronounced with fast films and fast screens (Fig. VII-11). Radiographic mottle increases also with increasing radiation energy because the amount of energy transferred to the screen upon absorption of a photon depends on the energy of the photon; consequently, a given radiographic density will have a higher quantum mottle if it resulted from the absorption of a lower number of high energy photons than if a higher number

FIG. VII-11. Radiographic mottle.

Left slow screen (calcium tungstate)

Right fast screen (barium lead sulfate)

(From Rossmann, Ref. 10.)

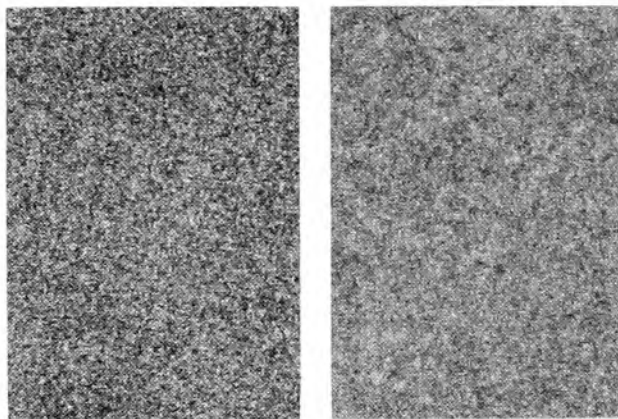
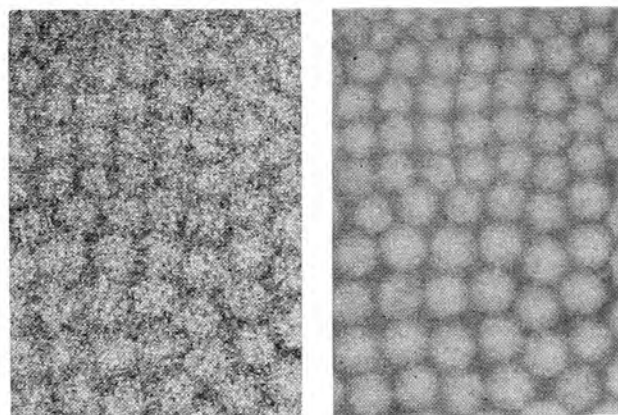


FIG. VII-12. Effect of radiographic mottle on visibility of low contrast detail.

Left radiograph made with a medium-speed screen-film system

Right radiograph made with a 200-times slower screen-film system (same screens as on left)

(From Rossmann, Ref. 10.)



of lower energy photons were used. The presence of radiographic mottle is detrimental to the visibility of low contrast detail, as shown in Fig. VII-12, and this undesirable "noise" factor can be reduced only by using a greater number of photons in the examination, i.e., by using a "slower" image-forming system.

Radiographic mottle represents the recording by a given image-converting system of the statistical fluctuations, or "noise," in the x-ray image, and any image-converting system in diagnostic radiology, such as a fluoroscopic screen or an image amplifier, exhibits its counterpart.

NOISE X-RAY PHOTONS

The term "noise" in information theory applies to signals which do not carry useful information and the presence of which interferes with information transfer in the system used. In diagnostic radiology the major contribution to noise in the radiologic image consists of x-ray photons scattered out of the primary beam by attenuation in the object under examination and which reach the radiologic image. The attenuation of the x-ray beam takes place mostly by scattering and thus without a great loss in the total number of photons present; and when the scattered photons reach the plane of the radiologic image, they supply the major component of noise.

The characteristic photons emitted upon photoelectric interactions in body tissues do not contribute appreciably to noise. In the soft tissues photoelectric interactions are relatively infrequent (Chapter III) and the energy of the characteristic photons is so low that they seldom reach the plane of the radiologic image. In bone photoelectric interactions are more probable; however, the most energetic characteristic photons of calcium, which carry an energy of approximately 4 keV, are rapidly absorbed in the immediate vicinity of bone and do not contribute appreciably to image noise. The only characteristic radiation generated in clinical examinations which is sufficiently energetic to reach with any probability the plane of the x-ray image is excited in high atomic-number contrast materials such as iodine and barium. The K-characteristic photons from these elements have an energy of approximately 30 keV and have a fair probability of interfering with the x-ray image. It should be noted, however, that such photons are present only in examinations carried out with a contrast material, and that furthermore the percentage of the primary photons interacting with the contrast material as compared to all the photons involved in the examination is small. Consequently, the contribution of these characteristic photons to noise can also be neglected when compared with the major component of the x-ray image noise—scattered radiation.

Scattered X-Ray Photons

The major portion of photon noise in the x-ray image is contributed by Compton scattering. In soft tissues coherent scattering represents less than

25% of Compton interactions for 20 keV photons and decreases rapidly with increasing photon energy. At 50 keV coherent scattering is only 6% of Compton interactions, and this component of scatter is therefore omitted in the present discussion.

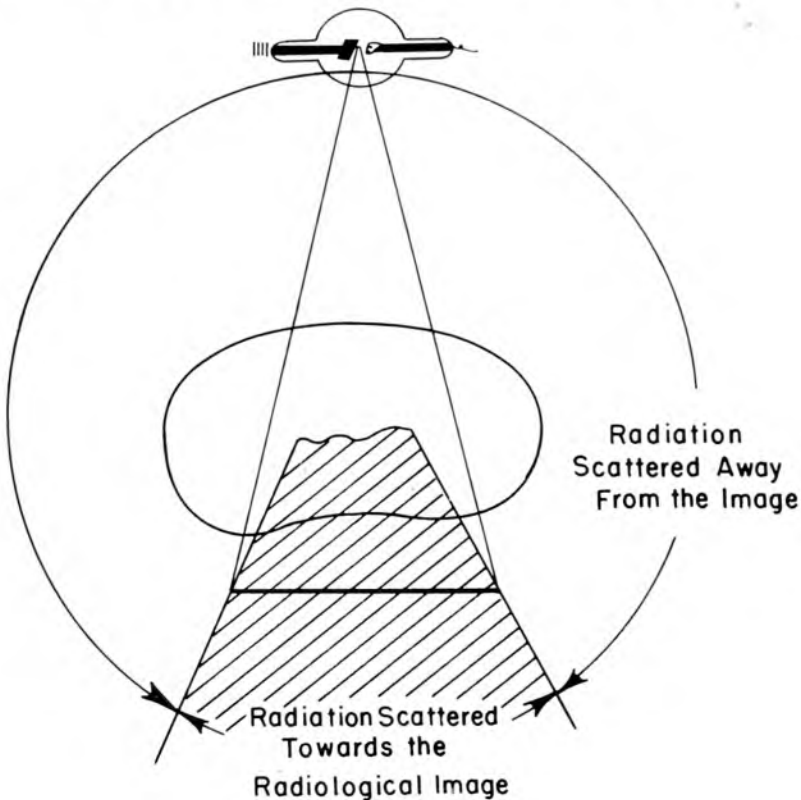
The spectral distribution of x-rays scattered in soft tissues can be determined by calculation. Bruce and Johns (Ref. 13) have studied the spectra of x-rays scattered in low atomic-number materials by a combination of an analytic and the "Monte Carlo" method. The details of the calculations are outside the scope of this book, and only a qualitative discussion of scattered radiation with some experimental results is included in this section.

The spectral distribution and number of scattered photons reaching the plane of the x-ray image depend primarily on three factors: (1) the energy of the incident x-radiation, (2) the area and shape of the field used in the examination, and (3) the thickness of the material under examination.

The mean energy of the scattered radiation that reaches the plane of the x-ray image, particularly for small fields of irradiation, is not much lower than that of the incident radiation because of a combination of the following factors:

1. In the diagnostic x-ray energy range only little energy can be transferred to the Compton electron. For example, in a single Compton interaction a 50 keV photon may lose a maximum of 17% of its energy. The

FIG. VII-13. Solid angle subtended by radiologic image at examined part.



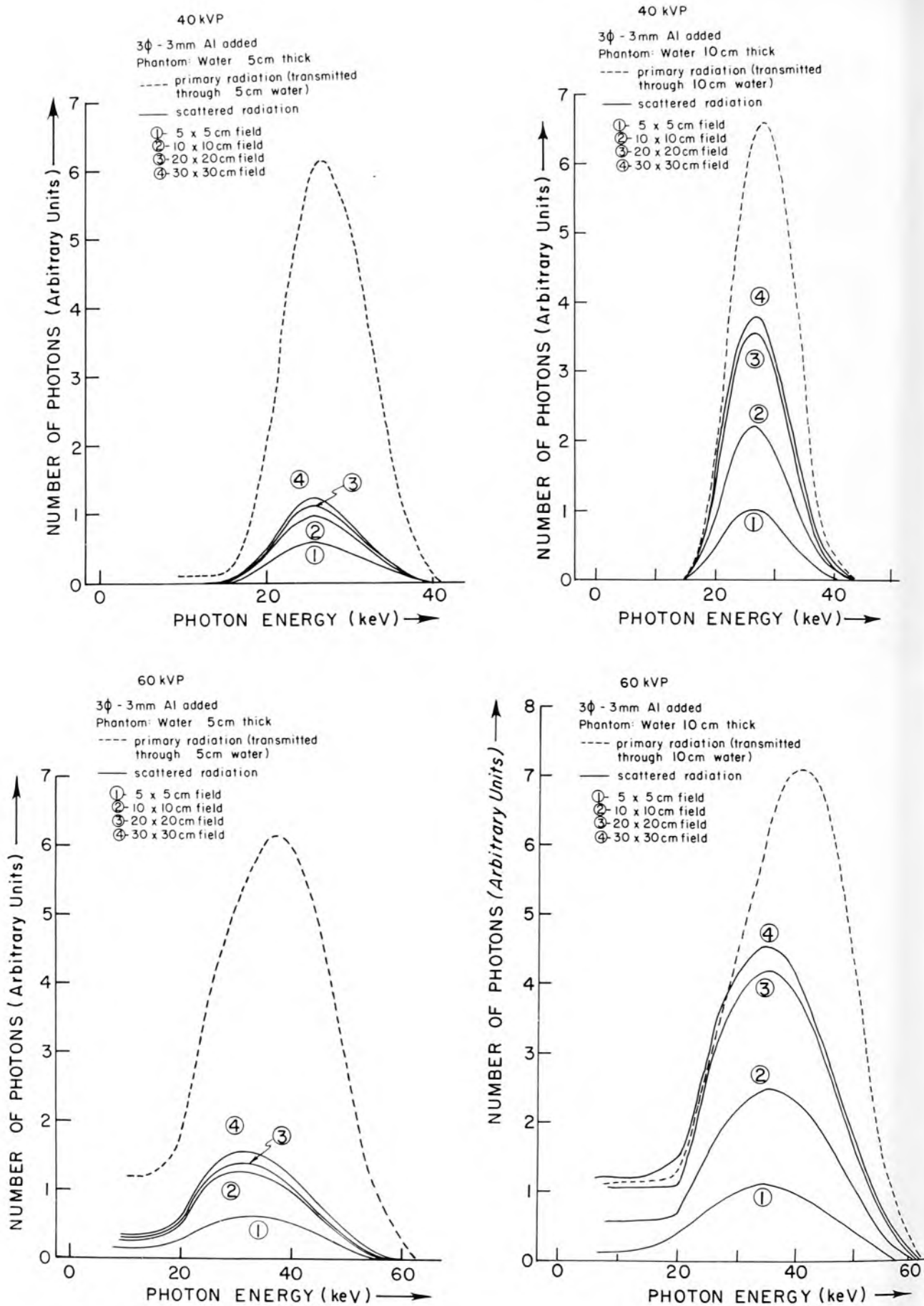


FIG. VII-14. Influence of field size, thickness of part examined, and radiation energy on scattered radiation.

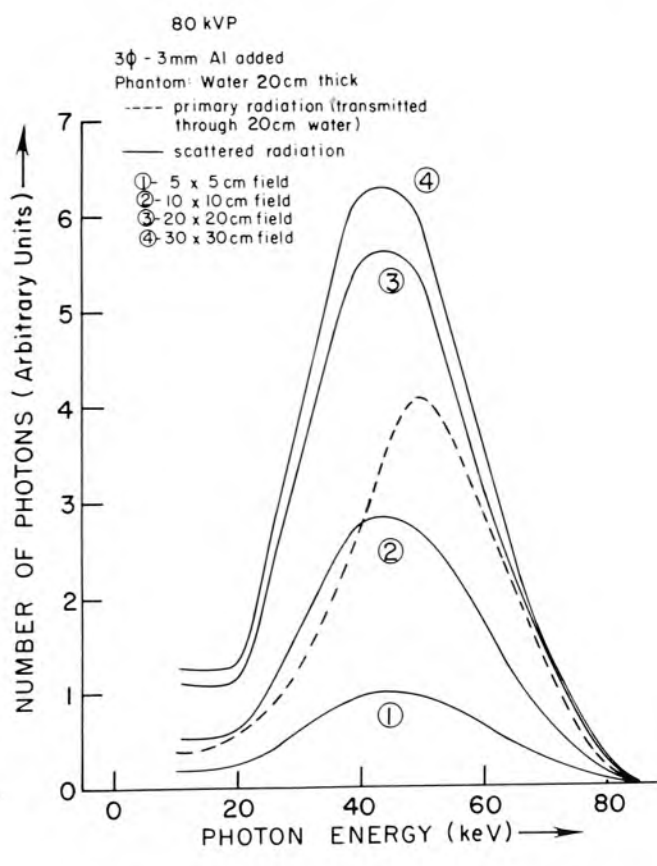
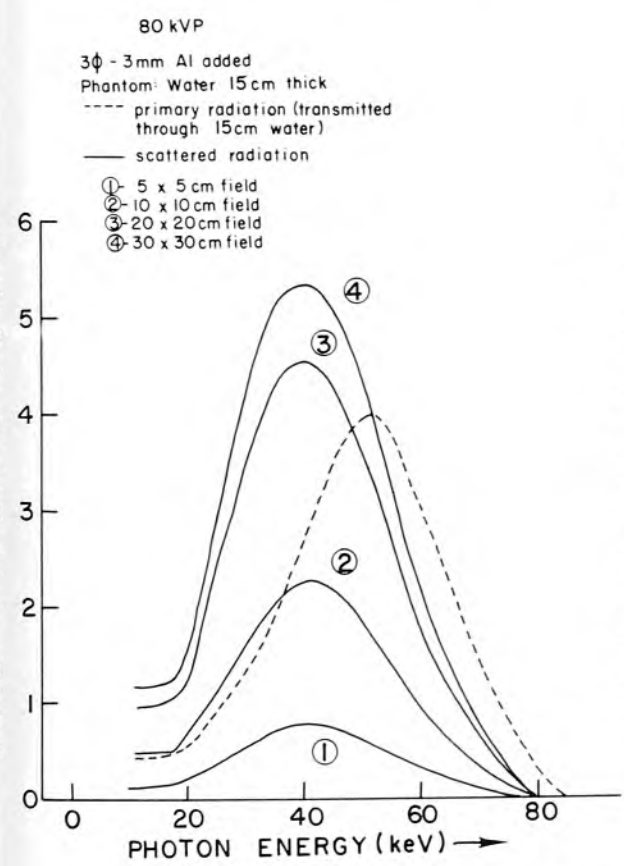
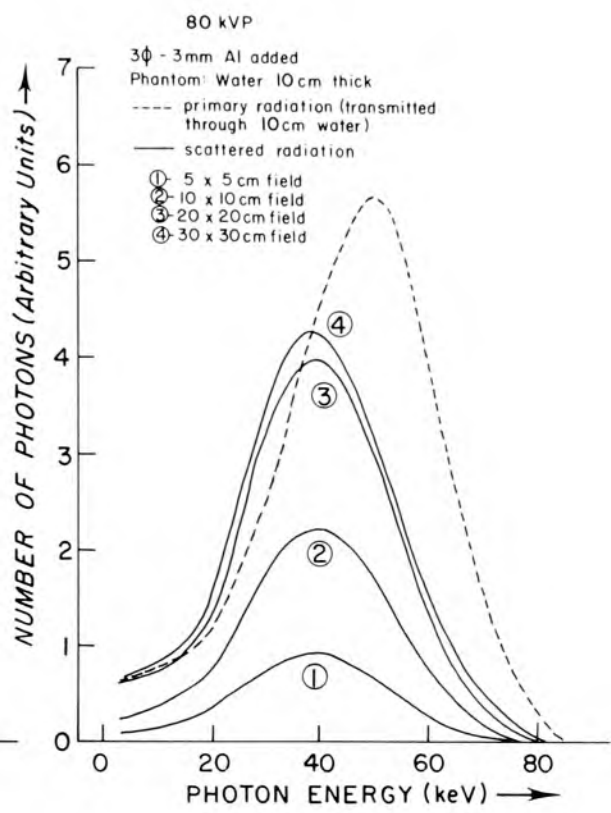
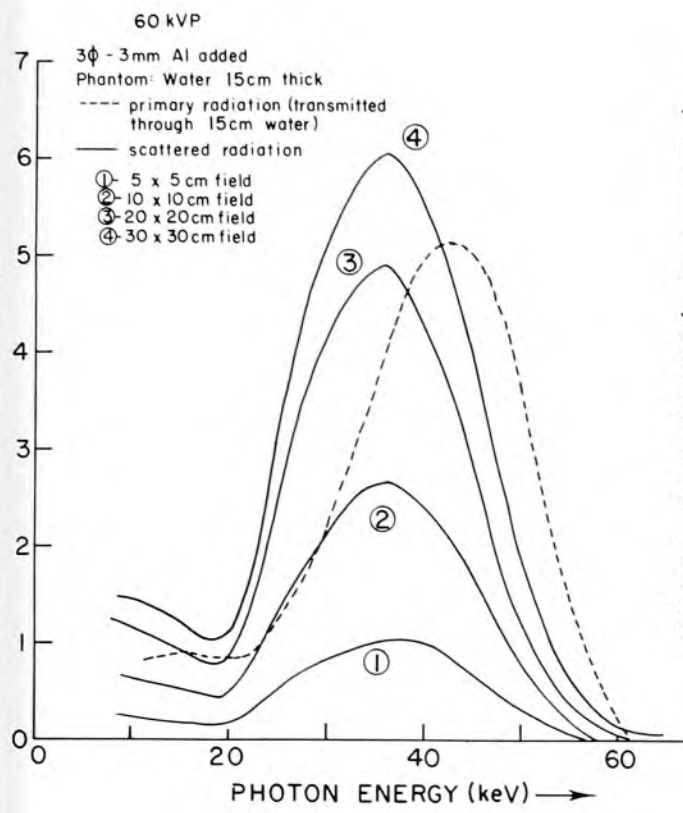


FIG. VII-14 (Continued).

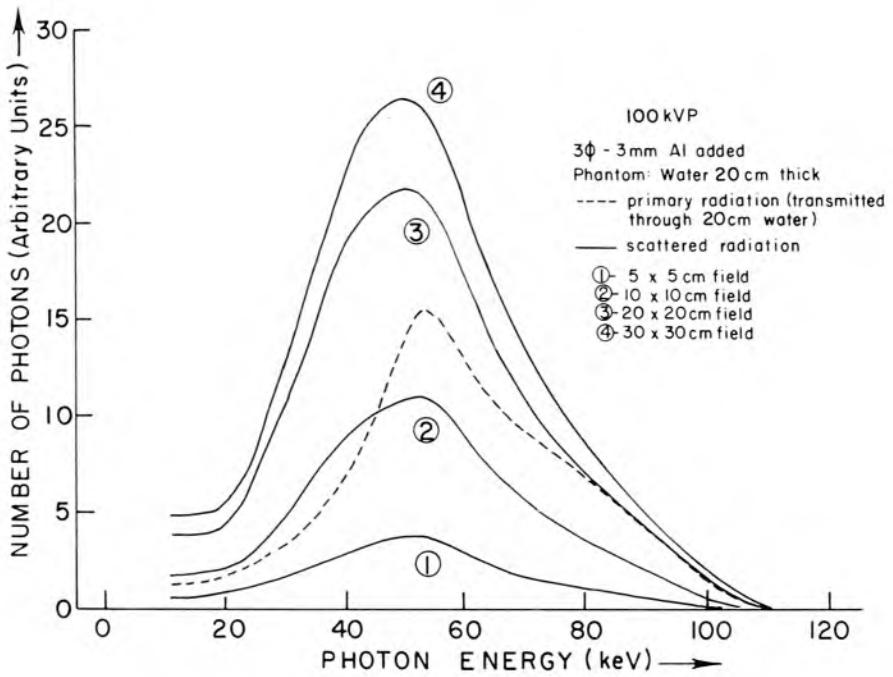
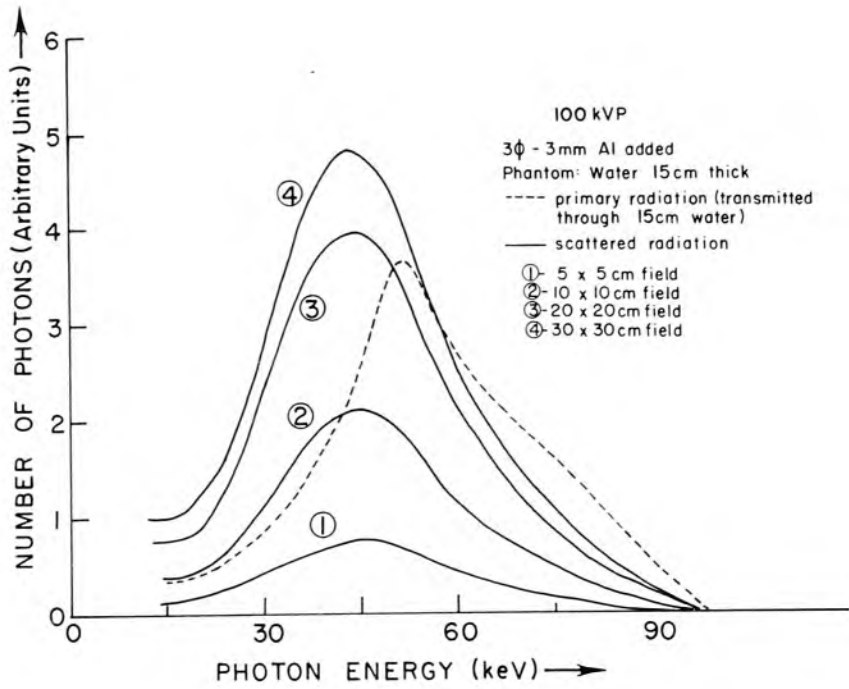


FIG. VII-14 (Continued).

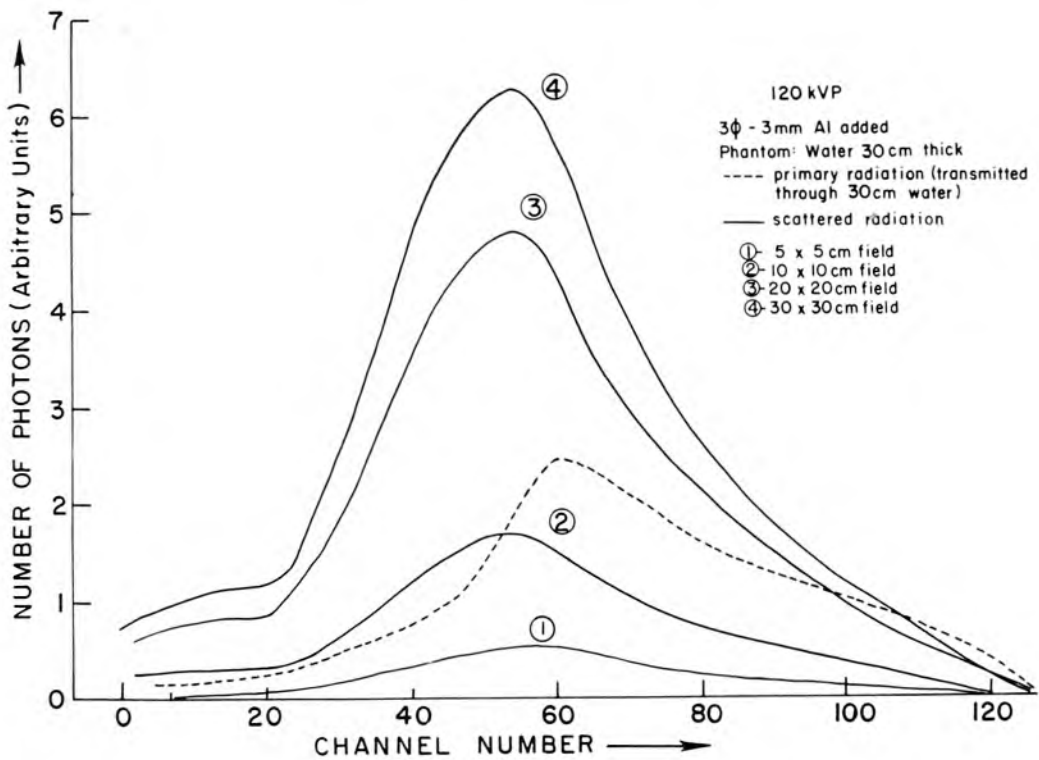
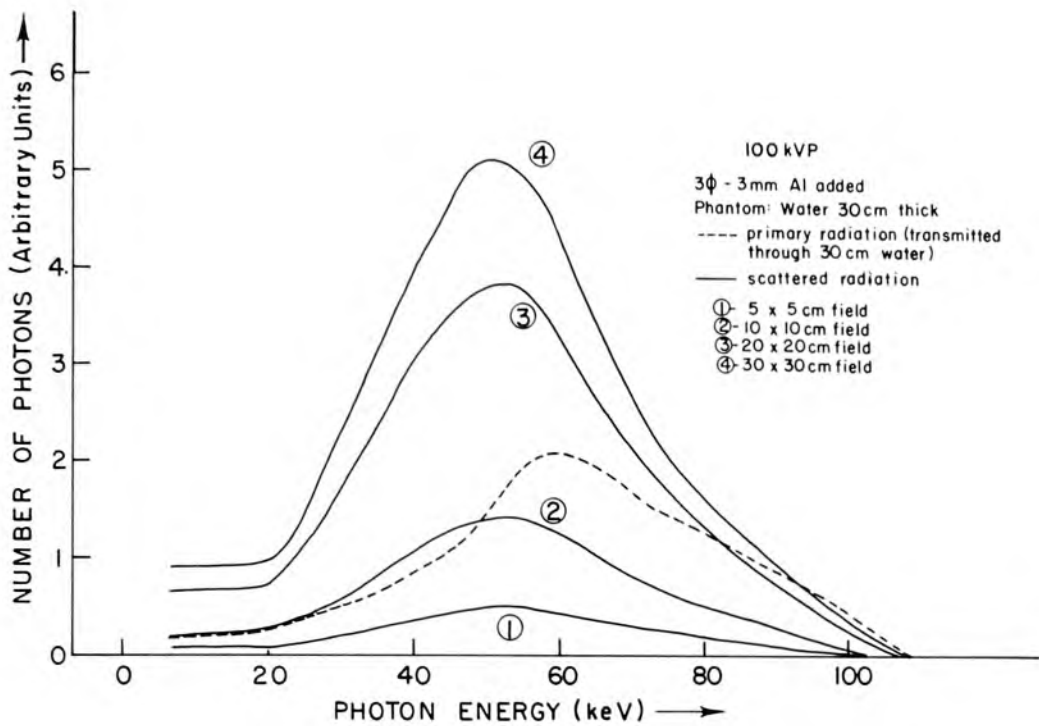


FIG. VII-14 (Continued).

$$C_{a,b} = \frac{B_a - B_b}{B_a} \times 100$$

$C_{a,b}$ = Contrast (a,b)
 B_a, B_b = Radiation Transmitted by a and b

$$C_{a+s,b+s} = \frac{40-35}{40} \times 100 = 12.5\%$$

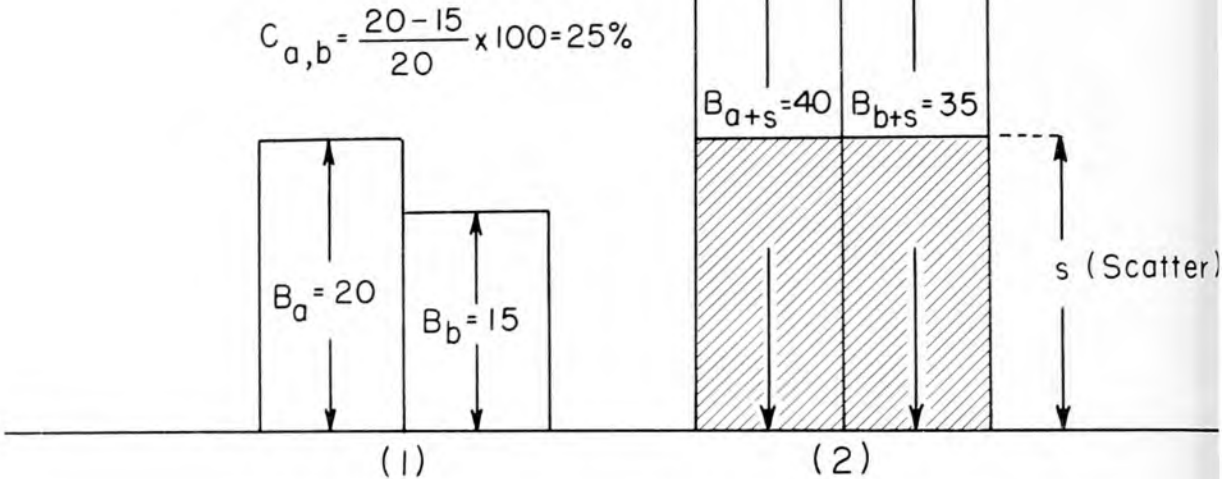


FIG. VII-15. Influence of scatter on contrast.

- 1 contrast $C_{a,b}$ without scatter
- 2 contrast $C_{a+s, b+s}$ with scatter present

Opposite two radiographs of the same pelvis showing the effect of scatter on contrast

- A** radiograph exposed without grid (scatter present); **technique** 80 kV_p, 25 mAs
B radiograph exposed with grid interposed between pelvis and film (large fraction of scatter removed); **technique** 80 kV_p, 100 mAs

maximum energy transfer occurs for backward scattering; for lower angles of scattering even less energy is transferred (Chapter III, section on the "Compton Effect"). The energy of a photon can be appreciably reduced by multiple scattering. However, the probability for a photon of reaching the plane of the image decreases with the number of scattering events because the solid angle subtended by the radiologic image at the patient is smaller than the solid angle of escape (Fig. VII-13).

2. The scattered photons that have a high probability of reaching the radiologic image are scattered at a small angle with respect to the interacting photons, and small angle scattering results in transfer of little energy to the interacting electron.

3. Higher energy photons are scattered with a greater probability in the



A



B

FIG. VII-15 A and B (*Legend on opposite page*).

forward direction than lower energy photons and therefore exhibit a greater probability of reaching the radiologic image.

4. The scattered radiation is depleted of lower energy photons by filtration in the tissues, between the point of interaction and the radiologic image.

The above factors are interrelated in a complex fashion, and their relative importance is a function of incident radiation energy, field size, volume of tissue irradiated, and distance between the plane of the radiologic image and the source of scatter. For the reasons discussed the amount of scattered radiation reaching the plane of the radiologic image increases rapidly with the energy of the interacting x-rays.

The influence of field size, thickness of material interposed in the x-ray beam, and x-radiation energy is shown in Fig. VII-14. An increase in field size increases the probability of scattered x-ray photons to reach the x-ray image; and the thickness of the absorber produces a similar effect. It should be noted that the shape of the field also plays a role in scattered radiation; a narrow elongated field contains less scattered radiation than a circular field of the same area because a greater number of scattered photons escape the narrow field.

Effect of Scattered Radiation on the Radiologic Image

The scattered x-ray photons that reach the radiologic image deteriorate it by reducing contrast. This effect is illustrated in Fig. VII-15. In Fig. VII-15(1) it is assumed that no scattered radiation reaches the x-ray image. The contrast between the two areas a and b is 25%. In Fig. VII-15(2) it is assumed that scattered radiation equal to the amount of radiation transmitted by Area a is present in the x-ray image. The contrast between Areas a and b is now of only 12.5%. This example shows that although the relative amount of radiation transmitted by two areas has not changed, the contrast

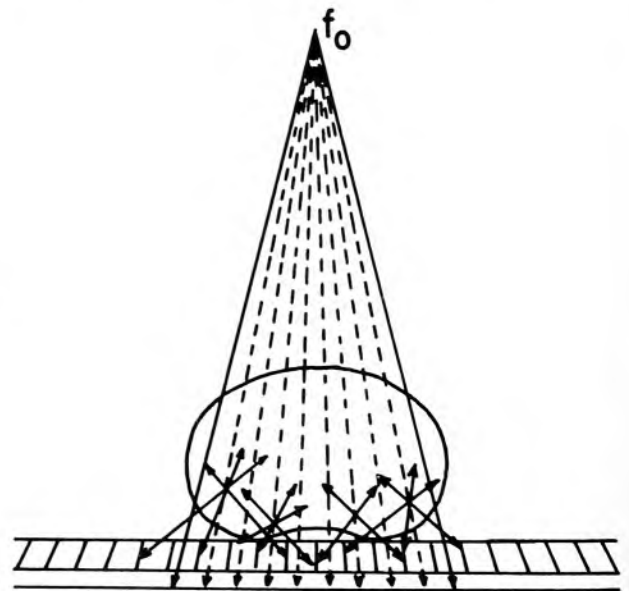


FIG. VII-16. Principle of grid operation.

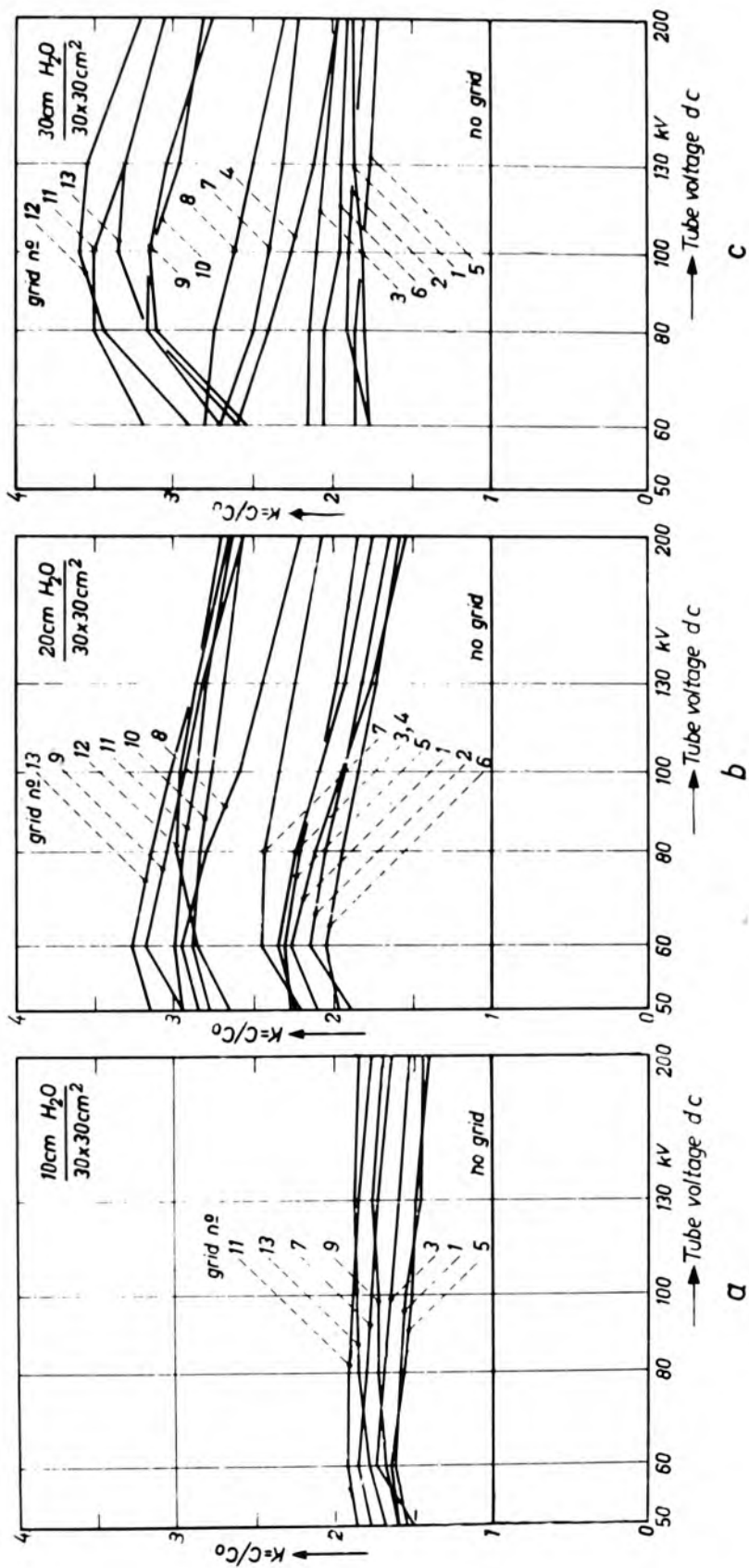
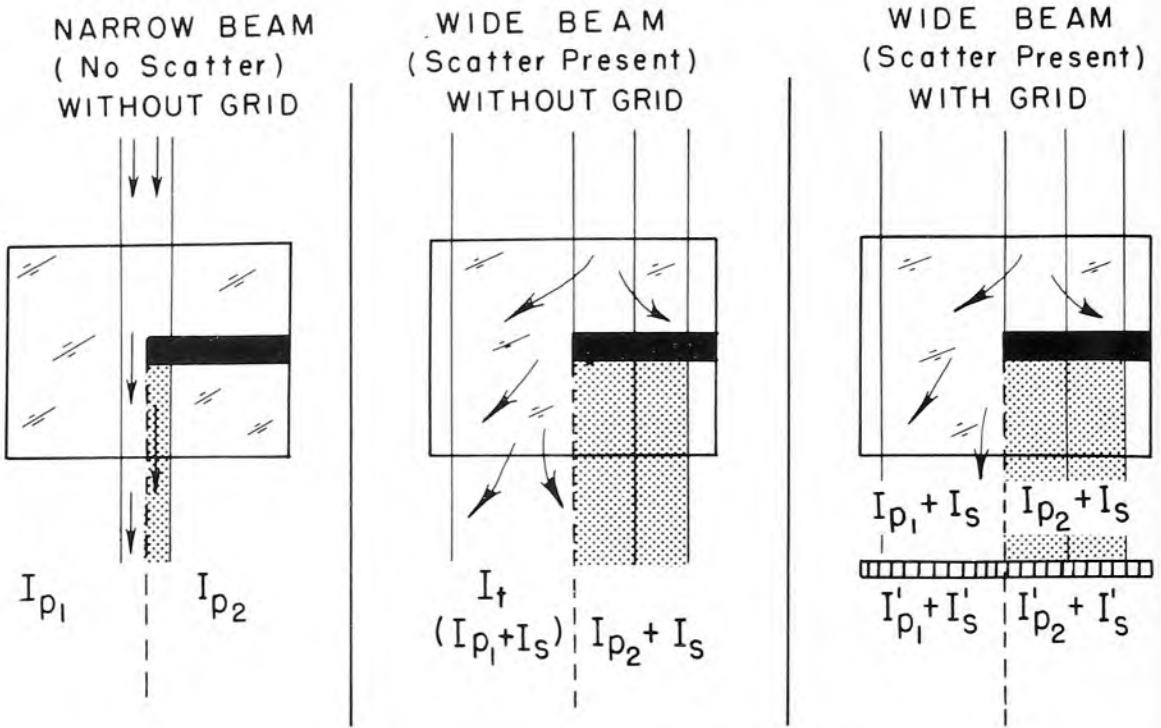


FIG. VII-17. Contrast improvement factors of 13 grids measured at various x-ray tube voltages with water phantoms 10, 20, and 30 cm thick (a, b, and c, respectively). (From *Hondius Bolding, Ref. 16.*)

TABLE VII-1. Parameters Used in the Evaluation of a Grid



Equation

$$\begin{aligned}
 (1) \quad & \frac{1}{k} = \frac{C_0}{C_p} \\
 & = \frac{I_{p1}}{I_t} \\
 (2) \quad & K = \frac{C}{C_0} \\
 & = \frac{T_p}{T_t} \\
 (3) \quad & C_p = \frac{I_{p1}}{I_{p2}} \\
 (4) \quad & C_0 = \frac{I_{p1} + I_s}{I_{p2} + I_s} \\
 (5) \quad & C = \frac{I'_{p1} + I'_s}{I'_{p2} + I'_s} \\
 (6) \quad & \frac{C_0}{C_p} = \frac{1}{1 + (I_s/I_{p1})} = \frac{I_{p1}}{I_t} \\
 (7) \quad & \frac{C}{C_p} = \frac{1}{1 + (I'_s/I'_{p1})} = \frac{I'_{p1}}{I'_t}
 \end{aligned}$$

between them is reduced by the presence of scattered radiation. This reduction in contrast is reproduced in the optical image and reduces its diagnostic value. Scattered radiation affects seriously the quality of most radiologic examinations (see Fig. VII-15(3)) (Ref. 14). Reduction of contrast by scattered radiation may result in rendering imperceptible details that may be of diagnostic importance.

X-RAY GRIDS¹

Scattered radiation in the radiologic image can be reduced by the use of a grid (Fig. VII-15(3)). *Grids*, *roentgen grids*, *x-ray grids*, and *scattered-ray grids* (Ref. 15) are different terms designating the same device invented by Bucky (Ref. 16) with the purpose of reducing selectively scattered radiation in the x-ray image.

An x-ray grid is composed of a series of strips of material relatively opaque to x-rays, such as lead, separated by strips of material considerably more transparent to x-rays. Figure VII-16 illustrates the working principle of an x-ray grid. The grid is relatively transparent to the radiation that originates in the focal spot of the x-ray tube and is transmitted by the object examined; and it is relatively opaque to scattered photons that impinge on the grid at angles different from that of the transmitted radiation.

Terminology

Both *stationary* and *moving grids* are used in radiology. Moving grids are set in motion during the x-ray exposure by means of a driving mechanism,

¹ Most of the discussion on x-ray grids is based on the excellent analysis by Dr. W. Hondius Boldingh (Ref. 16). The author is grateful to Dr. Boldingh and to the Philips Company for their authorization to reproduce their material.

KEY TO SYMBOLS^a

k = Contrast reduction factor of scattering medium

K = Contrast improvement factor of a grid

C_p = Contrast without scattered radiation (no scattering material used)

C_0 = Contrast with scattered radiation (scattering material used)

C = Contrast with grid in place

I_p = Intensity of primary radiation

I_s = Intensity of scattered radiation

I_t = Intensity of total radiation

I_{p2} = Radiation transmitted through examined object

I_{p1} = Radiation transmitted through area adjacent to examined object

I'_{p1} = I_{p1} radiation transmitted through grid

I'_{p2} = I_{p2} radiation transmitted through grid

I'_s = I_s radiation transmitted through grid

T_p = I'_p/I_p = Transmission of primary radiation through grid

T_s = I'_s/I_s = Transmission of scattered radiation through grid

T_t = I'_t/I_t = Transmission of the total radiation through grid

^a From NBS Handbook 89 (Ref. 15) and Hondius Boldingh (Ref. 16).

an accessory called a *Bucky* or *Potter-Bucky*. A *linear grid* is composed of plane strips that are parallel in the direction of their longest dimension. A linear grid is said to be *parallel* when the planes of the strips are parallel. A linear grid is *focused* when the planes of the strips converge to a line virtually parallel to the grid surface; this line is called *convergence line*. A *cross grid* is composed of two linear grids assembled in such a way that the direction of their strips form an angle; if this angle is 90 degrees, the grid is *orthogonal*. The convergence lines of the linear grids in a cross grid intersect at the *convergence point*. The distance between the convergence line, or the convergence point, and the grid surface is called the *focusing distance* for the grid. The perpendicular distance between the x-ray tube focus and the grid surface is the *focus-grid distance* (Ref. 15).

A typical x-ray grid is made of lead strips approximately 0.05 mm thick and about 3 mm high, separated by the *interspace material* which is relatively transparent to x-rays (usually an organic compound or aluminum). The separation between the centers of the lead strips is approximately 0.3 mm. These figures vary depending on the grid construction. For example, the number of lead strips per millimeter of grid may vary from approximately 10 to 50 strips per centimeter. The number of strips affects the distance between the strips (Ref. 15).

The reduction of contrast in the radiologic image due to scatter radiation can be expressed by the contrast reduction factor k (Ref. 16), which is equal to the ratio of the contrast obtained with and without the presence of scattered radiation (Table VII-1, Eq. (1)). The purpose of the grid is to reduce the contrast reduction factor by reducing scattered radiation in the x-ray image. The effectiveness of a grid in accomplishing this purpose can be measured by the contrast improvement factor K , which is defined as the ratio of the x-ray contrast with and without the grid (Fig. VII-17). The contrast improvement factor can also be defined in terms of the transmissions of primary and scattered radiations through the grid (Table VII-1, Eq. (2)), independently of contrast.

Contrast Improvement Factor

The contrast improvement produced by a grid depends on the spectral energy distribution of radiation used and on the volume of scattering material exposed to radiation. Table VII-2 includes values of the contrast improvement factor K for a series of grids measured under conditions suggested by the ICRU (Ref. 15) (Figs. VII-18 and VII-19). Figure VII-20 shows a series of plots of the improvement achieved with a series of grids, as a function of tube voltage and thickness of scattering material in the beam. The following conclusions can be drawn from Fig. VII-17: The relative quality of the different grids tested expressed as the relative value of the contrast improvement factor appears to be independent (1) of the voltage range used and

TABLE VII-2. Characteristics of 13 Measured Grids^a

Grid no.		Strips				Lead content				Characteristics (100 kV, 20 cm H ₂ O)		
Thick- ness d (μ)	Height h (mm)	Dis- tance D (μ)	Strip density N (cm^{-1})	Grid ratio $r = h/D$	r/N (cm)	Volume V ($10^{-4} \text{ cm}^3/\text{cm}^2 = \mu$)	Weight P (mg/cm ²)	Prim. transm. T_{pn} (%)	Bucky factor B_n	Contrast improvement factor K_n		
1 ^b	50	1.1	27	3.4	0.12	150	170	67.5	2.9	1.95		
2 ^c	50	2 × 1.1	25	2 × 3.1	0.25	270	310	57	3.4	1.95		
3	50	2.5	24	7	0.29	300	340	69	3.05	2.1		
4	30	2.5	40	11	0.27	300	340	69	3.05	2.1		
5	60	2	29	7	0.24	350	390	72.5	2.9	2.1		
6	80	2	24	6	0.25	380	430	72.5	2.55	1.85		
7	50	3.5	23	9	0.39	400	460	67	3.5	2.35		
8	30	3.5	38	15	0.39	400	460	68.5	3.8	2.6		
9 ^d	50	2 × 2.5	24	2 × 7	0.58	600	680	58.5	5.0	2.95		
10	50	4.5	28	15	0.54	630	720	64	4.35	2.8		
11	60	4.6	27	15	0.56	730	830	68.5	4.2	2.85		
12	60	6	22	15	0.68	790	900	64	4.6	2.95		
13	70	4.5	27	15	0.56	850	960	60.5	5.0	3.0		

^a From Hondius Bolding (Ref. 16).

^b Aluminium-interspaced grid.

^c Aluminium-interspaced cross grid (about 2 × No. 1).

^d Cross grid (2 × No. 3).

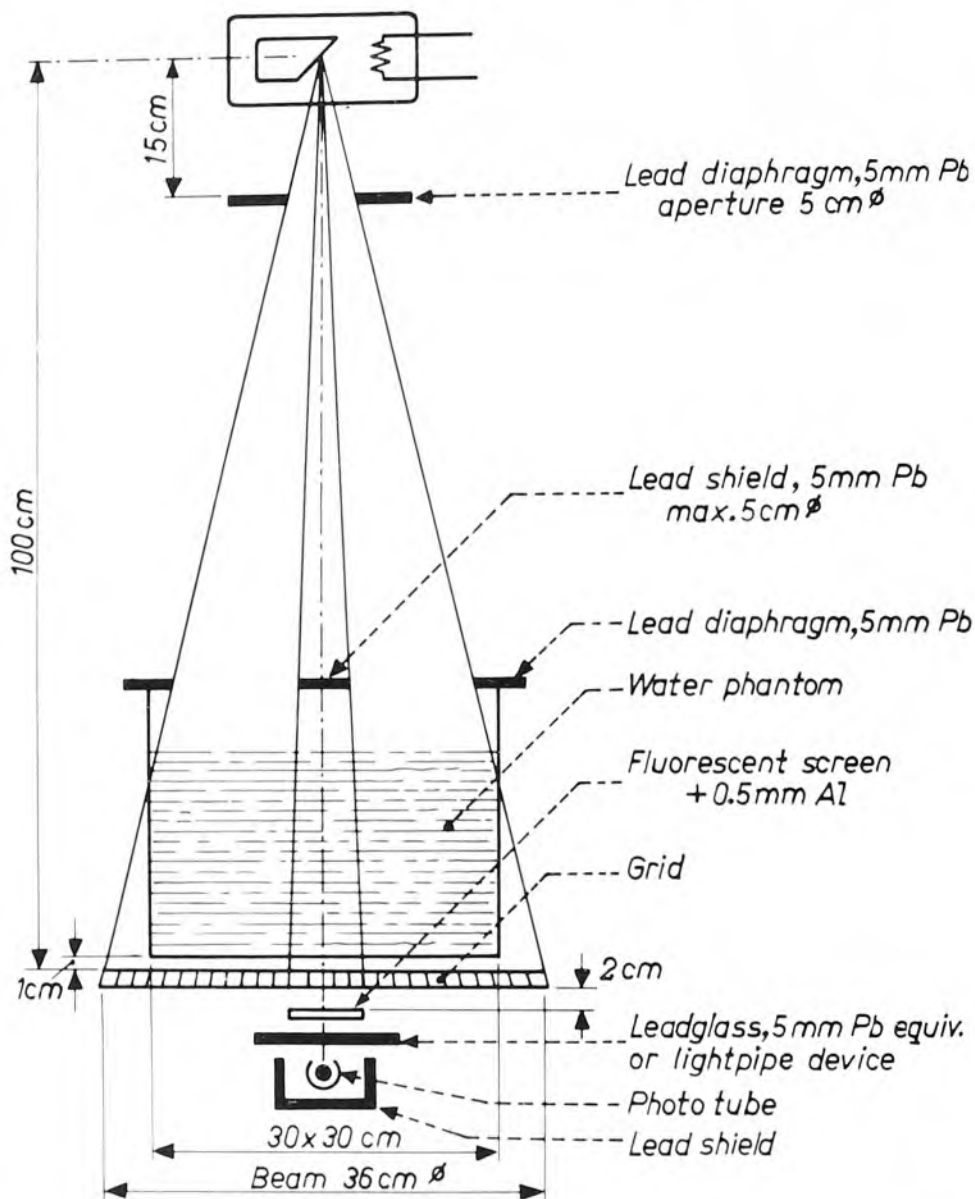


FIG. VII-18. Apparatus for measuring scattered and total radiation.
(From Hondius Boldingh, Ref. 16.)

(2) of the phantom thickness. Therefore from the standpoint of the contrast improvement factor, a given screen can be superior to others independently of the radiation used and the volume of scattering material present.

Selectivity

Various other parameters have been used in characterizing the performance of grids, such as (1) the *loss factor* $V (= 1 - T_p)$, which is a measure of the loss of primary radiation passing through the screen; (2) the *clean-up factor*, or efficiency $\eta (= 1 - T_s)$, and (3) the *Bucky factor* B , which is equal

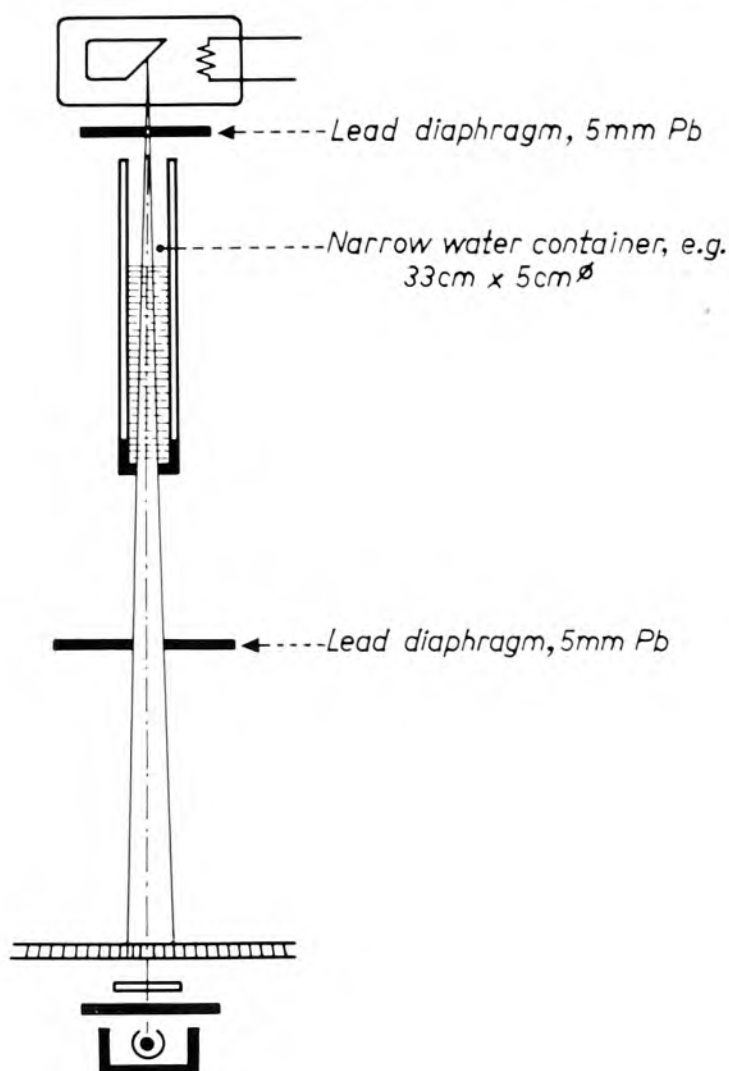
to the total incident radiation divided by the total transmitted radiation

$$(1/T_t).$$

One of the more useful of these factors, suggested by Waard (cited in Ref. 16) and Reiss (cited in Ref. 16) is the *selectivity* Σ of a grid; it is equal to T_p/T_s . The relation between the contrast improvement factor K and the selectivity Σ is shown in Fig. VII-21 for various values of I_s/I_p . It is apparent that Σ is a complex function of K , and that a considerable difference between the Σ 's of two grids may not necessarily result in an appreciable increase in the contrast improvement factor K . Therefore, although the selectivity Σ is useful from the standpoint of screen design, it is not as useful in its final evaluation as the contrast improvement factor K (Ref. 16).

FIG. VII-19. Apparatus for measuring primary radiation.

(From Hondius Boldingh, Ref. 16.)



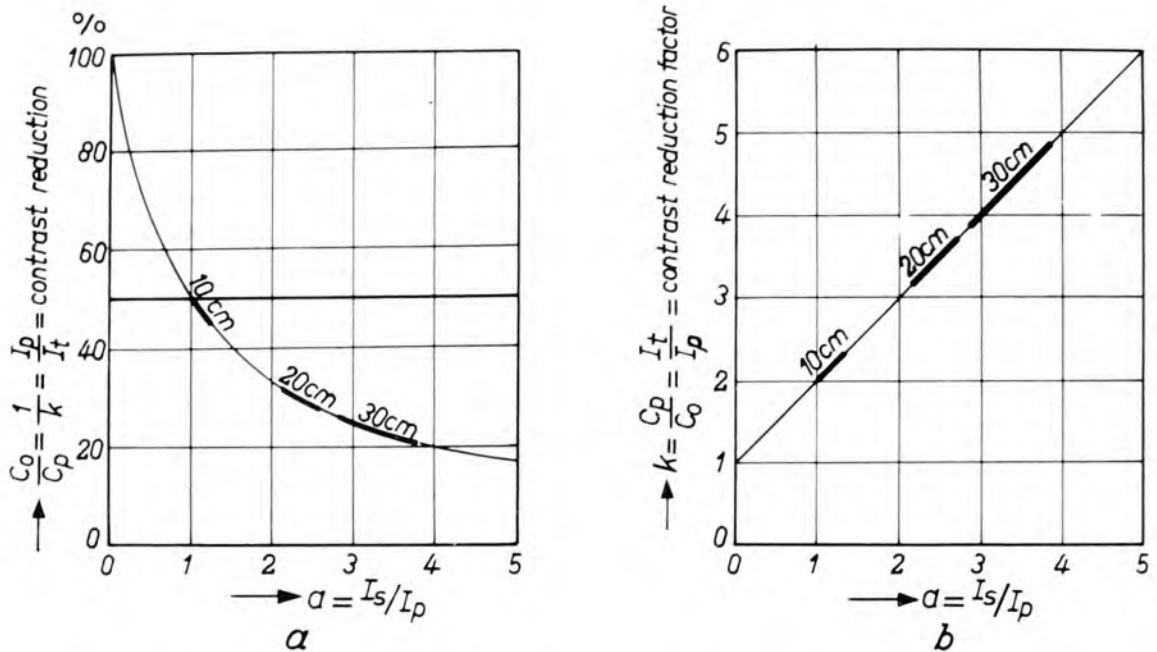


FIG. VII-20. Contrast reduction (a) and contrast reduction factor k (b) as a function of I_s/I_p . Heavy lines indicate values for 10, 20, and 30 cm of water for x-ray tube voltages ranging from 60 to 200 kV. (From Hondius Boldingh, Ref. 16.)

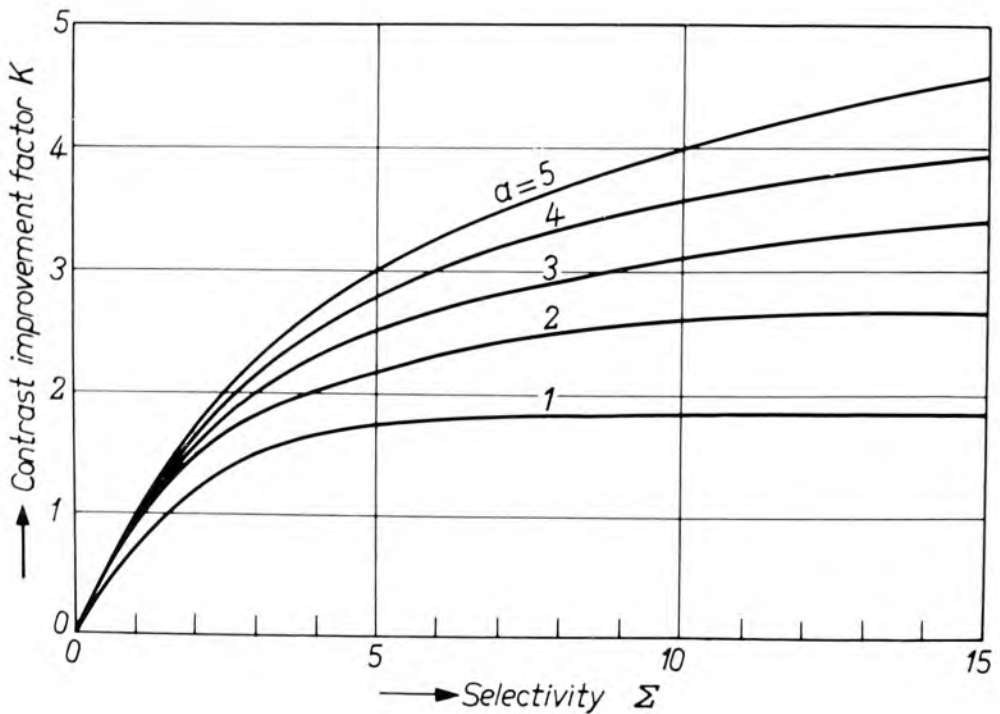


FIG. VII-21. Contrast improvement factor K as a function of selectivity for various values of $a = I_s/I_p$. (From Hondius Boldingh, Ref. 16.)

FIG. VII-22. Grid ratio.

Typical values:

$$d = 0.05 \text{ mm}$$

$$D = 0.3 \text{ mm}$$

$$h = 3.6 \text{ mm}$$

$$r = 12$$

Grid ratio:

$$r = \frac{h}{D}$$

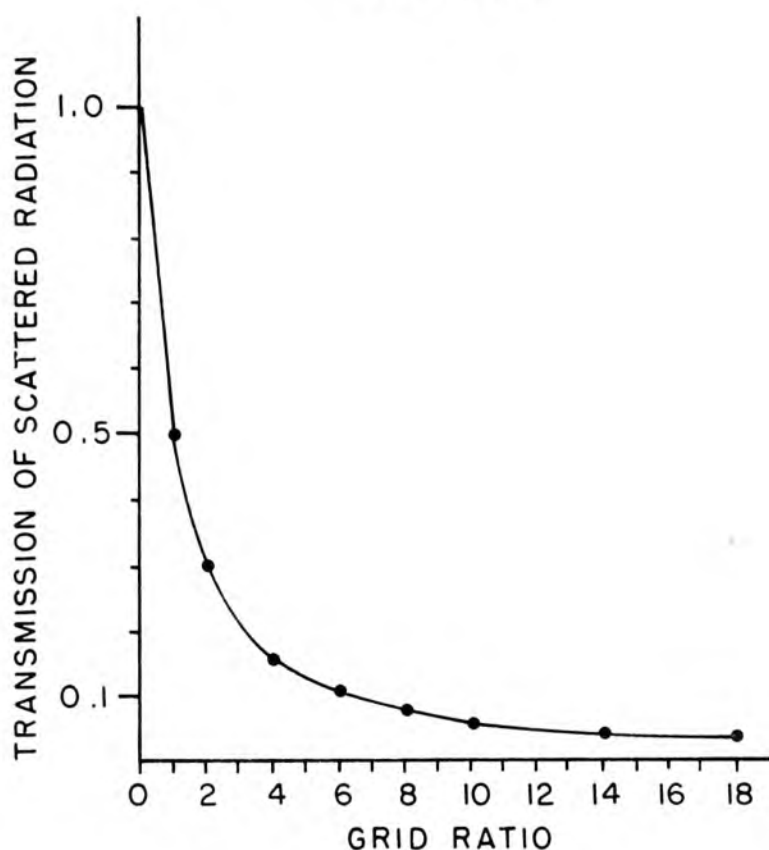
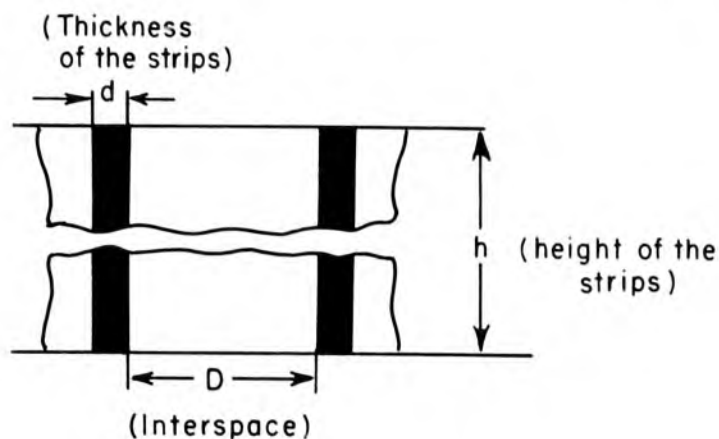


FIG. VII-23. Transmission of scattered radiation by an ideal grid versus grid ratio. (Courtesy of Sven Ledin and The Elema Shönander Co.)

Grid Ratio

The grid ratio r is defined as the ratio between the height of the strips h and the distance D which separates them, as follows:

$$r = \frac{h}{D}$$

The grid ratio is a parameter widely used in qualifying commercial x-ray grids (Fig. VII-22).

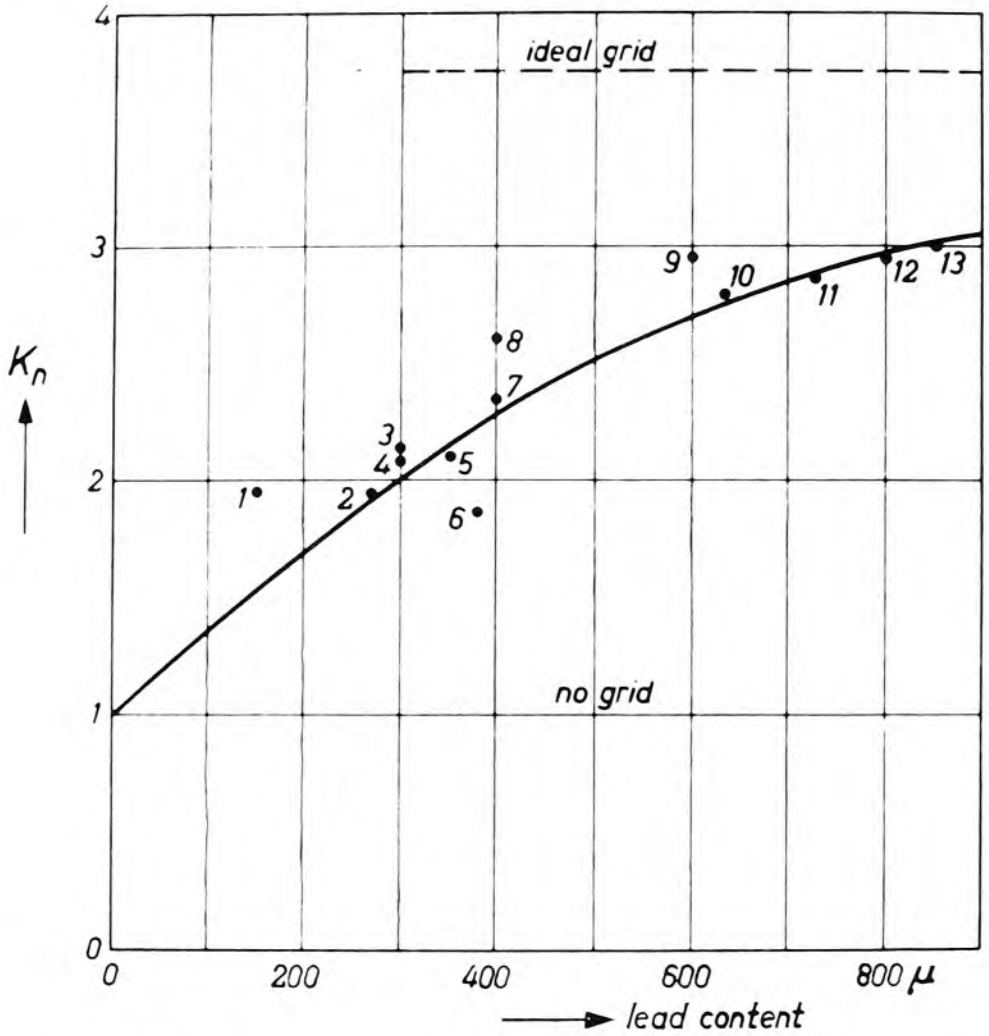


FIG. VII-24. Contrast improvement factor K_n (100 kV dc, 2 cm water, 30×30 cm² field) as a function of lead content. (From Hondius Boldingh, Ref. 16.)

X-ray grids are usually constructed with ratios of about 5 to 16. The quality of a grid, expressed as the percentage of scattered radiation removed versus grid ratio, is shown in Fig. VII-23. It is apparent that only little improvement is achieved beyond a ratio of 8; and, as will be shown later in this chapter, high ratio grids present serious practical disadvantages. For this reason the majority of the grids used in diagnostic radiology are built with ratios lower than 12.

The advantage of the grid ratio over the previously discussed methods of expressing grid quality is that the ratio is a physical characteristic of the grid and is independent of radiation energy and scattered radiation. Unfortunately, grid ratio is a suitable method for the comparison of contrast-improving qualities of grids only if the number of strips per unit length (strip density) of the compared grids is kept constant, as was the case in the early days of grid development. In modern grids strip density varies over

wide limits, and under such circumstances reliance on the grid ratio may be misleading (Ref. 16).

Lead Content

The lead content P of a grid is defined as the mass of the lead in the grid per unit surface area. Lead content can be used as a rough but easily determinable index of the contrast improvement produced by a grid (Refs. 15 and 16) (Fig. VII-24), *provided the grid is efficiently constructed*. An example of an inefficiently constructed grid is a lead sheet that even with a high lead content is a poor selective absorber of scattered radiation.

Focus-Grid Decentering

Sometimes the focal spot of the x-ray tube is displaced from the convergence line of a focused linear grid or from the convergence point of a focus

FIG. VII-25. Transmission of primary radiation through grid, as a function of angulation error or lateral decentering. (Courtesy of Sven Ledin and The Elema Schönander Co.)

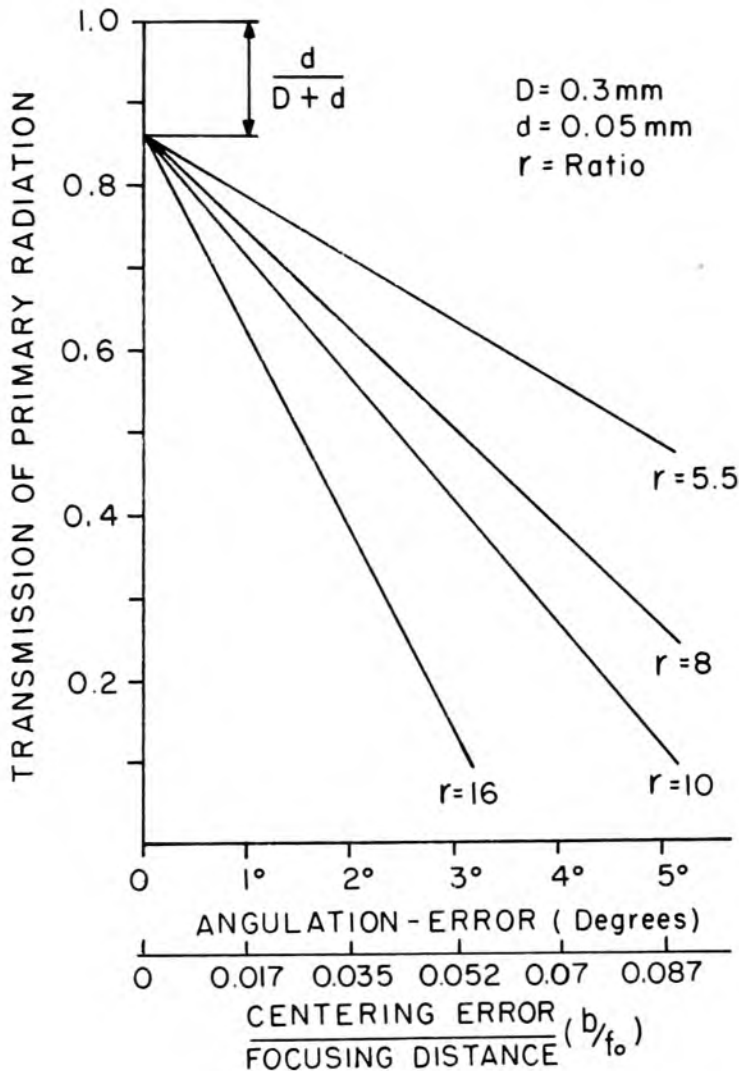
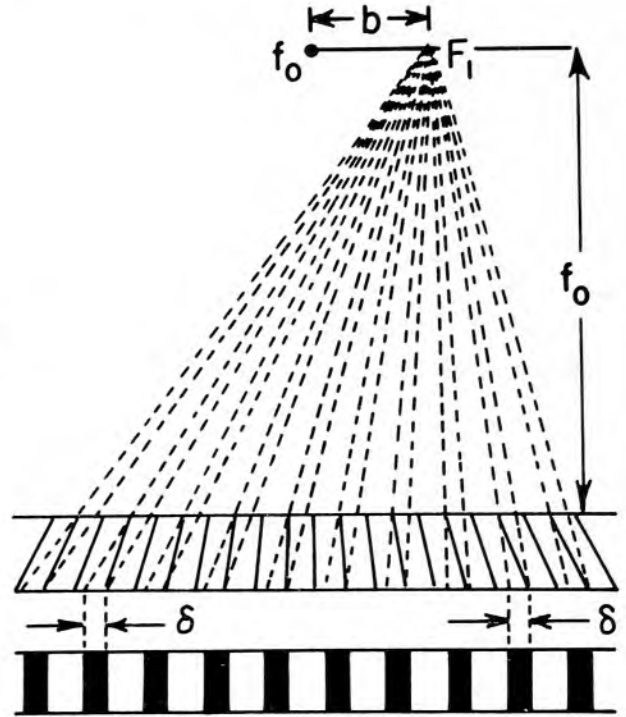


FIG. VII-26. Effect of lateral decentering of grid on shadows cast by grid strips.



cross grid. Decentering results (1) from the displacement of the x-ray tube focal spot in a plane parallel to the grid (lateral decentering), (2) from the variation of the focus-grid distance, or (3) from a combination of (1) and (2). Decentering of the focal spot with respect to the grid may occur accidentally because it is often difficult to position accurately an x-ray tube; it may also occur because decentering is inherent in the use of a focused moving grid; and sometimes practical considerations dictate the use of a grid at a distance other than its focusing distance.

Focus-grid decentering results in an increase in the shadow area cast by the grid strips, with consequent reduction in the transmission of primary radiation.

Lateral Decentering—Angulation Error. In a well-centered x-ray tube-grid combination the shadow cast by the strips is nearly equal in width to their thickness, and the percentage of the primary radiation intercepted by the strips is equal to

$$\frac{d}{D + d} \times 100,$$

where d is strip thickness and D is the distance separating the strips (Fig. VII-25).

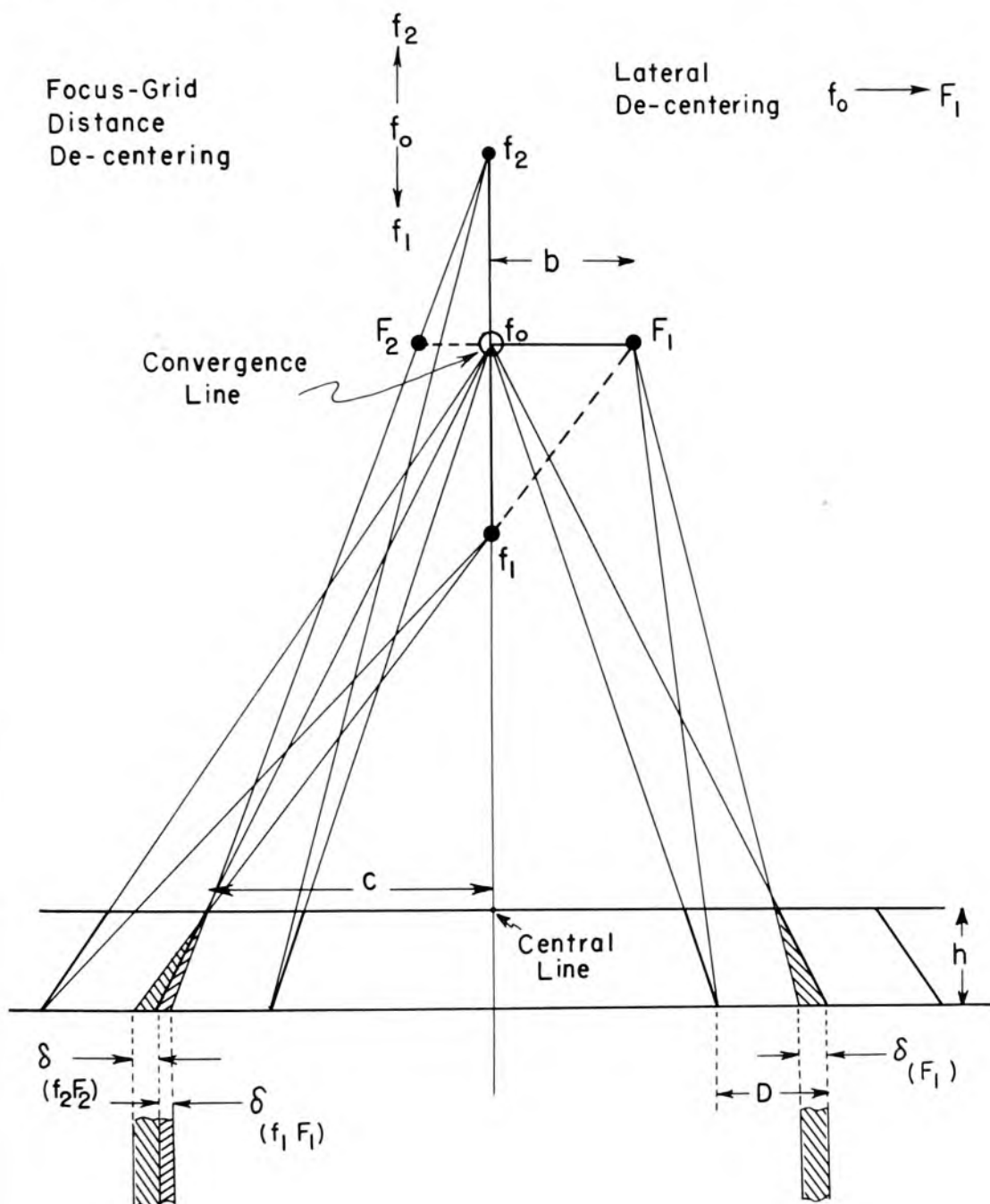
Lateral decentering of the x-ray tube by a distance b results in an increase in width of the shadow cast by each one of the strips by a quantity δ , which is uniform throughout the area of the grid (Figs. VII-26 and VII-27). The

increase δ is equal to

$$\delta = \frac{hb}{f_0},$$

where h is the thickness of the grid, b is the lateral decentering distance, and f_0 is the focal distance of the grid. The relative loss of primary radiation resulting from a lateral decentering b is equal to δ/D , or rb/f_0 .

FIG. VII-27. Effect of lateral decentering and focus-grid distance decentering on shadows cast by grid strips.



Lateral decentering occurs also when a well-centered grid is tilted in such a fashion that the planes of the strips are angulated with respect to the radiation. Such angulation error can be measured by the angle formed by the planes of the strips and the direction of the x-radiation. The tangent of this angle is equal to b/f_0 , and the relative loss of primary radiation consequent to angulation error can also be expressed as follows:

$$\frac{\delta}{D} = r \tan \alpha = \frac{rb}{f_0} \quad (1)$$

This equation shows that the relative loss of primary radiation resulting from lateral decentering or angulation error is proportional to the grid ratio r and to the displacement and inversely proportional to the focal distance of the grid. For example, if an error of 1 cm in the lateral centering of a grid with a ratio of 12 and a focusing distance of 100 cm occurs, the relative loss of primary radiation is $12 \times \frac{1}{100} = 12\%$.

The motion of a moving grid always results in lateral decentering. The amplitude of the excursion of commercial moving grids varies between 1 and 3 cm, which results in a maximum decentering of 5 to 15 mm. Under the particularly unfavorable circumstances of a high ratio grid with wide amplitude of displacement and a short focusing distance, the motion of a grid may result in lateral decentering losses of about 20% of the primary radiation.

Focus-Grid Distance Decentering. A grid-x-ray tube system is also decentered when there is a difference between the focusing distance of the grid and the focus-grid distance, although this system may be correctly centered laterally. Focus-grid distance decentering results in a spread of the strips' shadows, increasing gradually in magnitude with increasing distance from the central line (Fig. VII-28). Such decentering does not produce any effect at the central line. In contrast to lateral decentering, which results in uniform loss in transmitted primary radiation across the grid, focus-grid distance decentering is revealed by a loss in radiation that is symmetrical with respect to the central line. The fractional loss in primary radiation δ/D at a distance c from the central line is given by

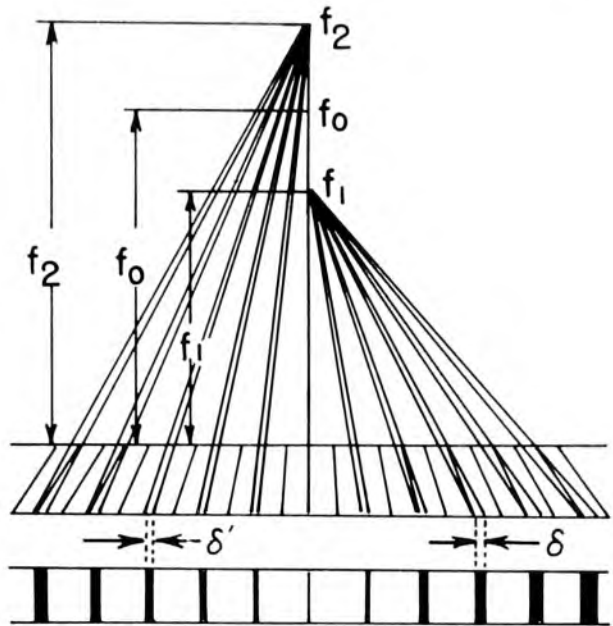
$$\frac{\delta}{D} = rc \left(\frac{1}{f_1} - \frac{1}{f_0} \right) \quad \text{for } f_1 < f_0 \quad (2)$$

and

$$\frac{\delta}{D} = rc \left(\frac{1}{f_0} - \frac{1}{f_2} \right) \quad \text{for } f_2 > f_0 \quad (3)$$

where r = grid ratio, c = distance from the central line, f_0 = grid focusing distance, and f_1 and f_2 = focus-grid distances (Ref. 16) (Fig. VII-27). If the differences $f_0 - f_1$ and $f_2 - f_0$ are small with respect to f_0 (small centering

FIG. VII-28. Effect of focus-grid distance decentering on shadows cast by grid strips.



error), Equations (2) and (3) can be simplified, respectively, to

$$\frac{\delta}{D} = rc \left(\frac{f_0 - f_1}{f_0^2} \right), \quad (2a)$$

or

$$\frac{\delta}{D} = rc \left(\frac{f_2 - f_0}{f_0^2} \right), \quad (3a)$$

$$\frac{\delta}{D} = \frac{rc \Delta f_0}{f_0^2}, \quad (4)$$

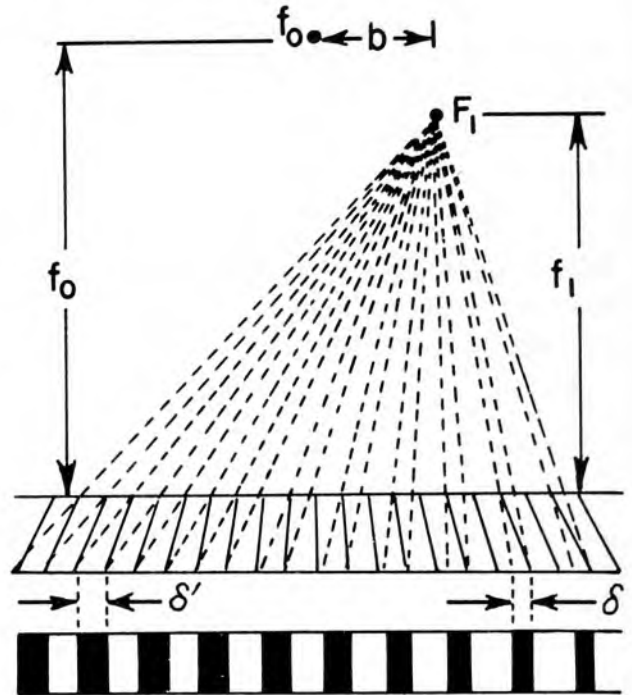
where $f_0 - f_1$ and $f_2 - f_0 = \Delta f_0$.

The following conclusions can be drawn from Equations (2), (3), and (4):

1. The fractional loss of primary radiation is directly proportional to the grid ratio and to the distance from the central line.
2. Focus-grid distance decentering away from the grid results in a smaller loss of primary radiation than when an equal displacement occurs toward the grid. Indeed, for a given displacement, the numerators of Equations (2) and (3) are equal, but the denominators in the case of displacement away from the source are greater than for a displacement of the focus toward the grid.
3. If decentering is small, the loss of primary radiation is proportional to the centering error and inversely proportional to the square of the grid focusing distance (Eq. 4).

Comparison of Focus-Grid Distance Decentering and Lateral Decentering. The loss of primary radiation due to lateral and focus-grid distance decentering exhibits the following common points: Both effects are (1) proportional to the grid ratio, (2) proportional to the decentering distance,

FIG. VII-29. Effect of combined lateral decentering and focus-grid distance decentering on shadows cast by grid strips.



and (β) inversely proportional to the focusing distance (Fig. VII-29). Therefore, low ratio grids with long focusing distances require less critical centering than high ratio grids with short focusing distances. The focusing distance of a grid is determined by the focus film distance used in the examination, and usually this parameter cannot be easily altered. On the other hand, the selection of a grid with a high ratio is made only in an attempt to increase the reduction of scattered radiation. As was shown in Fig. VII-23, the plot of the transmission by a grid of scattered radiation versus grid ratio first exhibits a sharp drop, followed by a considerably flatter area; beyond a grid ratio of 8 to 10, the reduction in the transmission of scattered radiation is reduced. On this basis it appears that the use of grids with ratios higher than approximately 8 is not efficient, because a relatively small gain in absorption of scattered radiation is obtained at the cost of extreme criticalness in grid centering.

Lateral grid centering is more critical than focus-grid distance centering. This can be shown by comparing the ratios of primary radiation losses resulting from the same lateral and focus-grid distance decentering:

The loss of primary radiation resulting from lateral decentering is given by Equation (1) (p. 274):

$$\left(\frac{\delta}{D}\right)_{\text{lat}} = \frac{rb}{f_0}$$

The loss of primary radiation resulting from focus-grid distance decentering, assuming that the amount of decentering is small with respect to f_0 , is

given by Equation (4):

$$\left(\frac{\delta}{D}\right)_{f-g} = \frac{rc\Delta f_0}{f_0^2}$$

If the lateral decentering distance is assumed to be equal to the focus-grid decentering distance, then $b = \Delta f_0$ and the ratio of the losses of primary radiation by lateral and focus-grid decentering is equal to

$$\frac{(\delta/D)_{\text{lat}}}{(\delta/D)_{f-g}} = \frac{f_0}{c} \quad (5)$$

Equation (5) shows that the ratio of the primary radiation losses for a given lateral decentering to the primary radiation losses for the same focus-grid distance decentering is equal to the focusing distance of the grid divided by the distance from the central line to the point where the losses are evaluated. The distance c is equal at most to one-half of the width of the grid, which is usually considerably smaller than the focusing distance. For example, for a 14×17 in. grid with a focusing distance of 40 in., $f_0/c = 40/7 = 5.7$; this means that under the described circumstances, at 7 in. from the central line the reduction of the intensity of the primary radiation due to lateral decentering is approximately 6 times greater than that for focus-grid distance decentering. This difference between the two types of decentering is illustrated in Fig. VII-27, where the losses in primary radiation subsequent to focus-grid distance decentering from f_0 to f_1 at c is equal to the losses resulting from the lateral decentering from f_0 to F_1 . Conversely, the primary losses resulting from a decentering from f_0 to f_2 are identical to the lateral decentering losses resulting from the decentering f_0 to F_2 .

Focus-grid distance centering in radiologic practice is not critical, particularly for grids with long focusing distances and low ratios, so that these grids can be used over a certain range of focus-grid distances without appreciably causing unequal absorption of primary radiation.

The selection of the focus-grid distance limits between which a grid can be used in practice depends on (1) the accepted reduction of primary radiation at a specified distance from the central line, (2) the grid ratio and the focusing distance, and (3) the uncertainty of the lateral decentering which contributes to the primary radiation losses.

The ICRU (Ref. 15) defines focus-grid distance limits as follows: "The limits are so defined, using the nominal or stated values of ' f_0 ' and ' r ' and an average lateral decentering of 1 cm of the tube focus, that a loss of 50 percent (for cross grids 25 percent) is obtained at 15 cm from the central line of the grid."

Moving Grids

In many radiologic examinations the grid is attached to a driving mechanism which sets it in motion during the x-ray exposure with the purpose of

blurring out the shadows cast by the absorption of radiation in the strips. Parallel, focused, and cross grids are so set in motion. Different mechanisms are used to operate moving grids; some move the grid once during the exposure; some communicate a rapid back-and-forth motion to the grid (reciprocating grids); and others produce a sinusoidal motion.

In addition to the blurring effect achieved, the operation of a moving grid differs in two other respects from that of a stationary grid with the same characteristics: (1) The excursion of a focused moving grid results in unavoidable lateral decentering with subsequent reduction in transmitted primary radiation. Usually, because of the short excursion of the grid this loss is not greater than about 20% (Ref. 16). (2) The x-ray image of a uniform distribution of radiation transmitted through a moving grid consists of a uniform distribution of photons. A stationary grid of identical characteristics tested under the same conditions supplies an x-ray image composed of the shadows cast by the grid strips and, in the interspace areas, a photon density greater by about 15% than in the image obtained with a moving grid. Thus, both in the moving and in the stationary grid the number of primary photons that are transmitted per unit area is the same, except that in the case of the stationary grid these photons are "compressed" between the strips.

The above considerations tend to favor slightly the use of stationary grids, although from the practical standpoint these factors appear to be of little consequence in clinical radiology. A more serious drawback in the use of moving grids are the disadvantages associated with a Bucky, which is costly and subject to failures, does not perform well for very short exposures, and may introduce an undesirable motion of the film. For these reasons, and because of the availability of grids with large numbers of strips per unit area (over 100 strips per inch), which render grid strip shadows almost unnoticeable, there is a tendency to abandon moving grids in favor of stationary grids.

Cross Grids

A cross grid is a structure composed of two linear grids having the same focusing distance, which are superimposed in such a fashion that their strips form an angle. If this angle is 90 degrees, the cross grid is said to be orthogonal. Most cross grids are orthogonal.

According to ICRU recommendations, the grid ratio r_c of a cross grid is

$$r_c = 2 \times r_e,$$

where r_e is the grid ratio of each one of the linear grids composing the cross grid. Although it appears theoretically possible to blur out the strip shadows of a cross grid by moving it (Ref. 17), moving cross grids are not often used in radiology.

In general terms, the performance of a cross grid is almost identical to that of a linear grid of the same grid ratio and the same lead content, with the following exceptions. The square pattern exhibited by cross grids when they are operated with focus-grid distance decentering is somewhat more pleasing to the eye than the linear pattern obtained with a linear grid of similar performance, and the cross grid provides a slightly better absorption of scattered radiation than a linear grid of similar characteristics. These advantages of cross grids must be weighed against the following disadvantages: They transmit less primary radiation, and they exclude oblique beam techniques, which are possible with linear grids. At this time not enough data are available to establish a clear-cut difference between the performances of cross grids and linear grids.

Grid Strips

Ideally, grid strips should be infinitely thin to absorb no primary radiation edgewise, and be completely opaque to scattered radiation striking their surface. These desirable features dictate that the strips be made of a material exhibiting the highest linear x-ray absorption coefficient for the scattered radiation. This suggests the use of a high atomic-number and high density element.

Two additional theoretical factors must be taken into account in the choice of strip material. The absorption of the relatively low energy x-rays used in diagnostic radiology in high atomic-number materials takes place mostly by photoelectric effect. Consequently, of two absorbers having different atomic numbers, the one with the lower atomic number may be more opaque to x-rays than the other absorber in a given photon energy range because of the relative positions of the K absorption peaks of the two elements, and the absorption of scattered x-rays in the strips by photoelectric effect results in the emission by the absorber of its characteristic radiation. In a grid constructed with high atomic-number material, the L-characteristic radiation is of no consequence because its energy is so low that it is almost completely absorbed in the interspace material of the grid. However, if the energy of the scattered radiation absorbed by the strips is sufficiently high to stimulate the emission of the K-characteristic radiation of the strip material, this radiation may escape the grid and reduce the contrast of the x-ray image. Grid fluorescence produced by the absorption of high-energy scattered radiation reduces the usefulness of a grid and also suggests the use of the highest possible atomic-number element as strip material to raise the energy limit of the photons that can excite the fluorescence of the grid.

The above considerations show that the selection of strip material is complex and should take into account not only the density and atomic number of the material but also the spectral distribution of the x-radiation with which the grid is to be used.

Practically all grids used in diagnostic radiology contain lead strips. Lead (atomic number 82, density 11.0 g/cm³) is cheap and relatively easy to handle, and offers a good compromise for the construction of grids. However from the theoretical standpoint lead is inferior in several respects to some other elements. Table VII-3 shows a series of elements that compare

TABLE VII-3. Atomic Number and Density of Some High Atomic-Number Metals

Element	Atomic number	Density (g/cm ³)
Tungsten	74	19.0
Platinum	78	21.4
Gold	79	19.3
Lead	82	11.0
Uranium	92	16.7

Adapted from *Handbook of Chemistry and Physics*, Ref. 18.

favorably with lead for the construction of grids. Platinum and gold, in spite of their slightly lower atomic numbers, are superior to lead because of their considerably greater densities, and gold grids have been constructed for use in radiology. The high cost of these two elements prohibits their use on a wide scale. The lower atomic number of tungsten is also counterbalanced by its high density, and the usefulness of tungsten grids has been demonstrated (Ref. 19). Uranium, with higher atomic number and higher density than lead, appears to be an excellent choice for the construction of grids (Ref. 20). A comparison of the linear x-ray attenuation coefficients for tungsten, lead, and uranium (Fig. VII-30) shows that there is "jockeying" between the superiority of uranium and tungsten over lead. Table VII-4 includes a comparison of the tenth-value layer (thickness of absorber which reduces the number of x-ray photons impinging on it by a factor of 10) of lead with the tenth-value layer of uranium for x-rays generated approximately between 30 and 200 kV_p. It is quite apparent that practically over this entire energy range uranium is considerably superior as grid strip material. In spite of these advantages, uranium grids are not used because of the difficulties involved in their construction.

Grid Interspace Material

The main purpose of the material between the strips of a grid is to provide structural support for the fragile, thin lead strips. In most commercially

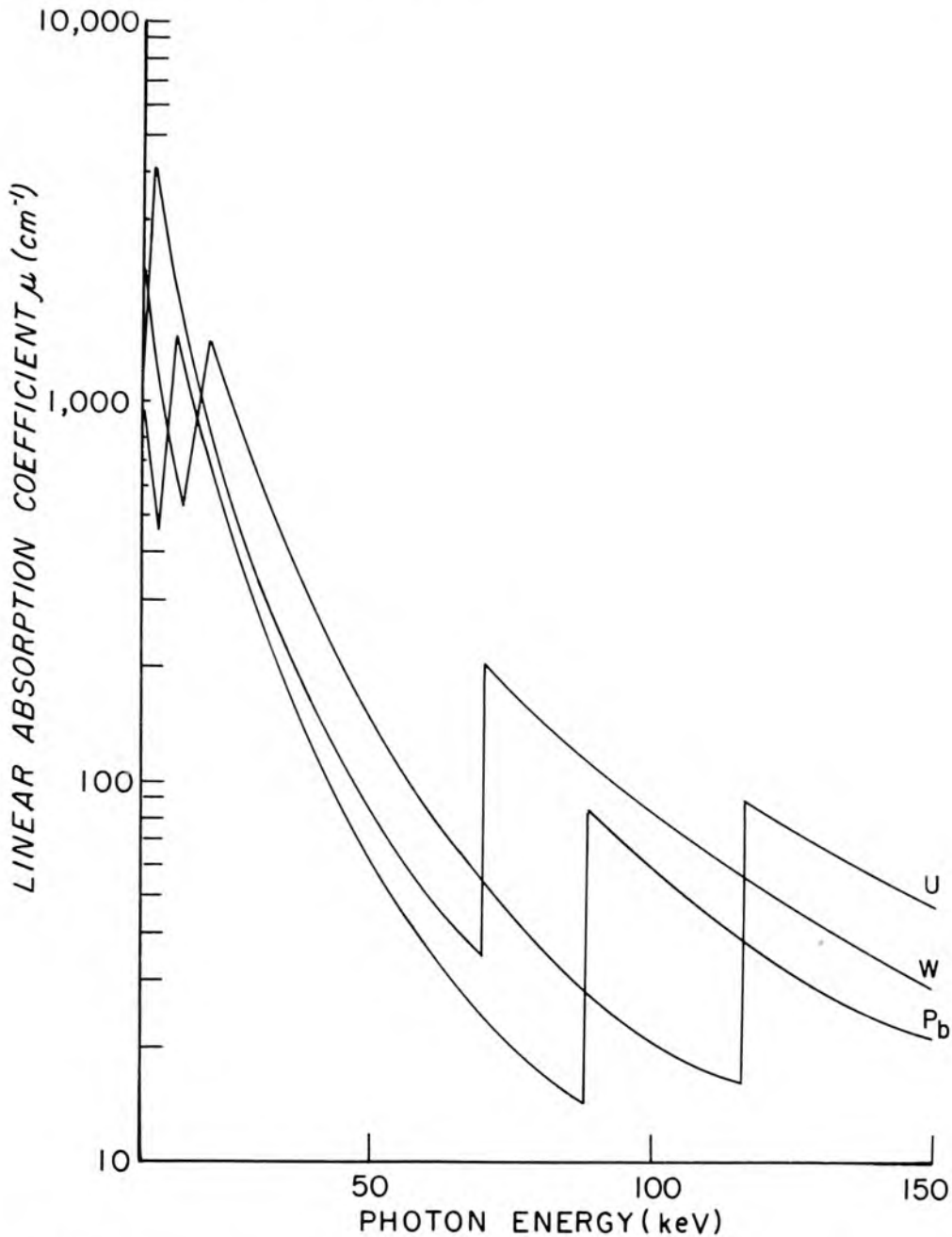


FIG. VII-30. Linear x-ray absorption coefficients for lead, tungsten, and uranium, as a function of photon energy. (Data from Siegbahn, K.: Beta and Gamma Ray Spectroscopy. New York. Interscience, 1955.)

manufactured grids the interspace material is either aluminum or some organic compound. The advantage of using organic compounds is that they absorb appreciably less primary radiation than aluminum (Figs. V-5 and V-9, Chapter V). On the other hand, aluminum is a better absorber for scattered radiation which does not strike the strips, and therefore the presence of aluminum may improve the contrast improvement factor of a

TABLE VII-4. One-Tenth-Value Layer of Uranium and Lead as a Function of X-Ray Energy

Peak energy (keV)	Added filtration (cm)	Half-value layer (cm)	Effective energy (keV)	$\frac{1}{10}$ -value layer for lead (cm)	$\frac{1}{10}$ -value layer for uranium (cm)	Ratio $\frac{1}{10}$ -V.L. lead to $\frac{1}{10}$ th-V.L. uranium
27.5	0	0.1 Al	22	0.004	0.0016	2.5
60	0.32 Al	0.425 Al	35	0.019	0.0075	2.5
80	0.32 Al	0.65 Al	48	0.032	0.013	2.4
115	0.32 Al	0.9 Al	60	0.044	0.025	1.8
140	0.3 Al	0.075 Cu	74	0.051	0.033	1.5
200	0.3 Al	0.1 Cu	81	0.064	0.038	1.7
120	0.3 Cu +0.1 Al	0.15 Cu	100	0.055	0.053	1.0
200	0.3 Cu +0.1 Al	0.25 Cu	130	0.102	0.058	1.8

grid (Ref. 21). This advantage is difficult to assess, and at this time is still somewhat controversial (Ref. 16). Technically, aluminum is a good grid interspacing material because it is hard, uniform, and nonhydroscopic, which prevents deformity of the lead strips during the manufacturing process. Furthermore, because of the hardness of aluminum, grids interspaced with aluminum appear to be more resistant in every-day use than grids using organic material and in many instances show better uniformity of construction than grids interspaced with organic material.

REDUCTION OF SCATTERED RADIATION BY DISTANCE

It is also possible to reduce the intensity of scattered radiation in the radiologic image by increasing the distance between the image plane and the examined object. Inasmuch as the scattered radiation is produced in the object, its intensity in the image plane is strongly dependent on the distance that separates the image from the object. This method is not as effective at high energies as at lower energies because of the small-angle, near-forward scattering of higher energy radiation. It is sometimes incorrectly referred to as air filtration. The reduction of scattered radiation by distance is accomplished at the cost of sharpness because of the increase in geometric unsharpness when the distance between the radiologic image and the examined object is increased.

UNSHARPNESS IN RADIOLOGIC EXAMINATIONS

The resolution in the optical image of a radiologic examination, whether this image is viewed directly on a fluorescent screen as in fluoroscopy or whether it is recorded on a photographic emulsion, is considerably lower than that resolution limited only by the statistical fluctuations of the photons that form the image. This occurs because at all levels, both at the generating and the retrieving of information, the various components of the x-ray apparatus contribute to the degradation of the image by producing unsharpness. The different forms of unsharpness are compounded in the final optical image and, together with statistical fluctuations, limit the resolution of the image.

The unsharpness contributed by the information generating system (x-ray tube, examined object) appears in the radiologic image as geometric unsharpness. The radiologic image is further deteriorated by the unsharpness introduced when it is converted into an optical image.

Geometric Unsharpness (Penumbra)

The focal spot of an x-ray tube is a surface of finite dimensions rather than a point source of radiation, and the shadow cast by any object intercepting the x-ray beam is surrounded by a zone of unsharpness. This zone of unsharpness is called geometric unsharpness, or *penumbra*, because its formation is identical in principle to that of the optical penumbra surrounding a shadow (*umbra*) cast by a finite-sized source of light.

X-ray penumbra can be explained as follows: A finite-sized source of x-rays can be regarded as a number of point sources of radiation distributed over the area of the focal spot. When an object is interposed in the beam of radiation, three zones are formed: (1) a zone where the radiation emitted by all the point sources of radiation is intercepted by the object (shadow), (2) a "light" zone where none of the sources is covered by the object; and (3) between these two zones, a third transitional zone—the penumbra—where only a certain number of point sources are covered. If radiation is emitted uniformly by the target, the number of photons across the penumbra varies linearly from the shadow to the "light" zone.

The width of the zone of geometric unsharpness is given by

$$U_F = F \times \frac{d}{D}, \quad (6)$$

where U_F is the width of the penumbra or geometric unsharpness, F is the width of the focal spot, d is the distance between the object and the point where the unsharpness is measured, and D is the distance between the focal spot and the object examined (Ref. 22) (Fig. VII-31). It is apparent that geometric unsharpness can be reduced by (1) reducing d , (2) increasing D , or (3) by reducing F .

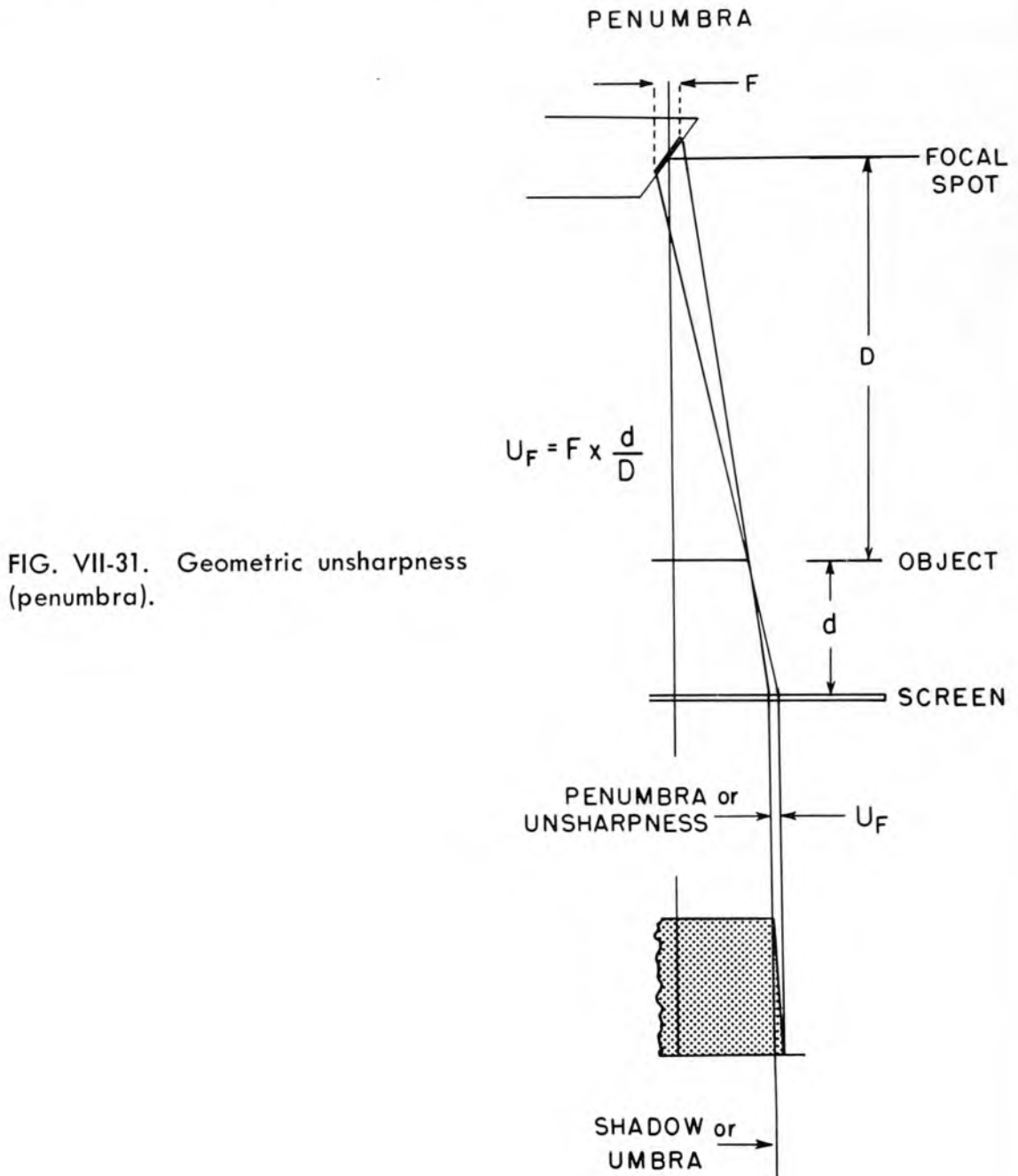


FIG. VII-31. Geometric unsharpness (penumbra).

Geometric unsharpness also results from the motion of either the examined object or the x-ray tube focus during the examination. Such unsharpness is referred to as *motion unsharpness* (Ref. 22) (Fig. VII-32). If the object moves by a distance Δm_F during the exposure, the width of the motion unsharpness zone U_{mO} is given by

$$U_{mO} = \Delta m_F \times \frac{D + d}{D}. \quad (7)$$

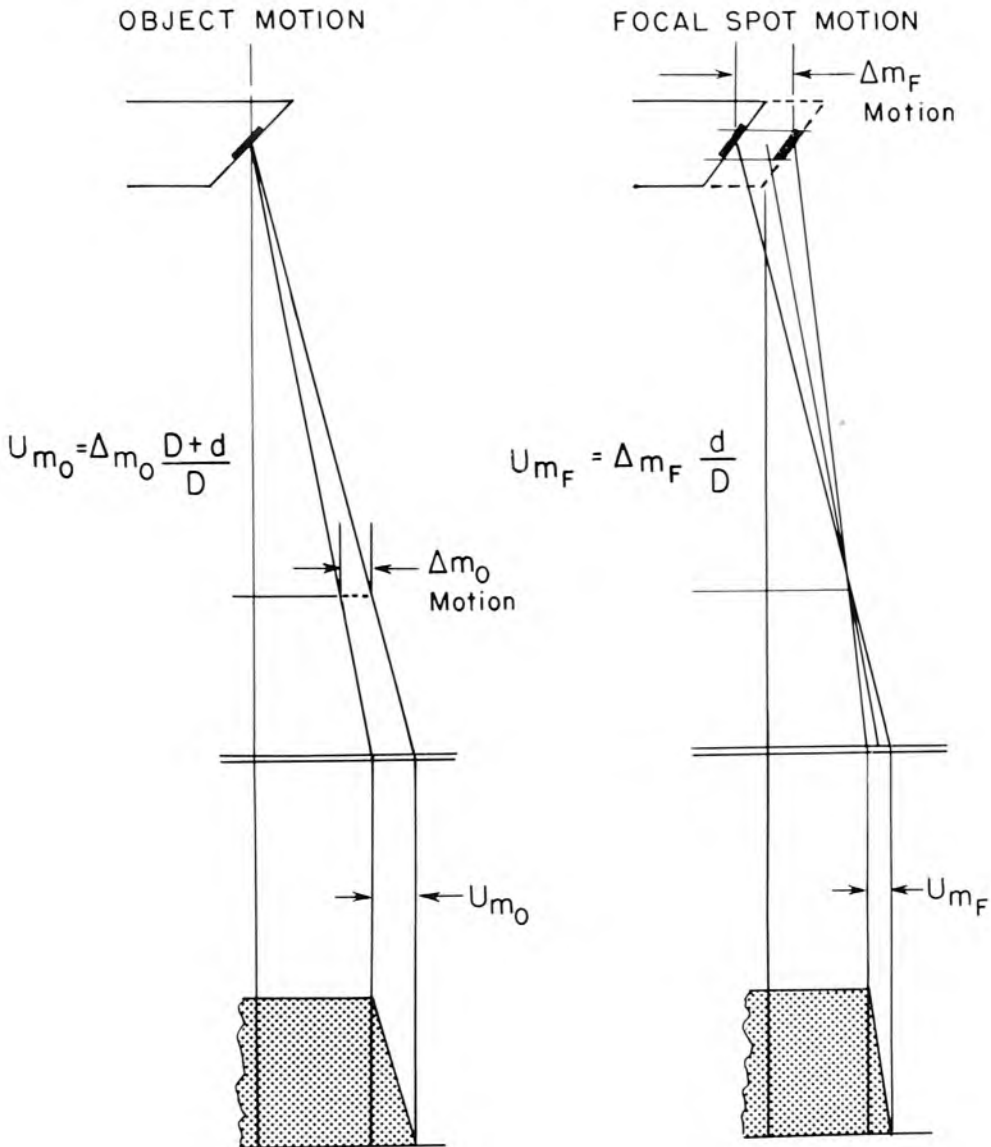
If the focal spot of the x-ray tube moves by a distance Δm_F during the exposure, the resulting geometric unsharpness is given by

$$U_{mF} = \Delta m_F \times \frac{d}{D} \tag{8}$$

It should be noted that the motion of the focal spot during the exposure results in an unsharpness identical to that produced by a focal spot having the width Δm_F .

The relative influence of object and x-ray tube motion on motion unsharpness is expressed by the ratio of the unsharpnesses produced by an

FIG. VII-32. Motion unsharpness.



equal displacement during exposure of the object and of the tube, as follows:

$$\frac{U_{mO}}{U_{mF}} = \left(\Delta m_F \times \frac{D+d}{D} \right) \div \left(\Delta m_F \times \frac{d}{D} \right).$$

If $\Delta m_O = \Delta m_F$, then

$$\frac{U_{mO}}{U_{mF}} = \frac{D}{d} + 1. \quad (9)$$

The ratio of the unsharpnesses approaches 1 only if d becomes much greater than D . Under conditions normally encountered in radiologic examinations, D is greater than d , and for the same displacement, object motion results in a wider zone of geometric unsharpness than tube motion. In a typical examination, D is approximately five times greater than d , and the ratio U_{mO}/U_{mF} is of the order of 6. This means that for the same displacement, object motion produces a zone of unsharpness six times wider than tube motion. This example emphasizes the importance of keeping the patient immobile during the examination, and also points out the relative lack of importance of focal spot motion, particularly if the distance d is small with respect to D . These relationships are experimentally demonstrated in dental radiography where, although the usually poorly supported x-ray tube swings widely during the exposure, little geometrical motion unsharpness shows on the film because of the close proximity of the examined object to the film. Motion unsharpness due to focal spot displacement can be reduced to zero by bringing the object in contact with the screen or film ($d = 0$). On the other hand, unsharpness motion due to the motion of the object can never be reduced to zero. If $d = 0$, motion unsharpness is equal to the displacement of the object.

MINIMUM SEPARATION
FOR RESOLVING A & B

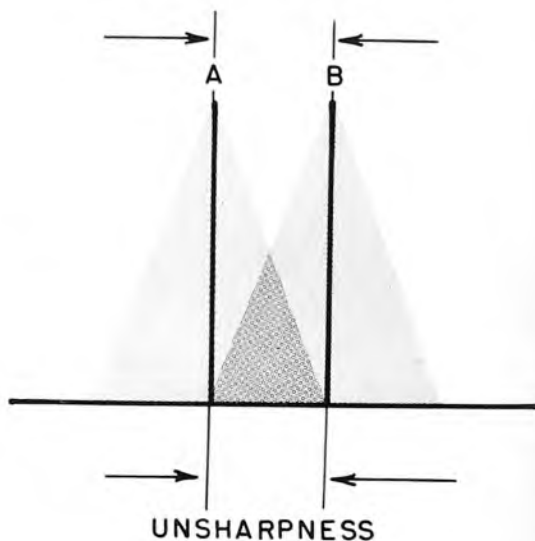


FIG. VII-33. Unsharpness and resolution.

Unsharpness results in loss of resolution, and two points can be resolved by a system exhibiting unsharpness only if the distance which separates them equals or exceeds the half-width of the zone of unsharpness (Figs. VII-33 and VI-3).

Unsharpness Contributed by Image Conversion

The conversion of the radiologic image to an optical image by means of screens, film, or screen-film combinations is accomplished at the cost of additional unsharpness. (Unsharpness in image amplifiers is discussed in Chapter VIII.)

Screen unsharpness is due to diffusion, in the phosphor layer, of the light photons produced by the absorption of x-ray photons. A less important component of screen unsharpness is contributed by the diffusion through the screen of the characteristic x-radiation excited in the phosphor by the absorption of x-rays. The diffusion of light in the screen depends mainly on crystal particle size, thickness of the screen, and transparency of the phosphor matrix to the light emitted. The density distribution of the unsharpness produced by a screen is difficult to evaluate because of the complexity of the factors involved. An approximate measure of the width of the unsharpness zone can be deduced from the resolving power of the screen by assuming that the separation between two resolved lines must be at least equal to the half-width of the zone of unsharpness. The resolution of x-ray screens varies from about 2.5 lines/mm for fluoroscopic screens to 14 lines/mm for high-resolution intensifying screens (Table VI-2). These two figures correspond to a width of unsharpness from 400 to 70 μ .

A better method of expressing screen unsharpness consists in determining the modulation transfer function of the screen by means of its line spread function (Ref. 3). As pointed out by Morgan et al. (Ref. 3), the most important factor affecting the detail recording capabilities of screens and film-screen combinations is amplitude distortion. Consequently, the expression for the modulation transfer function of these systems may be limited to a representation of the amplitude response versus frequency. Figure VII-6 shows sine-wave amplitude response characteristics of five types of screens commonly used in radiology.

Unsharpness contributed by the film is, in most clinical radiologic examinations, a component negligible with respect to either geometric or screen unsharpness. Figure VII-7 shows the sine-wave amplitude response of a typical radiographic film. A comparison of Figs. VII-6 and VII-7 shows that the detail recording capabilities are considerably superior in the film than in the screen; for example, the amplitude response is reduced in the film by 50% for 20 cycles/mm, while the same distortion occurs in the screen at a frequency of only 2 cycles/mm. Film resolution is a limiting factor in the detail-recording capability of a radiographic examination only in examinations of extremities carried out without intensifying screens. In

TABLE VII-5. Components of Unsharpness in Typical Radiologic Examinations

Examina- tion	Focal spot size (cm)	Focus- object distance D (measured to the midline) (cm)	Object- screen distance d (measured from the midline) (cm)	Screen used	Film used	Geometric unsharpness $U_F = F \times \frac{D}{d}$ (mm)	Screen unsharp- ness (mm)	Film unsharp- ness (mm)	Total unsharp- ness (mm)	Resolving power for 100% contrast ^b (lines/mm)
Hand	0.1	92	2	none	no-screen	0.02	0	0.07	0.09	22
Chest	0.2	185	15	medium speed	standard speed	0.15	0.25 ^a	0.04	0.44	4.5
Abdomen	0.2	85	15	medium speed	standard speed	0.35	0.25 ^a	0.04	0.64	3
Skull	0.1	90	10	medium speed	standard speed	0.11	0.25 ^a	0.04	0.40	5

^a From Handbook of Radiology, Ref. 24.

^b Reciprocal of half-width of unsharpness (Fig. VII-33).

such examinations, focal spot-size geometric unsharpness is reduced because of the small distance between the object and the film; and if no motion occurs, film unsharpness is the major component of the total unsharpness in the examination.

Total Unsharpness and Detail-Recording Capability of Radiographic Systems

The total unsharpness recorded by the film in a radiographic examination is equal to the sum of the unsharpness contributed by each one of the components of the apparatus used in obtaining the recorded image. Table VII-5 shows total unsharpness and the relative contribution of each one of the components in various typical radiographic examinations. Motion unsharpness was omitted in these examples as it was assumed that the exposures were sufficiently short to stop motion.

Table VII-5 shows: (1) With the exception of the examination of a hand,

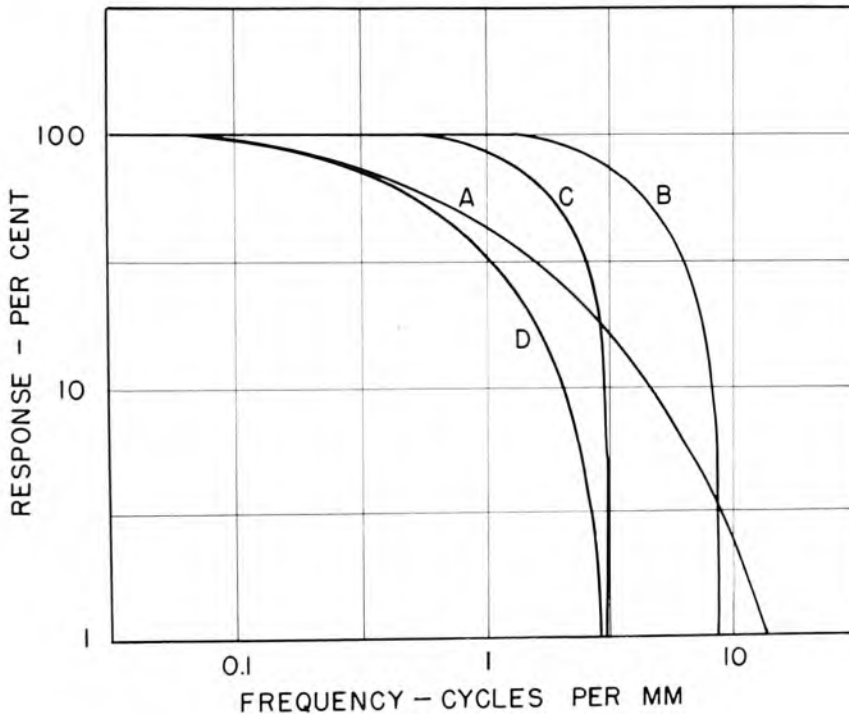
FIG. VII-34. Modulation transfer function. Individual frequency response functions of the components (A, B, and C) of a radiographic system and the composite frequency response function of all three components operating simultaneously (D).

A typical radiographic film exposed with intensifying screens

B 1 mm focal spot with 90 cm object-focal spot distance and 10 cm object-film distance

C motion of the object traveling a distance of 0.3 mm during exposure

D total system frequency response (modulation transfer function) derived by multiplying responses of each one of the components A, B, and C for each frequency
(From Morgan, Ref. 23.)



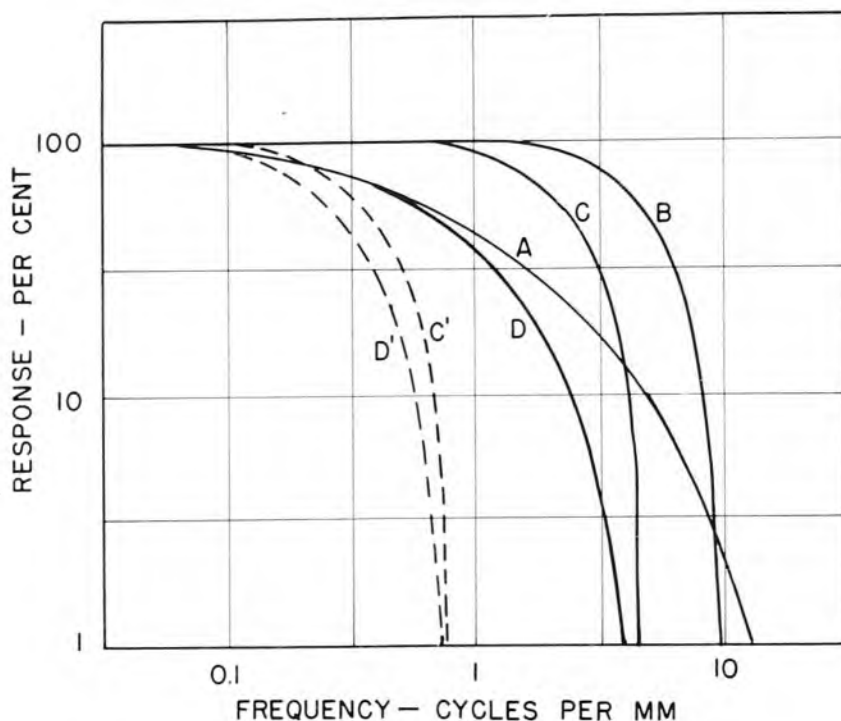


FIG. VII-35. Effect of varying levels of anatomic motion on the recording capability of a radiographic system.

A film-screen combination

B 2 mm focal spot with 180 cm object-focal spot distance and 10 cm object-film distance

C motion of the object traveling 0.25 mm during exposure

C' motion of the object traveling 1.5 mm during exposure

D total system modulation transfer function for Motion C

D' total system modulation transfer function for Motion C'

(From Morgan, Ref. 23.)

carried out under conditions which reduce geometric unsharpness because of the short distance between the object examined and the film, film unsharpness contributes 10% or less of the total unsharpness. (2) The contribution of screen unsharpness in these examinations contributes about one-half of the total unsharpness. (3) At short focal film distances, considerable reduction of unsharpness can be achieved by the use of a small focal spot size. (4) If the object examined had moved by as little as 1 mm during any one of the examinations, the resultant motion unsharpness would have exceeded the sum of the other unsharpnesses.

The above study should be regarded as only qualitative. A considerably superior method for the evaluation of the detail-recording capability of a radiographic system consists in determining the modulation transfer function for the examination. This can be accomplished either by measuring this function for the whole system, or by evaluating the modulation transfer

functions for each of the components of the system and by compounding their relative contributions (Ref. 23). The latter approach offers the advantage of showing the relative contribution of each one of the components of the system to the quality of the resulting image.

Figure VII-34 shows the modulation transfer functions of three components of a radiographic system and the composite frequency response function of all three components. The influence of motion on the modulation transfer function of a radiographic system is shown in Fig. VII-35. It is apparent from Fig. VII-35 that System D is capable of recording detail of the order of 1 mm without great distortion, whereas System D' is not. It is interesting to note that Functions D' and C' are not very different, which indicates that in Examination D', motion is primarily responsible for loss of detail.

REFERENCES

1. VAN ALLEN, W. W., and MORGAN, R. H.: Measurement of resolving power of intensifying screens. *Radiology* 47:166, 1946.
2. ROSSMANN, K.: Modulation transfer function of radiographic systems using fluorescent screens. *J. Opt. Soc. Amer.* 52:774, 1962.
3. MORGAN, R. H., BATES, L. M., GOPALARAO, U. V., and MARINARO, A.: The frequency response characteristics of x-ray film and screens. *Amer. J. Roentgen.* 92:426, 1964.
4. ROSSMANN, K.: Measurement of the modulation transfer function of radiographic systems containing fluorescent screens. Presented at the Meeting of the American Association of Physicists in Medicine, Chicago, Nov., 1964.
5. ROSSMANN, K., and SEEMANN, H. E.: Detail visibility in radiographs: theoretical study of the effect of x-ray absorption in the object on the edge sharpness of radiographic images. *Amer. J. Roentgen.* 85:366, 1961.
6. ROSSMANN, K.: Detail visibility in radiographs: an experimental and theoretical study of geometric and absorption unsharpness. *Amer. J. Roentgen.* 87:387, 1962.
7. ROSSMANN, K., LUBBERTS, G., and CLEARE, H. M.: Measurement of the line spread function of radiographic systems containing fluorescent screens. *J. Opt. Soc. Amer.* 54:187, 1964.
8. ROSSMANN, K.: Image forming quality of radiographic screen-film systems: the line spread function. *Amer. J. Roentgen.* 90:178, 1963.
9. CLEARE, H. M., SPLETTSTOSSER, H. R., and SEEMANN, H. E.: An experimental study of the mottle produced by x-ray intensifying screens. *Amer. J. Roentgen.* 88:168, 1962.
10. ROSSMANN, K.: Spatial fluctuations of x-ray quanta and the recording of radiographic mottle. *Amer. J. Roentgen.* 90:864, 1963.
11. STURM, R. E., and MORGAN, H. R.: Screen intensification systems and their limitations. *Amer. J. Roentgen.* 62:617, 1949.
12. ROSSMANN, K.: Modulation transfer function of radiographic systems using fluorescent screens. *J. Opt. Soc. Amer.* 52:774, 1962.
13. BRUCE, W. R., and JOHNS, H. E.: The spectra of x-rays scattered in low atomic number materials. *Brit. J. Radiol.*, Suppl. 9:1, 1960.

14. REISS, K. H.: Scattered radiation and characteristic film curve. *Radiology* 80:663, 1963.
15. Methods of Evaluating Radiological Equipment and Materials. *International Commission on Radiological Units and Measurements (ICRU)*, NBS Handbook 84. Washington, D.C., U.S. Government Printing Office, 1962.
16. HONDIUS BOLDINGH, W.: Grids to Reduce Scattered X-Rays in Medical Radiography. Philips Research Reports Supplements, #1, Eindhoven, Netherlands, Philips Research Laboratories, 1964.
17. MATTSSON, O.: Practical photographic problems in radiography. *Acta Radiol.*, Suppl. 120:85, 1955.
18. HODGMAN, C. D., WEAST, R. C., and SELBY, S. M., eds.: *Handbook of Chemistry and Physics*, 41st ed. Cleveland, Ohio, Chemical Rubber Publishing Co., 1959.
19. REISS, K. H.: Wolfram-Viellinienraster, ein neues Hilfsmittel der Röntgendiagnostik. *Röntgen- u. Laboratoriumspraxis*. 14:222, 1961.
20. TER-POGOSSIAN, M., and LEDIN, S.: Uranium x-ray grids. *Radiology* 75:797, 1960.
21. LEDIN, S.: *The Physical Background of Contrast in Roentgenograms with Special Regard to Scattered Radiation*. Thesis, Stockholm, 1952.
22. GLASSER, O., QUIMBY, E. H., TAYLOR, L. S., WEATHERWAX, J. L., and MORGAN, R. H.: *Physical Foundations of Radiology*, 3rd ed. New York, Hoeber, 1961.
23. MORGAN, R. H.: The frequency response function. *Amer. J. Roentgen*. 88:175, 1962.
24. MORGAN, R. H., and CORRIGAN, K. E., eds.: *Handbook of Radiology*. Chicago, Ill., Year Book, 1955.

(VIII)

THE FLUOROSCOPIC EXAMINATION

The term fluoroscopy refers to diagnostic radiologic examinations in which the optical image supplied by a luminescent x-ray screen is observed by the radiologist. A lead glass plate protects the radiologist against the x-radiation passing through the screen. Fluoroscopy is mostly used for the radiologic examination of dynamic processes; it is sometimes preferred to radiography in static studies when time does not allow the processing of film.

The fundamental difference between radiography and fluoroscopy lies in the fact that in fluoroscopy the optical image supplied by the x-ray screen is observed directly, while in radiography the image is first recorded on film and then observed, usually by transmitted light.

It would seem that no difference should exist between the qualities of the images obtained by the two methods, or perhaps that the fluoroscopic image should be superior to the radiographic image because of the absence of possible unsharpness, which is introduced by the use of film. The fact is that the image quality in fluoroscopy is considerably lower than in radiography because of the following: During a fluoroscopic examination the patient is usually exposed to radiation for a period of time which is seldom shorter than 1 min, and which may be as long as 20 to 30 min. The radiation exposure rate must be kept low to avoid excessive total exposure of the patient. Thus, fluoroscopy must be carried out with low x-ray photon fluences. This situation affects the fluoroscopic image in two related ways: (1) the fluoroscopic image is considerably dimmer than the radiograph observed under normal conditions of viewing, and (2) the fluoroscopic image is formed by a considerably smaller number of x-ray photons per unit area than the radiographic image. Both factors affect the quality of the fluoroscopic image by the magnitude of the statistical fluctuations of the photons involved. The quantitative study of the influence of these factors on the fluoroscopic image requires an understanding of the limitations of visual acuity at low light levels.

VISION AT LOW LUMINANCE LEVELS—SCOTOPIC VISION

Vision is the acquisition of information about an object by means of light that is either emitted or reflected by that object. The image of the object examined is formed by the optical system of the eye on the retina. The human retina contains two types of receptors sensitive to light—the cones and the rods. The highest density of cones is found in the fovea centralis, and their number per unit area decreases from the center to the periphery of the retina (Ref. 1). There are practically no rods in the central portion of the fovea, and their number first increases radially from the center of the fovea, reaches a maximum, and then decreases to the periphery. The sensitivity of cones and rods to light probably does not differ much; however, the excitation of rods is linked to larger fields of the retina than that of the cones so that for a given amount of light per unit area falling on the retina, the rod system is considerably more sensitive than the cone system (Ref. 2). The difference in sensitivity between rods and cones depends on the wavelength of the exciting light. At 5000 Å the rod system is about 100 times more sensitive than the cones while the two systems exhibit similar sensitivities at 6500 Å. Another difference between cone and rod vision is that cones are sensitive to both the intensity and the wavelength of light falling on them and are able to distinguish color, while rods are only sensitive to light intensity and are unable to produce color vision.

The response of the retina to light depends on the number of light photons impinging upon it, and in the study of the visual observation of an object it is necessary to define a parameter which is related to the number of light photons originating in the object and traveling in the direction of observation. This parameter is the *luminance*, or brightness, of the object.

The luminance B of a surface is expressed as the luminous flux F per unit solid angle ω per unit projected area A , as follows:

$$B = \frac{F}{A \times \omega} \quad (1)$$

The luminance of a surface is (1) independent of the distance between the observer and the surface, and (2) it is not altered when an optical system is introduced between the eye of the observer and the object. The luminous flux can be defined as “the quantity characteristic of radiant flux which expresses its capacity to produce a luminous sensation evaluated according to the values of relative luminous efficiency” (Ref. 3).

The unit of luminous flux is the lumen (lm). The commonly used unit of luminance is the lambert (L), which is the luminance of a perfectly diffusing surface emitting 1 lm/cm². Another unit of luminance, recommended by ICRU (Ref. 3), is the candela per square meter (cd/m²). This unit is equal to $\pi \times 10^{-4}$ lamberts (1 cd/m² = $\pi \times 10^{-4}$ L) and is convenient to

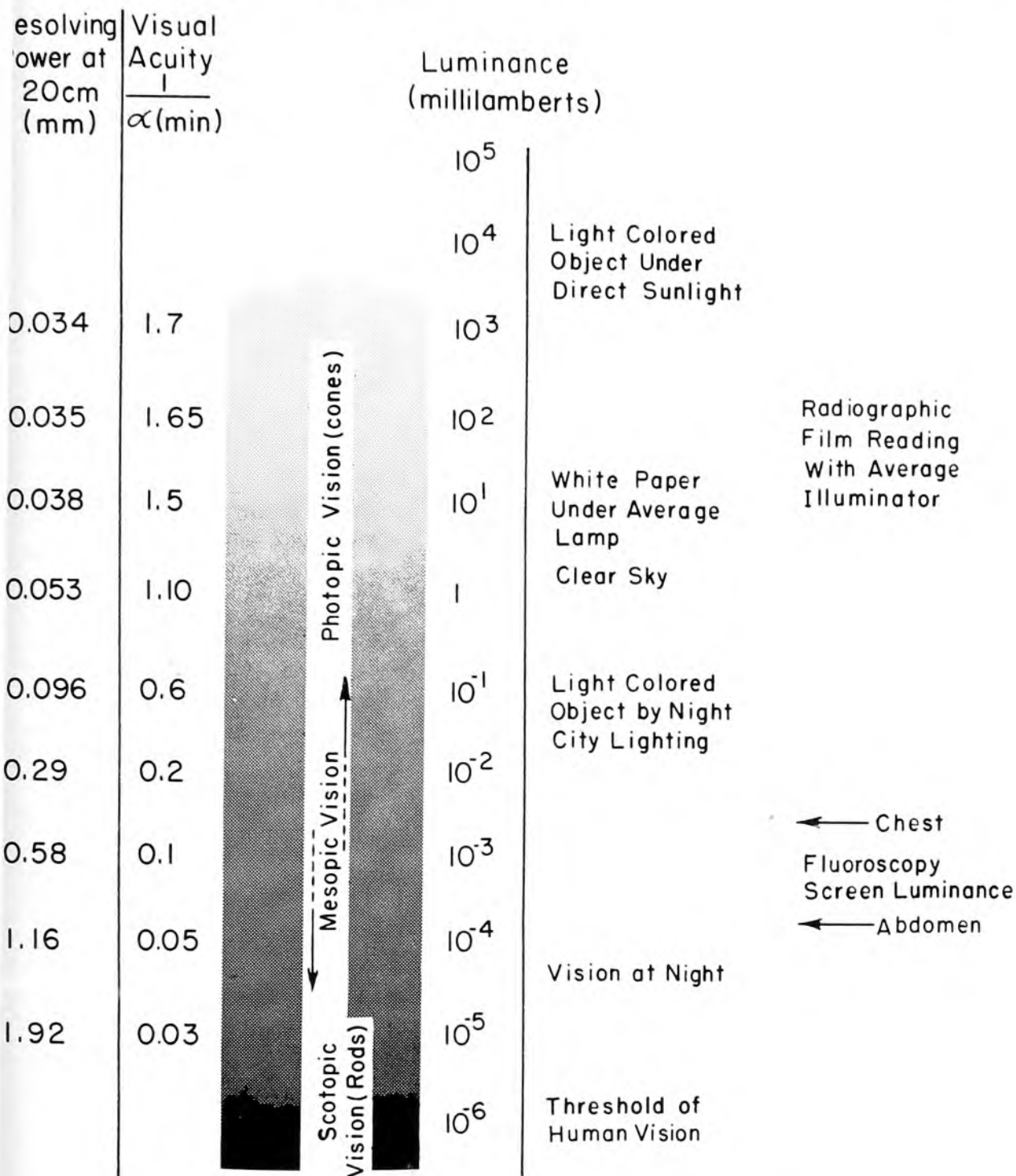


FIG. VIII-1. Scale of luminances commonly encountered.

use in certain photometric calculations. Figure VIII-1 gives a reference scale of luminances commonly encountered.

In normal vision the luminance of observed objects increases from a low value of approximately 10^{-2} millilambert (mL) ($1 \text{ mL} = 10^{-3} \text{ L}$) up to extreme values such as 10^8 and 10^9 mL, the luminance of the sun. In this range

of luminance human vision is said to be *photopic*. In photopic vision the retinal photoreceptors used are the cones, which provide high visual acuity, color vision, and relatively low sensitivity to light. If a "photopic" eye is placed in darkness its sensitivity to light increases, as shown in Fig. VIII-2. Photopic vision changes to a transitional state referred to as *mesopic* vision to reach the *scotopic* or night vision stage.

This increase in the sensitivity of the eye, which is referred to as *dark adaptation*, consists in the change from cone photoreceptor vision to the high sensitivity-low resolution rod vision. The dark adaptation curve (Fig. VIII-2) exhibits a discontinuity after approximately 5 to 8 min, which results from the transition of cone vision to rod vision. This discontinuity separates photopic vision from scotopic vision. It is interesting to note that if the test field is centered upon the fovea, where there are practically no rods, only the first portion of dark adaptation is observed. In a period of approximately 30 min the dark adaptation curve flattens out and after that period shows only a slight improvement of sensitivity with time. The fully adapted scotopic eye is approximately 10,000 times more sensitive than the photopic eye. (A test for scotopic vision is the demonstration of absence of color vision.)

The sensitivity of scotopic vision is extremely high. After a period of dark adaptation of several hours, the human eye is sensitive, under optimal conditions, to as few as 5 to 14 photons absorbed simultaneously in the retina (Ref. 1). In this respect the eye is about as sensitive as a photomultiplier tube. The range of sensitivity of the human eye is also remarkable. Vision encompasses luminances from 10^{-6} to over 10^{-6} mL. This sensitivity range is divided nearly evenly between photopic and scotopic vision.

Because of the unequal distribution of cones and rods in the retina, high-resolution photopic vision is carried out mostly in the center of the visual field (in the fovea), while the sensitivity of scotopic vision increases from the center of the visual field to about 20 degrees, where the rod population is denser. Thus, peripheral vision is more important in the dark-adapted eye, which is relatively blind in the central area where rods are scarce.

The ability of the eye to resolve detail can be expressed either as *visual acuity*, which is defined as the reciprocal of the angle, measured in minutes, that separates two contours barely recognized as distinct, or as *resolving power*, which is the distance between barely recognizable contours at a given viewing distance. (The concepts of visual acuity and resolving power are considerably more complex than these definitions imply. In this context the definitions are, however, adequate.) The maximum visual acuity of the human eye lies between 1.5 and 2. This maximum visual acuity is limited by the distance between the centers of adjacent cones in the middle of the fovea centralis, which is of the order of 2 to 2.3μ (Refs. 4 and 5).

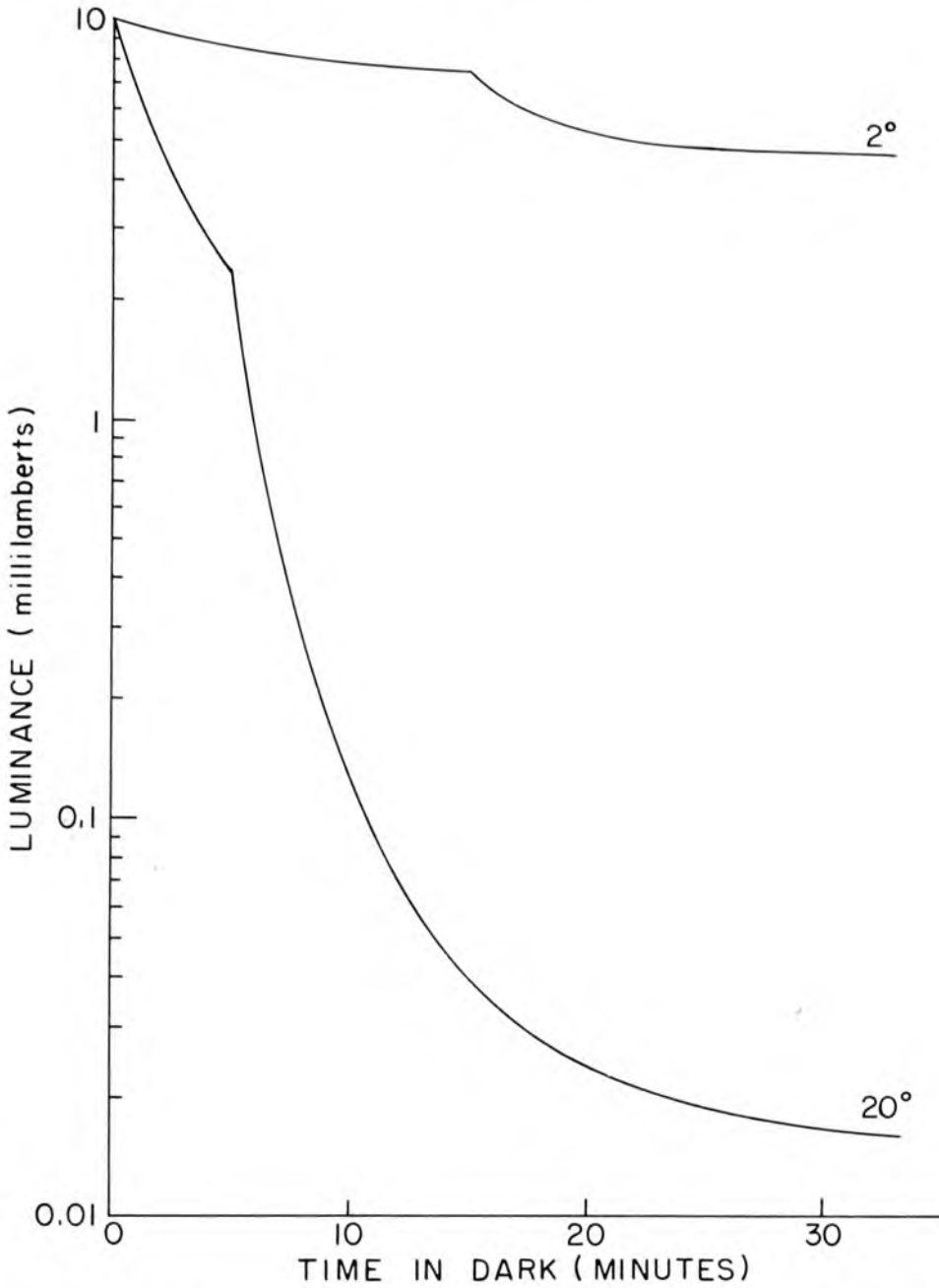


FIG. VIII-2. Dark adaptation as a function of time for two test fields of different areas centered on the fovea. Discontinuities can be regarded as transitions from photopic to scotopic vision. Note that for the small field (2 degrees) the break is minimal because of the scarcity of rods in the fovea. (Adapted from Hecht et al., Ref. 15.)

The visual acuity of the human eye decreases with decreasing luminance of the observed object to a low value of 0.03 for luminance of about 10^{-5} mL. A decrease in visual acuity with decrease in light intensity occurs also in eyes as different from those of man as insect eyes. This phenomenon is not well explained on the basis of present knowledge of the physiology

of the eye alone. Improvement in visual acuity with increased luminance cannot be explained by the contraction of the pupil in bright light and subsequent improvement in the optical system of the eye, because this phenomenon is also observed with artificial pupils, which do not contract and therefore do not provide for a change in optics for different light intensities. Furthermore, the occurrence of this phenomenon in insect eyes, which have a considerably different optical system from that of man, also invalidates this hypothesis. A partial explanation is that at high intensities the observer uses the central portion of the retina, which corresponds to high visual acuity, and as the intensity of light decreases, peripheral portions, which are known to provide lower acuity, are used. This is the explanation for the decrease in visual acuity in the transition from photopic to scotopic vision resulting from the lower resolution of the rod system as compared to that of the cone system. However, this explanation fails to take into account the continuous loss in visual acuity with decreasing light intensity in the scotopic region while the same region of the retina continues to be used (Ref. 4). A possible theory for variation in the visual acuity of the same portion of the retina for different illumination involves the assumption that more detecting elements are activated as the illumination level decreases (Ref. 6). Thus, at different illumination levels the same area of the retina would exhibit functional mosaics of photoreceptors having different resolutions (Ref. 1). Whether this theory is correct or not, the decrease in visual acuity in the lower luminance region, can certainly be explained on the basis of *statistical fluctuations in the small number of photons used by the retina in acquiring information* (Refs. 1 and 7).

Scotopic Visual Acuity and Statistical Fluctuations

In vision, information is transferred by means of light photons, and this information is extracted by the photoreceptors in the retina by absorption of photons. The maximum amount of information thus gathered, and therefore the maximum resolution obtainable, is limited by the statistical fluctuations in the number of photons absorbed by the retina. (See also section on "Statistical Nature of Radiologic Image," Chapter VI.) Intuitively it would seem that the luminous flux producing the retinal image is so intense that statistical fluctuations could not play an appreciable role in visual acuity. This concept is true in photopic vision but is not justified at the lower intensity levels of scotopic vision, as shown by the following calculations:

The number of photons entering the eye pupil per unit time during vision is equal to the luminous flux entering the pupil (a measure of the radiant energy flux entering the eye) divided by the energy carried by each light photon. The luminous flux F entering the eye pupil is given by a rearrangement of Equation (1):

$$F = B \times \omega \times A$$

where B is the luminance of the object viewed, ω is the solid angle subtended by the object at the eye, and A is the area of the pupil. If B is expressed in candela per square meter, ω in steradians, and A in square meters, F is expressed in lumens.

To find the number of light photons involved in the vision of a low luminance object, let us assume a radiologist is viewing at a distance of 20 cm a fluoroscopic screen that is perpendicular to the line of vision. Under typical conditions encountered in fluoroscopy the luminance B of the screen may be 10^{-3} mL or

$$B = \frac{10^{-2}}{\pi} \text{ cd/m}^2 = 3.183 \times 10^{-3} \text{ cd/m}^2.$$

The number of light photons emitted per 1 mm^2 of the screen and entering the pupil of the eye can be calculated as follows:

1. The solid angle subtended by 1 mm^2 of the screen surface at the pupil of the eye, placed at a distance of 20 cm, is equal to

$$\omega = \frac{1 \text{ mm}^2}{400 \text{ cm}^2} = 0.25 \times 10^{-4} \text{ sr.}$$

2. The illumination impinging upon the pupil of the eye of the observer under the above circumstances is

$$\frac{F}{A} = B \times \omega = 3.183 \times 10^{-3} \times 0.25 \times 10^{-4} = 0.8 \times 10^{-7} \text{ lx.}$$

(The lux (lx) is a unit of illumination of a surface equal to 1 lm/m^2) (Ref. 8).

3. The diameter of the pupil at such a low light intensity level is about 8 mm, which gives a pupillary area of about 50 mm^2 ; therefore the luminous flux entering the eye is

$$F = B \times \omega \times A = 0.8 \times 10^{-7} \times 50 \times 10^{-6} = 4 \times 10^{-12} \text{ lm.}$$

4. The lumen, a unit of luminous energy, equals under scotopic conditions approximately 5.73×10^{-4} watts (W) for light with a wavelength of 5070 \AA . Therefore the total energy flux impinging on the pupil is

$$4 \times 10^{-12} \times 5.73 \times 10^{-4} = 2.3 \times 10^{-15} \text{ W}$$

or

$$2.3 \times 10^{-8} \text{ erg/sec.}$$

5. The energy hn carried by each light photon ($\lambda = 5070 \text{ \AA}$) is 3.9×10^{-12} erg. Therefore the energy flux of 2.3×10^{-8} erg/sec is produced by a photon flux n on the pupil of

$$n = \frac{2.3 \times 10^{-8}}{3.9 \times 10^{-12}} = 6 \times 10^3 \text{ photons/sec.}$$

Not all the photons entering the eye reach the retina; a fraction is lost at the interface between the air and the cornea, and others are lost in the

optical system of the eye before reaching the retina. Of the photons reaching the retina, only about 10% are absorbed in the visual purple of the rods. Thus, probably only 1 to 5% of the photons impinging upon the pupil are utilized by the retina (Refs. 1 and 9). Of the 6×10^3 photons/sec entering the pupil in the above example, only 60 to 300 photons/sec may produce useful stimuli in the rods. This figure represents the rate at which the photons emitted by 1 mm² of the viewed screen are absorbed by the rods.

The statistical quality of the picture thus captured by the retina depends on the total number of photons absorbed, and this number is equal to the product of the photon flux and the period of time over which the eye is capable of accumulating information. In contrast to detectors such as photographic emulsions, which are capable of accumulating information practically indefinitely, the temporal summation of the human eye exposed to a flux of photons is limited to about 0.2 sec. For a period up to 0.2 sec the effect is proportional to the total number of photons received. This period of time during which summation of light effects occurs is referred to either as *retinal action time* (Ref. 1) or *storage time* of the eye (Ref. 7). After that period of time, however, the photon stimuli are no longer additive.

In the example previously discussed the maximum number of photons that determine the statistical quality of the image seen by the eye is equal to the photon flux r multiplied by the retinal action time, or 300 photons/sec/mm² \times 0.2 sec = 60 photons/mm². This number represents the photons absorbed by the retina under the described conditions out of the total number emitted by 1 mm² of a screen having a luminance of 10^{-3} mL. It is apparent that so small a number is appreciably affected by statistical fluctuations. Rose (Ref. 7) has demonstrated that the reduction in visual acuity of the human eye at low luminance levels can be completely explained by these statistical fluctuations.

Scotopic Vision and the Fluoroscopic Examination

The quality of a radiograph is not limited by the statistical fluctuations of the light photons affecting the retina. As shown in Fig. VIII-1, radiographs are usually examined at light levels which can be made as high as desirable to maximize visual acuity. Under such circumstances the statistical fluctuations of the light photons result in a loss of detail that is negligible with respect to either the statistical fluctuations of the x-ray photons responsible for the radiographic image or for the unsharpness produced by the screens or other factors affecting the quality of the radiographic image.¹

¹ The physical aspects of fluoroscopy and the relationship between the physiology of vision and the limitations of fluoroscopic examinations are thoroughly discussed in Chamberlain's historical Carman Lecture entitled "Fluoroscopes and Fluoroscopy" (Ref. 14).

In fluoroscopy the low luminance of the screen places it in the low scopic vision region (Fig. VIII-1), and the statistical fluctuations of the light photons utilized by the retina profoundly affect the quality of the examination. That the number of light photons utilized by the eye in a typical fluoroscopic examination is small was shown in the previous section.

STATISTICAL FLUCTUATIONS, CONTRAST, AND IMAGE PERCEPTIBILITY

The importance of statistical fluctuations in fluoroscopy has been described by Sturm and Morgan (Ref. 10).

The relation between the statistical fluctuations of photons forming a visual image and the dimension of the smallest perceptible structure of this image can be determined as follows (Ref. 7):

If an image is formed by an average number of quanta N , this number is subject to statistical fluctuations that are approximately equal to the square root of N . The minimum visually perceivable variation in the number of photons, ΔN , is proportional to \sqrt{N} :

$$\Delta N = k \sqrt{N}, \quad (2)$$

where k is the threshold signal-to-noise ratio of a human eye. The numerical value of k is, at this time, not firmly established, and measured k values of about 2 to 5 (Refs. 7, 11, and 12) have been reported. If it is assumed that $k = 2.5$, then a signal must be at least 2.5 times greater than the root mean square of the noise before it can be recognized by the eye (Ref. 7).

The minimum perceptible contrast (threshold contrast), C_{\min} is given by $(\Delta N/N) \times 100$. When $k = 2.5$, then

$$C_{\min} = \frac{\Delta N}{N} \times 100 = \frac{2.5}{\sqrt{N}} \times 100. \quad (3)$$

The quanta number N can also be expressed in terms of photon flux n (number of photons emitted per unit time per unit area), as follows:

$$N = nt \times A, \quad (4)$$

where t is the time of summation of photons and A is the area of the smallest perceptible image. In this case Equation (3) becomes

$$C = \frac{2.5}{\sqrt{nt} \times \sqrt{A}} \times 100. \quad (5)$$

The square root of the area of the smallest perceptible image, \sqrt{A} , is approximately equal to the linear dimension of this image, and

$$\sqrt{A} = \delta = \frac{2.5}{C \sqrt{nt}} \times 100, \quad (6)$$

where δ is the linear dimension of the smallest perceptible image with a contrast C . In this equation, n is the smallest value reached by the x-ray or light photon (or in certain cases, particles) flux (particle fluence) in the formation of the visual image. Sturm and Morgan (Ref. 10) have demonstrated good agreement between visual performance measured under fluoroscopic conditions and the linear dimensions of minimum perceptible images predicted by calculation for different contrasts.

If there is multiplication of photons at some stage of the examination, such as occurs in the conversion of x-ray photons into light in an x-ray screen, the lower value of the photon flux determines the limit of the statistical perceptibility of the examined object. It should be noted that if, in a given image-forming system, the photon flux passes through a series of stages of high and low values, the lowest value of the flux determines the maximum image perceptibility allowed by statistical fluctuations.

The stage of the examination at which the statistical information reaches its lowest level is called *quantum sink* (Ref. 13). In practice each stage contributes to the statistical degradation of the image, and usually the image perceptibility is worse than predictable by the lowest value of the photon flux. If at some stage of an image-forming system the photon flux is much lower (for instance, by a factor of 10) than at any of the other stages, then the statistical fluctuations of the other stages can be neglected and the statistical image quality is completely determined by the low stage (quantum sink).

Equation (6) applies to radiography as well as to fluoroscopy. In fluoroscopy the time t is the retinal action time, while in radiography it is the exposure time of the film. In radiography the lowest photon level occurs, as shown in Fig. VIII-3, with the absorption of x-ray photons in the screen. After that stage there is photon multiplication, when the energy of the x-ray photons is converted into light in the screen. In radiography statistical fluctuations of photons do not play an appreciable role because the resolution observed on the radiograph is much inferior to the limitations imposed on the system by statistical fluctuations. It is possible, however, that with fast radiographic screens the subsequent lowering of the number of photons used may result in deterioration of the quality of the roentgenographic image because of statistical fluctuations (Chapter VII, section on "Radiographic Mottle").

Statistical Fluctuations in Fluoroscopy: Comparison with Radiography

In fluoroscopy, photon fluctuations play a determining role in limiting the minimum perceivable detail; in radiography they do not. This difference between fluoroscopy and radiography results from the considerably smaller number of photons both at the x-ray and light stages utilized in the formation of the fluoroscopic image. The following example illustrates this difference:

Assume (1) a radiographic examination of a 25-cm thick abdomen carried out with the following technique:

X-ray tube voltage: 80 kV_p
 Tube current times exposure time: 100 mAs
 Focus-film distance: 36 in.
 Exposure: 1 mR on the screen,

and (2) a fluoroscopic examination of the same part carried out as follows:

X-ray tube voltage: 80 kV_p
 Tube current: 3.3 mA
 Exposure time: 30 sec
 Tube current times exposure time: 100 mAs
 Exposure rate: 2 mR/min on the screen.

The dose of radiation delivered to the patient is the same in Examinations (1) and (2).

The radiographic examination results from approximately 30×10^6 photons/cm² impinging on the screen-film combination. This number of photons per unit area corresponds to an exposure of 1 mR (Chapter XI) which produces an optical density of 1 on standard-speed x-ray film exposed with two medium-speed intensifying screens (Fig. VI-33). The x-ray photons are absorbed in the screens and converted to light photons, as shown in Fig. VIII-3. The light photons in turn are completely absorbed in the film.

During the fluoroscopic examination the same total number of photons impinges per square centimeter on the fluoroscopic screen, however, because of the limited temporal summation of the eye, the fluoroscopic image at any time during the examination consists only of the photons accumulated during the storage time of the eye of 0.2 sec. Thus, in the fluoroscopic examination the number of x-ray photons/cm² impinging on the screen which may contribute to the formation of the image is given by

$$\text{photon flux} = \frac{30 \times 10^6}{30 \text{ sec}} \text{ photons/cm}^2 = 10^6 \text{ photons/cm}^2/\text{sec},$$

and the total number of photons accumulated during the storage time of the eye (0.2 sec) is 2×10^5 photons/cm² (Fig. VIII-3).

Of the 30×10^6 photons/cm² impinging on the screen-film combination, approximately 30%, or 1×10^7 photons/cm², are absorbed in the screen and converted into light photons. The light photons escaping the screens are completely absorbed in the photographic emulsion, and this energy is utilized in producing photographic grains in the emulsion. On the average, 200 light photons are required to render one photographic grain developable, and there is a drop in the number of information-carrying quanta between the screens and the photographic emulsion. This drop, however, is not

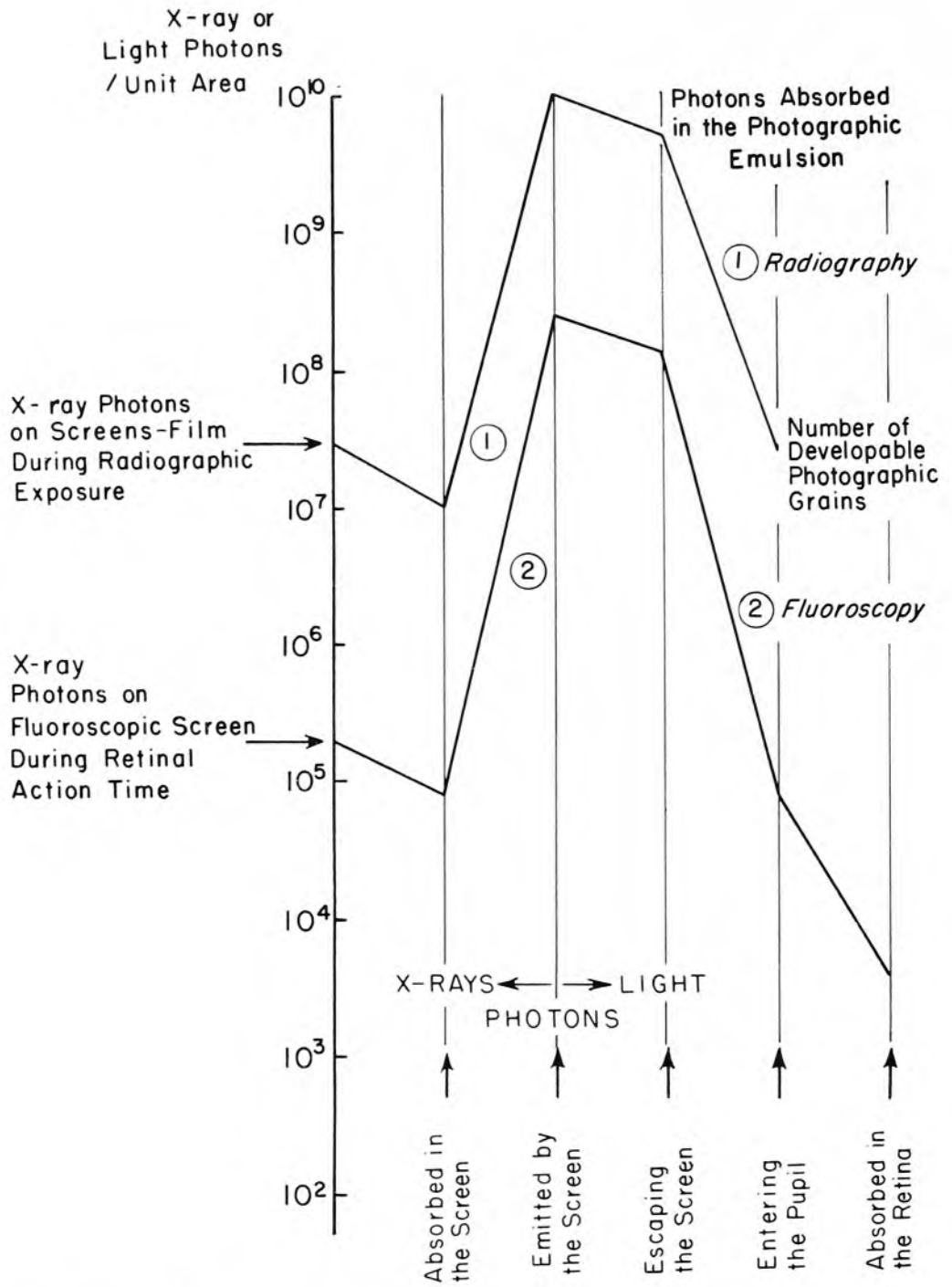


FIG. VIII-3. Quantum levels in the various stages of image conversion.
 1 radiography
 2 fluoroscopy

sufficient to use up the quantum gain achieved in the screens by the conversion of x-ray photons into light photons, and the quantum sink occurs in radiography at the stage of the absorption of x-rays in the screens. Thus the statistical quality of the radiographic image, under the conditions of this discussion is determined by 1×10^7 photons/cm².

In fluoroscopy, only about 1 photon out of 50,000 provided by the fluoroscopic screen is utilized in the retina of the observer, mostly because of the small solid angle subtended by the pupil of the eye at the screen, and also because only a small percentage of the light photons entering the pupil are utilized by the retina (see Section 2). This loss of photons exceeds the photon multiplication achieved in the screen, and in fluoroscopy the quantum sink occurs in the retina of the observer. Of the 2×10^5 photons/cm² impinging on the fluoroscopic screen per 0.2 sec, only 4×10^3 photons/cm² are utilized in the formation of the image, and this number determines the statistical quality of the examination. Thus, for the same dose of radiation delivered to the patient, the quantum sinks are:

For radiography, 1×10^7 quanta/cm²

For fluoroscopy, 4×10^3 quanta/cm².

Statistical Fluctuations and Image Perceptibility in Fluoroscopy

The x-ray apparatus used in fluoroscopy is capable of resolution similar to that of a radiographic system. Although the fluoroscopic screen, because of greater thickness and larger particle size (Table VI-2), contributes greater unsharpness than the radiographic screen, the two apparatus are not too different in resolution capabilities because in the majority of examinations, the most important component of unsharpness is contributed by the large size of the focal spot of the tube used (Table VII-5). However, in most fluoroscopic examinations the resolution achieved is considerably lower than in radiographic examinations because of photon statistical fluctuations which limit the resolution of the image obtained, rather than unsharpness inherent in the apparatus.

The limits imposed by photon fluctuations on the maximum resolution achieved in fluoroscopy can be deduced from the measured visual acuity at fluoroscopic luminance levels. The fluoroscopic luminance range extends from 10^{-4} to 10^{-2} mL, with corresponding visual acuities from 0.05 to 0.20. If the screen is viewed from a distance of 20 cm, the corresponding resolving power varies from 1.16 to 0.3 mm corresponding approximately to 0.6 to 3 lines/mm resolved. It should be noted that the better resolving power figure corresponds to a particularly high luminance level encountered only in the fluoroscopy of thin parts. A comparison of these figures with the resolution capabilities of the screens used in fluoroscopy shows that in most of the fluoroscopic luminance range, statistical fluctuations limit, the quality of the image, and that only at particularly high luminance levels do

statistical fluctuations allow resolutions to equal the capabilities of the screens.

REFERENCES

1. PIRENNE, M. H.: *Vision and the Eye*. London, Chapman and Hall, 1948.
2. ENOCH, J. N.: Private communication.
3. Methods of Evaluating Radiological Equipment and Materials. *International Commission on Radiological Units and Measurements (ICRU)*, NBS Handbook 89. Washington, D.C., U.S. Government Printing Office, 1962.
4. O'BRIEN, B., and MILLER, N. D.: *A Study of the Visual Acuity in the Central Retina*. Wright Air Development Center Technical Report #53-198.
5. HECHT, S., and MINTZ, A. U.: The visibility of single lines at various illuminations and the retinal basis of visual resolution. *J. Gen. Physiol.* 22:593, 1939.
6. HECHT, S.: The relation between visual acuity and illumination. *J. Gen. Physiol.* 11:255, Jan. 1928.
7. ROSE, A.: Sensitivity performance of the human eye on an absolute scale. *J. Opt. Soc. Amer.* 38:196, 1948.
8. LEGRAND, Y.: *Light, Colour and Vision*. New York, Wiley, 1957.
9. ROSE, A.: Quantum effects in human vision. *Adv. Biol. Med. Physics* 5:211, 1957.
10. STURM, R. E., and MORGAN, R. H.: Screen intensification systems and their limitations. *Amer. J. Roentgen.* 62:617, 1949.
11. OOSTERKAMP, W. J.: Image intensifier tubes. *Acta Radiol.*, Suppl. 116:497, 1954.
12. WEBSTER, A. W., and WIPFELDER, R.: Limitations of Combined Image Amplifier-Television Systems for Medical Fluoroscopy. Institute of Radio Engineers Transactions on Biomedical Electronics, 150-155, 1962.
13. NIKLAS, W. S.: "Conversion Efficiencies of Conventional Amplifiers," in *Technological Needs for Reduction of Patient Dosage from Diagnostic Radiology*, ed. by Janower, M. L. Springfield, Ill., Thomas, 1963.
14. CHAMBERLAIN, W. E.: Fluoroscopes and fluoroscopy. *Radiology* 38:383, 1942.
15. HECHT, S., HAIG, C., and WALD, G.: The dark adaptation of retinal fields of different size and location. *J. Gen. Physiol.* 19:321, 1935.

(IX)

X-RAY IMAGE INTENSIFICATION

FLUOROSCOPIC X-RAY IMAGE INTENSIFICATION

As shown in Chapter VIII, the improvement of the perceptibility of images in fluoroscopy can only be achieved by raising the level of the quantum sink in the image, as Sturm and Morgan have demonstrated (Ref. 1). This can be accomplished by increasing the flux of x-ray photons used in the examination. However, this solution is unacceptable because it means increasing the always undesirable exposure of the patient to radiation.

Another solution to the problem is apparent from Fig. VIII-3. The quantum sink in the examination occurs with the absorption of photons by the retina. The low value reached by the photon level at the retina results from the combination of two factors: (1) loss of photons in the eye and, mainly, (2) loss of photons between the screen and the eye pupil resulting from the small value of the solid angle subtended by the screen at the pupil. These losses more than use up the photon multiplication achieved when x-ray photon energy is converted into light photons in the fluoroscopic screen. While Factor (1) cannot be altered, the desired improvement of the statistical quality of the image can be achieved by raising the number of light photons per solid angle that reach the pupil. This can be accomplished by increasing the luminance of the image supplied by the screen. The statistical quality of the image is thus improved until the low level of the light photons exceeds the number of x-ray photons absorbed in the screen. At that point the latter number becomes dominant because of its fluctuations, and further multiplication of light photons reaching the retina does not affect appreciably the statistical quality of the image.

The calculation of the light amplification required for a one-to-one correspondence between the number of x-ray photons absorbed in the screen and the number of light photons absorbed in the retina includes a certain number of parameters the exact value of which is not well determined. With the parameters shown in Fig. VIII-3 the value calculated for this gain is about $\times 20$. Sturm and Morgan (Ref. 1) suggest that no improve-

ment in usual performance is to be expected beyond a gain factor of 30 to 50 over the luminance of a Patterson B-2 fluoroscopic screen (E. I. du Pont de Nemours & Co., Inc.).

Although no improvement can be expected in statistical image perceptibility from raising the photon flux in fluoroscopy by a factor greater than approximately 20, it is still desirable to raise the luminance to a greater value for two reasons: (1) If sufficient luminance can be achieved, fluoroscopy can be carried out without dark adaptation. The luminance gain required for bringing a dim fluoroscopic image to the photopic vision level is about $\times 1000$. (2) If this condition is fulfilled, the "cone" photopic central vision would allow better acuity than peripheral "rod" scotopic vision.

The above discussion shows that the statistical quality of a fluoroscopic examination can be improved without an increase in the dose of radiation delivered to the patient by (1) raising the light flux reaching the retina by a factor of at least 20 and (2) further increasing the luminance of the image to the photopic vision level. The improvement in detail perceptibility thus achieved is limited by the statistical fluctuations of the x-ray photons absorbed in the screen. It is interesting to note that the concept of raising the luminance of the x-ray screen in fluoroscopy, developed on the basis of retinal physiology (Ref. 2), was suggested well before Sturm and Morgan (Ref. 1) demonstrated on the basis of Rose's work (Ref. 3) that image perception in fluoroscopy was in fact limited by statistical fluctuations of light photons and established quantitatively what gain in image perceptibility could be achieved by raising the light photon flux emitted by a fluoroscopic screen.

FLUOROSCOPIC X-RAY IMAGE INTENSIFIERS

The luminance of a fluoroscopic screen cannot be increased 1000-fold, or even much less, by intrinsic means for the following reason: The fluoroscopic screen converts the x-ray image into an optical image composed of a greater number of photons per unit area. This multiplication of photons in the conversion process is possible because the energy carried by each x-ray photon is sufficient to create, under normal conditions of fluoroscopy, approximately 20,000 light photons having a wavelength corresponding to the fluorescence of the screen. Fluoroscopic screens, however, exhibit a conversion efficiency of only 10 to 15%, and the absorption of an x-ray photon in the screen results in the emission of only about 2000 to 3000 light photons. Even if a 100% efficient screen could be devised, its luminance would be increased by only a factor of about 7 to 10 over conventional screens. Thus, if a greater gain in photon multiplication is required, the fluoroscopic screen must be replaced by a different image converter, into which energy is fed in addition to the x-ray beam to permit the desired photon multiplication. Such an image converter is referred to as an *x-ray image intensifier*, and it is

STOPPED

Reading here -

see christensen

go to ch. XI

defined as "a device which converts instantaneously an x-ray pattern into a corresponding light image of higher energy density" (Ref. 4).

The replacement of a fluoroscopic screen by an x-ray image intensifier is made to fulfill two purposes: (1) To provide the receptors of the retina of the observer with an image having a photon flux greater than the lowest value reached at any stage of the system that converts the x-ray image into light. Under these circumstances, for each x-ray photon absorbed in the sensing detector of the image converter, more than one light photon reaches the photoreceptors in the retina, and the statistical quality of the image obtained depends only on the fluctuations of the absorbed x-ray photons. (2) To supply an optical image having a luminance sufficiently high to place it in the photopic vision range of the observer.

It should be noted that although all currently used x-ray image intensifiers attempt to accomplish both purposes, it is not inconceivable that an intensifier could be designed to fulfill only the first purpose; also, Purpose (2) could be fulfilled without achieving Purpose (1).

X-ray image intensifiers can be classified into the following categories according to the physical method applied in achieving intensification: (1) x-ray image intensifier tubes or light amplifier tubes, (2) x-ray image scanning systems (television systems), and (3) solid-state x-ray intensifiers.

In many instances x-ray image intensification is accomplished in more than one step. For example, the optical image supplied by an x-ray image intensifier tube may be further intensified by the use of either a light amplifier tube or an image scanning system embodying a television chain, as shown in Fig. IX-1.

X-Ray Image Intensifier Tubes

The device most widely used in x-ray image intensification is the x-ray image intensifier tube, which is an image converter sensitive to x-rays. An image converter is a device that converts a photon image into another photon image of higher energy density. Vacuum tube image converters were described as early as 1934 (Ref. 5). Image converters have been used during World War II in the form of "snooper-scopes" for the observation of the enemy at night by converting an infrared image into a visible image of higher energy density. Light intensifier tubes have been widely used in astronomy in the observation and photographic recording of celestial bodies of low visibility. A neutron image converter was patented in 1942 (Ref. 6). One of the first applications of this principle for fluoroscopic image intensification was made by Langmuir (Ref. 7). In 1948, Coltman (Ref. 8) described an x-ray image intensifier tube the principle and design of which are embodied with minor alterations in modern tubes.

An x-ray image intensifier tube can be defined as "a vacuum tube containing an input screen which converts an x-ray pattern into an electron pattern, and in which the electrons are accelerated and focused

IMAGE-TUBE X-RAY IMAGE INTENSIFIERS

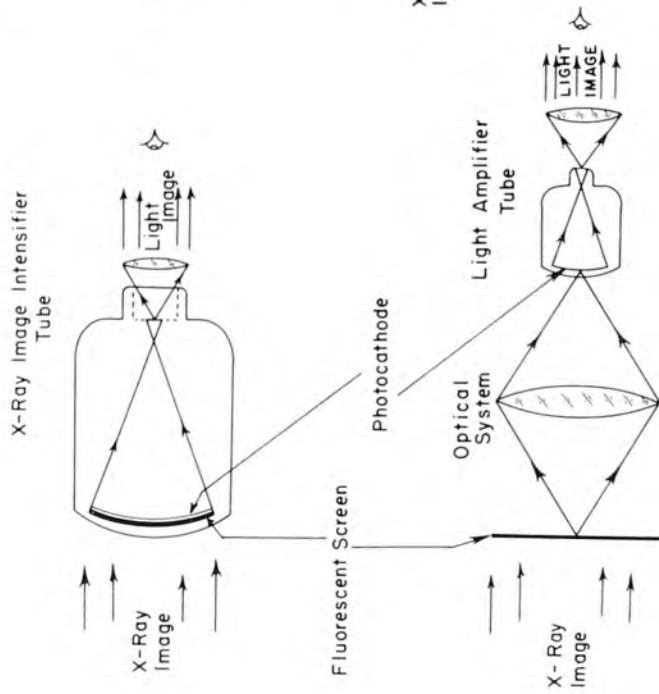
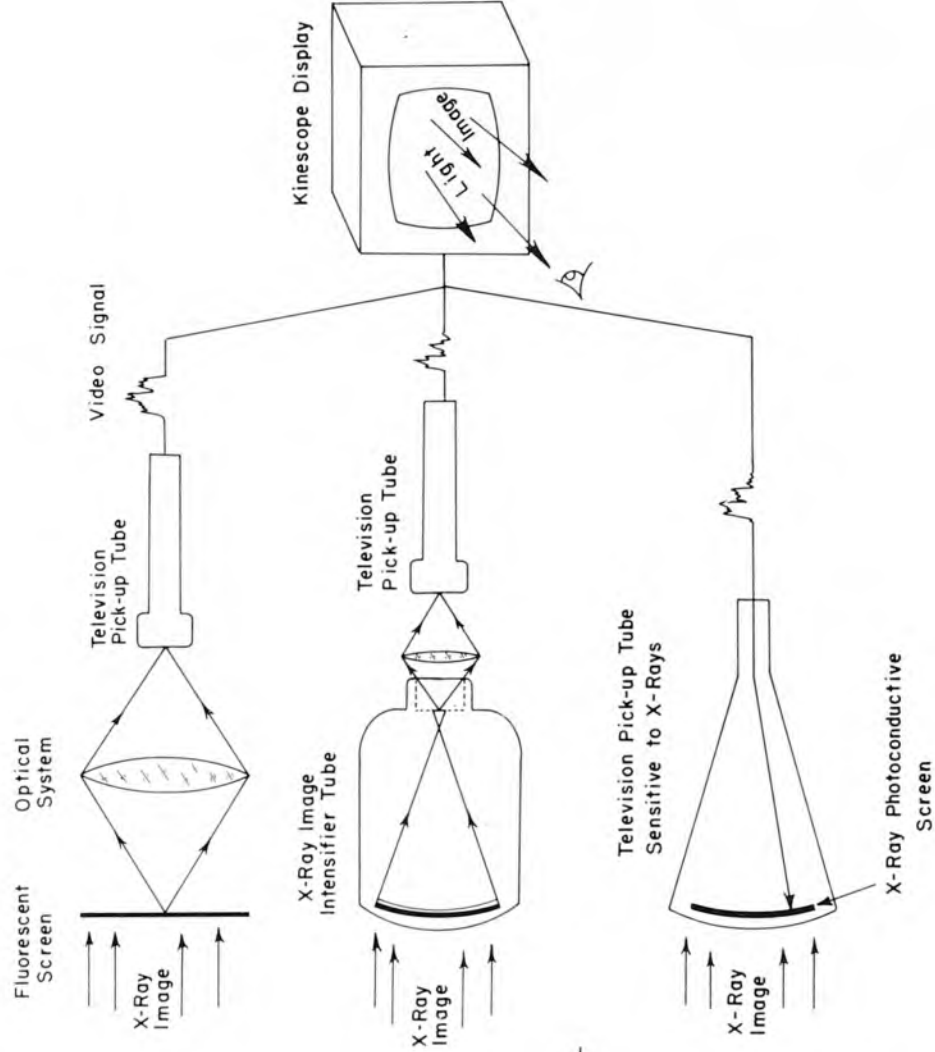


IMAGE SCANNING SYSTEM



SOLID STATE X-RAY IMAGE INTENSIFIER

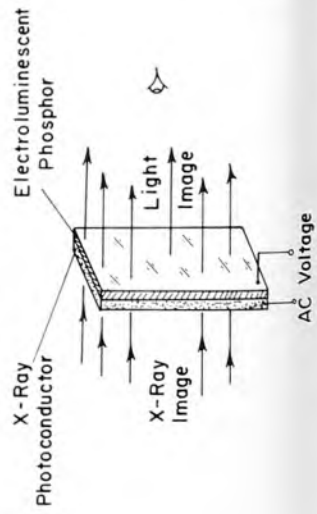


FIG. IX-1. X-ray image intensifier systems.

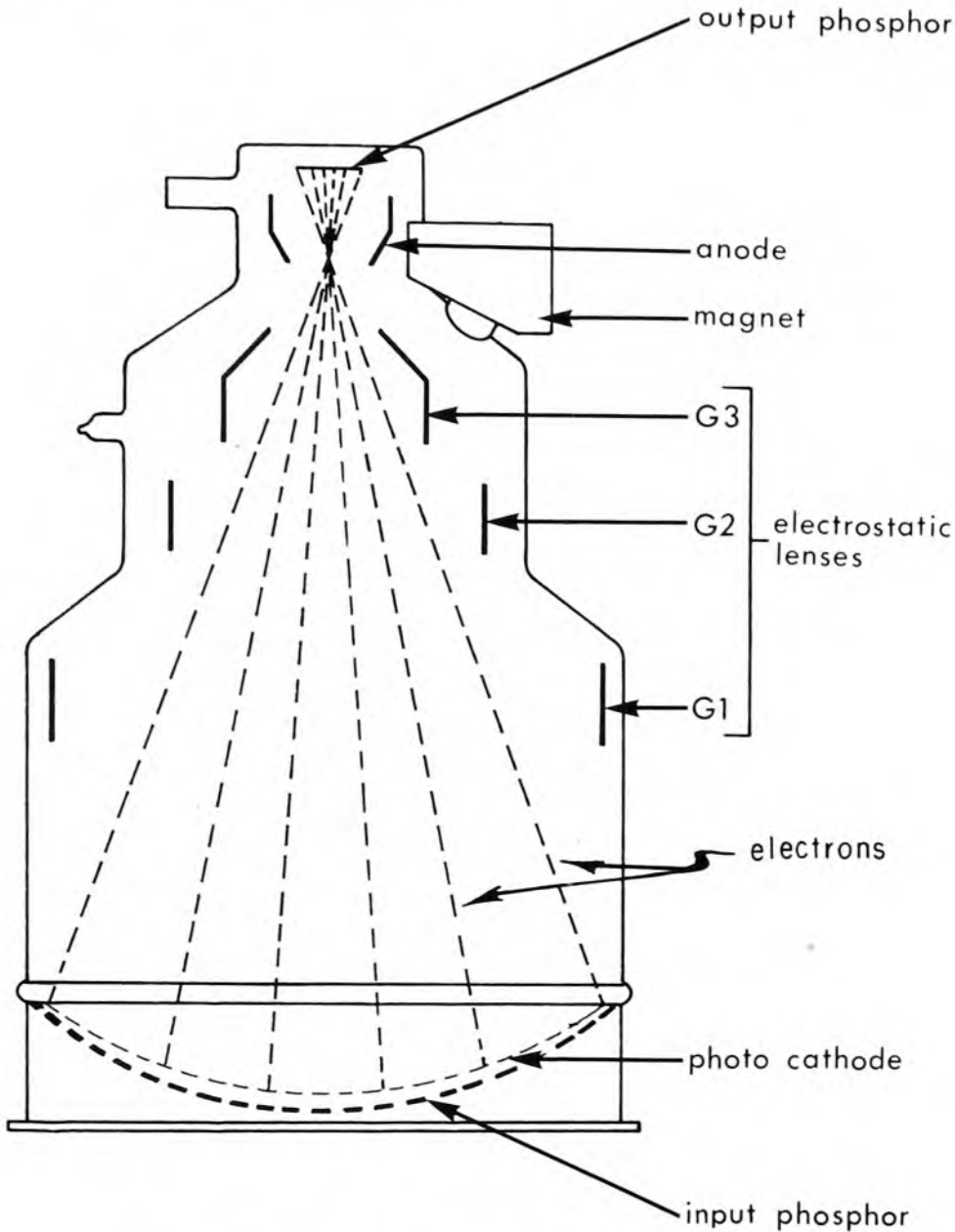


FIG. IX-2. Diagram of x-ray image intensifier tube.

(Courtesy of Machlett Laboratories, Inc.)

onto an output screen which converts the electron pattern into a light image of higher intensity." (Ref. 4). Basically, the x-ray image intensifier tube is a light intensifier tube optically coupled with a fluorescent screen which converts the x-ray image into a light image.

Figure IX-2 shows the cross section of a typical x-ray intensifier tube. The device is made of an evacuated glass envelope containing the following elements: (1) a composite input screen-photocathode, (2) an electrostatic electron lens system, (3) an anode, and (4) an output screen.

The input screen may be deposited on a concave, thin aluminum backing

and is usually composed of zinc cadmium sulfide crystals embedded in a resin matrix. The screen, the purpose of which is to convert x-ray energy into light, is very similar in characteristics to a conventional x-ray fluoroscopic screen (Table VI-2), and serves as substrate for a photocathode. Photocathodes are commonly made of alkali or alkali metals (for example, Sb-CsO and Sb-K-Na-Cs) (Ref. 9). A barrier layer is sometimes provided between the phosphor and the photoemitter to prevent the vapors of the alkali metals (such as cesium), which are commonly used in activating photoemitters, from deactivating the fluorescent screen (Ref. 9).

The optical image formed by the fluorescent screen is converted by the photocathode into an electron image. The electrons forming this image are accelerated between the photocathode and the anode by a potential difference of approximately 30,000 V and are electrostatically focused by the electron lens system to form on the viewing screen an image smaller than the radiographic image. The electron image is converted into a visible image in the viewing screen. The latter is a fluoroscopic screen containing the same phosphor as the input screen (zinc cadmium sulfide), but of smaller particle size because the smaller diameter of the viewing screen requires a finer-grain phosphor for a given resolution. The screen is aluminized to increase its conversion efficiency, to prevent the accumulation of electric charges, and to protect the phosphor from poisoning by alkali metal vapors. The above description applies to one particular type x-ray image intensifier tube only, and other designs have been used; for example, some intensifiers have different electron lens systems.

The diameter of the x-ray image that can be observed by the intensifier is determined by the diameter of the input screen. This diameter in most commonly used tubes varies from 5 to approximately 8 in., although tubes with a field of about 12 in. have been also constructed. The diameter of the viewing screen is usually 1 in. (Fig. IX-3), although smaller output diameter tubes have been built, and at least one image intensifier embodies an output screen 3 in. in diameter.

Intensification Factor—Brightness Gain. The intensification factor of an x-ray image intensifier is usually expressed as *brightness (luminance) gain*, which is the luminance of the viewing screen of the intensifier while its input screen is exposed to a given flux of x-rays, divided by the luminance of a Patterson B2 fluoroscopic screen (E. I. du Pont de Nemours & Co., Inc.) exposed to an identical x-ray flux. The brightness gains produced by typical commercial x-ray intensifier tubes vary from about 1000 to 6000.

Brightness gain results from two unrelated factors: (1) *flux gain* G_F , and (2) *minification gain* G_M .

Flux gain G_F is produced in the tube by acceleration of the electrons between the photocathode and the anode. The absorption of the accelerated electrons in the output screen results in the emission by the screen of a greater number of light photons than were necessary to generate the elec-

trons in the photocathode. In a typical x-ray image intensifier this gain results in a brightness gain of about 50.

The electrons formed at the photocathode are not only accelerated in the tube but are also focused onto the output screen by means of an electrostatic lens thereby forming an image of reduced size with respect to the input screen. The number of electrons striking the viewing screen per unit area is greater than the number of electrons emitted by the photocathode per unit area by a factor called the minification gain G_M . This factor is equal to the ratio of the areas of the two screens:

$$G_M = \frac{A_i}{A_v} = \left(\frac{D_i}{D_v}\right)^2, \quad (1)$$

where A_i and A_v are the areas of the input and viewing screens, respectively, and D_i and D_v are their respective diameters. For example, an intensifier tube with an input screen 8 in. in diameter and an output screen 1 in. in diameter, has a minification gain of $(8/1)^2 = 64$.

It should be noted that a gain in luminance by minification cannot be achieved by reducing the size of an optical image by means of an optical system, for example by a lens. This difference between optical and electronic minification can be explained as follows: In light optics, according

FIG. IX-3. Two different diameter (Machlett Dynascope 6-in. and 9-in.) x-ray image intensifier tubes. Photograph shows output screens of tubes. (Courtesy of Machlett Laboratories, Inc.)



F = luminous flux
 B, B' = luminance
 $F = B \omega df = B' \omega' df'$
 since $\omega df = \omega' df'$
 $B = B'$ luminance unchanged

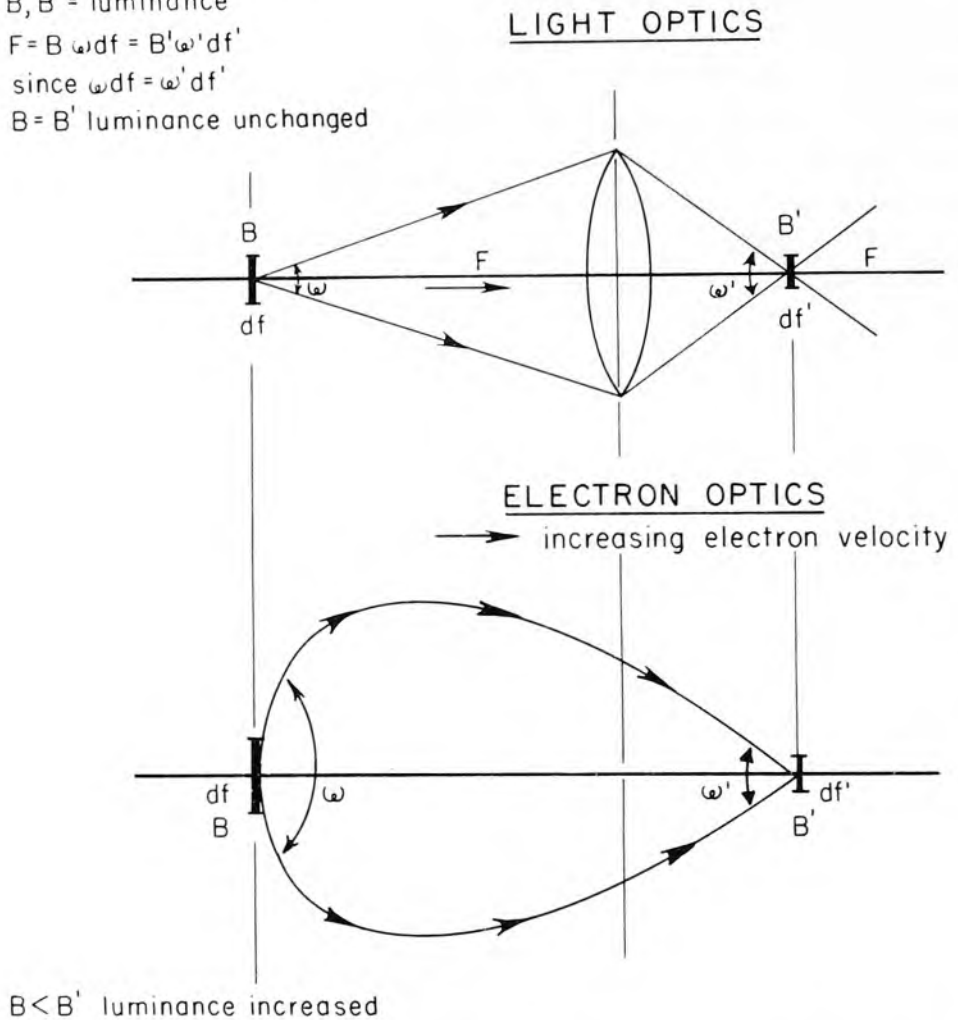


FIG. IX-4. Comparison of a light optics system (luminance B' of image is equal to luminance B of object) with an electron optics system (luminance B' of minified image is greater than luminance B of object). (Adapted from Teves and Tol, Ref. 10.)

to Abbe's law, the luminance of an observed object remains unchanged if an optical system is introduced between the observer and the object, however, only if the object and the image are located in a medium of uniform refractive index. If the refractive index on the object side is lower than on the image side, there may be gain in brightness. This, in fact, is the situation in the image intensifier. In electron optics the quantity representing the index of refraction is determined by the velocity of the traveling electrons. Because of the acceleration of the electrons between the photocathode and the output screen, the index of refraction between the two electrodes can be considered as continuously changing to reach a maximum value before the electrons are stopped in the output screen (Ref. 10).

The trajectories of the continuously accelerating electrons are curved, and

a large percentage of the electrons emitted by a surface element df are collected into a solid angle ω' (Fig. IX-4). Thus, in an image intensifier, minification gain is achieved by the focusing of electrons by an electric field, and both flux gain and minification gain are due to the effect of an accelerating electrostatic field (Ref. 10).

An important characteristic of the minification gain achieved in an x-ray image intensifier tube is, that although this factor increases the luminance of the viewing screen, it does not affect the number of quanta (particles or photons) per resolution element at any stage of the image-forming system. Thus, gain by minification cannot improve the statistical quality of the image supplied by the intensifier.

The total luminance gain G accomplished by an x-ray intensifier tube is equal to the product of the flux gain and the minification gain:

$$G = G_F \times G_M. \quad (2)$$

In a typical tube with an input screen diameter of 8 in., an output screen diameter of 1 in., and a flux gain equal to 50, the total luminance gain, with the aid of Equation (1), is given by $G = 50 \times (8/1)^2 = 3200$.

It is apparent from the above discussion that flux gain and minification gain contribute in different ways to the performance of an x-ray intensifier tube, and that the parameter "brightness gain" can be misleading. Indeed, there can be a difference in the imaging qualities of two x-ray intensifier tubes producing the same brightness gain if one tube achieves its total gain by a greater contribution of flux gain than minification gain.

This difficulty can be overcome by describing an intensifier by its *conversion efficiency*, which is equal to the ratio of light photons emitted by the viewing screen to the number of x-ray photons incident on the input screen (Ref. 9). This ratio is a measure of the improvement of the quantum flux in the image-forming system. The usefulness of brightness gain by minification lies in bringing the luminance of the fluoroscopic image from the scotopic to the photopic region of vision.

X-Ray Image Intensifier Tube Performance. The intrinsic resolution (exclusive of quantum fluctuations) of x-ray image intensifier tubes is mainly determined by the thickness and structure of the input screen and by the quality of the electron optics. In some tubes, the input fluorescent screen is made thinner than conventional fluoroscopic screens in an attempt to improve resolution at the expense of opacity of the screen to x-ray photons. Good electron optics are easier to achieve in smaller-diameter tubes. In large-diameter tubes resolution decreases at the edges owing to inadequate electron focusing. In these larger tubes, a compromise is usually achieved by keeping the resolution throughout the surface of the tube constant, though lower than for a smaller-diameter tube. In other tubes peripheral distortion is tolerated to gain increased central resolution. Oosterkamp

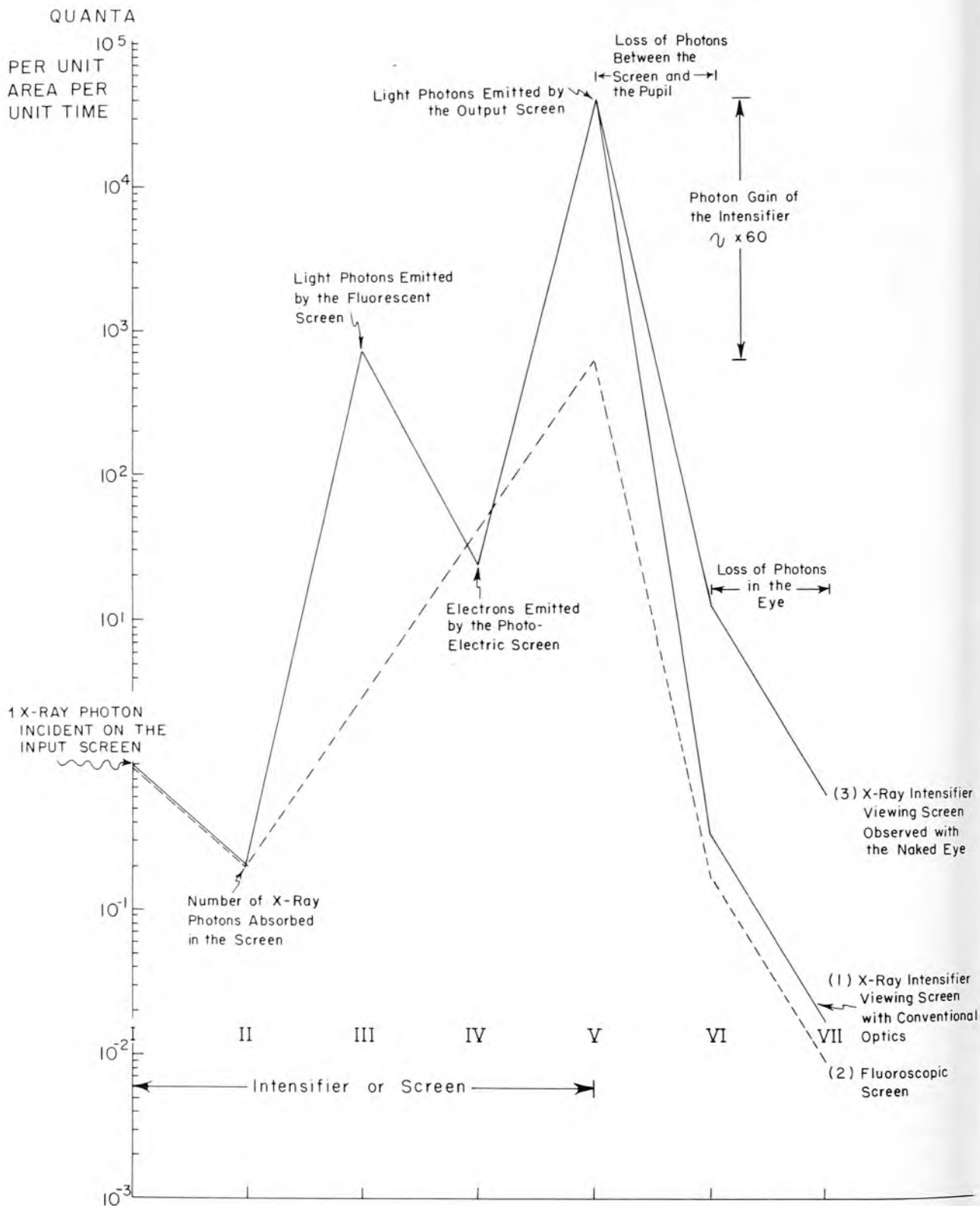


FIG. IX-5. Quantum levels reached in different stages of image conversion in three different systems.

- 1 x-ray image intensifier tube fitted with conventional magnifying optics
 - 2 fluoroscopic screen
 - 3 output screen of x-ray image intensifier tube observed with the naked eye
- (Adapted from Niklas, Ref. 9.)

(Ref. 11), for a particular tube, quotes a resolving power of about 0.4 mm, which corresponds to a resolution of about 2.5 lines. Generally the resolution of modern x-ray intensifier tubes is of the order of 2 lines/mm, which is a little inferior to that of fluoroscopic screens.

Dark adaptation is unnecessary for fluoroscopy aided by an x-ray image intensifier tube because the gain of most currently used tubes exceeds 1000, which is sufficient to bring most fluoroscopic images into the photopic region of vision.

The statistical fluctuations of an image supplied by an x-ray intensifier tube are determined by the quantum levels at the different stages of the conversion of the x-ray image into the intensified optical image (Refs. 1, 9, 11-13). Figure IX-5 shows a comparison between the fate of a single x-ray photon impinging on an x-ray image intensifier tube and on a conventional fluoroscopic screen. In this study (Ref. 9) the assumption is made that the fluorescent screen of the image intensifier and the fluoroscopic screen have identical x-ray absorption properties. This assumption is justified by the fact that both the thickness and the composition of the input fluorescent screen in a typical x-ray intensifier tube (Table VI-2) are nearly identical to those of a conventional fluoroscopic screen. Figure IX-5 shows that the number of light photons emerging from the viewing screen of the x-ray intensifier tube is approximately 60 times greater than that escaping the fluoroscopic screen. This figure represents the flux gain of the tube. It should be noted that at no time in this study is the minification gain taken into account because this factor does not influence photon statistics. Between the viewing screen of the x-ray intensifier tube fitted with conventional optics (Graph 1) and the pupil of the eye, there is a drop of light photons considerably greater than that observed in the fluoroscopic screen (Graph 2), with the result that at the pupil of the eye (Stage VI), the photon flux supplied to the pupil by the intensifier is only twice that supplied by the conventional fluoroscopic screen. This difference between the x-ray intensifier fitted with an optical system and the fluoroscopic screen observed with the naked eye is due to the following:

When a fluoroscopic screen is observed by the naked eye at a distance of approximately 20 cm, approximately one out of every 3000 photons emitted by the screen reaches the eye. The image intensifier supplies a considerably minified picture of the screen, and the latter must be observed by means of an optical system with a long optical path (approximately 100 cm) (Ref. 9). The use of the optical system results in a considerable loss of light photons, and only one photon per 80,000 emitted by the viewing screen reaches the pupil of the eye. *This loss of light photons in the optical system all but erases the flux gain achieved by the image intensifier.* Of course, if the output of the image intensifier were observed with the naked eye, the flux gain would be retained, as shown in Fig. IX-3. Unfortunately, the small size of the image precludes direct viewing.

It should be noted that the results of this study (Fig. IX-5) (Ref. 9) were determined by a particular screen and a particular intensifier system. Comparison of another fluoroscopic screen with another x-ray intensifier tube system which differs from the one selected in the above study by the absorption of x-rays in the input screen may yield a somewhat different figure for the improvement achieved by the system over a conventional fluoroscopic screen. The results shown in Fig. IX-5 should be considered qualitative rather than quantitative. Nevertheless, the final conclusion that x-ray intensifier tubes which are coupled to the eye of the observer by "conventional" optics fall short of their purpose of raising the light photon flux per unit solid angle reaching the eye pupil above the lowest level of statistical fluctuations is valid (Refs. 9 and 14).

It is apparent, therefore, that one should not expect a great improvement in the statistical quality of the image supplied by a conventional x-ray intensifier tube over that of a fluoroscopic screen. However, radiologists using x-ray intensifier tubes agree that they are able to see better detail than with a fluoroscopic system. This difference can be partially explained by the slight improvement in quantum flux achieved by the apparatus, but is probably mostly due to the fact that the intensifier allows higher-resolution cone vision.

Two-Stage X-Ray Intensifier Tubes

The previous discussion points to the desirability of raising the photon flux gain of a conventional x-ray intensifier tube. Technical difficulties, however, prevent a significant improvement in photon flux of such tubes. A more practical solution for raising the photon flux of the output image of the intensifier tube consists in coupling the output image to a light-amplifying device. This second-stage light amplifier may be a television system (see subsequent sections in this chapter) or a light amplifier tube. The amplification produced by such an image converter must result in raising the light flux; gain by minification is neither useful nor desirable at this stage.

Figure IX-6 shows a two-stage x-ray image intensifier tube (Refs. 9 and 15) designed for high flux gain. This tube is composed of a conventional first-stage x-ray image intensifier optically coupled in tandem by fiber optics to a second-stage light amplifier tube. Both stages are enclosed in the same vacuum envelope. The use of fiber optics in the optical coupling between the output screen of the x-ray image intensifier and the input screen of the light amplifier results in excellent light coupling efficiency. A comparison of some characteristics of a two-stage x-ray image intensifier tube with a conventional single-stage tube is shown in Table IX-1.

It is apparent from Table IX-1 that an appreciable improvement of flux gain can be achieved by using a two-stage tube. Two-stage tubes are at this time still in the experimental stage.

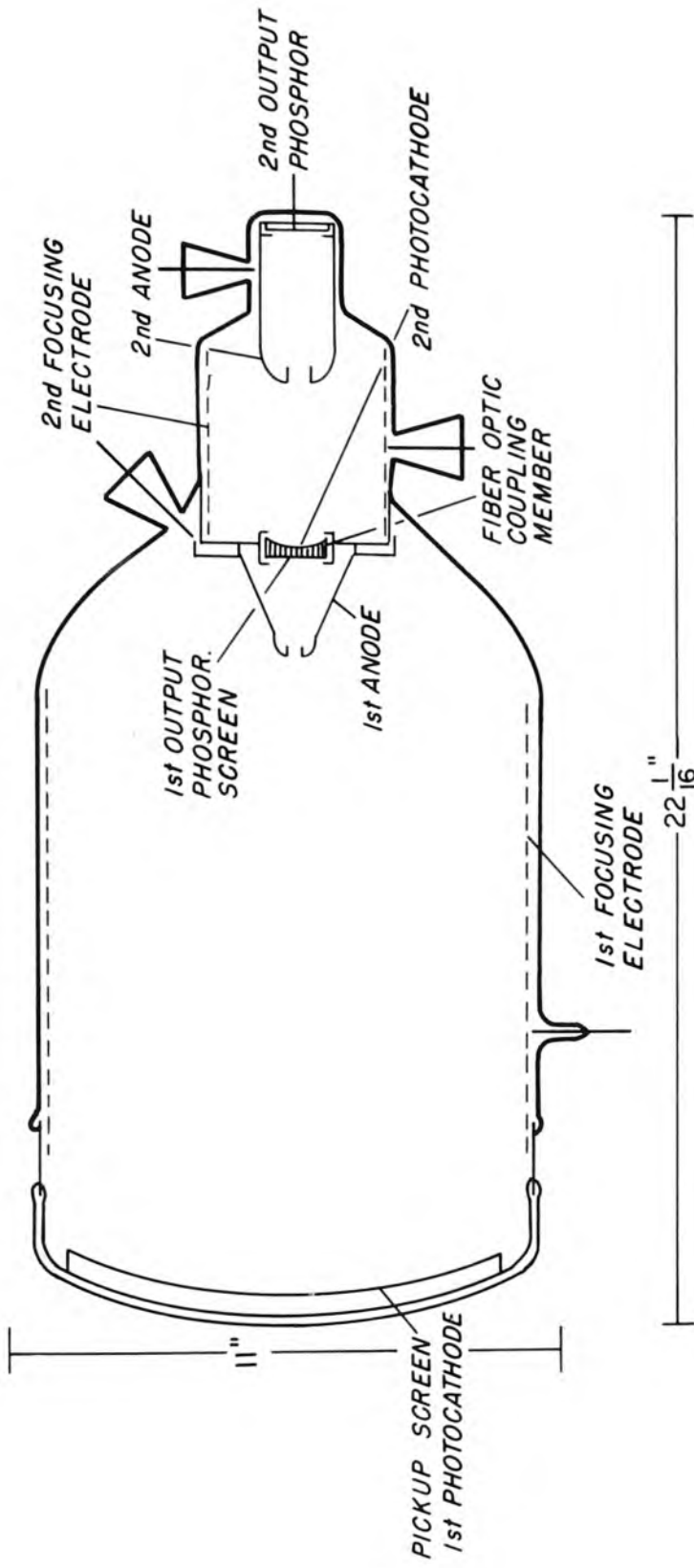


FIG. IX-6. Two-stage x-ray intensifier tube.
 (Courtesy of The Rauland Corp.)

TABLE IX-1.

Conventional single-stage x-ray image intensifier (Rauland R-6175, Type B)		Two-stage experimental x-ray image intensifier (Rauland R-6205)	
Anode potential:	33 kV	Total anode potential:	62 kV
Input screen:	22 cm	Input screen:	22 cm
Minification ($1/M$):	7.5	Minification ($1/M$):	17
Flux gain:	about 50	Over-all flux gain:	930
Brightness gain:	3000	Brightness gain:	270,000
Over-all conversion efficiency: 23×10^3 light photons per incident x-ray photon		Over-all conversion efficiency: 400×10^3 light photons per incident x-ray photon	

From Niklas (Ref. 9).

Light Amplifier Tube X-Ray Image Intensifiers

X-ray image intensification can be achieved by means of a device consisting of a fluoroscopic screen optically coupled with a light amplifier tube. This method of x-ray intensification is identical in principle with x-ray image tube intensification. In both systems the x-ray image is converted into a light image, and the light image is intensified by the same type of light amplifier. The two systems differ in the location of the fluorescent screen. In the x-ray image intensifier the screen is contained in the vacuum envelope that houses the light amplifier; it is in intimate contact with the photocathode and is an integral part of the image converter. In the system discussed here, the screen is separate from the light amplifier.

Figure IX-7 shows a cross section of such an x-ray intensifier, referred to by the trade name of Cinelix Image Intensifier (Old Delft Company, Delft, Holland). This system has a circular fluorescent screen with a diameter of 12.5 in. coupled by means of mirror optics to a light amplifier tube. The screen, which is similar in composition and structure to a conventional fluoroscopic screen, is optically coupled to the light amplifier tube by means of a Bouwers concentric-mirror optical system with a focal ratio of $f/0.68$. The advantage of using a mirror system rather than a conventional transmission lens system is that, for comparable physical dimensions, the mirror system exhibits a considerably higher light gathering efficiency. The diameter of the light intensifier photocathode is 80 mm, with a viewing screen 16 mm in diameter. The image supplied by the output screen can be viewed by means of an optical system, or the screen can be optically coupled to a television system (see section on "Television Chain-X-Ray Intensifier Tube Combinations").

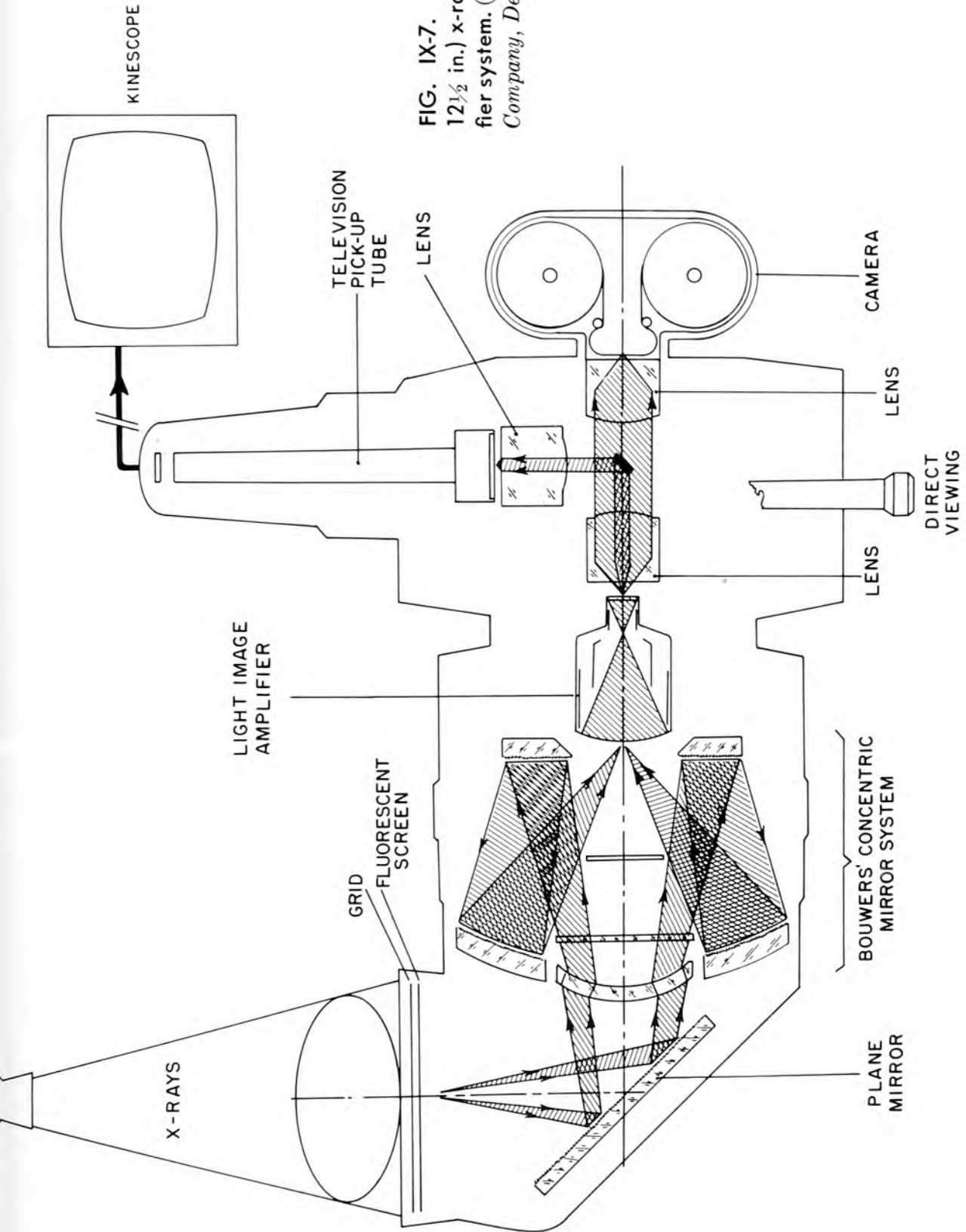


FIG. IX-7. Cinelix (Cinelix 12½ in.) x-ray image intensifier system. (Courtesy Old Delft Company, Delft, Holland.)

In the system described above, the optical coupling between the fluoroscopic screen and the photocathode, although achieved by means of an excellent optical system, is inferior to the direct contact between the fluorescent screen and the photocathode in x-ray intensifier tubes. The Cinelix system, however, offers the following advantages over the conventional x-ray intensifier tubes: (1) The diameter of the input screen is somewhat larger than the largest tubes made. (2) The screen can be changed at will; thus, if high speed is desired at the cost of some resolution, the conventional screen can be easily replaced by a thicker, coarser screen. (3) The cost of replacement of the small-sized light amplifier tube is less than that of the costlier x-ray intensifier tube. (4) The small-diameter image intensifier tube may achieve better peripheral resolution than larger tubes.

X-RAY IMAGE SCANNING SYSTEMS—TELEVISION SYSTEMS

X-ray image intensification can be achieved by converting the radiologic image into an electrical signal by means of a scanning system and, after suitable amplification, converting the signal into an optical image on a television display screen. At present, the most widely used scanning systems for x-ray intensification are relatively conventional closed-circuit television chains, which are used in one of two ways: (1) The television camera is optically coupled to a fluoroscopic screen and the optical image supplied by the screen is intensified by the electronic circuitry of the television chain. (2) The television camera is optically coupled to an x-ray image intensifier, which may be either an x-ray image intensifier tube or a Cinelix-type apparatus, and the optical image supplied by the x-ray intensifier is then displayed, usually magnified, on the television monitor screen.

In a television camera the device which converts an optical image into a modulated electrical signal is the *pickup tube*. Two types of pickup tubes with different characteristics are used in television cameras: the Vidicon tube and the Image Orthicon tube. Choice between a Vidicon and an Image Orthicon pickup tube for a given application in x-ray intensification is usually dictated by the characteristics of the tube. In certain instances, however, either type can be used, and the choice is not clear-cut.

Vidicon and Image Orthicon Television Pickup Tubes

A Vidicon pickup tube (Figs. IX-8 and IX-9) is made of an evacuated glass envelope that contains (1) a two-layer photoconductive input screen, (2) an electron gun producing a narrow beam of accelerated electrons, and (3) a series of electrostatic grids which control the electron beam. The electron beam is focused onto the input screen and is made to scan the screen by means of external focusing and horizontal and vertical deflecting coils. In addition, an external coil or a permanent magnet regulates the alignment of the electron beam within the evacuated tube. The input screen is de-



FIG. IX-8. Television pickup tubes.

Top Vidicon

Bottom Image Orthicon

posited on the glass envelope inside the tube, and is composed of a transparent conductive layer in intimate contact with a photoconductive surface which is an insulator in the dark but becomes conductive when struck by light. The transparent conductive layer is maintained at a positive potential. When an optical image is formed on the photoconductive surface, the dark areas remain nonconductive while the conductivity of the lighted areas becomes proportional to the amount of light absorbed. When the electron beam scanning the photoconductive surface strikes a lighted area, a current flows through the tube. This current constitutes the picture signal supplied by the tube.

Vidicon tubes are structurally simple, are resistant to shocks and to changes in temperature, and are relatively inexpensive. On the other hand, their sensitivity to light is relatively low and they exhibit a "stickiness" or persistence of the particularly bright areas of the image. Some modern Vidicon tubes, such as the RCA 7735A, are relatively free from this undesirable feature. Because of their low gain, Vidicon tubes are used in tandem with some image intensifying system.

An Image Orthicon pickup tube (Figs. IX-8 and IX-9) consists of an evacuated glass envelope containing the following structures: (1) a photocathode input screen, (2) a target structure composed of a fine metal mesh in close proximity to a very thin glass target (magnesium oxide targets are also used), (3) an electron gun producing a narrow beam of electrons, (4)

VIDICON

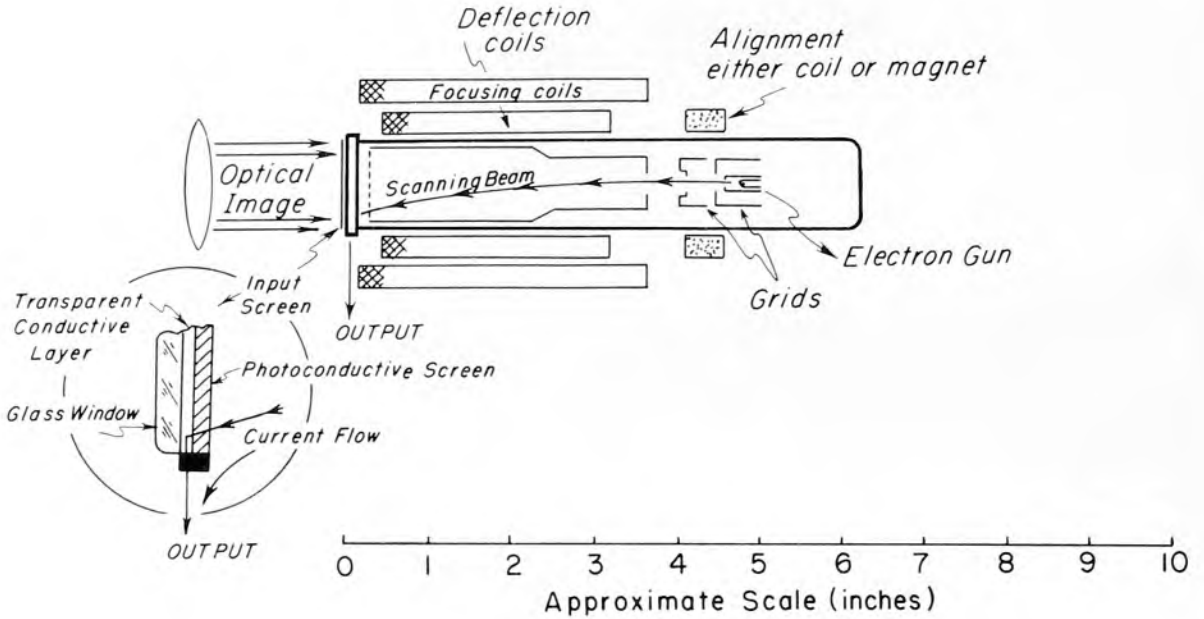


IMAGE ORTHICON

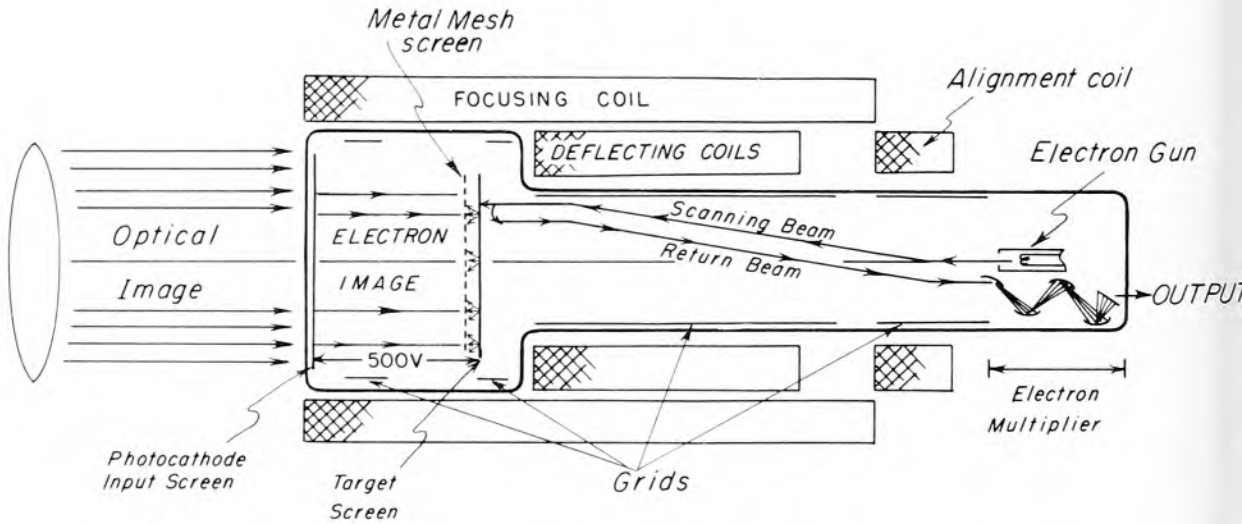


FIG. IX-9. Schematic diagram of components of television pickup tubes.

Top Vidicon

Bottom Image Orthicon

an electron multiplier structure, and (5) a series of grids maintained at suitable potentials to keep the electrons within the tube in the proper trajectories. The electrons in the vacuum glass envelope are subjected to magnetic fields generated by a series of coils external to the tube. A focusing coil produces a magnetic field parallel to the axis of the tube, which prevents the electrons from diverging from the axis of the beam. Two sets of deflect-

ing coils, one set acting in a horizontal direction and the other in a vertical direction, provide two variable magnetic fields, 90 degrees one from the other, which provide the scanning action of the beam of electrons. Finally, an alignment coil permits the alignment of the axis of the electron beam with respect to the magnetic field.

When an optical image is incident upon the photocathode input screen of an Image Orthicon tube, electrons are emitted by the screen, and their number at any point is proportional to the luminance of the optical image. The optical image is thus converted into an electron image. The electrons supplied by the photocathode are accelerated by approximately 500 V and focused by the combined action of the external magnetic field and the internal electric field onto the anode target. The anode target is a thin film of glass (or magnesium oxide in some high-sensitivity Orthicons) which has a high resistance in the target plane and a low resistance in a direction perpendicular to the target plane. When the target is struck by the accelerated electrons originating in the photocathode, secondary electrons are released by the target. The number of these secondary electrons depends on the nature of the target material and is typically about 3 secondary electrons per primary incident electron. These secondary electrons are collected by a metallic mesh (about 750 openings per inch) placed near the target and on the side of the photocathode. The emission of electrons by the target leaves a pattern of positive charges on the target corresponding to the electron image supplied by the photocathode. The other side of the target is scanned by the beam of electrons generated by the electron gun and focused by the external focusing coil. The energy of the electrons forming the beam is controlled by the tube potential in such a fashion that the electrons reach the target with substantially no energy, and are absorbed by the positively charged areas until the latter are neutralized. When the electron beam is directed against areas of the target that are not positively charged, the electrons are not absorbed but return toward the back end of the tube and are focused onto the first dynode of the electron multiplier system (see Chapter XI, section on "Photomultiplier Tubes"). Thus, the positive charge pattern on the target modulates the intensity of the scanning electron beam by depleting the beam. The returning electron beam is amplified about 1000 times in the electron multiplier system, and the output of the Image Orthicon consists of the collected current of the electron multiplier. The electric signal supplied by the Orthicon tube is then further amplified and otherwise handled by electronic circuitry. The efficiency of the modulation of the electron beam in an Orthicon tube does not exceed 25% (Ref. 16). The scanning time of an Orthicon tube is approximately $\frac{1}{30}$ sec.

The statistical fluctuations of the output signal of an Image Orthicon tube are contributed by (1) the statistical fluctuations in the image supplied by the target, and (2) the statistical fluctuations of the electrons in the scanning beam. At high light levels, the number of electrons used in the

scanning beam can be large, and the quality of the image is limited only by the statistical fluctuations of the target image. On the other hand, when the Image Orthicon tube is operated at low light levels, the modulation of the scanning beam represents only a small fraction of the scanning beam current. Under such circumstances it becomes necessary to decrease the electron flux in the scanning beam to raise the percentage of modulation, and a limit to the statistical quality of the signal supplied by the tube is set by the statistical fluctuations of the electrons in the scanning beam (Ref. 17). Thus, at low signal levels, the signal-to-noise ratio of an Image Orthicon tube is undesirably low because of the unavoidable presence of a relatively high noise level contributed by the fluctuations of the scanning electron beam. If modulation is low, the signal may be completely overshadowed by tube noise. For that reason, in spite of high gain, Image Orthicon tubes are not particularly suited for the intensification of very low intensity signals.

Standard Orthicon tubes have a diameter of approximately 3 in., with a photocathode diameter of about 1.5 in. A larger-diameter Image Orthicon (diameter 4.5 in., cathode diameter 3.6 in.), which is particularly useful for x-ray image intensification, was described by Banks (Ref. 16).

Image Orthicon pickup tubes are widely used in commercial television applications. These tubes are relatively temperature dependent and fragile. Exposure of an energized Image Orthicon tube to excessive light may cause permanent damage to the target.

Television Circuits and Resolution

The electronic circuitry used in connection with a pickup tube in a television chain imposes limits on the maximum resolution which can be achieved by the chain. The vertical and horizontal resolutions in a television chain-converted image are determined by different parameters of the electronic circuit, and may be different in a given chain.

Scanning—Vertical Resolution. Whether a television chain includes a Vidicon or an Image Orthicon pickup tube, the image is collected in the tube by a beam of electrons scanning the image area by means of a horizontal sweep. Under the circumstances the vertical resolution of the image converted in the television system cannot exceed the number of horizontal scanning lines per unit length.

In United States television broadcasting systems, the television image is scanned by 525 horizontal lines in $\frac{1}{30}$ sec. The scanning consists of a back-and-forth motion (*active* and *retrace* sweeps) of the beam, but information is carried by the electron beam only during its active travel in one direction. The lines are not scanned consecutively: one field consists of the scan of even lines and the next of odd lines. The interlaced lines of two fields form one television frame in $\frac{1}{30}$ sec.

The total number of 525 lines is not utilized in forming the image, be-

cause approximately 40 lines are wasted during the time taken by the beam to return from the bottom of the image to start a new field at the top, and only about 485 lines are available for the vertical resolution of the image. Certain television systems use a greater number of lines. In x-ray image intensification 837- and over 1000-line television chains are used.

Horizontal Resolution. In a television chain the image is coded by modulation (variation in intensity) as a function of time of the scanning electron beam during the active horizontal sweep. The frequency of the electrical signal thus obtained (rate of modulation per unit time) is proportional to the speed with which the electron beam scans a horizontal line. This frequency is related to the number of lines used in the chain, as shown in the following example:

Assume that the image of a grid composed of 500 vertical lines opaque to light, separated by areas transparent to light, is formed on the input screen of a pickup tube included in a 525-line television chain. The modulation of the scanning beam in the tube consists of 500 rises in intensity during one horizontal sweep time. The number of lines scanned in $\frac{1}{30}$ sec is 525; therefore a horizontal sweep (one line) is made in about $63 \mu\text{sec}$ ($\frac{1}{30}$ sec \div 525 lines = 63×10^{-6} sec/line). This time is divided between the active horizontal sweep and the retrace, which takes about $11 \mu\text{sec}$. Therefore the time left for a horizontal sweep in a 525-line system is about $52 \mu\text{sec}$. The frequency of the electrical signal modulated 500 times during one horizontal sweep (rate of modulation per second) is

$$\frac{500}{52 \times 10^{-6} \text{ sec}} = 9.6 \times 10^6 \text{ cycles, or 9.6 megacycles.}$$

This electrical signal is transferred undistorted by the television chain only if the electronic circuitry has a frequency *bandpass* of 9.6 megacycles per second or greater. If the bandpass of the circuitry is lower, for example 4.8 megacycles, then the resolution of the system cannot exceed 250 lines. Thus, the horizontal resolution of a television chain is determined by the number of horizontal lines and by the bandpass of the electronic circuitry used. Any increase in the number of lines requires a proportional increase in the bandpass of the circuitry if horizontal resolution is to be kept constant. A television chain with 875 horizontal lines requires a circuit with a bandpass of about 16.5 megacycles to be capable of achieving a horizontal resolution of 500 lines. (A resolution of 500 lines is expressed in television terminology as 1000 *television lines*—both lines and interspaces are counted.)

Conventional television broadcasting is done with a bandpass of about 4 megacycles, which limits the horizontal resolution to about 230 lines (460 television lines).

Target Underscanning. The resolution capabilities of a television chain that includes an Image Orthicon pickup tube can be increased by *target*

underscanning, which consists in reducing electronically the area of the Orthicon target scanned by the electron beam. This results in more television lines per unit length at the expense of observed area size. The resolution of the Orthicon chain increases proportionally with the ratio of the underscanned area to total target area (Ref. 18). Thus, an 875-line system underscanned by a ratio of 2 to 1 should exhibit a resolution of about 1600 lines. Target underscanning is comparable to optical magnification by means of Image Orthicon systems.

Image Orthicon Television Chain X-Ray Intensifier

An Image Orthicon television chain optically coupled to a fluoroscopic screen can be effectively used in raising the luminance of the image x-ray screen. The desirable features of such a system are as follows: (1) The brightness gain which can be achieved by means of an Orthicon television chain is sufficiently high to raise the photon flux of the image at the retina of the observer well above the x-ray photon flux absorbed by the fluoroscopic screen. (2) With a high-resolution television chain (large number of lines, suitable circuit frequency bandpass, and large-diameter Orthicon tube) the resolution in the final image is limited only by the quality of the image supplied by the fluoroscopic screen. (3) The image supplied by the system is sufficiently large for direct observation. (4) Several remote monitors can be used simultaneously. (5) Different fluoroscopic screens can be used as required by the type of examination conducted. (6) Image brightness and contrast can be controlled electronically.

The use of Orthicon television chains for x-ray image intensification was described by Morgan and Sturm (Ref. 19). The apparatus developed by these authors consisted of a 3-in. diameter Image Orthicon tube with associated electronic circuitry, optically coupled to a standard fluoroscopic screen by means of an optical mirror system. The luminance gain achieved with this apparatus was 300 to 1000 times in chest fluoroscopy and 1000 to 3000 times in fluoroscopy of the abdomen. The reported screen luminance was of the order of 3 ft-L. However, the measured performance of this apparatus in image perceptibility was only slightly superior to conventional fluoroscopy.

Image Orthicon x-ray image intensifiers are commercially available from Marconi Instruments, Ltd. (St. Albans, Herts, England). The Image Orthicon used in the Marconi intensifier is a 4½-in. tube with a photocathode of 3.625 in., which is appreciably larger than the 1.5-in. diameter photocathode used in conventional 3-in. tubes. The optical system coupling the Image Orthicon tube to the fluoroscopic screen is a mirror system developed by Bouwers of Delft, Holland.

The influence of a large photocathode Orthicon tube and of a particularly efficient light-gathering system on the statistical quality of the image supplied by such a system was studied by Banks (Ref. 16). Figure IX-10

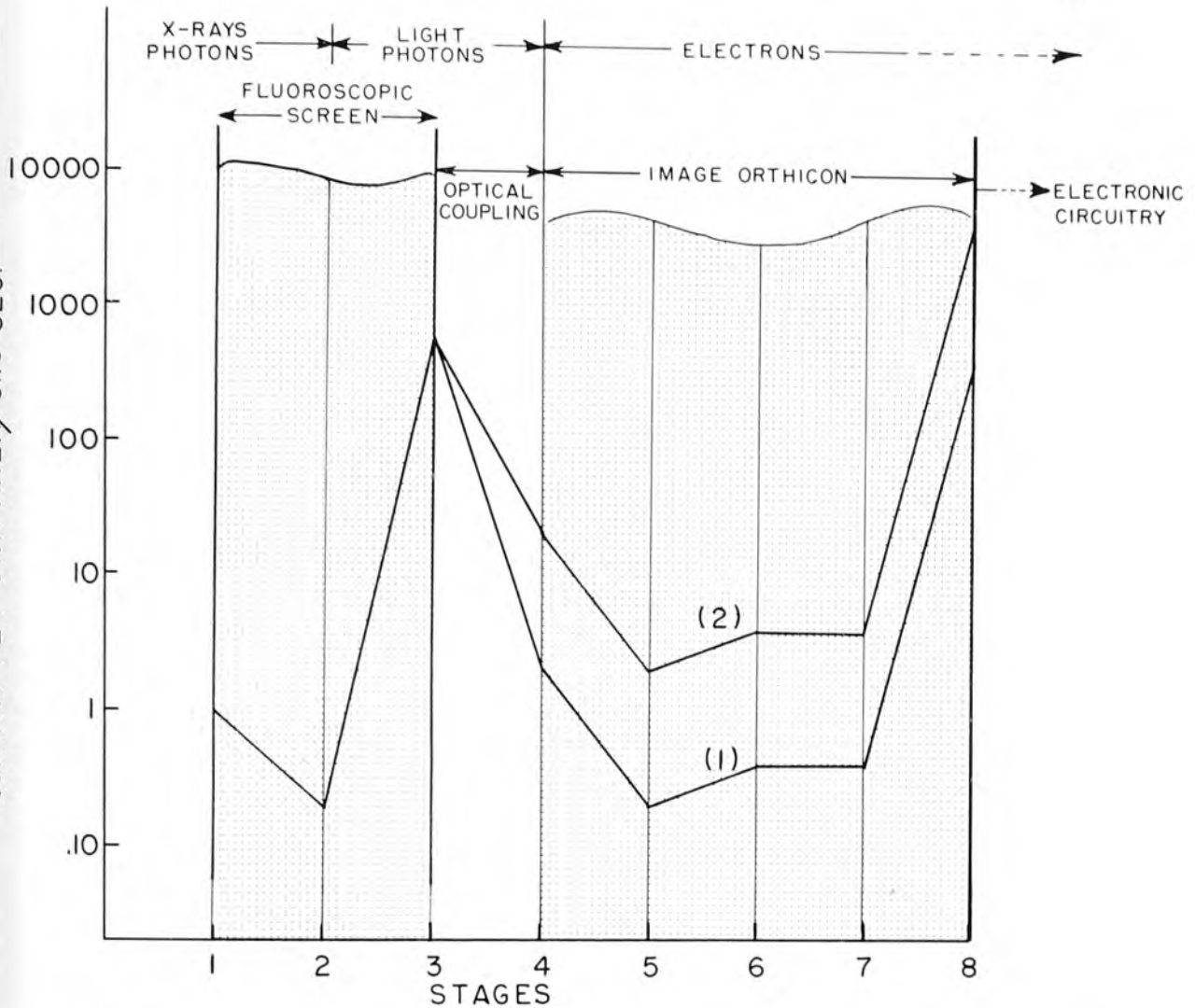


FIG. IX-10. Quantum levels reached in different stages of image conversion in two different systems.

1 fluoroscopic screen coupled by means of lens optics ($f/1$) to a 3-in. Orthicon tube
 2 same fluoroscopic screen coupled by means of Bouwers mirror optics ($f/0.7$) to a $4\frac{1}{2}$ -in. Orthicon tube.

(Adapted from Banks, Ref. 16.)

shows the quantum levels reached during the different stages of image conversion in two television x-ray intensifiers which differ in their Image Orthicon photocathode diameters and in the couplings of their optical systems. Graph 1 corresponds to a system with a 3-in. Orthicon tube (photocathode diameter 1.5 in.) coupled to the fluoroscopic screen by an optical system with an f -number of $f/1$; in Graph 2 the Orthicon used is a $4\frac{1}{2}$ -in. tube (photocathode diameter 3.625 in.) optically coupled by a Bouwers mirror system with a numerical aperture of $f/0.7$.

The first three stages of image conversion are determined by the fluoro-

scopic screen used. The only difference in this portion of image conversion with a conventional fluoroscopic examination is that the integration time used in television viewing is equal to about 0.16 sec. It is shorter than the storage time of the eye because of the loss of integration of information by blanking between television frames (Ref. 13). However, since the photon numbers plotted in Fig. IX-10 are expressed in arbitrary units, the integration time does not intervene numerically. In Stage 1, a single x-ray photon, after passing through the patient, impinges upon the fluoroscopic screen. The probability of this photon for being absorbed in the screen is approximately 20%; in Stage 2, 0.2 photon is absorbed in the screen giving rise to approximately 600 light photons in Stage 3 (approximately 3000 light photons are produced in a conventional screen per x-ray photon absorbed). Stage 4 corresponds to the number of photons collected by the optical system coupling the Image Orthicon tube to the fluoroscopic screen.

The fraction of light photons collected by an optical system having an f -number f , an optical transmission T , and a linear magnification M is given by

$$\frac{N_c}{N_e} = \frac{M^2}{(M + 1)^2} \times \frac{T}{4f^2}, \quad (3)$$

where N_e is the number of photons emitted by the screen and N_c is the number of photons collected by the optical system (Ref. 16). The transmission factor of the optical system was assumed to be 0.6. In System 1, only 1 light photon out of 500 emitted by the fluoroscopic screen reaches the photocathode of the Orthicon tube, while in System 2, because of better optics and lower minification, 1 photon out of 50 reaches the tube. Thus, a gain of approximately 10 is achieved in System 2 as compared to System 1. From there on, it is assumed that both systems handle the image in an identical manner. This situation, in fact, does not illustrate accurately the relative performances of the 3- and 4½-in. tubes. The 4½-in. Orthicon tube exhibits a lesser loss in quanta at the photon-electron conversion stage than the 3-in. tube because of a more efficient photosurface (Sb-Cs(O) type) of the photocathode (Ref. 16). This factor was omitted from the values shown in Fig. IX-10 to emphasize the improvement achieved by increasing the size of the photocathode and by using a more efficient optical system. Approximately 10 x-ray photons are required to release 1 electron from the photocathode of the tubes, resulting in a drop of 10 units from Stage 4 to Stage 5. When the photoelectrons strike the target screen at Stage 6, there is a multiplication of electrons by a factor of 3, and the charge deposited is doubled. The transition from Stage 6 to Stage 7 consists in the modulation of the scanning beam by the charge on the target screen, and there is no appreciable loss in electrons in this stage. Finally, the transition from Stage 7 to Stage 8 corresponds to the electron multiplication

of the return scanning beam by the electron multiplier. The electron gain thus achieved is about 1000. From there on further electron multiplication may be achieved by electron circuitry.

It is apparent that in System 1 (Fig. IX-10) an approximately equally low number of quanta is reached at Stage 2, where x-ray photons are absorbed in the fluoroscopic screen, and at Stage 5, where photoelectrons are emitted by the photocathode of the Image Orthicon. Thus, these low values contribute equally to the statistical deterioration of the image. In System 2, on the other hand, the number of photoelectrons emitted by the photocathode is approximately ten times greater than the low value reached by the x-ray photons in the screen, and therefore the image intensifier does not contribute appreciably to the statistical deterioration of the image supplied by the fluoroscopic screen. This corresponds to the performance of the ideal image intensifier in fluoroscopy (Ref. 1). The theoretical improvement in minimum perceptible contrast which can be achieved with this system over conventional fluoroscopy is discussed in the section on "Contrast Perceptibility Improvement by Image Intensification" of this chapter.

Television Chain-X-Ray Intensifier Tube Combinations

The weakness of x-ray intensification by means of an Image Orthicon tube alone lies in the fact that at low light levels the performance of the tube is poor because of its low signal-to-noise ratio (see section on "Vidicon and Image Orthicon Television Pickup Tubes" above). This weakness can be overcome by optical coupling of the Image Orthicon tube to the output screen of an x-ray image intensifier tube (or of a Cinelix-type system). In such a tandem, image intensification is accomplished in two stages: (1) The low intensity image is first intensified by the image tube, which is a "low noise" system well suited for the detection of weak signals, and (2) the output image of the intensifier tube is further intensified by the Orthicon tube. In this two-stage system the Image Orthicon tube is supplied with a relatively intense signal and operates with a more favorable signal-to-noise ratio than if the Orthicon alone had to provide the full intensification.

Fluoroscopic x-ray intensification so achieved also offers advantages over the use of an intensifier tube alone; in particular, this combination improves the statistical quality of the observed image by providing a more efficient coupling between the eye of the observer and the observed image than that achieved by the "long" optical coupling conventionally used in magnifying the input screen of an intensifier tube.

Efficient optical coupling between the photocathode of the television pickup tube (either Vidicon or Image Orthicon) and the output screen of an x-ray intensifier tube is easy to accomplish, because both the image intensifier output screen and the television pickup photocathode are of

about the same diameter (about 1 in.). The efficiency of light photon transfer from the intensifier tube to the photocathode of the television pickup tube is given by Equation (3):

$$\frac{N_c}{N_e} = \frac{M^2}{(M + 1)^2} \times \frac{T}{4f^2}$$

Since no magnification M is required, the equation is reduced to

$$\frac{N_c}{N_e} = \frac{T}{16f^2}$$

If, for example, the f -number of the system used is 1 and the transmission T of the optical system is 0.6, a conservative figure, then $N_c/N_e = 0.037$, which means that approximately 4% of the photons emitted by the intensifier screen reach the photocathode of the pickup tube.

The optical image thus supplied to the pickup tube is further intensified, as discussed in the previous section, until it reaches the monitor screen and is then viewed by the observer. It should be noted that although there is a considerable loss in light photons in the transmission of the monitor image to the retina of the observer, this loss is about the same as in the observation of the fluoroscopic screen (as shown in Fig. VIII-3, Chapter VIII). This loss does not affect the statistical quality of the image because it is more than compensated by the flux gain produced by the television chain. Figure IX-11 shows that in a television chain-x-ray intensifier tube combination, the lowest number of image-forming photons occurs with the absorption of x-ray photons in the input screen of the x-ray intensifier tube, and that this number is at least an order of magnitude lower than any of the other levels; thus this system fulfills the statistical requirements of an ideal image intensifier.

A television chain with a Vidicon pickup tube can also be used to advantage in tandem with either an x-ray intensifier tube or a Cinelix system. Although the gain of the Vidicon tube does not allow as much brightness control as that of the Image Orthicon tube the addition of a Vidicon tube to an image intensifier tube still offers the other advantages of a television chain. The persistence of the Vidicon image ("stickiness") does interfere with the perceptibility of moving objects (Fig. IX-12). However, considerable progress has been made in the design of modern Vidicon tubes, both from the standpoint of gain and persistence. Vidicons such as the RCA 7735A or the Philips Plumbicon are considerable less "sticky" than the Vidicon tube used in Fig. IX-12, and a more modern Vidicon would probably differ even less from the Orthicon (Ref. 28). Because of their simplicity and improvement in performance, modern Vidicons, have become increasingly more attractive for use in connection with x-ray image intensifiers.

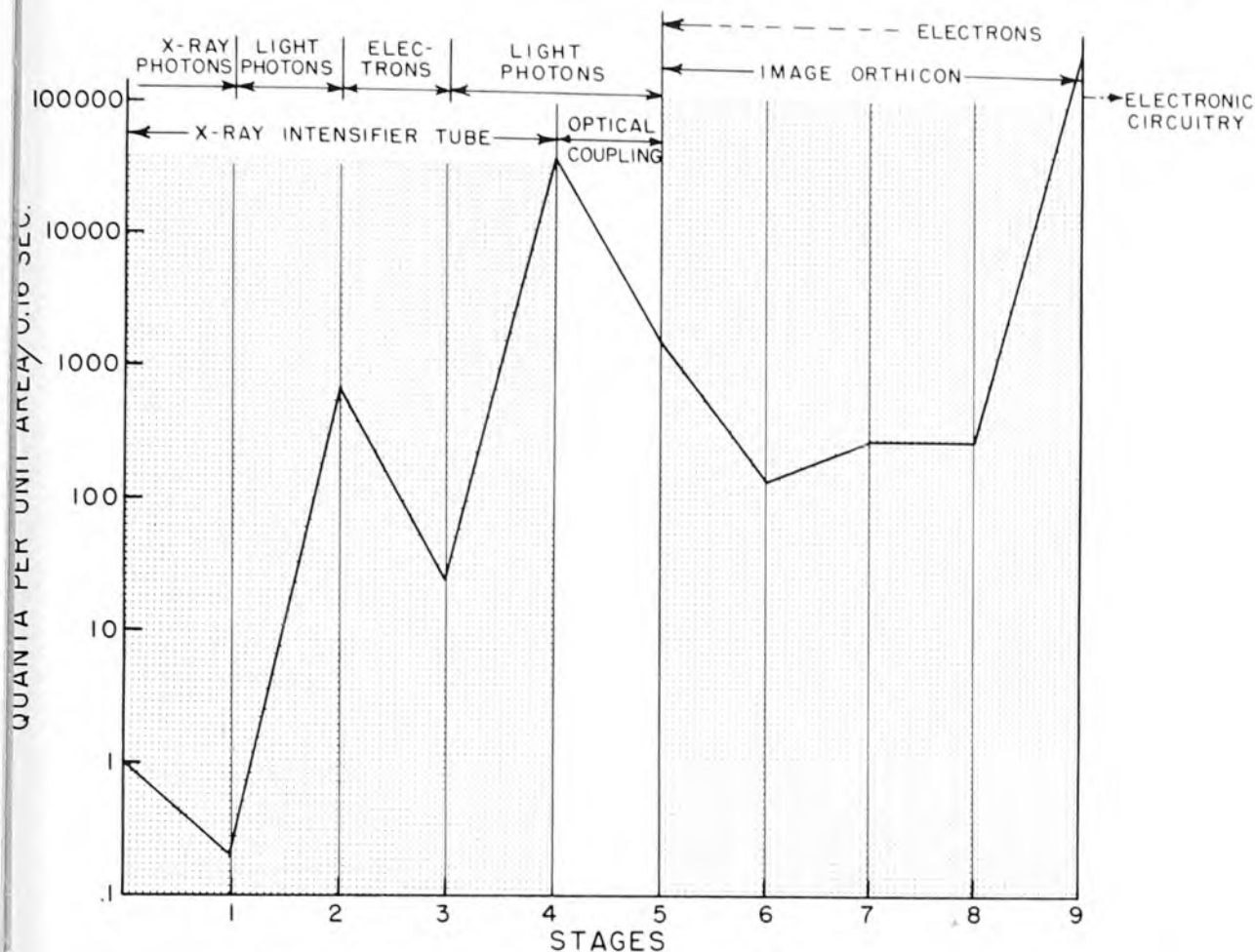


FIG. IX-11. Quantum levels reached in different stages of image conversion in x-ray image intensifier system consisting of x-ray intensifier tube optically coupled ($f/1.0$) to an Image Orthicon television chain. The quantum levels in the x-ray image intensifier tube (Stages 1-4) are the same as those shown in Fig. IX-5 (Stages II-V). The quantum levels in the Orthicon chain (Stages 5-9) are the same as those shown in Fig. IX-10 (Stages 4-8).

Other X-Ray Scanning Television Intensifiers

Television pickup tubes directly sensitive to x-ray have been developed (Ref. 20) for the purpose of achieving x-ray image intensification. The x-ray-sensitive photocathode of these tubes is generally of the photoconductive type (selenium or lead oxide), and the principle of operation is similar to that of a conventional Vidicon pickup tube. X-ray intensifiers using such tubes have been tested but have never been very successful.

X-ray image intensification has also been achieved by scanning the part to be examined by a narrow beam of x-rays (Refs. 21-23). The apparatus used for this purpose consists of an x-ray tube of special design which provides a narrow pencil of x-radiation that can be made to scan the field to

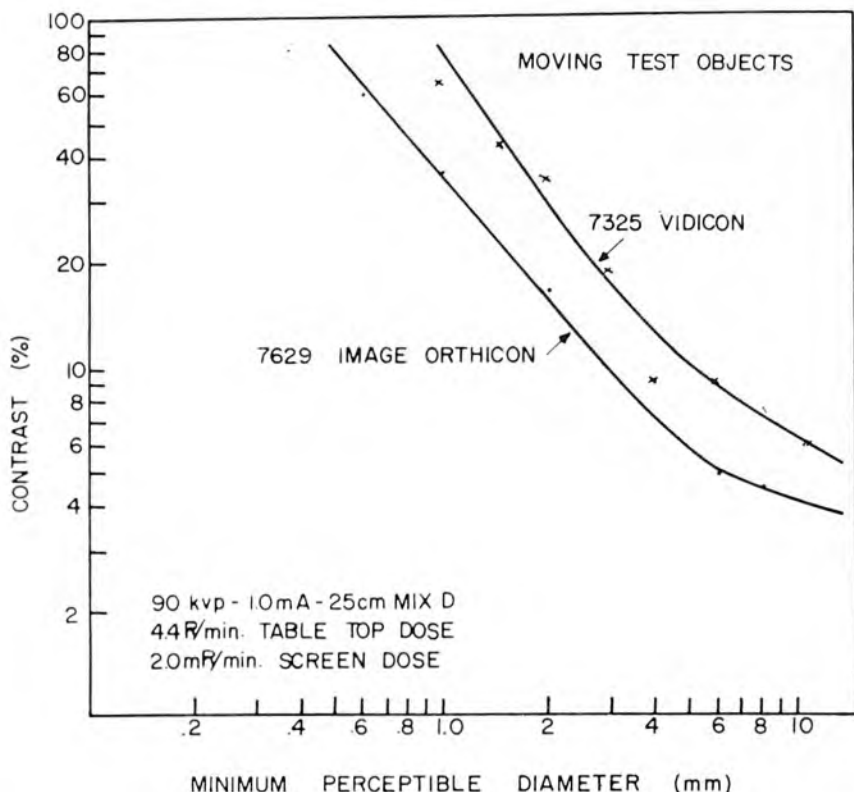


FIG. IX-12. Comparison, by means of moving test objects, of image perceptibility with an x-ray image intensifier tube optically coupled to a television chain with Vidicon pickup tube; Image Orthicon pickup tube. (From Webster and Wipfelder, Ref. 27.)

be examined. After passing through the examined part the pencil of x-rays impinges upon a scintillation counter which converts the x-ray energy into an electrical signal. The electrical signal is converted into an optical image on a television screen which is scanned in synchrony with the x-ray beam. To this date, these systems have not been applied to clinical work.

SOLID-STATE X-RAY INTENSIFIERS

All the previously described modes of x-ray image intensification utilize electrons traveling in a vacuum. X-ray intensification can also be achieved by the perturbation of electrons in semiconducting solids. This method of intensification has been called *solid state intensification*, *photoconductive-electroluminescent intensification*, or *panel-type intensification*. Various possible mechanisms have been proposed in the application of semiconductors in x-ray intensification (Ref. 24). A solid-state x-ray intensifier which shows promise was developed by Kazan (Ref. 25). This device is based on the combined application of two properties possessed by some semiconductors: photoconductivity and electroluminescence.

A form of photoconductivity consists in the enhanced conductivity of

a semiconductor when it is exposed to x-rays. This phenomenon is due to the fact that the absorption of x-rays in this material results in the creation of high energy electrons which through a series of collisions generate a large number of secondary electrons. The presence of these secondary electrons increases the electrical conductivity of the material. It is also possible that the creation of positive space charge also increases the conductivity in the dielectric (Ref. 24). Electroluminescence is the property possessed by certain materials to convert electrical energy into light photons.

The solid-state x-ray intensifier described by Kazan is composed of a stack of the following elements (Fig. IX-13): (1) a photoconductor layer, (2) an opaque insulating layer, and (3) an electroluminescent layer covered by a transparent conducting layer. An alternating voltage is applied to this panel. This intensifier operates as follows:

When an x-ray image is formed on the photoconductor, the panel becomes more conductive in the areas struck by x-radiation, and the x-ray image is converted into an image composed of variations in the conductivity of the first layer. The variation in conductivity of the first layer results in a variation of the electrical potential applied to the electroluminescent

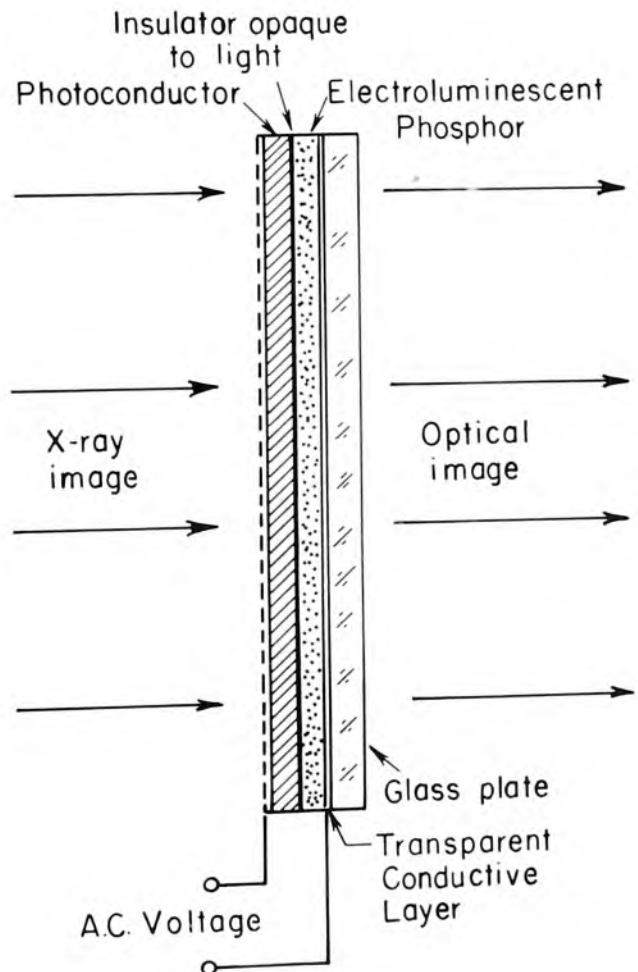


FIG. IX-13. Solid-state x-ray image intensifier. (After Kazan, Ref. 25.)

layer. The latter in turn emits a light image that corresponds to the x-ray image imprinted on the photoconductor. The electroluminescent phosphor (copper-activated zinc sulfoselenide—Zn(SSe)) is a powder bonded in plastic. When exposed to direct current the phosphor exhibits negligible electroluminescence, on the other hand, if alternating current is applied, it luminesces intensely with the emission of yellow-green light. The photoconductor is powdered cadmium sulfide, also bonded with plastic. The luminance of such a panel is over 100 times greater than that of a Patterson CB2 fluoroscopic screen when they are exposed to equal x-ray fluxes. Unfortunately, the long decay time of the image formed on such a panel precludes its practical use in fluoroscopy, and such intensifiers are at this time of no practical use in diagnostic radiology.

CONTRAST PERCEPTIBILITY IMPROVEMENT BY IMAGE INTENSIFICATION

All x-ray image intensifiers used currently in fluoroscopy fulfill adequately one of their purposes, which is to raise the luminance of the image supplied to the pupil of the radiologist to a level which does not require dark adaptation and which permits high resolution cone vision. However, as shown in the previous sections, there are wide differences between x-ray intensifier systems in their ability to reduce the influence of statistical fluctuations on the quality of the image which they supply and thereby improve detail perception.

The performance of an x-ray intensifying system can be expressed and compared with that of other systems by the minimum perceptible contrast per unit resolution element in the image supplied by the intensifier. The limit imposed by statistical fluctuations on the minimum perceptible contrast for a given resolution element is given by Equation (3) of Chapter VIII:

$$C_{\min} = \frac{k}{\sqrt{N}} \times 100,$$

where N is the minimum level reached by the number of photons per resolution element in the image-forming system and k is the threshold signal-to-noise ratio of the human eye the value of which lies between 2 and 5. When $k = 2.5$, then

$$C_{\min} = \frac{2.5}{\sqrt{N}} \times 100.$$

It should be kept in mind that an ideal image intensifier supplies an image with a minimum perceptible contrast at best equal to that of the radiologic image impinging upon the intensifier, because under no circumstances can the statistical accuracy of the image supplied by the intensifier exceed that of the radiologic image.

The following example is a quantitative comparison, under typical conditions of fluoroscopy, between the contrast perceptibility improvements achieved by three intensifier systems and a fluoroscopic screen: Assume the fluoroscopic examination of a 25-cm thick abdomen carried out with 90 keV_p x-rays and with a skin exposure rate of 1 R/min. This exposure rate for 90 keV_p x-rays results from a photon flux of about 300×10^8 photons/cm²/min (Chapter XI, Table XI-4). The attenuation of 90 keV_p x-rays in 25 cm of water-equivalent material reduces the photon flux by approximately 300 (Fig. V-9, Chapter V); and, neglecting beam divergence, the exposure rate in the transmitted beam is about 3 mR/min, with a photon flux of 10^8 photons/cm²/min, or 1.66×10^6 photons/cm²/sec. The number of photons integrated during the storage time of the eye (0.2 sec) is

$$1.66 \times 10^6 \text{ photons/cm}^2/\text{sec} \times 0.2 \text{ sec} = 3.3 \times 10^5 \text{ photons/cm}^2.$$

The minimum perceptible contrast for a resolution element of 1 cm² in the radiologic image is

$$C_{\min} = \frac{2.5}{\sqrt{3.3 \times 10^5}} \times 100 = 0.43\%.$$

Table IX-2 shows the minimum perceptible contrast achieved when the above x-ray image is converted to an optical image by (1) a fluoroscopic screen; (2) an x-ray image intensifier tube fitted with conventional magnifying optics; (3) the same x-ray image intensifier tube optically coupled with an Image Orthicon television chain; or (4) a television image intensifier. It should be noted that in the television systems the integration time is only 0.16 sec, which is shorter than the storage time of the eye of 0.2 sec because of blanking between television frames.

It is apparent that on theoretical grounds Systems 3 and 4 are superior to System 2. The theoretical improvement in minimum perceptible contrast achieved over conventional fluoroscopy by means of System 2 and System 3 is in good agreement with experimental results (Ref. 26).

Figure IX-14 (Ref. 27) shows experimentally determined relationships between minimum perceptible diameter and contrast for (1) a fluoroscope; (2) an x-ray image intensifier tube with conventional optics; (3) a Vidicon television chain optically coupled to the x-ray intensifier tube; and (4) two Image Orthicon television chains coupled to the x-ray image intensifier tube.

Results (Fig. IX-14) show (1) definite superiority of the intensifiers over the fluoroscope, (2) superiority of one of the Image Orthicon television chains (5820) over optical viewing at low contrast levels (difference between the 7626 and 5820 Orthicons is explained by the greater noise level of the 7626 tube (Ref. 27)), and (3) general agreement between theory and ex-

TABLE IX-2. Comparison of Minimum Perceptible Contrast in Four Different X-Ray Systems

X-ray system	Minimum perceptible contrast for 1-cm ² resolution element <i>in x-ray image^a</i> ($3.3 \times 10^5 hn / \text{cm}^2 / 0.2 \text{ sec}$)	Location of lowest photon level (quantum sink)	Number of photons per 1-cm ² resolution element at lowest level ^a (hn / cm^2)	Minimum perceptible contrast for 1-cm ² resolution element ^a
(1) Fluoroscopic screen	0.43 %	retina	3300/0.2 sec ^{b,e}	~4 %
(2) X-ray image intensifier tube with conventional optical system	0.43 %	retina	5500/0.2 sec ^{b,d}	~3 %
(3) X-ray image intensifier tube coupled with an Image Orthicon TV chain	0.43 %	input screen	$5 \times 10^4 / 0.16 \text{ sec}^b$	~1 %
(4) Image Orthicon TV intensifier (4½" Orthicon Bouwers mirror optics)	0.43 %	input screen	$5 \times 10^4 / 0.16 \text{ sec}^b$	~1 %

^a Resolution element 1 cm² in size in the full-scale image of the object under examination.

^b Twenty percent of the x-ray photons impinging on the screen are absorbed.

^c Twenty x-ray photons absorbed in the screen result in 1 light photon absorbed in the retina of the observer.

^d Twelve x-ray photons absorbed in the screen result in 1 light photon absorbed in the retina of the observer.

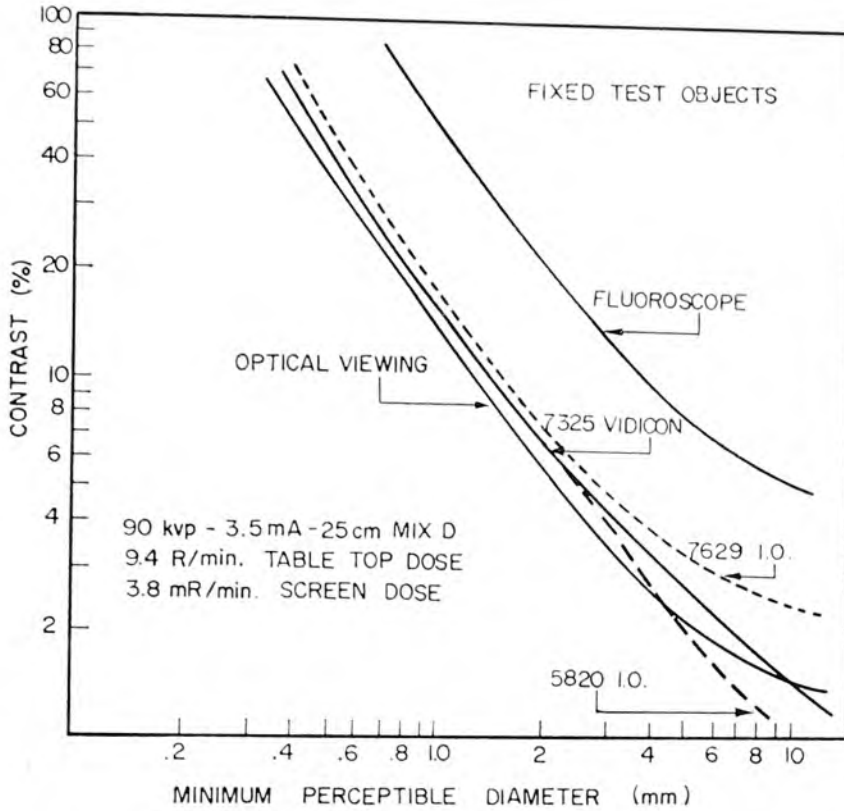


FIG. IX-14. Minimum perceptible diameter versus contrast, experimentally determined with several x-ray image intensifiers. (From Webster and Wipfelder, Ref. 27.)

perimental determination of the relationship between minimum perceptible diameter and minimum perceptible percent contrast (Table IX-2). (The minimum perceptible area is approximately equal to the square of the minimum perceptible diameter.)

REFERENCES

1. STURM, R. E., and MORGAN, R. H.: Screen intensification systems and their limitations. *Amer. J. Roentgen.* 62:617, 1949.
2. CHAMBERLAIN, W. E.: Fluoroscopes and fluoroscopy. *Radiology* 38:383, 1942.
3. ROSE, A.: Sensitivity performance of the human eye on an absolute scale. *J. Opt. Soc. Amer.* 38:196, 1948.
4. *Methods of Evaluating Radiological Equipment and Materials.* NBS Handbook 89. Washington, D.C., U.S. Government Printing Office, 1963.
5. HOLST, G., DEBOER, J. H., TEVES, M. C., and VEENEMANS, C. S.: An apparatus for the transformation of light of long wave length into light of short wave length. *Physics* 1:297, 1934.
6. U.S. Patent No. 2,270,373 (1942) granted to Hartmut I. Kallmann.
7. U.S. Patent No. 2,198,479 (April 23, 1940) granted to I. Langmuir.
8. COLTMAN, J. W.: Fluoroscopic image brightening by electronic means. *Radiology* 51:359, 1948.

9. NIKLAS, W. F.: "Conversion Efficiencies at Conventional Image Amplifiers," in *Technological Needs for Reduction of Patient Dosage from Diagnostic Radiology*, ed. by Janower, M. L., Springfield, Ill., Thomas, 1962.
10. TEVES, M. C., and TOL, T.: Electronic intensification of fluoroscopic images. *Philips Technical Review* (Philips Company) 14(#2):33, 1952.
11. OOSTERKAMP, W. J.: Image intensifier tubes. *Acta Radiol.*, Suppl. 116:497, 1954.
12. MORGAN, R. H.: Development and State of X-Ray Television Intensification in America. Proceedings of the 9th International Congress of Radiology, 1959, p. 23.
13. DOLON, P. J., and NIKLAS, W. F.: "Quantum Statistics of X-Ray Image Intensifying Systems for Fluoroscopy," in *The Reduction of Patient Dose by Radiologic Instrumentation*, ed. by Moseley, R. D. Springfield, Ill., Thomas, 1964.
14. MORGAN, R. H.: Screen Intensification and Cineradiography. Lecture, Meeting of the American Roentgen Ray Society, Miami Beach, Fla., 1961.
15. DOLON, P. J., and NIKLAS, W. F.: Gain and Resolution of Fiber Optic Intensifier. Image Intensifier Symposium, Ft. Belvoir, Va. 1961, sponsored by NASA and the U.S. Army Engineer Research and Development Laboratories.
16. BANKS, G. B.: Television pick-up tubes for x-ray screen intensification. *Brit. J. Radiol.* 31:619, 1958.
17. MORTON, G. A., and RUEDY, J. E.: "The Low Light Level Performance of the Intensifier Orthicon," in *Advances in Electronics and Electron Physics, Symposium on Photoelectronic Image Devices*, New York, Academic Press, 1960, pp. 183-293.
18. MANNING, W. H., JR.: The TV telescope. *Astronautics and Aerospace Eng.* 1(6):36, 1963.
19. MORGAN, R. H., and STURM, R. E.: The Johns Hopkins fluoroscopic screen intensifier. *Radiology* 57:556, 1951.
20. SMITH, C. W.: "An X-Ray Sensitive Photo-Conductive Pickup Tube," in *Photo-Electronic Image Devices, Advances in Electronics and Electron Physics*, vol. 12, New York, Academic Press, 1960. [Good bibliography]
21. MOON, R. G.: Discussion of Symposium on Screen Intensification. *Amer. J. Roentgen.* 62:637, 1949.
22. MOON, R. G.: Amplifying and intensifying the fluoroscopic image by means of a scanning x-ray tube. *Science* 112:389, 1950.
23. GREATOREX, C. A.: "Image Intensification Using a Flying Spot X-Ray Tube," in *Photo-Electronic Image Devices, Advances in Electronics and Electron Physics*, vol. 12, New York, Academic Press, 1960.
24. WILLIAMS, F. E.: Electroluminescence and light amplifying phosphors applied to fluoroscopic image intensification. *Amer. J. Roentgen.* 75:77, 1956.
25. KAZAN, B.: A solid state amplifying fluoroscope screen. *Amer. J. Roentgen.* 79:709, 1958.
26. WEBSTER, E. W., and WIPFELDER, R.: Limitations of Combined Image Amplifier Television Systems for Medical Fluoroscopy. Institute of Radio Engineers Transactions on Biomedical Electronics, April, 1962, pp. 150-155.
27. WEBSTER, W. W., and WIPFELDER, R.: Contrast and detail perception in television and cine systems for medical fluoroscopy. *J. Soc. Motion Picture Television Eng.* 73:617, 1964.
28. WEBSTER, E. W.: Personal communication. March 1965.

(X) CINEFLUOROGRAPHY— PHOTOFLUOROGRAPHY

X-RAY CINEMATOGRAPHY (ROENTGEN CINEMATOGRAPHY)

X-ray cinematography, or roentgen cinematography, consists of the cinematographic recording of a radiologic image.¹ The potential usefulness of the dynamic recording of a radiologic image by cinematography was recognized as early as 1896 when MacIntyre demonstrated to the members of the Glasgow Philosophical Society a moving picture film obtained by serially projecting pictures exposed by means of x-rays of a frog's leg in motion. MacIntyre's experiments were described in the Archives of Skiagraphy (Ref. 1).

MacIntyre attempted two approaches to achieve x-ray cinematography. First he recorded by means of an ordinary camera the optical image formed by the radiologic image on a potassium platino-cyanide fluorescent screen. This method was found to be too slow. Then he recorded the radiologic image directly on photographic film which was allowed to pass in front of an aperture in a thick lead covering protecting the camera from x-radiation. Although MacIntyre in his early attempts was unable to record rapid motion, he nevertheless succeeded in recording by x-ray cinematography the motion of a frog's leg slowed down by anesthesia.

MacIntyre's early work exhibits two particularly interesting aspects: (1) He successfully combined for his purpose two techniques both of which had been discovered within about one year of his work, radiography and cinematography. (2) He applied to his purpose two different techniques of x-ray cinematography, the direct exposure of a photographic emulsion to x-rays and the cinematographic recording of a fluoroscopic image. Both techniques have since been used in x-ray cinematography. The two approaches used by MacIntyre are commonly called the direct and the indirect method, respectively, of cinematography.

¹ The reader interested in the history of the development of x-ray cinematography is referred to Refs. 2 and 3.

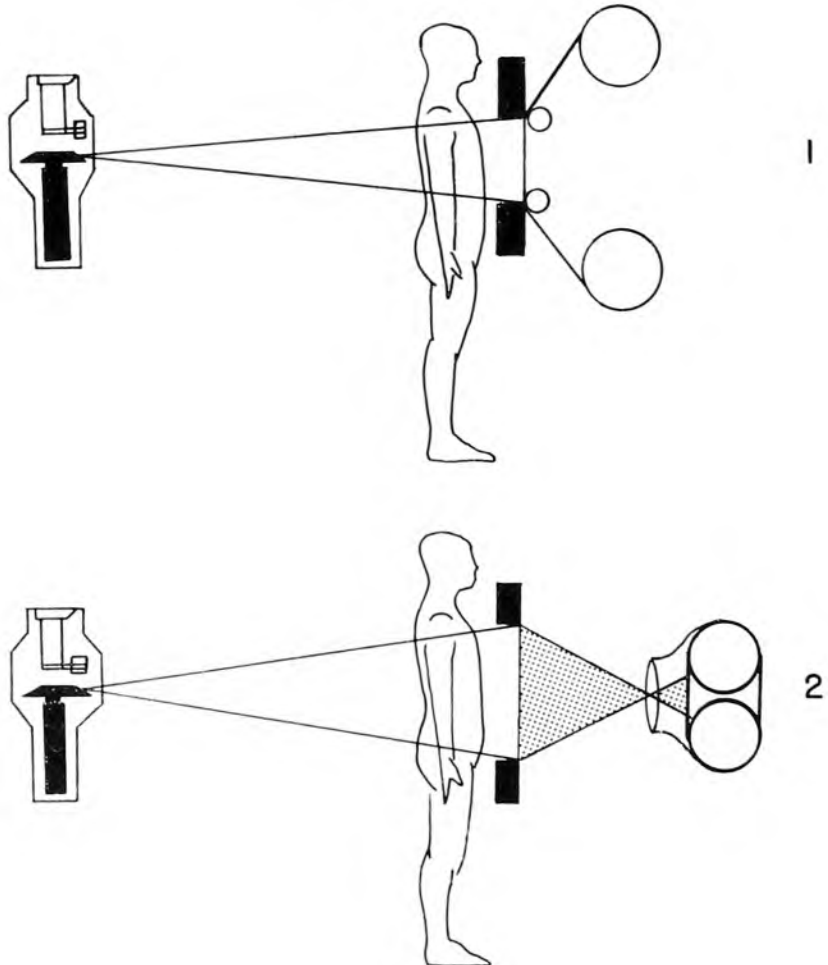
DIRECT AND INDIRECT METHODS OF X-RAY CINEMATOGRAPHY

X-ray cinematography may be defined as the cinematographic recording of a radiologic image such that the recording of this image, in terms of the number of exposures per unit time, is compatible with the usual standards for cinematography (Ref. 4). This definition establishes a distinction between the cinematographic recording of the radiologic image and serial radiography or serial fluorography, which consist in the serial recording of the radiologic image at a lower image frequency rate either by means of radiography or fluorography.

The direct method of x-ray cinematography (Fig. X-1,(1)) consists in exposing photographic film either directly or in contact with one or two intensifying screens to the radiologic image. The film is either in the form of a roll, and is serially exposed by means of a camera, or cut film may be used and exposed by means of a serial film changer (Refs. 2 and 3). The

FIG. X-1. Cinefluorography.

- 1 direct
- 2 indirect



dimensions of the radiologic image recorded by direct x-ray cinematography cannot exceed the size of the film because the radiologic image cannot be reduced in size. In general, the dimensions of the recorded field exceed the size of conventional cinematographic film, and the recorded image must be reduced in size and printed on cinematographic film for projection by a conventional motion picture projector. If the radiologic image to be recorded is sufficiently small in size, it can be recorded directly on film suitable for projection without minification. In this manner successful direct x-ray cinematography has been carried out on 70mm film (Ref. 5).

The quality of the image recorded by direct x-ray cinematography is excellent. On the other hand, the mechanical problems presented by the rapid transport of film are formidable, and although good apparatus have been developed to expose as many as 12 films as large as 14×14 in. per second, such a frequency is inadequate for cinematography (Ref. 4) and the devices are used only for serial radiography.

Smaller films (70mm) (Ref. 5) have been successfully used for direct x-ray cinematography with a suitably high number of exposures per unit time to achieve true cinematographic effect. However, the small size of the radiographic image thus recorded considerably reduces the usefulness of such a system. At this time the direct method of x-ray cinematography is practically abandoned in diagnostic radiology.

Indirect x-ray cinematography (Fig. X-1,(2)) consists in the cinematographic recording of the fluoroscopic image formed on a conventional fluoroscopic screen or on the output screen of an image intensifier by means of a cinematographic camera optically coupled to the screen. This method of x-ray cinematography is commonly referred to as *cinefluorography*, and this term will be used throughout this text.

Cinefluorography of the optical image by a conventional fluoroscopic screen yields images of good quality. Unfortunately, the light emitted by a fluoroscopic screen under standard conditions of fluoroscopy does not exceed a few microlumens per square centimeter (Ref. 6), and while such light output is adequate for a visual fluoroscopic examination after suitable dark adaptation, it is insufficient for the exposure of photographic film in the short period of time (about $\frac{1}{40}$ sec) required for cinematography. Under the circumstances, suitable film density, even with very fast photographic emulsions, can be obtained only by increasing the x-ray flux to a level intolerable for safety reasons in diagnostic radiology. Under the circumstances, while cinefluorography with a conventional fluoroscopic screen remains an acceptable method for the examination of experimental animals, this method has for all practical purposes been rejected in clinical diagnostic radiology. Currently, and with the exception of specialized research projects, cinefluorography is carried out with the help of some type of x-ray intensifier. The different components of a modern cinefluorographic unit are shown in Fig. X-2.

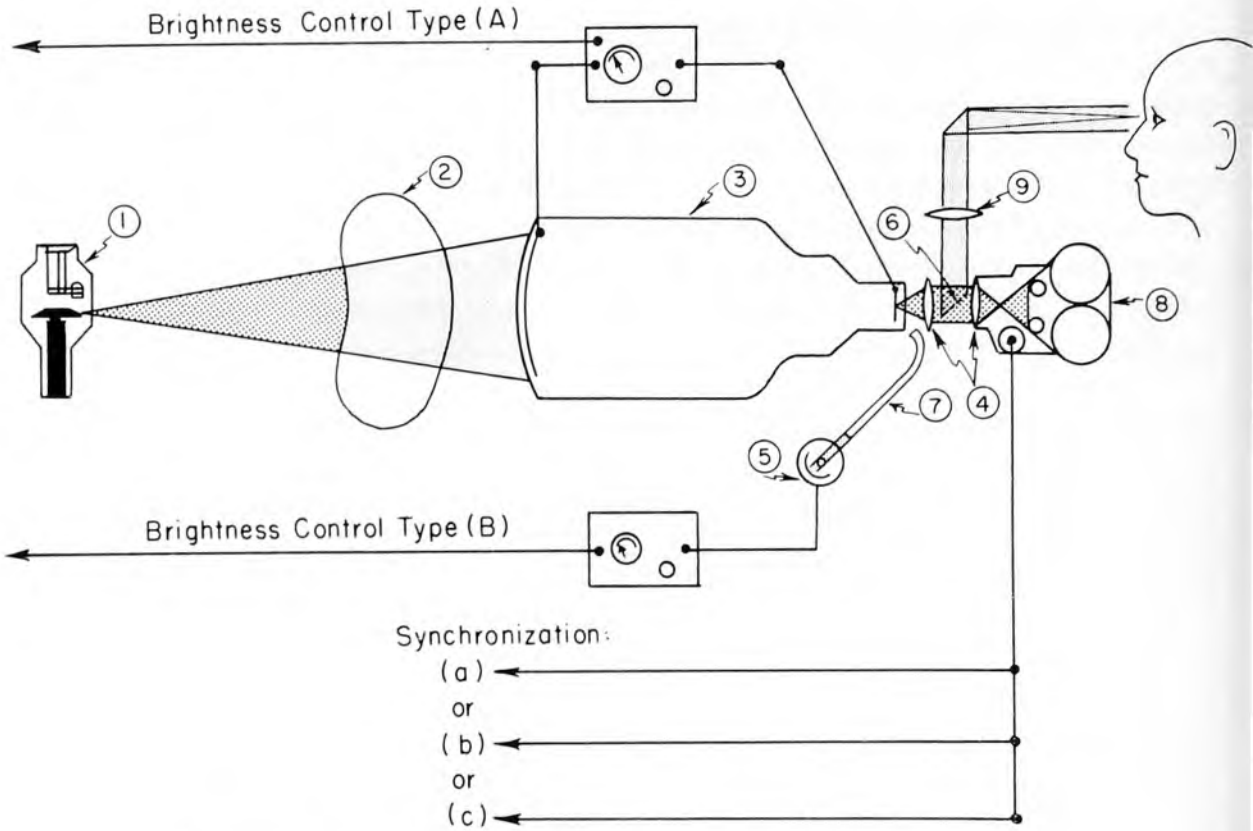


FIG. X-2. Schematic diagram of a typical cinefluorographic system.

- 1 x-ray tube
- 2 part examined
- 3 x-ray intensifier tube
- 4 lenses
- 5 photomultiplier tube
- 6 partially reflecting mirror used to monitor the image during recording
- 7 light pipe
- 8 cinematographic camera
- 9 field lens

Brightness control Type A is based on measurement of intensifier tube current. Brightness control Type B is based on measurement, by means of photomultiplier tube, of light emitted by screen of intensifier. Synchronization is controlled by camera motor, which supplies electrical signal either to: (a) thyatron tubes in circuit of x-ray generator; (b) grid-control tube; or (c) Dynapulse switching tube, or others.

THE X-RAY UNIT IN CINEFLUOROGRAPHY

The source of x-radiation commonly used in a cinefluorographic unit is, with minor modifications, a conventional diagnostic x-ray unit which has either a full-wave rectified generator or a constant potential generator. The current rating of the generator need not exceed 50 mA. The generator should be capable of delivering 150 kV to the x-ray tube. The primary

circuit of the generator used in cinefluorography usually requires thyatron control both for brightness control and synchronization (see the next two sections) (Ref. 7).

The x-ray tube should be able to withstand a current of up to 50 mA for several minutes and a voltage of up to 150 kV. Grid control tubes have been found to be useful in cinefluorography because they can supply well-defined pulses of radiation. For the latter reason the Dynapulse circuit may also be used in cinefluorography.

Synchronization in Cinefluorography

In cinefluorography it is desirable (1) to energize the x-ray tube only while the shutter of the camera is open, and (2) if the x-ray generator produces x-rays in pulses, to synchronize the opening of the shutter with the x-ray unit to admit a constant number of pulses per exposure. The term *synchronization* in cinefluorography refers to these two concepts.

Nonsynchronized Systems. Cinefluorography can be successfully carried out without synchronization between the production of x-rays and the opening of the shutter in the cinematographic camera. This method, however, exhibits the following disadvantages:

1. While the film is advanced in the camera (pull-down time) and while the camera shutter is closed (shutter-closed time), the examined patient is needlessly exposed to x-rays. In most cinematographic cameras the shutter-open phase is about 170 degrees (Fig. X-3), which means that the shutter remains closed for about one-half of the time and half of the radiation exposure of the patient is diagnostically useless. Special cameras with pull-down times and shutter-open phases of 270 degrees (Cinelix system) are used in cinefluorography partially to overcome these drawbacks.

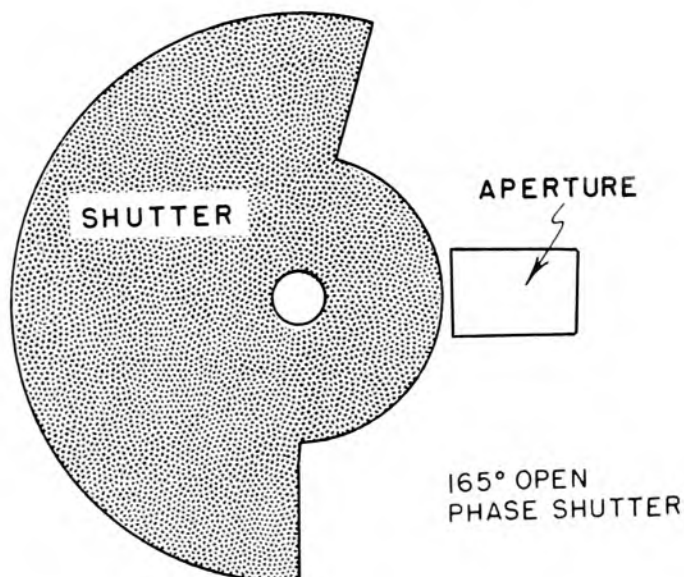


FIG. X-3. Cinematographic camera shutter.

2. The production of x-rays during the shutter-closed period results in unnecessary loading of the x-ray tube.

3. If a pulsating voltage is applied to the x-ray tube, such as is the case with a full-wave rectified circuit, absence of synchronization between the camera shutter opening and the production of x-rays may for short exposures result in unequal exposures of different frames (Ref. 7). This occurs because a constant shutter-open time of the camera may encompass a varying number of x-ray pulses. The relative variation of exposure thus produced increases with a reduction in the number of pulses occurring within the shutter-open time. This difficulty is for all practical purposes negligible for low frequency exposures but becomes a serious drawback of non-synchronous cameras operated with exposure rates greater than 30 frames/sec. Obviously this difficulty does not occur with x-ray systems energized by constant potential generators such as a three-phase 12-pulse generator (Chapter IV).

Synchronized Systems. Synchronization can be achieved relatively simply in cinefluorography by using a camera with equal shutter-open and shutter-closed times driven by a synchronous motor. Under these circumstances, no matter what difference in phase exists between the shutter opening and the pulsation of the x-ray beam, this difference in phase remains constant, and all frames are equally exposed.

The system, however, does not overcome the problems created by the production of x-rays during the film pull-down time, and the majority of clinically used cinefluorographic units employ a device which prevents the production of x-rays during the camera shutter-closed time. This device is a commutator and brush system attached to the synchronous motor, which provides an electrical signal synchronized with the shutter-open and shutter-closed phases of the camera. This electrical signal may be used to turn the x-ray beam on and off in a variety of ways. It may be used for the control of a pair of thyatron tubes connected "back to back" in the primary circuit of the high voltage transformer of the x-ray generator (Fig. X-4), allowing the x-ray circuit to be energized only during the shutter-open time. Or, the signal may be used for triggering either the switching tube in a dynapulse circuit or a grid control tube, either of which in a cinefluorographic system provides for short x-ray exposures independent of the number of frames per second used.

When synchronization is achieved by the use of thyatrons in the primary circuit of a half-wave rectified circuit, both time and magnitude of the exposure are inversely proportional to the number of frames per unit time (exposures increase at ratios of 1 to 2 to 4 for 30, 15, and $7\frac{1}{2}$ frames/sec, respectively). In the cinefluorographic recording of fast motion long exposures at a low frequency may be undesirable. This difficulty can be corrected by synchronizing the firing angle of the thyatron switching tubes to produce equal, short exposures independent of the number of frames per

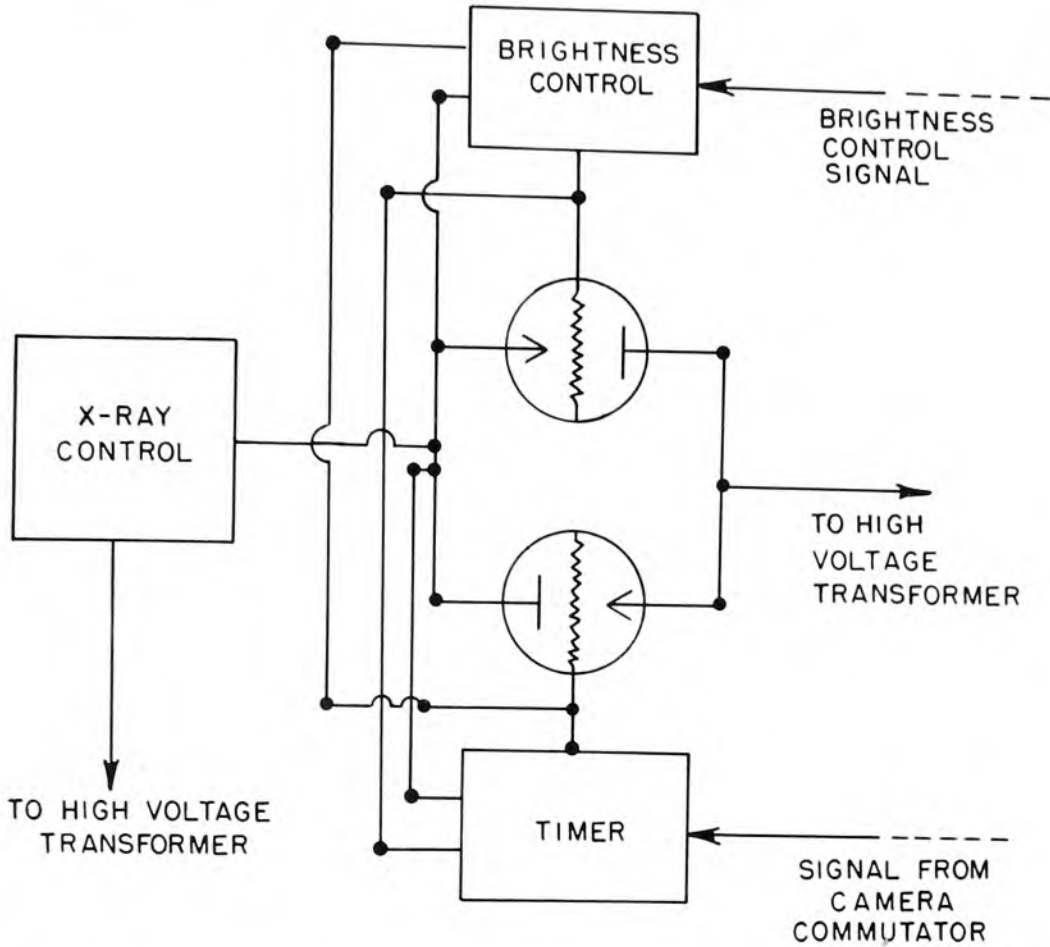


FIG. X-4. Block diagram of circuit used in cinefluorography for synchronization and brightness control. Synchronization and brightness are controlled by two thyristors connected "back to back" which control voltage supplied to primary circuit of x-ray generator.

unit time, which improve the sharpness of the x-ray images on the film (Ref. 7).

Cinefluorography carried out with x-ray intensifier systems which embody a television link presents special problems in their synchronization. These problems are discussed under "Kinefluorography."

Brightness Control

During cinefluorography the transmission of x-rays by the examined part may vary because the field of examination is moved, for example, from chest to abdomen; or because the attenuation of x-rays in the examined part is modified by the introduction of a contrast medium. The latter occurs frequently in cinefluorography of the gastrointestinal tract during the introduction of barium. A change in x-ray transmission results in a change in the brightness of the output screen of the x-ray intensifier, which in turn is re-

flected by a change in film exposure. Photographic film used in cinefluorography is generally high in contrast and short in latitude (see section on "Characteristics of Film used in Cinefluorography") and variations in exposure may result in images of unsuitable densities. It is consequently desirable to maintain the brightness of the output screen of the x-ray image intensifier within relatively narrow, preset limits. This is accomplished by the use of a brightness control circuit, which is included in most cinefluorographic units (Figs. X-2 and X-4).

Two brightness control systems are widely used in modern cinefluorography. In the first, a portion of the light emitted by the output screen of the x-ray intensifier is directed either by means of a plastic light guide or a small mirror to a photomultiplier tube which responds to this light stimulus by generating an electric current proportional to the intensity of the light received (Fig. X-2a). This current in turn is used to control the kilovoltage and the current of the x-ray tube by changing the firing angle of the thyratron tubes included in the primary circuit of the x-ray generator (Fig. X-4). The control can be either automatic or manual. The manual procedure involves reading the photomultiplier tube current on a meter and maintaining the meter reading within preset values by manual control of the x-ray circuit. This method of brightness control is similar to phototiming previously discussed (p. 147).

Another method for controlling brightness consists in measuring the current flowing between the input and output screens of the intensifier, as shown in Fig. X-2b and using this current to control the x-ray tube output by means of a system similar to the one described above.

Although most brightness control systems control both the kilovoltage and the current of the x-ray tube, they differ, in the relative amount of control of kilovoltage and tube current. Brightness control must be preset to a given value that depends on the speed of the film to be used in the examination and on the type of examination to be carried out. The exact setting for brightness control of a given cinefluorographic system is determined by empirical means. Brightness control systems function well and are very useful adjuncts to cinefluorography.

X-RAY IMAGE INTENSIFIERS FOR CINEFLUOROGRAPHY

The x-ray image intensifiers used in cinefluorography are conventional fluoroscopic x-ray image intensifiers (Chapter IX) adapted for cinefluorography. At this time there are no x-ray image intensifiers specifically designed for cinefluorography. Perhaps one exception is the development of an x-ray image intensifier tube with an output screen 7.4 cm in diameter (Rauland Corporation), approximately three times greater than that of conventional tubes. This tube is particularly suited for 35mm cinefluorography and 70mm photofluorography (see under "Film for Cinefluorography").

THE OPTICAL SYSTEM IN CINEFLUOROGRAPHY

The image supplied by the x-ray intensifier must be optically coupled to the photographic film in the camera. Most image intensifiers provide an image on their output screen approximately 1 in. in diameter. (Cinefluorography carried out with x-ray image intensifiers including a television chain present certain specific problems which are discussed under "Kinefluorography.") Usually the optical coupling between the output screen of the image intensifier and the photographic film is achieved by means of lenses, although it is not inconceivable that either mirror optics or fiber optics could be used for this purpose. Because of the desirability of reducing as much as possible the dose of x-radiation delivered to the patient during cinefluorography, it is important to achieve efficient optical coupling in the system, and therefore lenses having high relative apertures (low f -number) are used for this purpose. The lens system most commonly used in cinefluorography consists of a tandem of collimator lens and camera lens, as shown in Fig. X-5. The output screen of the x-ray image intensifier is placed in the focal plane of the collimator lens which provides a parallel beam of light for the camera lens. The camera lens produces an image of the output screen on the photographic film which is placed in the focal plane of the lens. In this arrangement both lenses are used at their infinity focus, and the magnification thus achieved is equal to the ratio of the focal lengths of the two lenses (Ref. 8). The high aperture lenses used for this purpose are generally composed of multiple elements assembled in a relatively long-barreled structure.

A factor that imposes undesirable limitations on the optical system used in cinefluorography is *vignetting*. The form of vignetting that is particularly troublesome in a tandem lens system is illustrated in Fig. X-6. All the light emitted by the object and impinging upon the collimator aperture is transmitted by the collimator in a cone the cross section of which is represented by the heavily shaded triangle. Around this cone, in the lightly shaded zones, only a portion of the light emitted by the outer edges of the object is transmitted. Thus, if the camera lens is placed in Position B, where its aperture intersects the zones outside the heavily shaded triangle, the image produced by the camera lens will exhibit a peripheral drop in illumination. This loss of light at the periphery of the image is referred to as vignetting. On the other hand, if the camera lens is placed in Position A, where the heavily shaded area completely fills the lens aperture, or if the lens is placed in any position to the left of A, vignetting would not be apparent on the image supplied by the camera lens.

Figure X-6 reveals that vignetting can be reduced (1) by bringing the camera lens as close to the collimator lens as possible; although even if the two lenses are in contact, a certain amount of vignetting may still occur within the lenses themselves, particularly if they are of the long barrel

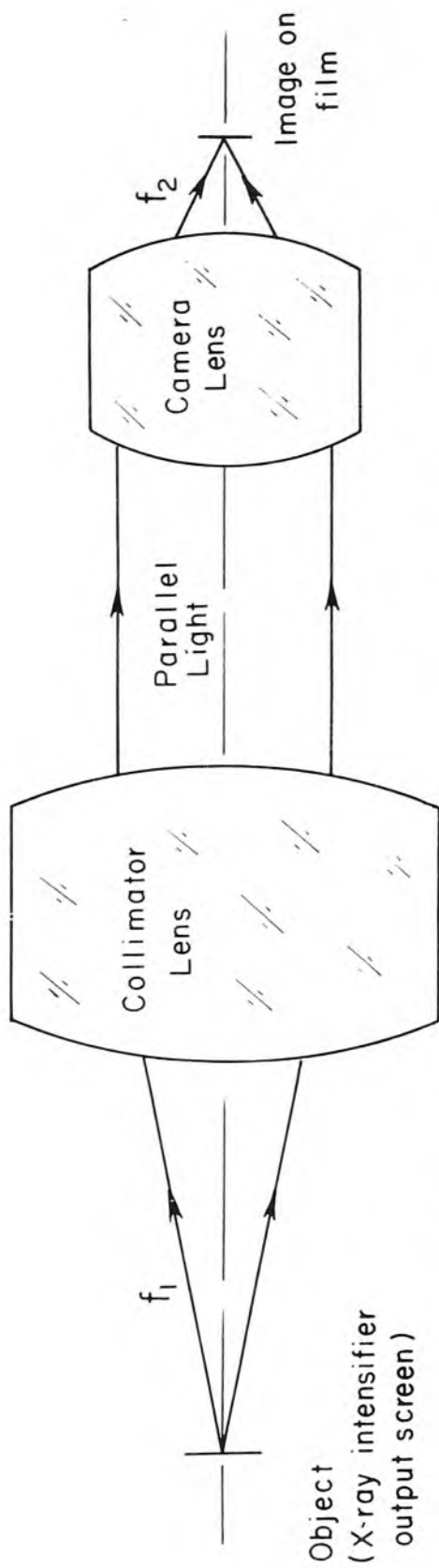


FIG. X-5. Two-lens tandem optical system used in cinefluorography for coupling x-ray image intensifier with camera.

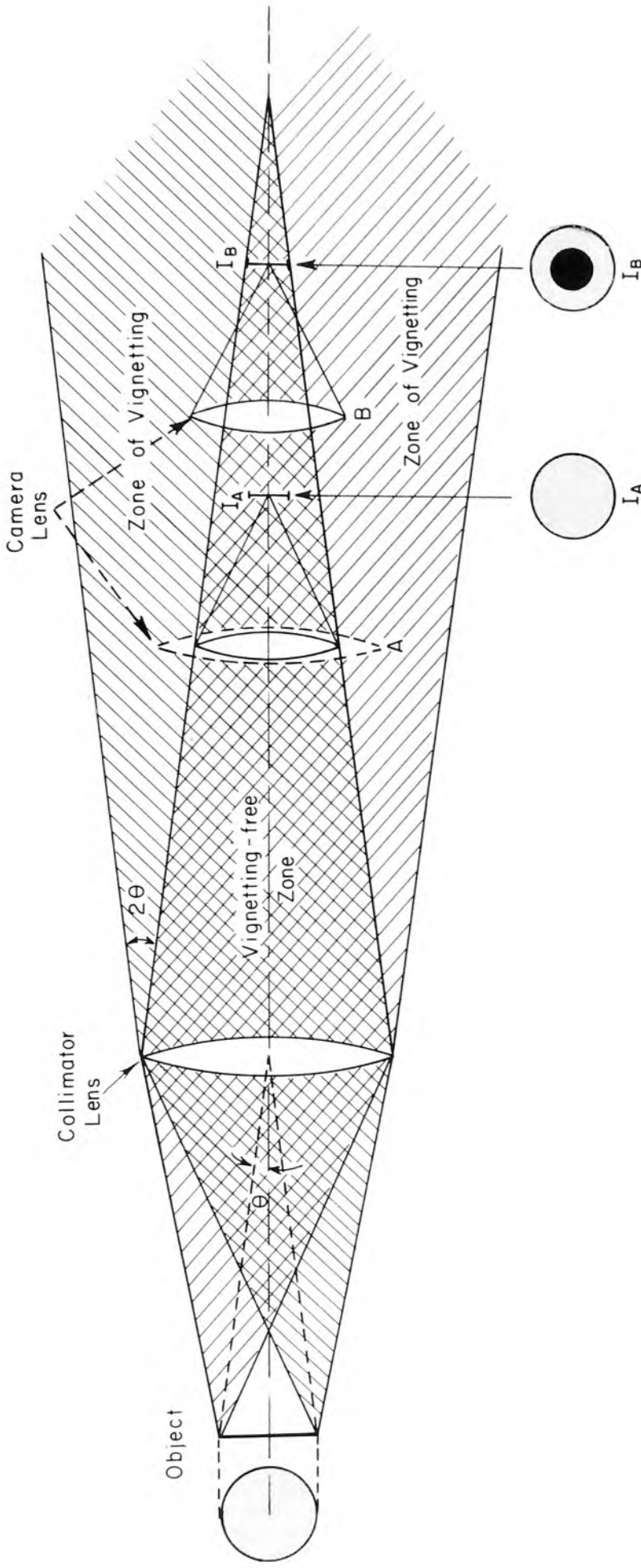


FIG. X-6. Vignetting in a two-lens tandem. When camera lens is placed in Position A, image I_A provided by lens is uniformly illuminated. If same lens is placed to right of A (Position B), image I_B thus provided exhibits zone of decreased illumination at its periphery. This effect is called "vignetting." A camera lens with a larger aperture (dotted outline) placed at A also shows vignetting because it intercepts the zone of vignetting.

type (loss of light in the lens mount itself); (2) by using a camera lens with an aperture diameter smaller than that of the collimator lens (a larger lens placed at A may exhibit vignetting, while a smaller one does not); and (3) by using lenses with relatively long focal lengths to reduce the angle of divergence of the parallel beam.

Therefore, to avoid vignetting, the following restrictions should be imposed on the design of the lens system:

1. The distance between the camera lens and the collimator lens should be as small as possible. However, because of various practical considerations, one of them being the desirability of placing a mirror between the two lenses for the purpose of monitoring the image (on "Image Monitoring"), this condition may not be easy to achieve.

2. The camera lens aperture must be smaller than that of the collimator lens. This means that if the same f -number is used for the collimator lens and the camera lens, the focal length of the camera lens must be shorter than that of the collimator lens, and the system will minify the image of the output phosphor. If a 1-to-1 ratio is desired between the output phosphor of the image intensifier and the image projected on the film, then the camera lens must have an f -number greater than that of the collimator lens, with consequent loss in light gathering efficiency.

3. If the collimator lens is to have the desirable long focal length it must have a large diameter, if a low f -number is to be achieved, and a large diameter requires a costly piece of glass.

It is apparent from these considerations that unless one is willing to sacrifice a large amount of light the image recorded on the film will be smaller in diameter than the image supplied by the output phosphor of the image intensifier.

The following example (Fig. X-7) illustrates the restrictions imposed on an optical system by vignetting (see also Fig. X-6). An x-ray image intensifier tube with an output screen 25 mm in diameter is optically coupled to a camera by a tandem of lenses composed of (1) a collimator lens having a focal length of 100 mm, a maximum aperture diameter of 66 mm, and $f/1.5$ and (2) a camera lens having a focal length of 40 mm, a maximum aperture diameter of 40 mm, and $f/1.0$.

The focal length of the collimator lens is sufficient to clear the well (Fig. X-8) which is sometimes provided for technical reasons around the output screen of some x-ray image intensifier tubes, and to provide a sufficiently small angle of divergence that will result in a reasonably long vignetting-free zone. The focal length of the collimator lens is also sufficiently short to provide a high aperture ratio ($f/1.5$) with a lens aperture diameter of reasonable size (maximum aperture 66 mm).

The aperture of the camera lens must be appreciably smaller than that of the collimator lens to avoid vignetting. Furthermore, it is desirable to provide some distance between the collimator lens and the camera lens to

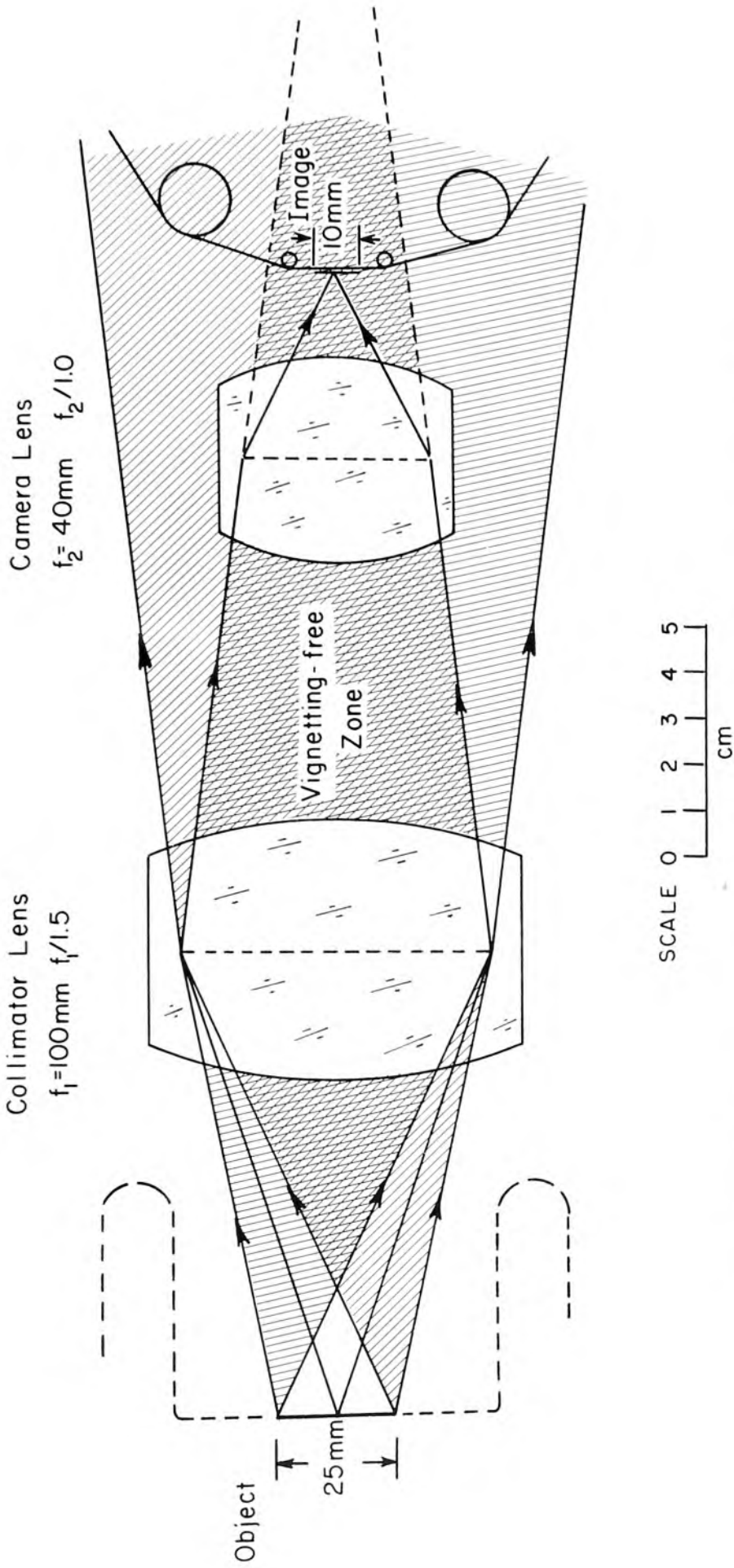


FIG. X-7. Possible combination of lenses for cinefluorography, coupling typical 25-mm (1-in.) x-ray image intensifier output screen to 16mm film. Characteristics and location of lenses are such as to avoid vignetting and to provide adequate space between them for insertion of a beam splitter (shown in Fig. X-8).

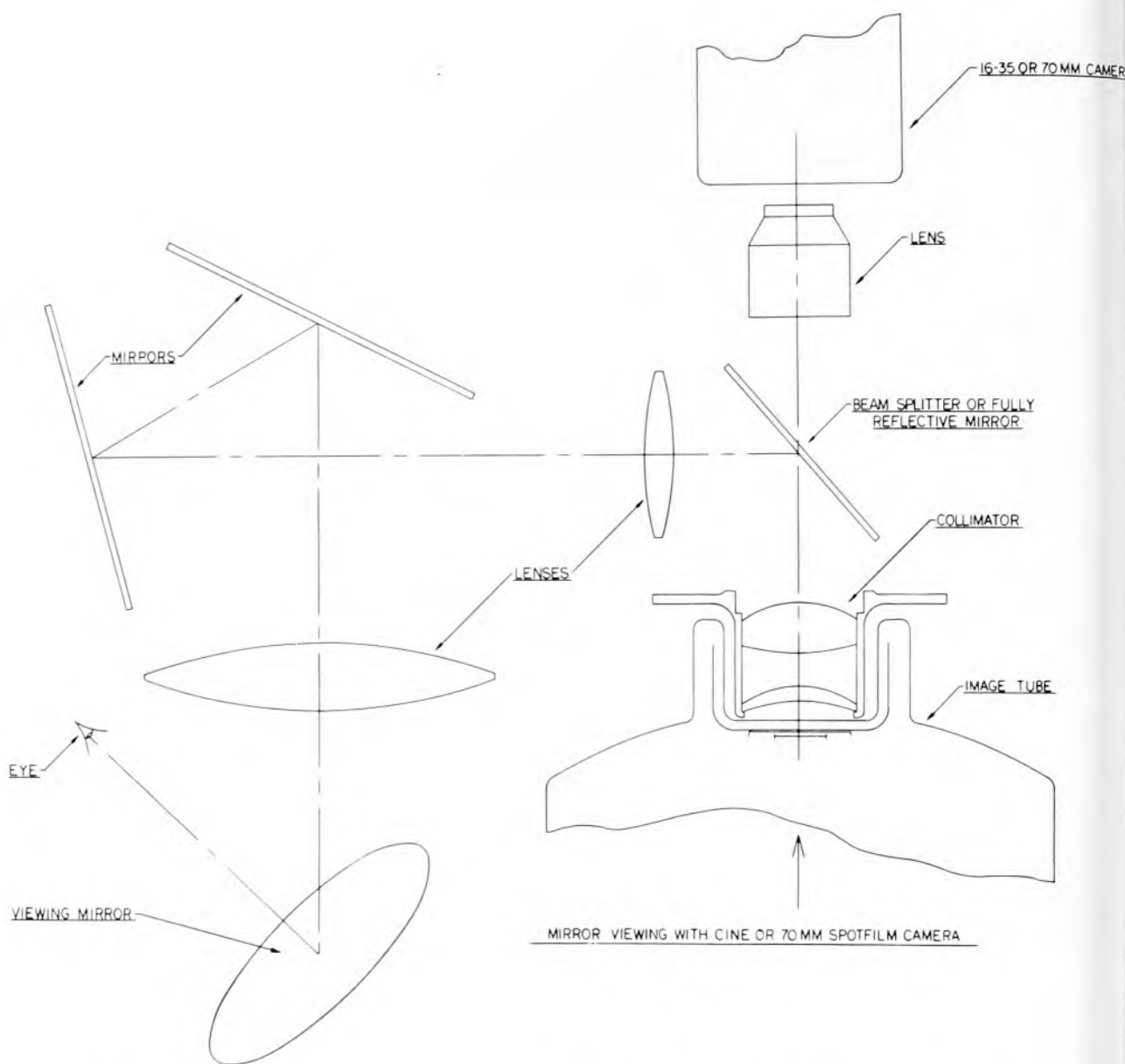


FIG. X-8. Scale diagram of typical optical system used in coupling x-ray image intensifier tube with either a 16mm or 35mm camera for cinefluorography, or with a 70mm spot film camera. Image monitoring and fluoroscopy carried out by optical system.

Lens Ratings

	Focal length	f -number
Collimator	56 mm	1.0
16mm camera lens	25 mm	0.95
35mm camera lens	75 mm	1.5
70mm camera lens	175 mm	2.5
Field lenses	175 mm 350 mm	

provide room for a mirror for the monitoring system. A camera lens with a maximum aperture diameter of 40 mm produces a vignetting-free image for a distance between the nodal planes of the two lenses of about 10.5 cm. The camera lens provides a distance of approximately 5 cm between the glass surfaces of the collimator lens and the camera lens which are facing each other. The camera lens, of course, should also have a high aperture ratio, and therefore its focal length must be kept short. The selection of a 40-mm focal length provides a desirable $f/1.0$.

The system of lenses described above results in an image minification of

$$\frac{f_1}{f_2} = 2.5,$$

where f_1 is the focal length of the collimator lens and f_2 the focal length of the camera lens. Therefore, the image of the 25-mm output screen of the image intensifier is approximately 10 mm in diameter. Such an image can be reasonably well recorded on standard 16mm film (see under "Film for Cinefluorography") with a slight loss of image in the vertical direction.

In the above example, if instead of using 16mm film to record the image supplied by the image intensifier it is desired to fill a 35mm frame, which is approximately twice as large, the camera lens must be replaced by a lens having a focal length twice as long. However, the maximum diameter of the camera lens aperture must remain the same to prevent vignetting. Under the circumstances, the f -number of the 35mm camera lens must be $f/2.0$. Since the illuminance of the image provided by a lens is inversely proportional approximately to the square of the f -number, the use of 35mm film instead of 16mm film results in a reduction of illuminance by a factor of 4.

It is therefore inefficient to attempt to record on 35mm film the image supplied by an image intensifier with a small-diameter output screen. On the other hand, if the output screen of the x-ray image intensifier is larger in diameter (for example, 50 or 75 mm), then the 35mm frame can be efficiently filled with the aid of a low f -number lens. For this reason x-ray intensifier tubes having larger output screens are designed to be used in connection with 35mm film. The argument also holds for even larger film, such as 70mm. A 70mm image can be obtained either by using a longer focal distance camera at the cost of light (lower f -number) (Fig. X-8), or by starting with a larger diameter image of the output of the image intensifier tube.

Cameras for Cinefluorography

The cameras used in cinefluorography are not fundamentally different from the cameras used in conventional cinematography. Two cameras that have been extensively adapted for cinefluorography are (1) the 16mm

Kodak cine special camera modified for synchronous operation of 7.5, 15, 30, and 60 frames/sec, to be used in connection with full-wave rectified circuits; and (2) the 35mm Arriflex camera, which has a continuous variable speed drive providing from 8 to 64 frames/sec. The more modern cinefluorographic systems have been fitted with cameras specifically designed for the purpose but which are not fundamentally different from conventional cameras and are therefore not further discussed in this text.

IMAGE MONITORING DURING CINEFLUOROGRAPHY

In cinefluorography, as in cinematography, it is desirable to monitor visually the recorded image. This is usually accomplished by diverting by means of a partially transparent mirror placed between the collimator and the camera lens a portion of the light that forms the image of the output screen of the image intensifier. The diverted imaging beam can be used either (1) to form an image by means of an optical system, to be observed by the radiologist, or (2) to form an image on the input screen of a television pickup tube that is displayed on a monitor, also to be observed by the radiologist (Fig. X-9).

The partially transparent mirror used for this purpose is designed to reflect only 5 to 10% of the light, thus 95 to 90% of the light is used by the camera and only a negligibly small fraction of light is used for monitoring. It should be noted that the intensity of the beam of x-rays required for cinefluorography is at least ten times higher than that used in fluoroscopy with image intensifiers; consequently, even the small percentage of light diverted is adequate to supply an image of brightness at least equal, if not superior, to that obtained in image-intensified fluoroscopy. This image, however, is affected by flicker resulting from the synchronization of the x-ray beam with the camera. (The system can be used for fluoroscopy without cinefluorography, in which case the partially transparent mirror is replaced mechanically by a fully reflecting mirror; the intensity of the beam of radiation used may then be reduced by a factor of at least 10, usually closer to 50.)

Direct Image Monitoring

The optical system used for direct monitoring of the cinefluorographic image without the help of a television chain consists in general of a field lens (collector lens) that collects the bundle of parallel light beams emerging from the collimator lens and forms an image which can be observed by the radiologist (Ref. 8). The image formed by the field lens can be observed without loss of field of vision or of light only if the eye of the observer is placed within the *exit pupil* of the optical system, which is the projected image of the aperture of the collimator lens formed by the field lens (Fig. X-10). If the diameter of the exit pupil is smaller than the separation between the pupils of the eyes of the observer (*pupillary distance*), only

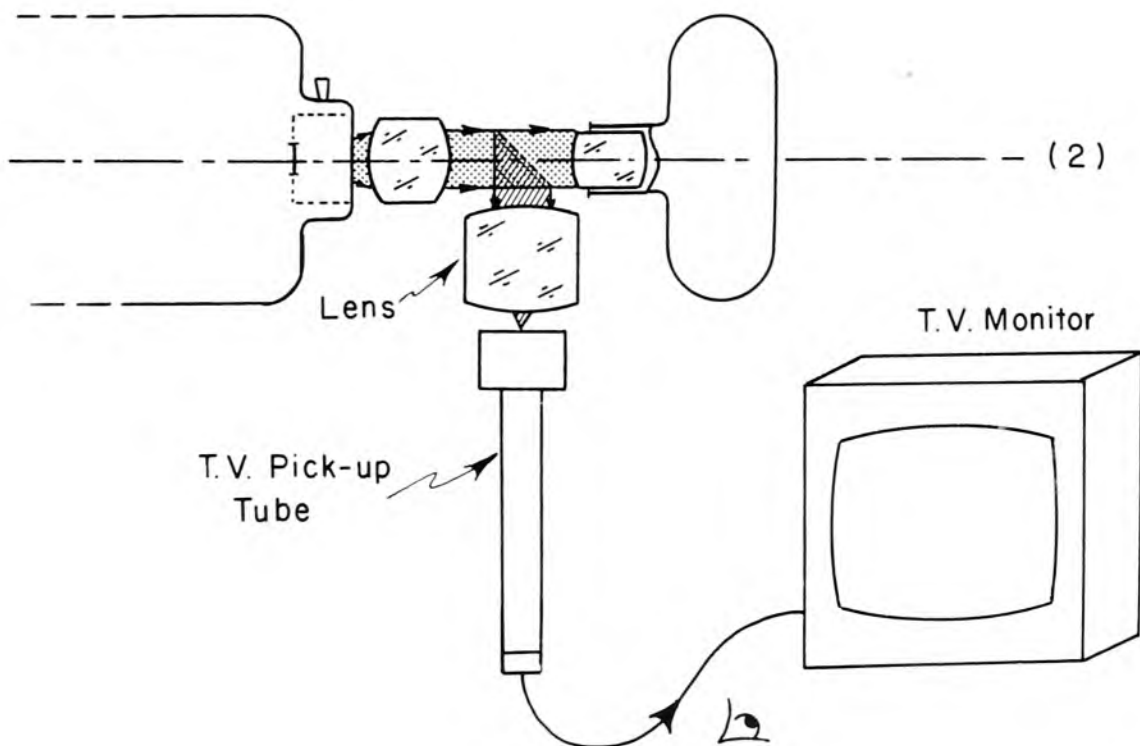
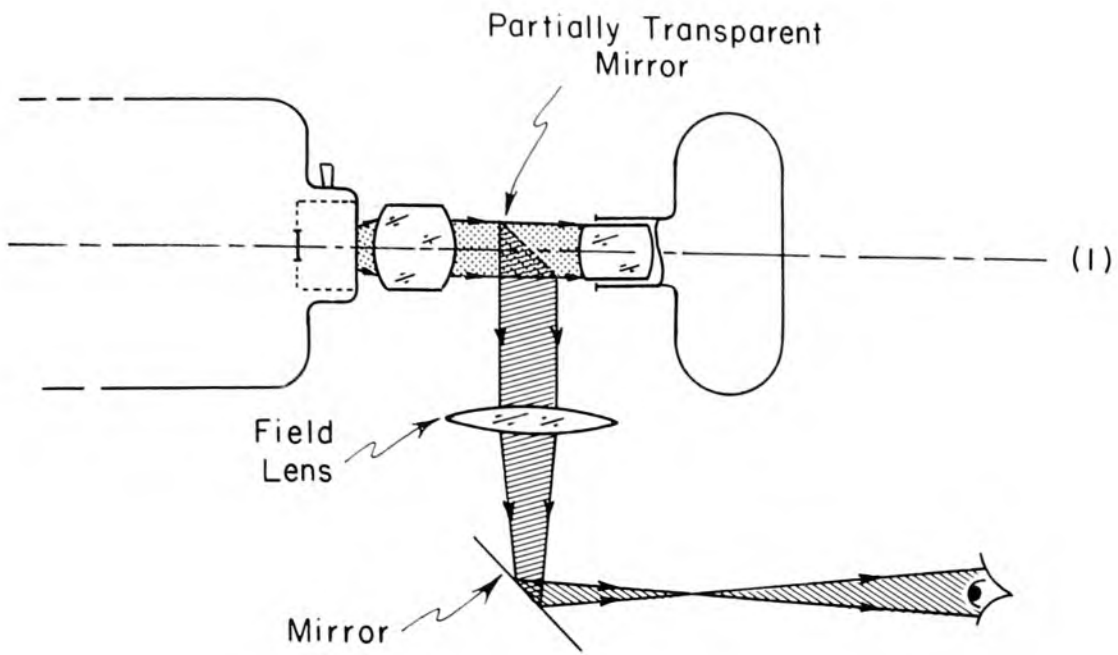


FIG. X-9. Image monitoring in cinefluorography.
 1 direct optical monitoring
 2 television monitoring

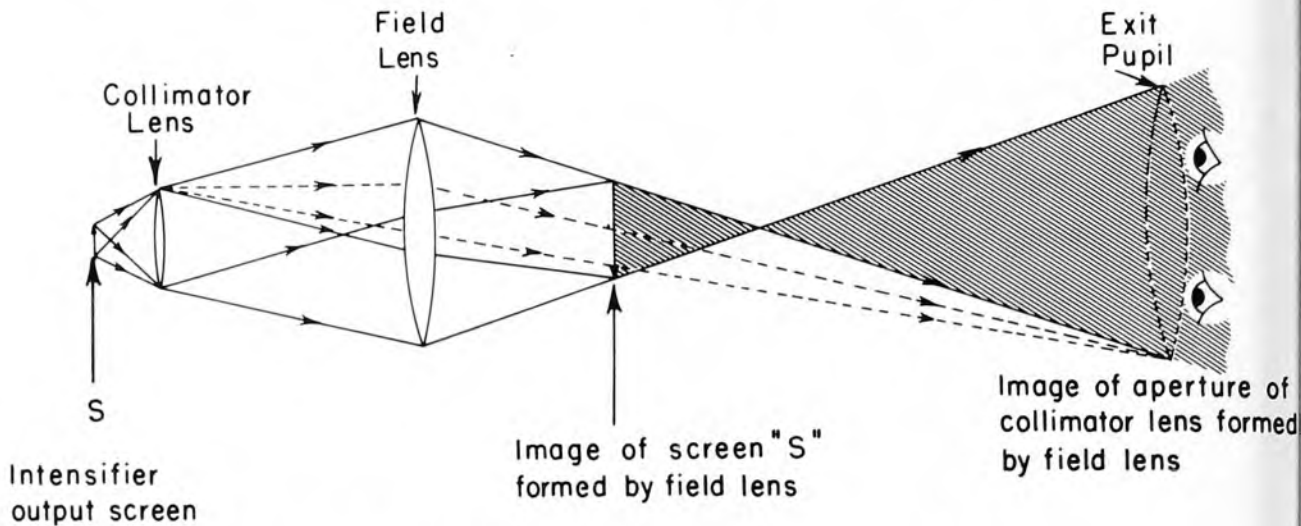


FIG. X-10. Exit pupil in cinefluorography monitoring.

monocular vision is possible. On the other hand, if the exit pupil is equal to or greater than the pupillary distance, the image of the screen can be observed by both eyes simultaneously, which is highly desirable. Most optical systems for viewing in fluoroscopy with image intensification are designed to provide a sufficiently wide exit pupil to make binocular observation possible.

A second purpose of the field lens is to magnify sufficiently the image of the relatively small output screen of the image intensifier. This magnification should allow comfortable observation at a viewing distance not shorter than approximately 20 cm because the human eye is incapable of easy focusing at shorter distances. Unfortunately, the diameter of the exit pupil and the magnification of the optical viewing system are inversely proportional to each other, and the design of the system must compromise between these two factors, which are also related to the f -number of the objective lens. The addition of a second lens to the optical system can increase its magnification and still retain an adequate exit pupil diameter for binocular vision. Usually several plane mirrors are also incorporated in the optical system to bring the observed image into a convenient position for observation during fluoroscopy or cinefluorography (Ref. 8). A typical optical viewing system is shown in Fig. X-8.

The system described allows only one individual to observe the image because there is not sufficient room to accommodate two pairs of eyes within the exit pupil. This situation may be remedied by diverting part of the image by means of a partially transparent mirror introduced in the optical path of the image. Thus, two observers may view the image simultaneously; however, the image of each observer is dimmer because of the division of light.

A purely optical system for the viewing of an image supplied by an

x-ray image intensifying system offers the advantage over an electronic system of being less expensive and free from electronic malfunction. On the other hand, the disadvantages of this system are as follows: (1) Only one, or perhaps two individuals are able to utilize the system simultaneously, when under certain circumstances it may be desirable to show the procedure to a greater number of observers. (2) The relatively narrow exit pupil of the system obliges the observer to keep his eyes within a relatively narrow beam of light, with an undesirable fading of the image when one of the eyes is displaced out of the field of the exit pupil. (3) In certain radiologic procedures accomplished with the help of image intensification and cinefluorography, such as cardiac catheterization, it is sometimes awkward for the individual who performs the procedure to be restricted in the position of his head by the exit pupil of the system.

Because of these disadvantages, many cinefluorographic units as well as fluoroscopic image intensifiers have a television chain added to their purely optical viewing system, or utilize television monitoring alone.

Television Monitoring

Television monitoring during cinefluorography is achieved by focusing by means of a lens the bundle of parallel beams diverted by the partially transparent mirror onto the input screen of a television pick-up tube (either a Vidicon or an Image Orthicon) and by displaying the image formed by the television chain on the screen of a kinescope (Figs. X-9, (1), X-11, and X-12). The diameter of the input screen in conventional television pick-up tubes is about the same as that of the output screen of the image intensifier, and efficient optical coupling between them is relatively easy to achieve with a conventional lens. The quality of the television chain selected for the purpose (number of lines in frequency bandpass of the electronic system) determines the quality of the image displayed on the monitor, which may be as good as that supplied by the output of the image intensifier.

Television monitoring in cinefluorography offers three main advantages over optical monitoring: (1) The image can be displayed simultaneously on several kinescopes remote from the image intensifier system, thus allowing a number of individuals to observe the procedure. (2) Monitoring of radiologic procedures by television is easier than by means of optical systems because in television systems the position of the head of the observer is not restricted by the exit pupil of the optical system. (3) The contrast of the image supplied by the television chain can be altered electronically, which under certain circumstances may improve the quality of the observed image.

The main disadvantages of television monitoring are: (1) relatively high cost, (2) they are subject to malfunction, as any other electronic system, and (3) synchronization is required between the x-ray unit and the television system.

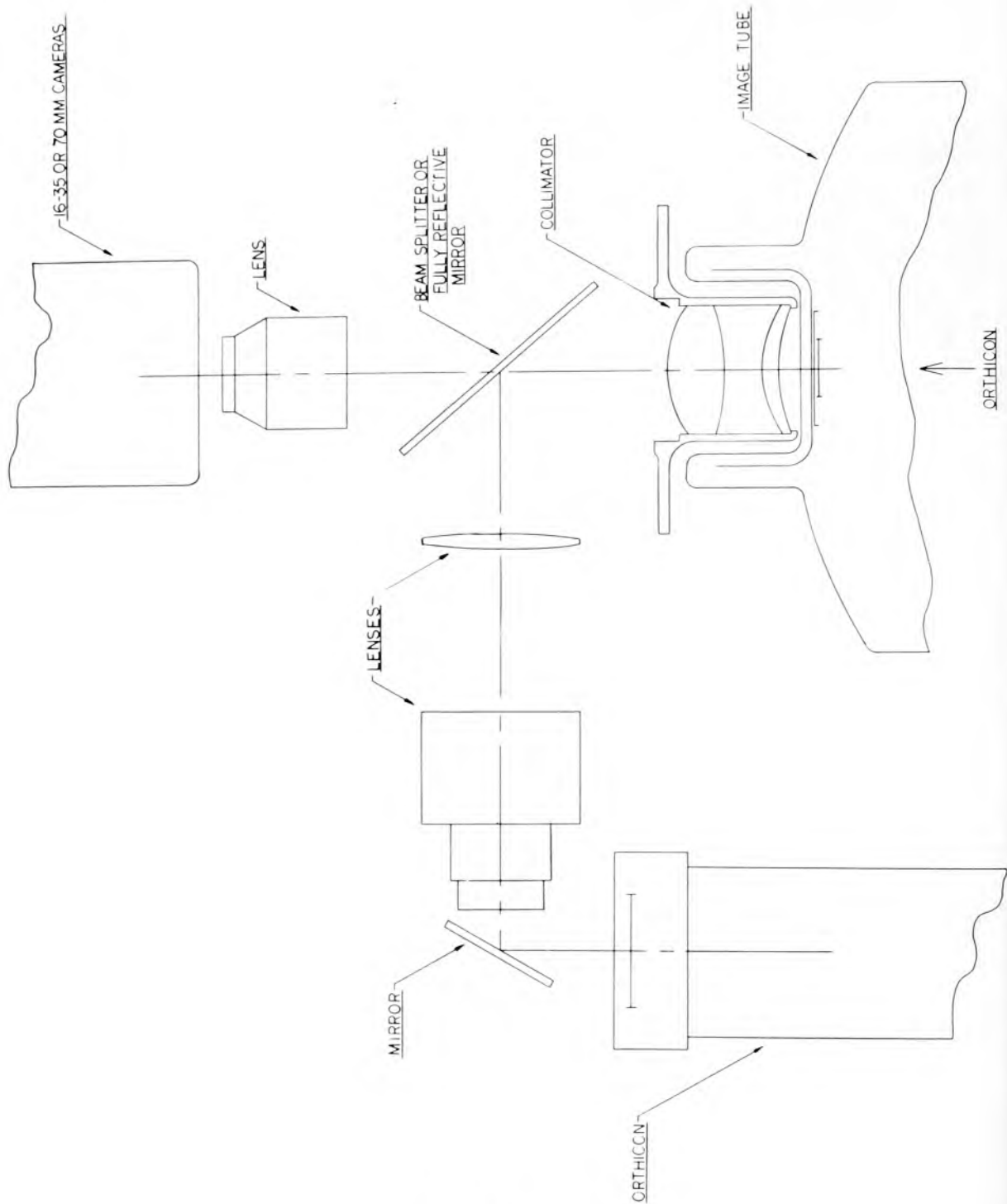


FIG. X-11. Scale diagram of same system as in Fig. X-8, with Image Orthicon television monitoring. Television lens $f = 100$ mm, $f/2.3$.

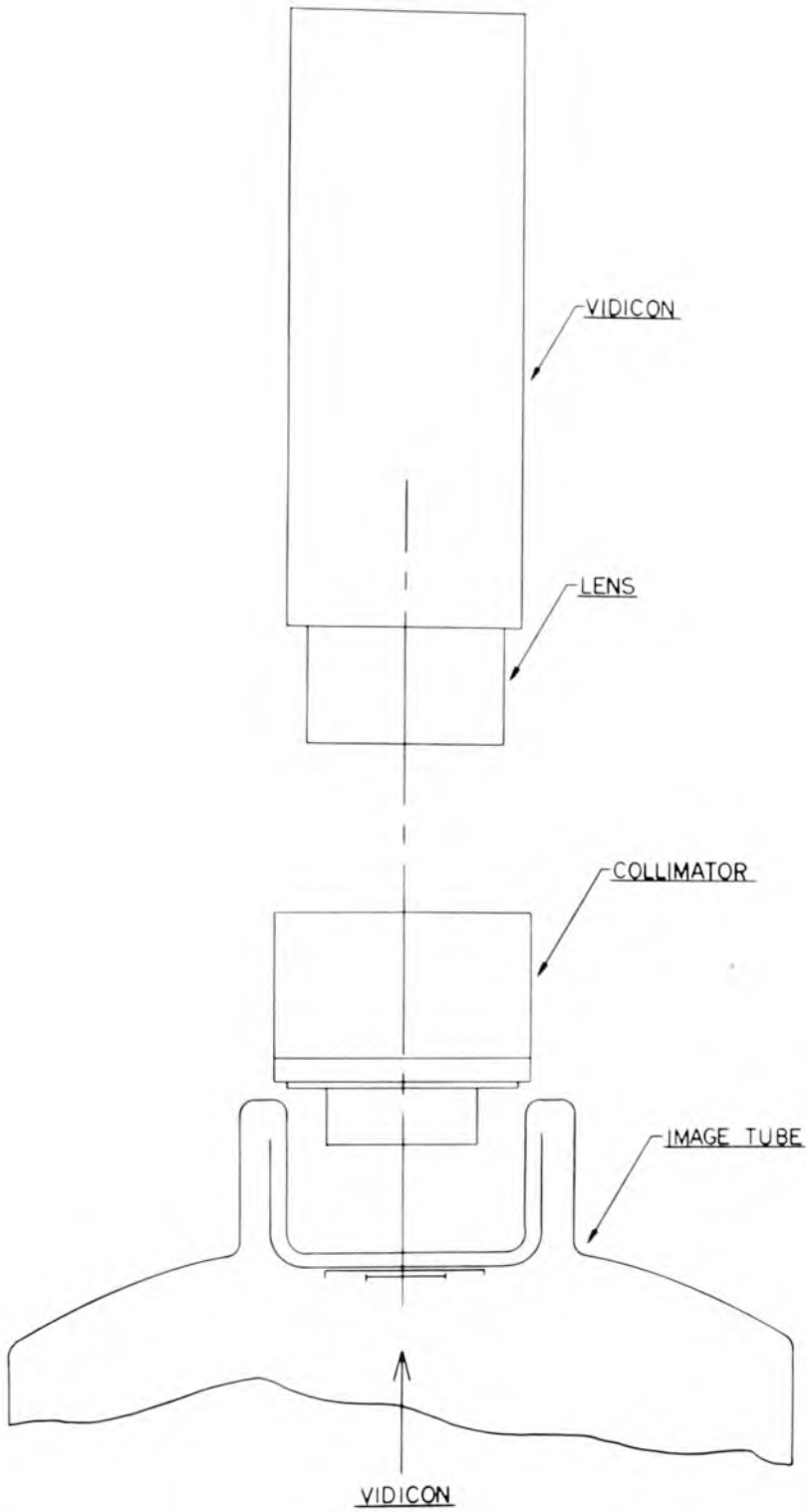


FIG. X-12. Scale diagram of optical system for direct coupling of x-ray image intensifier tube with Vidicon television pickup tube.

Collimator $f = 75 \text{ mm}, f/1.1$

Television lens $f = 37 \text{ mm}, f/1.0$

FILM FOR CINEFLUOROGRAPHY

16mm Versus 35mm Film

The cinefluorographic image is usually recorded on 16mm- or 35mm-wide film. The use of 70mm film for this purpose encounters difficult problems, particularly in the design of suitable lenses. Furthermore, it appears, as will be shown in this section, that 35mm film is capable of recording all the detail the other components of the cinefluorographic systems are capable of supplying, and therefore the use of wider film is not warranted.

A camera using 16mm-wide film takes 40 frames per foot of film, and the dimensions of each frame are 10.5 mm \times 7.5 mm; while a 35mm camera takes only 16 frames per foot of film, and the frames are 20 mm \times 18 mm (Ref. 9). Thus the area of a 35mm-film picture is approximately four times greater than that of a 16mm-film picture; therefore, approximately four times as many silver halide grains are exposed per resolution element in a photograph taken on 35mm film than if the same image were reduced to the size of a 16mm-film frame. It appears, therefore, that 35mm cameras should be preferred to 16mm cameras in cinefluorography from the standpoint of better detail resolution. In fact, the greater resolution achieved per resolution element by means of 35mm film as compared to 16mm film has little bearing on the quality of the image obtained with cinefluorographic systems presently available, because components other than the film limit the resolution of the systems to such an extent that full advantage cannot be taken of the film resolving power. On the other hand, the difference in size between 35mm and 16mm frames may affect not only the resolution but also the light gathering efficiency of the optical system in cinefluorography by altering the required minification of the output screen of the image intensifier. This effect can be illustrated by the following example:

Consider a cinefluorographic system consisting of a 5-in. diameter input x-ray intensifier tube, of suitable optics, and of a 16mm camera. The diameter of the input screen is reduced in such a system to the minimum dimension of the 16mm frame, which is 0.75 cm, by a factor of about 17. If the x-ray image intensifier is of particularly good quality, it is capable of resolving approximately 3 lines/mm (Table VI-1, Chapter VI) (most image intensifiers exhibit a lower resolving power). Thus the film, in order to reproduce faithfully the image incident upon the input screen of the image intensifier, must be capable of resolving at least $17 \times 3 = 51$ lines/mm. This resolving power is well within the capabilities even of particularly fast film (Table X-1), and under these circumstances the resolving power of the film does not limit the quality of the image. The resolving power of the camera used in producing the image on the film varies from approximately 40 to 50 lines/mm for average cameras to high values of 80 to 100 lines/mm for better apparatus

TABLE X-1. Characteristics of Some Films Used for Cinefluorography

EASTMAN KODAK FILMS

(Courtesy of X-Ray Sales Division, Eastman Kodak Company)

I. Photography of Image Intensifier Output Phosphor

Film ^a	Sensitivity	Speed ^b	Contrast ^c	Resolving power ^d (lines/mm)
Kodak Cineflure	orthochromatic	100	1.75	80
Kodak Linagraph Shellburst	panchromatic	70	1.75	100
Kodak Double-X Negative	panchromatic	100	1.30	89
Kodak Plus-X Negative	panchromatic	40	1.30	80

II. Photography of Television Displays (Kinescope Recording)

Kodak special TV cinefluorographic film (a range of contrast may be achieved by varying developing time)

III. Printing Material

Kodak fine grain positive film (a contrast of about 2.0 can be achieved)

DU PONT FILMS

(Courtesy of E. I. du Pont de Nemours & Company, Inc.)

I. Photography of Image Intensifier Output Phosphor

#931: Panchromatic, high-speed reversal film, contrast about 1.75 (Ref. 21)

#936: Panchromatic, very fine grain, medium speed, wide latitude negative film; contrast about 1.5 (Ref. 21)

#140: Panchromatic, fine grain, high contrast film (see characteristic curve in Chapter VI, Fig. VI-17)

II. Photography of Television Displays

#834: Fine grain, high speed-low contrast emulsion for the photography of either positive or negative images on kinescopes; sensitivity ultraviolet, violet, and blue

^a Kodak Rapid X-Ray Developer, 7 min, 68°F.

^b Kodak Cineflure assigned a speed of 100; speed based on exposure required to reach a net density of 0.85.

^c Contrast based on average gradient of the characteristic curve over a log exposure range of 0.9 (i.e., a subject contrast of 8:1), centered about a net density of 0.85.

^d Resolving power based on microscopic examination of these films when used to photograph a resolving power test chart having a contrast of 6.3:1; a "perfect" optical system was employed.

(Ref. 9). Thus, in order to match the quality of the image supplied by the x-ray image intensifier, a "good" camera must be selected.

Consider now a cinefluorographic system composed of a 9-in. diameter input x-ray image intensifier coupled to a 16mm camera. The minification achieved by such a system is approximately 30, and the film must be capable

of recording $30 \times 3 = 90$ lines/mm (Ref. 14). This value is borderline for the resolving power of the film, and particularly for the camera used. Indeed, a particularly good camera must be used to be able to record such detail.

On the other hand, if the same x-ray image intensifier (9-in. diameter input screen) were used in connection with a 35mm camera, the minification factor would be only 12.5, and the maximum resolution required from the film and the camera would be only about 50 lines/mm, which is an easy requirement to fulfill both for the camera and the film. It should be remembered that a resolution of 3 lines/mm is better than that achieved by most x-ray image intensifiers. This means that in this example particularly stringent conditions were imposed on the camera and the film.

The above example shows that the use of a 16mm camera in conjunction with a 5-in. diameter input x-ray image intensifier does not result in an appreciable loss in resolution, while if a larger input image intensifier is used, particularly if the instrument is capable of high detail rendition, a 35mm camera is to be preferred. However, with use of small-diameter image-intensifier output screens (1 in. or less) it is not practical to develop a 35mm optical glass system that competes in speed with a 16mm system, and the choice of a 35mm camera coupled with a 1-in. diameter image-intensifier output screen results in a system which is about four times slower than if the image intensifier were coupled to a 16mm camera (see under "Optical System in Cinefluorography"). Under these conditions, because of the desirability of using faster systems, 16mm cameras are generally preferred to the 35mm size.

The difficulties encountered in coupling efficiently the image intensifier to a 35mm camera can be partially resolved by using an intensifier with a larger-size output screen (see p. 355). Such x-ray image intensifier tubes have been constructed but are not widely used because they exhibit a considerably lower luminance gain owing to smaller minification gain. They are usable only for cinefluorography because their low gain does not render them particularly attractive for direct image-intensified fluoroscopy. (They can be used to advantage in connection with Orthicon television chains.)

The above discussion shows that the use of larger film, such as 70mm, does not appreciably improve the quality of the cinefluorographic image if the procedure is carried out with image intensifiers presently available.

Film Characteristics

The wavelength of the light emitted by the output screen of an image intensifier used for fluoroscopy must fall within the sensitivity range of the human eye, and preferably in a high sensitivity range. For this reason the phosphors in the output screens of image intensifiers fluoresce usually in the yellow-green range. Consequently, cinefluorography can be carried out only with films which encompass yellow and green light in their sensitivity response. (An exception is the kinescopic recording of blue-fluorescent kine-

scope screens.) X-ray film, which is sensitive only in the ultraviolet and blue-violet, is unsuitable for cinefluorography as it is practiced now. It is not inconceivable that an ultraviolet fluorescing phosphor could be incorporated in the output screen of an image intensifier to be used only for cinefluorography to the exclusion of visual observation. Such a system, however, would present the serious drawback of requiring quartz optics.

Orthochromatic emulsions, which are sensitive to ultraviolet, blue, and green light, and *panchromatic* emulsions, the response of which approximates that of the human eye and covers a broad sensitivity spectrum from violet to red, are suitable for cinefluorography.

In addition to suitable wavelength sensitivity, photographic film used in cinefluorography should exhibit three desirable characteristics: high speed, high contrast, and fine grain (Ref. 10). *High speed* is desirable to carry out cinefluorography with a minimal dose of radiation for the patient and to reduce possible motion blurring by reducing exposure time. *High contrast* puts in evidence structures having relatively low subject contrast. *Fine grain* allows good reproduction of detail. These three characteristics depend on the composition of the photographic emulsion used on the film, and also, but to a lesser degree, on the developing of the film after exposure. In general, if developing is increased either by increasing time or temperature, or by using a more "energetic developer," both the speed and the graininess of the exposed film are increased.

Any two of the three characteristics can be improved at the expense of the third (Ref. 10). For example, a high speed-high contrast film is grainier than a high speed-low contrast film; conversely, a high speed-fine grain film exhibits relatively lower contrast than a lower speed emulsion. It should be noted that the graininess of a particularly high speed-high contrast film is considerably enhanced by the fact that quantum mottle (Chapter VII), resulting from the statistical fluctuations of the relatively low number of x-ray photons required for a suitable exposure with a fast film, is superimposed over the inherent graininess of the film. Furthermore, graininess is enhanced by the high contrast of the film.

In summary, the choice of film for a given cinefluorographic examination depends on a compromise between the dose of radiation to which the patient can safely be exposed, the contrast desired, and the detail reproduction desired. Which of the three factors can be sacrificed to enhance the others is a personal choice of the radiologist who performs the examination. Table X-1 lists some physical characteristics of films commonly used in cinefluorography.

Negative and Reversal-Type Films

Under normal conditions of photography the areas of the film exposed to light become opaque to light after suitable processing because of the presence of silver particles, while the unexposed areas are transparent to light

because of the removal of unexposed silver salts during processing. Such film is referred to as a *negative* because it reproduces light areas as black, and vice versa. The negative is printed on light-sensitive paper to produce a *reversed positive*. If desired a negative film can be printed in a reversed form to produce a *positive*. Diagnostic radiology is usually carried out with negative films.

Certain photographic films are made to produce a positive image directly without passing through the intermediary step of making a negative. Such films are called *reversal films*. To achieve its purpose, a reversal film must be subjected to *reversal processing*. This procedure involves processing the exposed film under normal conditions to produce a negative on the film; then, removing the negative image thus formed by dissolving the exposed particles; and re-exposing to light the film thus treated, thereby exposing the previously unexposed particles of silver halide. When this film is processed normally, it produces a positive image of the photographed object. Reversal films are useful whenever a positive image suitable for projection is to be obtained in the shortest period of time.

Reversal-type films are widely used in cinefluorography. However, rather than to reversal processing they are subjected to normal, negative-type processing to produce an image comparable to a radiograph. This approach provides an image of high contrast. Under certain circumstances it is desirable to produce a positive-type image either for the purpose of obtaining several negative copies or for enhancing the contrast on the print. Indeed, when a negative is printed, the contrast obtained is equal to the product of the contrasts of the negative and the print emulsion. Also, under certain circumstances, it may be desirable to transfer an image formed on 35mm film onto a 16mm print with the purpose of increasing the contrast and also obtaining a narrower film which is sometimes more convenient to project than the bulkier 35mm film. For this type of transfer, reversal processing is employed.

RECORDING THE CINEFLUOROGRAPHIC TELEVISION IMAGE

The cinematographic recording of a fluoroscopic image supplied by an x-ray intensifier that includes a television chain can be achieved either (1) by recording by means of a cinematographic camera the image formed on the screen of the television monitor, or (2) by recording the electrical signals into which the image has been translated by the television pickup tube on magnetic video tape, without the help of photographic film.

Kinefluorography

The cinematographic recording of a fluoroscopic image displayed on a television monitor (*kinescope*) is often called *kinefluorography* (Ref. 11). In most television systems the image is scanned at the rate of 30 frames/sec, and usually kinefluorography is carried out by synchronizing the

camera to this frequency. However, slower frequencies of recording can be achieved by omitting a certain number of fields from recording. For example, a rate of 24 frames/sec can be achieved by using a camera fitted with a shutter-open phase of 144 degrees, which is open only 40% of the time. Under these conditions, the film is exposed to 1 field ($\frac{1}{60}$ sec), but the following $1\frac{1}{2}$ fields are omitted ($\frac{1}{40}$ sec). Another and simpler method of synchronization at rates lower than 30 frames/sec consists in recording an integer number of television fields per film frame (Ref. 12).

Synchronization in kinescopic recording can also be achieved by presenting the information on the kinescope on a single repetitive line and by recording each following raster line (line forming the television image) sequentially on a continuously running film (Ref. 12). In this system the camera moves the film continuously at the rate of one frame per scanning time. It should be noted that a similar type of system is used in video tape recording.

In kinefluorography it is also possible to achieve greater frequencies than 30 frames/sec by recording only a fraction of the interlacing fields that form the image. For example, in the more conventional television systems which provide 2 fields per frame in $\frac{1}{30}$ sec, one can record 1 television field per photographic frame, thus achieving a frequency of 60 frames/sec. Other television systems provide a frame composed of 3 interlaced fields, each scanned in $\frac{1}{60}$ sec, and kinescopic recording may be carried out by recording 1, 2, or 3 of these fields per photographic frame. This approach, however, results in less information recorded per photographic frame.

Video Tape Recording in Cinefluorography

The image coded in the form of an electrical signal by a television pick-up tube can be recorded on magnetic video tape. This method, which is widely used in commercial television, has been successfully applied in cinefluorography.

A video tape system is capable of recording all the information supplied by a television chain, provided the information-coding capability of the tape is sufficient to accommodate all the information supplied by the television chain. The information-coding capability of the tape is expressed in megacycles per second, and in order to record all the information available the frequency response of the video tape must at least be equal to the bandpass frequency of the television system. For example, a video tape recorder with a frequency response of about 3 megacycles is capable, with a suitable display system, of supplying a horizontal resolution of approximately 280 lines for the total field. If such a system is used for the recording of an image supplied by a 1000-line television system with a 20-megacycle bandpass, the recording capabilities of the video tape system will not match the information presented and the recorded image

will be of lower resolution quality than that supplied by the television chain (Chapter IX).

The image recorded on video tape can be displayed at will on a kine-scope and, if desired, recorded on photographic film by a kinescope recorder. Video tape can be erased and reused a large number of times; 400 possible erasures and recordings are quoted by manufacturers of video tape equipment.

COMPARISON OF CINEFLUOROGRAPHY, KINEFLUOROGRAPHY, AND VIDEO TAPE RECORDING

The photon gain achieved in image-intensified fluoroscopy by the insertion of a television chain, which provides efficient optical coupling between the eye of the observer and the intensified image (Chapter IX), does not take place in cinefluorography. Indeed, in most cinefluorographic systems the quantum sink occurs with the absorption of x-ray photons by the input screen of the image intensifier, and the statistical quality of the image remains the same whether it is processed by a purely optical system and recorded on film or whether a television chain is included in the system.

Kinefluorography offers two main advantages over cinefluorography: electronic control of the brightness gain and electronic control of contrast. In cinefluorography the brightness gain of the image intensifier has a fixed value, and while film exposure can be reduced by stopping down the aperture of the camera lens, photographic exposure can be increased over the maximum value achieved by this system only by increasing the x-ray flux. A kinefluorographic system, on the other hand, allows a wide variation of the brightness gain by varying the gain achieved in the television link. Such an increase in gain allows kinefluorographic recording with very low doses of radiation for the patient. It should be noted, however, that reduction in the dose of radiation under these circumstances also results in a statistical deterioration of the image obtained; and for comparable statistical image quality, a kinefluorographic system is not superior to a cinefluorographic system. Under certain circumstances, however, the quality of the required examination may be sacrificed in favor of reducing the dose of radiation for the patient. This compromise can be reached in a kine-scope system but is impossible in present cinefluorographic systems.

The television chain in a kinefluorographic system also allows a wide range of contrast control which is sometimes desirable in the examination of a particularly low contrast object. Contrast control is absent in cinefluorography.

The advantages of kinefluorographic systems are accompanied by the following drawbacks: (1) Kinescopic recording in a conventional system requires approximately $\frac{1}{30}$ sec per photographic frame, which is the time required for the complete interlacing of 1 television frame. Shorter kine-

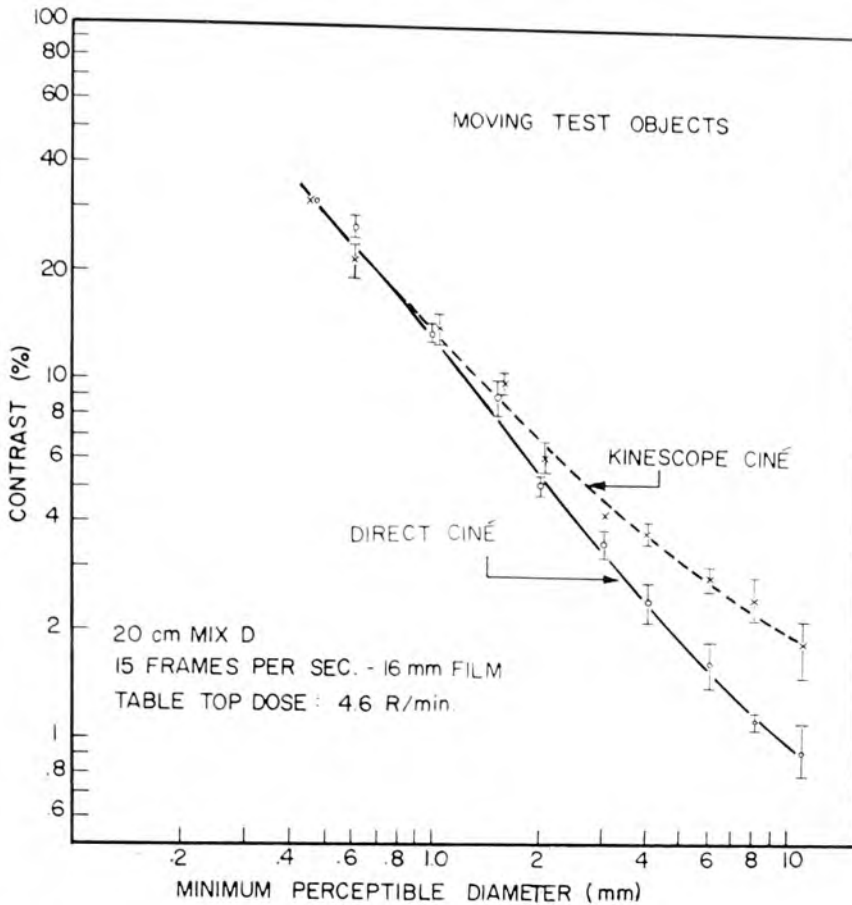


FIG. X-13. Comparison of cinefluorography using (1) direct cine recording from output screen of x-ray image intensifier tube; (2) kinescope recording from Image Orthicon television chain coupled with same x-ray intensifier tube. Both tests were carried out under the same x-ray conditions and with moving objects. (From Edward W. Webster and the J. Soc. Motion Picture Television Engrs., Ref. 11).

scopic exposures can be achieved by recording only one scan of the line interlace, but these short exposures are achieved at the cost of loss of information per photographic frame. (2) The resolving power of a kinefluorographic system is limited by the number of raster lines, the scanning spot size, the bandwidth of the system, and the noise introduced in the system by even the best electronic circuitry (Ref. 12).

At this time, it appears that the best films recorded by cinefluorographic systems are superior in quality to the best films recorded from a kinescope (Ref. 12). Kinefluorographic recordings appear to be noisier than cinefluorographic recordings and subject to spurious shadows that reduce the perception of large details at low contrast (Fig. X-13) (Ref. 11).

Video tape recording of a fluoroscopic image offers the obvious advantage of not requiring photographic processing. The examination recorded on video tape can be viewed immediately after completion by displaying the image stored on the tape on a conventional kinescope. If needed, the tape

can be stored and replayed as often as desired. If, on the other hand, a permanent record is not needed, the tape can be erased and reused again several hundred times.

Video tape recording has the advantages of a system that includes a television chain, such as brightness and contrast control, and also its disadvantages, such as limitation in exposure frequency due to scanning, loss in resolution due to scanning spot size, noise, etc. A major disadvantage of video tape recording, however, is of technical nature. While it is possible to record on video tape all the information supplied by a television chain, this can be achieved only if the frequency response of the video tape recorder is at least as broad as that of the television system supplying the information. Thus, high-resolution television systems may require a tape frequency response as high as 20 megacycles. Video tape recorders capable of such a frequency response are currently unavailable for radiologic use. The frequency response of the best commercial equipment does not exceed about 5 megacycles, and most of the video tape recorders widely available for radiology have a bandpass of about 3 megacycles. Video tape recorders with a frequency response of the order of 3 megacycles limit the horizontal resolution to less than 300 lines, which is considerably lower than the capabilities of a good cinefluorographic system.

At present, the quality of the image recorded by a cinefluorographic system appears to be slightly superior to that obtained in kinefluorography, and is considerably superior to the image recorded by means of presently available video tape systems. The practical advantages offered by video tape recording in many instances make this method quite desirable, provided high resolution in the recorded image is not required.

PROJECTORS FOR CINEFLUOROGRAPHIC FILM

The analysis of cinefluorographic and kinefluorographic examinations poses requirements which are not fulfilled by conventional motion picture projectors. Dreisinger (Ref. 13) has proposed the following desirable features for analytic projectors specifically designed for cinefluorography: (1) They should permit the film to run in either direction. (2) Projection rates should be variable approximately between 1 and 16 frames/sec. (3) Instantaneous forward and reverse actions, and a mechanism for expeditious change from normal to single-frame projection, and back again, should be provided. (4) Remote control of the apparatus should be possible. (5) Flicker-free projection at low rates of speed is desirable.

Although the above conditions are not met by conventional motion picture projectors, most of these features are found in editing machines for cinematographic film. These machines, however, should provide better definition, more light intensity, and larger pictures to be useful for the analysis of cinefluorographic film (Ref. 13).

Several projectors are available commercially that incorporate most of

the above desirable features. Some have been designed for purposes quite different from cinefluorography, while others were specifically adapted for this purpose.

The beaded screens conventionally used for viewing motion pictures are inadequate for cinefluorography because of loss of detail occurring in the motley structure of the screen; consequently, screens of finer grain are preferable.

IMAGE QUALITY IN CINEFLUROGRAPHY

The upper limit of the quality of the image recorded by means of cinefluorographic systems presently available is limited by the image-forming ability of the x-ray image intensifier used. As discussed earlier in this chapter, the image-forming capabilities of the optical system that couples the film with the x-ray image intensifier, and that of the film used, are in most modern systems capable of better resolution than that achieved by the image intensifier. The best presently available x-ray image intensifiers are capable of resolving 2, perhaps 3 lines/mm, and such is the limit of the resolving power of the better cinefluorographic systems.

This upper limit of the resolution of a cinefluorographic system applies only to situations where the statistical fluctuations in the image handled by this system do not appreciably affect resolution. In practice, however, the upper limit of resolution (established by the unsharpness introduced by the image-forming system) is never reached because the resolution achieved by the system is limited at a lower level by the statistical fluctuations of the image-forming quanta.

Figure X-14 shows the levels reached by the information-carrying quanta (which may be x-ray photons, light photons, electrons, or grains in the photographic emulsion) in a cinefluorographic system. (Image statistics in x-ray intensifying systems are discussed in Chapter IX.) The light photons emitted by the output screen of the image intensifier are conducted by the optical system to the photographic film, and sensitize grains in the photographic emulsion there; in both processes there is a loss in quanta.

The efficiency of the optical system coupling between the output screen of the intensifier and the film can be calculated by Equation (3) given in Chapter IX:

$$\frac{N_c}{N_e} = \frac{M^2}{(M + 1)^2} \times \frac{T}{4f^2},$$

where N_c/N_e is the fraction of photons collected by the optical system, M is the linear magnification of the system, f is the f -number of this system, and T is its optical transmission.

The efficiency of a typical photographic emulsion in converting light photons into photographic grains is of the order of 0.005 (Ref. 14).

Figure X-14 shows that under typical conditions of cinefluorography

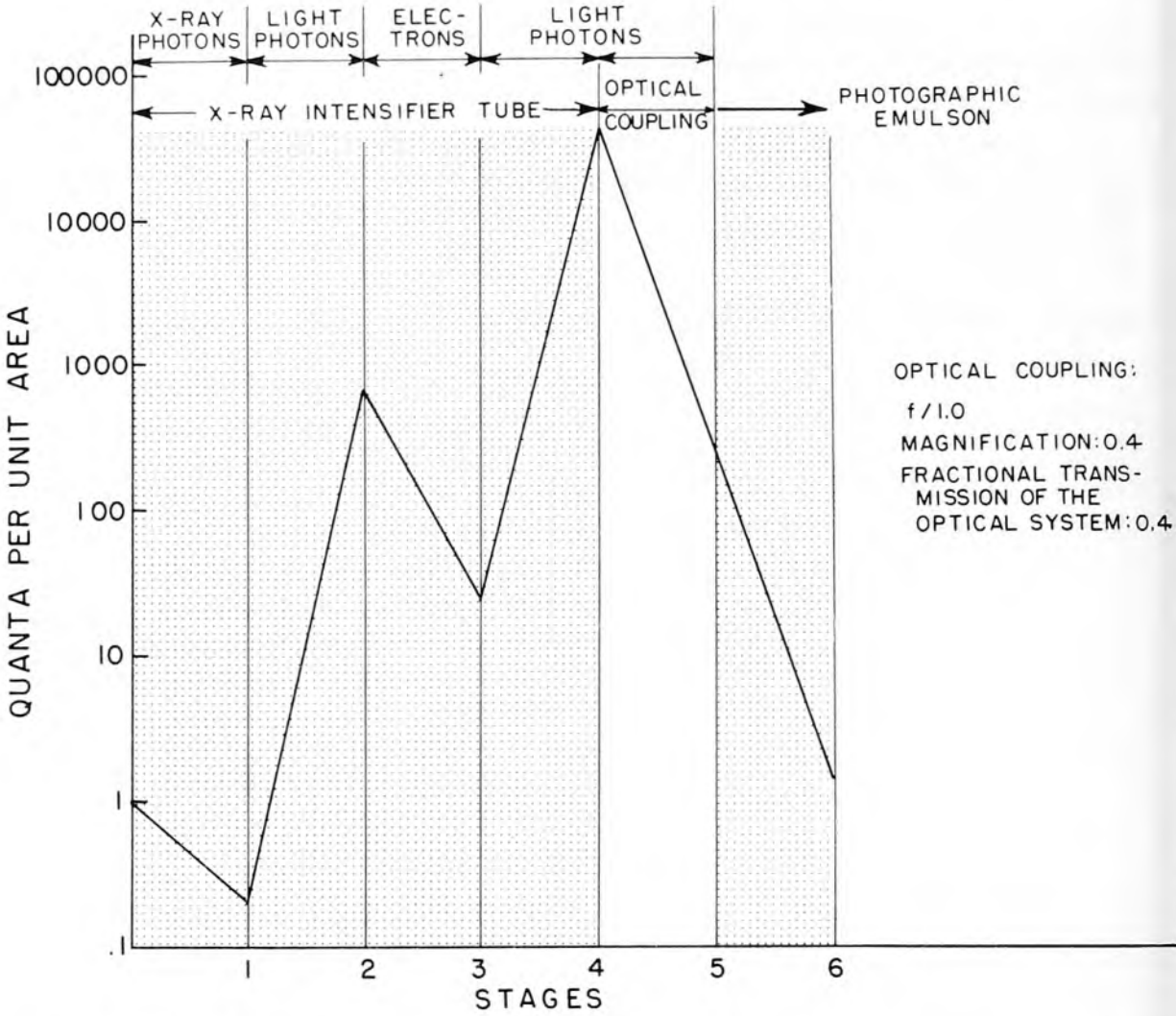


FIG. X-14. Quantum levels reached in different stages of image conversion in a cinefluorographic system.

Optical coupling $f/1.0$
 Magnification 0.4
 Fractional transmission of the optical system 0.4

the losses in information-carrying quanta between the output screen of the x-ray image intensifier and the final image formed on the photographic emulsion are not sufficient to use up the quantum gain achieved by the x-ray intensifier after the absorption of x-ray photons by its input screen. Under the circumstances, the lowest level of statistical information (quantum sink) in this system occurs with the absorption of x-ray photons by the intensifier input screen, and this level is not affected by the balance of this system. It should be noted that in Fig. X-14 that the quantum level in the photographic emulsion is only slightly higher than the quantum sink. Under these conditions a lower-efficiency image intensifier and/or a lower-efficiency optical system introduced into the cinefluorographic

system may result in lowering the quantum level at the photographic emulsion level below the previous quantum sink (Ref. 14). It is therefore important to use high-gain image intensifiers and efficient optics in cinefluorography.

The number of photons per unit area determines the statistical quality of the cinefluorographic image, and this number varies widely with the energy of the x-radiation used in the examination and particularly with the characteristics of the cinefluorographic system used (such as x-ray image intensifier gain, light-gathering power of the optical system used, speed of film, etc.). For example, a cinefluorographic system that employs a high-gain image intensifier and fast film produces an image of a given photographic density with a lower number of photons striking the input screen of the image intensifier than if a lower gain intensifier were used with a slower film and slower optics. Therefore the statistical quality of the image obtained with the slow cinefluorographic system is superior to that obtained with the high gain system because the slow system utilized a greater number of the photons the radiologic image originated. In a typical cinefluorographic examination carried out with 90 keV_p x-rays, the radiation exposure at the input screen of the image intensifier may be of the order of about 50 μR per frame. (It should be noted that cinefluorographic examinations are carried out with considerably lower and considerably higher radiation exposures per frame.) Such an exposure carried out with a radiation energy under consideration corresponds approximately to 1.5×10^6 photons/cm² (Table XI-4, Chapter XI) on the input screen. If it is assumed that approximately 20% of these photons are absorbed in the input screen, the statistical quality of the final image obtained is determined by approximately 3×10^5 photons/cm². It is interesting to compare this value with the number of photons per unit area forming a fluoroscopic image without x-ray intensification. Under typical conditions in the fluoroscopic examination of a 25-cm thick abdomen, carried out with 90 keV_p x-rays, the statistical quality of the image obtained is determined by approximately 3300 photons/cm² (Table IX-2, Chapter IX). A comparison of this figure with the number of photons responsible for the cinefluorographic image obtained under these conditions show that the latter is formed by about 10 times as many photons. Thus one would expect superior image perceptibility per cinefluorographic frame. This situation has been verified experimentally. Webster and Wipfelder (Ref. 11) have shown that for the same exposure rate the cinefluorographic recording of an object with 10% contrast resulted in a minimum perceptible diameter of a little less than 2 mm, while a fluoroscopic examination of the same object gave a minimum perceptible diameter of about 7 mm (Fig. X-15). This comparison was carried out with moving test objects.

In conclusion, the upper limit of the resolution that can be achieved by a cinefluorographic system depends mostly on the resolution of the x-ray

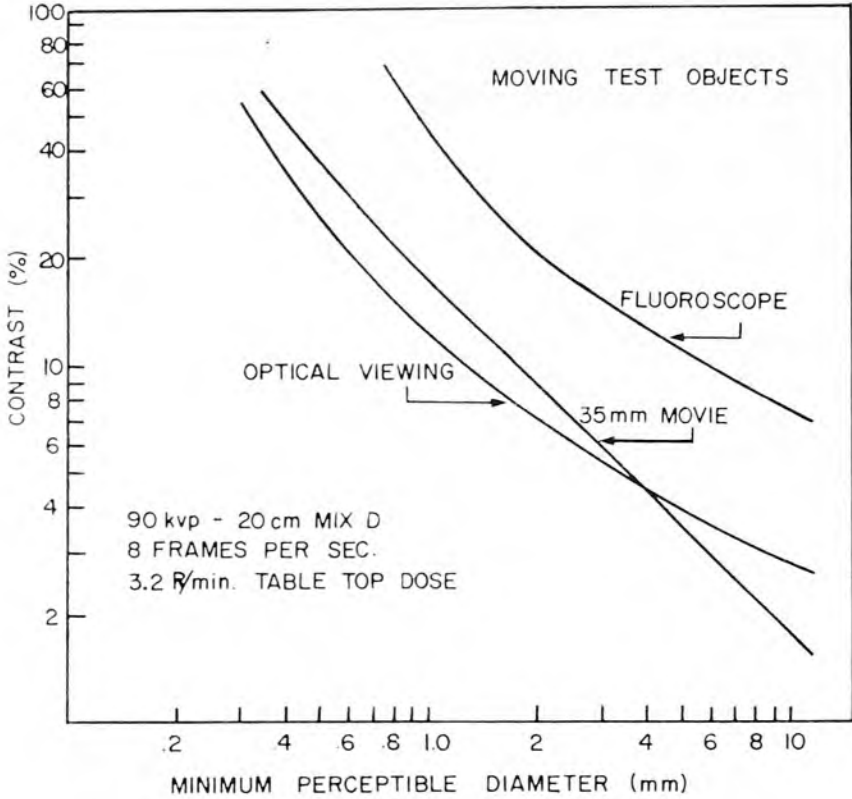


FIG. X-15. Comparison of performance of (1) conventional fluoroscopy; (2) x-ray image intensifier with direct viewing; (3) cinefluorographic recording on 35mm film of image supplied by x-ray intensifier. The same moving test objects and constant x-ray factors were used with all systems tested. (From Edward W. Webster and the J. Soc. Motion Picture Television Engrs., Ref. 11.)

image intensifier. However, while the type of equipment used has some influence on the quality of the image obtained (Ref. 14), detail and contrast perceptibility of the image supplied by a given cinefluorographic system is mostly determined by the x-ray photon flux of the radiologic image, which in turn depends on the x-ray dose rate emerging from the examined part. Good agreement has been found between the minimum perceptible diameter obtained experimentally by a cinefluorographic system and the minimum perceptible diameter for the same object contrast calculated on a theoretical basis which assumed that the image perceptibility is determined only by statistical fluctuations.

RADIATION EXPOSURE IN CINEFLUOROGRAPHY

The radiation exposure of the patient resulting from a cinefluorographic examination is a function of the desired quality of the recorded image because, as shown in the previous section, the quality of this image is primarily determined by the number of x-ray photons responsible for its exposure. Under such circumstances, the dose of radiation delivered to the patient

upon cinefluorographic examination of a given part may vary widely. The range in radiation dose has an upper limit. It is futile to raise the statistical quality of the examination beyond the point where statistical fluctuations in the image affect resolution to a lesser degree than the unsharpness introduced by the system. In practice, however, this upper limit is never reached because it occurs with radiation intensities intolerably high from the health standpoint. A situation in which the statistical fluctuation of the x-ray photons did not affect appreciably the resolution of the image was encountered when cinefluorography was carried out without image intensification (direct cineradiography). It is interesting to note that these early techniques produced very high quality images which can no longer be produced in modern cineradiography because of the influence of statistical fluctuations. Thus, in modern cinefluorography the quality of the image depends strongly on the patient's radiation tolerance.

From the theoretical standpoint there is no lower limit of radiation exposure below which cinefluorography is impossible. Indeed, with very high image intensification it is possible to obtain a film density suitable for visual inspection with only a small number of x-ray photons impinging upon the input screen of the intensifier. Of course under such circumstances the quality of the image is poor because of the magnitude of the influence of statistical fluctuations. Practical diagnostic cinefluorography is carried out with radiation exposures having an upper limit of approximately 20 R/min to the skin, and a lower limit of about 1 R/min. In some examinations these limits are exceeded (Refs. 15-18).

PHOTOFLUOROGRAPHY (FLUROGRAPHY)

Photofluorography is a diagnostic radiographic technique whereby the optical image supplied by a fluorescent screen is recording photographically by means of a still camera.

After processing, the image recorded on the film, which is reduced in size with respect to the image supplied by the fluorescent screen, is examined by the radiologist usually with a magnifying viewer. There are three main reasons why photofluorography is preferred to conventional radiography for certain examinations: (1) The cost of the smaller-sized photofluorographic film is lower per examination than that of radiographic film. (2) Multiple exposures are easy to achieve with photofluorographic cameras loaded with a large amount of film, while cameras for multiple exposures with large-size radiographic film are bulky and complicated. (3) The storage of photofluorographic film requires less space than that of the larger-size radiographic film.

These advantages of photofluorography over radiography are, however, achieved at the cost of resolution and radiation exposure of the patient per examination. The disadvantages of photofluorography result from the following factors: The fundamental difference between radiography and photofluorography is that in radiography the exposure of the film is achieved by

bringing it in contact generally with two screens, while in photofluorography the film is coupled to one fluorescent screen by means of an optical system which projects a reduced image of the screen. The use of an optical system always results in loss of light photons the magnitude of which is mainly determined by: (1) minification, (2) the f -number of the optical system, and (3) the light transmission of the system. In photofluorography the conversion of the radiologic image into an optical image by the fluorescent screen is achieved under less favorable conditions than in radiography. In radiography, usually two screens are used and the x-radiation transmitted by the first screen is partially utilized by the second screen in forming the optical image. In photofluorography, on the other hand, a single screen is used, and the radiation escaping this screen is wasted from the standpoint of the examination. The combination of these two factors renders photofluorography a less efficient method of radiographic examination from the standpoint of conversion of the radiologic image into the optical image than conventional radiography, and various steps must be taken in the design of a photofluorographic apparatus to reduce the gap between the two methods.

The phosphor used in photofluorographic fluorescent screens is either zinc sulfide, which fluoresces with the emission of blue light (4400 Å), or zinc cadmium sulfide, which fluoresces in the yellow-green (5300 Å) (Chapter VI, Table VI-2). In these screens the phosphor particle size and the thickness of the phosphor layer are similar to that used in fluoroscopic screens. The resolving power of photofluorographic screens is of the order of 2 to 5 lines/mm, which is appreciably less than that achieved with intensifying screens (Chapter VI, Table VI-2). It should be noted that a resolving power identical with or better than that obtained with intensifying screens could be achieved in fluorographic screens by reducing the thickness of the phosphor layer and/or particle size. This improvement, however, would be accomplished at the cost of screen speed.

TABLE X-2. Specifications of 70mm and 4×4 in.
Mirror-Optics Photofluorographic Systems

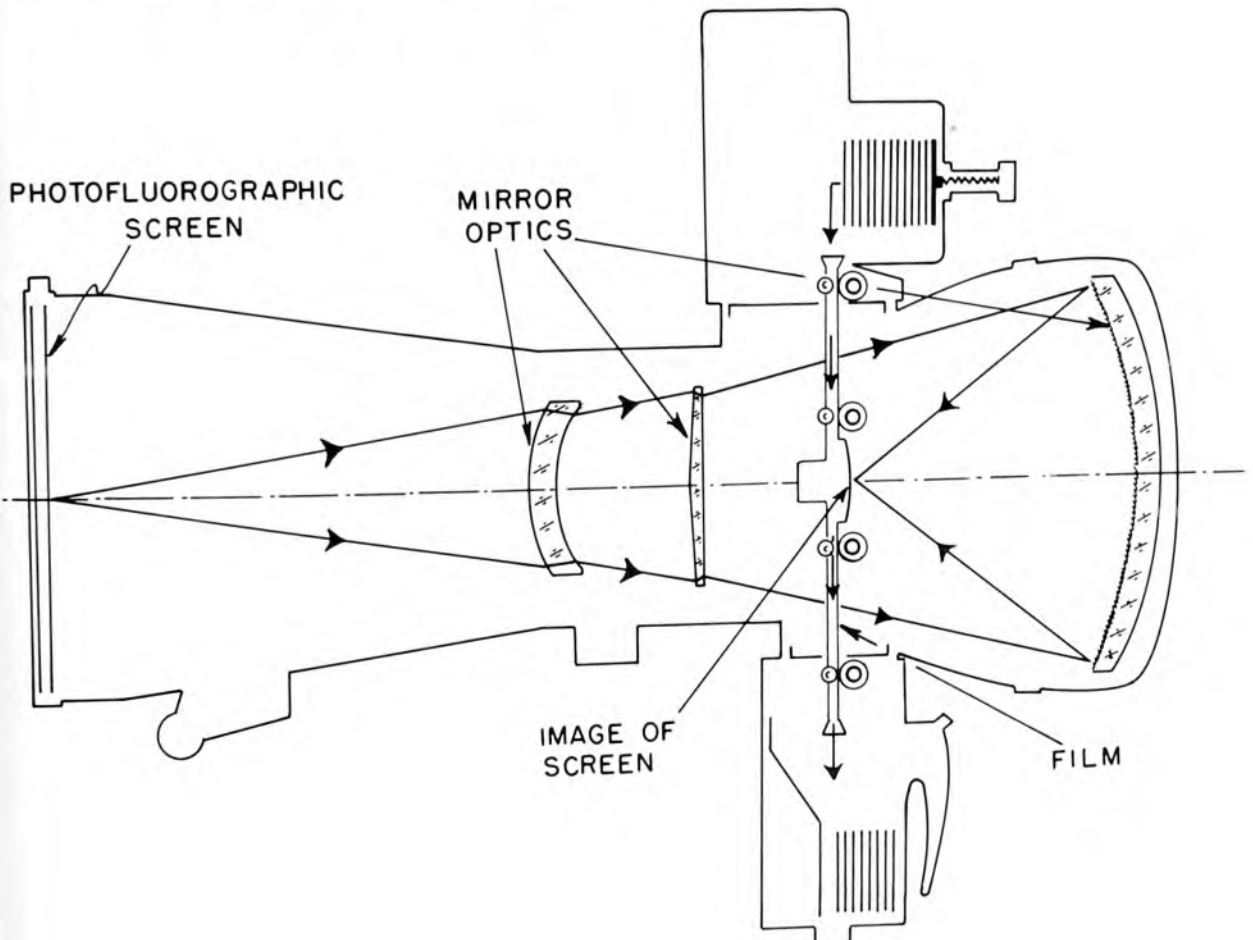
	70mm	4×4 in.
General relative aperture	$f/0.63$	$f/0.65$
Focal length	160 mm	213 mm
Image size	63×63 mm	90×90 mm
Film size (nominal)	70×70mm roll film	4×4 in. cut film
Screen size	16×16 in.	16×16 in.
Reduction factor	6.3:1	4.4:1
Weight of camera (without cassette)	141 lbs	198 lbs

Courtesy of Aerojet Delft Corporation, Plainview, N.Y.

The optical system used in photofluorography in coupling the fluorescent screen to the film must be made as efficient as possible with the purpose of collecting a large fraction of the light emitted by the screen. Conventional optical transmission systems are used in photofluorography. It is, however, difficult with such systems to achieve an f -number smaller than approximately 1.5. On the other hand, the optical coupling between the screen and the film can be achieved efficiently by using mirror optics with an f -number of the order of 0.6 (Table X-2) (Fig. X-16). The use of mirror optics with $f/0.63$ as compared to transmission optics with $f/1.5$ increases the light-gathering efficiency of this system by a factor of about $(1.5/0.63)^2 = 5.7$. Under these conditions there is great advantage in the use of mirror optics for this purpose as compared to more conventional transmission lenses.

The photographic film commonly used in photofluorography is either 70mm "roll film" or 4×4-in. "cut film" (Table X-2). The emulsion may be either blue sensitive for use with zinc sulfide screens or green sensitive for

FIG. X-16. Photofluorographic unit using Bouwers mirror optics (Odelca 100-XVII-S). (Courtesy of The Old Delft Co., Delft, Holland.)



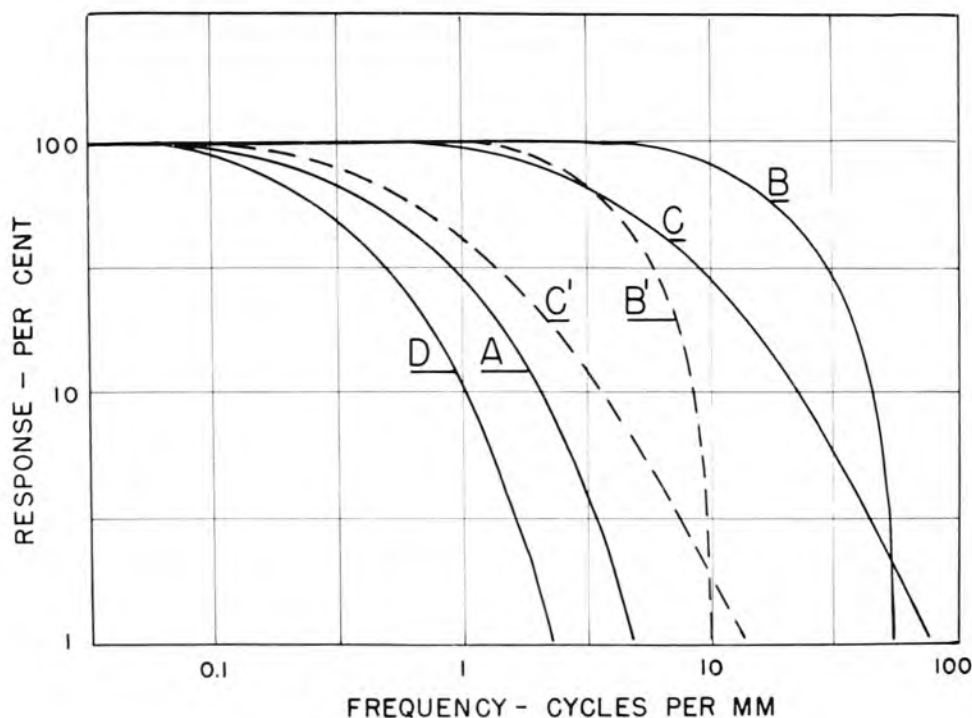
use with zinc cadmium sulfide screens. Characteristic curves of sensitive photofluorographic film are shown in Fig. VI-17, Chapter VI.

The resolution achieved by means of presently available photofluorographic systems is inferior to that achieved in radiography, mainly because of the greater unsharpness introduced by the input screen of the photofluorographic system. The quality of the image in photofluorography is mostly affected by the unsharpness of the screen (Ref. 20). Figure X-17 shows the modulation transfer functions for a photofluorographic system, suitably corrected for minification.

The analysis of photon statistics in a photofluorographic system (Fig. X-18) shows that the quantum sink is reached in the photographic emulsion with the number of photographic grains exposed. This occurs because even in the best optical system presently available the loss of light that occurs in the coupling of the photographic emulsion to the screen, combined with the statistical loss that occurs in the conversion of light photons into photographic grains (approximately 200 light photons per photographic grain

FIG. X-17. Modulation transfer function. Frequency response functions for components of photofluorographic system, showing corrections required by image minification of system.

- A contribution of fluoroscopic screen
 - B uncorrected contribution of typical lens
 - C uncorrected contribution of photofluorographic film
 - B' and C' contributions of B and C corrected for minification M
 - D composite response of system
- (Courtesy of Russell H. Morgan and the Amer. J. Roentgen., Ref. 19.)



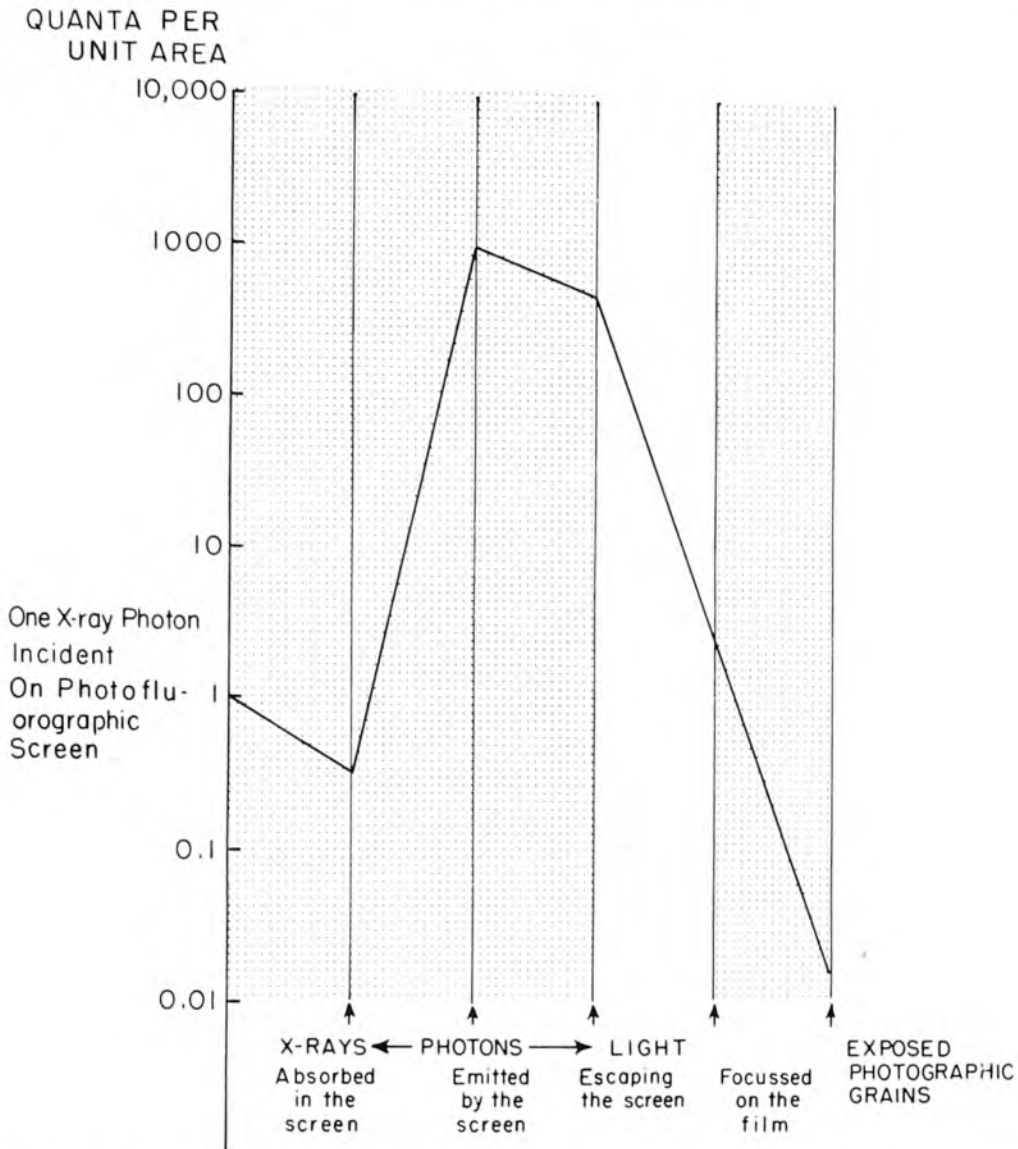


FIG. X-18. Quantum levels reached in various stages of image conversion in photofluorographic system.

developed), more than uses up the photon gain achieved in the conversion of x-ray energy into light in the photofluorographic screen. It appears, therefore, that a statistical gain could be achieved in photofluorography by the use of x-ray intensification. This approach appears to be very promising, and many cinefluorographic systems are now fitted with photofluorographic cameras either of the 70mm or of the 4×4-in. format (Table X-2). Potentially these systems are capable of better resolution than the conventional photofluorographic systems, because image intensification provides a statistically superior image and theoretically without loss of resolution due to unsharpness. It should be noted, however, that at this time the resolution achieved by straight optical systems appears to be superior to that obtained

with image intensifiers because of purely technical limitations such as loss in resolution at the edges of image intensifier tubes which may be overcome in the future. With image intensification, photofluorography is potentially capable of supplying radiographic images of quality approaching that achieved in present-day radiography, and because of the many advantages inherent in the use of small-size film, it is probable that this technique will gain considerable importance in diagnostic radiology.

REFERENCES

1. MACINTYRE, J.: X-ray records for the cinematograph. *Arch. (Clinical) Skiagraphy* 1:37, April 1897. (Also in *Lancet*, 920, March 27, and 1706, June 19, 1897.)
2. JARRE, H. K.: "Roentgen Cinematography," in *The Science of Radiology*, ed. by Glasser, O. Springfield, Ill., Thomas, 1933.
3. MICHAELIS, A. R.: *Research Films in Biology, Anthropology, Psychology and Medicine*. New York, Academic Press, 1955.
4. TRISTAN, T. A.: "Methods of Cinefluorography," in *Cinefluorography*, ed. by Ramsey, G. H., Watson, J. S., Jr., Tristan, T. A., Weinberg, S., and Cornwell, W. S. Springfield, Ill., Thomas, 1960.
5. WEINBERG, S. A., WATSON, J. S., and RAMSEY, G. H.: Cinefluorography technical refinements. *Amer. J. Roentgen.* 75:63, 1956.
6. DAUVILLIER, A.: Anwendung der Grundlagen des Fernsehens in der Röntgenologie: der "Radiophot." *Fortschr. Röntgenstr.* 40:638, 1929. Translated from: *Rev. gén. Elect.* 1928, 23 January, IIIrd Congr. Int. Radiol. Paris 1931, p. 229. *Research films in biology, anthropology, psychology, and medicine*, New York, Academic Press, 1955.
7. EULER, F. J.: "Synchronization in cinefluorography," in *Cinefluorography*, ed. by Ramsey, G. H., Watson, J. S., Jr., Tristan, T. A., Weinberg, S., and Cornwell, W. S. Springfield, Ill., Thomas, 1960.
8. KINGSLAKE, R.: "Recording Equipment Lenses," in *Cinefluorography*, ed. by Ramsey, G. H., Watson, J. S., Jr., Tristan, T. A., Weinberg, S., and Cornwell, W. S. Springfield, Ill., Thomas, 1960.
9. BLOOM, W. L., JR.: *Image Intensification and Recording Principles*. Technical Service, X-Ray Dept., General Electric Company, 1962.
10. CORNEY, G. M.: "Photographic Aspects of Cinefluorography," in *Cinefluorography*, ed. by Ramsey G. H., Watson, J. S., Jr., Tristan, T. A., Weinberg, S., and Cornwell, W. S. Springfield, Ill., Thomas, 1960.
11. WEBSTER, E. W., and WIPFELDER, R.: Contrast and detail perception in television and cine systems for medical fluoroscopy. *J. Soc. Motion Picture Television Engrs.* 73:617, 1964.
12. MILLER, E. R.: "Kinescopic Recording of Fluoroscopic Information: Usefulness and Limitations," in *The Reduction of Patient Dose by Diagnostic Radiologic Instrumentation*, ed. by Moseley, R. D., Jr., and Rust, J. H. Springfield, Ill., Thomas, 1964.
13. DREISINGER, F. W.: "Analytical Projectors for Cinefluorography," in *Cinefluorography*, ed. by Ramsey, G. H., Watson, J. S., Jr., Tristan, T. A., Weinberg, S., and Cornwell, W. C. Springfield, Ill., Thomas, 1960.

14. MORGAN, R. H.: The performance of screen intensification and cinefluorographic systems. *Amer. J. Roentgen.* 86:1027, 1961.
15. TRISTAN, T. A., and QUICK, R. S.: "Radiation Dose in Image Intensifier Cinefluorography," in *Cinefluorography*, ed. by Ramsey, G. H., Watson, J. S., Jr., Tristan, T. A., Weinberg, S., and Cornwell, W. S. Springfield, Ill., Thomas, 1960.
16. MATSUDA, H., NAGAOKA, T., TAKAI, G., and NINOMIYA, K.: Medical applications of x-ray television. *Amer. J. Roentgen.* 85:352, 1961.
17. HALE, J., GEORGE, D. L., EPPERSON, R. D., and TRISTAN, T. A.: "Physical Factors in Cinefluorography," in *The Reduction of Patient Dose by Diagnostic Radiologic Instrumentation*, ed. by Moseley, R. D. Springfield, Ill., Thomas, 1964.
18. HENNY, G. C.: "Dose Aspects of Cinefluorography," in *Technical Needs for Reduction of Patient Dosage from Diagnostic Radiology*, ed. by Janower, M. L. Springfield, Ill., Thomas, 1963.
19. MORGAN, R. H.: The frequency response function. *Amer. J. Roentgen.* 88:175, 1962.
20. NAWIJN, A.: Modulation transfer and quality of mirror cameras for photo-fluorography. *Röntgen-Blätter* 16(#7)(Supplement), 1963.
21. WATSON, J. S., JR., and WEINBERG, S.: "Evaluation of Equipment, Films and Processing for Cinefluorography," in *Cinefluorography*, ed. by Ramsey, G. H., Watson, J. S., Jr., Tristan, T. A., Weinberg, S., and Cornwell, W. S. Springfield, Ill., Thomas, 1960.

(XI) RADIATION DOSIMETRY: UNITS AND INSTRUMENTATION

QUALITY AND QUANTITY OF X-RADIATION (Refs. 1 and 16)

X-radiation is described by two variables: quality and quantity. The *quality* of a beam of x-rays is the energy of the x-ray photons of which the beam is composed. If the x-radiation consists of monochromatic (monoenergetic) photons, the quality of the beam is the energy carried by these photons. If the beam is composed of photons of various energies, the quality of the radiation is expressed as the *spectral distribution* of these photon energies as a function of their number (Chapter II, under "X-Ray Spectrometry"). The unit of x-ray quality (energy) most commonly used is the *electron volt* (Chapter I, under "Work and Energy"). Other units of energy, such as the *erg*, can also be applied to this purpose.

The *quantity* of x-radiation in a beam in diagnostic radiology can be usefully expressed in two different ways. It can be expressed as the number of particles (photons) per unit area. This quantity is called *particle fluence* or *fluence* (Φ) (Table XI-1), and is expressed as

$$\Phi = \frac{N}{a}, \quad (1)$$

where N is the number of photons entering a sphere of cross-sectional area a . The quotient

$$\phi = \frac{\Phi}{t}, \quad (2)$$

where t is time, is called the *particle flux density* or *flux density* or *particle fluence rate*. This quantity ϕ represents the number of photons per unit area per unit time in a beam of x-rays. Fluence is measured in reciprocal area units (area^{-1}), and the particle flux density is expressed in reciprocal area-reciprocal time units (Table XI-1).

It is convenient to express the quantity of x-radiation in terms of fluence or particle flux density when the variable studied is the number of

TABLE XI-1. Table of Quantities and Units Used in Radiology

Name	Symbol	Units	
		egs	Special
Energy imparted (integral absorbed dose)		erg	g rad
Absorbed dose	D	erg g ⁻¹	rad
Absorbed dose rate		erg g ⁻¹ sec ⁻¹	rad sec ⁻¹
Particle fluence, or fluence	Φ	cm ⁻²	
Particle flux density	ϕ	cm ⁻² sec ⁻¹	
Energy fluence	F	erg cm ⁻²	
Energy flux density, or intensity	I	erg cm ⁻² sec ⁻¹	
Exposure	X	esu g ⁻¹	R (roentgen)
Exposure rate		esu g ⁻¹ sec ⁻¹	R sec ⁻¹
Mass attenuation coefficient	μ/ρ	cm ² g ⁻¹	
Mass energy absorption coefficient	μ_{en}/ρ	cm ² g ⁻¹	
Mass stopping power	S/ρ	erg cm ² g ⁻¹	
Average energy per ion pair	W	erg	eV

Adapted from the NBS Handbook 84 (Ref. 16).

photons, and not their energies. Such is the case, for example, in the statistical study of the radiologic image, where the variable of importance is the number of photons per unit area.

The quantity of x-radiation can also be expressed in terms of *energy fluence* (F) as follows:

$$F = \frac{E_F}{a}, \quad (3)$$

where E_F is the sum of the energies of the particles that pass through an area a . The energy fluence is the total energy carried by the x-radiation per unit area.

The *energy flux density* or *intensity* (I) is the quotient F/t , where F is the energy fluence and t is time:

$$I = \frac{F}{t} = \frac{E_F}{at}. \quad (4)$$

This quantity is also called *energy fluence rate*. The energy fluence rate, or intensity of x-radiation, represents the total energy carried by the radiation incident per unit area per unit time. Energy fluence is measured in units of energy per unit area and intensity is measured in units of energy per unit area per unit time (Table X-1). (All the defined quantities apply also to radiations other than x-rays.)

The interaction of x-rays with matter results in a transfer of energy from

the beam of x-rays to the medium where the interaction takes place. The amount thus transferred is referred to as *absorbed dose* (D), which is defined as

$$D = \frac{E_D}{m}, \quad (5)$$

where E_D is the energy imparted by ionizing radiation to a mass of matter m . The unit of the absorbed dose D of ionizing radiation is the rad, which equals 100 ergs/g. The *absorbed dose rate* is the quotient D/t , where D is the absorbed dose in ergs and t is the time. The absorbed dose rate is expressed in rads per unit time (Table X-1).

Radiation Exposure—the Roentgen (Ref. 16)

A necessary factor in the quantitative study of the effects of radiation in matter is the absorbed dose. Unfortunately, the direct measurement of x-radiation dose is difficult. This purpose may be accomplished by using a calorimeter which allows the measurement of the heat generated in the absorber under study subsequent to the absorption of radiation. Unfortunately, the doses of radiation commonly measured are equivalent to only 10^{-3} to 10^{-5} cal (Ref. 2). Such small quantities of heat are difficult to measure and require the use of extremely sensitive calorimeters which are not practical for routine radiation dose measurements.

One of the simplest methods for the detection and measurement of x-radiation consists in detecting and measuring the ionization produced by this radiation in a gas. The presence of ions in a volume of gas is readily detected and their number easily measured by means of an ionization chamber with suitable auxiliary circuitry. Such a system measures the energy lost by the x-radiation in ionizing the gas. If the ionization chamber is sufficiently large to convert all the energy of the incident x-ray beam into ions, then the quantity measured by the chamber represents the total energy carried by the x-ray beam. However, the x-ray beam usually dissipates only a fraction of its energy in forming the ions which are collected in the ionization chamber, and the measurement thus obtained is only proportional to, not an absolute measure of, the absorbed dose of radiation in the particular chamber under consideration. Under the circumstances it is useful to express the presence of x-radiation at any point in terms of the number of ions produced by the x-radiation in a given mass of gas, and refer to this number as the *exposure*. The number of ion pairs formed by a given amount of x-radiation in a given mass of gas depends on the nature of the gas, and consequently the definition of exposure must take into consideration the nature of the gas used. Radiation exposure (X) is defined as

$$X = \frac{Q}{m}, \quad (6)$$

where Q is the sum of the electric charges of all the ions of one sign produced in air when all the electrons liberated by the photons in a volume element of air of mass m are completely stopped in air.

The unit of exposure is the *roentgen* (R), and

$$1 \text{ R} = 2.58 \times 10^{-4} \text{ coulomb/kilogram (C/kg).}$$

With present techniques it is difficult to measure exposure when the photon energies involved lie above a few MeV or below a few keV (Ref. 16). It should be noted that the above definition of the roentgen is quantitatively equal to the older definition of the roentgen as “the quantity of x- or gamma-radiation such that the associated corpuscular emission per 0.001293 grams of air produces in air ions carrying 1 esu of quantity of electricity of either sign.” (Ref. 3.)

The *exposure rate* is defined as the quotient X/t , where X is the exposure and t is time. Exposure rate is expressed in roentgens per unit time.

Roentgens, Rads, and Photons

The relationship between radiation exposure (expressed in roentgens) and the dose thereof absorbed in air (expressed in rads) can be derived from the definition of the roentgen.

One roentgen is defined as the creation of a charge of 2.58×10^{-4} C/kg of air.

The elementary charge, e , equals 1.60210×10^{-19} C (Table XI-6), therefore 1 C equals approximately 6.242×10^{18} electron charges. The average energy (W_{air}) expended in air for the formation of one ion pair is equal to 33.7 eV (Ref. 1). Consequently, the creation of a charge of 1 C in air requires an expenditure of energy of

$$6.242 \times 10^{18} \times 33.7 = 2.103 \times 10^{20} \text{ eV/C.}$$

Since 1 eV equals 1.602×10^{-12} erg, the energy corresponding to the creation of 1 C in air is equal to

$$2.103 \times 10^{20} \times 1.602 \times 10^{-12} = 3.37 \times 10^8 \text{ ergs/C.}$$

Therefore, 1 R, by definition, corresponds to an expenditure of energy of

$$2.58 \times 10^{-4} \times 3.37 \times 10^8 = 8.69 \times 10^4 \text{ ergs/kg.}$$

Since, by definition, 1 rad equals 100 ergs/g, the above expenditure of energy corresponds to a dose of approximately 0.87 rad. Thus, in air, the absorbed dose of x-rays is approximately 0.87 rad per roentgen.

The above calculation is valid only if the following conditions are met: (1) The mass of air must be uniformly exposed to 1 R, and it must be surrounded on all sides by the same material with a thickness at least equal to the range (distance travelled by the electron) of the secondary electrons created by the irradiation. (2) The x-radiation must have a quantum energy

greater than 20 eV corresponding to an energy range where the value of W_{air} is assumed to be constant (Ref. 1).

The above relationship between the roentgen and the dissipated energy applies for substances with an x-ray absorption energy dependence similar to that of air (see section on "Air-Equivalent Thimble Ionization Chambers"). Since in the low energy range the energy dependence of the absorption of x-rays is mostly dependent on the atomic number, a substance is *air equivalent* if its atomic number is close to the effective atomic number of air, which is equal to approximately 7.64 (Ref. 4). It should be noted that the number of rads per roentgen for air is independent of energy for radiation with energy greater than 20 eV.

The relationship between radiation exposure and absorbed dose of radiation for media other than air (or which are not air equivalent) is given by the equation

$$D_{\text{med}} = 0.87 \cdot \left[\left(\frac{\mu_{\text{en}}}{\rho} \right)_{\text{med}} \div \left(\frac{\mu_{\text{en}}}{\rho} \right)_{\text{air}} \right] \cdot X = fX, \quad (7)$$

where D_{med} is the absorbed dose in the medium exposed to radiation, 0.87 is the ratio rad/R for air, μ_{en}/ρ are the respective *mass energy absorption coefficients* of the medium and of air, X is the radiation exposure in roentgens, and f is the ratio rad/R (conversion factor) for the medium (Ref. 1). If the radiation used is not monochromatic, the mass energy absorption coefficients for the medium and for air are evaluated for the total energy spectrum of the radiation used (Table XI-3).

The ratio of the mass energy absorption coefficient of a given medium to that of air varies in general with radiation energy (Table X-2), and consequently the factor f also varies with radiation energy, particularly for low x-radiation energies and for substances with an effective atomic number very different from that of air, such as bone (Table XI-2). For low energies, photoelectric absorption, which is strongly energy- and atomic-number dependent, is the determining factor in the value of the energy absorption coefficient. On the other hand, for media with an effective atomic number close to that of air, such as water and muscle (Chapter V), the factor f does not vary appreciably with radiation energy because the energy absorption coefficients of these substances vary in a manner similar to that of air (Tables XI-2 and XI-3).

X-ray energy fluence F and x-ray photon fluence Φ can be derived from the exposure value as follows: The exposure of 1 R in air corresponds to an absorbed dose of 0.87 rads, and 1 rad equals 100 ergs/g. Therefore the energy absorbed in air per roentgen is 87 ergs/g.

The energy absorbed per gram is equal to the energy fluence F multiplied by the mass energy absorption coefficient μ_{en}/ρ . Therefore the energy fluence F equals

$$F = 87 \div (\mu_{\text{en}}/\rho)_{\text{air}} \text{ ergs/cm}^2/\text{R}.$$

TABLE XI-2. Values of Mass Energy Absorption Coefficients and Factor *f*

Photon energy <i>MeV</i>	Mass energy-absorption coefficient, (μ_{en}/ρ) , cm ² /g																$f = 0.869 \frac{(\mu_{en}/\rho)_{med}}{(\mu_{en}/\rho)_{air}}$						
	H	C	N	O	Na	Mg	Al	P	S	A	K	Ca	Poly- styrene (C ₈ H ₈) _n	Perspex, plexi- glass, lucite (C ₅ H ₈ O ₂)	Poly- ethylene (CH ₂) _n	Bakelite (C ₆ H ₃ O ₇)	Water	Air	Com- pact bone ^b	Muscle ^b	Water Air	Com- pact bone ^b Air	Muscle ^b Air
0.010	0.0099	1.94	3.42	5.50	15.4	20.9	26.5	40.1	49.7	62.0	77.0	89.8	1.79	2.92	1.66	2.43	4.89	4.66	19.0	4.96	0.912	3.54	0.925
0.015	0.0110	0.517	0.916	1.49	4.43	6.09	7.65	11.9	15.2	19.4	24.6	28.9	0.478	0.788	0.444	0.651	1.32	1.29	5.89	1.36	.889	3.07	.916
0.20	0.133	.203	.360	0.587	1.77	2.47	3.16	5.00	6.41	8.31	10.5	12.5	1.88	.311	.176	.257	0.523	0.516	2.51	0.544	.881	4.23	.916
0.30	0.186	.0392	.102	.163	0.482	0.684	0.880	1.45	1.85	2.46	3.12	3.75	.0561	.0892	.0534	.0743	.147	.147	0.743	.154	.869	4.39	.910
0.40	0.230	.0306	.0465	.0700	.194	.274	.351	0.570	0.731	0.974	1.25	1.52	.0300	.0426	.0295	.0368	.0647	.0640	.305	.0677	.878	4.14	.910
0.50	0.270	.0226	.0299	.0410	.0966	.140	.176	.282	.361	.484	0.626	0.764	.0229	.0288	.0232	.0259	.0394	.0384	.158	.0409	.892	3.58	.926
0.60	0.305	.0203	.0244	.0304	.0637	.0845	.104	.166	.214	.284	.367	.443	.0211	.0243	.0218	.0226	.0304	.0292	.0979	.0312	.905	2.91	.929
0.80	0.362	.0201	.0218	.0239	.0369	.0456	.0536	.0780	.0971	.124	.158	.191	.0213	.0226	.0224	.0217	.0253	.0236	.0520	.0255	.932	1.91	.939
1.0	0.406	.0213	.0222	.0238	.0334	.0372	.0372	.0500	.0599	.0725	.0909	.111	.0228	.0235	.0241	.0227	.0252	.0231	.0386	.0252	.948	1.45	.948
1.5	0.485	.0246	.0249	.0252	.0258	.0275	.0282	.0315	.0351	.0368	.0433	.0488	.0264	.0267	.0280	.0261	.0278	.0251	.0304	.0276	.962	1.05	.956
2.0	0.530	.0267	.0267	.0271	.0265	.0277	.0275	.0292	.0310	.0302	.0339	.0367	.0287	.0289	.0305	.0283	.0300	.0268	.0302	.0297	.973	0.979	.963
3.0	0.573	.0288	.0289	.0289	.0289	.0278	.0290	.0283	.0301	.0278	.0304	.0319	.0310	.0311	.0329	.0305	.0320	.0288	.0311	.0317	.966	0.938	.957
4.0	0.587	.0295	.0296	.0296	.0284	.0293	.0287	.0287	.0301	.0274	.0299	.0308	.0317	.0319	.0337	.0312	.0329	.0296	.0316	.0325	.966	.928	.954
5.0	0.589	.0297	.0297	.0297	.0284	.0293	.0287	.0287	.0300	.0271	.0294	.0304	.0319	.0320	.0339	.0314	.0330	.0297	.0316	.0327	.966	.925	.957
6.0	0.588	.0296	.0296	.0296	.0283	.0292	.0286	.0287	.0297	.0270	.0291	.0301	.0318	.0319	.0338	.0313	.0329	.0296	.0315	.0326	.966	.925	.957
8.0	0.573	.0288	.0289	.0289	.0276	.0285	.0278	.0280	.0287	.0261	.0282	.0290	.0310	.0311	.0329	.0305	.0321	.0289	.0306	.0318	.965	.920	.956
1.0	0.555	.0279	.0280	.0280	.0267	.0275	.0269	.0270	.0280	.0252	.0272	.0279	.0300	.0301	.0319	.0295	.0311	.0280	.0297	.0308	.965	.922	.956
1.5	0.507	.0255	.0255	.0255	.0243	.0250	.0246	.0245	.0254	.0228	.0247	.0253	.0274	.0275	.0291	.0270	.0283	.0255	.0270	.0280	.964	.920	.958
2.0	0.464	.0234	.0234	.0234	.0225	.0232	.0227	.0228	.0235	.0212	.0228	.0234	.0252	.0252	.0267	.0247	.0260	.0234	.0248	.0257	.966	.921	.954
3.0	0.398	.0204	.0204	.0205	.0199	.0206	.0201	.0204	.0210	.0193	.0208	.0213	.0219	.0220	.0232	.0216	.0227	.0205	.0219	.0225	.962	.928	.954
4.0	0.351	.0184	.0186	.0187	.0184	.0191	.0188	.0192	.0199	.0182	.0199	.0204	.0197	.0198	.0208	.0194	.0205	.0186	.0199	.0203	.968	.930	.948
5.0	0.316	.0170	.0172	.0174	.0173	.0181	.0180	.0184	.0192	.0176	.0193	.0200	.0181	.0183	.0191	.0179	.0190	.0173	.0186	.0188	.964	.934	.944
6.0	0.288	.0160	.0162	.0166	.0166	.0175	.0174	.0179	.0187	.0175	.0190	.0198	.0170	.0172	.0178	.0168	.0180	.0163	.0178	.0180	.960	.949	.949
8.0	0.249	.0145	.0148	.0154	.0154	.0167	.0169	.0175	.0184	.0172	.0190	.0197	.0153	.0156	.0160	.0153	.0165	.0150	.0165	.0163	.956	.956	.944
10.0	0.222	.0137	.0142	.0147	.0147	.0163	.0167	.0174	.0183	.0173	.0191	.0201	.0144	.0147	.0149	.0144	.0155	.0144	.0159	.0154	.935	.960	.929

^a See footnote 4.
^b See footnote 5.

From NBS Handbook 85 (Ref. 1).

TABLE XI-3. Mean Conversion Factor \bar{f} in Compact Bone and Muscle for Various X-Ray Spectra

\bar{f}		Tube potential (kV _p)	HVL	
Muscle (rad/R)	Compact bone (rad/R)		mm Al	mm Cu
0.92	3.99	50	0.25	0.01
0.92	4.00	80	1.8	
0.92	3.63	100	4.2	0.18
0.93	2.79	140	4.5	0.19
0.94	1.94	250		1.25

Adapted from NBS Handbook 85 (Ref. 1).

The energy fluence F is equal to the photon fluence Φ multiplied by the energy hn carried by each photon, as follows:

$$F = \Phi \times hn. \quad (8)$$

If F is expressed in ergs/cm², Φ in photons/cm², and hn in keV, the formula becomes

$$F = \Phi \times 1.602 \times 10^{-9} \times hn,$$

1 keV being equal to 1.602×10^{-9} erg. Since the energy fluence per roentgen is $87/(\mu_{en}/\rho)_{\text{air}}$, the particle (photon) fluence per roentgen becomes

$$\Phi = \frac{54.3 \times 10^9}{(\mu_{en}/\rho)_{\text{air}} \times hn} \quad \text{photons/cm}^2/\text{R}.$$

Table XI-4 lists particle fluence and energy fluence per roentgen and the mass energy absorption coefficient for air as functions of photon energy.

X-RAY DOSIMETRY¹

X-ray dosimetry consists in measuring either (1) parameters which are intrinsic to the beam of x-rays, such as quality and quantity, or (2) the absorbed dose of radiation in a medium resulting from the exposure of this medium to radiation. In either case, x-ray dosimetry consists of the quantitative determination of the interaction of x-rays with matter.

In the diagnostic energy range, the interaction of x-rays with matter results in a transfer of energy from the radiation to electrons which in turn

¹ For further study the reader is referred to the excellent text entitled *Radiation Dosimetry*, edited by Hine and Brownell (Ref. 5). Report 10b of the International Commission on Radiological Units and Measurements (ICRU), entitled "Physical Aspects of Irradiation," National Bureau of Standards Handbook 85 (Ref. 1), includes a broad study of various methods used in x-ray dosimetry and an extensive bibliography on this subject.

TABLE XI-4. Particle Fluence, Energy Fluence, and Mass Energy Absorption Coefficient, as Functions of Photon Energy^a

Photon energy (MeV)	Particle fluence Φ (photons/cm ² /R) ($\times 10^8$)	Energy fluence F (ergs/cm ² /R)	Mass energy absorption coefficient $(\mu_{en}/\rho)_{\text{air}}$ (cm ² /g)
0.010	11.7	18.7	4.66
0.015	28.1	67.4	1.29
0.020	52.6	169	0.516
0.030	123	591	0.147
0.040	212	1360	0.0640
0.050	283	2270	0.0384
0.060	310	2980	0.0292
0.080	288	3690	0.0236
0.100	235	3770	0.0231
0.15	144	3470	0.0251
0.20	101	3250	0.0268
0.30	62.8	3020	0.0288
0.40	45.9	2940	0.0296
0.50	36.6	2930	0.0297
0.60	30.6	2940	0.0296
0.80	23.5	3010	0.0289
1.00	19.4	3110	0.0280
1.50	14.2	3410	0.0255
2.00	11.6	3720	0.0234
5.00	6.28	5030	0.0173
10.00	3.77	6040	0.0144

^a Calculated from data in NBS Handbook 85 (Ref. 1).

$$\Phi = \frac{54.3 \times 10^{12}}{(\mu_{en}/\rho)_{\text{air}} h\nu \text{ (in keV)}} \quad \text{photons/cm}^2/\text{R}$$

$$F = \frac{87}{(\mu_{en}/\rho)_{\text{air}}} \quad \text{ergs/cm}^2/\text{R}$$

lose their energy by excitation and ionization. Therefore, the interaction of x-rays with matter can be detected and measured by methods leading to the detection and measurement of excitation and ionization. A number of physical interactions can be used for x-ray dosimetry. Most of the methods used fall into one of the following categories: (1) detection of ions in gases, (2) calorimetric determination of the energy dissipated by radiation in a given medium, (3) photographic dosimetry, based on the density produced on a photographic emulsion by x-radiation, (4) chemical dosimetry, based on the magnitude of chemical reactions that take place as a result of irradiation,

(5) scintillation dosimetry, based on the luminescence produced by radiation in certain crystals and amorphous media, and (6) solid state dosimetry, which may be based on one of several radiation-induced phenomena such as changes in optical density, photoluminescence, thermoluminescence, or conductivity changes (Ref. 1).

The methods for the determination of x-ray quality were discussed in Chapter II. The purpose of the following sections is to discuss three methods particularly useful in the determination of x-ray quantity in diagnostic radiology: (1) ionization dosimetry, (2) photographic dosimetry, and (3) scintillation dosimetry.

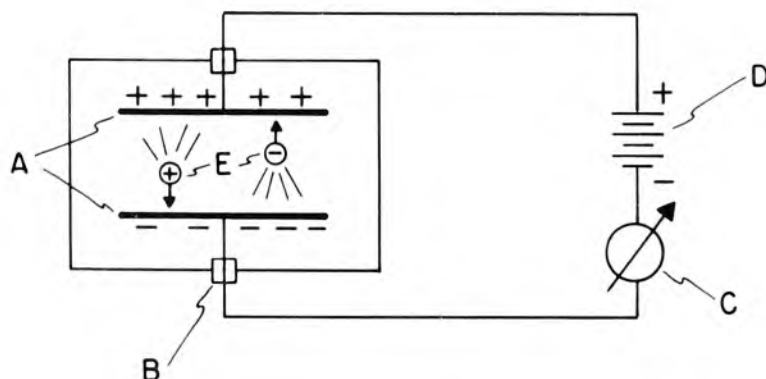
IONIZATION DOSIMETRY

Ionization in gases consequent to irradiation and measured in ionization chambers provides the most widely used method of x-ray dosimetry. An ionization chamber is composed of two electrodes which may be constructed in a variety of shapes, separated by a volume of gas. An electric field is maintained between the two electrodes by connecting them to a source of electricity (Fig. XI-1). A meter capable of measuring electric current or charge is connected in the ionization chamber circuit. Various gases can be used in ionization chambers. However, air is most commonly used for x-ray dosimetry.

The exposure of an ionization chamber to x-rays results in the production of ions in the gas of the chamber. As these ions are subjected to the action of the electric field between the electrodes, the positive ions drift toward the negatively charged electrode while the negative ions drift toward the positively charged electrode. The ionization electrons travel towards the anode

FIG. XI-1. Principle of operation of ionization chamber.

- A electrodes
- B insulator
- C current- or charge-measuring device
- D source of electricity
- E ions



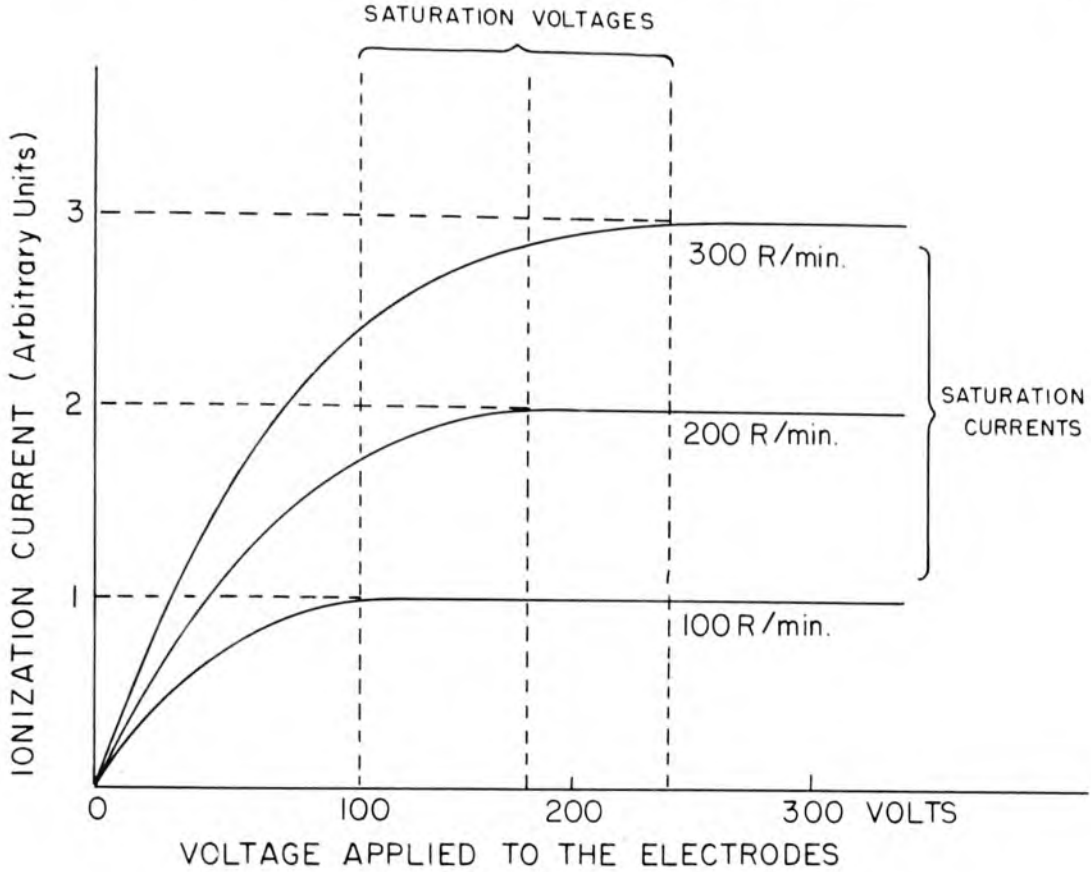


FIG. XI-2. Saturation currents in ionization chamber.

considerably faster than the heavier, positive ions. In electronegative gases, the electrons formed by ionization may attach themselves to neutral atoms thereby forming heavy negative ions. This process is called *electron attachment* (Ref. 6). During this drift of the ions toward the electrode that carries a charge opposite to theirs, electrons may be captured by positive ions. This process, called *recombination*, results in the formation of a neutral atom or molecule which is no longer acted upon by the electric field. The ions that do not undergo recombination transfer their charges to the electrodes in the chamber, and a current is thus generated in the ionization chamber circuit. The magnitude of this current is proportional to the number of charges collected per unit time, and can therefore serve as a measure of the beam of radiation striking the chamber.

Saturation Voltage

The ions formed in the gas of an ionization chamber tend to recombine unless they are rapidly swept by the electric field and collected by the electrodes. Figure XI-2 shows a family of curves obtained by plotting the current measured in an ionization chamber versus voltage applied to the electrodes for various intensities of radiation. All the curves exhibit a

region where the ionization current increases as the voltage applied to the electrodes is raised. In this region there is considerable recombination of ions, and the increase in current observed is due to the fact that an increase in voltage results in a greater number of ions reaching the electrodes. All curves, however, reach exponentially a plateau, and above a given value (saturation voltage) an increase in voltage does not result in an appreciable change in current (saturation current). The saturation current corresponds to the situation where most of the ions formed in the chamber are collected before they can recombine. The saturation voltage increases with increasing radiation intensity because the probability of recombination is greater for higher ion density; thus, high radiation levels in an ionization chamber require higher saturation voltages.

For a given ionization chamber the saturation voltage depends not only on the maximum ion density to be generated in the chamber, but also on the physical structure of the chamber itself. In general, for a given voltage applied to the electrodes, the reduction of the distance between the electrodes increases the electric field and thus reduces the chance of recombination by reducing the distance traveled by the ions before collection.

In most ionization chambers used for x-ray dosimetry in diagnostic radiology, an electric field of about 250 V/cm, resulting from a few hundred volts applied to the electrodes of the chamber, is suitable to achieve saturation (Ref. 4).

Free-Air Standard Ionization Chamber

The free-air standard ionization chamber is an instrument designed to measure radiation exposure directly in roentgens. It is a primary standard in the sense that it is designed to satisfy the requirements for the definition of the roentgen, and it is not calibrated against another ionization chamber.

The definition of the roentgen is based on the expression for a given electric charge produced by ionization in a given mass of air. Consequently, the experimental realization of an instrument capable of measuring roentgens directly must incorporate (1) a method of defining a mass of air, and (2) a method for collecting and measuring all the charges produced by ionization subsequent to the irradiation of this mass of air.

In the free-air standard ionization chamber (Fig. XI-3) a volume of air is defined by that portion of a collimated beam of x-rays (shaded area in Fig. XI-3) entering the chamber which is equal in length to the collector electrode. The electrodes are parallel plates generating an electric field of 100 V/cm. The electric field is shaped by guard plates and guard wires in such a fashion that the lines of force of the electric field are perpendicular to the collector electrode in the collecting area. The ionization current is measured by means of an electrometer which is usually connected

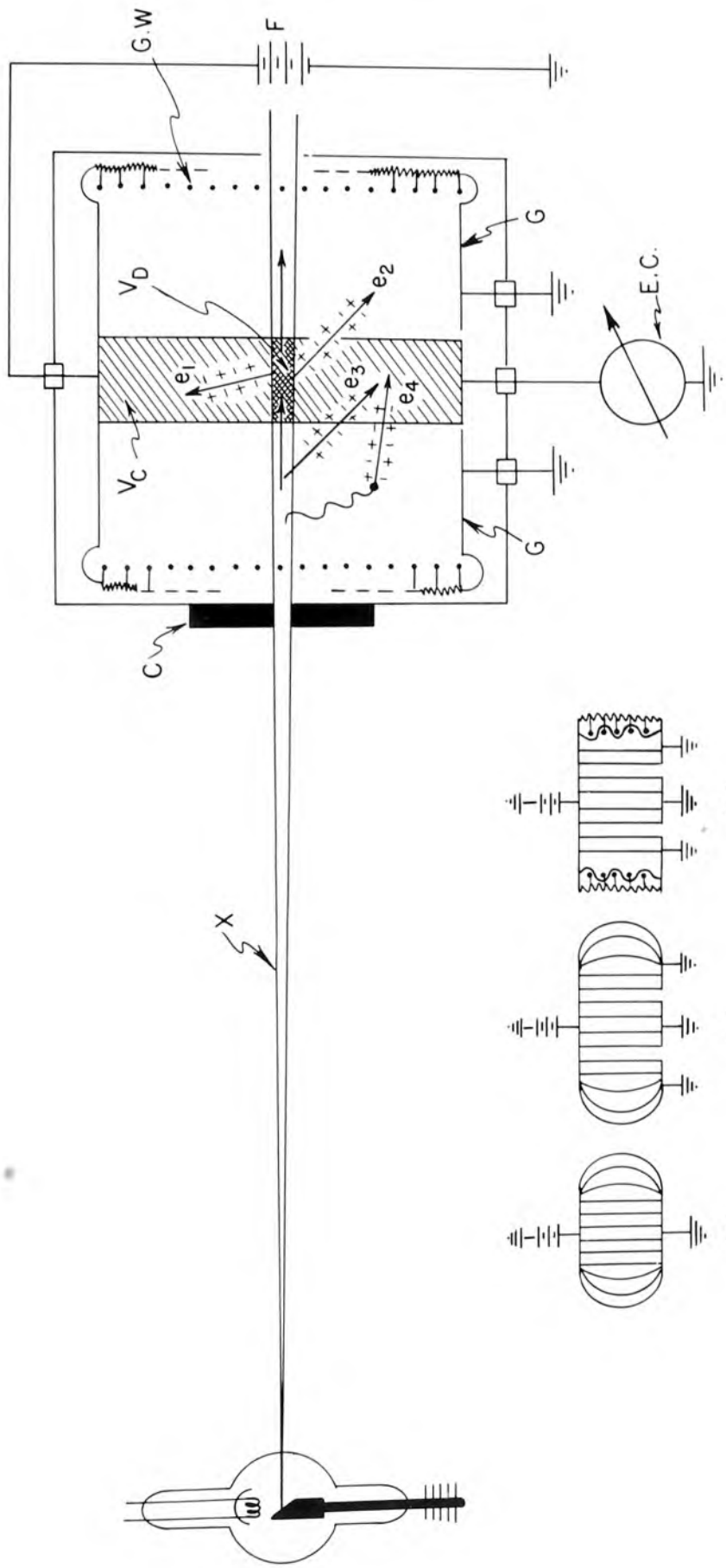


FIG. XI-3. Schematic diagram of parallel-plate free-air ionization chamber. (Adapted from Wyckoff and Attix, Ref. 7.)

and operated in such a fashion as to maintain the collector electrode as nearly as possible to the potential of the guard plates, which are usually maintained at ground potential (Ref. 7). The distance between the electrodes and the defined volume of air must be at least equal to the range of the secondary electrons produced by the radiation to be measured in air. This precaution must be observed to ensure the collection of all the charges produced by the secondary electrons resulting from the interactions of x-rays in the defined volume of air. The loss of electrons (E_2) from the volume where ion collection takes place is compensated by the entry into this volume of electrons (E_3) originating outside the defined volume. Electrons produced by scattered photons outside the defined volume (E_4) are unwanted in the measurement, but their contribution is generally small.

The mass of air involved in the measurement can be calculated from the measured volume by applying suitable corrections for temperature and pressure.

Standard free-air ionization chambers of different designs have also been constructed. Free air chambers calibrated against a standard free-air chamber are used as secondary standards.

Thimble Ionization Chamber

Free-air ionization chambers, because of their bulk and their relative lack of mobility, are unsuitable, for most applications in x-ray dosimetry, with the exception of radiation standardization. Most x-ray measurements are usually achieved by means of *thimble ionization chambers*. The term thimble ionization chamber includes a large number of instruments of various sizes and shapes with a sensitive volume which may be as small as a few cubic millimeters or as large as several cubic centimeters. A thimble ionization chamber consists of a shell often made of some plastic material that surrounds a volume of gas which contains two electrodes (Fig. XI-4). Usually one of the electrodes in the chamber is a wire located in the axis of the cylindrical shell, and the second electrode is a conductive coating deposited on the inside of the shell (Fig. XI-4, bottom). It should be noted that a great number of other electrode arrangements can be used in thimble chambers.

The thimble chamber is connected to a source of electricity and to some electric-current or charge measuring device, generally an electrometer. Although different gases can be used in thimble chambers, air is used most often, either at atmospheric or at higher pressures.

When a thimble chamber is exposed to x-rays, most of the ionizations taking place in the gas result from secondary electrons which are produced subsequent to x-ray photon interactions in the walls of the chamber. Only a small percentage of the ionization in a thimble chamber results from the absorption of x-rays in the gas itself, because the probability of x-ray



FIG. XI-4. Thimble ionization chamber (Victoreen Condenser-R Meter Model 570), with charger and electrometer (*top*). At *bottom* is shown a cross section of thimble ionization chamber attached to condenser. Chamber is open to air, and readings must be corrected for temperature and pressure.

absorption is considerably greater in the shell than in the gas-filled cavity due to the relatively low density of the latter.

Thimble ionization chambers are most useful in radiation dosimetry if their design and construction are such that they fulfill the following three criteria: (1) electronic equilibrium is achieved within the chamber, (2) the chamber fulfills the requirements of the Bragg-Gray relation, and (3)

the chamber is air equivalent in the radiation energy range for which it was designed.

Electronic Equilibrium. A state of electronic equilibrium is said to exist at a point within a medium if every electron leaving an infinitesimal volume surrounding this point is replaced by another electron originating outside the volume. Under equilibrium conditions, the energy dissipated in the volume by the electrons is equal to that which would have been dissipated in the volume if all the electrons originating in it would have dissipated their energy within this volume (Ref. 1).

Electronic equilibrium in the measuring volume of a free air chamber is achieved by surrounding this volume with a thickness of air at least equal to the range of the secondary electrons produced by the x-radiation measured in air. In the thimble ionization chamber, electronic equilibrium is achieved by surrounding the gas volume with a shell the thickness of which is at least equal to the range of the secondary electrons produced by the x-radiation to be measured in the material composing the shell.

★ **The Bragg-Gray Relation.** The mathematical relationship between the ionization produced in a small gas-filled cavity provided in a solid medium subjected to irradiation and the energy absorbed in the medium is referred to as the Bragg-Gray theory, or Bragg-Gray relation, a concept introduced by Bragg and developed by Gray (Ref. 4):

$$D = J_m \times W \times s_m, \quad (9)$$

where D is the absorbed dose per gram of material, J_m is the number of ion pairs formed per gram of gas, W is the average energy expended by the ionizing particles in the gas in forming one pair of ions, and s_m is the ratio of the stopping power per unit mass of medium to the stopping power per unit mass of the gas. The ratio s_m is also equal to the ratio of the energy dissipated per unit mass of the solid medium by the electron flux, divided by the energy dissipated per unit mass of gas by the same electron flux. In the practical application of the Bragg-Gray relation, the gas used is generally air, for which W_{air} is equal to 33.7 eV. Tables of mass stopping power, or mass stopping power ratio relative to air for various elements, have been compiled (Refs. 1 and 8).

The Bragg-Gray relation is valid only if the following conditions are fulfilled (Ref. 4). (1) The gas-filled cavity within the solid is so small that the amount of energy lost by the electrons within the cavity is small; which means that most of the electrons entering the cavity also escape it, so that the presence of the cavity does not alter appreciably the electron flux within the medium. (2) A negligibly small number of photons interact with the gas in the cavity directly, and most of the electrons responsible for the measured ionization originate in the medium rather than in the cavity. (3) The rate of energy absorption throughout the cavity is constant, therefore the size of the cavity must be small with respect to the radiation field

gradient. (4) If the cavity is used for the determination of radiation exposure, the wall thickness must be sufficient to exclude all electrons originating outside the medium.

The Bragg-Gray relation is particularly useful in radiation dosimetry because it allows the determination of the energy dissipated by x-radiation within a solid medium by measuring the ionization produced in a gas-filled cavity. An extreme application of the Bragg-Gray relation consists in measuring the absorbed dose in air exposed to x-rays. In this case the gas cavity and the surrounding medium are identical in nature.

Air-Equivalent Thimble Ionization Chamber. A thimble ionization chamber constructed in such a fashion as to fulfill the requirements of the Bragg-Gray relation provides a measurement proportional to the energy dissipated by the x-radiation in the material that composes the shell of the chamber. Thus, if a thimble chamber is constructed of aluminum, the reading supplied by the chamber when used to measure x-ray beams of various energies and intensities provides a measure of the relative energy dissipated by these radiations in aluminum. If a thimble chamber is to be used to measure radiation exposure in air, then the wall material must have a stopping power identical to that of air. Under these circumstances, the Bragg-Gray relation Equation (9), is reduced to

$$D = J_m \times W_{\text{air}}, \quad (10)$$

s_m being equal to 1. The above expression gives the dose absorbed in air, which is proportional to the exposure. The determination of the absorbed dose in air exposed to x-rays, carried out in the section on "Roentgens, Rads, and Photons," above, made use of this equation.

Since the stopping power of any material depends upon its effective atomic number, an air-equivalent thimble ionization chamber must have a shell with an effective atomic number equal to that of air, which is 7.64 (Ref. 4). Although it is difficult to construct an ionization chamber which is air equivalent for all x-ray energies, a number of ionization chambers which are nearly air equivalent over a broad energy range have been constructed (Figs. XI-4, XI-5, and XI-6).

Condenser Ionization Chamber. The electronic circuitry associated with a thimble ionization chamber may be designed either to measure ionization current or ionization charge. A particularly useful form of thimble ionization chamber is the condenser (capacitor) ionization chamber, which consists, in general, of an air-equivalent thimble chamber permanently connected to a condenser (Fig. XI-4). In this apparatus the source of electricity that provides the electric field in the ionization chamber is the condenser, which is charged to a given potential by means of an external charging device. When the chamber-condenser combination is placed in the field of radiation to be measured, the ionization current in the chamber partially discharges the condenser (Fig. XI-7). After exposure, the poten-

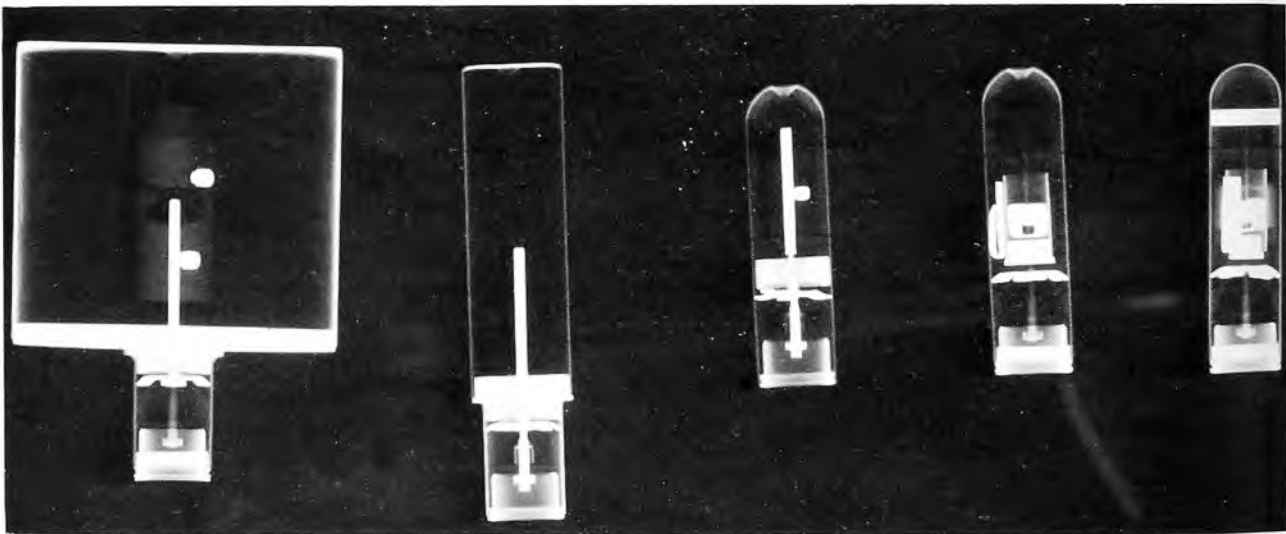
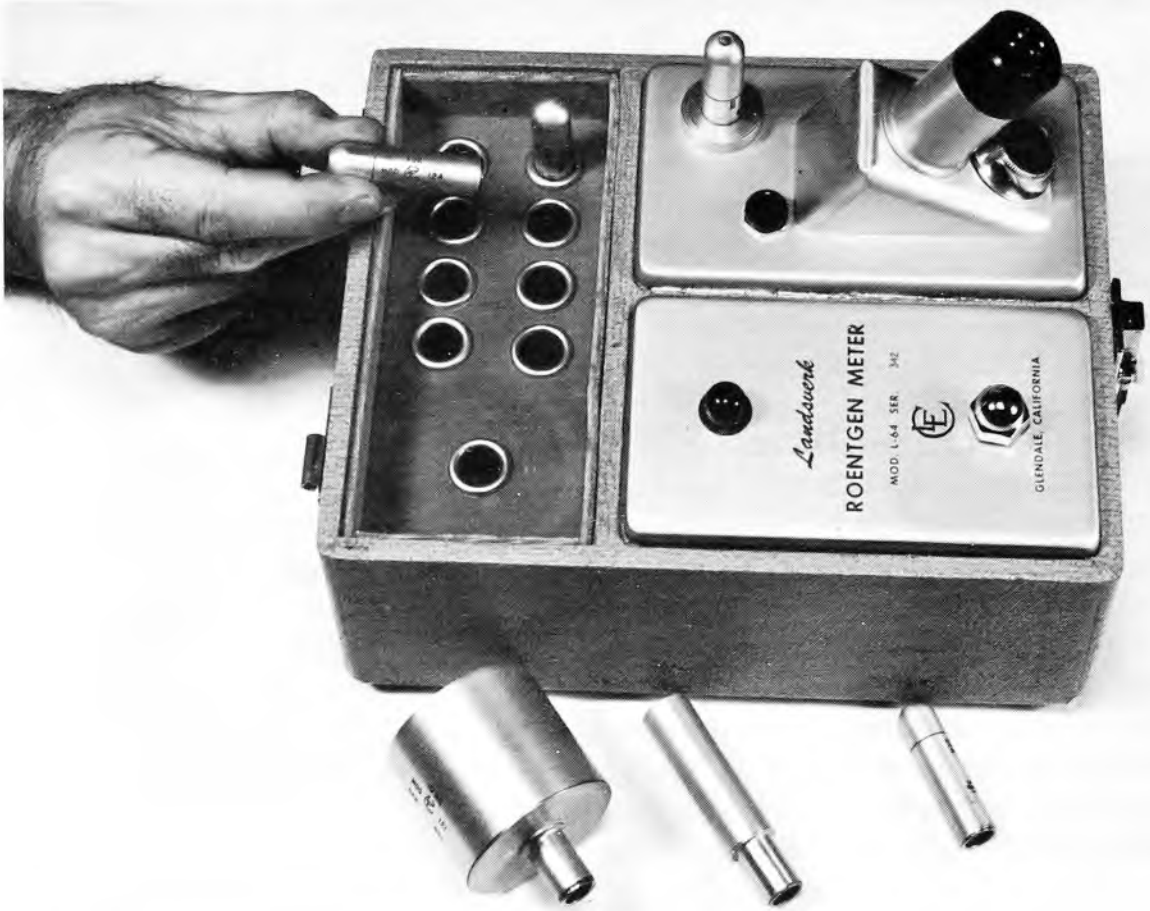


FIG. XI-5. Thimble ionization chambers (Landsverk Roentgen Meter Model L-64), with charger and electrometer. Different-sized chambers used with same charger and electrometer exhibit different sensitivity ranges resulting from the different volumes of chambers in which ionization takes place. Electrical capacity of all chambers is the same. Ionization chambers are sealed off, and readings are independent of temperature and pressure.

Bottom radiograph of chambers



FIG. XI-6. Portable ionization chamber survey meter (Victoreen Survey Meter Model 440). Instrument is designed to measure exposure rates, and is mostly used for measuring stray x-radiation.

tial across the partially discharged condenser is measured by an electrometer. Since the difference of potential across the condenser is proportional to the remaining charge, the reduction in the difference of potential across the condenser subsequent to radiation exposure is a measure of the charge lost by the ionization chamber, and is therefore proportional to the exposure.

Air-equivalent thimble ionization chambers utilized in the measurement of radiation exposure are never used as primary standards; they are always calibrated directly or indirectly against a standard free-air ionization chamber.

PHOTOGRAPHIC DOSIMETRY

The exposure of a photographic emulsion to x-rays results in an increase in the opacity to light of the processed emulsion. The density thus achieved can be measured by photoelectric means and related to the radiation exposure, thus providing a method of dosimetry (Refs. 1 and 9).

The latent photographic image produced in a photographic emulsion exposed to x-rays results from the energy deposited in the photographic grains by electrons generated by the absorption of x-rays in the film or its vicinity. Therefore the density on the film is a measure of the amount of

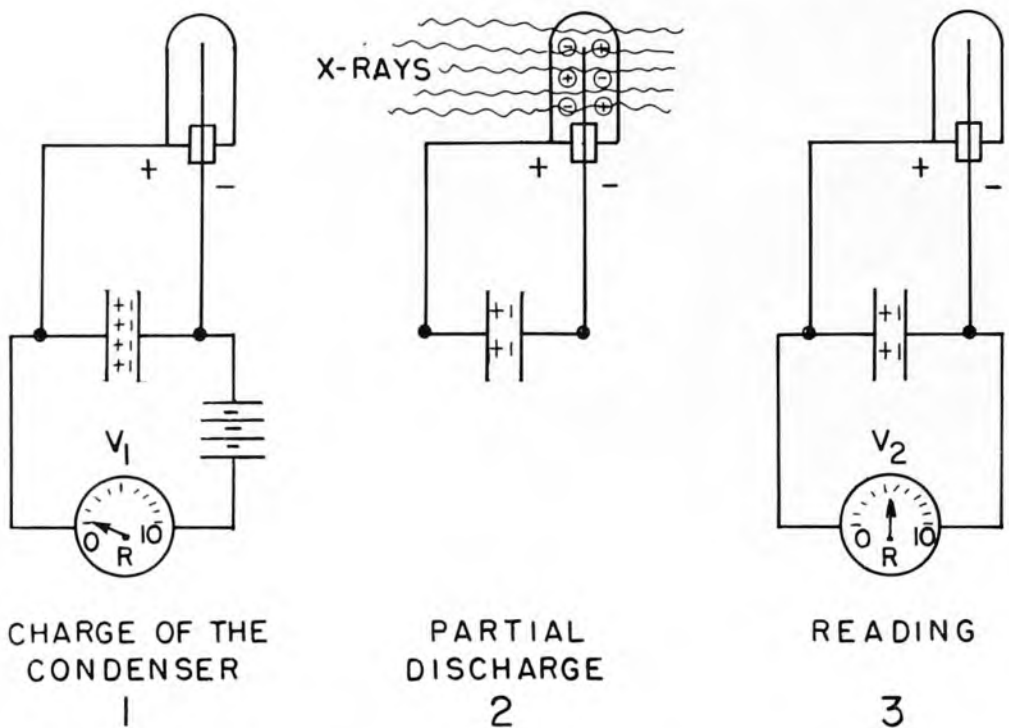


FIG. XI-7. Condenser thimble ionization chamber.

- 1 condenser is charged until voltage between electrodes reaches a given value (0 on electrometer scale)
- 2 ionization chamber is exposed to radiation, which causes leakage of portion of condenser charge, with consequent drop in voltage
- 3 after exposure, voltage across condenser is measured by electrometer. Loss of voltage is proportional to charge lost by condenser (Chapter IV, section on "Switching Tube X-Ray Circuits").

energy dissipated by the x-radiation in the emulsion and its immediate vicinity. Because in the diagnostic energy range the absorption of x-rays in photographic emulsions takes place mostly by photoelectric interactions in bromine and silver, the response of photographic emulsions to radiation exposure is strongly photon energy dependent (Fig. VI-28, Chapter VI). In view of this limitation, photographic dosimetry of x-rays is useful only if one is interested in determining the absorbed radiation dose in the photographic emulsion, or, if the spectral distribution of the radiation is sufficiently well known, to calibrate the photographic film with x-radiation having an identical spectral distribution. But in the diagnostic energy range it is of little interest to determine the absorbed dose of radiation in photographic emulsions, and it is difficult to reproduce for calibration purposes the spectral distribution of the radiation to be measured.

Thus, photographic dosimetry is of little value unless one can correct by some means the response of the photographic emulsion to radiation and obtain a linear or near-linear response between radiation exposure and

density over a wide photon energy range. This purpose can be achieved by covering the photographic film with various metallic filters to reduce the undesirable energy dependence (Refs. 1, 9, and 10).

In spite of the use of metallic filters, photographic x-ray dosimetry is not sufficiently accurate for general use in the diagnostic range, and the method is used only for personnel monitoring by means of film badges, where it is quite adequate and widely used.

SCINTILLATION DOSIMETRY

X-ray scintillation dosimetry is carried out by means of scintillation detectors. Scintillation detectors are based on the property of certain substances, called phosphors, to emit flashes of light, or scintillations, when struck by ionizing radiations. It should be noted that the phenomenon of scintillation is nothing else but luminescence, which was discussed in Chapter VI. A scintillation detector (Figs. XI-8 and XI-9) is composed of a phosphor optically coupled to a photomultiplier tube which translates the flashes of light supplied by the phosphor when struck by ionizing radiations into electrical pulses. These electrical pulses are usually amplified in magnitude and sometimes sorted according to their heights by means of an electronic circuit.

Phosphors Used in Scintillation Dosimetry

A number of substances that may be crystalline or amorphous, solid or liquid, inorganic or organic, have provided useful phosphors for scintillation dosimetry. Table XI-5 lists a number of these phosphors which are used in the detection of ionizing radiation by scintillation techniques. A comparison with Table VI-2, Chapter VI, will show that some of the phosphors incorporated in x-ray screens are also used as scintillation phosphors.

One of the most widely used phosphors in scintillation dosimetry is crystalline sodium iodide activated with thallium. This phosphor is desirable because it exhibits a particularly high conversion efficiency and a high effec-

FIG. XI-8. Block diagram of a scintillation dosimeter.

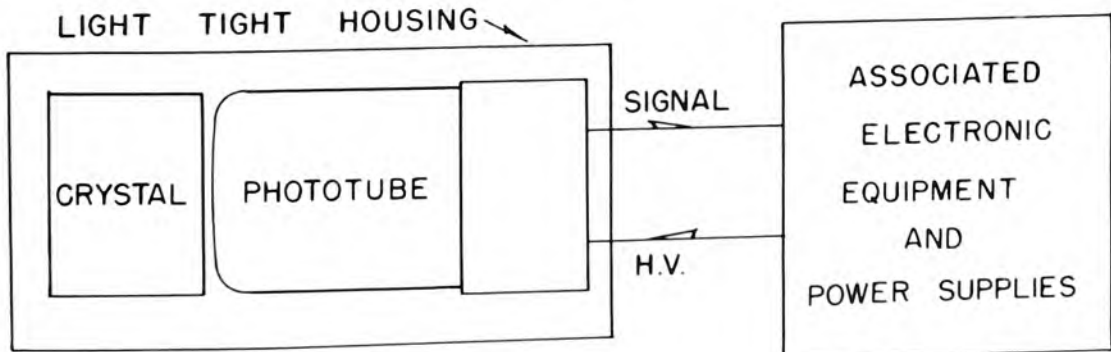




FIG. XI-9. Scintillation detector and component parts.

Top and *Middle* phosphor (NaI(Tl) crystal) and photomultiplier tube (Dumont)
Bottom radiograph of scintillation detector showing internal structure of photomultiplier tube

TABLE XI-5. Physical Properties of Phosphors Used in Scintillation Techniques^a

Phosphor	Composition	Effective atomic number (Z_{eff})	Density (g/cm ³)	Wavelength of radiation emitted (Å)	Conversion efficiency (%)	Decay time (10 ⁻⁶ sec)	Refractive index
Sodium iodide activated with thallium	NaI(Tl)	50 (Ref. 17)	3.67 (Refs. 11, 17)	4100 (Ref. 17)	13 (Ref. 18)	0.3 (Ref. 11)	1.7 (Ref. 17)
Anthracene	C ₆ H ₄ :(CH) ₂ :C ₆ H ₄	5.8 (Ref. 17)	1.25 (Ref. 17)	4400 (Ref. 18)	5 (Ref. 18)	0.03 (Ref. 18)	
Liquid (Ref. 17)							
Scintillating solute, <i>p</i> -terphenyl; solvent, xylene; concentration, 5 g solute per liter solvent.	C ₆ H ₄ (CH ₃) ₂ (xylene)	5.6	0.87	3700	~2	0.007	1.5
Plastic (Ref. 17)							
Scintillating solute, terphenyl; solvent, polystyrene; concentration, 31 g solute per liter solvent.	C ₆ H ₅ CH:CH ₂ (styrene)	5.7	1.06		~1.5	~0.005	1.59

^a Physical properties of other phosphors used in scintillation techniques are listed in Table VI-1, Chapter VI.

TABLE XI-6. Physical Constants and Formulas

Constant	Symbol	Value
Speed of light in vacuum	c	2.997925×10^{10} cm sec ⁻¹
Elementary charge	e	4.80298×10^{-10} esu 1.60210×10^{-19} coulomb
Electron rest mass	m_e	9.1091×10^{-28} g
Protons rest mass	m_p	1.67252×10^{-24} g
Gravitational constant	G	6.670×10^{-8} dyn cm ² g ⁻²
Planck's constant	h	6.6256×10^{-27} erg sec
Avogadro constant	N_A	6.02252×10^{23} molecules gram-mole ⁻¹
Boltzmann constant	k	1.38054×10^{-16} erg ° K
1 electron volt	eV	= 1.6021×10^{-12} erg
1 calorie	cal	= 4.184×10^{-7} erg
1 micron	μ	= 10^{-4} cm
1 angstrom	Å	= 10^{-8} cm
For conversion of electromagnetic radiations into energy:		Multiples and submultiples:
Energy (in keV) = $\frac{12.398}{\lambda \text{ (in } \text{Å})}$		Symbol
		10 ⁶ mega M
		10 ³ kilo k
Unified atomic mass unit:		10 ⁻³ milli m
$\frac{1}{12}$ the mass of the ¹² C nuclide		10 ⁻⁶ micro μ

From NBS Misc. Publ. 253 (Ref. 2, Chapter I).

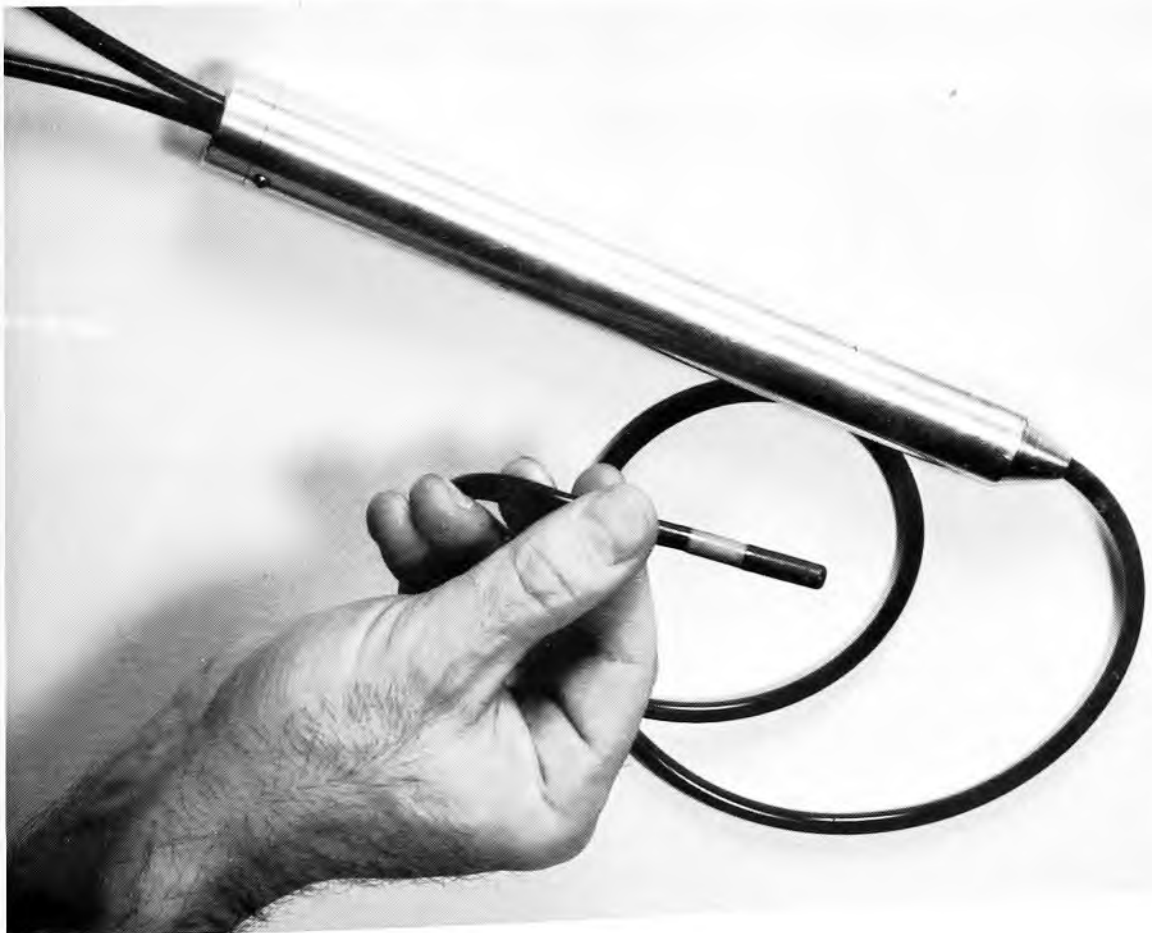
tive atomic number, which in many instances is a desirable feature because it results in a high absorption coefficient for x- and gamma-rays. On the other hand, sodium iodide is highly hygroscopic and must be protected from humidity. The latter purpose is usually achieved by enclosing the crystal in an aluminum, airtight chamber with a transparent window that allows light photons generated in the phosphor to escape (Fig. XI-9).

In many applications of scintillation techniques, particularly in x-ray exposure dosimetry, a high atomic-number phosphor is undesirable if air equivalence is to be achieved, and organic phosphors are preferred. One of the oldest phosphors used for this purpose is crystalline anthracene, which exhibits a desirably high conversion efficiency, although not as high as that of thallium-activated sodium iodide (Table XI-5). More recently, a number of plastic phosphors have become available. In general, most of these phosphors exhibit a lower conversion efficiency than anthracene; however the plastic phosphors can be obtained in any size or shape, while large crystals of anthracene are difficult to obtain. Several organic liquids (Table XI-5) have also been found to be useful scintillators but are seldom used in scintillation dosimetry of x-rays.

Optical Light Coupling

The light generated by the ionizing radiation within the phosphor must be efficiently transferred to the photocathode of the photomultiplier tube. This is usually accomplished by covering all the surfaces of the phosphor, except the surface from which the light is guided to the photomultiplier tube, with a highly reflective coating and optically coupling the light escape surface of the phosphor to the photocathode of the photomultiplier tube. In some arrangements the surface of the phosphor is in intimate contact with the photocathode of the photomultiplier tube (Fig. XI-9), often with a layer of grease between them to prevent reflections between the crystalline surface and the glass surface of the phototube as much as possible. In some applications it is desirable to separate the phosphor from the photomultiplier; in such a case the optical coupling may be achieved by means of a rod of methyl methacrylate or quartz, or even a flexible fiber optics light guide (Fig. XI-10).

FIG. XI-10. Scintillation detector in which phosphor is optically coupled to photomultiplier tube by means of flexible fiber-optics light guide. Flexible probe is designed to be introduced into body cavities.



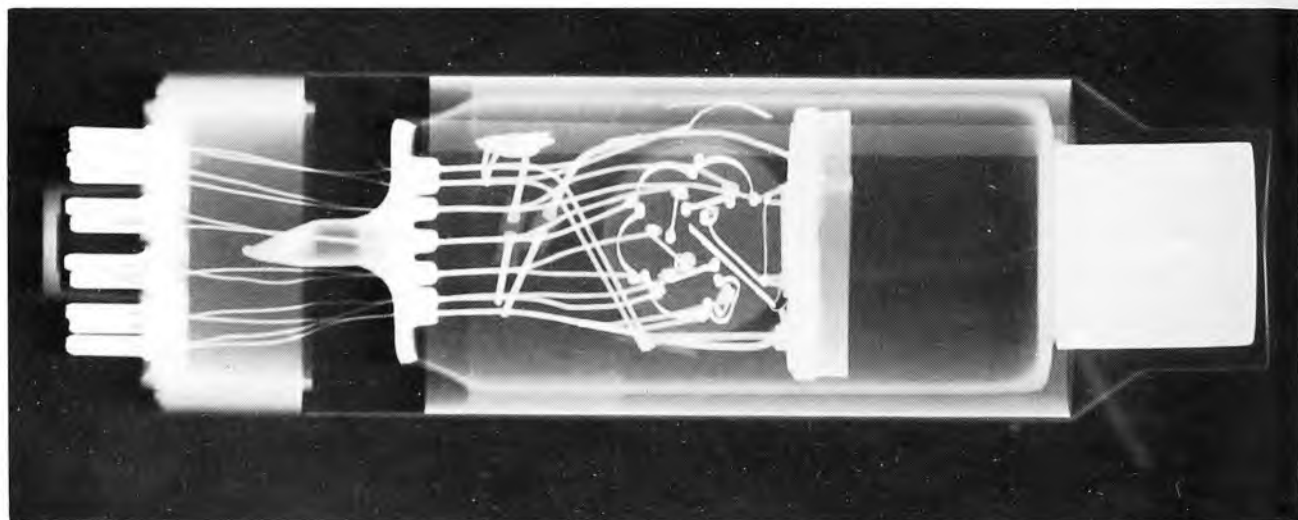
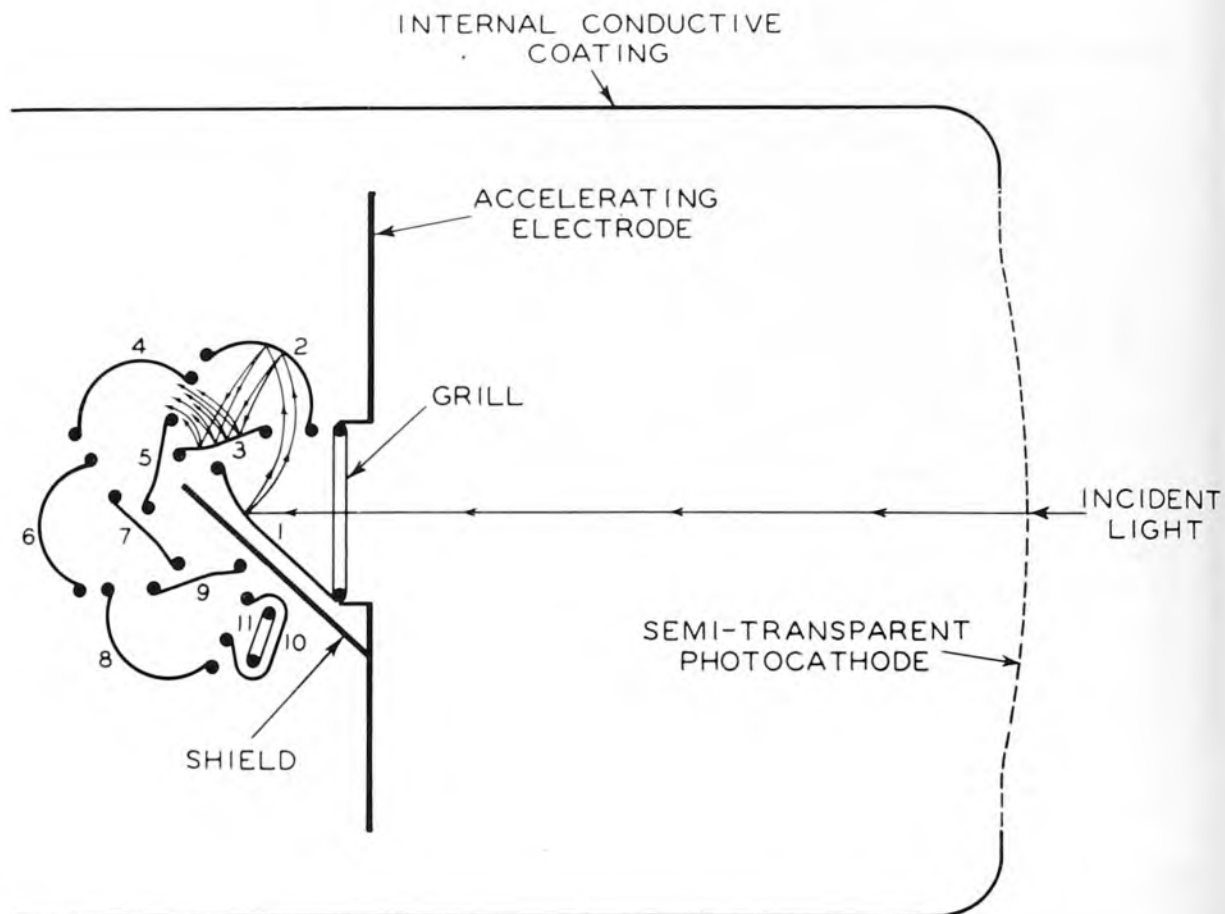


FIG. XI-11. *Top* schematic diagram of dynode structure of R.C.A. photomultiplier tube.

1-10 dynodes

11 anode

Below radiograph of scintillation detector constructed with R.C.A. photomultiplier tube (note difference in dynode design with tube shown in Fig. XI-9)

(Courtesy R.C.A. Company.)

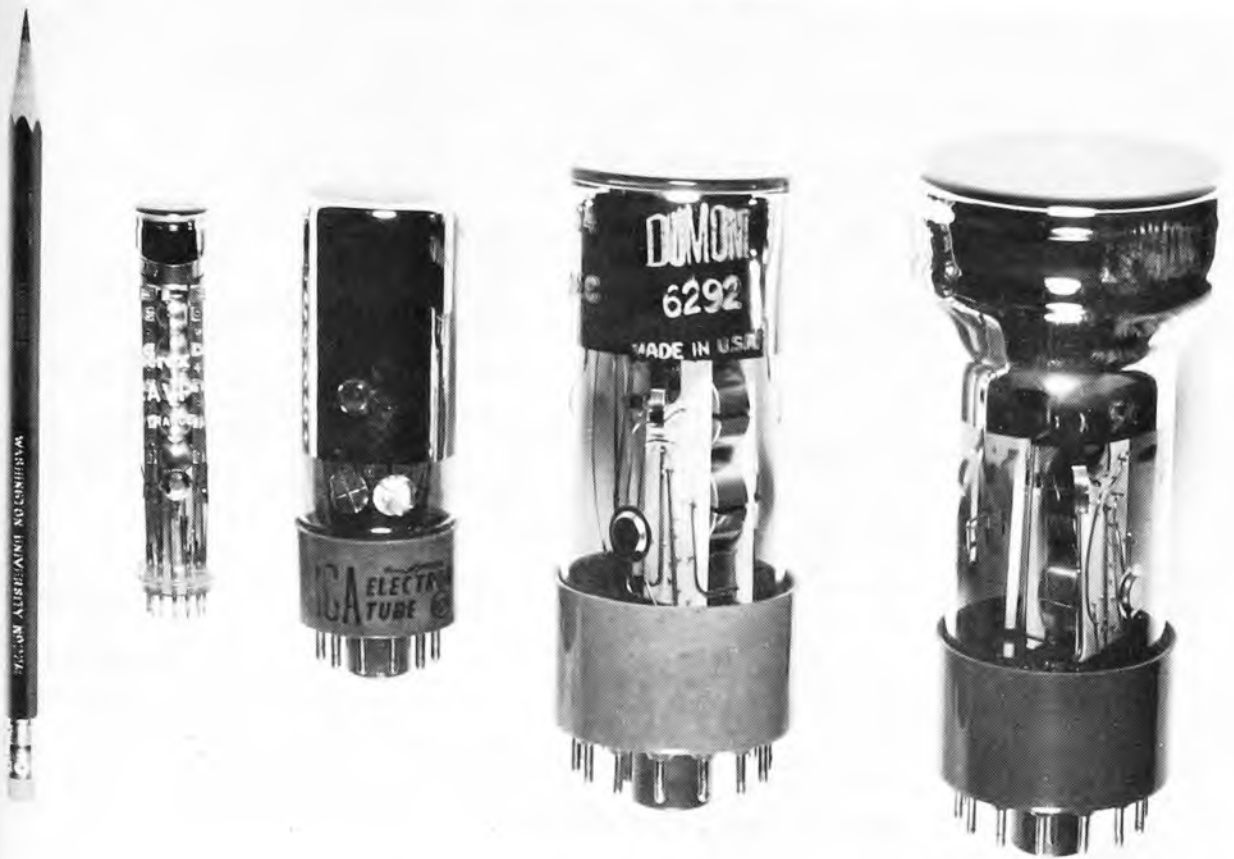


FIG. XI-12. Photomultiplier tubes.

Photomultiplier Tubes

A photomultiplier tube contains essentially three elements (Fig. XI-11): a photocathode in which light photons dislodge electrons; a series of electrodes, usually referred to as *dynodes*, the purpose of which is to multiply the electron flux supplied by the photocathode; and the anode or *collector*, which collects the avalanche of electrons produced by the dynodes (Refs. 11 and 12). The electron multiplication attained in photomultiplier tubes is of the order of $\times 10^6$. Photomultiplier tubes are extremely sensitive light detectors (Fig. XI-17) which can be constructed in a variety of sizes and shapes, depending upon the desired purpose (Fig. XI-12).

Electronic Circuitry Associated with Scintillation Detectors

The electronic circuit associated with a scintillation detector fulfills two purposes: (1) it supplies the high voltage required for the operation of the photomultiplier tube, and (2) it converts the electrical signals supplied by the photomultiplier tube into a form suitable for interpretation.

The operation of a photomultiplier tube requires electrical power in the

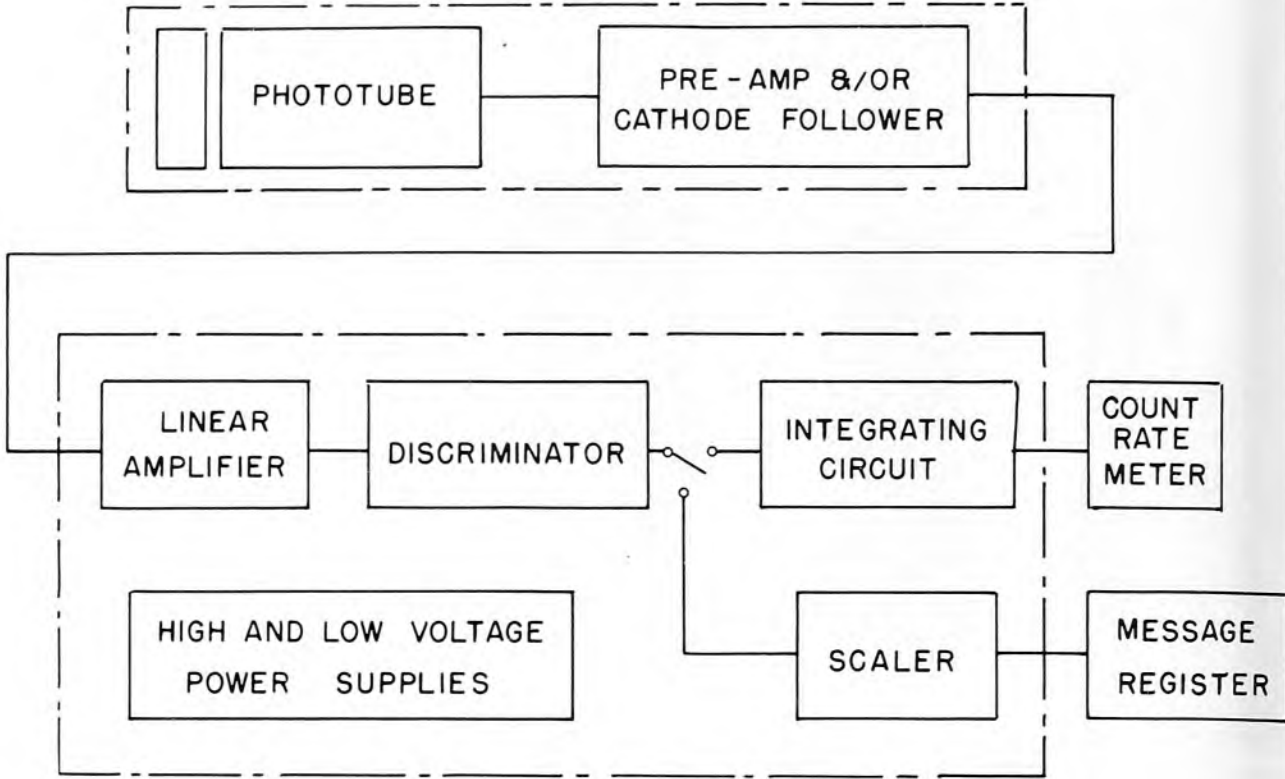
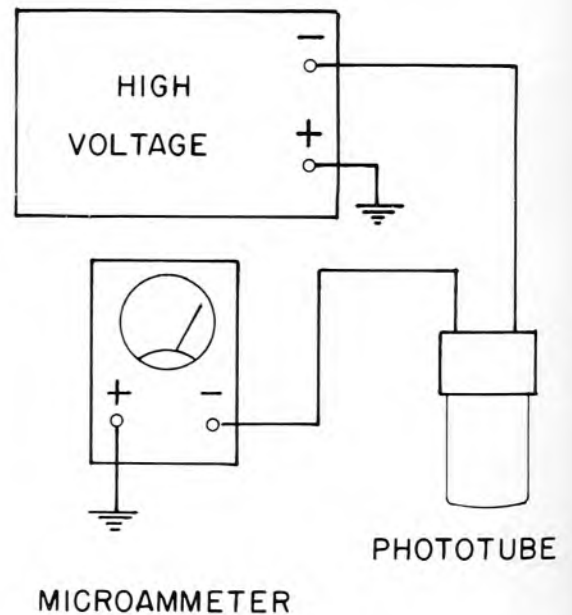


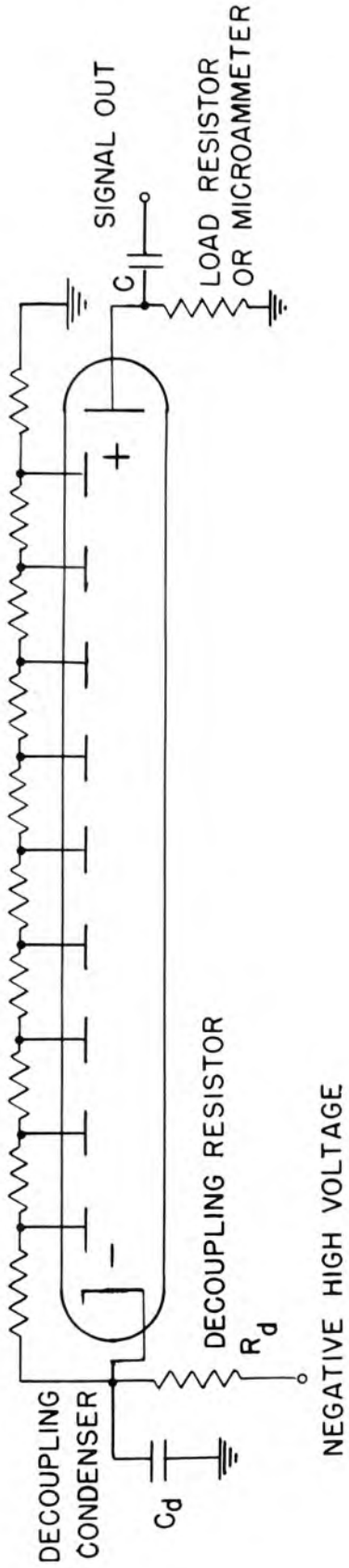
FIG. XI-13. Block diagram of a pulse photomultiplier tube circuit.

FIG. XI-14. Block diagram of a dc photomultiplier tube circuit.



form of high voltage, which is typically of the order of 1200 V in photomultipliers commonly used. The photomultiplier tube is connected in such a fashion that the photocathode is maintained at a high negative potential with respect to the collector, and this potential is nearly equally divided in steps among the dynodes (typically about 10 dynodes) by means of a *voltage divider* (Fig. XI-15).

VOLTAGE DIVIDING NETWORK RESISTORS - COMMONLY 100K TO 220K



VOLTAGE DIVIDING NETWORK RESISTORS

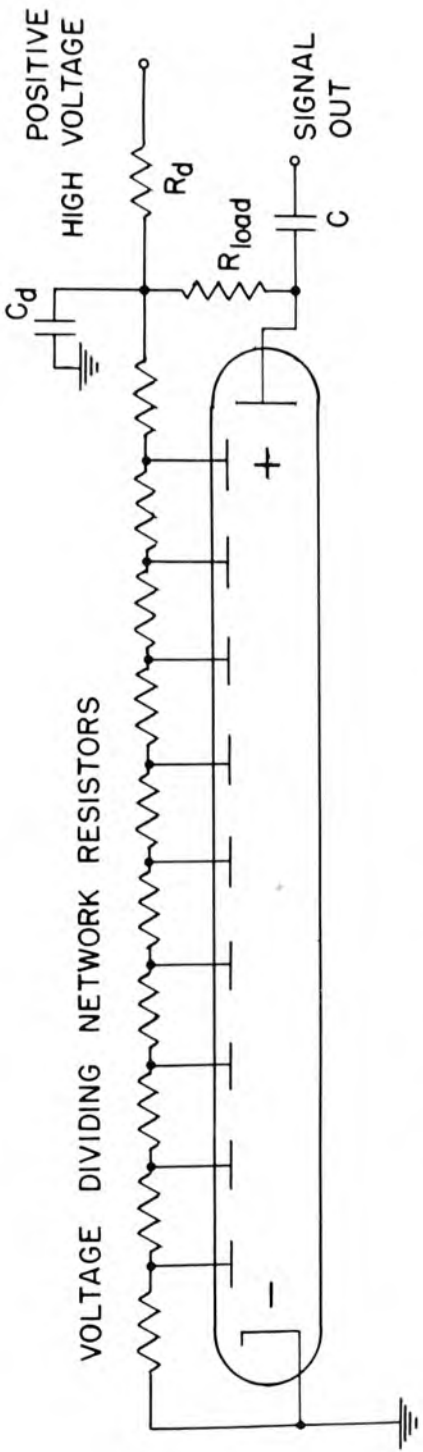


FIG. XI-15. Two wiring diagrams for photomultiplier tubes.

The signal supplied by the photomultiplier tube consists of electrical pulses the magnitudes of which are proportional to the flashes of light that initiate the electron avalanches. These pulses can be processed by one of two circuits—the pulse circuit or the dc circuit.

In the *pulse circuit*, the electrical pulses supplied by the photomultiplier tube are first amplified and then either recorded or further processed by a pulse analyzer circuit that sorts the pulses according to their heights (Figs. XI-14 and XI-15). The pulse height analyzer may be of the single channel type or it may sort simultaneously pulses into a large number of channels (for example, 400 channels). A pulse circuit with a pulse height analyzer is used in scintillation spectrometers (see Chapter II, section on “Scintillation X-Ray Spectrometry”).

The photomultiplier tube may also be connected to a dc microammeter, a vacuum-tube voltmeter, or a dc amplifier (Figs. XI-13 and XI-15). These circuits do not distinguish between individual pulses and only record the photomultiplier tube current proportional to the light intensity striking the photocathode.

Scintillation Techniques in X-Ray Dosimetry

Scintillation detectors are sensitive and versatile instruments which can be applied in a variety of ways in x-ray dosimetry. The electrical signal supplied by the photomultiplier tube is proportional to the amount of energy dissipated by an x-ray photon in the phosphor. Under the circumstances, if the thickness of the phosphor is sufficiently great to absorb almost completely the energy of a beam of x-rays, the signal supplied by the apparatus is proportional to the energy flux density or intensity of the x-ray beam. With suitable calibration, a scintillation detector can therefore be used for energy flux or intensity measurements. This purpose is usually achieved by connecting the photomultiplier tube to a dc circuit. If, on the other hand, the photomultiplier tube is connected to a pulse circuit followed by a pulse height analyzer, this combination allows for the measurement of energy fluence and spectral distribution of the radiation as well, and is called *scintillation spectrometer* (Chapter II). With a scintillation spectrometer the energy flux density of an x-ray beam can be determined by measuring the area under the spectral distribution curve, which is equal to the intensity of the beam.

For the above applications the selection of the phosphor material is not critical, and the only condition that the phosphor must fulfill is to be sufficiently thick to absorb all the radiation incident upon it. In the diagnostic energy range this condition is easily achieved with sodium iodide crystals approximately 2 cm thick (Fig. XI-16).

Scintillation detectors can also be used for the measurement of radiation exposures. For this purpose the phosphor must fulfill certain requirements. If the dimensions of the phosphor are large compared to the maximum range

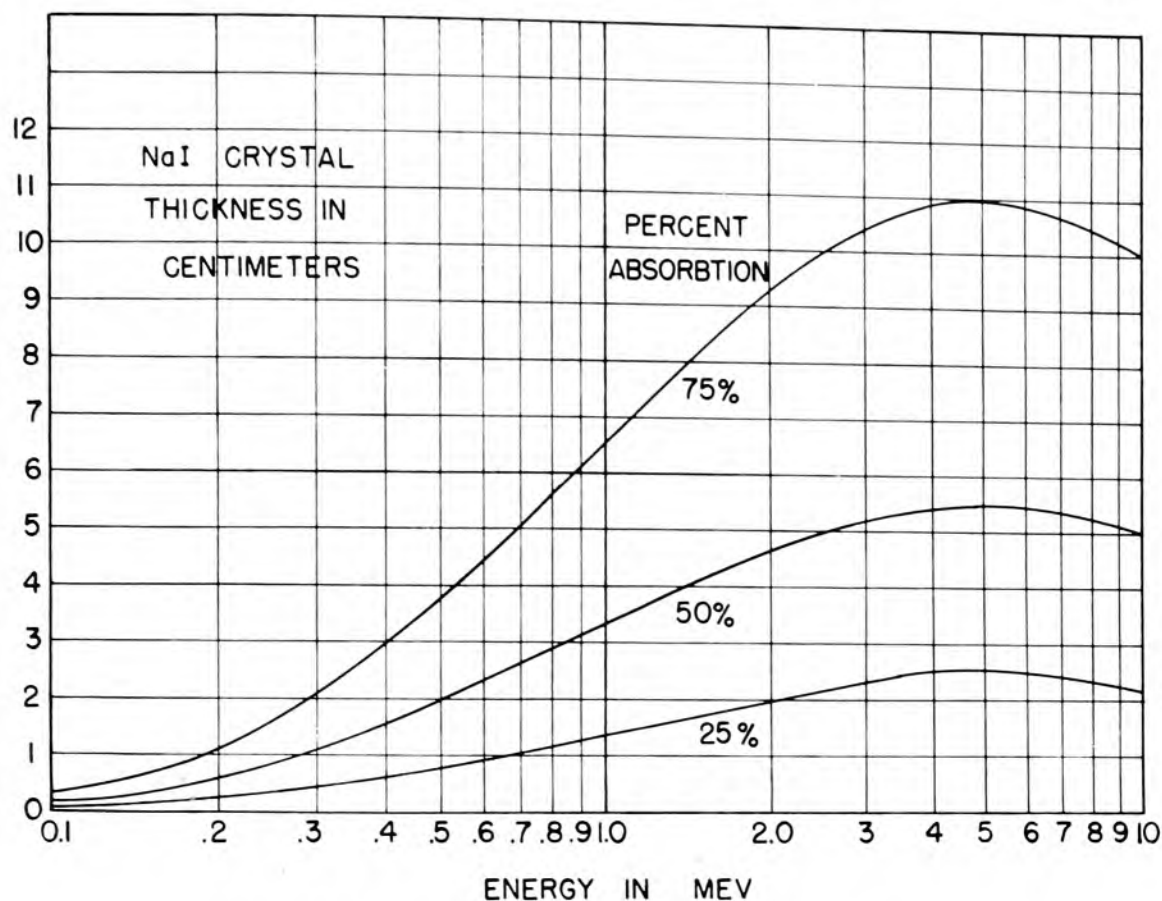


FIG. XI-16. Absorption of x-rays in sodium iodide.

of the secondary electrons produced in the phosphor by the incident x-radiation, and if these dimensions are small compared to $1/\mu_{en}$, the reciprocal of the energy absorption coefficient of the phosphor for the radiation to be measured, then the energy dissipated by the x-radiation within the phosphor, E_{phos} , can be related to that absorbed in an air-equivalent chamber with a sensitive volume equal to that of the phosphor (E_{air}) by the expression

$$\frac{E_{\text{phos}}}{E_{\text{air}}} = \frac{1 - e^{-t\mu_{en}}}{t\mu'_{en}}, \quad (11)$$

where μ_{en} and μ'_{en} are the linear energy absorption coefficients of the scintillator and air, respectively, t is the thickness of the phosphor presented to the beam of radiation, and e is the base of natural logarithms (Refs. 1, 13-15).

The variation of Equation (11) with photon energy depends on both the absorption coefficient and the thickness of the crystal. By a suitable selection of phosphor material, or by combining different phosphors, the detector can be made air equivalent over a wide range of energies. This has been accomplished by a number of combinations, such as anthracene and calcium tungstate; terphenyl dissolved in benzene and chlorobenzene; a polystyrene-based plastic phosphor combined with calcium tungstate; and a variety of

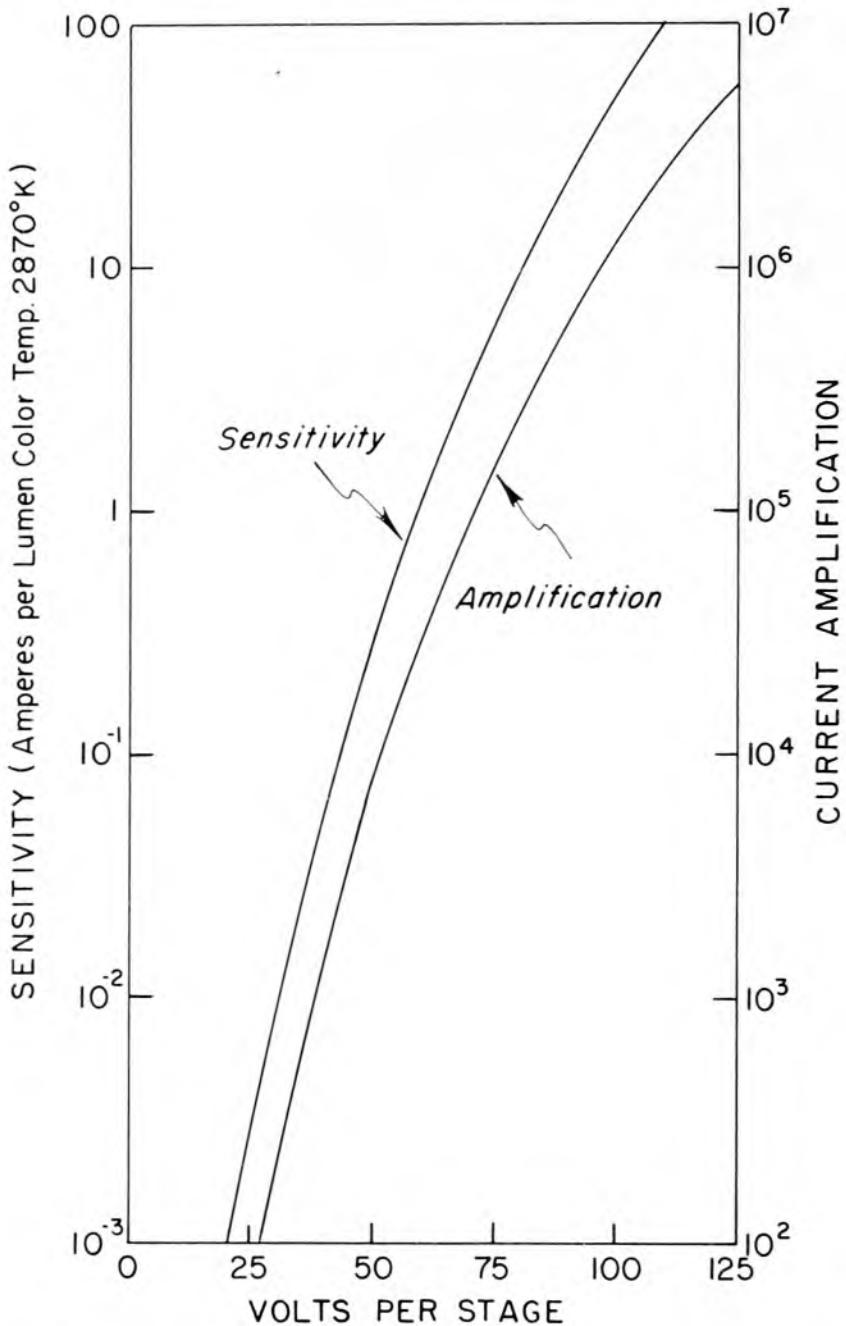


FIG. XI-17. Typical photomultiplier gain and light sensitivity as functions of dynode voltage.

other mixtures. Furthermore, other mixtures of phosphors may be made either soft-tissue equivalent, fat equivalent, or bone equivalent (Ref. 1). With all these combinations, the scintillation detector is connected to a dc circuit.

Scintillation detectors used in x-ray dosimetry are not suitable primary standards, and they must be either calibrated against an ionization chamber or some other device, or used only for relative measurements. Because of the strong dependence of the pulse heights of the photomultiplier tube on the

high voltage applied (Fig. XI-17), the constancy of the calibration of these instruments should not be relied upon, and they should be frequently recalibrated. Scintillation counters employ complex and expensive electronic equipment which may require a fair amount of servicing. Nevertheless, because of their high sensitivity and their ability to provide energy analysis, scintillation techniques are extremely valuable tools in x-ray dosimetry.

REFERENCES

1. "Physical Aspects of Irradiation." *International Commission on Radiological Units and Measurements (ICRU), Report 10b*. National Bureau of Standards Handbook 85. Washington, D.C., U.S. Government Printing Office, 1964.
2. GLASSER, O., QUIMBY, E. H., TAYLOR, L. S., WEATHERWAX, J. L., and MORGAN, R. H.: *Physical Foundations of Radiology*, 3rd ed., New York, Hoeber, 1961.
3. *International Commission on Radiological Units and Measurements (ICRU), Report 9*: National Bureau of Standards Handbook 78. Washington, D.C., U.S. Government Printing Office, 1959.
4. JOHNS, H. E.: *The Physics of Radiation*, 2nd ed. Springfield, Ill., Thomas, 1961.
5. HINE, G. J., and BROWNELL, G. L., eds.: *Radiation Dosimetry*. New York, Academic Press, 1956.
6. FRANZEN, W., and COCHRAN, L. W.: "Pulse Ionization Chambers and Proportional Counters," in *Nuclear Instruments and Their Uses*, vol. 1, ed. by Snell, A. H. New York, Wiley, 1962.
7. WYCKOFF, H. O., and ATTIX, F. H.: "Design of Free Air Ionization Chambers." National Bureau of Standards Handbook 64. Washington, D.C., U.S. Government Printing Office, 1957.
8. "Stopping Powers for Use With Cavity Chambers." National Bureau of Standards Handbook 79. Washington, D.C., U.S. Government Printing Office, 1961.
9. EHRLICH, M.: "Photographic Dosimetry of X and Gamma Rays." National Bureau of Standards Handbook 57. Washington, D.C., U.S. Government Printing Office, 1954.
10. WILSEY, R. B.: The use of photographic films for monitoring stray x-rays and gamma rays. *Radiology* 36:229, 1951.
11. PRICE, W. J.: *Nuclear Radiation Detection*. New York, McGraw-Hill, 1958.
12. SNELL, A. H.: *Nuclear Instruments and Their Uses*, vol. 1. New York, Wiley, 1962.
13. BRUCKER, G.: Energy dependence of scintillation crystals. *Nucleonics* 10(#11): 72, 1952.
14. ITTNER, W. B., and TER-POGOSSIAN, M.: Air equivalence of scintillation materials. *Nucleonics* 10(#2):48, 1952.
15. BELCHER, E. H.: Radiation dosimetry with scintillation detectors. *Brit. J. Radiol.* 26:455, 1953.
16. "Radiation Quantities and Units." *International Commission on Radiological Units and Measurements (ICRU), Report 10a*. National Bureau of Standards Handbook 84. Washington, D.C., U.S. Government Printing Office, 1962.
17. RAMM, W. J.: "Scintillation Detectors," in *Radiation Dosimetry*, ed. by Hine, G. J., and Brownell, G. L. New York, Academic Press, 1956.
18. MURRAY, R. B.: "Scintillation Counters," in *Nuclear Instruments and Their Uses*, vol. 1, ed. by Snell, A. H. New York, Wiley, 1962.

INDEX

- Absorbed dose, 384, Table, 383
Absorbed dose rate, 384, Table, 383
Absorber half-value layer, 40-42, 67-70
Absorber thickness
 effect on attenuation, 65-72
 effect on *Bremsstrahlung*, 29-31
Absorption coefficients, 89
Acceleration of electrons, 96-97
Air equivalence, 386
Air pockets, in diagnostic examination, 173
Alpha particle, 14
Alpha rays, 20
Aluminum
 as filter, 158-160, 165, 166, 168
 in grid interspace, 281-282
Amplitude distortion, in modulation transfer function, 242-243, 245
Angulation error, 271, 272-274, 275-277, 278
Annihilation radiation, 12, 86, 87
Anodes (targets) of x-ray tubes, 96-98, 100-105, 120
Anthracene, in scintillation detectors, 404, 411, Table, 403
Antiparticles, 13
Atomic number. *See also* Effective atomic number.
 effect on *Bremsstrahlung*, 31
 effect on photoelectric interactions, 75-77
Attenuation analysis, 59
Attenuation coefficients, 66-72, 88-90, Table, 71
 for bone, 172, 173
 for fat, 172, 173
 for iodine, 170, 171, 175
Attenuation coefficients (*continued*)
 for lead, 170, 171
 linear attenuation coefficient, 66-67, 88-90, Table, 71
 mass attenuation coefficient, Table, 383
 for water, 170, 171, 172
Attenuation spectrometry, 39-42
Attenuation of x-rays, 39-42, 64-72
 in air, 173-175
 in bone, 163, 166-168, 172, 173-175
 in contrast media, 169-171, 173, 175
 in fat, 160-162, 163, 172, 173-175
 in iodine, 170, 171, 173-175
 in lead, 170, 171
 in liver, 168-169
 in lung, 173-175
 mathematical equations, 64-72
 in muscle, 170, 171, 172, 173
 in water, 90-94, 173-175
Auger effect, 77
Autotransformers, 128, 129, 146
Average energy per ion pair, 25, 396, Table, 383
Back emission, 130
Barrier layer rectifiers. *See* Solid state rectifiers.
Baryon, 13, Table, 12
Base density, 227-229
Bent-crystal spectrometer, 54
Beryllium-window x-ray tube, 120, 121
Beta rays, 20
Binding energy, 17-18, 24, 34-35, Table, 19

- Body fluids
 attenuation in, 162-166, 173. *See also*
 Attenuation of x-rays in water.
 densities, 173
- Bone
 attenuation in, 163, 166-168, 172,
 173
 Compton effect in, 167, 173
 contrast, 176-183
 density, 173, Table, 173
 effective atomic number, Tables, 161,
 173
 electron density, Tables, 161, 173
 mass energy absorption coefficient,
 386, Table, 387
 photoelectric effect in, 167, 172, 173
- Bouwers mirror optics, 329-331
 in Image Orthicon television chain,
 Table, 338
 in photofluorography, 377
- Bragg-Gray relation, 396-397
- Bragg spectrometer, 52-53
- Bremsstrahlung*, 27-33
 effect of absorber thickness on, 29-31
 in lead, 32
 in tungsten, 32, Table, 37
 in water, 32
- Breast radiography. *See* Mammography.
- Brightness gain, 312-315
- Brightness control, 347-348
- Bucky, 264
- Bucky factor, 266, Table, 265
- Cable capacitance, effect on tube volt-
 age, 152-153, 154
- Calcium tungstate phosphors, 202, 205-
 206, 411, Tables, 196, 201
- Capacitor ionization chamber. *See* Con-
 denser ionization chamber.
- Capacitors, 142-143
- Cathode rays, 20
 in Hittorf-Crookes tube, 1-5
- Characteristic curve. *See under* Radio-
 graphic film.
- Characteristic radiation, 33-38
 energies, Table, 36
 intensities in tungsten, Table, 37
- Characteristic x-radiation. *See* Charac-
 teristic radiation.
- Cinefluorography, 342-375
 cameras, 355-356
 direct monitoring, 356-359
 film for, 362-366, Table, 363
 kinefluorography, 366-367, 368-370
 magnetic tape recording, 367-370
 negative film, 365-366
 optical coupling, 349-355
 projectors, 370-371
 radiation exposure, 374-375
 reversal film, 366
 synchronization, 345-347
 television monitoring, 357, 359-361
 video tape recording, 367-370
 vignetting, 349, 351-355
- Cinelix image intensifier, 320-322
 with television chain, 331-333
- Classical scattering of x-rays. *See*
 Thomson effect.
- Coherent scattering of x-rays. *See*
 Thomson effect.
- Collector (anode), 407
- Collisional interactions, 26, 27, 33-38
- Compton effect, 77-84
 angle of recoil electron, 79
 angle of scattering, 79, 80, 82, 83
 attenuation, 88-94
 contribution to noise, 252-260
 cross section, 83, 84
 energy transfer in, 80-83, Tables, 81,
 90
 linear attenuation coefficient, 88-89
 mass attenuation coefficient in nitro-
 gen, 94
 probability of occurrence, 84
- Compton interaction. *See* Compton
 effect.
- Compton scattering, role in noise produc-
 tion, 252-260
- Condenser ionization chamber, 395, 397-
 399, 400
- Contactors, 139, 141, 145, 146
- Contrast, 171-176, 192, 193
 film contrast, 213-215, 217, 222, 365,
 Table, 363
 improvement with grids, 263-282

- Contrast (*continued*)
influence of scatter on, 258, 260-263
radiographic contrast, 212-215
as result of difference in attenuation,
171-176
in soft tissues, 183
subject contrast, 212-215
variation with voltage, 176-183
- Contrast improvement factor, 261, 264-
266, 267, 268, 270, Table, 265
- Contrast media, 169-171, 173, 175, 252
- Contrast reduction factor, 264, 268
- Contrast transmission function. *See*
Modulation transfer function.
- Coolidge x-ray tube, 98, 99
- Counters, 39
- Critical energy, 24-25, Table, 25
- Cross section, 84
- Dark adaptation, 296, 297
- Decentering. *See under* Grids.
- Densities of human tissues, Table,
173
- Detectors, 38-39
- Deuteron, 13
- Diffraction, 43-54
of x-rays, 49-54, 57-59, 61
- Diffraction grating spectrometers, 47,
48, 50-54
- Diffraction gratings, 45-49, 51-54
- Direction of x-radiation, 33
- Dynamax "50," 110
target rating charts, 114
- Dynapulse circuits, 139-143, 152
- Dynapulse switching tube, 344
- Dynodes, 407, 408, 409
- Effective atomic number, 91-94
of bone, 173, Table, 161
of fat, 173, Table, 161
of muscle, 173, Table, 161
of water, 173, Table, 161
- Efficiency of x-ray production, 31-33
- Elastic collisions, 20-21, 23
- Electric charge, 8
- Electromagnetic radiation, 20-25
- Electron
acceleration methods, 96, 97
binding energy, 24, 34-35
energy, 11, Table, 12
interaction with matter, 26-38
mass, 11, Table, 12
monoenergetic electrons, 29
positive (positron), 12, 13, Table, 12
- Electron attachment, 391
- Electron density, 91-94
- Electron range, 27, 28
- Electron shells, 14-15
binding energy in, 17-18, 34-35,
Table, 19
transitions in, 34, 35
in tungsten, 16
- Electron transitions, 34, 35
- Emission analysis. *See* Fluorescence
analysis.
- Emulsions. *See* Photographic emulsions.
- Energy, 8-9
conversion to electron, 11
mass equivalence, 10-11
units, 9, 10, 23
- Energy fluence, 383, 386, 388, Tables,
383, 389
- Energy fluence rate. *See* Intensity.
- Energy flux density. *See* Intensity.
- Energy spectrum of x-rays. *See* Spectral
distribution.
- Excitation, 23-24
- Exposure rate, 385, Table, 383. *See also*
Radiation exposure.
- Fat
attenuation in, 163, 172, 173
Compton effect in, 161, 162, 173
density, Table, 173
effective atomic number, 173, Table,
161
electron density, 173, Table, 161
photoelectric effect in, 161, 162, 172,
173
- Field emission x-ray tubes, 121-124, 125
- Film. *See* Radiographic film. *Also under*
Cinefluorography; Photofluorog-
raphy.

- Film badges, 401
- Film bases, 208–209, 210
 base density, 227–229
 thickness, Table, 230
- Film sensitivity
 in cinefluorography, 364, 465, Table, 363
 to direct exposure, 225–226, 228, 229–231
 to screen exposure, 225–226, 228, 231–234
- Film speed
 in cinefluorography, 364, 365, Table, 363
 of radiographic film, 222–225, 226
- Filtration, 155–160. *See also* Attenuation.
 added, 156, 157, 158–160
 by aluminum, 158–160, 165, 166, 168
 by Compton effect, 156, 157
 by copper, 159, 160
 inherent, 156–158, Table, 157
 by photoelectric effect, 156, 157
 by water, 160, 165, 166, 168
- Flexible fiber-optics light guide, 405
- Fluence. *See* Particle fluence.
- Fluorescence, 194–199
- Fluorescence analysis, 59–62
- Fluorescence yield, 77, Table, 78
- Fluorescent radiation, 75
- Fluorography. *See* Photofluorography.
- Fluoroscopic image
 difference from radiographic image, 293
 intensification of, 307–322, 328–332, 336–339
- Flux density, 382, Table, 383
- Flux gain, 312–318
- Focal spot, 103–106
- Focal spot size, 246
- Force
 electrostatic, 7, 8, 13
 fields, 8
 gravitational, 7, 8
 nuclear, 13
- Free-air ionization chambers, 392–394
- Frequency response function. *See* Modulation transfer function.
- Fresnel bi-mirrors, 43, 44, 50
- Full-wave rectified circuits, 134
- Gamma rays, 26
- General radiation. *See* Bremsstrahlung.
- Generators, 97, 101
 in cinefluorography, 344–345
 ratings, 143–144
- Graininess, 238, 249–251, 365
- Grid control tubes, 117, 119–121
 in cinefluorography, 344, 345
- Grids, 260, 263–282
 aluminum-interspaced, 281–282
 Bucky factor, 266, Table, 265
 characteristics, Table, 265
 clean-up factor, 266
 cross grids, 264, 278–279
 decentering, 271–277
 grid ratio, 269–271
 lead, 264, 271, 280
 linear grids, 264
 loss factor, 266
 moving grids, 263, 277–278
 principle of operation, 260
 uranium, 280
- H and D curve, 209
- Half-value layer, 40–42, 67–70
- Hardening of x-ray beam, 156, 158
- Harmonic distortion, 242, 245
- Hittorf-Crookes tube, 1–6
- Illumination, 299
- Image monitoring, 356–361
 direct, 356–359
 television, 357, 359–361
- Image Orthicon pickup tube, 322–326, 328
 combination with x-ray image intensifier tube, 331–333, 337, 339, Table, 338
 statistical fluctuations, 325–326
 as x-ray image intensifier, 328–333
- Integral detectors, 39
- Intensity, 38, 383, Table, 383
 as function of absorber thickness, 29–31, 40–42
- Intensity spectrum, 38
- Interference, 43–49

- Ionization, 23–25
 Ionization chambers, 390–399
 Ionization timers, 147
 Iontomat, 147
- Kinefluorography, 366–367, 368–370
 Kinescope, 359, 366
- Laue spots, 57, 59
- Lead
 - attenuation coefficient, 281
 - Bremsstrahlung* in, 32
 - electron range, 28
 - in grids, 264, 271, 280
 - tenth-value layer, Table, 282
- Lead screens, 179
- Lepton (μ meson), 13, Table, 12
- Line radiation. *See* Characteristic radiation.
- Line spread function, 244–247
- Line x-radiation. *See* Characteristic radiation.
- Linear attenuation coefficient, 66–67, 88–90, Table, 71
- Liver, attenuation in, 168–169
- Luminance, 294–296
- Luminance gain. *See* Brightness gain.
- Luminous flux, 294, 298–300
- Lung, density, 173
- Magnetic tape recording, 208
 - in cinefluorography, 367–370
- Mammography, 182, 183
- mAs timer, 146
- Mass, energy equivalence, 10–11
- Mass absorption coefficient, in water, 94
- Mass attenuation coefficient, Table, 383
- Mass energy absorption coefficient, 386, Tables, 383, 387, 389
- Mass stopping power, 396, Table, 383
- Mean free path, 70
- Meson, 13, Table, 12
- Minification gain, 312–315
- Minimum perceptible contrast. *See also* Contrast.
 - Minimum perceptible contrast (*continued*)
 - comparison in different systems, Table, 338
 - in fluoroscopy, 301–302, 336–339
 - improvement by image intensification, 336–339
 - in x-ray image intensification, 331
 - Mirror optics, in photofluorography, 377, Table, 376
 - Modulation transfer function, 241–249, 251
 - as measure of unsharpness, 287, 289–291
 - in photofluorographic systems, 378
 - Monoenergetic (monochromatic) x-rays, 124, 127
 - Mottle, 249–252
 - effect of film-screen speed on, 251
 - effect of radiation energy on, 251–252
 - Muon, Table, 12
 - Muscle
 - attenuation in, 162–166, 172, 173. *See also* Attenuation of x-rays in water.
 - Compton effect in, 164, 165, 173
 - density, 173
 - effective atomic number, 173, Table, 161
 - electron density, 173, Table, 161
 - mass energy absorption coefficient, 386, Table, 387
 - photoelectric effect in, 164, 165, 172, 173
- Negative film 365–366
- Neutrino, 13 Table, 12
- Neutron, 11–13, Table, 12
- Noise, 252–263
- Nucleon, 15
- Nucleus, 14, 15
- Off-focus radiation, 105, 106
- Optical coupling
 - in cinefluorography, 349–355
 - in scintillation detectors, 405–410
- Organic phosphors, in scintillation detectors, 404, 411, Table, 403

- Pair production, 84-86
 attenuation coefficient, 88-89
 energy transfer in, Table, 90
- Panel-type intensification. *See* Solid-state x-ray image intensification.
- Particle fluence, 302, 382, 388, Tables, 383, 389
- Particle fluence rate. *See* Flux density.
- Particle flux density. *See* Flux density.
- Particles, 11-20, Table, 12
- Peak voltage, 152
- Penumbra. *See* Unsharpness, geometric.
- Personnel monitoring, 401
- Phase distortion, 242-243, 245
- Phosphorescence, 194-199
- Phosphors, 194-199, Table, 196
 anthracene, 404, 411, Table, 403
 barium lead sulfate, 206, Table, 201
 calcium tungstate, 202, 205-206, 411, Tables, 196, 201
 characteristics, 199, Table, 201
 in fluoroscopic screens, 206-207
 in intensifying screens, 205, 208
 light emission of, 204
 organic phosphors, 404, 411, Table, 403
 in photofluorographic screens, 206-207
 plastic phosphors, 404, 411, Table, 403
 in scintillation detectors, 401-404, 410-412, Table, 403
 sodium iodide, 401-404, 410, 411, Table, 403
 zinc cadmium sulfide, 207, 208, Table, 201
 zinc sulfide activated with silver, 207, Tables, 196, 201
- Photoconductive-electroluminescent intensification. *See* Solid-state x-ray image intensification.
- Photodisintegration, 86, 87-89
 attenuation coefficient, 88, 89
 energy transfer in, Table, 90
- Photoelectric effect, 74-77
 attenuation, 90-94
 attenuation coefficient, 88-89
 contribution to noise, 252
 direction of ejected photoelectron, 77
- Photoelectric effect (*continued*)
 energy transfer in, Table, 90
 mass attenuation coefficient in nitrogen, 94
 probability of occurrence, 75-77
- Photofluorography, 375-380
 film, 377-378
- Photographic emulsions, 208-209, 210, 229
 thickness, Table, 230
 use in x-ray dosimetry, 399-401
- Photographic x-ray film. *See* Radiographic film.
- Photomultiplier tubes, 402, 405-410
 in scintillation spectrometers, 54
- Photon, 11-12, Table, 12
- Photon fluence, 151. *See also* Particle fluence.
 effect on image quality, 186-192
 statistical fluctuations in, 186-192
- Photon flux. *See* Photon fluence.
- Photopic vision, 296
- Phototimers, 146
- Physical constants, Table, 404
- Pickup tubes in television. *See* Image Orthicon pickup tubes; Vidicon pickup tubes.
- Pinhole camera, use with x-ray tubes, 104-105
- Plastic phosphors, in scintillation detectors, 404, 411, Table, 403
- Point spread function, 244
- Poisson distribution, 187-189, 191
- Polyenergetic (polychromatic) x-rays, 42
- Positron, 12-13, Table, 12
- Potter-Bucky, 264
- Projectors, 370-371
- Proton, 11-13, Table, 12
- Pull-down time, 345-346
- Pulse circuit, 408-410
- Pulse height analyzer (discriminator), 54, 408-410
- Quantum, 22
- Quantum mottle, 249-251
- Quantum sink, 302
 in cinefluorography, 372-373

- Quantum sink (*continued*)
in fluoroscopy, 305, 307
with image intensification, 307
in photofluorographic systems, 378-379
in radiography, 305
- Quenching, 198
- Radiation exposure
in cinefluorography, 374-375
dosimetry, 384-385
measurement by scintillation detectors, 410-413
- Radiative interactions, 26-33
- Radioactivity, 15
- Radiographic film, 208-239
base density, 227-229
characteristic curve, 209, 212-216, 218-221, 225-226
density, 209-229
developing, 234-237, 238, 239
film latitude, 217, 222
fixing, 234-237
fog, 227-229
gamma, 213-215
graininess, 238, 249-251
granularity, 238
physical properties, Table, 230
processing, 234-237, 238, 239
reciprocity law, 226-227
resolving power, 238-239
sensitivity to direct exposure, 225-226, 228, 229-231
sensitivity to screen exposure, 225-226, 228, 231-234
sharpness, 238-239
speed, 222-225, 226
- Radiographic mottle. *See* Mottle.
- Rayproofing, 107
- Recombination, 391
- Resistors, 144, 145
- Resolution, 185-186, 192-193
in cinefluorography, 362-364, 371-374, Table, 363
components, Table, 288
effect of unsharpness, 283, 287
of eye, 296
- Resolution (*continued*)
in photofluorography, 376, 378
of screen-film systems, 241
in television chains, 326-328
of x-ray image intensifier tubes, 315-317
- Resolving power. *See* Resolution.
- Resonance absorption, 26
- Retinal action time, 300
- Reversal film, 366
- rms potential, 152
- Röntgen, Wilhelm Conrad, 1-6
- Roentgen cinematography. *See* X-ray cinematography.
- Roentgen grids. *See* Grids.
- Roentgen rays. *See* X-rays.
- Rotating anodes. *See under* X-ray tubes.
- Ruhmkorff induction coil, 1, 3, 129
- Saturation voltage, in ionization chambers, 391-392
- Scatter. *See* Compton scattering; Scattered radiation.
- Scattered radiation
contribution to noise, 252-260
determination, 246
effect on contrast, 258, 260-263
in high energy radiography, 182
reduction by distance, 282
reduction by grids, 260, 263-282
- Scattered-ray grids. *See* Grids.
- Scintillation counters. *See* Scintillation detectors.
- Scintillation detectors, 401-413
- Scintillation spectrometer, 54-57, 410
- Scotopic vision, 294-301
- Screen mottle, 249-251
- Screens, 199-208, Table, 201
efficiency, 202-204
fluoroscopic screens, 206-207
intensification factor, 234
intensifier input screens, 208
intensifying screens, 204-206, 207
photofluorographic screens, 206-207
resolving power, 200, 202, Table, 201
speed, 200, 202

- Selenium rectifiers, 133
 Self-rectified circuits, 130-131
 Sensitometric curve, 209
 Sensitometry, 208
 Serial fluorography, 342
 Serial radiography, 342
 Shutter-closed time, 345, 346
 Shutter-open time, 345, 346
 Signal-to-noise ratio
 of Image Orthicon tube, 326, 331
 threshold, of human eye, 336
 Silicon rectifiers, 133
 Sine wave response. *See* Modulation transfer function.
 Single-phase circuits, 130-131, 133-134, 139, 140
 Sodium iodide, in scintillation detectors, 401-404, 410, 411, Table, 403
 Soft tissues
 attenuation in, 162-166
 contrast, 176-183
 densities, Table, 173
 Solid state rectifiers, 132-133, 136
 Solid-state x-ray image intensification, 334-336
 Space charge, 121
 Spectral distribution
 for *Bremsstrahlung*, 29-31
 effect of tube voltage on, 151-155
 in tungsten, 37-38
 Spectrometry. *See* X-ray spectrometry.
 Spinning top, 147-149
 Standard deviation, 189-190
 Statistical fluctuations, 186-192
 effect on image quality, 186-192
 effect on radiographic image, 249
 in fluoroscopy, 300-306
 in radiography versus fluoroscopy, 302-305
 in scotopic vision, 298-301
 Step-down transformers, 128, 144
 Stereo Dynamax, 122
 Storage time of eye, 300
 Synchronization in cinefluorography, 345-347
 Switching tube circuits. *See* Dynapulse circuits.
 Targets of x-ray tubes. *See* Anodes.
 Television scanning, 326-328
 Tenth-value layer, Table, 282
 Tetrode, 142-143
 Thermal-field (TF) emission, 124
 Thermionic emission, 121-123
 Thermionic rectifiers. *See* Vacuum tube rectifiers.
 Thimble ionization chambers, 394-399
 Thomson effect, 72-74
 attenuation coefficient, 88-89
 contribution to noise, 252-253
 energy transfer in, Table, 90
 Thomson scattering of x-rays. *See* Thomson effect.
 Three-phase circuits, 134-139, 140
 Threshold contrast. *See* Minimum perceptible contrast.
 Thyatron tubes
 in cinefluorography, 344, 346, 347
 in x-ray timers, 146, 147
 Timers, 146-149
 Transformers, 127-129
 autotransformers, 128, 129, 146
 Ruhmkorff induction coil, 129
 step-down, 128, 144
 two-winding, 128, 129
 Transmittance, 209
 Triplet production, 85-86
 attenuation coefficient, 88, 89
 energy transfer in, Table, 90
 Tungsten
 attenuation coefficient, 281
 Bremsstrahlung in, 32, Table, 37
 characteristic radiation energy in, Table, 36
 characteristic radiation intensities in, Table, 37
 energy spectrum in, 37-38
 Uncertainty principle, 185-186
 Units, Tables, 383, 404
 barn, 84
 candela, 294
 cgs system, 8
 electron volt, 9, 10, 23, 382
 electrostatic unit of charge (esu), 8

- Units, (*continued*)
 erg, 9, 23, 382
 lambert, 294
 lumen, 294
 lux, 299
 rad, 385, Table, 383
 roentgen, 385, Table, 383
- Unsharpness, 193, 283-291
 components, Table, 288
 determination, 246
 film unsharpness, 287, 290, Table, 288
 geometric unsharpness (penumbra),
 101, 246, 283-287, 290, Table, 288
 motion unsharpness, 246, 284-287
 screen unsharpness, 287, 290, Table,
 288
- Uranium
 attenuation coefficient, 281
 in grids, 280
 tenth-value layer, Table, 282
- Vacuum tube rectifiers, 131, 132
 Valve tubes. *See* Vacuum tube rectifiers.
 Van de Graaff generator, 176
 Video tape recording, in cinefluoro-
 graphy, 367-370
 Vidicon pickup tube, 322-326
 combination with x-ray image intensi-
 fier tube, 331-333, 337, 339
- Vignetting, 349, 351-355
 Visual acuity, 296-300
 Voltage divider, 408, 409
 Voltage ripple, 134-137, 139, 154
 Voltmeters, 146, 152
- Water
 attenuation in, 93-94, 162-166
Bremsstrahlung in, 32
 Compton effect in, 164, 165, 173
 effective atomic number, 93, Table,
 161
 electron density, 93, Table, 161
 electron range, 28
 mass energy absorption coefficient,
 386, Table, 387
 photoelectric effect in, 164, 165
- Wave diffraction, 43-49
 Wave interference, 43-49
 White radiation. *See* *Bremsstrahlung*.
 Work, 8-9
- Xerography, 208
 X-radiation efficiency. *See* Efficiency of
 x-ray production.
 X-radiation intensity. *See* Intensity.
 X-ray cinematography, 341-375
 direct, 342-343
 indirect. *See* Cinefluorography.
 X-ray circuits, 129-143, 144-146
 X-ray diffraction, 49-54
 by crystals, 51-54, 57-59, 61
 X-ray diffraction gratings, 51-54
 X-ray diffraction spectrometers, 50-54
 X-ray energy spectrum. *See* Spectral
 distribution.
 X-ray film. *See* Radiographic film.
 X-ray grids. *See* Grids.
 X-ray image intensifiers, 308-339
 brightness (luminance) gain, 312-315
 in cinefluorography, 348
 Cinelix image intensifiers, 320-322
 conversion efficiency, 315
 flux gain, 312-318
 intensifier tubes, 309-320, 331-333,
 Tables, 320, 338
 light amplifier tubes, 320-322, 331-333
 minification gain, 312-315
 in photofluorography, 379-380
 resolution, 315-317
 scanning systems, 322-334
 television, 322-334
 two-stage intensifier tubes, 318-320,
 Table, 320
- X-ray intensity. *See* Intensity.
 X-ray reflection, 4
 X-ray screens. *See* Screens.
 X-ray spectrometers, 38-40
 X-ray spectrometry, 38-63
 attenuation spectrometry, 39-42
 diffraction spectrometry, 49-54
 interference spectrometry, 49-54
 scintillation spectrometry, 54-57
 X-ray spectroscopy, 57-62

- X-ray tubes, 97-127
- angulation of target, 103-104
 - anode damage, 102, 118
 - beryllium-window, 120-121, 183
 - in cinefluorography, 345
 - Coolidge tube, 98-99
 - cooling, 103-107
 - Dynamax "50," 110, 114
 - energy ratings, 112-117
 - field-emission, 121-124
 - gas tubes, 98, 99
 - grid-control, 117, 119-121
 - heat dissipation in, 103-107, 112
 - heat storage capacities, 113-117
 - housing, 107, 111
 - for monochromatic (monoenergetic)
x-rays, 124, 127
- X-ray tubes (*continued*)
- rating charts, 115-117
 - rotating anodes, 101-110
 - stationary anodes, 100-105, 120
 - stereo, 121-123
 - targets (anodes), 96-98, 100-110, 118,
120
 - use of pinhole camera with, 104-105
- X-ray tube voltage
- effect on x-ray energy spectrum, 151-
155
 - ratings, 107-117
- X-rays
- definition, 26
 - direction, 33
 - discovery, 1-6
 - distinction from gamma rays, 26